



<https://theses.gla.ac.uk/>

Theses Digitisation:

<https://www.gla.ac.uk/myglasgow/research/enlighten/theses/digitisation/>

This is a digitised version of the original print thesis.

Copyright and moral rights for this work are retained by the author

A copy can be downloaded for personal non-commercial research or study,
without prior permission or charge

This work cannot be reproduced or quoted extensively from without first
obtaining permission in writing from the author

The content must not be changed in any way or sold commercially in any
format or medium without the formal permission of the author

When referring to this work, full bibliographic details including the author,
title, awarding institution and date of the thesis must be given

Enlighten: Theses

<https://theses.gla.ac.uk/>
research-enlighten@glasgow.ac.uk

UPLIFT BEHAVIOUR OF CIRCULAR PLATE ANCHORS
IN COHESIONLESS SOILS

by

Abdelmalek Bouazza

(Ing. Civil, Ecole Polytechnique d'Alger)

Thesis submitted for the degree of
Doctor of Philosophy

Department of Civil Engineering
University of Glasgow

August 1990

ProQuest Number: 11007594

All rights reserved

INFORMATION TO ALL USERS

The quality of this reproduction is dependent upon the quality of the copy submitted.

In the unlikely event that the author did not send a complete manuscript and there are missing pages, these will be noted. Also, if material had to be removed, a note will indicate the deletion.



ProQuest 11007594

Published by ProQuest LLC (2018). Copyright of the Dissertation is held by the Author.

All rights reserved.

This work is protected against unauthorized copying under Title 17, United States Code
Microform Edition © ProQuest LLC.

ProQuest LLC.
789 East Eisenhower Parkway
P.O. Box 1346
Ann Arbor, MI 48106 – 1346

To my mother Nouara
and in the memory of my father Lakhdar

CONTENT

	page
ACKNOWLEDGEMENTS	vii
SUMMARY	viii
NOTATION	ix
CHAPTER 1: INTRODUCTION	
1-1 GENERAL	1
1-2 APPLICATIONS	2
1-3 TYPE OF ANCHORS	4
1-4 MODEL STUDIES	7
1-5 OBJECTIVE OF THE RESEARCH	8
CHAPTER 2: REVIEW OF PREVIOUS THEORETICAL AND EXPERIMENTAL WORK.	
2-1 INTRODUCTION	20
2-2 LIMITING EQUILIBRIUM ANALYSIS	21
2-2-1 Earth cone theory	21
2-2-2 Earth pressure theory	22
2-2-3 Shearing stress theory	23
2-2-4 Balla's theory	23
2-2-5 Mariuopol'skii theory	24
2-2-6 Matsuo's theory	26
2-2-7 Meyerhof & Adams theory	27
2-2-8 Vesic's theory	29
2-2-9 Clemence & Veesaert theory	31
2-2-10 Fadl's theory	32
2-2-11 Murray & Geddes theory	33
2-2-12 Saeddy's theory	33
2-2-13 Tagaya et al theory	34
2-2-14 Frydman & Shaham theory	35
2-3 DIMENSIONAL ANALYSIS	48
2-4 FINITE ELEMENT ANALYSIS	49

2-5	PROBABILISTIC METHOD	51
2-6	COMPARISON OF THEORETICAL METHODS	54
2-7	PREVIOUS EXPERIMENTAL WORK	57
	2-7-1 Form of the failure surface	57
	2-7-2 Load displacement behaviour	59
	2-7-3 Summary	62
2-8	PURPOSE AND SCOPE OF THE PRESENT WORK	62
CHAPTER 3: SOIL CHARACTERISTICS AND PREPARATION OF SAND BEDS		77
3-1	SOIL CHARACTERISTICS	77
	3-1-1 Origin of soils	77
	3-1-2 Properties of the sands	77
	3-1-2-1 Geometry of sand particles	77
	3-1-2-2 Particle shape determination	78
	3-1-2-3 Specific gravity	79
	3-1-2-4 Particle size distribution	79
	3-1-2-5 Limiting porosities	79
	3-1-2-6 Shear strength of sands	80
	3-1-2-7 Conclusions	81
3-2	SAND BED PREPARATION	92
	3-2-1 Creation of uniform sand beds	92
	3-2-2 Details of the raining device	94
	3-2-2 Uniformity of the sand beds	95
CHAPTER 4: LABORATORY TESTS OF MODEL ANCHORS		109
4-1	INTRODUCTION	109
4-2	VARIABLES	109
4-3	GENERAL DETAILS OF APPARATUS FOR LOAD TESTS	110

4-3-1	Electrical equipment	110	
4-3-2	Data acquisition	111	
4-3-3	Receiver tank	113	
4-3-3	Rig	114	
	4-3-3-1	Anchor assembly	115
	4-3-3-2	Loading assembly	115
	4-3-4	Method of assembly	116
	4-3-5	Positioning of anchor in sand for testing	116
	4-3-6	Air pressure control panel	117
	4-3-7	Method of loading	117
4-4	PRESENTATION OF TEST RESULTS	118	
	4-4-1	Dimensional analysis	118
	4-4-2	Test results	120
CHAPTER 5:	DISCUSSION AND COMPARISON OF TESTS RESULTS	136	
5-1	INTRODUCTION	136	
5-2	DISCUSSION OF THE PULL OUT RESULTS	137	
	5-2-1	Load displacement behaviour of a plate anchor	137
	5-2-2	Ultimate uplift resistance	138
	5-2-3	Effect of relative density and overburden pressure	139
	5-2-4	Effect of grain size	151
	5-2-5	Effect of grain shape	156
	5-2-6	Effect of grading	161
	5-2-7	Summary	166
5-3	COMPARISON OF PRESENT RESULTS WITH PREVIOUS THEORIES	167	
5-4	COMMENTS	170	

CHAPTER 6: THE STEREO PHOTOGRAMMETRIC METHOD FOR OBTAINING DISPLACEMENT AND STRAIN FIELDS	180
6-1 INTRODUCTION	180
6-2 LITERATURE REVIEW	181
6-2-1 Direct measurement	181
6-2-2 Photographic technique	181
6-2-3 X-ray technique	182
6-2-4 Other methods	183
6-2-5 Stereo photogrammetry technique	184
6-3 REVIEW OF PREVIOUS WORK	185
6-3-1 Laboratory based studies	185
6-3-2 Field based studies	187
6-4 STEREO PHOTOGRAMMETRIC METHOD	188
6-4-1 General description of the method	188
6-4-2 Recording the displacement field	189
6-4-3 Measurement of the displacement field	191
6-4-4 The measuring principles of the Zeiss Jena Stecometer	191
6-5 OUTPUT FROM THE ZEISS STECOMETER	193
6-6 MEASUREMENT OF DISPLACEMENT	194
6-7 COMPUTER PROCESSING OF DATA FROM THE STECOMETER	195
6-8 STRAINS COMPUTATION	195
6-9 ERRORS AND ACCURACY	197
6-10 UPLIFT TESTING PROCEDURE	199
CHAPTER 7: DISCUSSION OF THE STEREO PHOTOGRAMMETRIC TEST RESULTS	216
7-1 INTRODUCTION	216
7-2 DISCUSSION OF THE RESULTS	218

7-2-1	Uplift tests, shallow anchors $D/B=4$	218
7-2-1-1	Loose state, L. Buzzard sand	218
7-2-1-2	Dense state, L. Buzzard sand	219
7-2-2	Uplift tests, deep anchors $D/B=8$	221
7-2-2-1	Loose state, L. Buzzard sand	221
7-2-2-2	Dense state, L. Buzzard sand	222
7-2-3	Effect of grain size, grain shape and grading	245
7-2-3-1	Grain size	245
7-2-3-2	Grain shape	245
7-2-3-3	Grading	247
7-3	COMMENTS	248
CHAPTER 8:	PLATE ANCHORS BURIED IN TWO LAYERED SAND: EXPERIMENTAL AND THEORETICAL INVESTIGATION	263
8-1	INTRODUCTION	263
8-2	STEREO PHOTOGRAMMETRIC TESTS	265
8-2-1	Two layered soil, $D/B=4$, $\lambda=1$	265
8-2-2	Two layered soil, $D/B=6$, $\lambda=2$	266
8-3	THEORETICAL APPROACH	276
8-3-1	Determination of the ultimate uplift load	277
8-3-3-1	Two layered soil, $2 \leq D/B \leq 5$, $\lambda=1$	280
8-3-3-2	Two layered soil, $2 < D/B \leq 5$, $1 < \lambda \leq 4$	282
8-4	EXPERIMENTAL INVESTIGATION	287
8-5	COMPARISON OF THEORETICAL AND EXPERIMENTAL RESULTS	289
8-6	CONCLUSIONS	290

CHAPTER 9: DESIGN PROCEDURE	296
9-1 INTRODUCTION	296
9-2 DESIGN PROCEDURE	296
9-3 COMPARISON WITH PUBLISHED DATA	299
9-3-1 Comparison with model and field tests in subrounded sand	299
9-3-2 Comparison with model tests in subangular sand	301
9-3-3 Comparison with other field tests	301
9-4 EXAMPLE OF DESIGN	303
CHAPTER 10: CONCLUSIONS	296
10-1 GENERAL	318
10-2 CONCLUSIONS	318
10-3 SUGGESTIONS FOR FUTURE WORK	322
REFERENCES	323
APPENDIX I: COORDINATES TRANSFORMATION	332
APPENDIX II: FLOW CHART	337

NOTATION

The symbols in general use throughout the thesis are listed below. Symbols peculiar to a particular theory or part of the thesis are defined in the text when they occur.

A	: Anchor area
B	: Anchor diameter
B _c	: Container diameter
D	: Anchor Depth
D/B	: depth/diameter ratio
D ₅₀	: Grain size diameter
ID	: Relative density or Index of density
H	: Thickness of upper layer
Nu	: Breakout or uplift resistance factor
P	: Anchor load
P _{exp}	: Experimental ultimate uplift load
P _{the}	: Theoretical ultimate uplift load
P _u	: Uplift pressure
P _x	: X parallax
P _y	: Y parallax
R	: Roundness
U	: Uniformity
α	: Angle of inclination of the failure surface
γ	: Bulk density
δ	: Anchor displacement
δ _f	: Anchor displacement at failure
λ	: Upper thickness ratio
φ	: Angle of internal friction
Ψ*	: Sphericity

ACKNOWLEDGMENTS

The work described in this thesis was carried out in the Department of Civil Engineering at Glasgow University, under the general guidance of Professor D. Muir Wood.

I would like to express my appreciation to the head of department, D. Green, Professor H.B. Sutherland and Professor D. Muir Wood for the opportunity to do this work and for the use of the departmental facilities.

I wish to express my sincere thanks to my supervisor, Mr T.W. Finlay, for his invaluable advice, encouragement and help throughout the course of this work. His concern for me during difficult situations is also much appreciated.

The advice and assistance of Mr N. Welsh, Manager of the Department of Photography and Photogrammetry at NEL (East Kilbride) and Dr A. Tait, Department of Geography, is most gratefully acknowledged. The help of W. Henderson, T. Montgomery and A. Yuill has been indispensable in sorting out the myriad of small but troublesome problems encountered in the laboratory.

My special thanks go to my best friends Dr Pedro Pradal Roa and Dr Djamel Abderrahmane whose kindness and encouragement have been a great source of support to me over these years and also for tolerating my anti-social work habits and for providing such a welcome distracting influence.

Many thanks also to my friends and fellow research students Dr & Mrs Wei, Dr & Mrs Hytiris, O.A. Awolaye, Dr H. Jasem, E. Osman, S.E. Djellab, R. Manaa, K. Belkheir, A. Bensalem, Dr O. Famiyesin, A.R. Khan, H. Musavi, A. Bensmail, Dr S.A.W. Saad, Dr A.K. Mohammad, the CNERIB team, E. Joudeh, C. Begley, M. Johnson, C. Constantinou, S. Fulton, I. Solomon, Mr & Mrs Currie and the Latin American group whose warmth and companionship made my stay so memorable.

Last, but not least, I acknowledge with humble gratitude the boundless patience and encouragement of my mother to whom I dedicate this work.

SUMMARY

The work presented in this thesis describes an investigation into the behaviour of circular plate anchors embedded in dry cohesionless soils and subjected to vertical static uplift loading.

A review of previous theoretical and experimental work provides a good insight into, and justification for, this study. A small-scale laboratory test model was constructed for experimentation purposes. A large circular steel tank was used to contain sand which was uniformly deposited using a raining device (except for the dense well graded sand). A total of one hundred and thirty tests were completed in five different sands at densities varying from loose to very dense and using depth/diameter ratio (D/B) ranging from 2 to 12. A further 20 tests have been performed in a two layered system. A stereo photogrammetry technique was used to establish the different zone of displaced sand mass for shallow and deep anchors and a computer program was developed to facilitate computation of the results.

From the analysis of the results, it appears that the sand grain shape and grading have a profound influence on the behaviour of circular plate anchors embedded in sand. However, it was found that grain size did not have any effect on the pull out behaviour. Other influencing factors, such as the depth of embedment and relative density have also been examined. The stereo photogrammetry results showed that the extent and the shape of the zone of disturbed sand is also a function of the aforementioned parameters. Tests in the two layered system indicated that the ultimate uplift load and the mode of failure were dependent on the thickness of the upper layer and the strength of the different layers.

A theoretical analysis based on Fadl's (1981) work, was formulated in order to predict the maximum uplift load in a two layered system. Design charts for homogeneous soil have also been put forward. The validity of the design procedure was examined by comparing it with both model and field test results reported by previous investigators. A reasonable correlation has been achieved. Finally, a number of areas of related research considered suitable for further study have been outlined for the benefit of future investigators.

Chapter 1

INTRODUCTION

1-1 GENERAL

In civil engineering works a foundation is sometimes required to withstand tensile or uplift forces, and the stability of such a foundation will depend on the soil above it, just as a foundation under compressive load will depend for its stability on the soil underneath. Typical of these types of foundations are plate anchors which are needed to transmit the external forces on the structures into the soil in which the plate anchor is embedded. The present study examines the behaviour of such an anchor, embedded in cohesionless soil and subjected to vertical static loading (fig. 1-1).

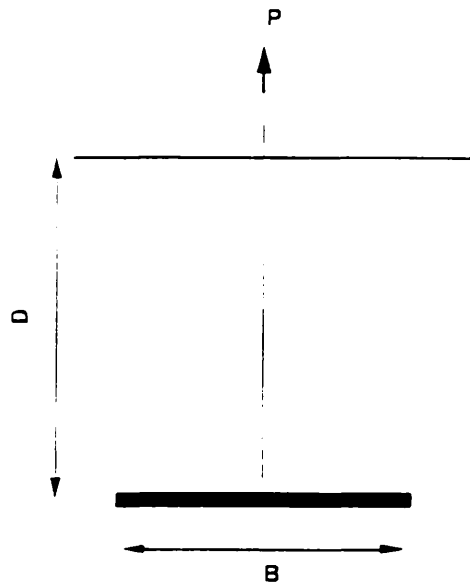


Fig. 1-1 Plate anchor under vertical uplift load.

Two methods by which a structure can be restrained are by dead weights and/or by mobilising the resistance of the surrounding soil. The use of 'dead load'

alone does not warrant elaboration as it is simply the weight of a block, made of concrete or steel, which provides the restraint. In the second, the anchor is placed within the soil, and the soil resistance acts together with the weight of the anchor to provide the restraint. This interaction of the soil and anchor forms the basis of the present investigation. The investigation forms part of a research programme which started 25 years ago at Glasgow University under the initiative of Professor Sutherland.

In this chapter, the principal anchor types and applications are described. Chapter 2 examines previous theoretical and experimental studies into the behaviour of plate anchors in cohesionless soil. Chapters 3 to 8 describe the various aspects of the present study, which is mainly experimental. Chapter 9 gives the design procedure and finally chapter 10 draws the thesis to a conclusion.

1-2 APPLICATIONS

Buried plate anchors have been used to stabilize structures for thousands of years. The oldest structures subject to uplift forces were tents. Anchors or stakes were commonly used to stabilize these structures. Modern anchors can be defined as structural members which transmit tensile forces from the main structure to the surrounding soil. They are generally attached to the structure with suitable anchor tendons.

Anchorage were primarily used for light structures until the middle of the nineteenth century when the first large suspension bridges were constructed. These bridges transmitted immense loads to the bridge foundations and permanent anchoring systems were designed to take these loads. The normal anchoring medium was rock. As structural engineering advanced, special light weight structures such as lattice

towers for radio and radar transmission were often subjected to wind loads creating reactions greater than the structure's own weight. Special tension anchoring systems were required to stabilize these structures.

Until recently the development of anchors had shown some semblance of gradualism, but with the proving of the ocean floor as an immense source of wealth an unprecedented expansion occurred in ocean exploration. Since the installation of the first fixed wooden oil platform in 6m depth of water in the Ship Shoal area of the Creole field off the coast of Louisiana in the U.S.A in 1947, oil platform construction has evolved steadily as offshore operations moved into deeper water thus requiring a greater sophistication in anchoring techniques. Consequently, the pace of research and development has quickened with a good deal of attention focussed on embedded anchors. A glance at table 1-1, where a list of operational and proposed floating systems is given, shows that most of the mooring systems use anchors.

Similarly on land, buried plate anchors are used extensively within the electric utility industry as the foundations for two or four legged lattice towers. Several case histories dealing with this type of foundation have been reported in literature. Weikart & Clemence (1987) described the use of anchors as a successful foundation system for electric transmission towers in the Rattlesnake Gulch and Bear Swamp sites in Central New York (USA) and more recently Dazinger et al (1989) reported the use of plate anchors for the Itaipu Transmission System (Brazil), stretching from Itaipu dam to Sao Paulo (900 Kms). In recent years there has been a substantial upsurge of interest, especially in North America, in foundations for transmission line towers. This interest follows on from the pioneering work carried out 20 or so years ago by Meyerhof & Adams (1968) under the auspices of the Ontario Hydro Electric Company. A recent survey conducted by the Electric Power Research

Institute (U.S.A) showed that about half of the existing towers in the United States, and about one third of those planned for construction in the next decade, use plate anchors (Kulhawy et al, 1987). The reason behind this boom is the substantial sponsorship of research on uplift resistance in the USA by power companies such as the Niagara Mohawk Power Corporation, the Houston Light and Power Company, the Southern California Edison Company etc.... In this domain the United Kingdom is lagging far behind. However, there is still hope that this trend will change and this is reflected by the comments made by Sutherland (1988) in the 28th Rankine lecture where he stated that:

" It will be interesting to see if the proposed privatisation of the Power Industry in the U.K will lead to similar sponsorship of field research in the uplift resistance as in the U.S.A".

The application of plate anchors in soil has also spread to stabilization of mobile homes (fig. 1-13), pipeline systems (Bobbit & Clemence, 1987, reported the use of plate anchors to stabilize large diameter pipelines in Indonesia), tieback excavation bracing systems and other structures (fig. 1-18). While it is not possible to describe all the applications, the examples given illustrate the versatility of the anchoring technique.

1-3 TYPE OF ANCHORS

Anchors have been seen to be efficient and cheap, and their applications are numerous. There are probably only two situations in which anchors can be envisaged to be impractical (Ponniah, 1984). Viz.,

- 1- If the foundation material is extremely stiff, problems may be encountered in anchor placement.
- 2- If the soil is very soft, the movements required to achieve the maximum loads may be unacceptable.

Plate anchors are among the most common types of anchor used in Civil Engineering construction. Others include grouted anchors, pile anchors and marine anchors.

- a- Grouted anchors

A grouted anchor consists of a steel tendon placed into a hole drilled in the soil which is subsequently grouted, most commonly using cement grout fig. 1-2. This type is considered where it is required to support large tensile loads in poor ground or to transmit these loads into stronger soil below the structure. Hanna (1982) gave detailed advice on the design and construction of grouted anchors for use in soil and rock.

- b- Pile anchors

The concept of a pile is that it relies on soil friction on the pile wall to resist vertical forces and on horizontal soil reaction to withstand horizontal forces. To improve the performance of a simple pile it is possible to build canisters or skirts around the top of the pile to increase lateral resistance, or to bell or under-ream the bottom of the pile to increase vertical resistance. Pile anchors (fig. 1-4) have been the subject of much research in recent years, principally because of their potential use as anchorages for tethered buoyant structures offshore. Nair & Duval (1982), Karal (1982) reported some typical uses of this type of foundation.

- c- Gravity anchors

The concept of the gravity anchor is simple (see fig. 1- 5). The anchor relies on self weight to resist vertical forces, and friction on the base to resist horizontal forces. They are used mainly in the marine environment, where they

are used to provide the restraint for ship's moorings. A detailed description of the gravity (deadweight) anchor is given by Taylor (1982).

- d- Suction anchors

Suction anchors rely for their effectiveness on a differential water pressure acting on a plate area of some sort, as illustrated in figs. 1-6 & 1-7. They can be deployed either on the sea bed (Wang et al, 1978, Larsen, 1989), or by using high pressure water jets, buried in the sea bed (Sahota, 1981). The major disadvantages are that they rely on regular or continuous pumping (if a pump stops the anchor reaches the end of its useful life). One possible application for suction anchors is in the mooring of wave energy converters (Karal, 1982).

- e- Marine anchors

Marine anchors are used for providing uplift resistance in shallow and deep water for the mooring of boats, buoys, ships and structures on the sea bed. A wide range of anchor types is used depending on the method of installation (fig. 1-8). Each type has particular advantages depending on the site and ground conditions and the load to be resisted. For example, the Gullfaks A platform, during near shore construction, was safely positioned by means of mooring systems using drag anchors embedded in the seafloor and other types of anchor embedded inland (see fig. 1- 16) (Roraas & Hagen, 1989). Stewart et al (1989) reported the use of large fluke anchors, in Middle Loch, Pearl Harbour, Hawaii, to preserve decommissioned naval vessels.

- f- Plate anchors

There are several types of plate anchor in use worldwide. They include

single or multiple helix anchors (Kulhawy,1985), the propellant embedded anchor (Taylor, 1982), spread anchors which include steel grillages, steel plates, precast concrete pads (Kulhawy, 1985), the "Hydropin" anchor (Kerr, 1976) and the "Duckbill" type of anchor (Gerrard & Cameron, 1988). These examples are illustrated in figs. 1-9 to 1-11 & 1-17.

The holding power of the embedded plate anchor is developed mainly by the weight and strength of the soil above it, and this will be discussed fully in the next chapter.

1-4 MODEL STUDIES

Model studies are used either to examine the validity of the assumption of a theoretical solution or to provide experimentally the answers to problems to which no satisfactory theoretical solution exists. Model testing may be classified under three categories, depending on the method and the objectives, James (1970)*.

The first category is where a prototype structure is modelled in all aspects. The size, distribution of stresses and any special ground conditions are scaled and represented in the model test. The conditions of similitude as discussed by Rocha (1957), have to be satisfied. The present study does not fall into this category because it is not intended to model a specific field situation but instead to obtain results which would have a wider application.

The second category is that in which the model tests are designed specifically to reveal stress and deformation information about a problem. It is not necessary that a full scale version of the problems exists, as the prime objective of this type of test is to investigate the soil- structure interaction, which will lead eventually to

* (After Stewart, 1988)

better design rules.

The third category is where the model anchor is considered to be a small prototype and the effect of chosen parameters on the anchor behaviour are investigated. The results expressed in dimensionless quantities have wide applications in the design of plate anchors in cohesionless soils.

These basic categories of model test are interrelated to a greater or lesser extent. The model tests undertaken in the present study fall into the second and third categories

1-5 OBJECTIVES OF THE RESEARCH

In general, the objective is to investigate the behaviour of circular plate anchors, vertically installed in dry cohesionless soils, when subjected to static uplift loads.

In particular, the objective is to investigate experimentally the effect of several variables controlling the behaviour of a plate anchor. Obviously the properties of the surrounding soils have a profound influence on the response of a loaded plate anchor. The effect of these properties, relative density, grain size, grain shape and grading, were carefully investigated. Another factor such as the effect of a layered system has also been examined. All experimental tests were conducted using a medium scale laboratory model. Design procedures, using data from the present investigation and from different parts of the world and based on soil properties, are proposed. The validity of laboratory test results and the predicted results were assessed by comparing them to each other and to those reported by previous investigators.

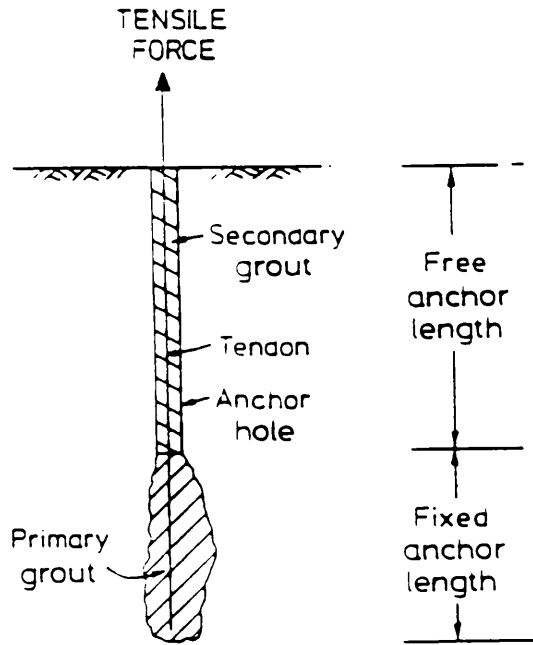


Fig. 1-2 Grouted anchor (after Hanna, 1982).

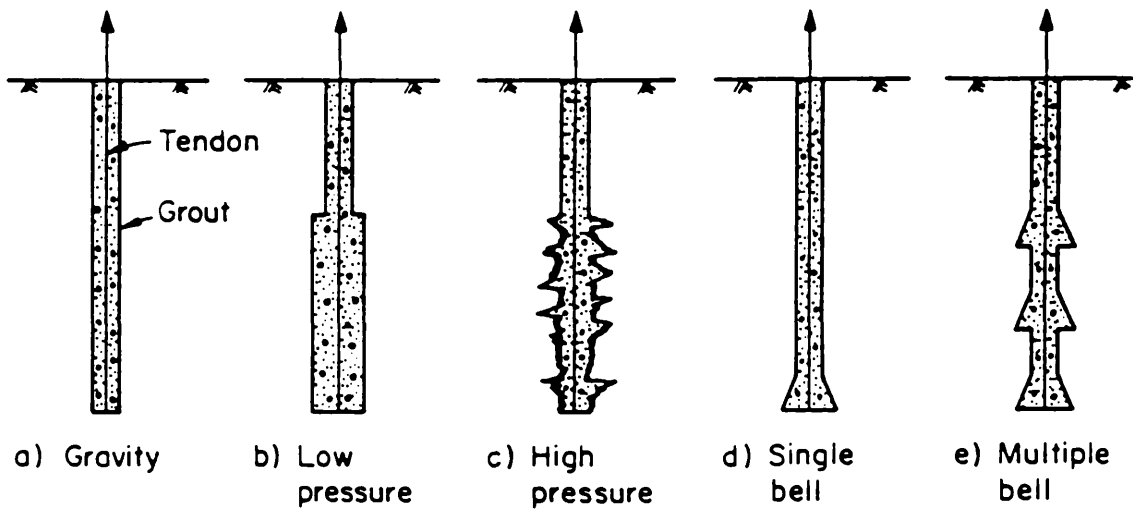


Fig. 1-3 Grouted anchor variations (after Kulhawy, 1985).

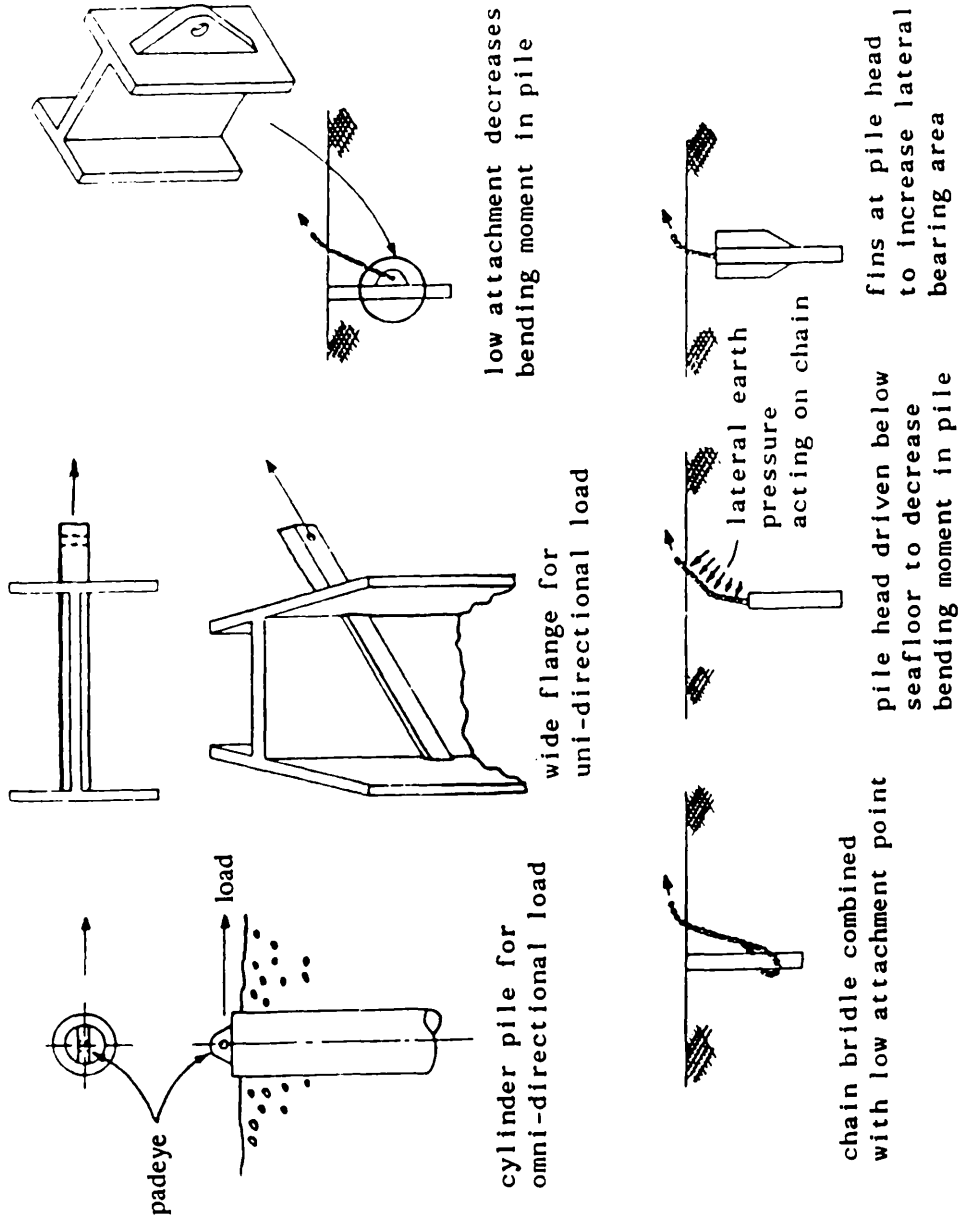


Fig. 1-4 Variations of the basic pile anchors (after Taylor, 1982).

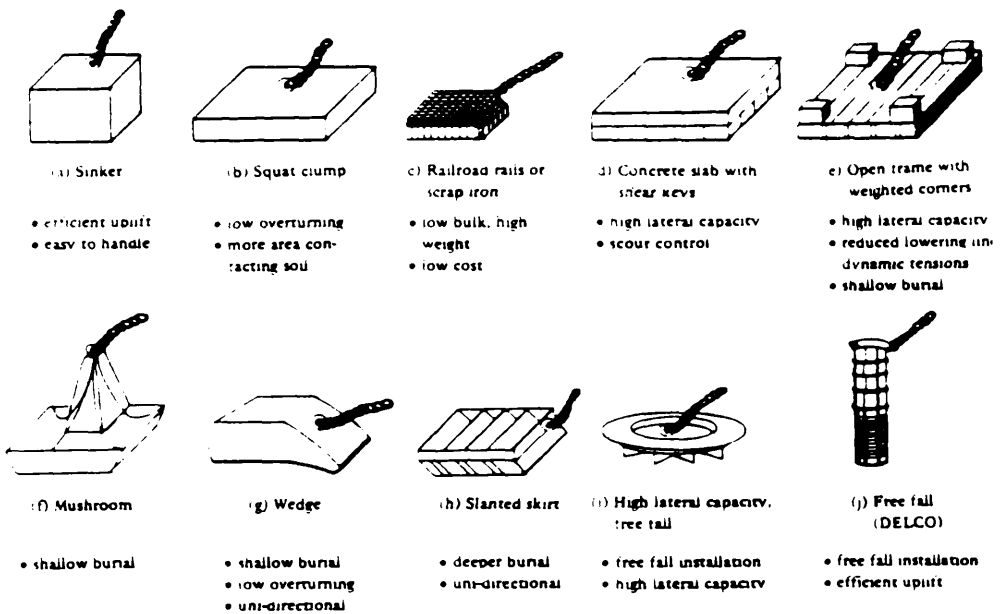


Fig. 1-5 Variations of the basic gravity anchors (after Taylor, 1982).

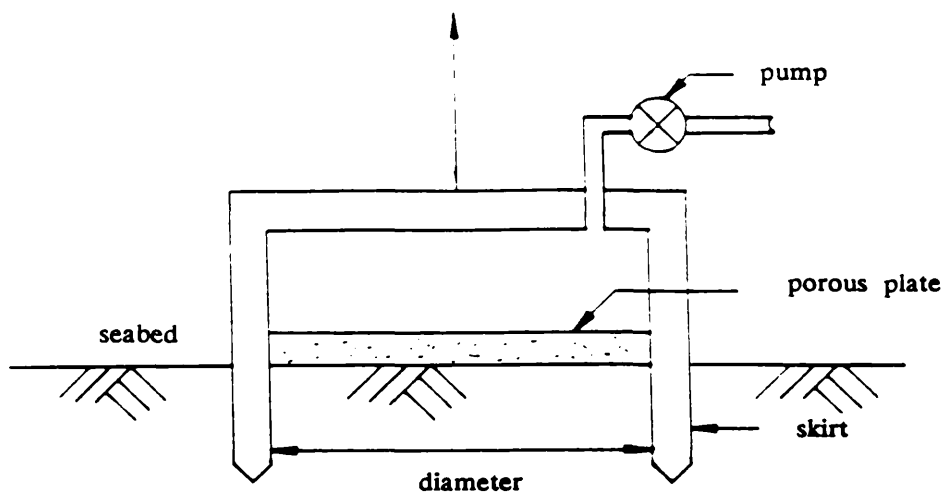


Fig. 1-6 Suction Anchor (after Wang et al, 1978).

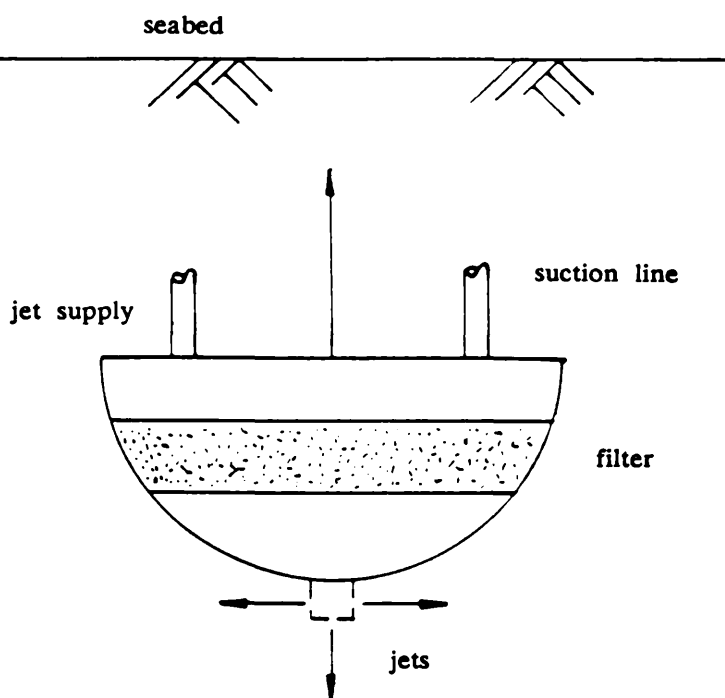


Fig. 1-7 Embedded suction anchor (after Sahota, 1979).

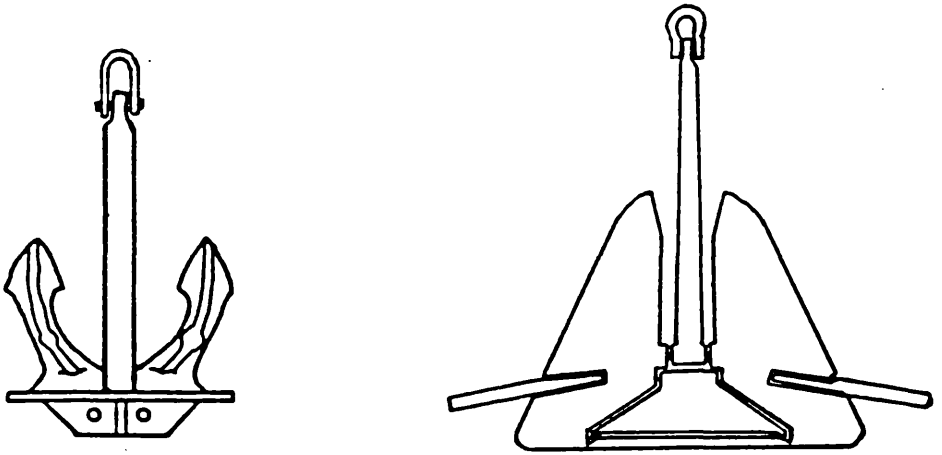


Fig. 1-8 Drag anchors (after Taylor, 1982).

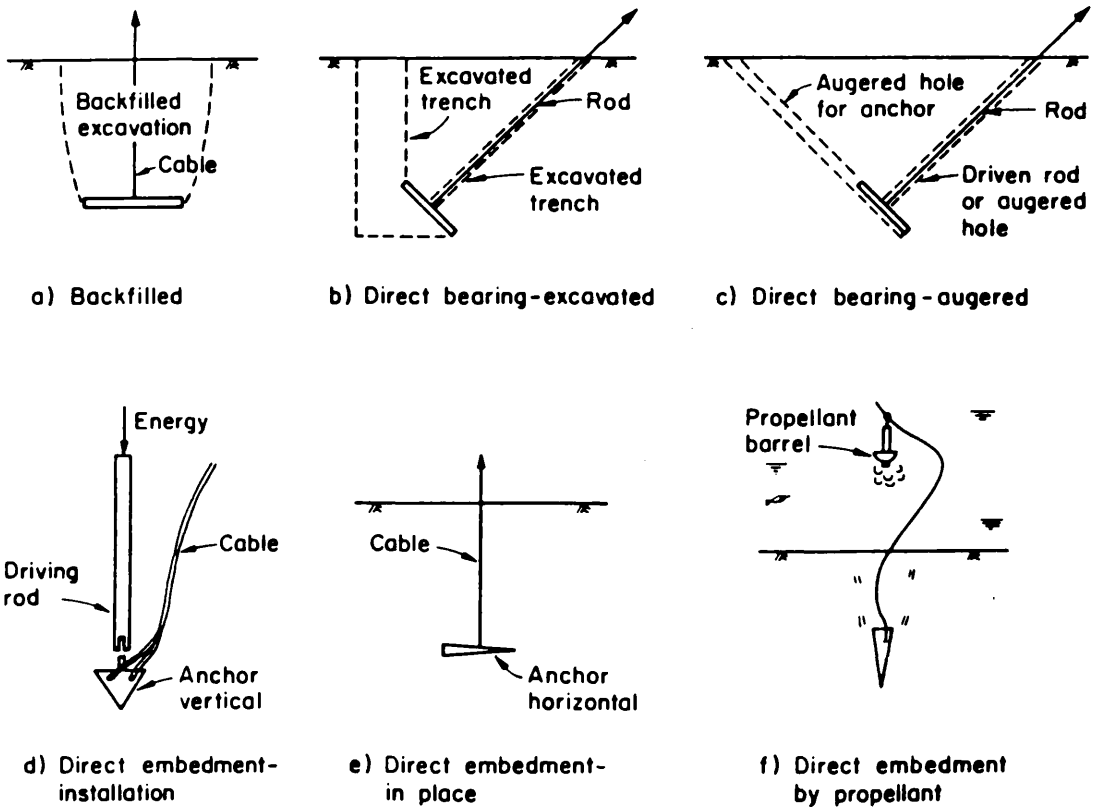


Fig. 1-9 Plate anchor variations (after Kulhawy, 1985).

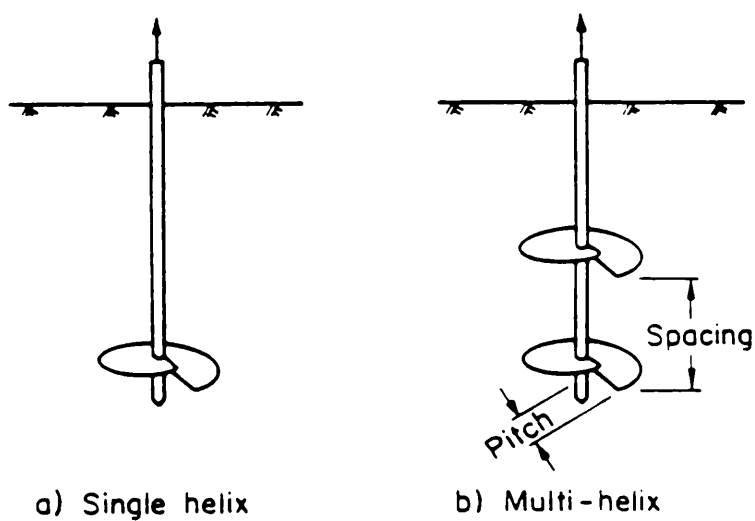


Fig. 1-10 Helical anchor variations (after Kulhawy, 1985).

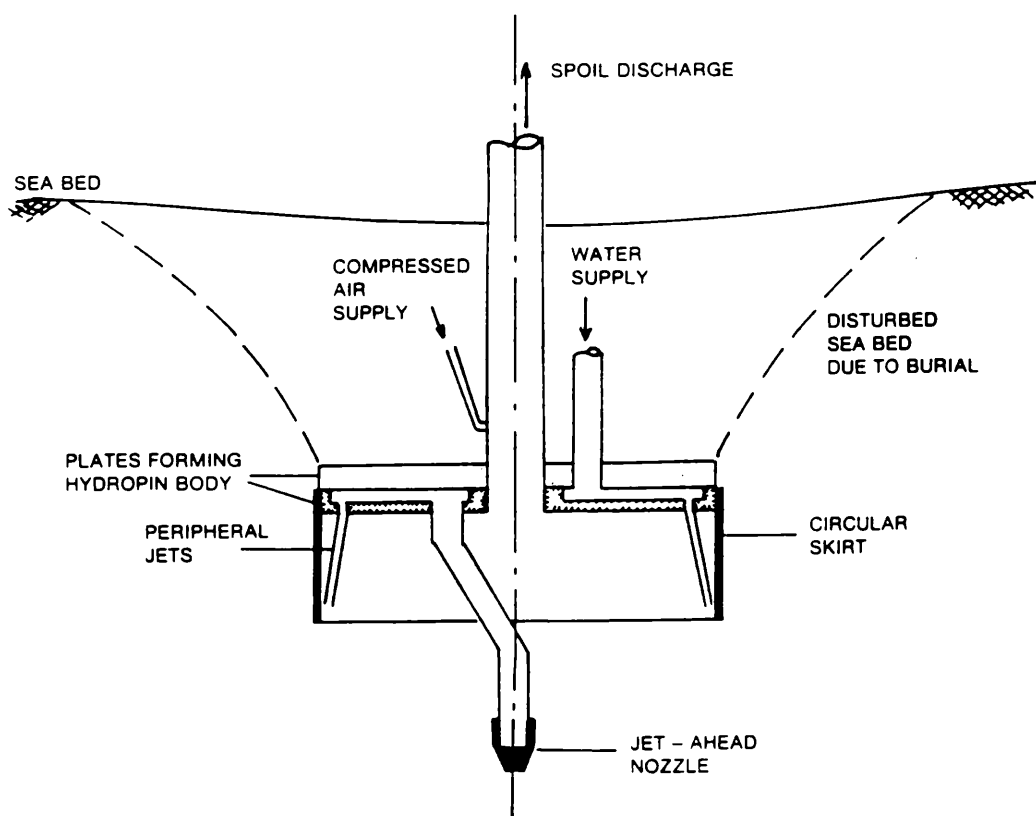
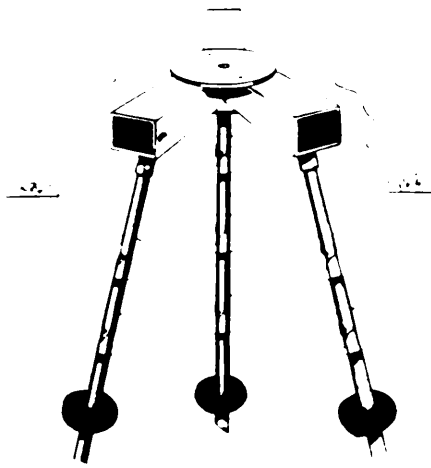
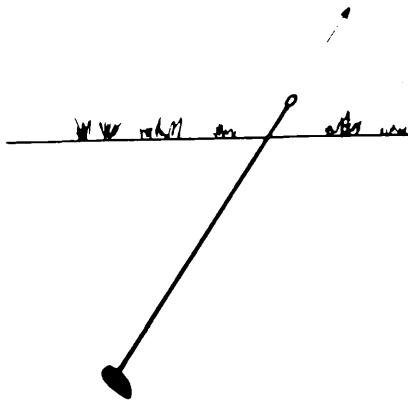


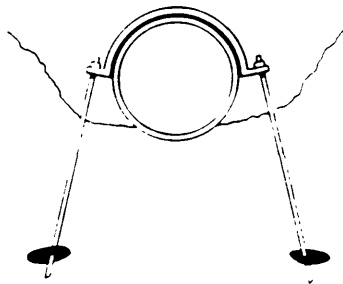
Fig. 1-11 Hydropin anchor (after Kerr, 1976).



Tower Foundation



Guy Anchor



Pipeline Anchor

Fig. 1-12 Typical anchor applications.

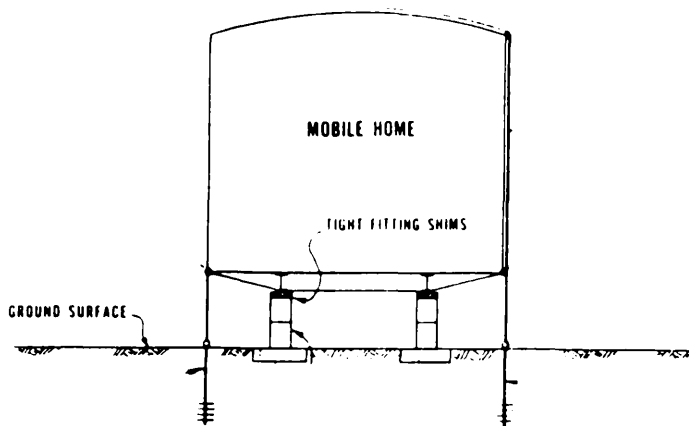


Fig. 1-13 Anchor foundations for mobile homes
(after Kovacs & Yokel, 1979).

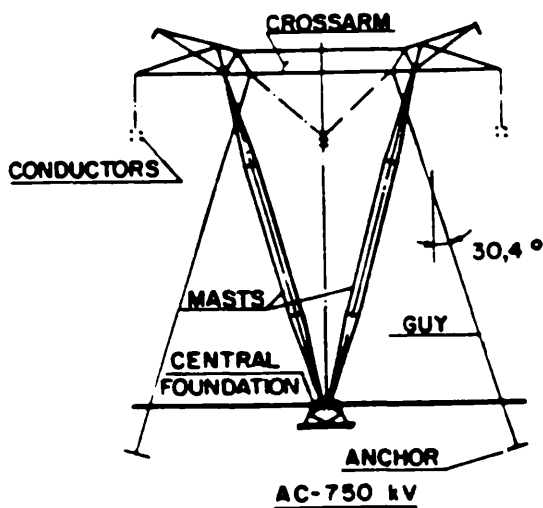


Fig. 1-14 Guyed tower foundations in the Itaipu Transmission System,
Brasil (after Danziger et al, 1989).

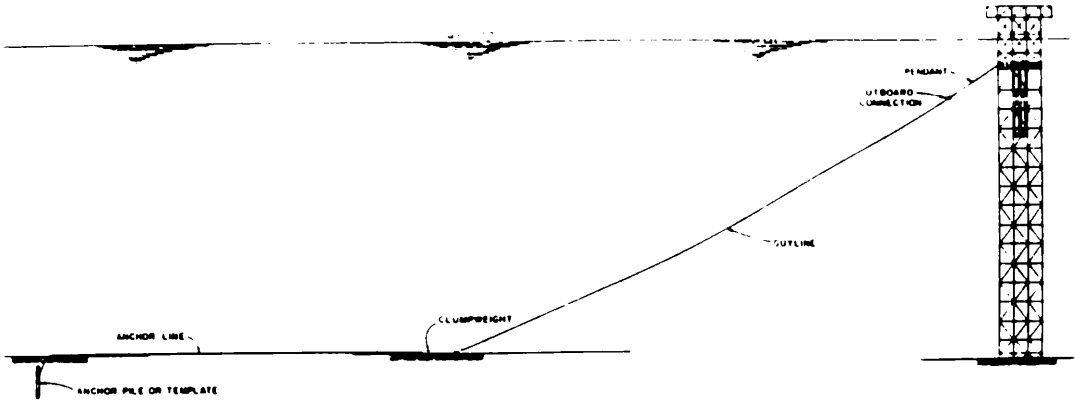


Fig. 1-15 View of a typical guyed tower mooring (after Nair & Duval, 1982).

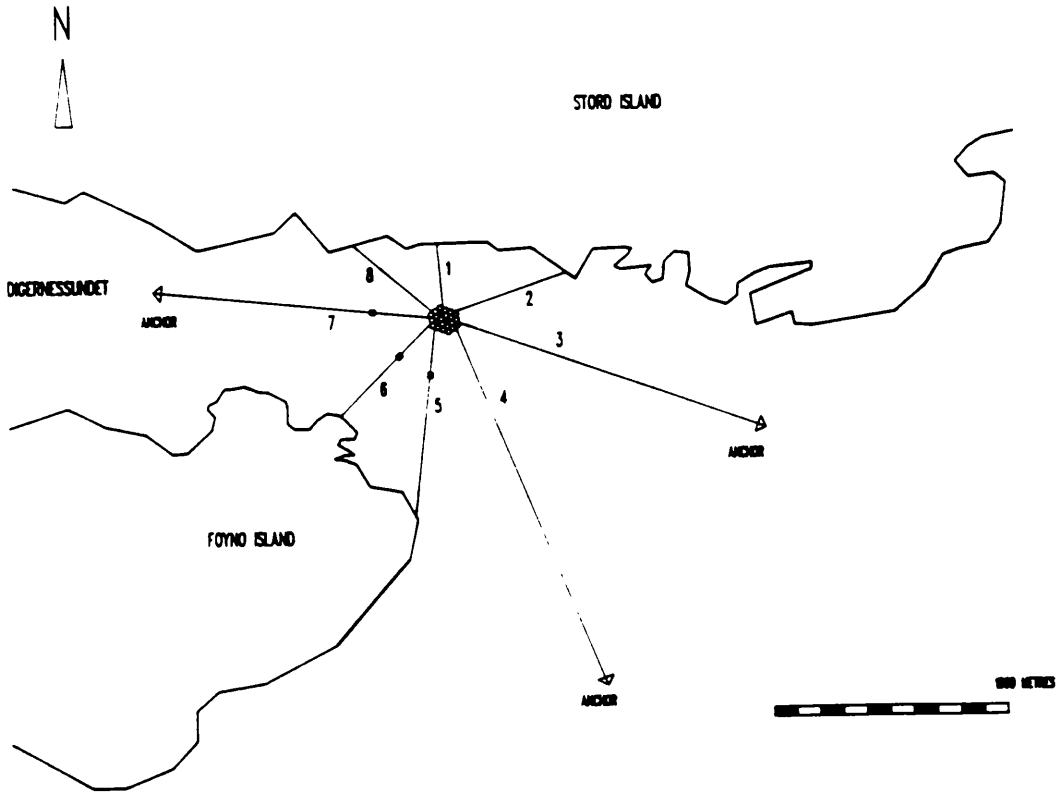


Fig. 1-16 Platform mooring arrangement at Stord, Norway (after Roraas & Hagen, 1989).

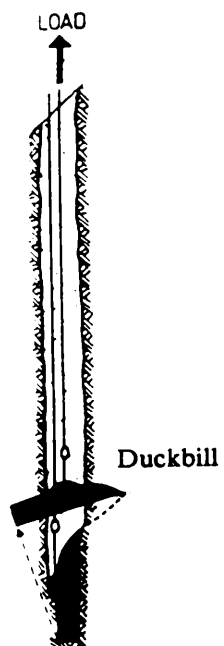


Fig. 1-17 Duckbill anchor system (after Gerrard & Cameron, 1988).

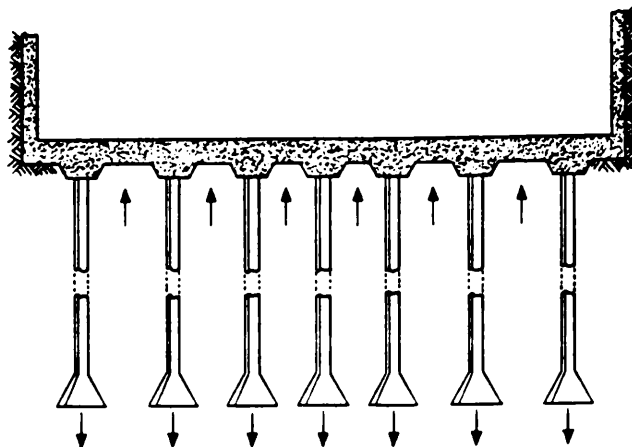


Fig. 1-18 Use of pile anchors to reduce heave of deep basement foundation.

Structure	Company	Material	Mooring	Payload (tonnes)	Production capacity (barrels/d)	Storage (barrels)	Status
Transworld 58 (semi-submersible)	Hamilton Bros. (Operator - N. Sea)	Steel	Spread anchor	N/A	70 000	N/A	Operating since 1975
Bideford Dolphin (semi-submersible)	Chevron (Operator - Mediterranean)	Steel	Spread anchor	N/A	N/A	N/A	Operating
Sedco 135 D (semi-submersible)	Petrobras (Operator - Brazil)	Steel	Spread anchor	1800*	N/A	40 000	Operating
Sedco 700 (semi-submersible)	Sedco	Steel	Spread anchor	2800*	N/A	86 000	Proposed
H3 (semi-submersible)	Aker	Steel	Spread anchor	2200*	N/A	N/A	Proposed
Tanker	Blehr & Tenvig	Steel	Spread anchor	20 000	100 000	270 000	Proposed
Floating platform	Sea Tank Co.	Concrete	Spread anchor	18 000	100 000	300 000	Proposed
Scotbuoy	Seven Seas Eng. Ltd.	Concrete/steel	Spread anchor	10 000	200 000	600 000	Proposed
Conprod	Norwegian Contractors	Concrete	Spread anchor	25 000	180 000	800 000	Proposed
Floating platform	Trans-Energy	Concrete	Spread anchor	10 000	N/A	500 000	Proposed
Big buoy	Torsvik	Steel	Spread anchor	10 000	150 000	160 000	Proposed
VAP 200	CFEM/IFP	Steel	Vertical tension leg	7000	100 000	-	Proposed
TPP	Aker	Steel	Vertical tension leg	14 000	N/A	-	Proposed
Arge 2000	Arge	Steel	Spread anchor	N/A	N/A	N/A	Proposed

* Operating check load

N/A = Information not available

Table 1-1 Floating production system structures
(after St John, 1980).

Chapter 2

REVIEW OF PREVIOUS THEORETICAL AND EXPERIMENTAL WORK

2-1 INTRODUCTION

The enormous increase in the application of anchors in civil engineering has shed more light on the anchor problem. The development from the early solution of the dead weight anchor to the more sophisticated ground anchor capable of holding the large uplift forces used nowadays shows the progress that has been made in solving the problem of uplift resistance.

Many investigators have presented theoretical solutions to the anchoring problem. Most of the theories are based on model scale studies in different types of soil. Shallow, deep, vertical and inclined anchors have been considered and various sizes and shapes of anchors, single or in groups, have been investigated to develop a relationship between anchor resistance, geometry and soil parameters.

Depending upon the depth of embedment of the anchor plate in the soil, the anchor is classified as either a shallow anchor or a deep anchor. In the former, the anchor is installed close to the surface of the soil, and the failure surface in the soil extends from the tip of the anchor to the ground surface with significant surface movements. Eventually a failure circle forms on the soil surface, well defined in cases of dense sand but poorly defined in loose sand. An increase in depth of embedment results in another type of failure in which the failure surface does not extend to the surface, but instead forms locally around the anchor. This type of failure mechanism exemplifies the deep anchor mode. The transition between the

two types of behaviour is termed the critical depth. Limiting equilibrium, finite element, and dimensional analysis techniques have been commonly used to analyse this problem, and the following sections review the theoretical and experimental work carried out to investigate the behaviour of vertical plate anchors embedded in cohesionless soils. For the purpose of clarity and comparison the expressions derived from the following theories are reduced (where possible) to the following form:

$$N_u = P_u/\gamma D \quad \dots\dots\dots(2.1)$$

where N_u = Breakout factor

and P_u = P/area of anchor

This allows comparison between the different methods on the basis of the dimensionless parameter N_u and the embedment ratio D/B .

2-2 LIMITING EQUILIBRIUM ANALYSIS

This is the most popular method. A failure surface whose form is based on field or laboratory observations is adopted and the force systems that are assumed to exist at failure are analysed.

2-2-1 Earth cone theory

This method was proposed by the Japanese Eletrotechnical Committee for the design of anchorages for transmission towers and described by Matsuo (1967). In this method, the ultimate uplift load is assumed to be equal to the dead weight of the anchor plus the weight of soil contained in the truncated cone as shown in fig.

(2-1). The ultimate uplift resistance, P , is given by:

$$P = w + \gamma (v - v_0) \dots\dots\dots (2.2)$$

Where;

w is the effective weight of the anchor.

v_0 is the volume of the footing below the ground surface.

v is the volume of the truncated cone and is

given by:

$$v = \frac{\pi D}{4} (B^2 + 2 B D \tan \alpha + \frac{4}{3} D^2 \tan^2 \alpha) \dots\dots\dots (2.3)$$

The quantity $(w - \gamma v_0)$ in equation (2.2) may be neglected in comparison with γv . Therefore the expression for the breakout factor may be written as:

$$N_u = 1 + 2 (D/B) \tan \alpha + 4/3 (D/B)^2 \tan^2 \alpha \dots\dots\dots (2.4)$$

2-2-2 Earth pressure theory

The earth pressure method, described also by Matsuo (1967) extended the scope of the earth cone method by adding a frictional component of resistance, fig. (2-2). The ultimate uplift load is assumed to be equal to the dead weight of the anchor, plus the weight of the soil contained in the cylinder above the anchor plus the vertical frictional component of resistance acting on the surface of this cylinder. The ultimate uplift resistance, P , is given as:

$$P = w + \gamma (v_1 - v_0) + F \dots\dots\dots (2.5)$$

Where the cylindrical volume of soil is:

$$v_1 = \frac{\pi}{4} B^2 D \dots\dots\dots (2.6)$$

and the vertical component of the limiting frictional force is:

$$F = \frac{\pi}{2} (K_0 \gamma D^2 B \tan \varphi) \dots \dots \dots (2.7)$$

Neglecting the term $(w - \gamma v_0)$ the breakout factor can be written as:

$$N_u = 1 + 2K_0 (D/B) \tan \varphi \dots \dots \dots (2.8)$$

2-2-3 Shearing stress theory

This theory is similar to the earth pressure theory. The only difference is that the vertical frictional component of resistance is replaced by a term which represents the shear force due to cohesion and friction, fig. (2-2). However, for a cohesionless soil the uplift resistance, P , is given by equation (2.5).

2-2-4 Balla's theory

Modern research on the uplift resistance of anchors was started by Balla (1961) who established experimentally the shape of the slip surfaces and proposed a method for the analysis of uplift forces based on these shapes. Balla assumed the slip failure surface to be an arc of a circle tangential to the edge of the anchor and intersecting the surface at an angle of $(\pi/4 - \varphi/2)$ as shown in fig. (2.3). The uplift resistance, P , is given by:

$$P = w_2 + w_3 + T_v \dots \dots \dots (2.9)$$

where, w_2 is the weight of the breaking out soil solid of revolution
and is given by:

$$w_2 = D^3 \gamma F_1 \dots \dots \dots (2.10)$$

where, F_1 is a factor depending on φ and D/B .

w_3 is the difference in weight between the anchor material
and the soil for the volume of the anchor shaft.

T_v is the vertical component of shearing over the slip
failure surface and is given by:

$$T_v = D^3 \gamma F_3 \dots \dots \dots (2.11)$$

where F_3 is a factor depending on φ and D/B .

Neglecting w_3 in relation to w_2 and T_v the breakout factor can be written as:

$$N_u = (F_1 + F_3) (D/B)^2 4/\pi \dots \dots \dots (2.12)$$

2-2-5 Mariuopol'skii theory

Mariuopol'skii (1965) assumed that the soil above the anchor was lifted and that failure occurred without sliding along the failure surface. He suggested that the development of tensile stresses resulted in a separation of a certain volume of earth in the form of a cone with a curvilinear generatrix as shown in fig. (2-4a). The ultimate uplift resistance was given as:

$$P = w + w_4 + \gamma v + Q \dots \dots \dots (2.13)$$

where; w is the weight of the anchor.

w_4 is the weight of the circular earth column above the
anchor plate.

v is the volume of the conical part of the entrained earth.

Q is the total cohesive force to failure along the lateral surface of the " separation cone " and is given by:

$$Q = \pi B \left[\tan \varphi \left(K \frac{\gamma}{4} D^2 + \int_0^D \frac{\sigma_r}{2} dz \right) \right] - \gamma v \dots\dots\dots (2.14)$$

where σ_r designates the additional radial stresses caused by pressing the anchor footing on to the overlying soil column.

After rearranging equation (2.9), the uplift resistance is given by:

$$P = w + \frac{\pi B^2}{4} \cdot \frac{\gamma D (1 + 2 K_0 D/B \tan \varphi)}{1 - 2n D/B} \dots\dots\dots (2.15)$$

where n is an empirical coefficient determined to be equal to 0.0025 φ .

Neglecting w in comparison to the second half of the expression, the breakout factor may be written as:

$$N_u = \frac{1 + 2 K_0 (D/B) \tan \varphi}{1 - 2 n (D/B)} \dots\dots\dots (2.16)$$

For deep anchors Marioupol'skii considered that the work of displacing the anchor through a distance, x, could be equated to the work required to expand a cylindrical cavity in the soil of height x from diameter B_0 to B and the work needed to overcome friction on the surface of the cone of soil formed above the anchor plate, fig. (2-4b). The ultimate uplift resistance is given by:

$$P = w + P_p \dots\dots\dots (2.17)$$

where P_p is the ultimate load transmitted to the soil by the anchor and is given by:

$$P_p = \frac{\sigma_r \pi B^2}{4 (1 - 0.5 \tan \varphi)} \dots\dots\dots (2.18)$$

2-2-6 Matsuo's theory

Matsuo (1967, 1968) developed an analysis which predicted the position of the failure surface on the assumption that it was composed of a combined curve of a logarithmic spiral rising vertically from the anchor edge and its tangential straight line meeting the ground surface at $(\pi/4 - \varphi/2)$, as shown in fig. (2-5). The position of the failure surface was found by selecting various centres for the logarithmic spiral such as O_0 . The analysis was similar to that of Balla in that a differential equation equivalent to Kotter's was used but with a different co-ordinate system to find the total vertical shearing resistance. The ultimate pull out load, P, for cohesionless soil was given by:

$$P = W + \gamma (B_2^3 K_1 - v_3) \dots\dots\dots (2.19)$$

where $v_3 =$ volume of anchor + shaft.

$B_2 =$ horizontal distance from the shaft centreline to the point where the log-spiral meets the straight line.

$K_1 =$ theoretical coefficient related to the depth of embedment, sliding surface and to the angle of internal friction.

The following expressions were derived in 1968, when Matsuo simplified the calculation involved in the uplift resistance equation presented in 1967 by assuming a constant center angle O_0 equal to 60° .

-1- for $0.5 \leq D/B < 1$

$$B_2^3 K_1 = (0.056 \varphi + 4.0) B^3 (D/B)^{(0.007 \varphi + 1.00)}$$

-2- for $1 \leq D/B < 3$

$$B_2^3 K_1 = (0.056 \varphi + 4.0) B^3 (D/B)^{(0.016 \varphi + 1.10)}$$

-3- for $3 \leq D/B < 10$

$$B_2^3 K_1 = (0.597 \varphi + 10.4) B^3 (D/3B)^{(0.023 \varphi + 1.30)}$$

Neglecting again ($w - \gamma v_3$) with respect to the rest of the expression (2.19), the breakout factor can be written as:

$$N_u = 4 B_2^3 K_1 / \pi B^2 D \dots\dots\dots (2.20)$$

2-2-7 Meyerhof & Adams theory

Meyerhof & Adams (1968) proposed a general uplift capacity theory which was complementary to the general bearing capacity theory Meyerhof (1951). A cylindrical failure surface was adopted extending vertically above the perimeter of the anchor as shown in fig. (2-6) and a theory was developed for the uplift resistance of a shallow strip footing. They assumed that the stresses on the curved failure surface would be approximately equal to the stresses developed along the cylindrical surface extending vertically above the perimeter of the anchor. The frictional stresses were calculated as in the friction cylinder method, by using earth pressure theory. Meyerhof & Adams modified their basic analysis by including an empirically derived shape factor to transform the plane stress system to the axisymmetric case which gave a suitable method for assessing the uplift resistance of a circular anchor. The ultimate uplift load, P , is given by:

$$P = \frac{\pi}{2} B \gamma D^2 s K_\mu \tan \varphi + w + w_s \dots\dots\dots (2.21)$$

where,

$$s = \text{shape factor} = 1 + m (D/B)$$

m is a coefficient depending on φ .

w_s is the weight of the lifted soil in the breaking out cylinder.

w is the anchor weight.

K_μ is the coefficient of lateral earth pressure during uplift and is given by:

$$K_\mu = K_{pv} / \tan \varphi \dots\dots\dots (2.22)$$

where, K_{pv} is the vertical component of the coefficient of passive earth pressure K_p and is given by:

$$K_{pv} = K_p \tan \delta \dots\dots\dots (2.23)$$

and, δ is the inclination of the passive earth pressure and is equal to $(2/3) \varphi$

Neglecting w the weight of the anchor, the breakout factor may be written as:

$$N_u = 2 (D/B) s K_\mu \tan \varphi + 1 \dots\dots\dots (2.24)$$

For deep anchors, Meyerhof & Adams suggested that the same failure will develop as for a shallow anchor but without reaching the ground surface as shown in fig. (2-6). The contribution of overburden pressure above the level where the extent of the failure stops was taken into account. Thus equation (2.21) becomes:

$$P = \frac{\pi}{2} (2 D - H) H \gamma B s K_\mu \tan \varphi + w + w_s \dots\dots\dots (2.25)$$

where, H is the vertical extent of the failure surface which was determined empirically.

The breakout factor is given as:

$$N_u = 2 H/B [2 - H/D]^s K_\mu \tan \varphi + 1 \quad \dots\dots\dots (2.26)$$

Table 2.1 Typical values for parameters in Meyerhof & Adams' theory

Friction angle, φ	0°	20°	25°	30°	35°	40°	45°
m	-	0.05	0.10	0.15	0.25	0.35	0.50
s_{\max}	-	1.12	1.30	1.60	2.25	3.45	5.50
critical depth, H/B	2.34	2.50	3.00	4.00	5.00	7.00	9.00
K_μ	-	0.85	0.89	0.92	0.94	0.95	0.95

2-2-8 Vesic's theory

Vesic (1971, 1972) presented a theory based on the expansion of a spherical cavity (axisymmetric case) by an internal pressure. In the shallow case the circular failure was assumed to extend from the expanded cavity to the ground surface, intersecting it at an angle α equal to $(\pi/4 - \varphi/2)$ as shown in fig. (2-7a). The ultimate pressure, P_{uc} , needed to break out a spherical cavity close to the surface of a semi infinite rigid plastic solid was given in terms of spherical cavity expansion factors F_c and F_q .

$$P_{uc} = c \bar{F}_c + \gamma D \bar{F}_q \quad \dots\dots\dots (2.27)$$

F_c and F_q depended on the shape and the relative depth of the cavity and the angle of internal friction. When equation (2.27) is applied to an anchor plate embedded in sand, it becomes:

$$P_{uc} = \gamma D \bar{F}_q \quad \dots\dots\dots (2.28)$$

where, \bar{F}_q is a plate breakout parameter and is given by:

$$\bar{F}_q = F_q + 1/3 (B/D) \quad \dots\dots\dots (2.29)$$

The ultimate breakout factor is given by:

$$N_u = F_q + \frac{1}{3} \frac{B}{D} \dots\dots\dots (2.30)$$

For deep anchors, Vesic assumed the same mode of failure as Mariuopol'skii and used a solution for the expansion of a cylindrical cavity, similar to that for a spherical cavity. The ultimate pressure, P_{uc} , was given as:

$$P_{uc} = \gamma D F'_q \dots\dots\dots (2.31)$$

Mariuopol'skii (1965) obtained the ultimate uplift capacity as:

$$P = \frac{\pi}{4} B^2 \frac{\sigma_r}{1 - 0.5 \tan\varphi}$$

For estimating the ultimate pressure, σ_r , Vesic showed that:

$$\sigma_r = \gamma D F'_q \dots\dots\dots (2.32)$$

where, F'_q is a cylindrical cavity breakout parameter.

Hence, the breakout factor, N_u , is given by:

$$N_u = \frac{F'_q}{1 - 0.5 \tan\varphi} \dots\dots\dots (2.33)$$

where, $F'_q = (1 + \sin\varphi) (I_r \sec\varphi)^{\sin\varphi} (1 + \sin\varphi)$

I_r represents the rigidity index of the soil defined in terms of strength characteristics, φ , and shear modulus of the soil as: $I_r = G/(\gamma D \tan\varphi)$

Vesic provided tables of the factors F_q and F'_q for both the axisymmetric and the plane strain case.

2-2-9 Clemence & Veesaert theory

Clemence & Veesaert (1978) approximated the curved form of the failure surface (for shallow anchors) by a straight line extending upward from the tip of the anchor and forming a truncated cone with an apex angle equal to the effective friction angle ($\alpha = \varphi$), fig. (2-8). They developed their theory by using this semi empirical failure surface and assuming that the normal stress on the sides of the surface was a linear function of depth. The value of K_0 was assumed to be constant with depth. The uplift resistance was expressed as:

$$P = \gamma V + \gamma K_0 \tan\varphi \cos^2(\varphi/2) \pi [BD^2/2 + 1/3 D^3 \tan(\varphi/2)] \dots\dots (2.34)$$

where, $V =$ volume of soil in the truncated cone

The first term in the equation is simply the weight of sand in the truncated cone. The second term is an expression for the shear resistance derived by integrating the shear stress over the failure surface.

Expressing equation 2.34 in terms of B,D and φ , the breakout factor, N_u , is given by the following:

$$N_u = 1 + 2/3 D/B \tan \varphi/2 + 4/3 (D/B)^2 \tan^2 \varphi/2 + K_0 \tan\varphi \cdot \cos^2 \varphi/2 \cdot (2 D/B + 4/3 (D/B)^2 \tan \varphi/2) \dots\dots(2.35)$$

2-2-10 Fadl's approximate theory

Fadl (1981) used the principles of the earth cone and earth pressure methods similar to Matsuo (1967). He adopted a simplified shape of failure surface, approximating the slightly curved form of the failure surface to a straight line intersecting the sand surface at an angle α as shown in fig. (2-9a). The angle α was defined in terms of relative density ID and angle of internal friction φ . The uplift resistance, P, was given as:

$$P = \frac{\pi D \gamma}{12} (8 D^2 \tan^2 \alpha + 12 B.D. \tan \alpha + 3 B^2) \dots\dots\dots (2.36)$$

where, $\alpha = M \varphi$, and $M = 0.25 [ID (1 + \cos^2 \varphi) + (1 + \sin^2 \varphi)]$

After rearranging equation (2.36) the breakout factor can be written as:

$$N_u = 8/3 (D/B)^2 \tan^2 \alpha + 4 (D/B) \tan \alpha + 1 \dots\dots\dots (2.37)$$

For deep anchors as shown in fig. (2-9b), Fadl assumed that the failure surface is limited at a distance below the ground surface (i.e local shear failure) and took into account the effect of the overlying soil. The uplift resistance, P, was given by:

$$P = \frac{\pi \gamma}{12} \left[8 H^2 (3D - 2H) \tan^2 \alpha + 12 H B (2D - H) \tan \alpha + 3 D B^2 + 6 K_0 (D - H)^2 (B + 2H \tan \alpha) \tan \bar{c} \varphi \right] \dots\dots (2.38)$$

where, $K_0 = 1 - \sin \varphi$, and $\bar{c} = ID \cdot \cos \varphi$

After rearranging equation (2.38) the breakout factor may be written as:

$$N_u = 8 (H/B)^2 (1 - 2/3 H/D) \tan^2 \alpha + 4 H/B [R + 2 - H/D] \tan \alpha + 2R + 1 \dots\dots\dots (2.39)$$

where, $R = [H/B.H/D - 2. H/B + H/D] K_0 \tan \bar{c} \varphi$
 H/B is the critical depth shown in fig. (2.9c)

2-2-11 Murray & Geddes theory

Murray & Geddes (1987) presented an equilibrium approach and a limit analysis approach based on the theory of plasticity. In the first approach the general failure configuration shown in fig. (2-10a) was adopted for a circular anchor, The ultimate uplift resistance is given by the weight of soil in the conical failure surface and the vertical component of the frictional resistance. The breakout factor N_u resulting from this analysis is given by equation (2.40a) where α is the angle of inclination of the failure surface.

$$N_u = [1 + 2 (D/B)(\sin \varphi + \sin \alpha)(1 + 2/3 (D/B)\tan \alpha (2 - \sin \varphi))] \dots\dots\dots (2.40a)$$

In the second approach (Fig. 2-10b) the collapse loading was determined by equating the work done by external forces, including the soil's self weight, to the internal dissipation of energy as a result of the soil's inherent shearing. However, since the soil under consideration was cohesionless and obeyed an associated flow rule, the dissipation of energy was taken as zero. A lower and an upper bound solution was proposed. The breakout factor resulting from this method is given by equation 2.40b.

$$1 \leq N_u \leq 1 + 2 D/B \tan \varphi (1 + 2/3 D/B \tan \varphi) \dots\dots\dots (2.40b)$$

2-2-12 Saeddy's theory

Saeddy (1975) formulated a solution for shallow anchors embedded in sand,

based on experimental observations and theories related to stress distribution in a semi infinite solid media. The above author assumed a logarithmic spiral failure surface starting tangentially upward from the anchor plate periphery and curving away from the centre line of the anchor, intersecting the ground surface at an angle of $(45^\circ - \phi/2)$ to the horizontal. Kotter's differential equation was used to calculate the distribution of shear stress on the failure surface. Non dimensional curves for the determination of the ultimate uplift capacity of shallow plate anchors were produced and are given in Fig. (2-13). In 1987, Saeddy extended his work to the case of a deep plate anchor. As with Fadl (1981), the failure surface was assumed to end at a level below the ground surface (see fig. 2-11) and a factor μ was introduced which took into account the effect of the compressibility of the soil. The total uplift force of the plate anchor was given as:

$$Q_u = \mu \sum \Delta Q_{ui} \quad \dots\dots\dots (2.41)$$

with $i = n$

where

$$\mu = 1.044 ID + 0.044$$

$$\Delta Q_{ui} = \pi \rho_i^2 [2\tau_i/\rho_i + \gamma] \Delta D_i$$

ρ_i = horizontal radius of breaking out soil mass.

τ_i = shear stress of soil along the failure surface.

ΔD_i = incremental depth

Another set of non dimensional curves has been produced and is shown in fig. 2.12.

2-2-13 Tagaya et al theory

Tagaya et al (1988) used Meyerhof's (1973) theory on anchors subjected to oblique loads. The ultimate pull out load for shallow anchors was given as:

$$P = 1/2 \gamma D^2/B K_b A + W \cos\alpha \dots\dots\dots(2.42)$$

where

$$K_b = 2 K_\mu \tan \varphi \text{ (for } K_\mu \text{ see section 2.2.7)}$$

A = anchor area.

W = weight of the anchor.

α = load inclination.

Neglecting the anchor weight and taking $\alpha=0^\circ$, the breakout factor may be written as:

$$N_u = D/B K_\mu \tan \varphi \dots\dots\dots(2.43)$$

For a deep anchor, the pull out resistance was obtained, as the failure mechanism of point bearing of a pile (Vesic, 1975) turned upside down, by the two dimensional failure mechanism shown in fig. (2.12a). The following breakout factor was obtained:

$$N_u = 1/2 (2 - \sin\varphi) \tan^2 (\pi/4 + \varphi/2) \exp (\pi/2 - \varphi) \tan\varphi \dots\dots\dots (2.44)$$

A design chart has been produced and is shown in fig. (2.12b)

2-1-14 Frydman & Shaham's theory

Frydman & Shaham (1989) proposed a method based on the work of Vermeer & Sutjiadi (1985) and Murray & Geddes (1987) who considered the equilibrium of a truncated wedge pulled out together with a rectangular plate; in both cases, they suggested the following upper bound to the breakout factor.

$$N_u = 1 + D/B \tan\varphi \dots\dots\dots (2.45)$$

Analysing data collected from literature and using statistical analysis Frydman & Shaham introduced a shape factor S (equ. 2.46) which was subsequently injected in expression 2-45 to give the breakout factor.

$$S = 1 + \frac{(B/L - 0.15)}{1 - 0.15} (S_{sq} - 1) \dots\dots\dots(2.46)$$

where; $S_{sq} = 1.51 + 2.35 \log (D/B)$

In the case of circular plate anchors, similarly to Ovesen (1981) they took B as the width of a square plate that would have the same area as the circular plate (i.e., $B = (\pi/4)^{\frac{1}{2}} B_c$, where B_c is the plate anchor diameter). The pull out capacity factor was then expressed as follows:

For dense sand ($D/B_c \leq 8$):

$$Nu = 2 (1 + (4/\pi)^{\frac{1}{2}} D/B_c \tan\varphi) (0.51 + 2.35 \log(4/\pi)^{\frac{1}{2}} D/B_c) \dots\dots\dots (2-47)$$

For loose sand, ($D/B_c > 1.8$):

$$Nu = 1.5 (1 + (4/\pi)^{\frac{1}{2}} D/B_c \tan\varphi) \dots\dots\dots (2-48)$$

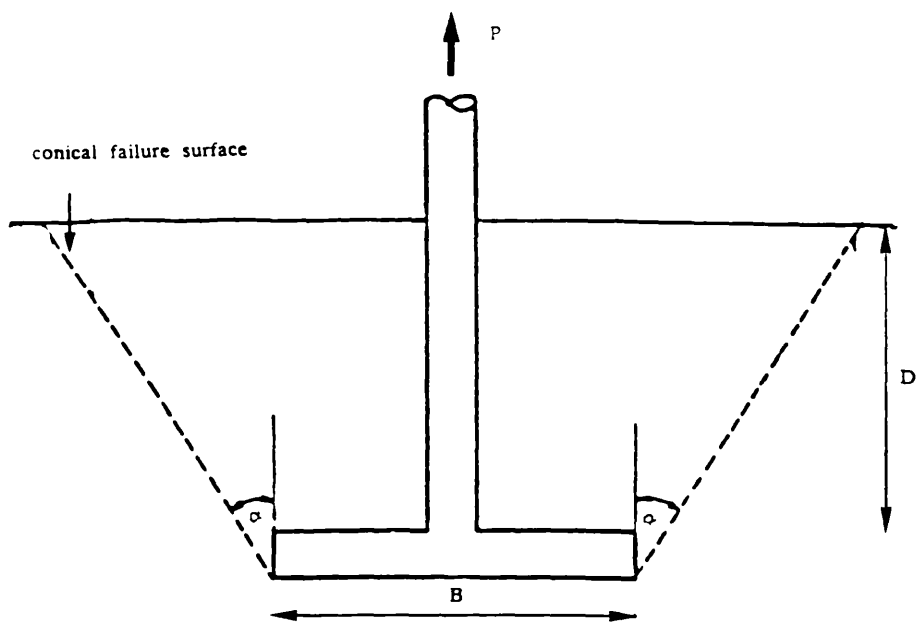


Fig. 2-1 Earth Cone Theory.

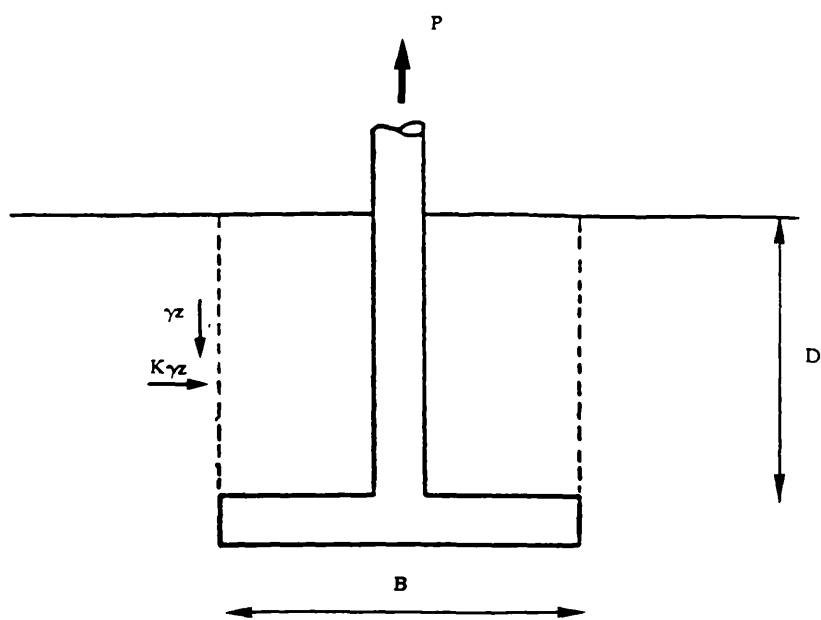


Fig. 2-2 Earth Pressure and Shearing Theories.

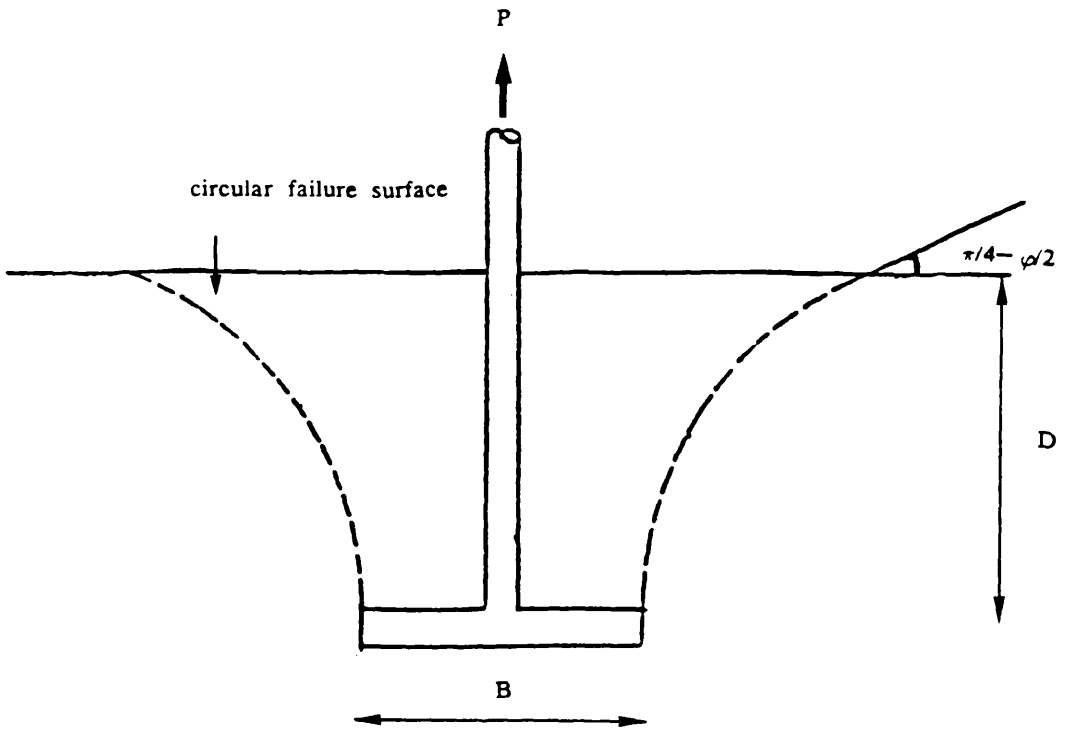


Fig. 2-3 Balla's Theory.

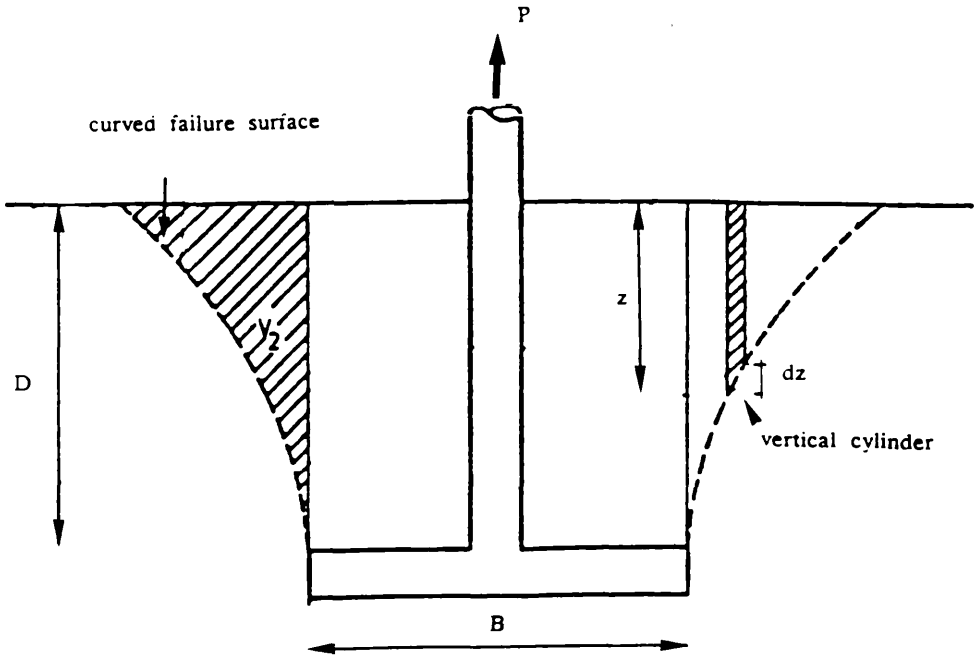


Fig. 2-4a Mariuopol'skii shallow Anchor Theory.

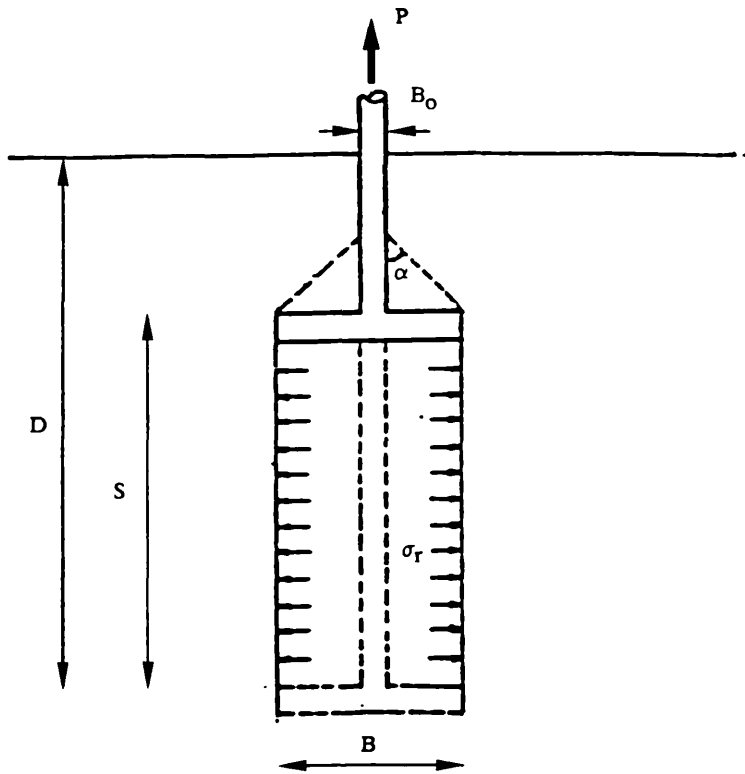


Fig. 2-4b Mariuopol'skii Deep Anchor Theory.

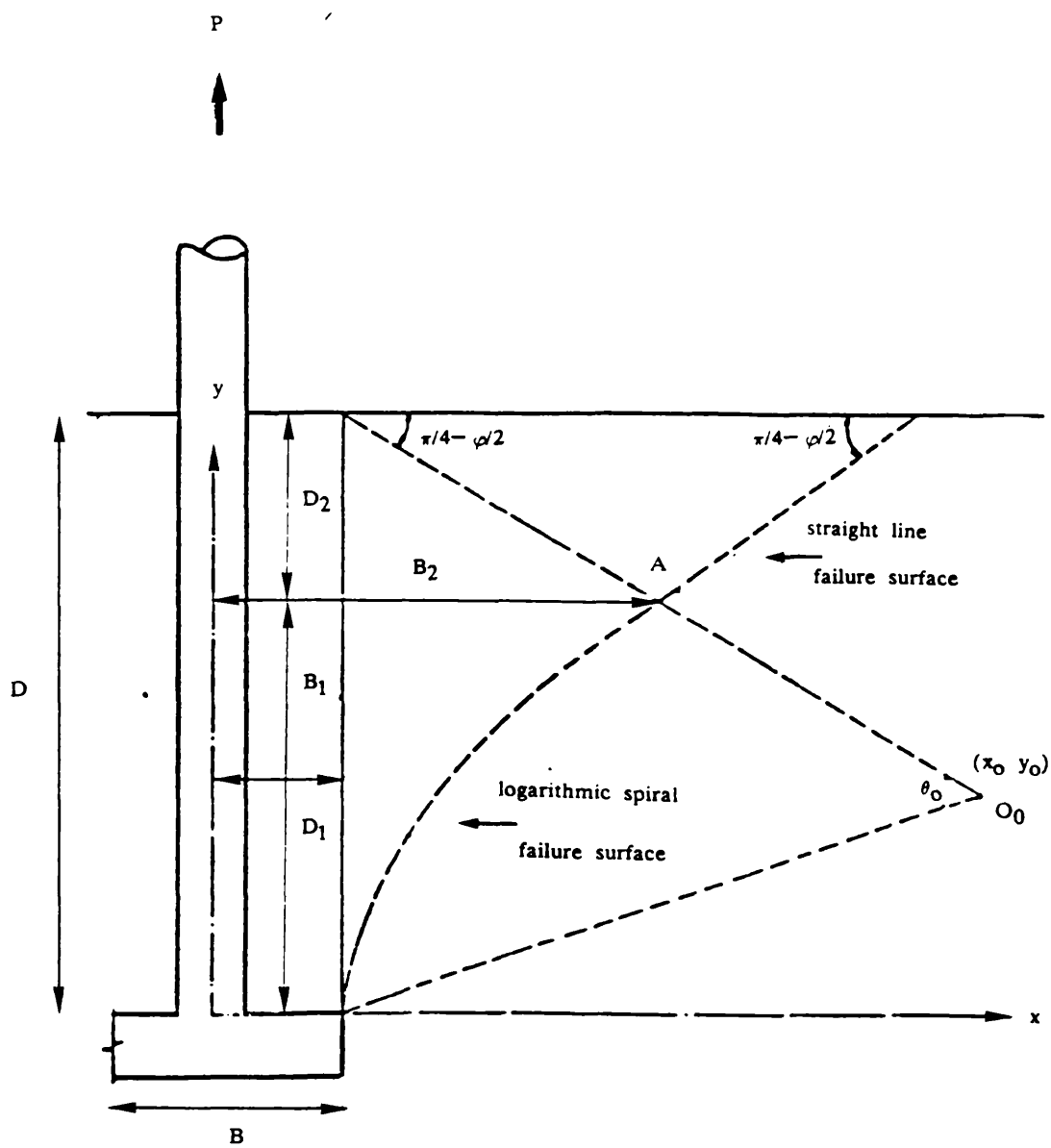


Fig. 2-5 Matsuo's Theory.

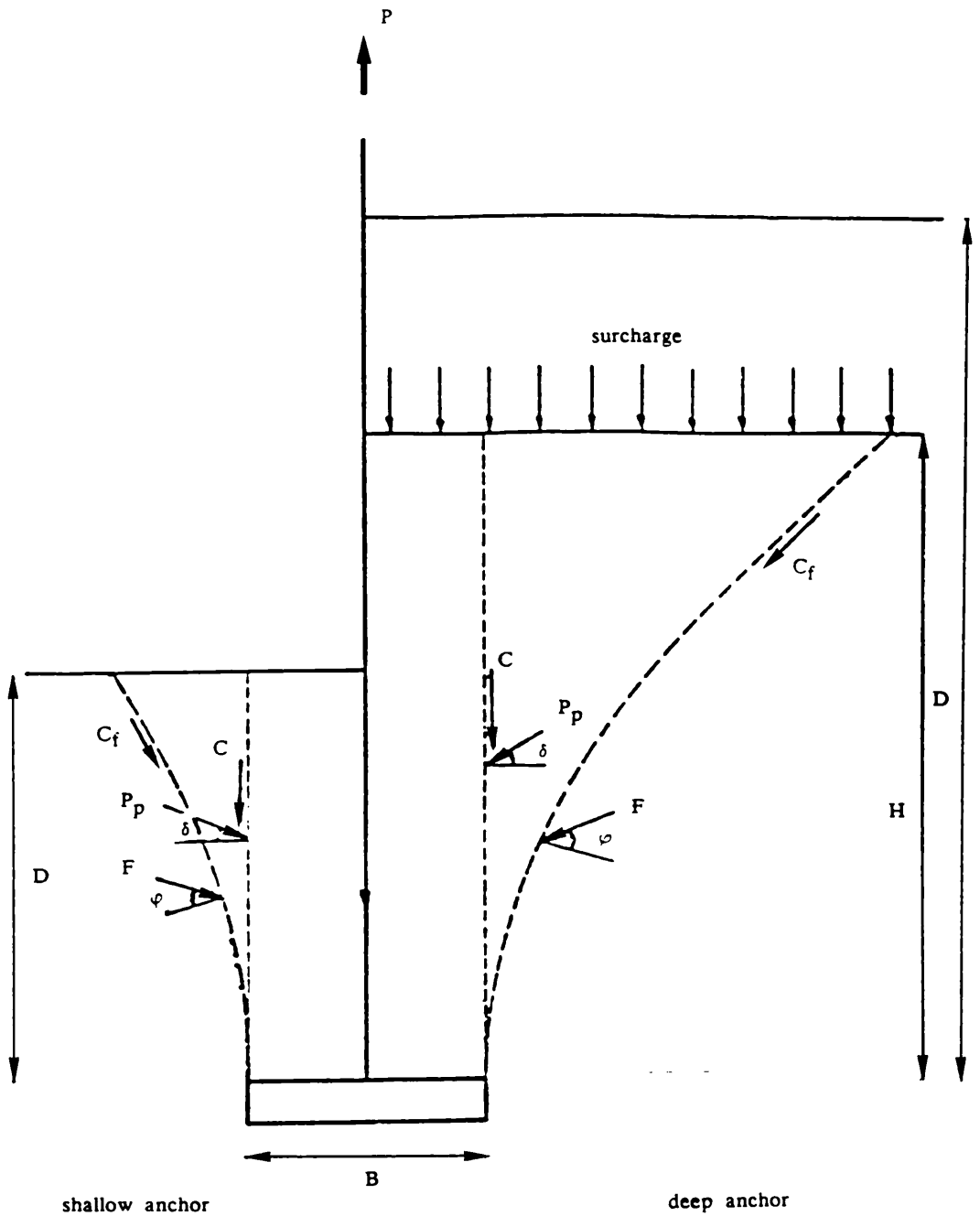


Fig. 2-6 Meyerhof & Adams' Theory.

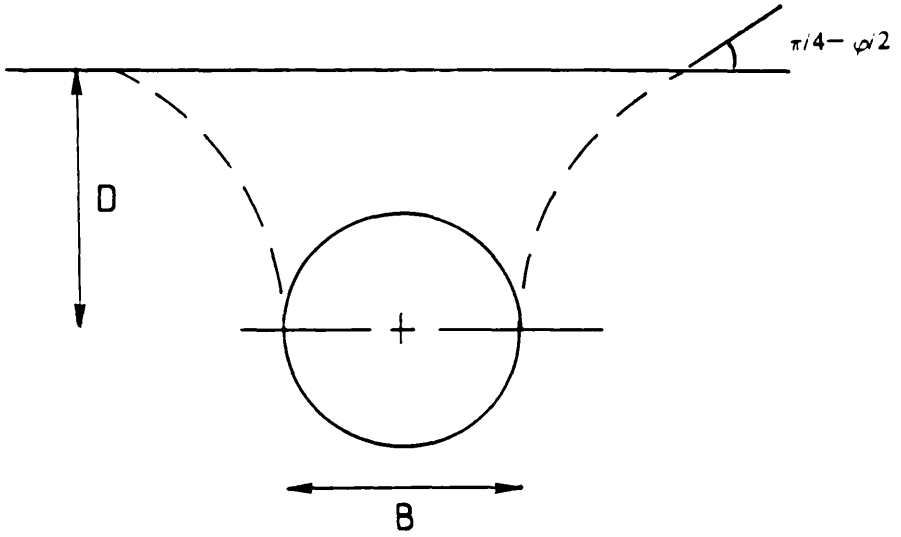


Fig. 2-7a Vesic's shallow anchor theory.

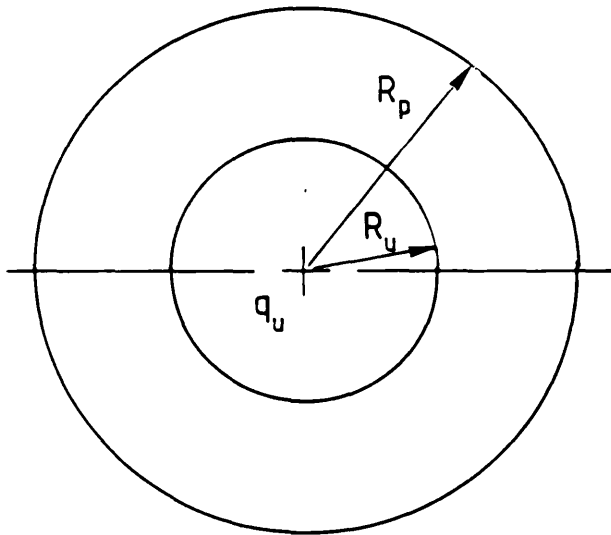


Fig. 2-7b Vesic's deep anchor theory.

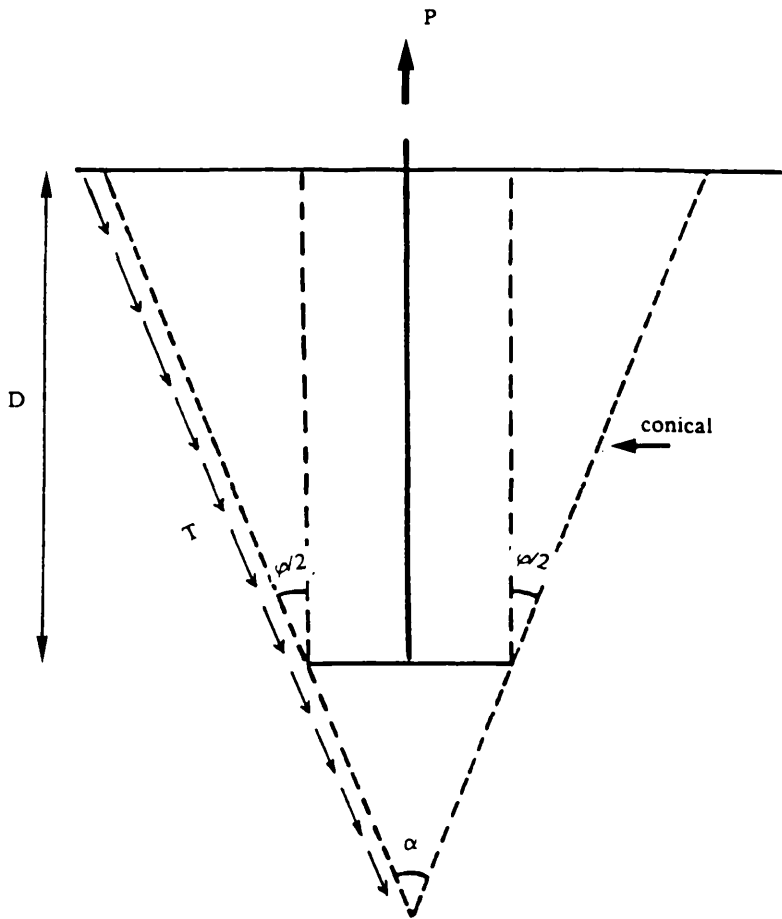


Fig. 2-8 Clemence & Veesaert's Theory.

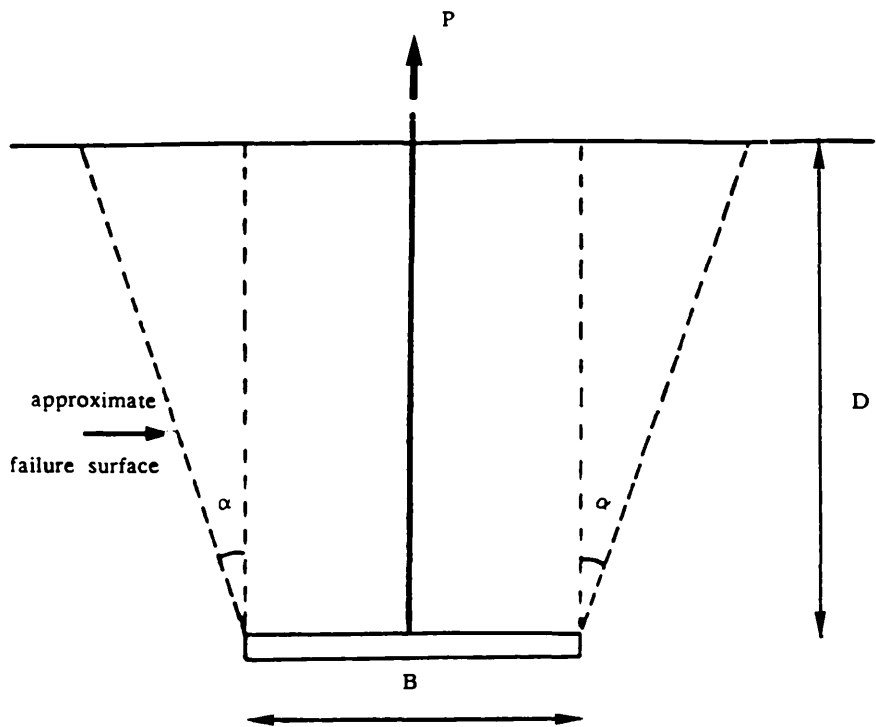
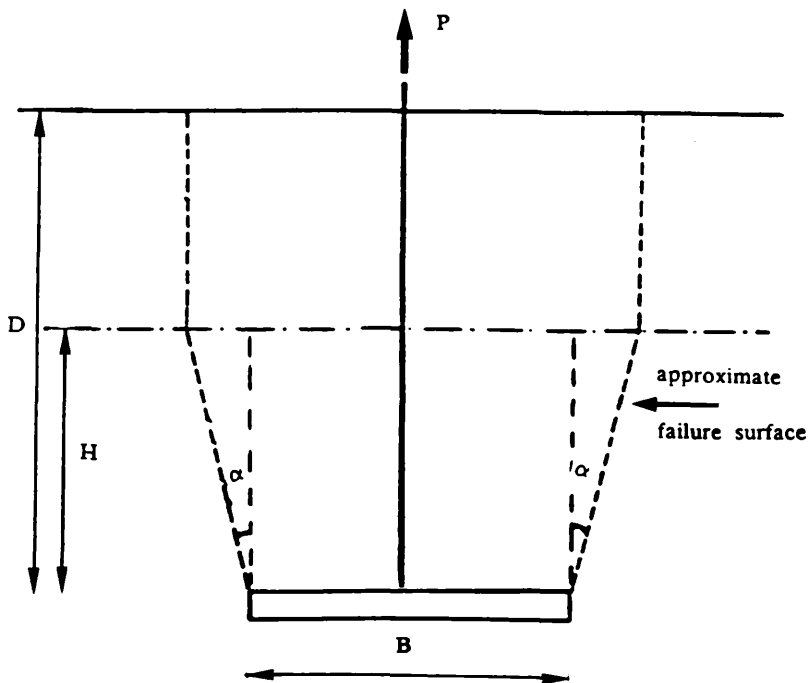


Fig. 2-9a Fadhil's shallow anchor theory.

Fig. 2-9b Fadhil's deep anchor theory.



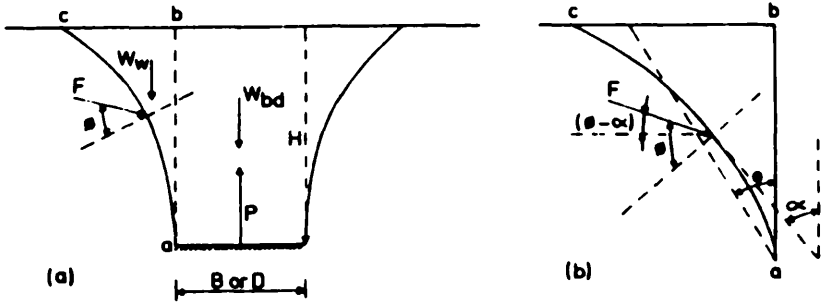
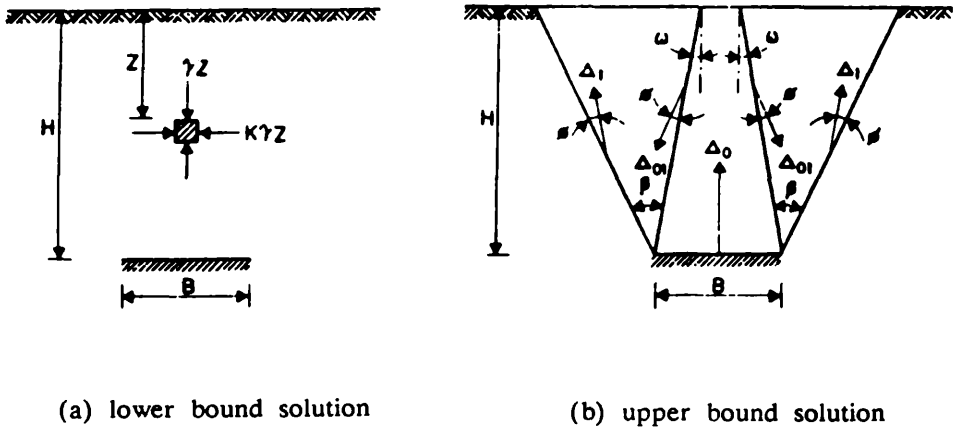


Fig. 2-10a Murray & Geddes theory (equilibrium approach)



(a) lower bound solution

(b) upper bound solution

Fig. 2-10b Murray & Geddes theory (limit analysis approach)

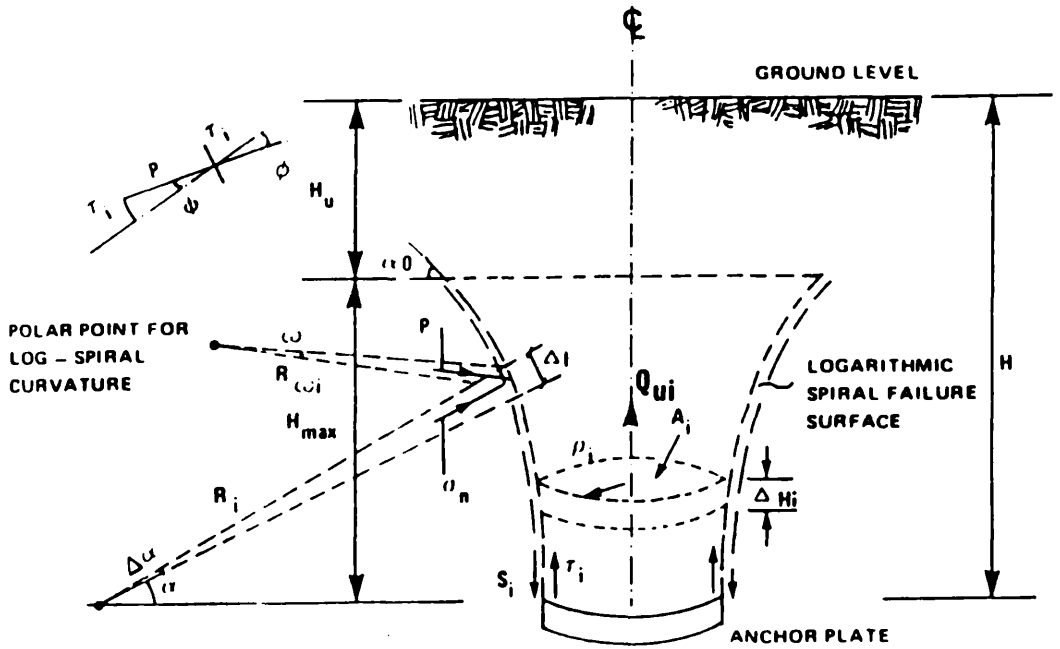


Fig. 2-11 Saeddy's Theory.

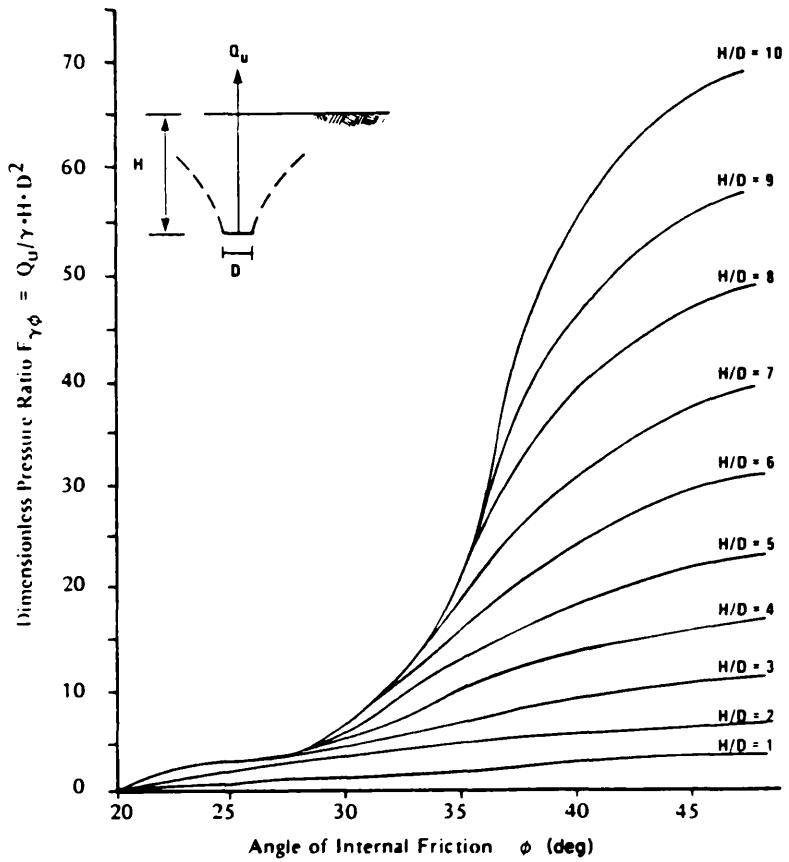


Fig. 2-12 Non Dimensional Curve for Determination of N_u (after Saeddy, 1987).

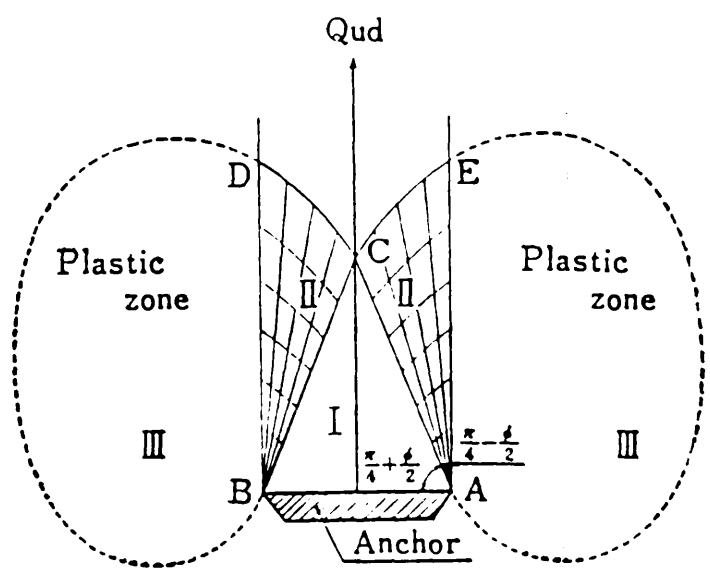


Fig. 2-12a Failure mechanism of a deep anchor (after Tagaya et al, 1988).

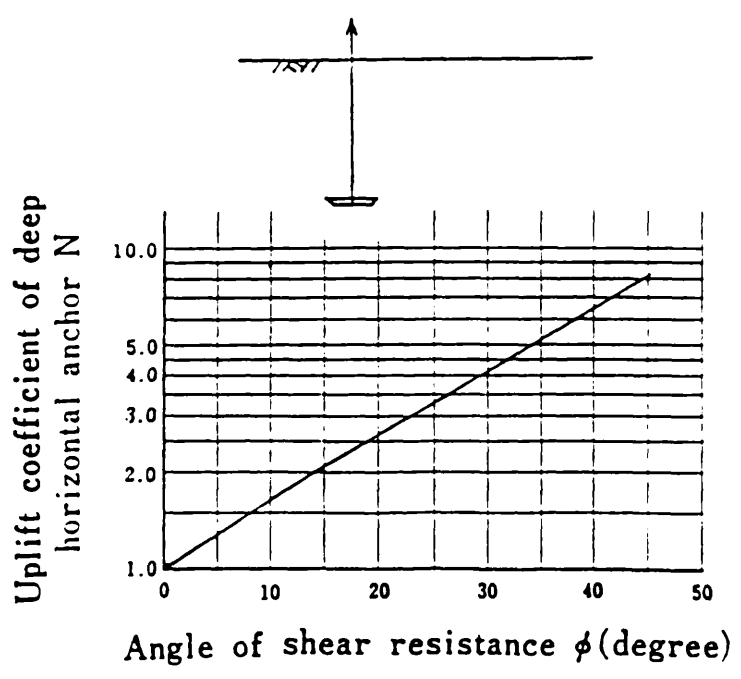


Fig. 2-12b Uplift coefficient of deep anchor (after Tagaya et al, 1988).

2-3 DIMENSIONAL ANALYSIS

Dimensional analysis has been applied to the results of a large number of model tests to determine empirically the relationships which govern the development of the maximum load that can be resisted by the model anchor. It can be applied to tests results in the field if an adequate knowledge of the parameters involved is available.

Sutherland (1965) used dimensional analysis to investigate the problem of raising a vertical shaft from a tunnel through the sea bed. The following relationship was obtained:

$$N_u = P_u / \gamma D = f [(D/B), \varphi] \dots\dots\dots (2.49)$$

It follows from the above equation that for a particular value of φ , the pull out factor depends only on depth/diameter ratio D/B . Laboratory tests on shallow anchors were carried out using disc plates with diameters ranging from 25 mm to 150 mm in dry and submerged sand. From the plots of N_u versus D/B the jacking force required to raise the shaft was predicted. The results of field tests agreed well with the experimental results when plotted on the same plots of N_u versus D/B (see figs. 2-15 & 2-16).

Baker & Kondner (1966) employed the same technique in their investigation, making a distinction between deep and shallow anchors and giving a separate dimensionless relationship for the two cases based on the experimental results. For a shallow anchor ($D/B \leq 6$) the dimensionless equation was expressed in the following form:

$$P/D B^2 \gamma = 3 + 0.67 (D/B)^2 \dots\dots\dots (2.50)$$

For a deep anchor it was given as:

$$(P/B^3\gamma - 170) B/b = 2800 + 470 (D/B) \dots \dots \dots (2.51)$$

where b = thickness of the anchor plate.

2-4 FINITE ELEMENT ANALYSIS

In keeping with the advances made in computers, numerical methods, including finite element methods, have become more sophisticated in their methods of solution. A wide range of geotechnical problems have been solved by the finite element technique. However, no satisfactory results have been reached yet in the domain of pull out of anchors embedded in cohesionless soils.

Rowe & Davis (1982) described a theoretical investigation on cohesionless soils in which consideration was given to the effect of anchor embedment, friction angle, dilatancy, initial stress state K_0 and anchor roughness. Their theoretical solution was based on an elastoplastic finite element analysis. The soil was assumed to have a Mohr Coulomb failure criterion and either an associated or a non associated flow rule. The anchor capacity was given by:

$$N_u = F_\gamma R_\psi R_k R_r \dots \dots \dots (2.52)$$

where F_γ is a basic anchor capacity factor

R_ψ , R_k and R_r are correction factors for the effect of soil dilatancy, initial stress state and anchor roughness respectively. The chart for these factors is given in figs.(2-17 & 2-18).

They also performed a number of pull out tests on strip anchors embedded in loose

sand (15% to 32% ID). Soil dilatancy was found to have a significant effect on anchor response and may appreciably increase the ultimate capacity of anchors in medium and dense sand. Their data have been compared with the theoretical results and an encouraging agreement found. However, there are doubts about some of their experiments. A value of high dilatancy angle ψ of 10° is questionable as a sand with $\psi = 33^\circ$ tends to be loose and little dilatant.

Tagaya et al (1983) investigated the pull out resistance of a shallow plate anchor by means of a two dimensional finite element based on Lade's constitutive equations. However, Dickin (1988) pointed out the inadequacy of their work since the above authors used the original incorrect version of Lade's equation.

Vermeer & Sutjiadi (1985) considered a long strip shallow anchor, adopting the failure mechanism shown in fig. (2-19) of a truncated wedge with an apex angle of 2ψ . This angle was found to coincide with the angle of dilatancy. The breakout factor was given as:

$$N_u = 1 + [D/B, D/L] \tan \varphi \cdot \cos \varphi_{cv} \dots \dots \dots (2.53)$$

where,

L = length of the strip.

φ_{cv} = angle of internal friction at constant volume.

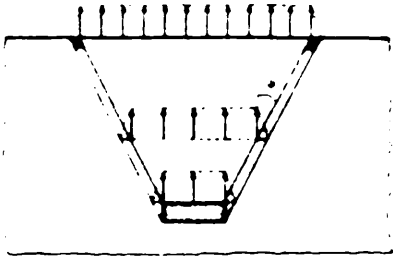


Fig. 2-19 Failure mechanism adopted by Vermeer & Sutjiadi.

An elastoplastic finite element computation was used to check the assumption made. The anchor problem was schematized to a passive trap door problem, and good agreement was found with the derived formula. However, Vermeer & Sutjiadi pointed out that for circular plates the formula is conservative in the sense that the limit load is underestimated.

Koutsabeloulis & Griffiths (1989) also schematized the anchor problem to a passive trap door problem (see fig. 2.30) and proposed a finite element solution which assumed that the soil behaved as an elastic, perfectly plastic material. The Mohr–Coulomb failure surface was used in conjunction with a non associated flow rule. The results obtained were presented (fig. 2–31) as expressions obtained empirically by curve fitting methods. The anchor breakout factor was given as:

$$N_u = N_{u,ps} [R_{\varphi}^{-(D/B)} R_{\varphi\theta}] \dots\dots\dots (2.54)$$

where R_{φ} and $R_{\varphi\theta}$ are parameters depending on φ as shown in fig. (2.31)
 $N_{u,ps}$ represents the breakout factor under plane strain conditions and is given by:

$$N_{u,ps} = D/B \sin (\varphi + \psi) + 1 \dots\dots\dots (2.55)$$

ψ = dilatancy angle.

2- 5 PROBABILISTIC METHOD

Ovesen (1981) investigated the uplift capacity of anchors embedded in cohesionless soil using both model and centrifuge tests. By means of curve fitting and statistical analysis the following ultimate uplift capacity formula has been devised

to present the results:

$$N_u = 1 + (4.32 \tan \varphi - 1.58) \cdot (D/B_e)^{3/2} \dots\dots\dots (2.56)$$

where B_e = equivalent side length of a square anchor.

The above equation can be used within the following limits:

$$D/B_e \leq 3.5 \text{ and } 29^\circ < \varphi \leq 42^\circ$$

Where φ is defined according to the Danish Code of Practice for Foundation Engineering (1977) by the following formula:

$$\varphi = 30^\circ - 3/U + (14 - 4/U)ID \dots\dots\dots (2.57)$$

Cragg et al (1986) took into account the variability in foundation strength and the wind load, ice load and wind on ice load acting on it. Hypothetical variations of a typical weather induced load and strength of a tower foundation are represented in Fig. (2-20). The shaded area in the region where these two distributions overlap, an area where load on the foundation may exceed its strength, represents the probability of foundation failure. Three modes of loading were considered. Wind, ice and wind on ice load distribution were expressed by the Gumbal type I distribution

$$F(p) = \exp [- \exp (B - P)/C] \dots\dots\dots (2.58)$$

where $F(p)$ = cumulative probability.

P = extreme weather induced load.

B, C = location and scale parameters.

The foundation uplift strength is assumed to follow the normal distribution which is expressed by:

$$F(s) = (1/\sigma (\pi)^{1/2}) \exp [- 0.5 (s-\mu)/\sigma] \dots\dots\dots (2.59)$$

where F(s) = the probability that strength will not exceed s.

s = foundation uplift strength.

μ = mean value of s.

σ = standard deviation of s.

A data base consisting of 160 foundation tests was assembled. The ultimate uplift resistance P was calculated from Meyerhof & Adams' expression (2.21). A normal distribution for foundation strength was derived and is shown below

$$\bar{P} = 1/4 [P_{++} + P_{+-} + P_{-+} + P_{--}] \dots\dots\dots (2.60)$$

and

$$\sigma_a = [1/4 \{ (P_{++})^2 + (P_{+-})^2 + (P_{-+})^2 + (P_{--})^2 \} - \bar{P}^2]^{1/2} \dots\dots (2.61)$$

where \bar{P} = mean ultimate uplift capacity.

σ_a = standard deviation of ultimate uplift capacity.

$$\text{and } P_{++,+,-,-+,-} = 0.5 \gamma \pi BD^2 s [K_{\mu} (+,+,-,-) \sigma_{K_{\mu}}] \tan(\bar{\varphi} +,-,+,- \sigma_{\varphi}) + W \dots\dots\dots (2.62)$$

A design chart was produced and is shown in fig.(2-21).

Trautman & Kulhawy (1988) produced a single generalised load displacement relationship for a shallow plate anchor (D/B < 3). A data base consisting of 75 load displacement curves was assembled and statistically processed. The above authors produced a design curve which is shown in Fig.(2-14).

2-6 COMPARISON OF THEORETICAL METHODS

Various methods of estimating the ultimate uplift factor N_u of plate anchors have been presented in preceding sections and illustrate the extent and the progress that has been made to find a general solution which can be applied to a variety of situations.

In the case of shallow anchors, initially the anchor was considered to be resisted only by the weight of the soil, as in the earth cone method, and subsequently the contribution of the soil through shear was included, as in all other methods. A further increasing level of sophistication is illustrated by the assumed failure surfaces, as linear and vertical in the shearing method, to circular in Vesic's method and then to the parabolic-linear surface in Matsuo's method. For deep anchors, Vesic extended Mariupolskii's approach by including a term for volume change Δv and the initial stiffness of soil I_r . Meyerhof & Adams considered the case of deep anchors as being analogous to a shallow anchor subjected to a surcharge and with the help of experiments provided a semi empirical solution. Fadl, and Saeddy assumed that the failure surface stopped below the ground surface and developed a solution which was in agreement with their experimental results (see figs. 2-26 & 2-27).

Application of these methods can result in a wide range of values. This is not surprising, because each method is based on specific, but differing assumptions regarding the form of the failure surface and the distribution of forces acting on the failure surface. The exception to this is the equation reported by Ovesen, which was derived from model and centrifuge tests.

The author has compared the results of many of the previous theories

proposed for the estimation of the ultimate uplift capacity of circular plate anchors, embedded in cohesionless soils. The results are given in a non-dimensional form using dimensional analysis. The estimated breakout factors N_u of shallow anchors ($D/B \leq 5.0$) are plotted in figs. (2-22 & 2-23) for loose and dense sand respectively. This range of D/B ratio has been chosen arbitrarily and serves merely to illustrate the differences in the theories considered. In fig.(2-22) all the curves are drawn for $\varphi = 30^\circ$, and the relative density I_D is assumed to be 20%. The curves of Matsuo and Fadl provide upper and lower bounds, respectively, to the values of uplift resistance factor. In fig. (2-23), the dense sand curves are drawn for $\varphi = 40^\circ$ and $I_D = 80\%$. The curve of Mariupolskii is rather peculiar, increasing very sharply to reach a breakout factor N_u of 40.0 at $D/B = 5.0$ a value 1.5 times the next highest value. Vesic and others have pointed out that the assumptions made by Mariupolskii in his initial reasoning on the failure mechanism of shallow anchors are arbitrary and not in agreement with the elementary theory of earth pressure. The scatter of the curves is less noticeable than in the loose case. Ovesen's (1981) formula is shown in both figures. For cohesionless soils, one would not expect much difference between the results from dimensionally similar models and centrifuge tests, as the body forces have little influence according to the simplified dimensionless group. The validity of this statement is further confirmed by the conventional model tests undertaken by Sutherland (1965) in connection with shaft-raising operations. These tests provided realistic upper and lower bounds to the prototype uplift resistance encountered in the field. Further evidence is presented in Ovesen's paper itself, where for plate anchors embedded in loose sand ($D/B \leq 3.5$) breakout factors from conventional and centrifugal tests were almost similar. Referring to fig. 2-23 the curves of Fadl (conventional test) and Ovesen are almost coincident. The corresponding curves for shallow anchors in loose soil fig. 2-22 have Ovesen's predictions greater than Fadl's. The reason for this discrepancy is probably due to the use, in the former, of an empirical formula for obtaining the angles of internal friction.

The deep anchor curves are presented in fig. (2-24 & 2-25) for loose and dense sand respectively for the same values of ϕ and ID used in the shallow case but with $6.0 \leq D/B \leq 14.0$. Vesic suggested the following variation of index of rigidity, $70 \leq I_r \leq 150$ for loose to dense sand, and these upper and lower bounds values were used in the present comparison together with $\Delta v=0$ (no volume change). Significant variations of N_u are observed, especially in dense sand where it can be seen that, for example at $D/B = 14.0$, Fadl's theory gives an N_u value over two times the next highest value. Vesic's deep anchor theory is independent of embedment ratio, but the lower limiting value is not specified. It was taken as $D/B=7$ to allow for the transition from shallow to deep anchor behaviour. This independence of embedment ratio is not consistent with experimental results. Vesic's theory is considered more relevant to deep anchor failure in cohesive soil (Ponniah, 1984).

Although the various authors obtained reasonable agreement between their predicted and experimental values, the maximum breakout factors predicted by various methods are not in good agreement with each other. The assumption made regarding the shape of the failure surface, the behaviour of the soil within this failure surface and the lack of information about the stress history of the soil was generally the cause of these discrepancies in the results. Most of the time, the failure surface and the shear behaviour of the soil along that surface was defined by the unit weight (γ) of the soil and its angle of internal friction ϕ . Esquivel Diaz (1967), recognizing the effect of the compressibility of the soil on the pull out resistance, suggested the need for its inclusion in any future theoretical analysis. Fadl (1981) and Saeddy (1987) did so and formulated the elaborate equations given in the preceding section which gave a reasonable agreement with some of the previous experiments. However, there is no general consensus as to which method is more appropriate for a given case.

2-7 PREVIOUS EXPERIMENTAL WORK

A considerable amount of laboratory scale testing has been carried out to understand the uplift behaviour of anchors. Two kinds of investigation have been considered. The first type of test focusses on determining the form of the failure surface associated with the development of the maximum load. The second type of test uses axisymmetric models to investigate the effect of the anchor configurations, engineering properties of the soil and type of loading on the load displacement behaviour of the anchor. In the following review it is intended to give a comprehensive survey of the most recent work on static uplift loads and therefore augment the work done by Fadl (1981).

2-7-1 Form of the failure surface

Several techniques have been used to observe the development of a failure surface. Generally the container in which the test was performed had a transparent side wall. Half section anchors and plane strain anchors were the most appropriate models used in this case. However, axisymmetric models have also been used despite the difficulty which one has to expect from such models. The following review will give a brief insight into the work done in this area during the last two decades.

Balla (1961) used half section models of anchors embedded in layers of natural and coloured sand to determine the form of the failure surface. The distortion of the coloured layers enabled the observation of a circular arc failure surface extending from the tip of the plate anchor to the ground surface.

Clemence and Veesaert (1978) used the same technique as above. The failure surface from the half anchor test on dense sand was recorded on film for analysis.

Overlaying photographic prints before and after each test using the reference grid lines provided a method by which the relative movement of the sand could be noted. The shape of the failure surface was generally curved from the base of the anchor to the sand surface.

Baker and Kondner (1966) performed a plane strain model test of a shallow plate anchor installed in a bed of dense sand which included coloured layers. A definite failure surface was observed and it was similar to the circular arc failure surface reported by Balla.

Maddocks (1978) used a stereo photogrammetric method to investigate the soil interaction of a plane strain model of a deep anchor ($D/B = 40.0$) embedded in dense sand. Sand grain movement was observed within a zone which extended ten times the anchor diameter on either side of the anchor and approximately twenty anchor diameters above the anchor. He concluded that anchor behaviour is more complex than predicted by assumptions of either uniform radial compression of the sand above the plate or a plastic response of the sand.

Carr (1970) used a plane strain model of a plate anchor embedded in a dense sand. Time exposure photography was used to observe the sand bed deformations at failure. A failure surface extending outwards from the anchor perimeter to the sand surface in a shallow arc was reported, the angle of intersection between the failure surface and the sand surface being greater than 45° . However, Carr reported that only relatively large sand displacements may be observed using the time exposure method, these occurring predominantly after the maximum load has been developed. He also monitored the sand movement in axisymmetric models by installing mechanical gauges around the plate anchor. It was reported that the main features of the interaction observed in the plane strain model are reproduced in an axisymmetric model.

Matsuo (1967) and Fadl (1981) performed axisymmetric model tests to assess the form of the failure surface. The sand layers were separated by a tracer layer of cement. After the anchor failed, the sand bed was moistened to set the cement and then half of the sand bed was carefully excavated to expose and measure the shape of the failure surface which was generally curved.

Frydman & Shaham (1989) used plane strain models of a plate anchor embedded in a dense sand. To obtain an indication of the location and shape of the shear surface bounding the uplifted soil mass during pull out, 2 mm diameter steel balls were placed in a triangular mesh on the sand surface adjacent to the glass face, and their movements were obtained from photographs taken at various stages of the test. It was found that failure occurred by uplift of a semi-rigid mass on shear bands inclined at about $20-23^{\circ}$ to the vertical.

2-7-2 Load displacement behaviour

Axisymmetric model anchors have been the object of testing for many years. These tests have been carried out to determine the factors involved in the uplift capacity and all have been concerned with determining the maximum load that can be developed by an anchor embedded in a given sand. The effect of depth of embedment, soil density, size of anchors and sand stress history were such factors.

Tsangarides (1978) investigated the effects of varying the pull out rate, the anchor shaft diameter and the anchor thickness on the ultimate pull out capacity of circular plate anchors. Tsangarides found that varying the pull out rate within the range 0.5 mm/min and 0.29 mm/min did not affect the load displacement behaviour of the plate anchor. The ultimate pull out resistance was reduced if the ratio of anchor diameter (B) to shaft diameter (B_s) was less than four for the same anchor

diameter, and the ultimate pull out capacity increased if the ratio of anchor thickness (t) to anchor diameter (B) was less than three.

Andreadis (1979) reported results on uplift tests conducted on cylindrical, circular, conical and fluke anchors. He concluded that the mode of failure of an anchor subjected to a pull out load was dependent essentially on the embedment ratio, the relative density of the soil and the shape of the anchor. The pull out capacity of a cylindrical and a circular anchor was found to be equal, the pull out capacity of a conical anchor was found to be approximately 15% less than in the circular case. This difference increased with increasing embedment ratio and was attributed to the ease with which sand grains could flow around the anchor as it moved upwards. The pull out resistance of the fluke anchor was found to be higher than the uplift capacity of a cylindrical anchor at shallow depth although at greater depth the fluke anchor displayed lower resistance than the three other types of anchors. A design chart was produced and is shown in fig.(2-28). He also reported on the effect of anchor installation procedures and concluded that systems which involved considerable loosening of adjacent sand, e.g. fluidisation, resulted in the anchor failing by punching into the overlying disturbed sand without a full transfer of load to the surrounding dense sand.

Fadl (1981) investigating the effect of relative density on the pull out resistance of a plate anchor reported the importance of relative density on anchor behaviour and concluded that the higher the relative density the higher the ultimate uplift load. The above parameter was subsequently included in the equations (2.36 & 2.38) derived to assess the ultimate uplift capacity in shallow and deep anchors.

Zakaria (1986) investigated the effect of installation disturbance on the pull out capacity of a plate anchor, an aspect somewhat elusive where there is relatively little guidance. The results showed that the zone of disturbance should be kept to one

anchor diameter in order to take full advantage of the anchor capacity (8% change in the pull out capacity from a homogeneous sand bed). When the zone of disturbance around an anchor embedded in dense to medium sand was increased to three anchor diameters, the pull out capacity was similar to that for the anchor as being pulled out from a bed which was wholly disturbed (see fig. 2-29).

Murray & Geddes (1987) showed that in dense sand the breakout factors for circular plate anchors were approximately 1.26 times those of square plate anchors.

Kulhawy et al (1987) described an experimental study of the effect of native soil density, and backfill density on the uplift capacity of plate anchors a problem similar to the one studied by Zakaria but with density as a parameter. The findings are summarized in the following table.

Table 2-2 Summary of Kulhawy et al (1987) results

increase in parameter	effect on capacity	conditions for which change in capacity is most pronounced
backfill density	increase	$D/B \geq 3.0$, dense native soil
native soil density	moderate increase	$D/B \geq 3.0$, dense backfill

Dickin (1988) described an experimental investigation on the uplift behaviour of plate anchors conducted in a centrifuge. The behaviour of a 25 mm rectangular anchor plate with different aspect ratios at embedment ratios D/B up to 8.0 in both loose and dense sand was studied. The model anchor was subjected to a centrifugal acceleration of 40 g, enabling the behaviour of a one meter wide anchor to be investigated. It was found that the ultimate uplift resistance and failure displacement both increased with embedment ratio, while anchor geometry had a marked influence

on the breakout factor and failure displacement which both reduced with increasing aspect ratios.

2-7-3 Summary

From the foregoing survey of experimental work carried out on uplift of plate anchors, it can be concluded that:

- (a)- The mode of failure and the breakout factor are dependent on the depth of embedment, stress history of the soil, the anchor geometry, the soil properties e.g. angle of shearing resistance and the relative density.
- (b)- The uplift capacity of a plate anchor can be reduced by the disturbance of soil caused around it during installation.
- (c)- Centrifugal test techniques can be applied with success to model the uplift behaviour of plate anchors and represents a very powerful tool.

2-8 PURPOSE AND SCOPE OF THE PRESENT WORK

The review shows that the interaction between a vertical uplift plate anchor and its surrounding soil has been the object of close investigation and many important parameters (D/B , ID , φ , stress history) influencing the plate anchor behaviour have been studied experimentally and theoretically. However no satisfactory analysis has been presented that will define the extent of the interaction. A survey of literature revealed that most of the published work on vertical uplift of plate anchors focussed mainly on the aspect of determining the breakout factor in one type of sand. The experimental details given in table 2-3 show that most of the

experiments were carried out, generally, in a uniform sand. This observation illustrates strongly the shortcomings of the previous theories which did not take into account the natural differences that exist in a sand. A typical example is given by Cragg et al (1986) in fig. 2-21 where, in the proposed design chart based on one type of sand, it can be seen that for $\phi = 36^\circ$ the sand is considered as dense which is not always true. Most of the theories developed did not yield good results except for the conditions under which they were established. The exception was Fadl's theory which showed a good agreement with some of the previous experiments. Nevertheless the validity of the formula for all types of sand has still to be proved.

It was felt that an experimental programme based on model tests in the laboratory was necessary. The primary object of the research was to study the behaviour of an embedded plate anchor during pull out in a range of granular soils. In particular, it was deemed that an understanding of the following factors would be of considerable interest in terms of their influence on the breakout factor and the shape of the failure surface.

- (i) The size of the sand particles.
- (ii) The grain shape of the sand particles.
- (iii) The grading of the soil.
- (iii) Effect of a layered system.

In this manner, trends in behaviour which cannot be identified because of the presence of other variables may be established and thus the behaviour of a plate anchor embedded in cohesionless soils may be more fully understood.

sources	sands used	D ₅₀ (mm)	U	grading	shape	maximum porosity (%)	minimum porosity (%)
Balla		0.25	2.0	----	----	----	----
Suther ^d .	Sizewell	0.17	1.8	uniform	subrou ^d	47.8	36.8
Baker & Kondner	Ottawa	----	---	uniform	-----	----	-----
Esquivel & diaz	Chatahoche	----	2.05	uniform	subang ^r	52.8	38.3
Matsuo	dry	0.50	2.0	uniform	-----	----	-----
Carr	concrete	0.40	1.9	uniform	-----	47.5	32.6
Clemence & Veesaert	river	----	1.4	uniform	subrou ^d	----	-----
Andreadis & al	Bush Farm	----	2.1	uniform	subang ^r	45.8	32.3
	Borough	----	1.4	uniform	subrou ^d	48.3	37.4
Fadl	L. Buzzard	0.75	1.8	uniform	subrou ^d	44.1	32.7
Zakaria	L. Buzzard	0.75	1.8	uniform	subrou ^d	44.3	32.7
Murray & Geddes	air-dried	0.25	2.0	uniform	subrou ^d	----	----

*Table 2.3 Properties of The Different sands
Used by Previous investigators.*

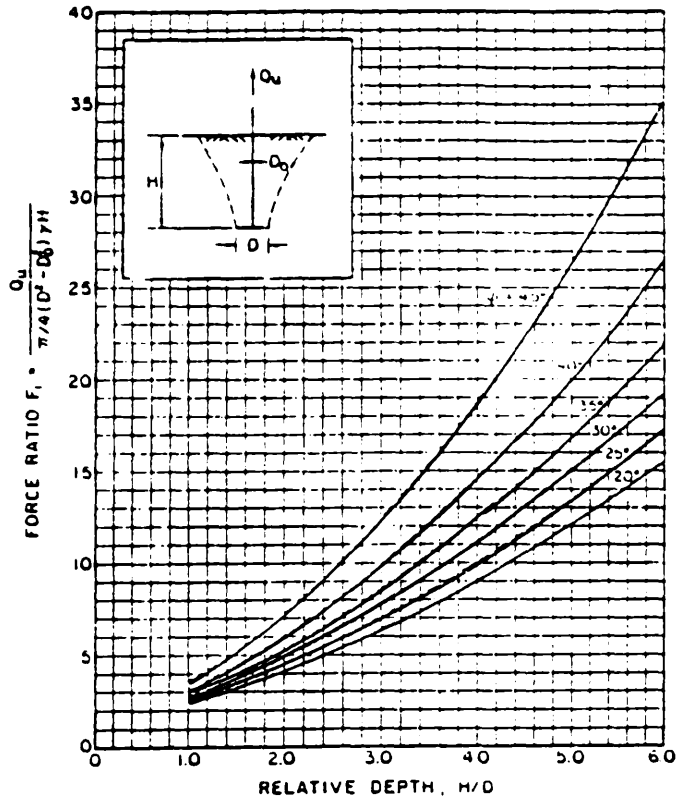


Fig. 2-13 Dimensionless Parameter Chart for Shallow Anchors (after Saedy, 1975).

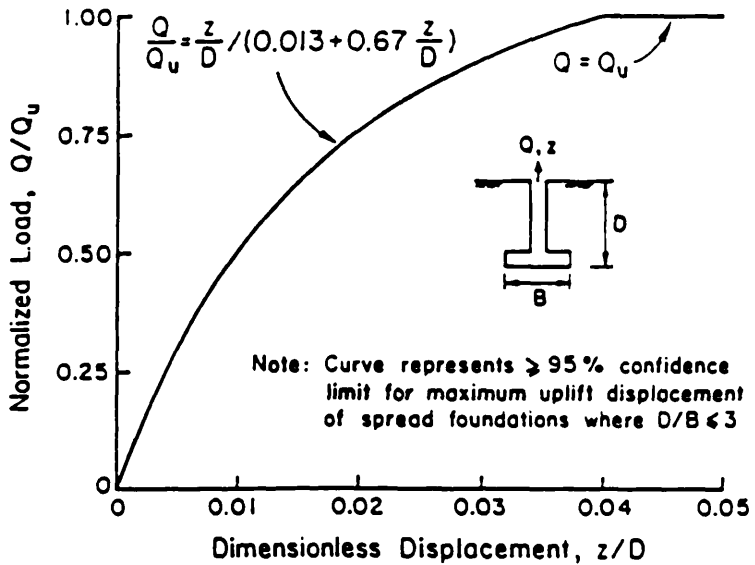


Fig. 2-14 Recommended Load Displacement Relationship for Design of Uplift Spread Foundations (after Trautmann & Kulhawy, 1988).

Fig. 2-15 Model test results for Design for Failure case at Sizewell (after Sutherland, 1965 & 1988).

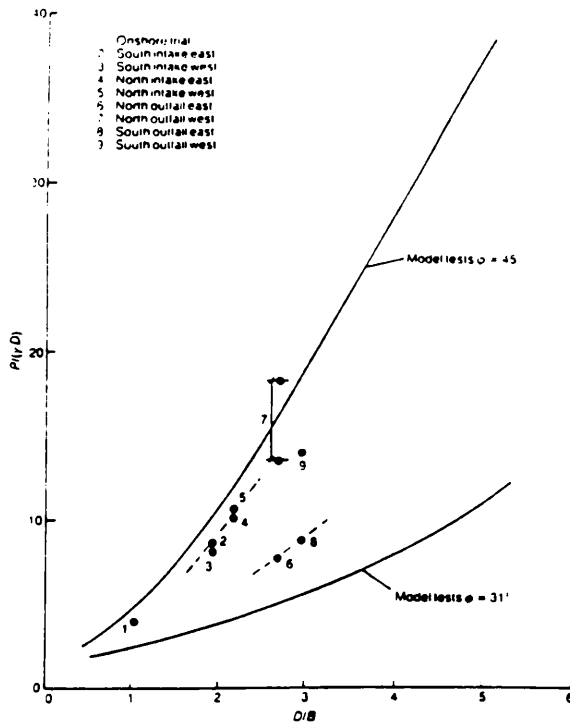
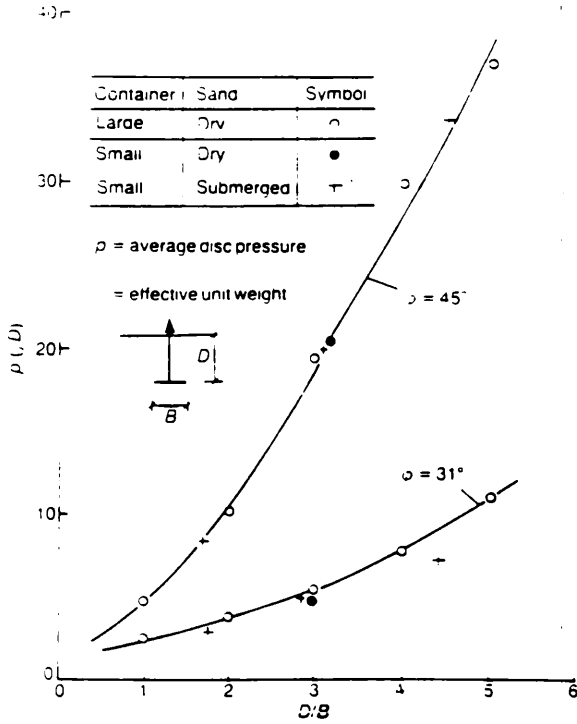


Fig. 2-16 Comparison of Model Test Results and Field Results (after Sutherland, 1965 & 1988).

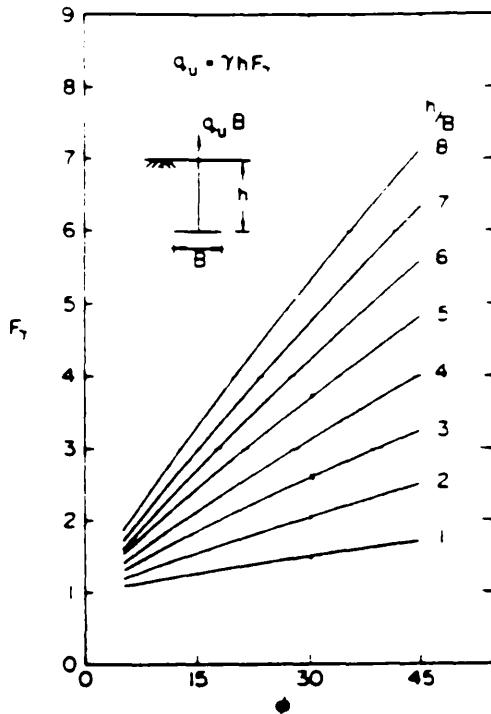


Fig. 2-18 Variation of Basic Anchor Capacity Factor F_γ with ϕ (after Rowe & Davis, 1982)

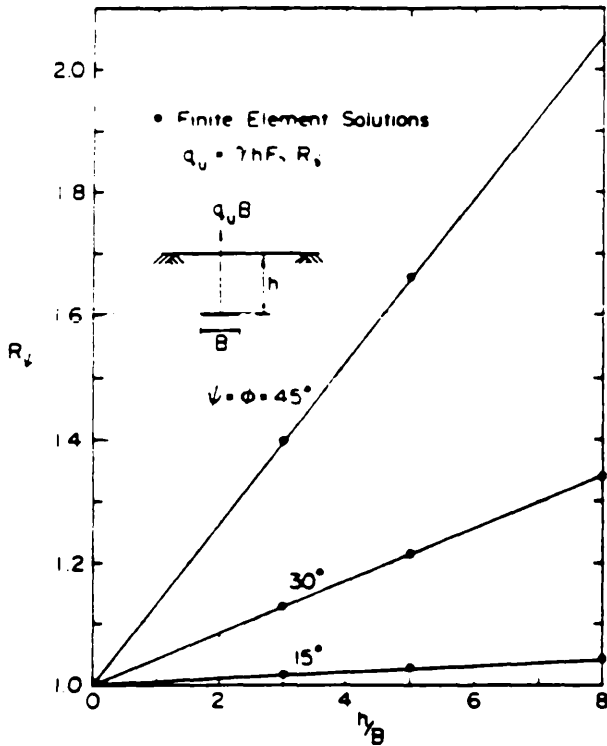


Fig. 2-17 Correction Factor for Effect of Dilatancy on Anchor Capacity (after Rowe & Davis, 1982).

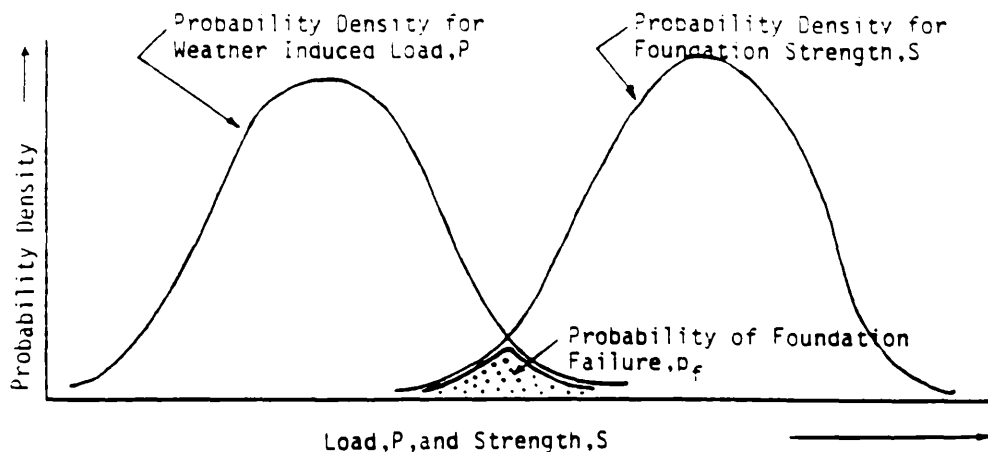


Fig. 2-20 Definition of Probability of Failure of a Foundation under Weather Induced Load (after Cragg et al, 1986).

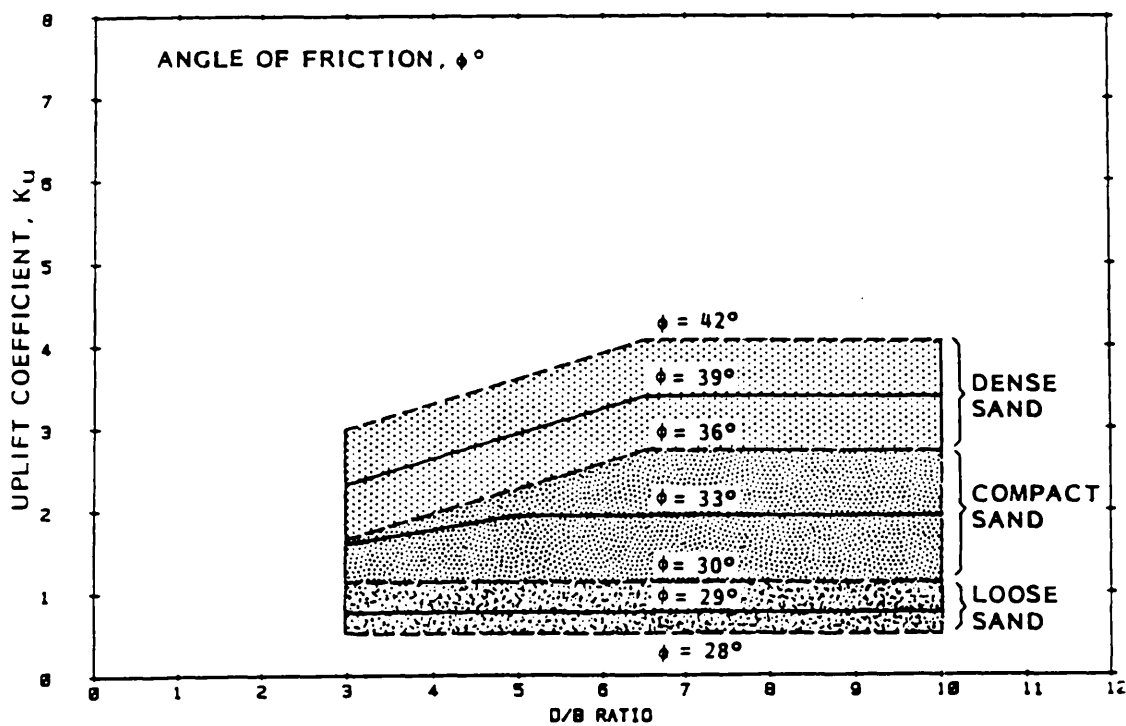


Fig. 2-21 Proposed Design Chart for Uplift Coefficients (after Cragg et al, 1986).

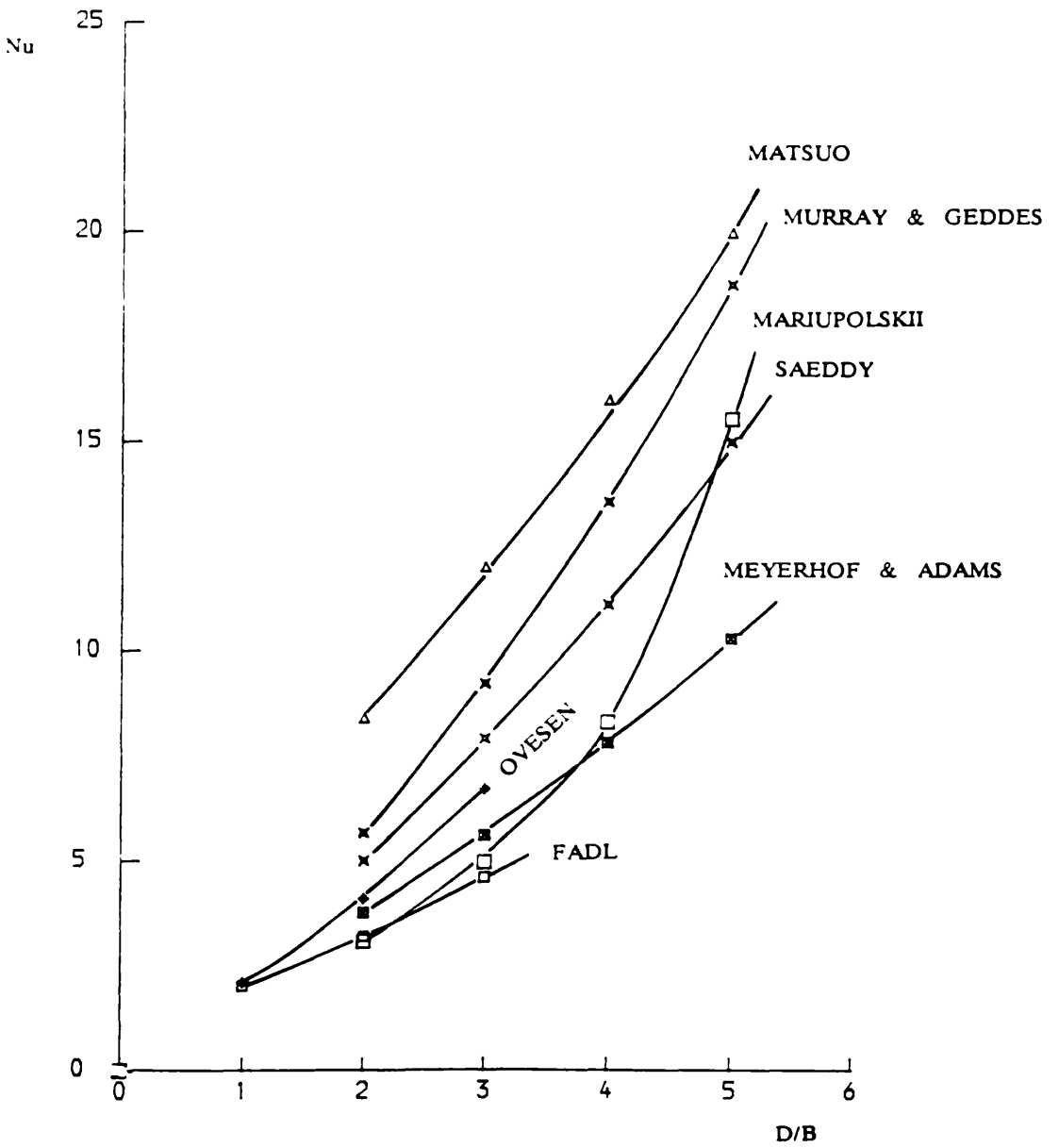


Fig. 2-22 Shallow Anchors: Comparison of Different Theories for Loose sand ($\phi = 30^\circ$).

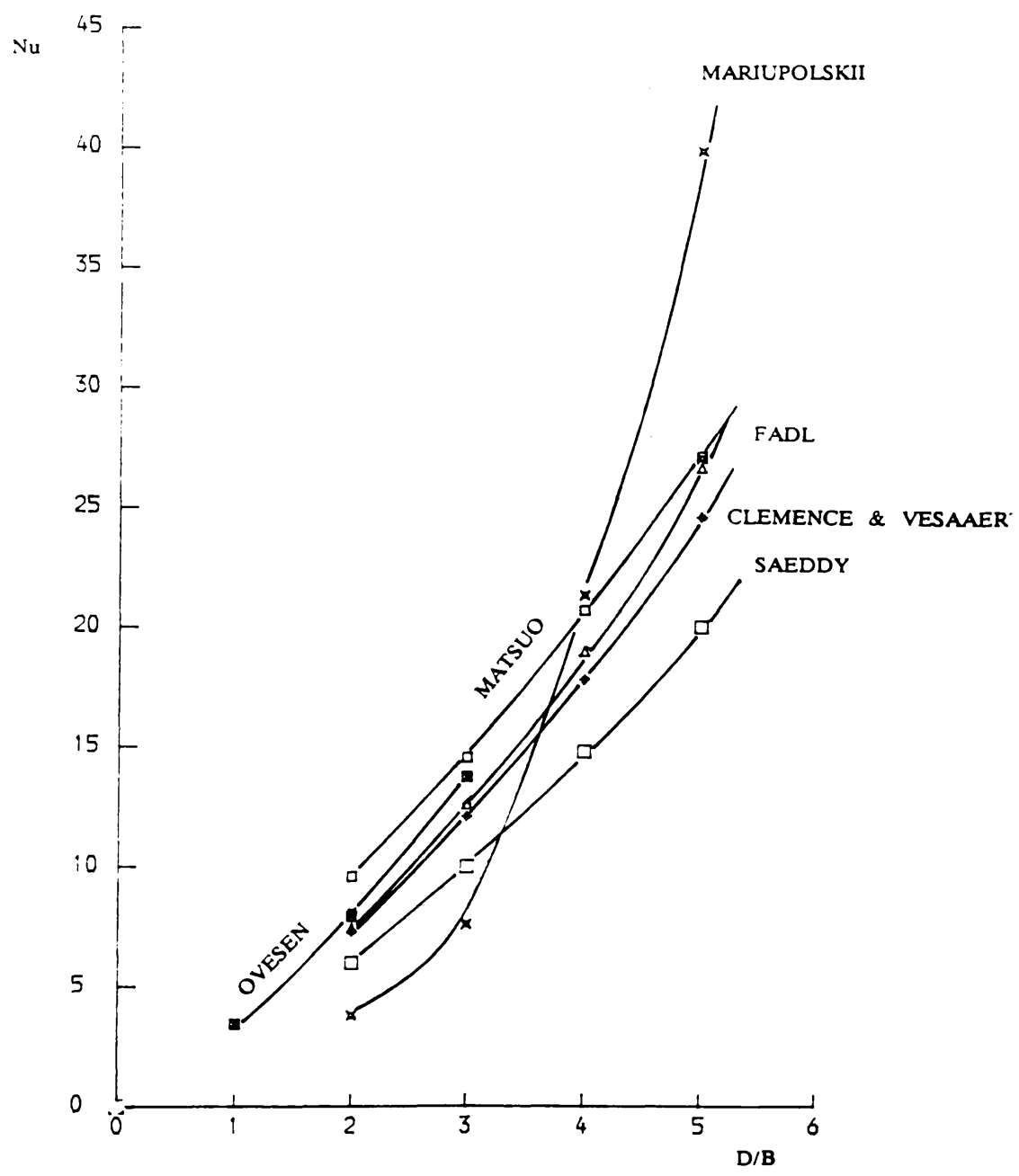


Fig. 2-23 Shallow Anchors: Comparison of Different Theories for Dense Sand ($\phi=40^\circ$).

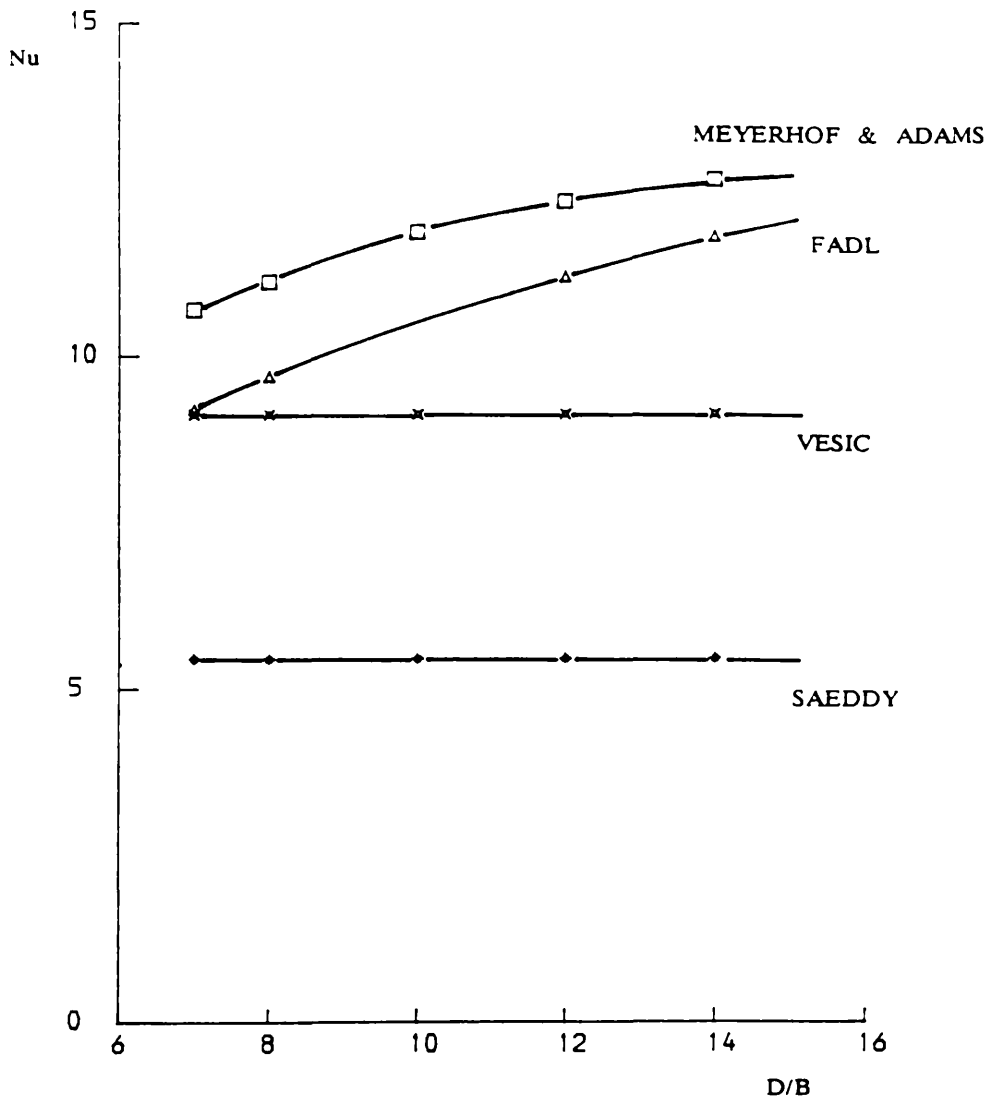


Fig. 2-24 Deep Anchors: Comparison of Different Theories for Loose sand ($\phi=30^\circ$).

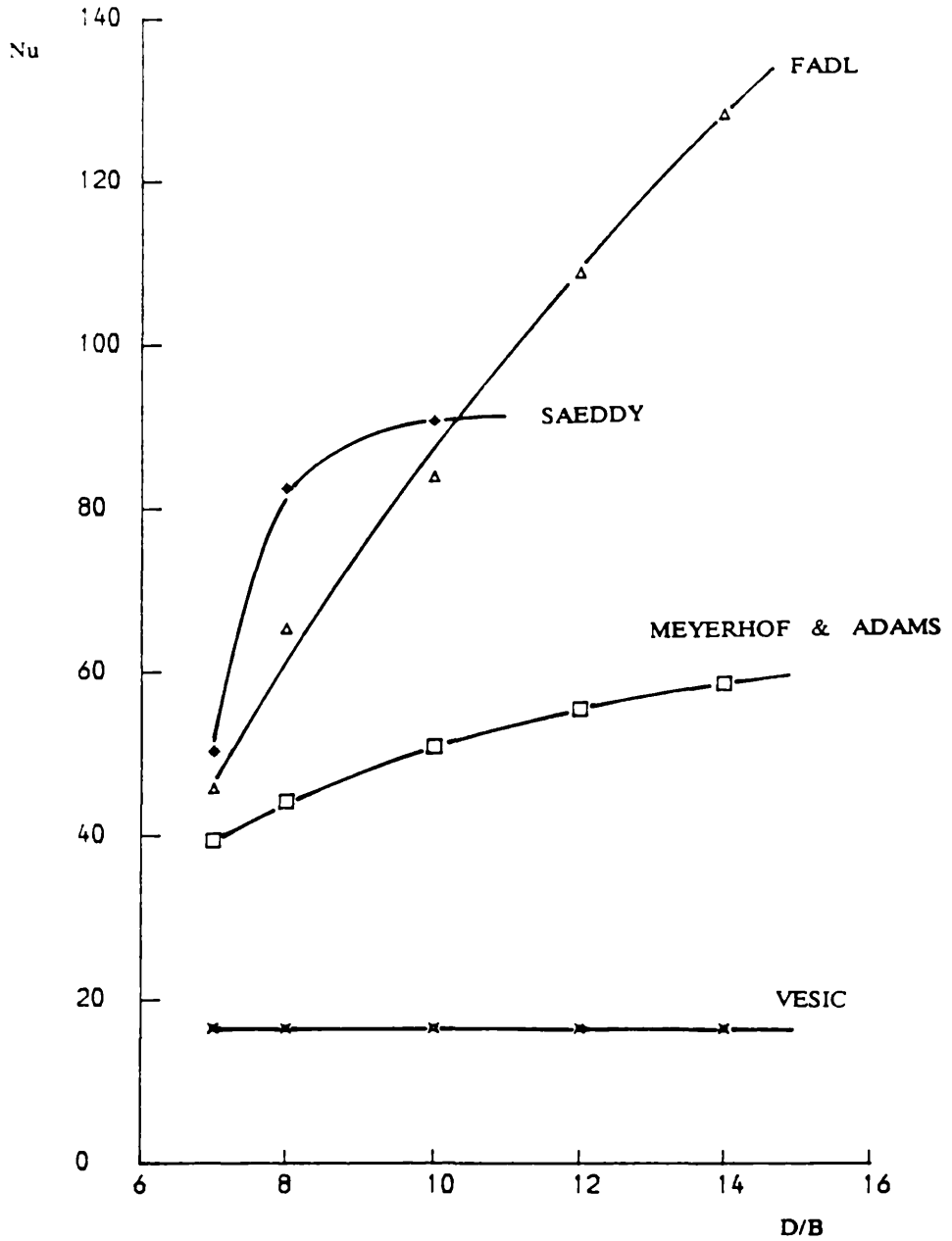


Fig. 2-25 Deep Anchors: Comparison of Different Theories for Dense Sand ($\phi = 40^\circ$).

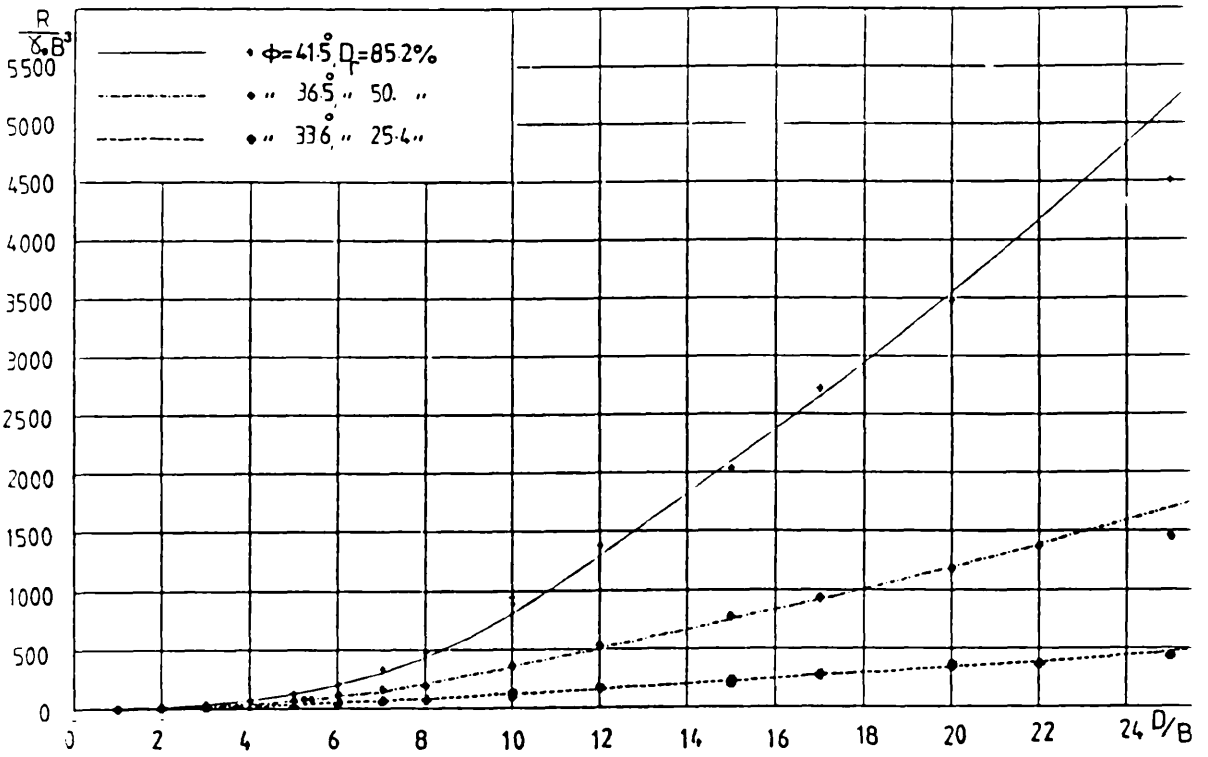


Fig. 2-26 Comparison of Fadl's Approximate Method with Model Test Results (after Fadl, 1981).

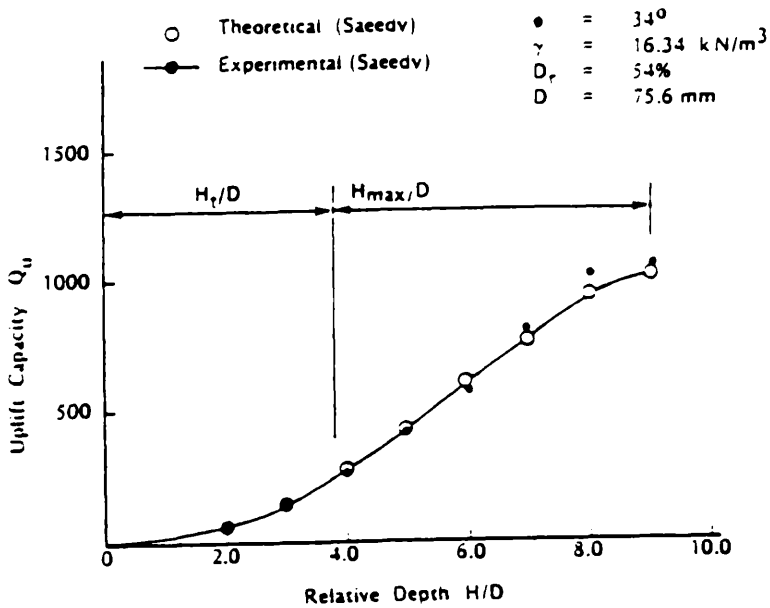


Fig. 2-27 Variation of Q_u with depth diameter ratio (after Saeddy, 1987).

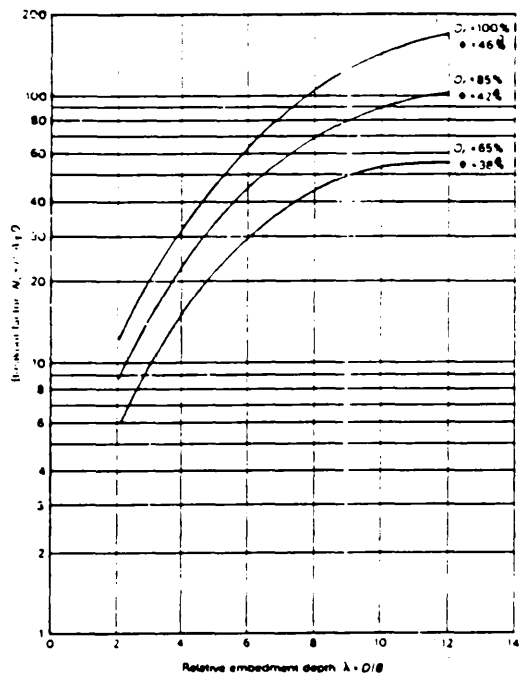


Fig. 2-28 Anchor Breakout Factor Relative Embedment Depth Design Curves (after Andreadis, 1981).

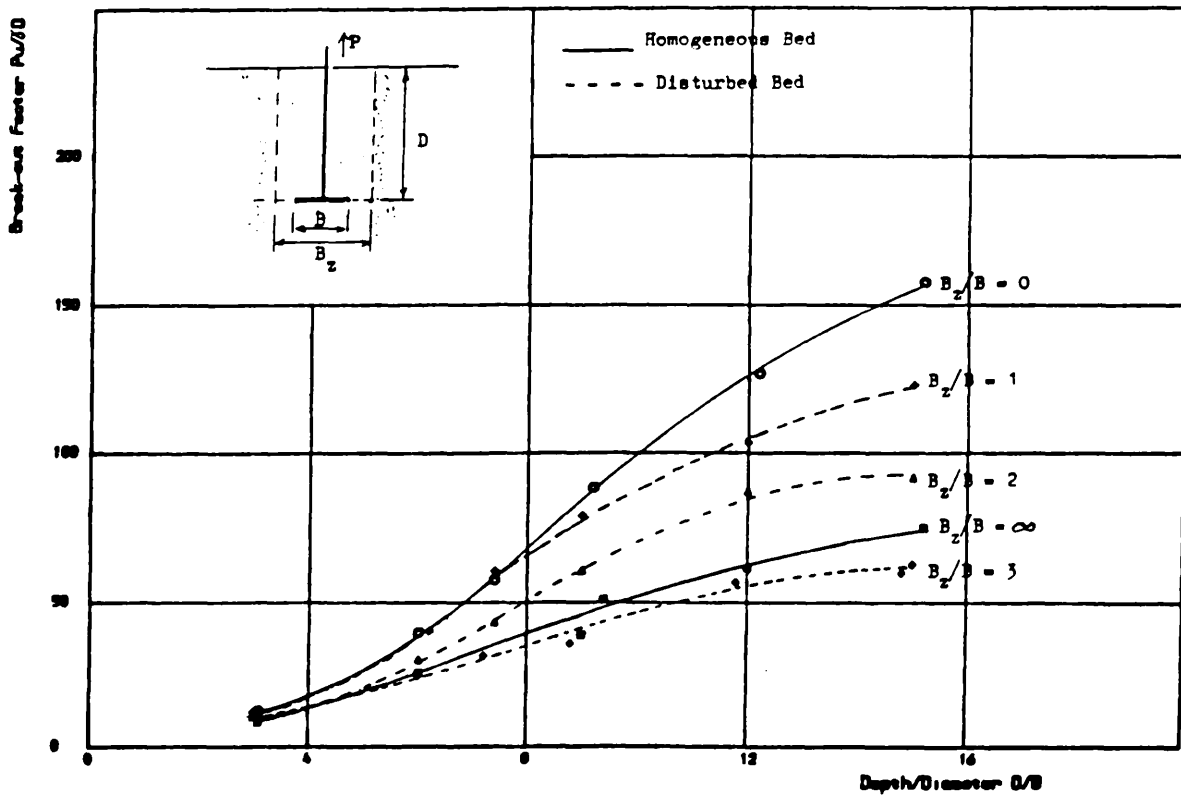


Fig. 2-29 Effect of Disturbed Zone on Anchor Breakout Factor (after Zakaria, 1986).

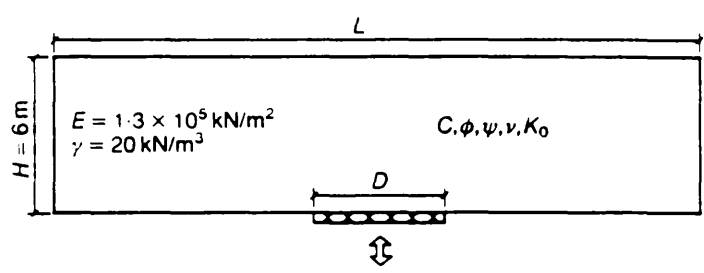


Fig. 2-30 Definition of the trap door problem (after Koutsabeloulis & Griffiths, 1989)

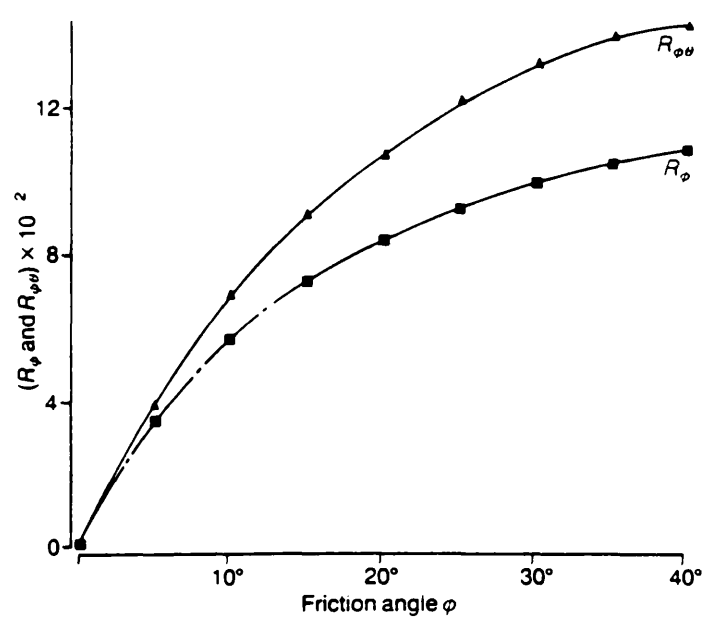


Fig. 2-31 Passive mode, axisymmetry: variation of R_{ϕ} and $R_{\phi\theta}$ with friction angle ϕ (after Koutsabeloulis & Griffiths, 1989).

sources	Shallow Anchors		Deep Anchors	
	BREAKOUT FACTOR N_u		BREAKOUT FACTOR N_u	
earth cone	$1 + 2 (D/B) \tan \alpha + 4/3 (D/B)^2 \tan \alpha$		--	
earth pressure	$1 + 2 K_0 (D/B) \tan \alpha$		--	
Balla	$4/\pi (D/B)^2 (F_1 + F_3)$		--	
Mariupolskii	$\frac{1 + 2 K_0 (D/B) \tan \alpha}{1 - 2 n (D/B)}$		$P_p / A\gamma D$	
Matsuo	$4 B_2^3 K_1 / \pi B^2 D$ up to $D/B=9$		--	
Meyerhof & Adams	$2 (D/B) s K_\mu \tan \varphi + 1$		$2 H/B (2 - H/D) s K_\mu \tan \varphi + 1$	
Vesic	$F_q + 1/3 (D/B)$		$F'_q / 1 - 0.5 \tan \varphi$	
Clemence & Vesaaert	$w^* + 2/3 D/B K_0 \tan \varphi \cos^2 \varphi / 2 [3 + 2(D/B) \tan(\varphi/2)]$		--	
Ovesen	$1 + (4.32 \tan \varphi - 1.58) (D/B_e)^{3/2}$		--	
Fadl	$8/3 (D/B)^2 \tan^2 \alpha + 4 (D/B) \tan \alpha + 1$		$8 (H/B)^2 (1 - 2/3 H/D) \tan^2 \alpha + 4 H/B [R + 2 - H/D] \tan \alpha + 2 R + 1$	
Murray & Geddes	$1 + 2 (D/B) (\sin \varphi + \sin \varphi/2) (1 + 2/3 (D/B) \tan \varphi/2)$		valid up to $D/B = 10.0$	
Saeddy			$1/A\gamma D \mu \Sigma \Delta Q_{ui}$	

Table 2-4 Summary of previous theories.

Chapter 3

SOIL CHARACTERISTICS AND PREPARATION OF SAND BEDS

3-1 SOIL CHARACTERISTICS

3-1-1 Origin of soils

Five types of sand were used in this investigation, Ballotini (glass beads), Leighton Buzzard and Lochaline sand which were already available in the laboratory, and Hyndford and Douglasmuir sand both of which were commercially available.

3-1-2 Properties of the sands

3-1-2-1 Geometry of sand particles

Two distinct parameters, sphericity and roundness, may be used to characterize the particle shape Wadell (1935). Sphericity, Krumbein (1941), is defined as the ratio of the volume of the particle to the volume of the smallest circumscribing sphere, and roundness is understood to be the ratio of the curvature of the corners and edges of the particle to the average curvature of the particle. Perfect sphericity and perfect roundness in a two dimensional view are both associated with a value of unity, and imperfect particles are characterized by values between zero and unity.

Sphericity, which is an absolute volumetric quantity in three dimensions can be measured in two dimensions by photographic techniques and estimated visually with consistent accuracy by the use of the Rittenhouse (1943) chart (See fig. 3-3);

roundness is visually estimated by means of a standard chart, such as that proposed by Krumbein (1941) (see fig. 3-2).

In this study, mean values of roundness and sphericity were used to quantify the particle shape characteristics of a given sand. Sands were classified according to Powers (1953) scale (see table 3-1).

Table 3-1 Roundness grades (after Powers, 1953).

Grade terms	Class intervals	Geometric means
Very angular	0.12-0.17	0.14
Angular	0.17-0.25	0.21
Subangular	0.25-0.35	0.30
Subrounded	0.35-0.49	0.41
Rounded	0.49-0.70	0.59
Well rounded	0.70-1.00	0.84

3-1-2-2 Particle shape determination

Grains from each particular sand were spilled randomly across a glass slide so that individual grains could be viewed through a microscope. As each grain came into view, quantitative values for its sphericity and roundness were estimated by comparing its shape with reference shapes depicted in the Rittenhouse and Krumbein charts and classified according to Powers scale.

A minimum of 50 grains from each sand were viewed in groups of 25 grains. Table (3-2) shows a set of typical test data for 50 grains of Leighton Buzzard sand. Table (3-3) presents the experimental results of the sphericity and roundness determination for each sand in terms of the mean values of the 50 grain groups. The mean roundness, R , varies from 0.27 to 0.98, whereas the mean sphericity, Ψ^* , varies only from 0.80 to 0.95. For a uniform sand, sphericity was found to vary with roundness as shown in fig. 3-4. The effect of shape can be characterized by just one shape parameter. Roundness, the more sensitive parameter, was adopted in the present investigation.

3-1-2-3 Specific gravity

The specific gravity for each type of sand was obtained using the British Standard method B.S 1377 (1975). The average of three tests on each soil was within 0.03, which was taken as representative of the sample. The values are given in table (3-3).

3-1-2-4 Particle size distribution

Sieve analyses were performed on the sands to B.S 1377 (1975). The resulting grading curves are shown in fig.(3-1).

3-1-2-5 Limiting porosities

The minimum and maximum porosities were determined by using the tests recommended by Akroyd (1957) and based on Kolbuszewski's (1948) tests. The minimum porosity was obtained using a vibrating hammer to compact the dry sand sample into a proctor mould. The maximum porosity was determined by filling a

proctor mould by pouring sand through a funnel with a small height of fall. The different values are shown in table (3-3). The average of five tests on each soil was taken as the representative value.

3-1-2-6 Shear strength of sands

Standard triaxial tests were performed on dry sand samples at low confining pressure σ_3 ranging from 15.0 to 80.0 Kn/m². The test procedure followed was generally similar to that described by Bishop and Henkel (1962). The size of the samples was 75.0 mm \times 38.0 mm diameter. The usual corrections were applied to the results. The controlled rate of strain (0.30 mm/min) method of applying the axial load to the sample was used. The loading system consisted of 1 ton Wykeham Farrance multispeed machine, the load being transmitted to the specimen by means of a loading ram, using a rotating bush to minimize the frictional forces (see fig.3-5). A self compensating air-water system was used to provide cell pressure. The axial load and axial deformation were respectively measured using a 1112 N-capacity (250 lbs) type D Sangamo load cell and a 25 mm travel Sensonics displacement transducer, both of them being connected to the data logger.

The relationship between relative density (ID) and angle of internal friction (ϕ) obtained from the triaxial tests for the four sands is shown in fig.(3-6). The data clearly show that except for Lochaline sand and Leighton Buzzard sand, the sands investigated have a separate and distinct relative density-friction angle relationship. The Ballotini (glass beads) have the smallest friction angles and exhibit the least increase in friction angle with increasing relative density, Lochaline sand and Leighton Buzzard sand with subrounded particles have intermediate friction angle values. Finally Douglasmuir sand (U=1.8) and Hyndford sand (U=5.5) with subangular particles have the highest friction angles. The influence of particle size

on the strength response of Lochaline sand and Leighton Buzzard sand was found to be insignificant (difference was about 0.5° and can be explained by the fact that although the two sands have the same shape, the roundness is slightly different). Also shown in fig. (3-6) the results obtained from Hyndford sand and Douglasmuir sand indicate that the effect of increased gradation is to increase the value of φ by about 2.5° (at the same relative density). To illustrate the effect of particle shape on the friction angle, the friction angles of the uniform sands at ID=40% and 70% have been plotted against the roundness of the particles in fig. (3-7). This shows that the friction angle is a function of particle shape and relative density. The friction angles decreased markedly with increasing particle roundness (or decreasing angularity).

The shear strength of the sand was found to be affected not only by the relative density and the roundness of the grains but also by the the grain size distribution. For a given grading the most angular grains give the highest shear resistance, but for a given relative density nothing can be said beforehand as the two factors, grain size curve and roundness, play a role. That the shear strength for a given relative density is greater for angular than rounded grains (Kolbuszewski, 1963), is true only in so far as all sands are characterized by the same grain size distribution curve (the same mean diameter D_{50} and the same uniformity)

3-1-2-7 Conclusions

- 1- A decrease in the particle roundness resulted in an increase in the angle of internal friction φ for sands at a given relative density, thus supporting the findings of Kolbuszewski & Frederick (1965), Holubec and a'Appolonia (1973), De Beer (1965) and Moroto (1989).

- 2- The particle size was found to have only a small effect on the angle of internal friction φ , the small difference registered being explained by the fact that Lochaline and Leighton Buzzard sands do not have the same roundness and sphericity although they have the same subrounded shape. Results reported by Vallerga et al, 1957 (Al- Hussaini, 1983) and Zelasko et al (1975) support the results of the present investigation.
- 3- It would be expected that a well graded and subangular sand would produce a better interlocking of grains and hence a larger angle of internal friction φ . It can be seen from fig.(3- 5) that the Hyndford sand produces the highest φ values, and thus illustrates this point. De Beer (1965) and Moroto (1989) reported an increase in shear strength due to improved gradation, hence confirming the present results.
- 4- A well graded sand will produce smaller porosities, since well graded soils, with a high uniformity coefficient U, have fines to fill the voids created by the larger grains thus forming a dense structure with a high unit weight. This is consistent with the findings of Koerner (1970).

Number of grains	ψ^*	R	Number of grains	ψ^*	R
1	0.82	0.45	1	0.82	0.40
2	0.82	0.42	2	0.83	0.41
3	0.83	0.43	3	0.81	0.41
4	0.81	0.43	4	0.82	0.42
5	0.82	0.45	5	0.82	0.45
6	0.81	0.48	6	0.81	0.41
7	0.81	0.47	7	0.81	0.47
8	0.81	0.47	8	0.81	0.48
9	0.81	0.41	9	0.81	0.41
10	0.82	0.42	10	0.82	0.39
11	0.85	0.42	11	0.82	0.45
12	0.82	0.48	12	0.81	0.42
13	0.81	0.45	13	0.82	0.42
14	0.82	0.43	14	0.82	0.42
15	0.82	0.43	15	0.83	0.42
16	0.83	0.43	16	0.84	0.43
17	0.82	0.41	17	0.81	0.43
18	0.81	0.45	18	0.82	0.41
19	0.83	0.45	19	0.82	0.43
20	0.81	0.41	20	0.83	0.42
21	0.82	0.42	21	0.82	0.44
22	0.81	0.43	22	0.82	0.44
23	0.81	0.40	23	0.82	0.40
24	0.81	0.40	24	0.82	0.41
25	0.83	0.41	25	0.83	0.43
Summation	20.48	10.85	--	20.49	10.62
Mean	0.819	0.434	--	0.82	0.425

**Table 3-2 Typical Data for Shape Determination
of Leighton Buzzard Sand**

	Ballotini glass beads	L. Buzzard sand	Lochaline sand	Douglasmuir sand	Hyndford sand
D_{50} (mm)	0.80	0.80	0.30	0.80	0.80
U	1.80	1.80	1.80	1.80	5.50
G_s	2.92	2.65	2.65	2.66	2.66
ψ^*	0.95	0.82	0.85	0.84	0.87
R	0.98	0.43	0.39	0.31	0.27
Shape	Well rounded	Subrounded	Subrounded	Subangular	Subangular
γ_{max} (Kn/m ³)	18.66	17.70	17.51	17.30	19.23
γ_{min} (Kn/m ³)	16.90	14.78	14.41	14.25	15.45
η_{max} (%)	42.10	44.20	45.60	46.40	41.90
η_{min} (%)	36.10	33.20	33.90	34.95	29.00

Table 3-3 Sands Characteristics

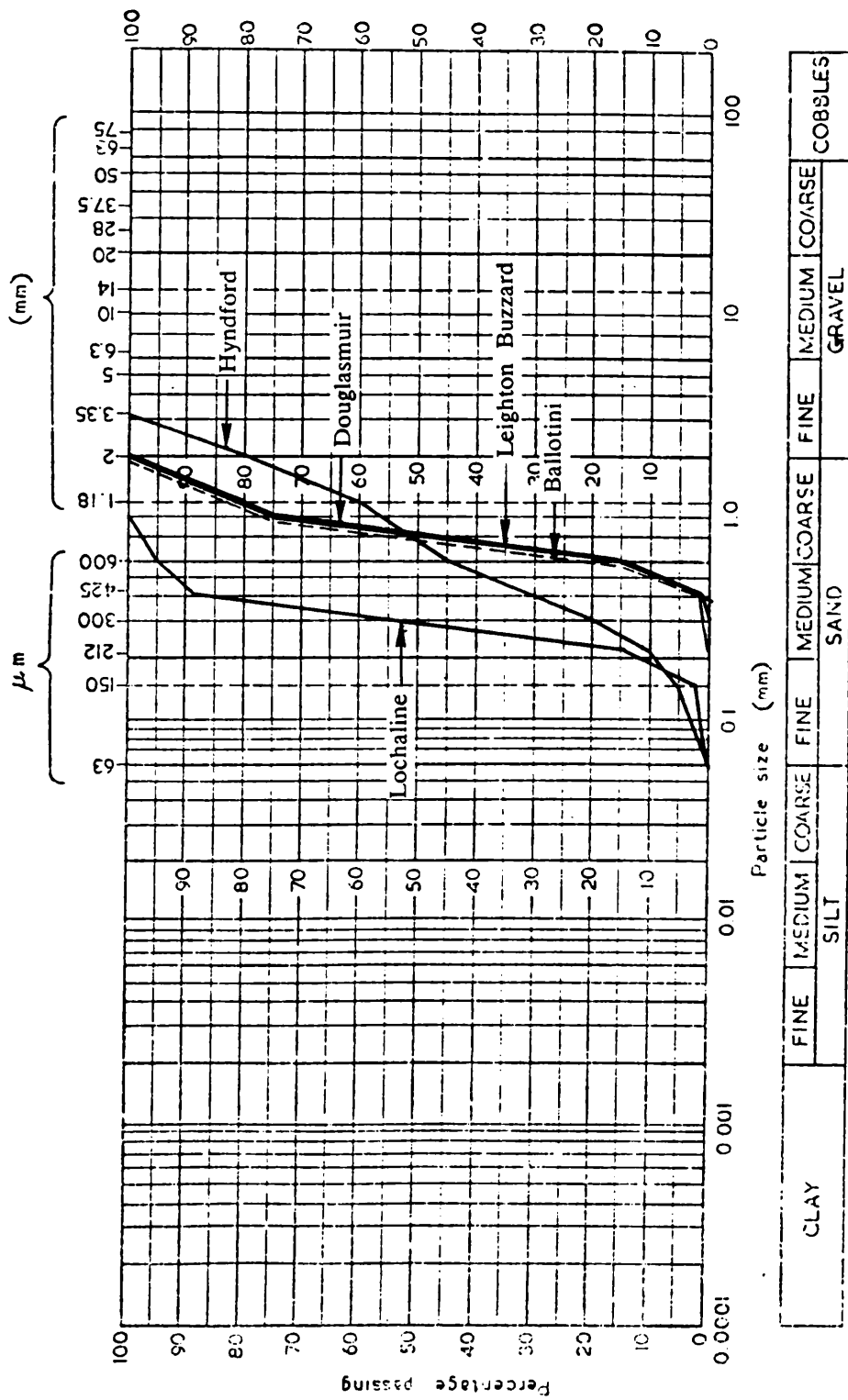


Fig. 3-1 Particle size distribution.

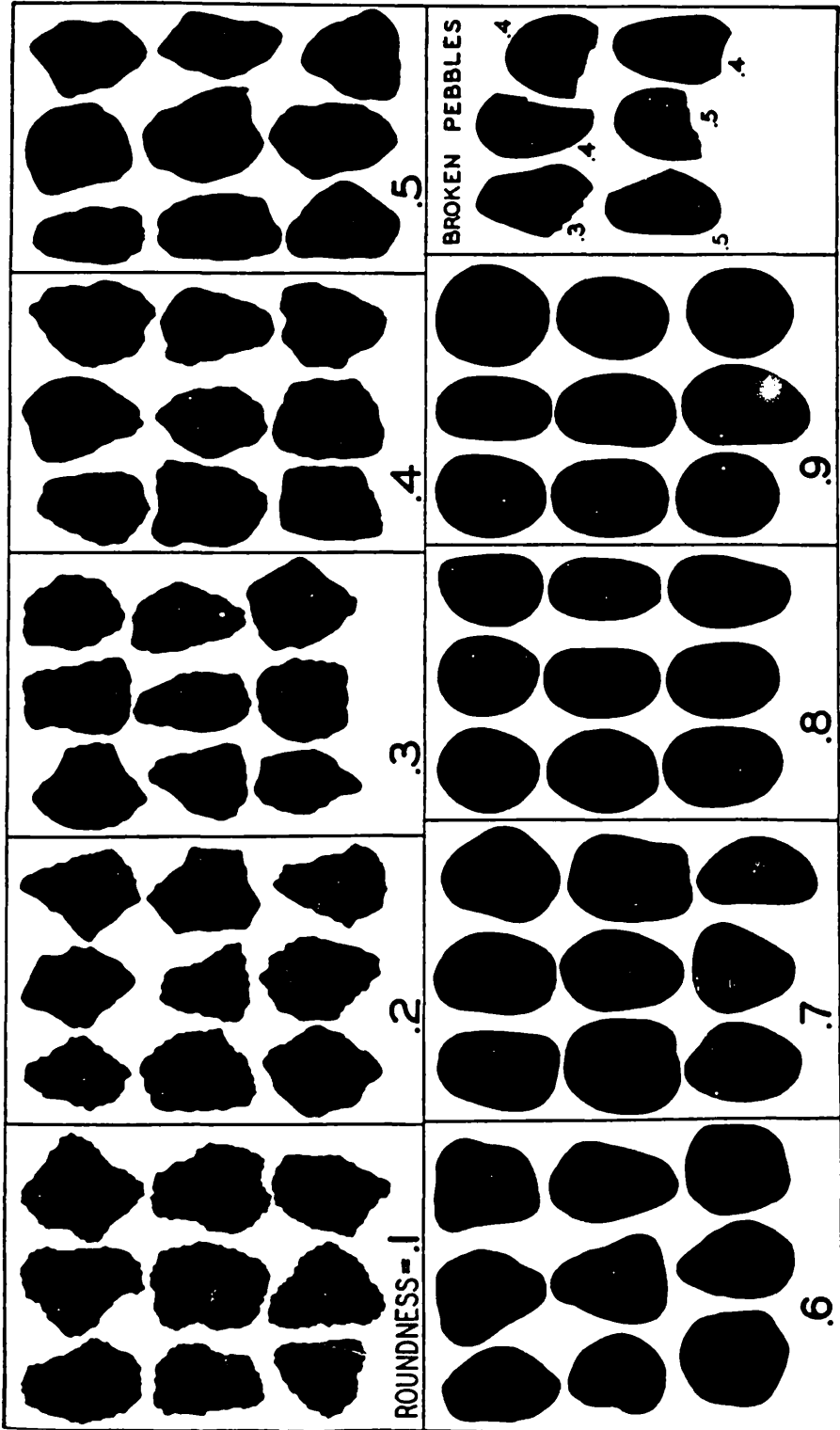


Fig. 3-2 Roundness chart (after Krumbein, 1941).

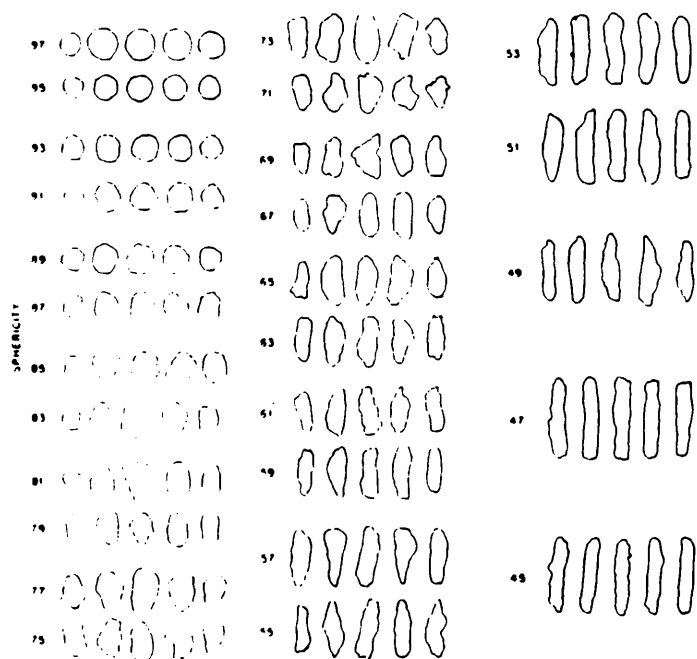


Fig. 3-3 Chart for determining visually the projection sphericity of sands (after Rittenhouse, 1943).

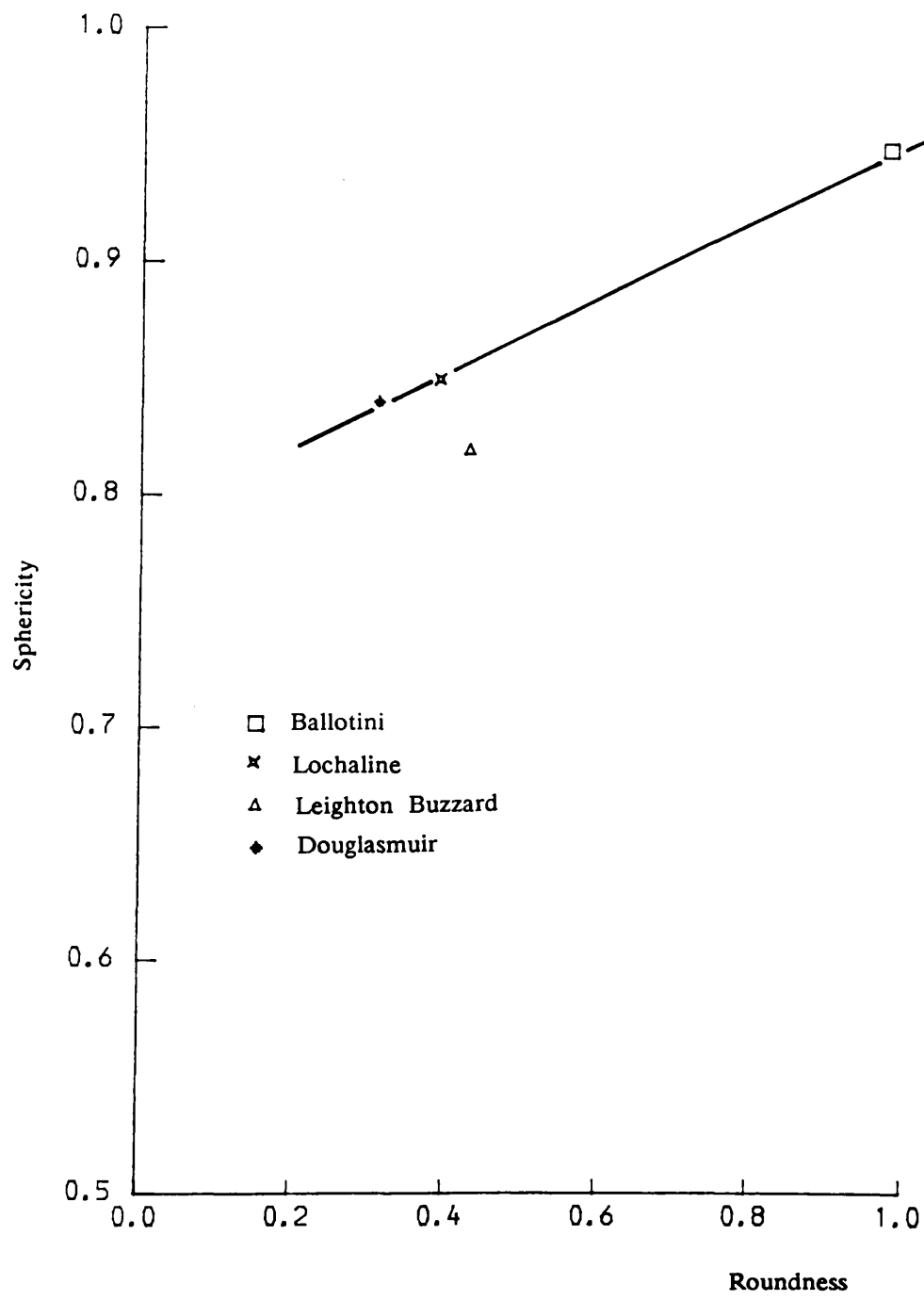


Fig. 3-4 Correlation of sphericity and roundness.

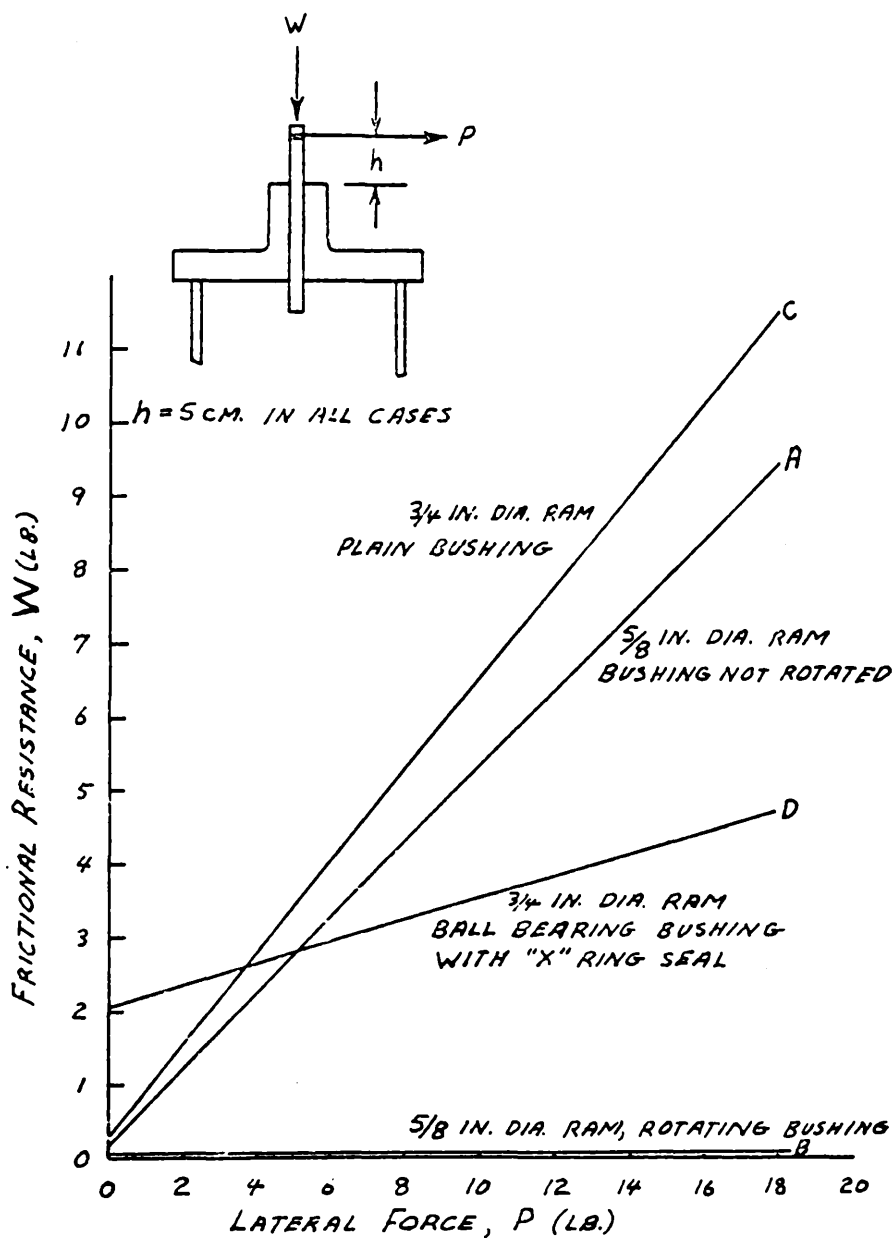


Fig. 3-5 Friction on Loading Ram (Freeman, 1970)*

* After Davie (1973)

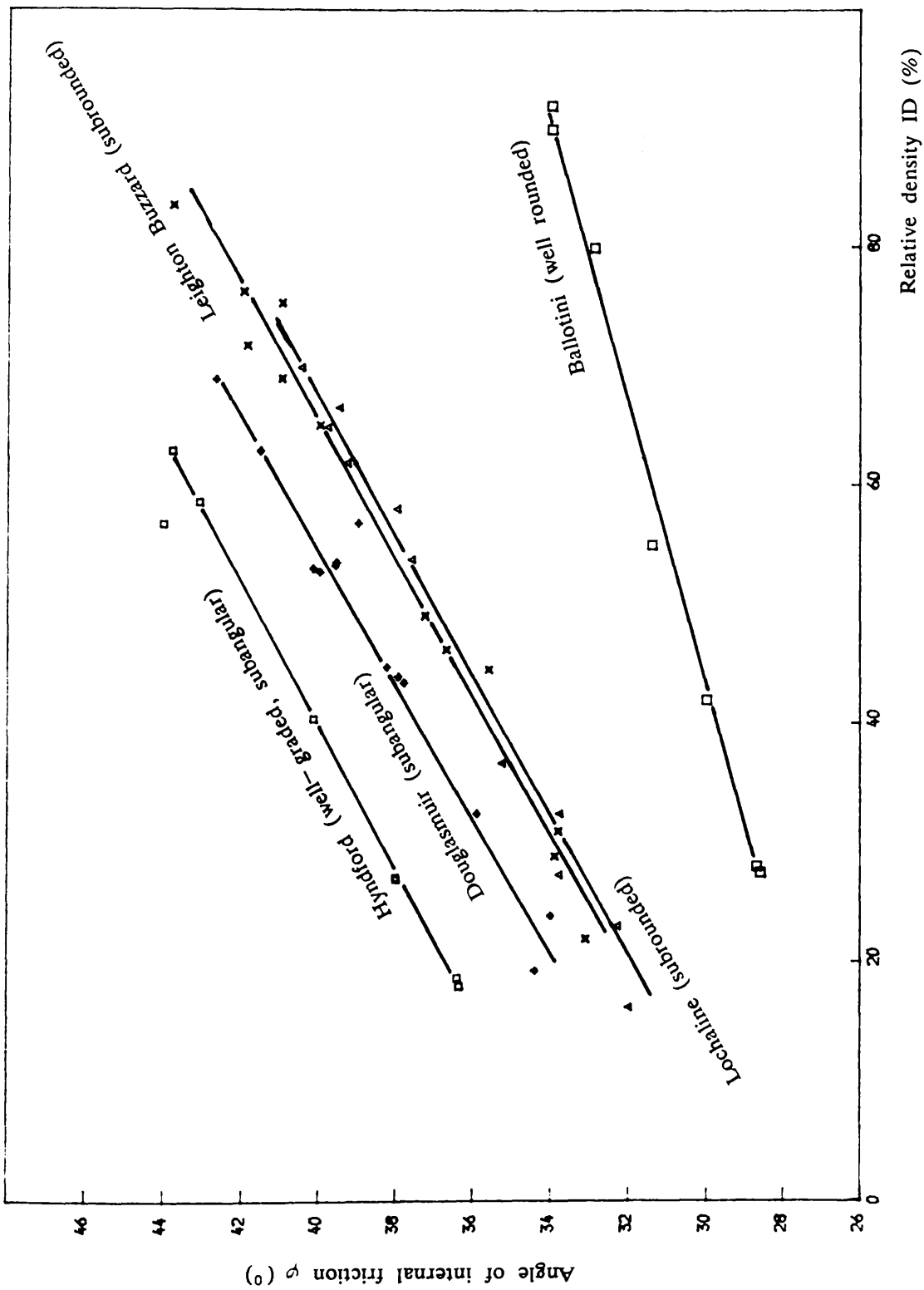


Fig. 3-6 Relationship between angle of internal friction and relative density.

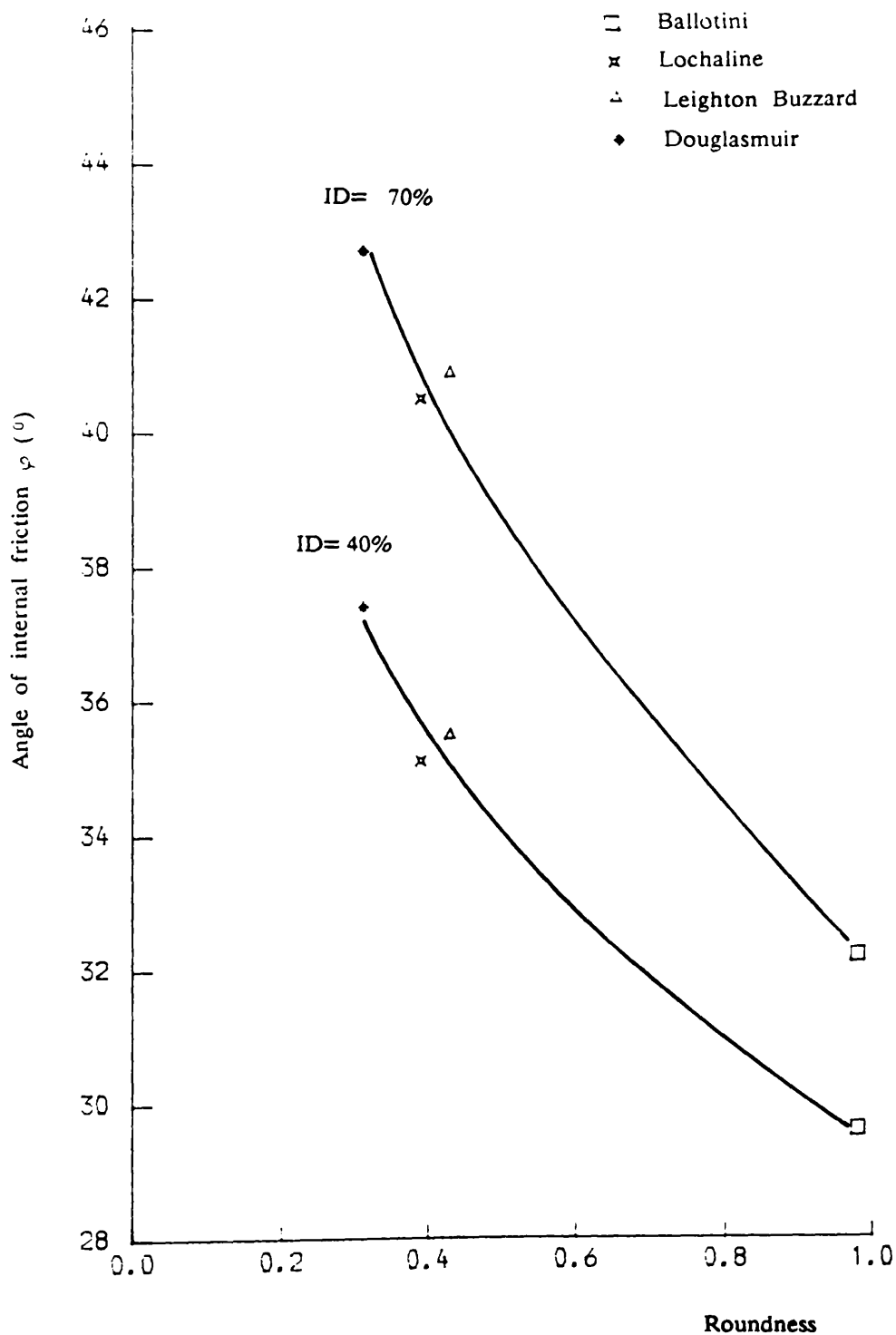


Fig. 3-7 Relationship between Roundness and angle of internal friction.

3-2 SAND BED PREPARATION

One of the most fundamental decisions to be made before the commencement of the test procedure is the choice of the method of preparation of the sand bed.

The main requirements of the present work were to provide fairly homogeneous and easily repeatable beds of sand over the entire programme of tests. Reconstituted samples of sand are often prepared in the laboratory by pluviation, where the sand is poured either through a concentrated opening or is rained from a surface which may cover the full cross-sectional area of the sample. Deposition in large size samples in model tests by the raining technique is carried out by some form of mechanism which traverses over the plan area of the sample. The pluviation technique is considered to approximate a natural deposition process.

3-2-1 Creation of uniform sand beds

The formation of sand beds of uniform porosity is a fundamental problem associated with all laboratory experiments involving cohesionless soils. There are several techniques of sand bed preparation, Butterfield & Andrawes (1970) divided them into two major groups:

- 1- Methods where the density is adjusted after deposition,
which are only suitable for dense sand beds.
- 2- Methods where the density is controlled during deposition.

Group 1 consists of methods involving vibration, tamping, stirring or fluidization using air. When the sand is placed in layers, tamping or stirring is usually employed to give a uniform density. Kulhawy et al (1979), Murray &

Geddes (1987), Tagaya et al (1988) and Dickin (1988) used this method. However, the protracted strenuous efforts involved in the stirring and tamping of soil layers is the main disadvantage of this method. Vibration or fluidization can also be applied to entire sand beds. The sand beds are usually prepared by placing, underwater, dry sand into the test tank and then vibrating (Andreadis, 1979; Low, 1986). A number of previous users such as Andreadis (1979), Harvey et al (1980) and Low (1986) have suggested that excess horizontal stresses can be introduced into sand beds created with this technique. On the other hand, the main advantage of this method lies in the simplicity of apparatus required, fair repeatability and the speed with which the soil bed can be prepared.

In group 2, the methods are based on the work of Kolbuszewski (1948), who showed that the density of a sand bed was a function of the intensity of deposition and the height of free fall of sand from a hopper to the sand surface. Two alternative deposition techniques are commonly used:

- i- Deposition using a controlled intensity rain of sand over the whole bed area.
- ii- Deposition using a controlled intensity sand curtain traversing the bed area.

Kolbuszewski and Jones (1961) used a controlled intensity sand raining technique, the sand being deposited in layers over the total surface area of bed. They constructed a hopper in which the intensity of deposition was controlled by varying the overlap of holes drilled in two plates at the base of the hopper. The hopper containing the sand could be mounted at any height directly above the sand container. This technique produced sand beds with very little variation in density between layers. Several investigators have used similar set-ups utilizing the sand

raining technique e.g. James (1965), Vaid & Negussey (1984), Das & Jin Kaun (1987) and Stewart (1988).

In the second technique the bed is built up of thin layers, each of which is produced from a falling curtain of sand discharged from a slot in a hopper, during every traverse of the hopper over the receiver tank. Various types of apparatus have been constructed based on this method (see Figs. 3-10 & 3-11), differing mainly in the technique used to control the intensity of deposition (Walker & Whitaker, 1967, Butterfield and Andrawes, 1970 and Fadl, 1981). However, there is the possibility of stratification when using this method, especially in the case of medium and loose deposits. This layering can be reduced by placing a diffuser mesh between the sand curtain and the bed James (1967).

In the present investigation the method of sand raining has been used as it proved successful and reliable in a previous project (Stewart, 1988). However in the case of Hyndford sand (well graded) air pluviation clearly resulted in segregation because of the finer particles lagging behind on account of their smaller velocities within the fixed height drop. Homogeneity of such pluviated samples was then questionable. In view of the above, vibration had to be used in order to achieve the desired densities for the laboratory pull out tests.

3-2-2 Details of the raining device

The hopper apparatus was required to produce a rain of sand grains, the velocity and intensity of which could be varied over wide limits. The velocity depended on the height of fall and so could be easily adjusted. The intensity depended on the diameter of the holes and so could be controlled by means of variable apertures. The raining device used is shown in fig.(3-12), the various components being:

- 5
- 1- Circular hopper of the same diameter as the test container.
 - 2- Moveable frame which allows the adjustment of the height of the hopper in order to maintain a constant height of fall of sand of 85 cm.
 - 3- Perforated discharge plates fixed to the bottom of the hopper to produce sand rain. Various discharge plates having perforations ranging from 2 mm to 13 mm diameter were used. Three rates of deposition, low, medium and high produced dense, medium and loose sand beds in the context of this investigation.
 - 4- Openable plates to retain sand while the hopper is filled.
 - 5- Sand tank, dimensions 500 mm diameter and 700 mm deep.
 - 6- Density pots.

In the present investigation the intensity of deposition was varied by using various plate apertures while the height of fall was kept constant by raising the portal frame and the hopper after each layer (75 mm thickness) was deposited. However, in the case of loose sand higher rates of pouring into the container trapped an air front mass ahead, the eventual escape of which caused a counter upward air current, thus reducing the impact energy and hence resulting in lesser compaction and layers shaped as shown in Fig.3-13. Density measurement showed that the formation of sand layers shaped in this way did not affect the homogeneity of the resulting sand bed, thus confirming the observations made by Stewart (1988).

3-2-3 Uniformity of the sand beds

The uniformity of a particulate mass is commonly tested by measuring the porosity, or alternatively the density, at different locations within the mass of soil.

Kolbuszewski pointed out that the state of the sand bed is best defined by the relative porosity or relative density, in terms of the maximum and minimum porosity which the particular sand can attain. However, the porosity alone cannot describe the state of packing of the sand grains Andrawes (1970). If the packing and density are uniform throughout the sand bed then the porosity of any part of the bed will be equal to the overall porosity.

Several methods of density measurement in the laboratory have been reported. These include the spoon penetration test (Gibbs & Holtz, 1957), vacuum sampling apparatus (Ovesen, 1962), X-Ray photography (Roscoe, 1967; Been, 1981; Morin, 1988), density pots (Butterfield & Andrawes, 1970) and density scoop (Trautman et al., 1985).

Different test conditions may require different measurement procedures, since no technique yet proposed is universally applicable. For example, the density scoop works well for medium to dense sands in the medium to fine grain size range but does not perform well with gravel sized particles. The cylinder and vacuum technique, which was developed at the Danish Geotechnical Institute, is a relatively easy procedure in which a steel tube is inserted into the sand and the sand within it is removed by vacuum and weighed. This technique has several of the same limitations as the density scoop. The X-Ray photography method have the advantage of being a non-destructive method. The changes in density of the material due to the change of porosity give rise to different levels of penetration by the X-rays and consequent shading of the photographic plates. A γ -ray technique, which scans the sand bed and records the penetration level point by point, was developed to provide qualitative measurement of the local voids ratios. All the previous methods made similar claims of good reproducibility, however based on the experience gained by Glasgow University through the extensive work of Fadhil (1981),

Zakaria (1986) and Stewart (1988), the author decided to use the density pots method with the following procedure.

First of all, the density pots must be calibrated by determining their volume. This was done by partially covering the top of the pot with a glass plate and weighing both the pot and the plate while dry. Next, water was carefully added to the pot maintaining a flat water surface with the glass cover. The pan was reweighed and the volume determined from the weight of water. The cylindrical pots were placed on the sand layer at the desired points to keep the pots apart from one another so that each pot was undisturbed by the removal of any other. The pots had a diameter of 75 mm and an internal depth of 50 mm with a knife-edged upper rim to prevent bouncing of sand particles into them. It is worth noting that the choice of diameter was based on the work of Kolbuszewski (1948a). He found that containers with diameter less than 75 mm gave rise to differences in measured porosities while containers with diameter greater than 75 mm caused little or no change in the measured porosity. After depositing the sand, the pots were carefully removed from the bed and the sand on the top was levelled off carefully with a steel straight edge. Knowing the mass of the sand collected in the pots, the density of that layer was evaluated. The same procedure was repeated for the next layer. The spreader was accordingly raised by 75 mm to correspond to the increase in sand layer depth in the tank so that a constant height of drop could be maintained. This was repeated until the required depth of bed was achieved.

In each test five pots were arranged. The average value was used to calculate the density, void ratio and porosity of the sand layer. The calculated porosity was taken to be the porosity of the sand layer at the mid-height of the measuring pot and the height of fall was considered to be from the mid-point of the discharge slot to this level. The calibration curve of the sand spreader is given in fig.(3-14). The results of the series of tests are given in tables 3-4 & 3-5.

Note:

- 1- The raining method was used to achieve dense, medium and loose densities for Lochaline, Leighton Buzzard and Douglasmuir sand.
- 2- Good repeatability of the sand beds was achieved using the above method. Three density tests were performed with each aperture.
- 3- A vibrating method was used to obtain the dense state for Hyndford sand. The sand was placed by bucket in the container and vibrated by a Kango hammer with a plate attachment to transmit the vibration to the sand in 50 mm layers. Repeatability of the dense sand bed when using this method is very difficult (the different values will be given in the next chapter). For medium loose and loose state, good reproducibility was achieved. A slight vibration lasting 10 seconds was used for the medium loose state, but for the loose state the sand was poured directly from a bucket into the container.

Pots N ^o	γ_{layer1} (Kn/m ³)	γ_{layer2} (Kn/m ³)	γ_{layer3} (Kn/m ³)	γ_{layer4} (Kn/m ³)	γ_{layer5} (Kn/m ³)	γ_{layer6} (Kn/m ³)
1	16.48	16.43	16.50	16.48	16.39	16.46
2	16.60	16.60	16.58	16.43	16.52	16.52
3	16.57	16.56	16.43	16.56	16.52	16.46
4	16.52	16.43	16.39	16.43	16.52	16.40
5	16.52	16.43	16.54	16.43	16.52	16.52
γ^*	16.53	16.52	16.49	16.47	16.49	16.47
e^*	0.603	0.604	0.607	0.609	0.607	0.609
n^*	37.62	37.65	37.77	37.85	37.77	37.85

γ^* = Average bulk density (Kn/m³) for each layer

e^* = Average void ratio for each layer

n^* = Average porosity for each layer

Table 3-4 Typical Results of Density Pot Tests in Lochaline Sand

Aperture 2 mm diameter

Height of Fall 85 cm

Apertures diameter	Ballotini glass beads	Lochaline sand	L. Buzzard sand	Douglasmuir sand	Hyndford sand
2	--	16.47	--	16.57	--
(mm)	--	0.032	--	0.044	--
γ^*					
sd					
4	18.60	--	17.28	--	--
(mm)	0.020	--	0.018	--	--
γ^*					
sd					
5	--	15.72	17.15	--	--
(mm)	--	0.084	0.020	--	--
γ^*					
sd					
7	17.78	--	--	16.09	--
(mm)	0.031	--	--	0.016	--
γ^*					
sd					
9	--	14.81	16.57	--	--
(mm)	--	0.014	0.033	--	--
γ^*					
sd					
10	--	--	--	--	16.95
(mm)	--	--	--	--	0.049
γ^*					
sd					
12	--	--	--	15.21	--
(mm)	--	--	--	0.055	--
γ^*					
sd					
13	--	--	15.63	--	16.59
(mm)	--	--	0.034	--	0.072
γ^*					
sd					

γ^* = mean bulk density (Kn/m³)
sd = standard deviation

Table 3-5 Summary of Density Tests Results

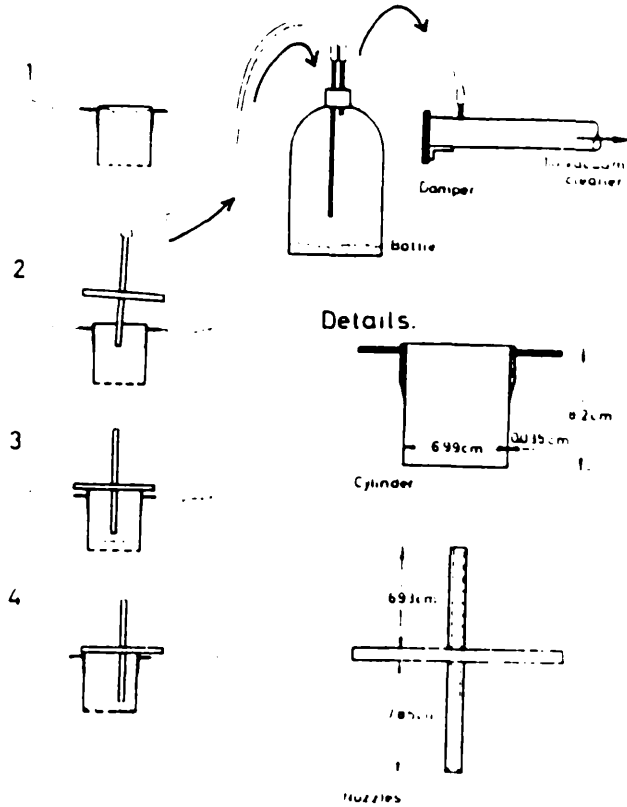
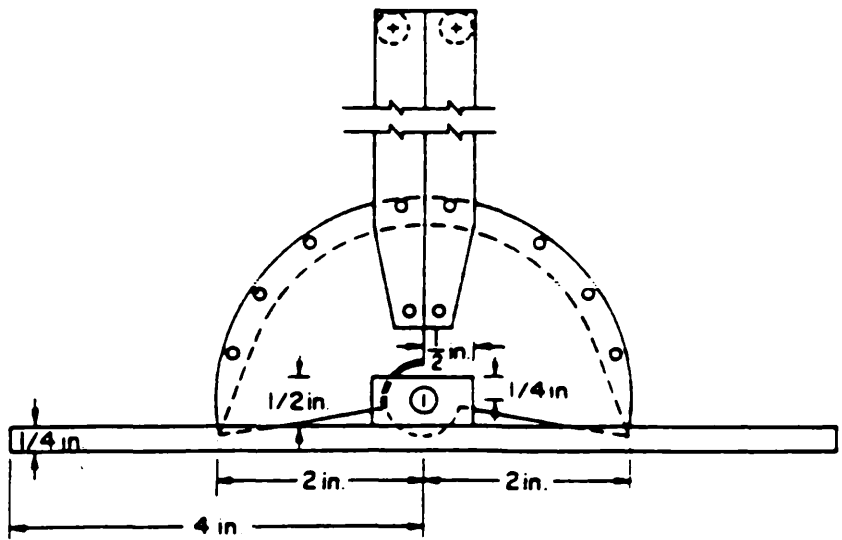


Fig. 3-8 Suction sampler method for density measurements (after Ovesen, 1962).



Side View

Fig. 3-9 View of the density scoop (after Trautmann et al, 1985).

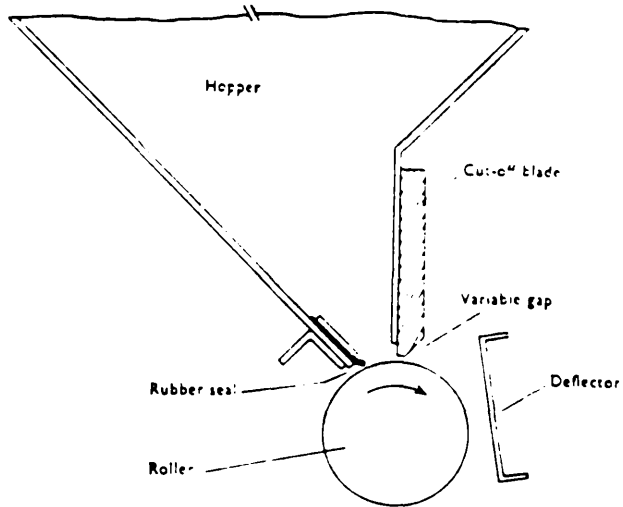


Fig. 3-10 Roller for controlling the flow of dry sand from the bottom of the hopper (after Walker & Whitaker, 1967).

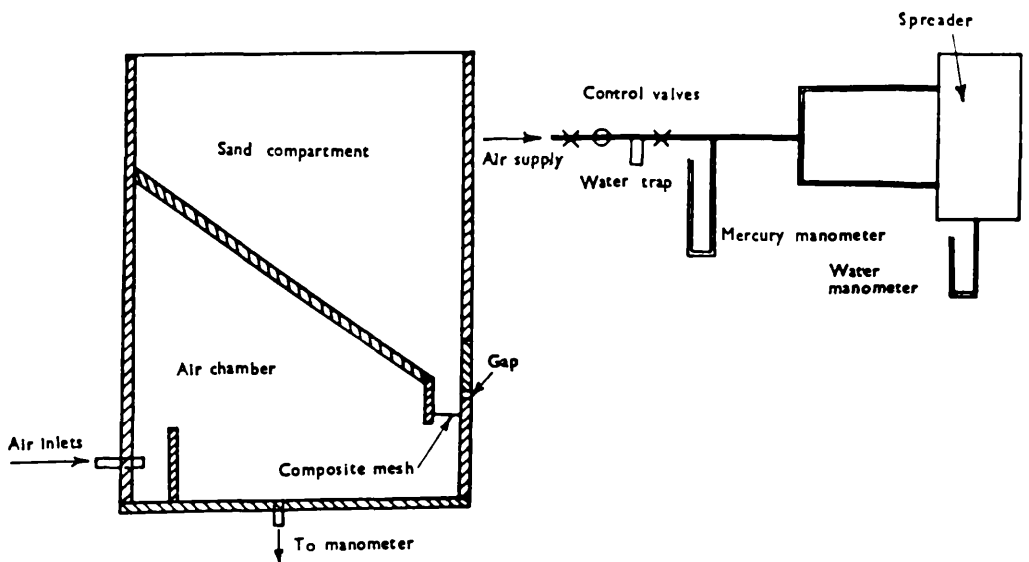
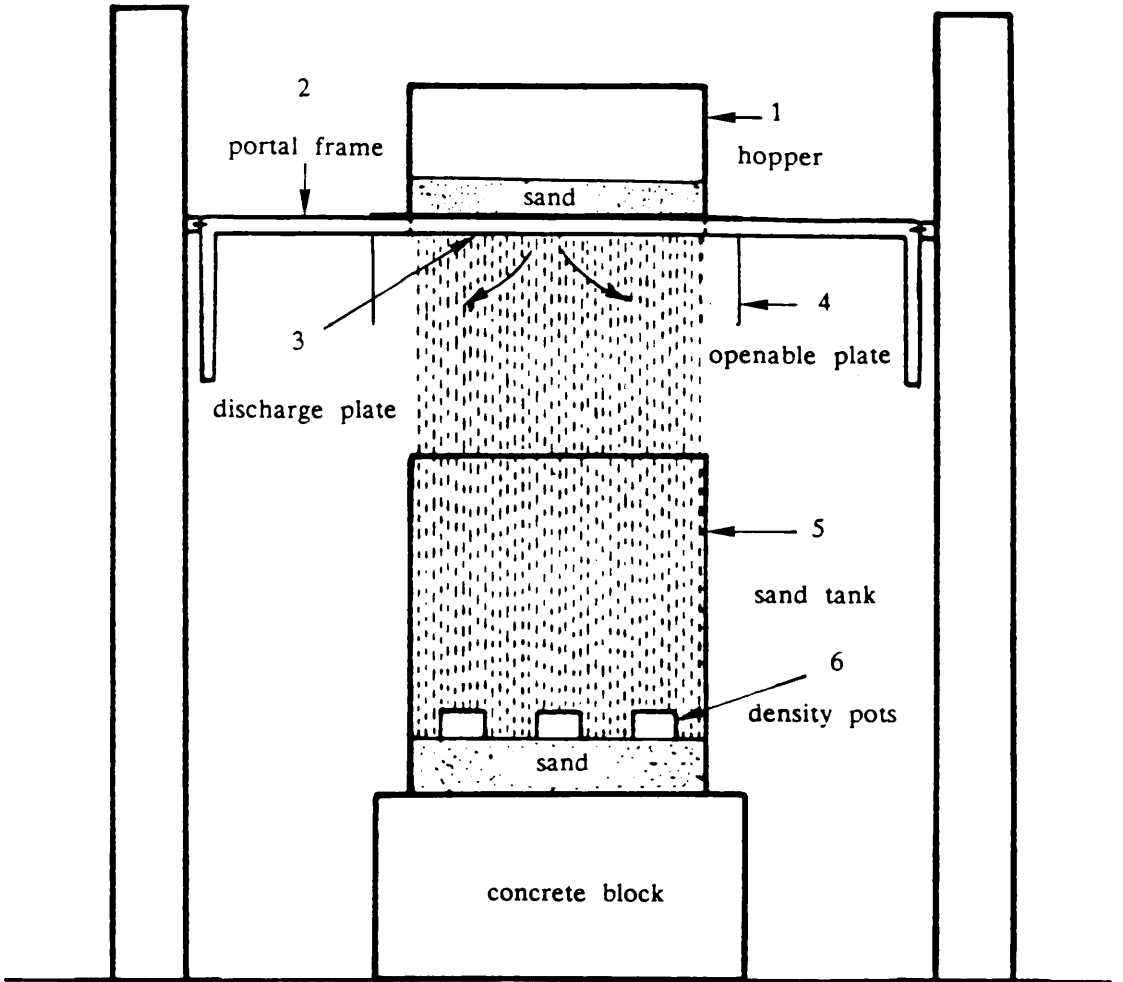


Fig. 3-11 Sand spreader (after Butterfield & Andrawes, 1970).

elevation



plan

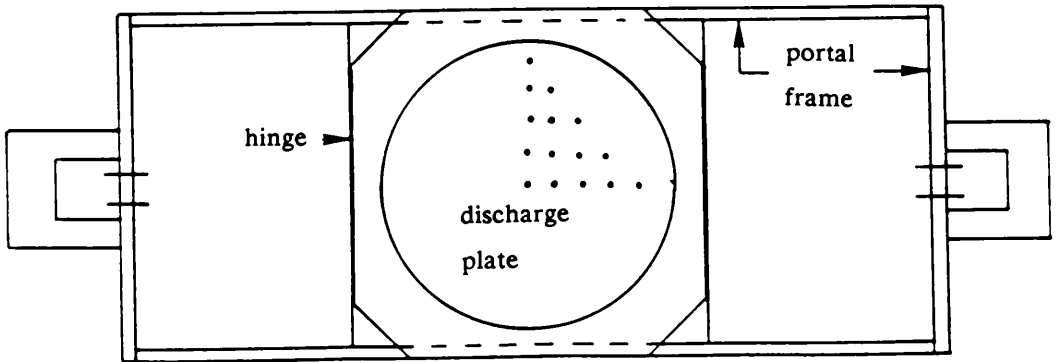


Fig. 3-12 Sand raining apparatus

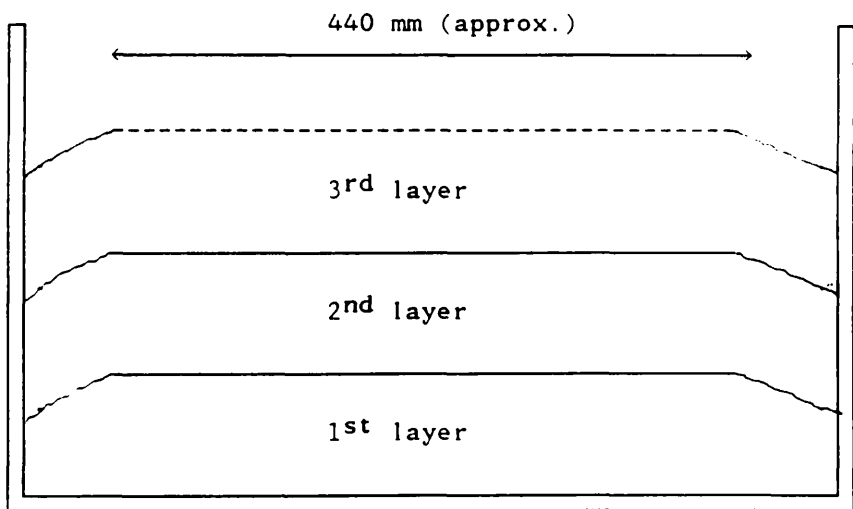


Fig. 3-13 Shape of sand layers in loose sand beds.

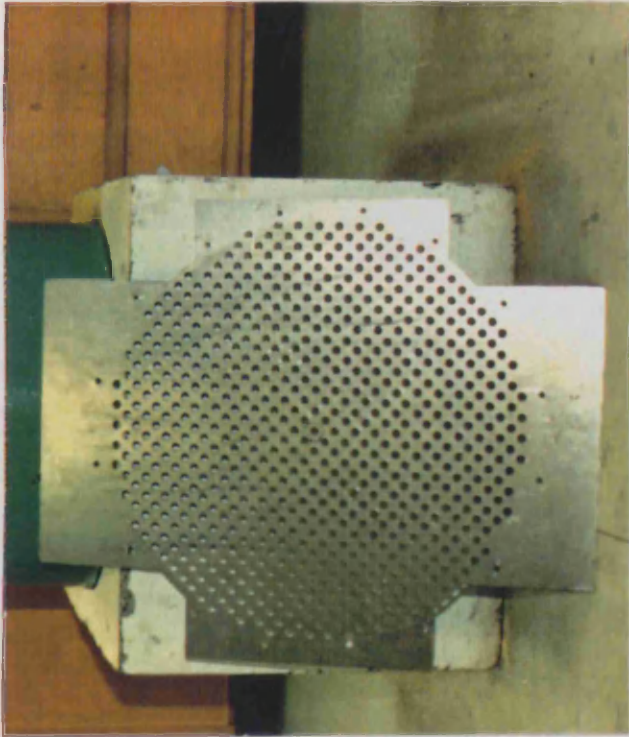


Plate 3-1 Type of sieve used in the present work.

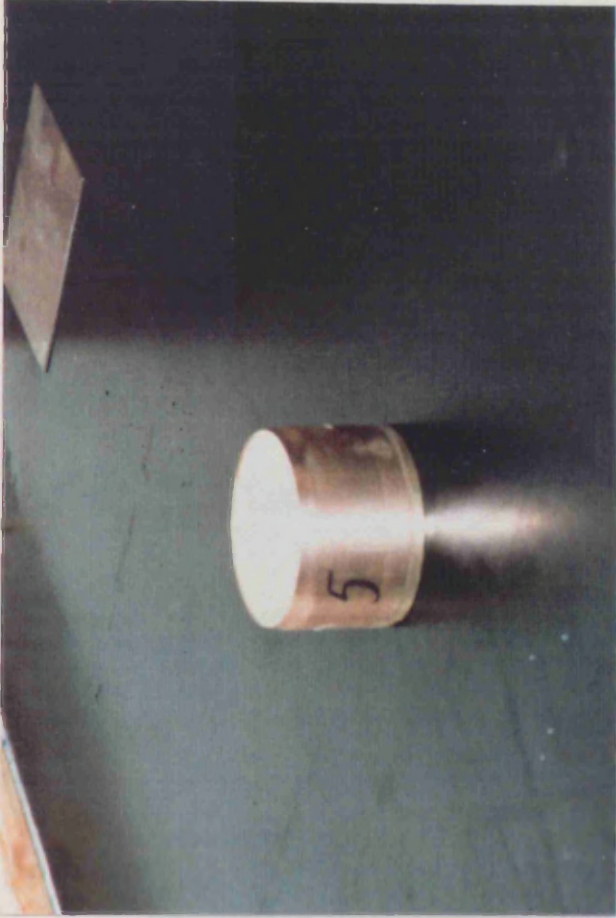


Plate 3-2 Density pot.

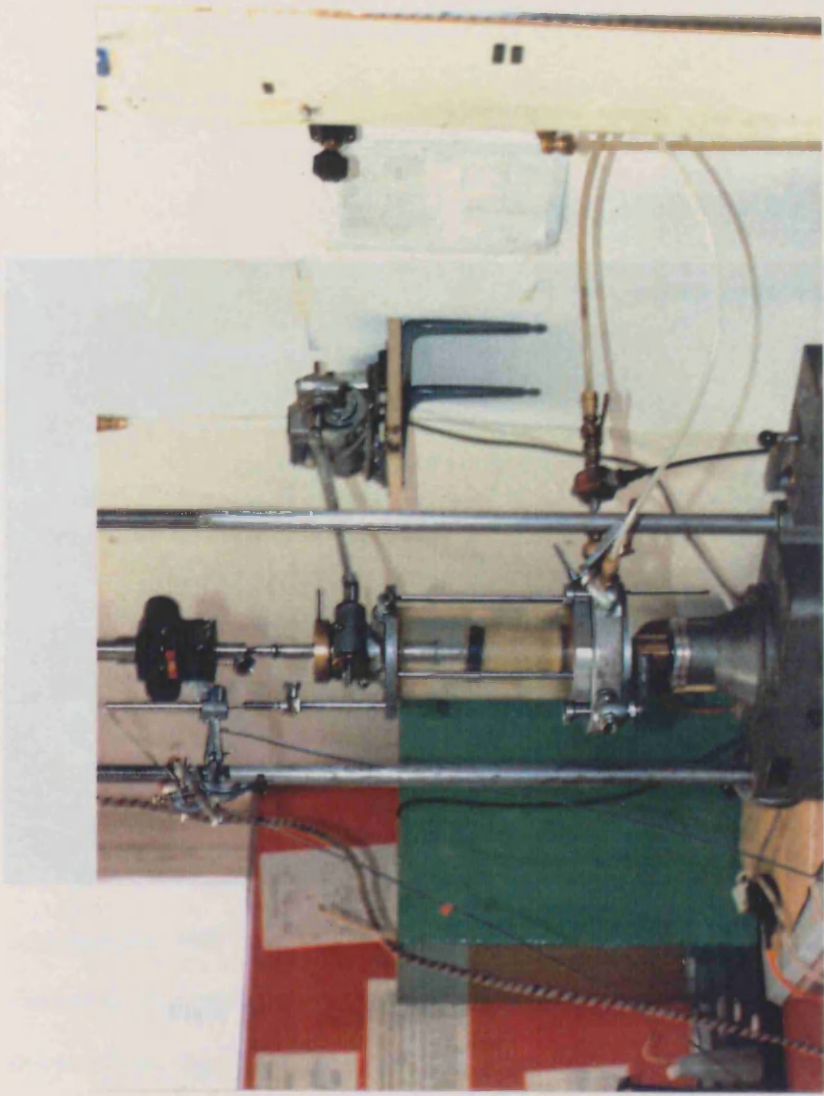


Plate 3-4 Triaxial test arrangement.

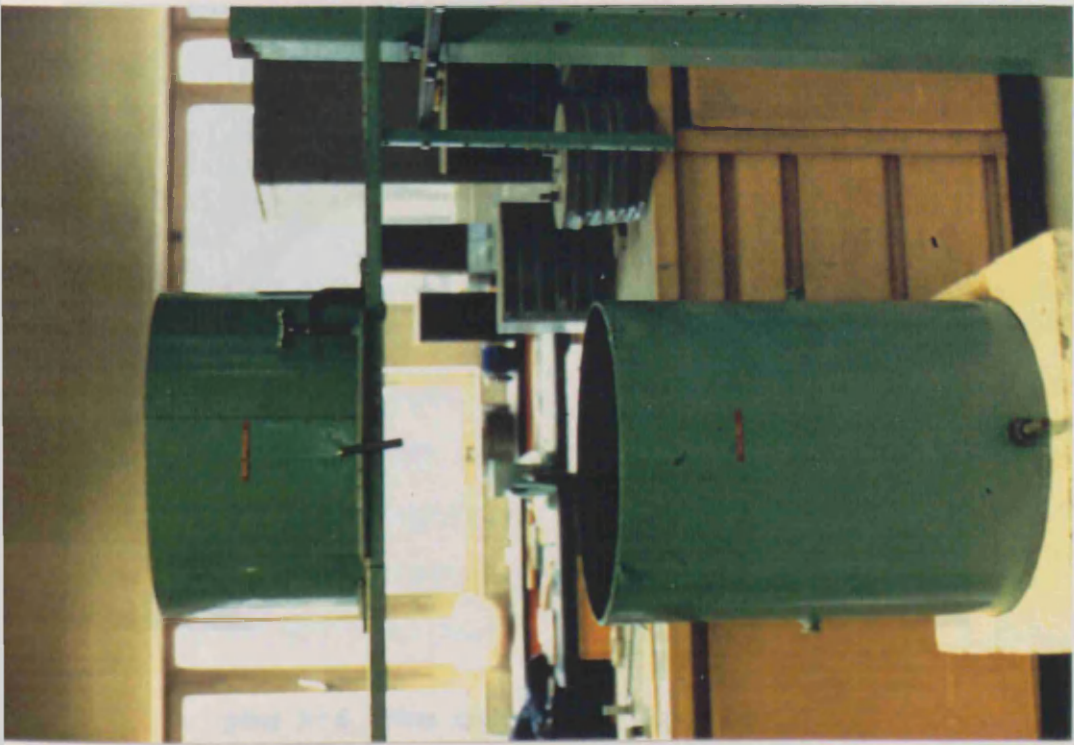


Plate 3-3 Test container and sand hopper.



Plate 3-5 sand raining in operation.

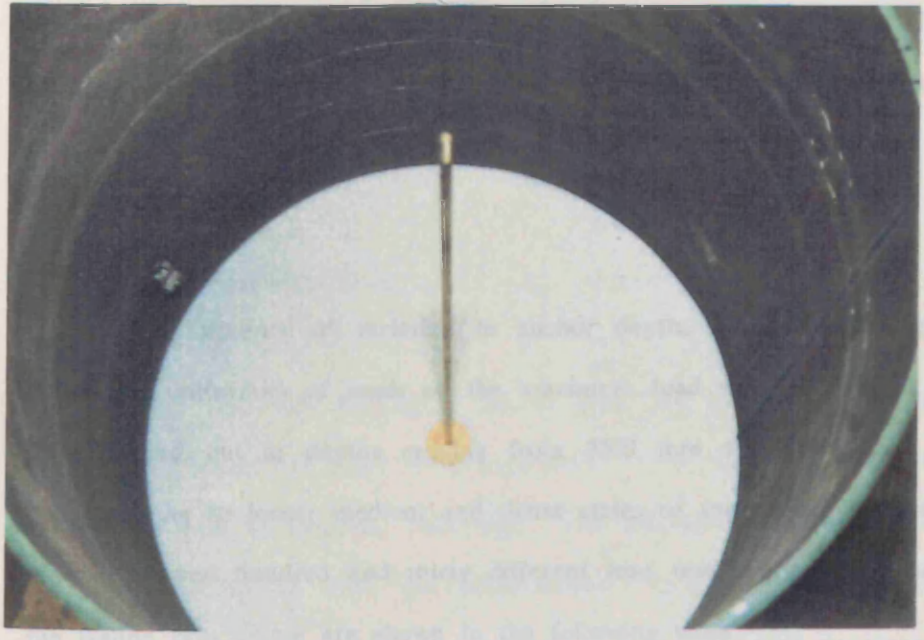


plate 3-6 Plate anchor before deposition of overburden.

Chapter 4

LABORATORY TESTS OF MODEL ANCHORS

4-1 INTRODUCTION

The experimental programme was designed to show to what extent variables such as depth of embedment, relative density, grain size, grain shape and uniformity coefficient influence the maximum uplift resistance and the failure surface. This chapter concerns the pull out tests on model anchors which were carried out in order to obtain experimental evidence concerning the magnitude of the failure load intensity for a number of different situations. The equipment used in the present investigation will be described as well as the loading method. The results will be discussed in chapter 5. The methods of forming uniform sand beds have been discussed in the previous chapter. It has also been shown that the spreader was capable of producing consistent density beds in the tank within a range of relative densities varying from 13% to 85% for a height of fall of 85 cm. The part dealing with the failure surface will be described and discussed in chapter 6 & 7.

4-2 VARIABLES

The influence of variation in anchor depth, sand densities, grain size, grain shape and uniformity of sands on the maximum load was investigated. Pull out tests were carried out at depths ranging from 75.0 mm to 450.0 mm. Three densities corresponding to loose, medium and dense states of the sands used were investigated. A total of one hundred and thirty different load tests were performed. Details of the testing programme are shown in the following table.

type of tests	load control tests		
	low density	medium density	high density
Sands			
Ballotini	---	9	10
Lochaline	7	9	11
L. Buzzard	7	10	20
Douglasm ^r	7	8	10
Hyndford	13	---	10

Table 4-1 Details of Testing Programme

4-3 GENERAL DETAILS OF APPARATUS FOR LOAD TESTS

The diagram of the apparatus used to perform the load tests is shown in fig.(4-1). Plate (4-1) shows a photograph of the apparatus. The main features are described below.

4-3-1 Electrical equipment

During the static loading of the anchors, the vertical loads and deflections at the top of the anchor shaft were monitored. The load was measured by a 2000 N-capacity type D Sangamo load cell. The displacements were measured by a 25 mm travel Sensonics type SR displacement transducer capable of detecting a movement of 0.02mm. The arrangement of load cell and displacement transducer

is shown in plate (4-2). These transducers produced analogue signals, which were mainly voltages in the present work, proportional to the magnitude of the respective physical quantity (load & displacement) produced. In practice, the recording of these analogue signals can be either in analogue or digital form.

4-3-2 Data acquisition system

Computer orientated automatic data acquisition and control systems are being increasingly used in laboratory, field and industrial applications, and generally fulfill two requirements.

- i- To measure simultaneously several parameters during a given test.
- ii- To obtain large volumes of data over a prolonged period.

This system replaces the manual means of obtaining test data by having the computer electronically monitor and record changes in test parameters via transducers. The data logging system, illustrated in fig . 4-4 , used in the present investigation comprises the following units.

- 1- Analogue transducers.
- 2- Signal conditioner.
- 3- Data logger, mini computer and output device.

-1- The analogue transducer

Basically, an analogue transducer is a device which detects a change in a physical quantity, such as force, and converts it into an equivalent change in voltage which can be recognised, read and recorded by a computer. Load cell and displacement transducers are examples of analogue transducers. Before carrying out the test, it was necessary to calibrate all transducers used. This was done by

calibrating the load cell to its maximum capacity against dead weights and the displacement transducer by the use of a micrometer. Recalibration was conducted on a regular basis thereafter to ensure consistency in their performance. Although calibration tests are considered as routine it must be remembered that this process is vital because the quality of the final results obtained relies heavily on the accuracy of the calibration factor. In the present investigation calibrations were regularly checked and found to be consistent.

- 2- The signal conditioner

The electrical resistance strain gauge type transducers employed tended to produce a voltage too small for the analogue-to-digital converter (A/D) to detect, therefore a signal conditioner was used to amplify the signals concerned to such a level as to render them detectable by the A/D converter. The signal conditioner used in the present work could accommodate 20 amplifiers mounted in two metal boxes (see plate 4-3). The zero and range controls available to each channel were adjusted so that the output from each transducer could be displayed in multiple fraction units of mV. To achieve this, each transducer was calibrated at a suitable sensitivity using the conditioner.

- 3- data logger, micro computer and output device

The data logger, (a Solartron) shown in plate 4-4, consisted of an analogue scanner, a data transfer unit and a digital voltmeter. During the operation, the Solartron hardware provided a channel sampling front to collect analogue signals from the transducers. The high speed A/D conversions were regulated by the built-in crystal controlled clock, a facility which is essential in automatic data logging operation. The micro computer used was a Commodore CBM 2001/B with

16 Kbytes memory capacity. The role of this computer in the system was to control the selection of sampling channel, frequency of sampling and other facilities that can be provided. All the data were transferred to an Epson printer which printed a continuous statement of date, time, channel number and transducer output.

There are several advantages in using the data logging system, the more distinctive ones being: (1) a neat and compact presentation of the results can be achieved with this system, (2) the system allows records to be made overnight, (3) the automatic records allow a high density of information to be obtained and, hence, a greater accuracy of the results.

4-3-2 Receiver tank

In designing a cylindrical test tank, the choice of its dimensions must be such that any possible influence of the boundary of the container on the behaviour of the plate anchor during a test is minimised, if not eliminated. This is a condition that should be satisfied in order that the prototype test situations for plate anchors are simulated at laboratory scale. Previous authors (Carr, 1970; Tsangarides, 1978; Andreadis, 1979) have carried out experiments to examine the extent of boundary effect due to the tank wall. They used the ratio of container diameter B_c to anchor diameter B as an indicator of potential side effects.

Carr (1970) conducted laboratory model anchor tests to determine the magnitude of the " zone of influence " around a loaded anchor. Specially designed sand movements gauges were used to measure sand movement around the anchor. He reported no movements in the zone outside $B_c/B > 8$. Tsangarides (1978) conducted a series of uplift tests in containers of various sizes. Using a 50 mm diameter anchor embedded in dense sand, Tsangarides found that for $D/B \leq 10.0$

the value of the pull out load was constant for tests in containers where $B_c/B \geq 12.0$. Tests in a container with $B_c/B = 6.0$ showed a sharp increase in the pull out load. Andreadis (1979) monitored the extent of soil disturbance during testing by introducing a stress monitoring method. Electronic soil pressure gauges were placed at locations throughout the depth of the sand bed. He reported that for $D/B \leq 8$ horizontal stresses become insignificant at distances over 15 times the anchor diameter and noted that the magnitude of horizontal stresses increased with increasing anchor diameter (D/B constant).

Considering the soil handling procedures and also on the basis of the previous findings the dimension of the tank diameter (500 mm) was chosen. The depth of the tank (700 mm) was adopted to enable the performance of deep anchor tests. The author has used a 37.5 mm and a 25.0 mm anchor diameter giving a ratio between test container diameter to anchor diameter (B_c/B) of 13 and 20 for the shallow and deep cases respectively, these values being judged adequate to avoid significant side effects.

The container was made from 6 mm mild steel plate into a right cylinder with a circular base plate welded to one end to form the bottom. It was placed on a block of concrete in order to dampen any vibrations from the laboratory floor.

4-3-3 Rig

The equipment used for the pull out test was the same for the four sands investigated. This test equipment can be divided in two parts.

- 1- Anchor assembly

- 2- Loading assembly

4-3-3-1 Anchor assembly

The anchor assembly comprised the following items:

- 1- Circular anchor plate
- 2- Anchor shaft
- 3- Pin
- 4- Anchor cap
- 5- Anchor support cap
- 6- Extension rod to load cell
- 7- Displacement datum
- 8- Centering device

Brass discs with smooth polished faces having diameters of 25 mm and 37.5 mm and 3 mm thickness were used (plate 4-6). Anchor shafts 3.5 mm or 6 mm diameter were screwed into the brass discs to make the anchor unit. It was assumed that the plate anchors were rigid enough to undergo negligible deformation compared to the soil during uplift resistance tests.

4-3-3-2 Loading assembly

The loading assembly consisted of the following items:

- 1- Air cylinder piston
- 2- Load cell
- 3- Yoke
- 4- Tie bars
- 5- Displacement transducer

The loading frame was built of 100 mm × 100 mm × 6 mm R.H.S. with

internal dimensions of 1400 mm horizontally and 1750 mm vertically. An air cylinder piston was bolted at the centre of the reaction frame. The distance between the support columns for the reaction frame was 1.5 m, large enough to allow a passage for a small mobile crane to lift and empty the container. The feet of these columns were each welded to a steel plate before being bolted to the laboratory floor. The bolted connection was strong enough to prevent the columns from moving while the tests were in progress. The reaction frame together with the air piston cylinder were temporarily removed while the sand bed was being formed in the container. A support rig was built for the reaction frame when it was detached from the columns.

4-3-4 Method of assembly

A centering rod which had a ring - like connection at the centre was carefully placed around the anchor shaft to minimize any lateral effects which might occur while the loading frame was being assembled.

A displacement datum was attached to the shaft as a means of recording the vertical motion of the anchor by an L.V.D.T. An anchor cap was screwed onto the upper threaded end of the shaft. A second and bigger cap called a supporting cap, suspended from a load cell through an extension rod, was sleeved into the anchor cap so that a pin could be inserted through a coaxial hole as shown in fig. 4-1.

4-3-5 Positioning of anchor in sand for testing

The supporting cross-beam together with the air cylinder piston mounted on it was removed temporarily from the support column to provide space for the

spreader. The portal frame was then fixed together with the hopper. The anchor was positioned on a 75 mm " foundation " layer of sand at the centre of the receiver tank. After deposition of the first layer, the portal frame was raised by 75 mm and the spreader was filled again with sand. The method of laying was repeated until the required depth of anchor embedment was achieved. Brass rod-holders were fixed to the anchor to avoid any movements. The experiment was now ready to proceed to test for ultimate static uplift load once the measuring devices were in place and operational.

4-3-6 Air pressure control panel

The air pressure control panel was fixed to one of the support columns of the reaction frame. The air pressure control panel is shown in fig. 4-2. The air supply from the central air compressor system was passed through an air filter and a manually controlled air regulator and read by a heavy duty air pressure gauge. It was then passed through a lubricator in its final stage before entering the air cylinder piston.

4-3-7 Method of loading

The static load tests which were carried out to determine the ultimate static uplift loads of the anchors were performed under load control (incremental loading) rather than displacement control. Andreadis (1979) and Zakaria (1986) showed that the load displacement characteristics of an anchor were not affected by this choice. At the start of the tests, pressure was slowly applied to the piston until the weight of the loading assembly was counter balanced. The piston pressure was then increased to apply the first load. The load increment was held for five minutes or until all further movement had ceased and then the next load was applied. As failure approached the load increments were decreased to 50% and 80% respectively.

Failure was indicated by a disproportional displacement while the load remain constant, the ultimate load was taken as that measured at the last load increment before total failure occurred.

4-4 PRESENTATION OF TEST RESULTS

In this section the results of the model uplift resistance tests performed by the author will be presented. The results of these tests will be compared and discussed in chapter 7.

4-4-1 Dimensional analysis

With many variables to consider, it is convenient to separate the most important ones and concentrate on them. One way of doing this is by dimensional analysis, which was introduced by Buckingham (1914) in his Π -theorem. It is used when the mathematical laws are not known but the factors affecting the phenomena are. It is also used to investigate the nature of the solution of physical problems and greatly reduces the number of the functionally related quantities to less than the number of physical quantities. In this respect, dimensional analysis is often helpful in establishing similitude between small scale tests and full scale tests as well as comparisons with different investigators' work

The Π -theorem states that a physical phenomenon which is a function of n physical quantities involving m fundamental units can be described in the functional form (Baker & Kondner, 1966).

$$F(\Pi_1, \Pi_2, \Pi_3, \dots, \Pi_{n-m}) = 0 \dots\dots\dots (4-1)$$

Where the Π -terms are the $(n-m)$ independent dimensionless products of the n physical quantities. The primary physical quantities for the uplift capacity of a circular plate anchor buried in sand are listed in table (4-2), a detailed description is given by Davie (1973) and Fadl (1981). The fundamental units chosen are force, length and time.

$$P = f(\gamma, D, B, \varphi, ID) \dots\dots\dots (4-2)$$

Table 4-2 Physical Quantities

physical quantities	symbols	fundamental units
uplift capacity	P	F
diameter of anchor	B	L
depth of embedment	D	L
unit weight of soil	Γ	FL^{-3}
angle of friction	φ	$F^0L^0T^0$
relative density	ID	$F^0L^0T^0$

Utilizing Buckingham Π - method the physical quantities yield the functional relationship:

$$Nu_c = \frac{R}{\frac{\pi}{4} B^2 \gamma D} = f(D/B, \varphi, ID) \dots\dots\dots (4-3)$$

Hence from the equation 4-3 it can be seen that for a given circular anchor plate embedded in cohesionless soil with known ϕ and ID:

- 1- Nu depends on D/B.
- 2- For a given ratio of D/B, Nu is constant and the value determined in a model test is applicable to the prototype problem.
- 3- For a given sand, when Nu is plotted against D/B, the complete solution is a family of curves each corresponding to particular ϕ and ID values.

The findings from the dimensional analysis e.g. equation 4-3 will be used to present the author's experimental results.

4-4-2 Test results

Table 4-3 shows the range of densities achieved in the present investigation and the method of sand placing. Tables 4-4 to 4-8 give a summary of the details and the results of all of the model uplift resistance tests performed by the author. The tables include details of the soil and the anchor used in each test, i.e. the anchor plate diameter B, the depth of embedment D, the bulk density of the sand γ . The dimensionless ratio D/B is also included. The ultimate uplift resistance pressure P_u for each test and the resulting breakout factor Nu are shown. The displacement of the anchor at ultimate uplift resistance, symbolized by δ_f , is also given in the tables.

Note:

The fifth series of pull out tests was conducted in Hyndford sand. Dense,

and medium loose sand states have been considered. The average densities for medium loose sands were 16.95 and 16.59 Kn/m^3 . The dense state was obtained by compaction achieved by a Kango hammer through a 49 mm diameter tamping plate (see plate 4-5) which was passed over each layer once. For each pass the tamping plate was placed on the sand surface for a duration of one minute. The tamping plate contained a small hole in the middle to allow the passage of the anchor shaft which was held by the centering device. The tamping plate was removed after compaction of each layer. The same procedure was repeated for the next layer till the required depth was reached. This method of placement of sand did not give repeatable densities. The densities achieved varied from 17.49 Kn/m^3 to 18.63 Kn/m^3 . The method of carrying out the pull out tests was similar to the previous series.

test series	sand	density γ (Kn/m ³)	relative density ID (%)	angle of internal friction ϕ (°)	state of packing	method of sand placing
1	Lochaline	16.47	66	39.7	dense	raining
		15.72	42	35.6	medium	
		14.81	13	32	loose	
2	L. Buzzard	17.28	85.5	43.7	v. dense	raining
		17.15	81	42.8	dense	
		16.57	60	39	medium	
		15.63	29	33.8	loose	
3	Douglasm ^r	16.57	76	43.7	dense	raining
		16.09	61	42.8	medium	
		15.21	31	36	loose	
4	Hyndford	17.49 to	60 to	43 to	dense to	compacted in layers poured from bucket
		18.63	92	47	v. dense	
		16.95	33	39	loose	
		16.59	23	37.2	loose	
5	Ballotini	18.60	97	34.9	v. dense	raining
		17.78	50	30.3	medium	

Table 4-3 Summary of test parameters

test N ^o	γ (Kn/m ³)	D (mm)	B (mm)	D/B	P (N)	P_u (Nmm ⁻² · 10 ⁻³)	N_u	δ_f (mm)
1	16.47	75.0	37.5	2	9.03	8.18	6.60	0.575
2	"	75.0	"	2	9.03	8.18	6.60	0.605
3	"	112.5	"	3	22.70	20.56	11.10	0.725
4	"	112.5	"	3	23.01	20.85	11.25	0.801
5	"	150.0	"	4	52.09	47.18	19.10	1.760
6	"	150.0	"	4	53.18	48.17	19.50	1.870
7	"	187.5	"	5	89.66	81.22	26.30	2.650
8	"	300.0	"	8	307.36	278.42	56.35	4.050
9	"	375.0	"	10	497.71	450.86	73.00	6.400
10	"	250.0	25.0	12	189.89	387.04	94.00	7.100
11	"	450.0	37.5	12	736.40	667.08	90.00	6.550
12	15.72	75.0	37.5	2	6.94	6.29	5.35	0.701
13	"	112.5	"	3	16.69	15.12	8.55	1.150
14	"	150.0	"	4	33.71	30.54	12.95	1.525
15	"	150.0	"	4	33.71	30.54	12.95	1.925
16	"	187.5	"	5	61.38	55.60	18.90	2.750
17	"	300.0	"	8	146.78	132.96	28.20	4.525
18	"	375.0	"	10	279.82	253.48	43.00	6.258
19	"	375.0	"	10	296.09	268.22	45.50	5.875
20	"	450.0	"	12	390.45	353.70	50.00	6.875
21	14.81	75.0	37.5	2	3.12	2.83	2.55	1.057
22	"	112.5	"	3	9.56	8.66	5.20	1.896
23	"	112.5	"	4	22.22	20.13	7.25	2.347
24	"	187.5	"	5	24.67	22.35	8.05	3.126
25	"	300.0	"	8	44.48	40.29	9.20	5.769
26	"	375.0	"	10	59.60	53.99	9.70	6.875
27	"	450.0	"	12	74.72	67.68	10.15	7.281

Table 4-4 Summary of Pull Out Test results in Lochaline sand.

test N ^o	γ (Kn/m ³)	D (mm)	B (mm)	D/B	P (N)	P _u (Nmm ⁻² · 10 ⁻³)	N _u	δ_f (mm)
28	17.28	75.0	37.5	2	13.47	12.21	9.40	0.155
29	"	112.5	"	3	30.96	28.05	14.40	0.175
30	"	150.0	"	4	63.16	57.21	22.10	0.555
31	"	150.0	"	4	63.16	57.21	22.10	0.610
32	"	187.5	"	5	121.87	110.40	34.10	0.875
33	"	187.5	"	5	126.57	114.46	35.40	0.923
34	"	200.0	25.0	8	137.59	280.44	81.15	2.750
35	"	250.0	"	10	251.16	511.92	118.50	3.425
36	"	250.0	"	10	245.86	501.12	116.00	3.201
37	"	300.0	"	12	381.51	735.94	150.00	4.121
38	"	300.0	"	12	386.09	744.77	151.80	4.219
39	17.15	75.0	37.5	2	10.62	9.62	7.50	0.225
40	"	75.0	"	2	11.94	10.81	8.40	0.273
41	"	112.5	"	3	26.55	24.05	12.45	0.325
42	"	150.0	"	4	58.42	52.92	20.10	0.723
43	"	187.5	"	5	103.56	93.81	29.20	1.121
44	"	300.0	"	8	412.91	374.04	72.70	2.942
45	"	225.0	25.0	9	177.90	161.15	94.00	4.326
46	"	300.0	"	12	308.96	600.52	122.40	5.258
47	"	300.0	"	12	323.11	628.00	128.00	5.214
48	16.57	75.0	37.5	2	7.96	7.21	5.80	0.538
49	"	112.5	"	3	17.49	15.84	8.50	0.841
50	"	150.0	"	4	47.79	43.29	17.40	1.561
51	"	187.5	"	5	78.33	70.79	22.85	2.310
52	"	236.0	"	6.3	155.34	140.72	35.80	2.851
53	"	300.0	"	8	288.11	260.99	52.50	4.127
54	"	300.0	"	8	330.60	299.48	60.25	4.231
55	"	375.0	"	10	468.68	424.56	68.30	5.169
56	"	386.0	"	10	509.84	461.85	71.85	5.288
57	"	450.0	"	12	634.94	700.91	94.00	6.671
58	15.63	75.0	37.5	2	3.98	3.60	3.10	1.132
59	"	112.5	"	3	13.28	12.03	6.50	1.651
60	"	165.0	"	4.4	34.52	31.27	12.10	3.487
61	"	230.0	"	6	83.61	75.74	21.10	4.501
62	"	300.0	"	8	118.16	107.04	22.80	5.157
63	"	337.5	"	9	151.36	137.11	26.10	6.113
64	"	450.0	"	12	232.34	210.47	29.10	7.801

Table 4-5 Summary of Pull Out Tests Results in Leighton Buzzard Sand.

test N ^o	γ (Kn/m ³)	D (mm)	B (mm)	D/B	P (N)	P_u (Nmm ⁻² · 10 ⁻³)	N_u	δ_f (mm)
65	16.57	75.0	37.5	2	13.26	12.02	9.70	0.350
66	"	75.0	"	2	13.26	12.02	9.70	0.374
67	"	112.5	"	3	39.83	36.08	19.35	0.612
68	"	150.0	"	4	69.04	62.54	25.20	0.925
69	"	187.5	"	5	110.20	99.83	32.10	1.500
70	"	225.0	"	6	200.48	181.70	48.70	2.450
71	"	300.0	"	8	459.38	416.14	83.70	4.225
72	"	300.0	"	8	467.42	423.43	85.20	4.543
73	"	225.0	25.0	9	189.86	386.97	103.80	2.450
74	"	225.0	"	9	189.86	386.97	103.80	2.975
75	16.09	75.0	37.5	2	11.95	10.82	9.00	0.815
76	"	75.0	"	2	11.95	10.82	9.00	0.789
77	"	150.0	"	4	50.45	45.71	18.95	1.723
78	"	187.5	"	5	82.31	74.55	24.70	2.218
79	"	187.5	"	5	83.82	76.02	25.20	2.301
80	"	300.0	"	8	346.25	313.66	68.00	5.437
81	"	300.0	"	8	313.34	283.83	58.80	5.321
82	"	225.0	25.0	9	142.06	289.55	80.00	3.451
83	15.21	75.0	37.5	2	7.17	6.50	5.70	1.214
84	"	75.0	"	2	7.12	6.50	5.70	1.312
85	"	150.0	"	4	31.27	31.25	13.70	2.188
86	"	231.5	"	6.2	84.19	83.28	23.55	4.217
87	"	300.0	"	8	124.80	113.02	24.80	5.347
88	"	337.5	"	9	153.02	138.60	27.00	6.141
89	"	337.5	"	9	159.24	144.25	28.10	7.109

Table 4-6 Summary of Pull Out Tests Results in Douglasmuir Sand.

test N ^o	γ (Kn/m ³)	D (mm)	B (mm)	D/B	P (N)	P_u (Nmm ⁻² · 10 ⁻³)	N_u	δ_f (mm)
113	18.60	75.0	37.5	2	9.55	8.65	6.20	1.150
114	"	82.5	"	2.2	9.99	9.05	5.90	1.236
115	"	75.0	"	2	8.16	7.39	5.30	0.875
116	"	67.5	"	1.8	5.47	4.96	3.95	1.125
117	"	86.25	"	2.3	12.13	10.99	6.85	1.025
118	"	77.5	25.0	3.1	6.72	13.69	9.50	0.425
119	"	135.0	37.5	3.6	28.55	25.86	10.30	0.550
120	"	138.75	"	3.7	31.05	28.13	10.90	0.440
121	"	187.5	"	5	55.24	50.05	14.35	2.775
121	"	132.5	25.0	5.3	20.49	41.77	16.95	2.450
122	17.78	75.0	37.5	2	5.79	8.65	3.90	1.150
123	"	86.25	"	2.3	7.62	6.90	4.50	1.453
124	"	105.0	"	2.8	10.92	9.89	5.30	1.854
125	"	120.0	"	3.2	16.50	14.93	7.00	2.725
126	"	135.0	"	3.6	16.69	15.12	6.30	1.352
127	"	142.5	"	3.8	23.35	21.15	8.35	1.400
128	"	150.0	"	4	20.31	18.40	6.90	1.425
129	"	187.5	"	5	33.12	30.00	9.00	3.125
130	"	"	"	5	32.38	29.33	8.80	3.225

Table 4-7 Summary of Pull Out Tests Results in Ballotini.

test N ^o	γ (Kn/m ³)	D (mm)	B (mm)	D/B	P (N)	P _u (Nmm ⁻² · 10 ⁻³)	N _u	δ_f (mm)
90	16.59	75.0	37.5	2	5.31	4.81	3.85	0.987
91	"	150.0	"	4	43.81	39.69	15.95	2.745
92	"	187.5	"	5	73.02	66.15	21.25	3.862
93	"	150.0	25.0	6	37.17	75.76	30.45	4.791
94	"	225.0	"	9	74.35	151.54	40.60	5.842
95	"	300.0	"	12	122.15	248.96	50.00	6.917
96	16.21	75.0	37.5	2	1.34	1.21	2.70	1.720
97	"	150.0	"	4	33.19	30.07	12.35	3.182
98	"	187.5	"	5	45.14	40.89	14.80	4.897
99	"	150.0	25.0	6	25.22	51.41	21.10	5.634
100	"	225.0	"	9	46.47	94.72	26.65	6.736
101	"	300.0	"	12	55.76	113.65	23.40	8.151
102	"	300.0	"	12	63.73	129.89	26.70	9.125
103	18.55	100.0	25.0	4	29.21	59.53	32.90	0.525
104	17.77	100.0	"	4	30.53	62.22	29.95	0.275
105	17.49	100.0	"	4	23.89	48.71	27.30	0.550
106	17.73	150.0	37.5	4	82.31	74.57	28.40	1.425
107	18.63	125.0	25.0	5	62.42	127.18	55.15	0.550
108	18.00	187.5	37.5	5	240.31	217.69	56.20	0.800
109	17.85	150.0	25.0	6	78.33	159.66	60.85	0.775
110	17.90	225.0	"	9	258.93	527.69	133.65	1.950
111	17.74	300.0	"	12	464.69	947.15	182.20	4.470
112	17.83	300.0	"	12	671.80	1369.30	262.00	3.620

Table 4-8 Summary of The Pull Tests Results in Hyndford Sand.

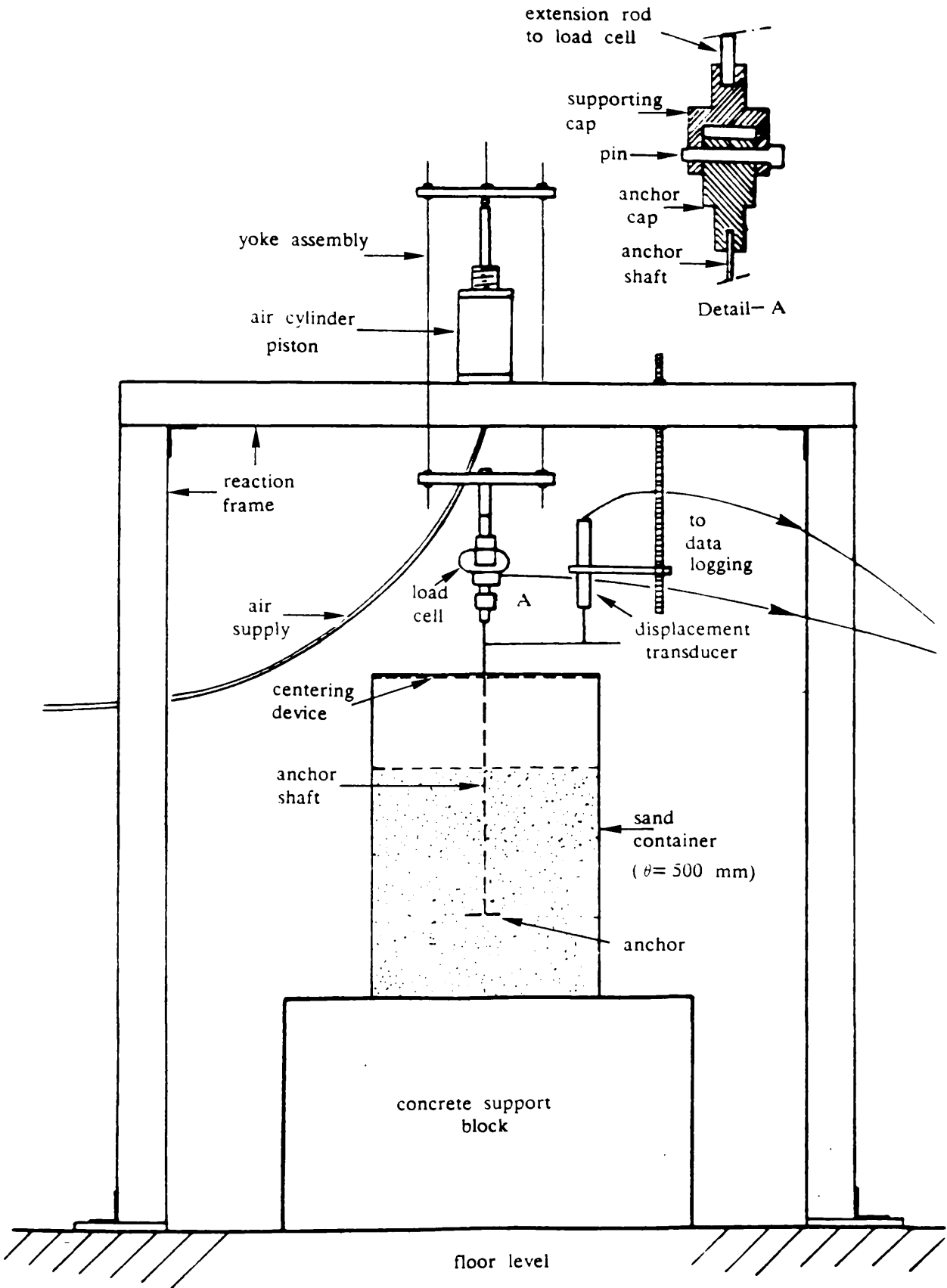
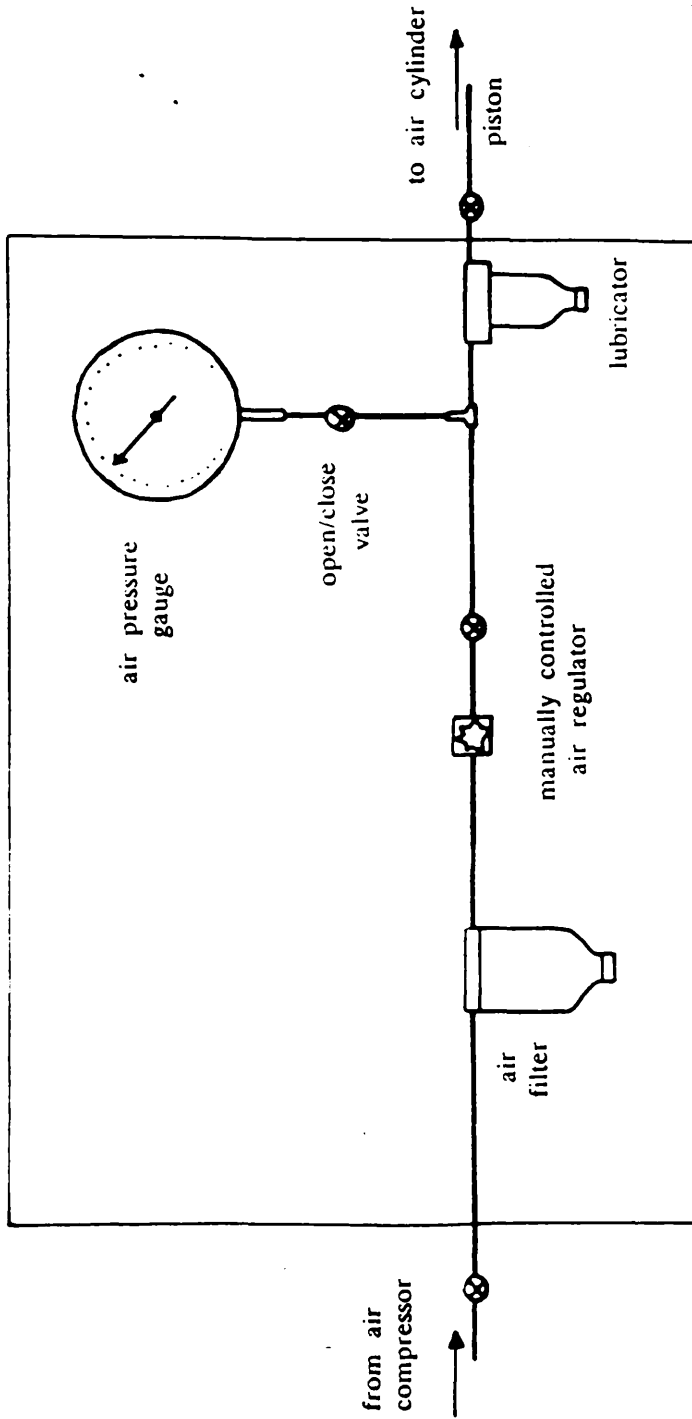


Fig. 4-1 Pull Out Set Up.

Fig. 4-2 Air Pressure Control Panel.



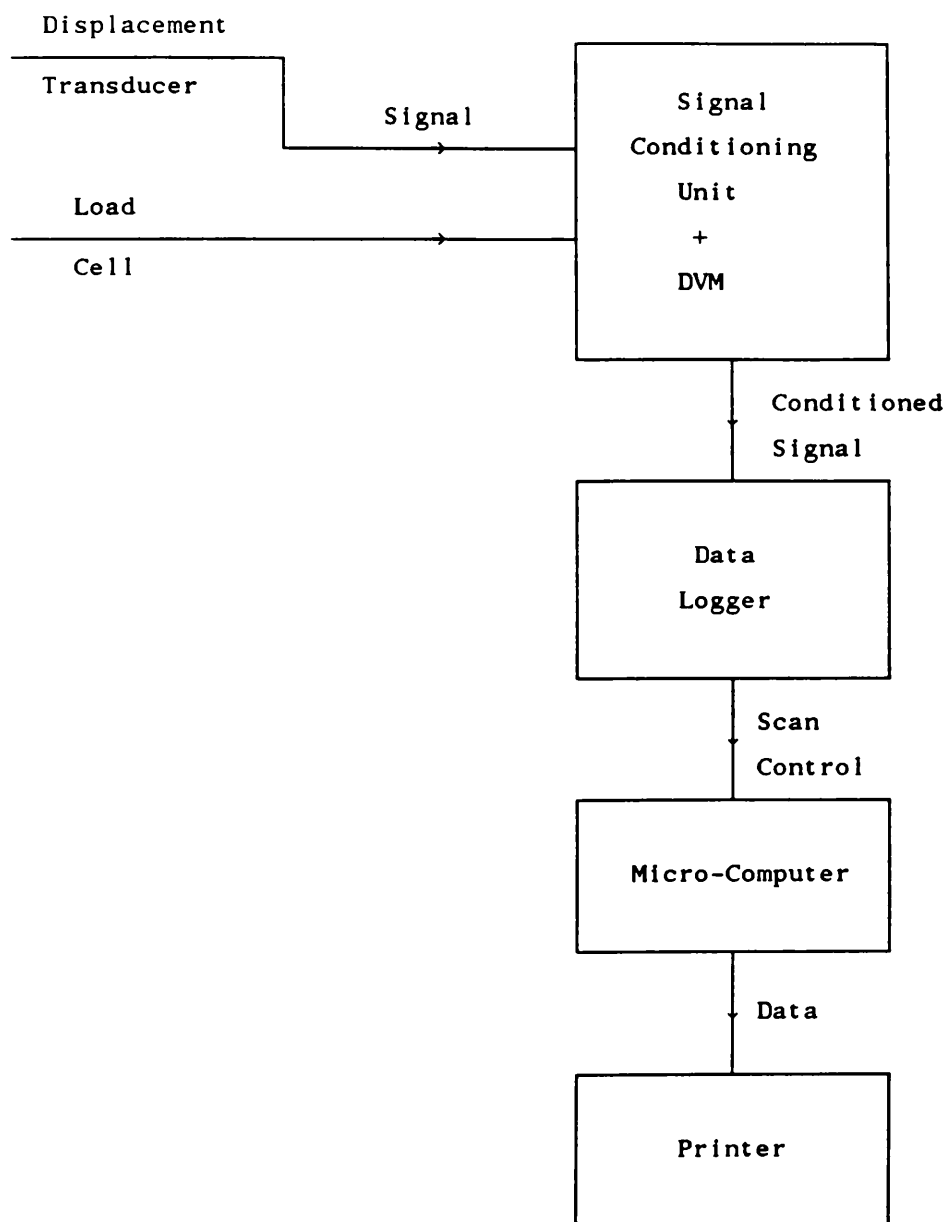


Fig. 4-3 Schematic of data acquisition system



Plate 4-1 Load controlled test arrangement.

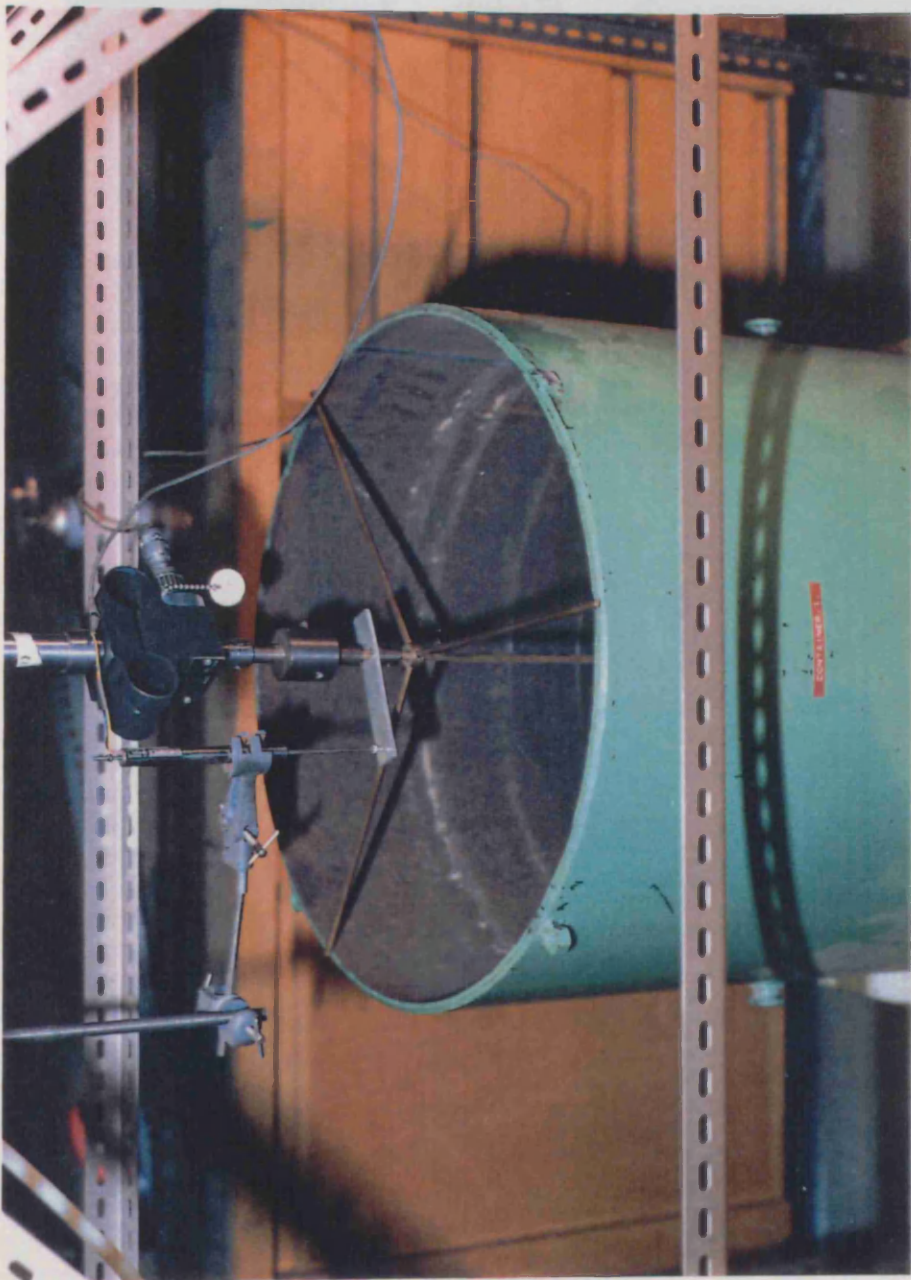


Plate 4-2 Anchor placement.

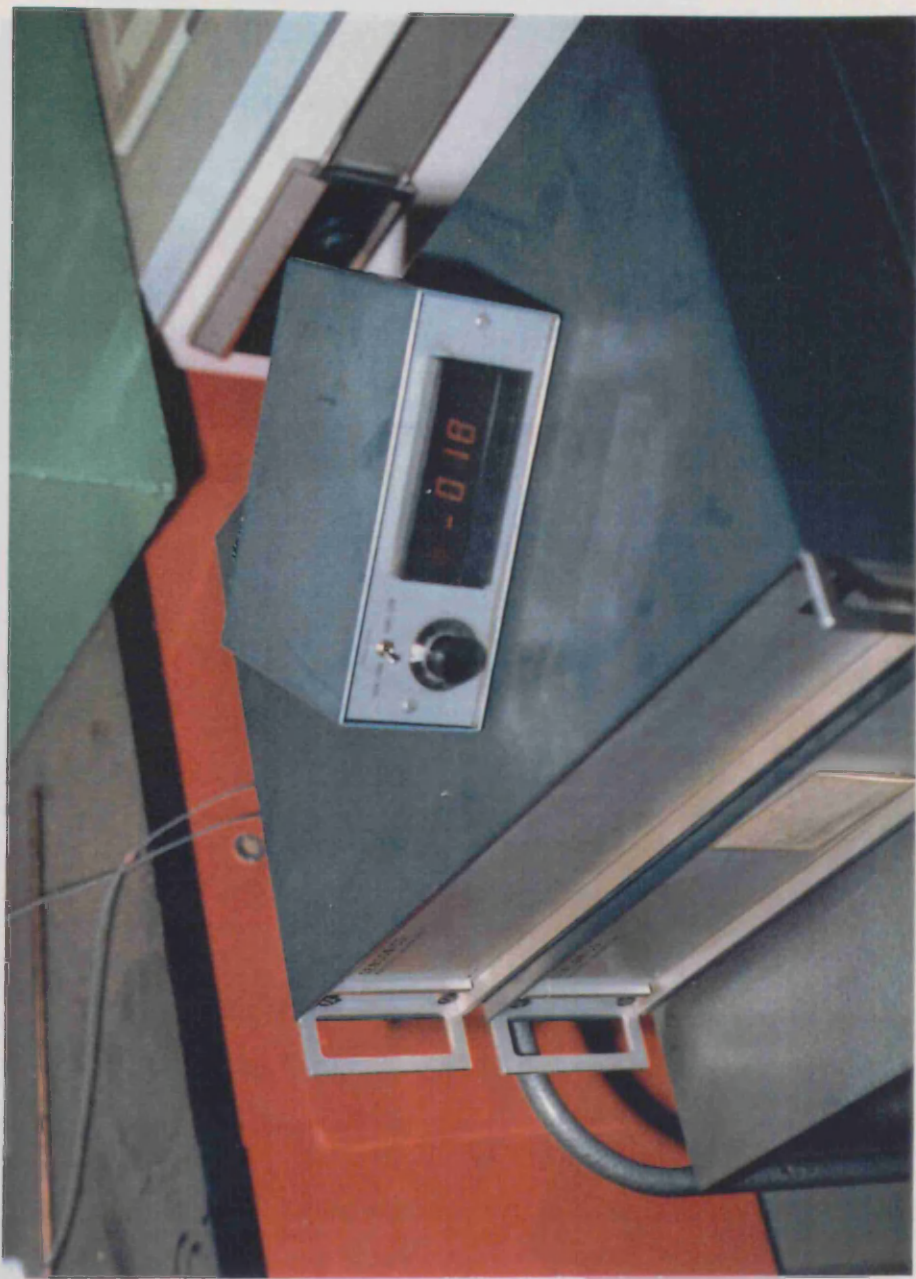


Plate 4-3 Satellite instrumentation box, signal amplification.



Plate 4-4 Data logging system.

Plate 4-4 Data logging system. (continued)

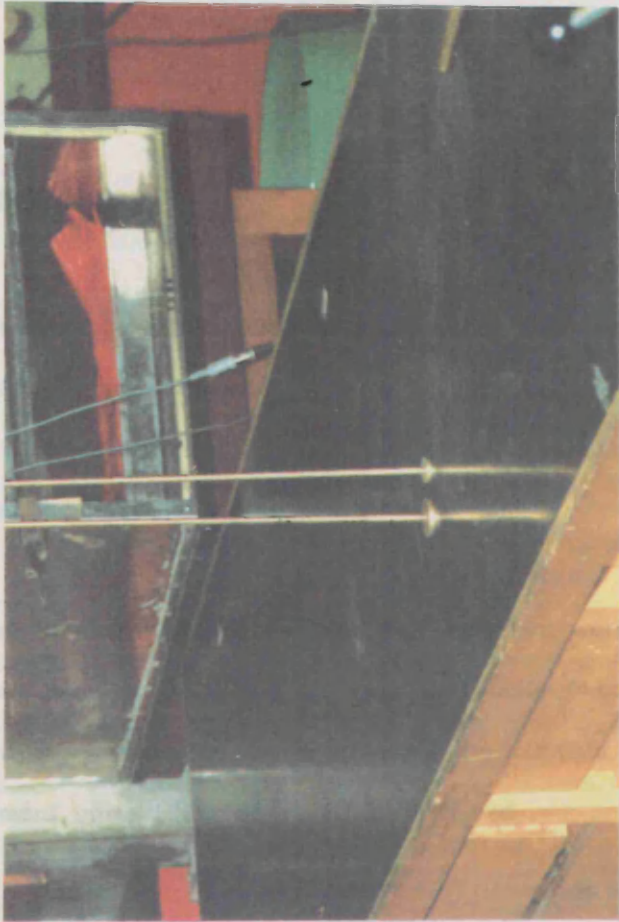


Plate 4-6 Plate anchors used in the present investigation.



Plate 4-5 Tamping plate used in the present investigation.

chapter 5

DISCUSSION AND COMPARISON OF TEST RESULTS

5-1 INTRODUCTION

In this chapter the results obtained from model uplift resistance tests conducted by the author will be discussed. The effect of depth of embedment, relative density, angle of shearing resistance, grain size, grain shape and grading of the sands on the breakout factors will be presented.

As stated in chapter 4 the pull out tests described were conducted under load control. Failure was generally reached when the anchor was rapidly lifted under a very small load increment. In the experiments the ultimate load was taken as the last load increment immediately before failure occurred.

In an attempt to present the results in a clear and logical way and also in view of the considerable amount of experimental data accumulated in the present investigation the author presents only typical data and general trends. Graphical methods of presentation are largely used, an explanation is made of the observations noted during the tests and the various parameters that have an important influence on the uplift capacity are analysed. Previous theories obtained by other investigators will be compared with the information presented in this study. The discussion of the results is divided in two sections for presentation purposes.

- A- Presentation of the pull out results.
- B- Comparison of the present results with previous work.

5-2 DISCUSSION OF THE PULL OUT RESULTS

5-2-1 Load displacement behaviour of a plate anchor

The difficulty of achieving the same relative density in the different sands investigated and the large number of pull out tests involved led to the presentation of typical load anchor displacement results in only one sand (Lochaline sand).

The plots presented in this section are all representative, the same trends and patterns being observed in the other sands. Fig. 5-1 shows a typical relationship between the uplift load P and the displacement δ of an anchor, embedded in medium loose sand, at any stage of the loading. The depth/diameter ratio D/B was taken as variable, density γ was kept constant. It can be seen that the effect of the overburden soil pressure is significant. The deeper the embedment, the higher the uplift load and anchor displacement.

Examination of the figures shows that the anchor exhibited a stiff, near linear, response for the early part of the loading range and, in the vicinity of the ultimate load, the displacement increased significantly before the peak load was attained. The load displacement diagrams also demonstrate that the displacement of the majority of the plate anchors at which the ultimate static resistance occurs is small for the particular case of Lochaline sand. This indicates that only a small displacement of the anchor is required to mobilize the frictional resistance of the sand. Fig. 5-2 shows that over 60% of the anchor displacement recorded at the development of the maximum load occurred during the application of the final 20% of the maximum load, a similar observation to that reported by Abu Taleb (1974). Fig. 5-3 presents the effects of relative depth of embedment on the uplift movement at failure. It can be seen that when the anchor is embedded at great

depth, the vertical movement is relatively high. As the anchor placement position approaches the soil surface, the bulb of pressure developing above the anchor is limited thus restricting the uplift movement of the anchor and leading to small values being attained at shallow depths.

The effect of relative density is depicted in figs. 5-4 & 5-5 where anchors with $D/B=5.0$ and 10.0 representing shallow and deep anchors respectively are considered. The density of sand was varied, with medium dense, loose medium and loose sands tested at densities, $\gamma=16.47, 15.72$ and 14.81 Kg/m^3 , corresponding to relative densities of 66%, 43% and 13% respectively. The two figures show the same trend, i.e. the denser the state of the sand, the higher the uplift load. Fig. 5-6 shows the effect of sand densification on the vertical displacement of the anchor, the movement at failure of the anchor surrounded by loose soil being approximately 1.6 times greater than for the same anchor embedded in dense soil. This was because the shear strength of the sand was rapidly mobilized when the anchor was pulled out of the dense sand. When the sand is denser, the degree of interlocking is high therefore the load from the anchor transferred to the sand was only required to breakout the soil mass rather than to first densify it.

5-2-2 Ultimate uplift resistance

The primary purpose of the present investigation was to find the values of the ultimate uplift resistance of a plate anchor embedded in different sands at various depths and to investigate the factors which influence these values.

The values of the ultimate uplift resistance factor N_u versus depth/diameter ratio (D/B) for the complete programme of model uplift resistance tests performed by the author are shown in figs. 5-7 to 5-11.

5-2-3 Effect of relative density and overburden pressure

A typical variation of ultimate pull out resistance with relative density is shown in fig. 5-12 for depth/diameter ratio D/B ranging from 3 to 12. A clear pattern emerges from this figure where it can be seen that the effect of the degree of densification of the soil is to greatly increase the uplift resistance of the anchor. Depending on the depth of embedment, increasing the relative density of the sand from very loose ($ID=13\%$) to dense condition ($ID=66\%$) increases the breakout factor from 3 to 5 times. The graph also show that for shallow anchors N_u bears a near linear relationship with ID as this latter varies from 13% to 66%. For deep anchors, significant deviations from the linear relationship are shown; it can be seen that the breakout factor N_u increases non linearly at a faster rate. An increase in ID will promote a greater compactness, and hence, a higher intergranular contact among the soil particles. Subsequently, this would mean an increase in the angle of internal friction φ of the sand surrounding the anchor, thus allowing larger shearing resistance to be developed during loading. Similar findings have been reported by previous workers such as Fadl (1981), Saeddy (1987) ... who have investigated the influence of soil relative density on the behaviour of a vertically uplifted plate anchor. They concluded that the influence of ID on the plate anchor capacity is significant.

Overburden pressure is the vertical pressure acting on a plane within a soil mass, generally produced by foundation pressure or by the self weight of the soil above the plane. A typical variation of the breakout factor with depth of embedment is shown in fig. 5-8, where it can be seen that the value of N_u increases rapidly with embedment ratio up to a certain value. As the D/B ratio increases and failure becomes more localised there is not the same dependence on depth as for the shallow anchor and the rate of increase diminishes and tends to become linear, thereby showing deep foundation behaviour. The transition depth

between a shallow and deep anchor is commonly called the critical embedment ratio $(D/B)_{cr}$. The linearity which is associated with the deep failure condition is consistent with minimal sand surface heave for $D/B > (D/B)_{cr}$ observed by Fadl (1981). Similar conclusions were derived by Kupferman (1974) who stated that when the critical depth of embedment was reached, the ultimate load of the anchor was related to the maximum passive arching stresses which the soil was capable of developing, and which in turn were related to the effective overburden pressure. This, therefore, led to the conclusion that the maximum load on a deeply embedded anchor would be proportional to the depth of embedment. Results from other investigators (Carr, 1970, Fadl, 1981) tended to support this conclusion.

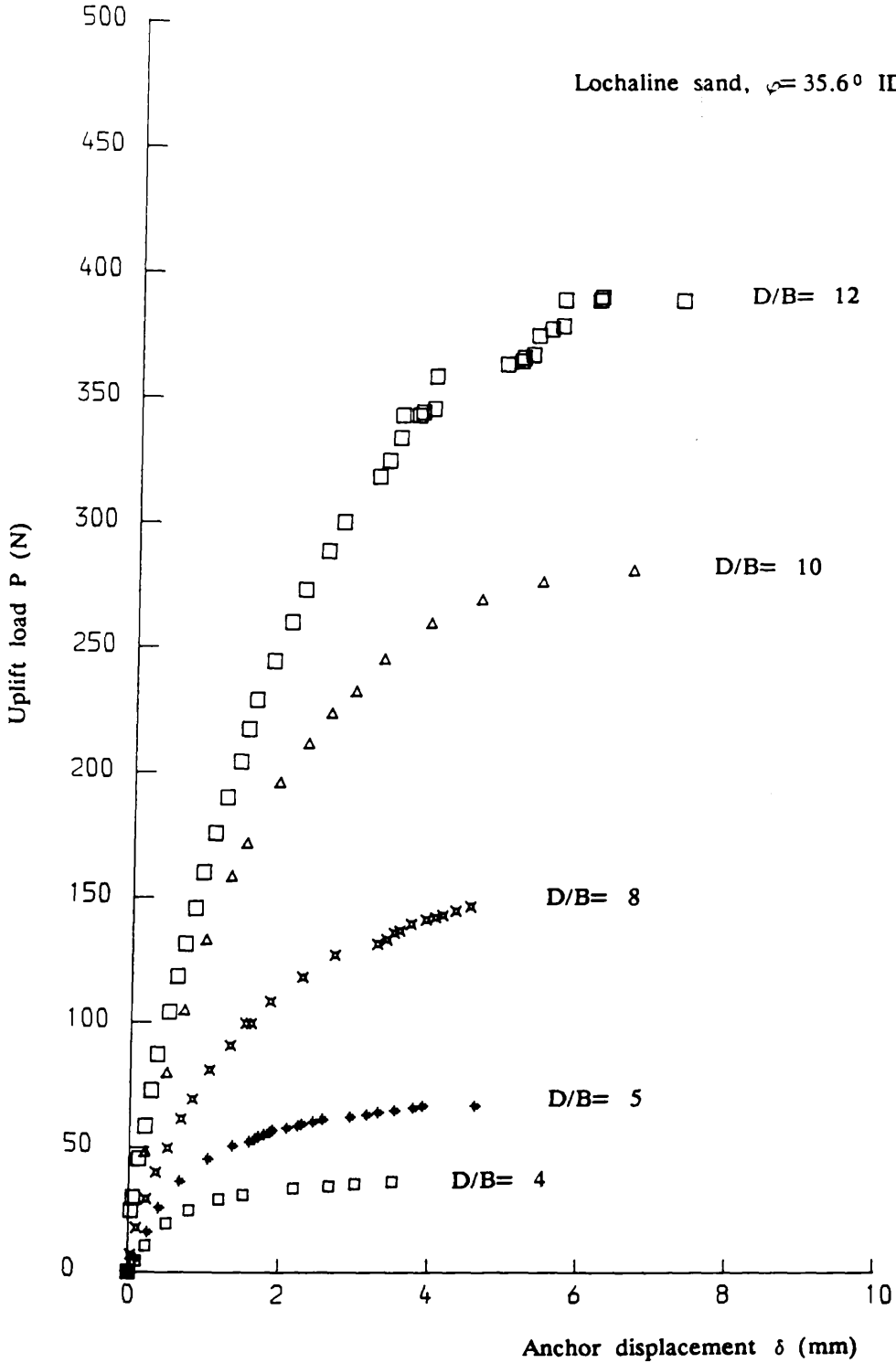


Fig. 5-1 Typical load-displacement relationship for different depth/embedment ratio

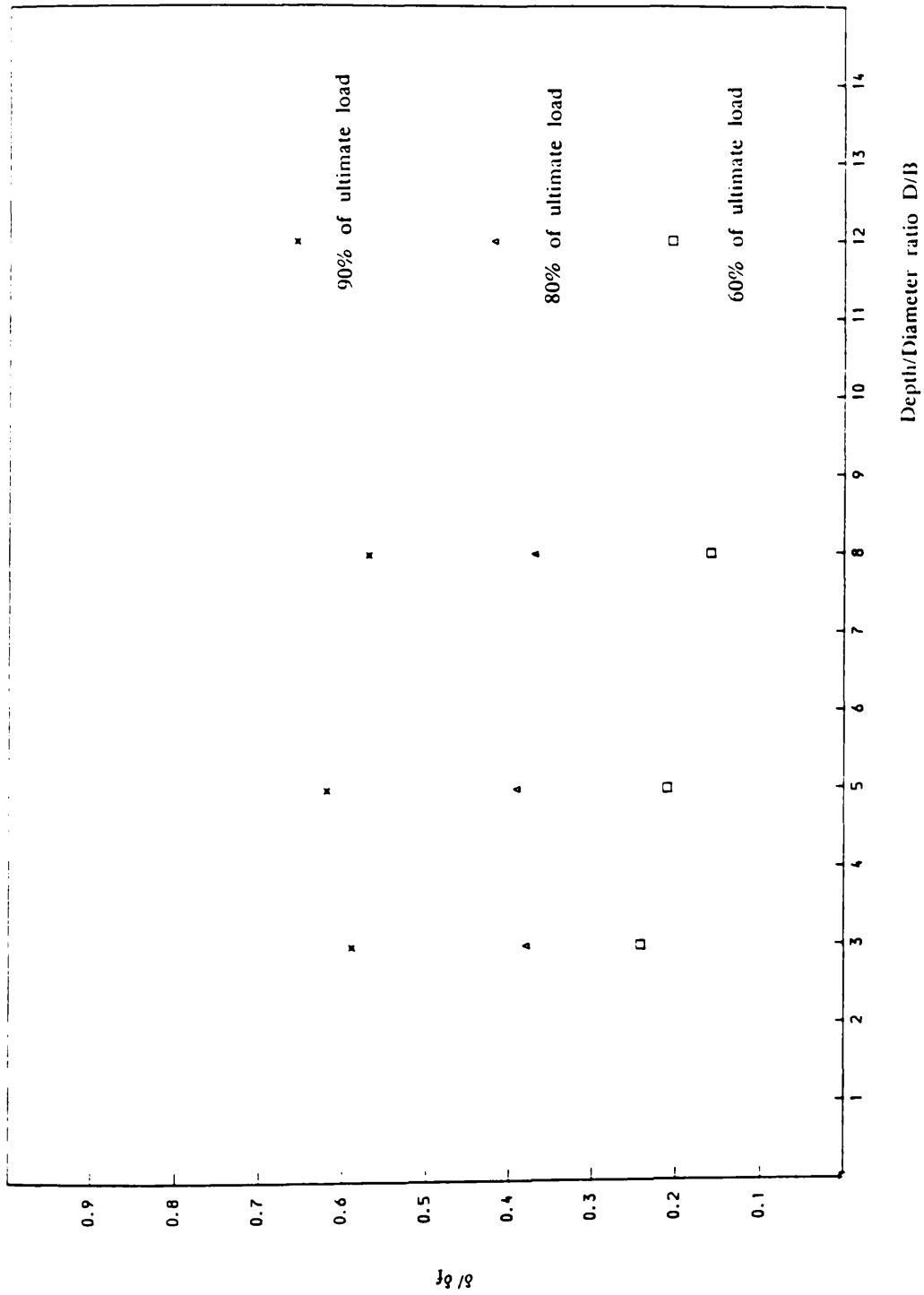


Fig. 5-2 Anchor displacement as a percentage of the displacement at failure vs depth/diameter ratio.

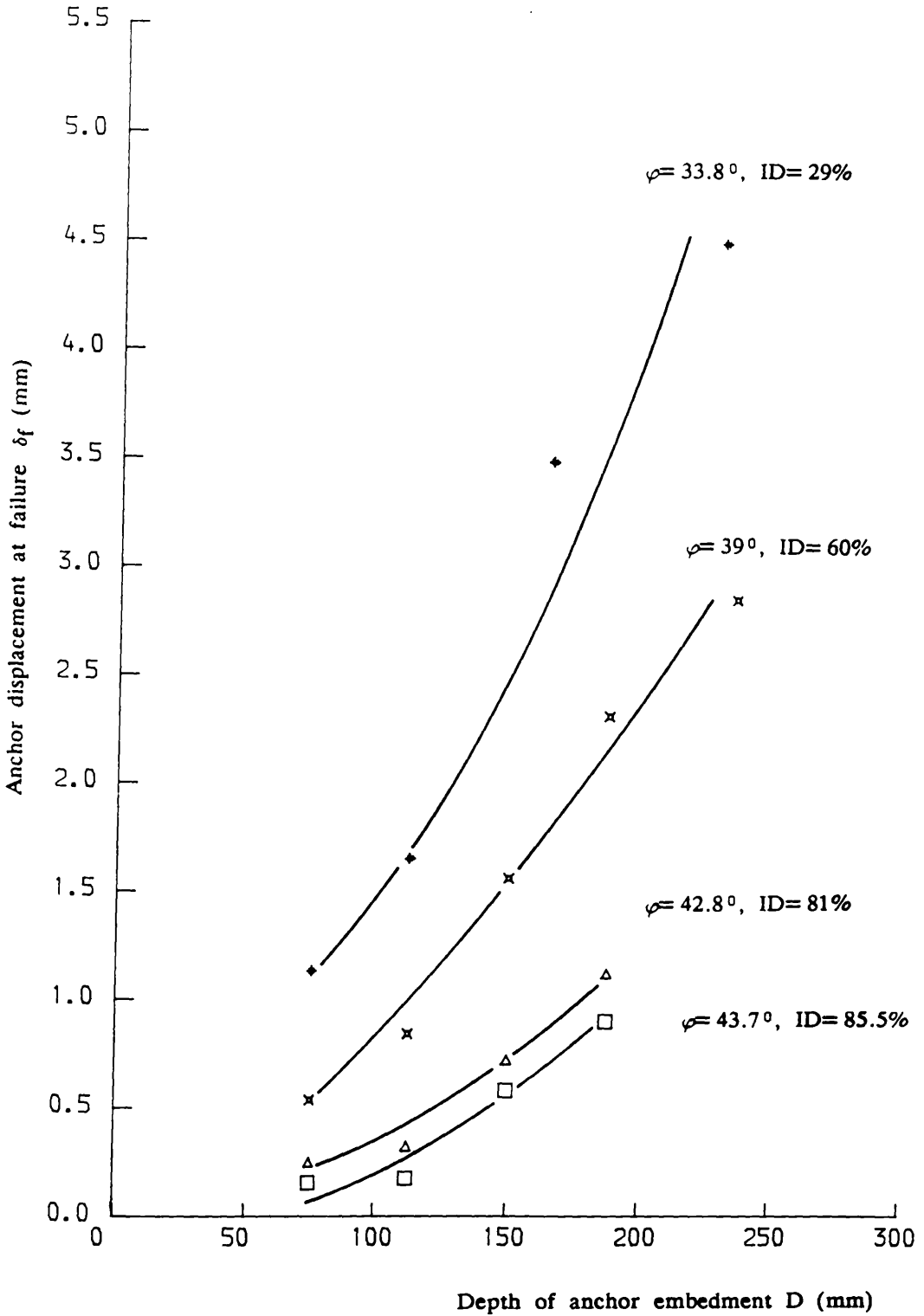


Fig. 5-3 Variation of the anchor displacement at failure vs depth of embedment for Leighton Buzzard sand.

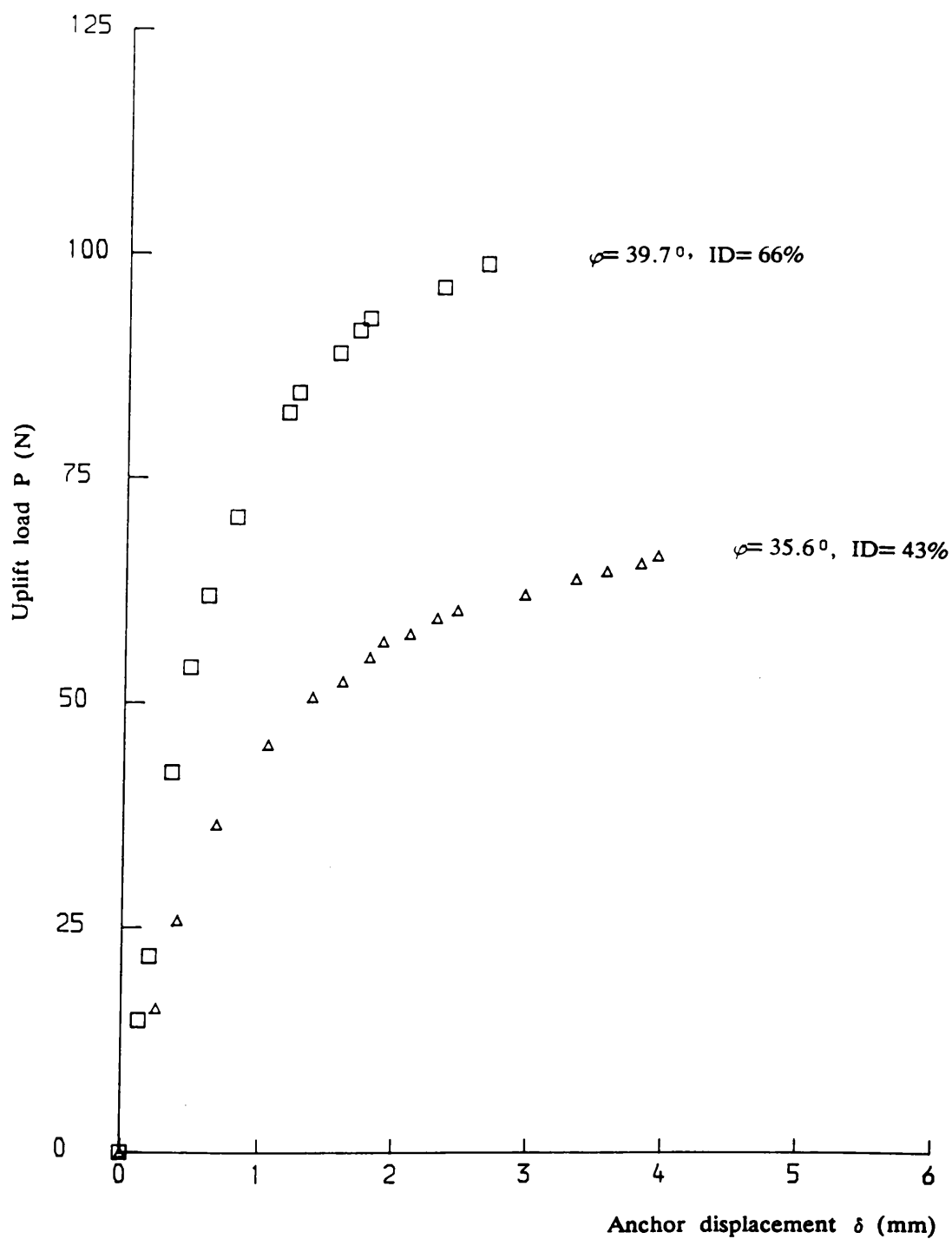


Fig. 5-4 Load-displacement relationship at different relative densities for Lochaline sand at $D/B=5$.

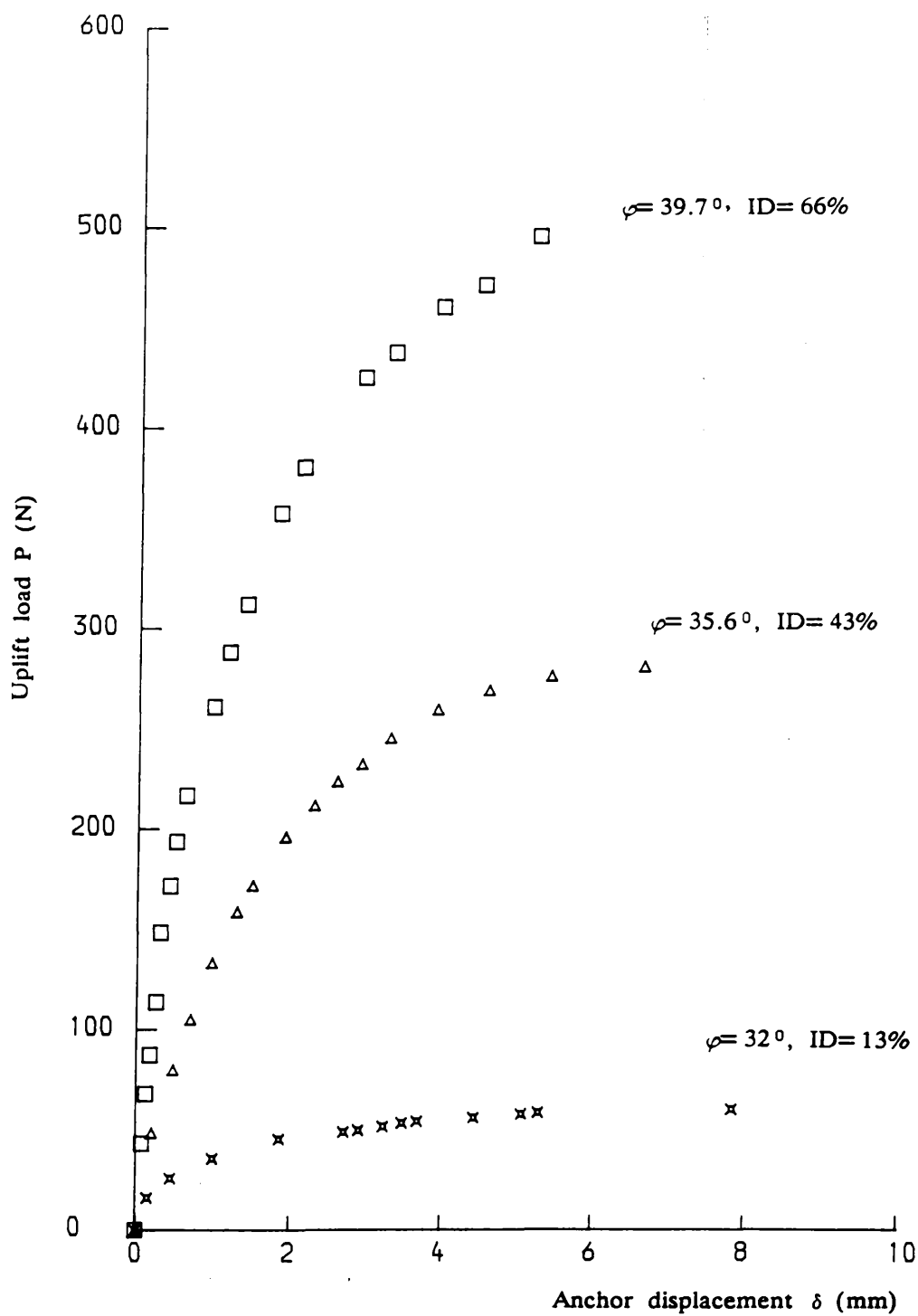


Fig. 5-5 Load-displacement relationship at different relative densities for Lochaline sand at $D/B=10$.

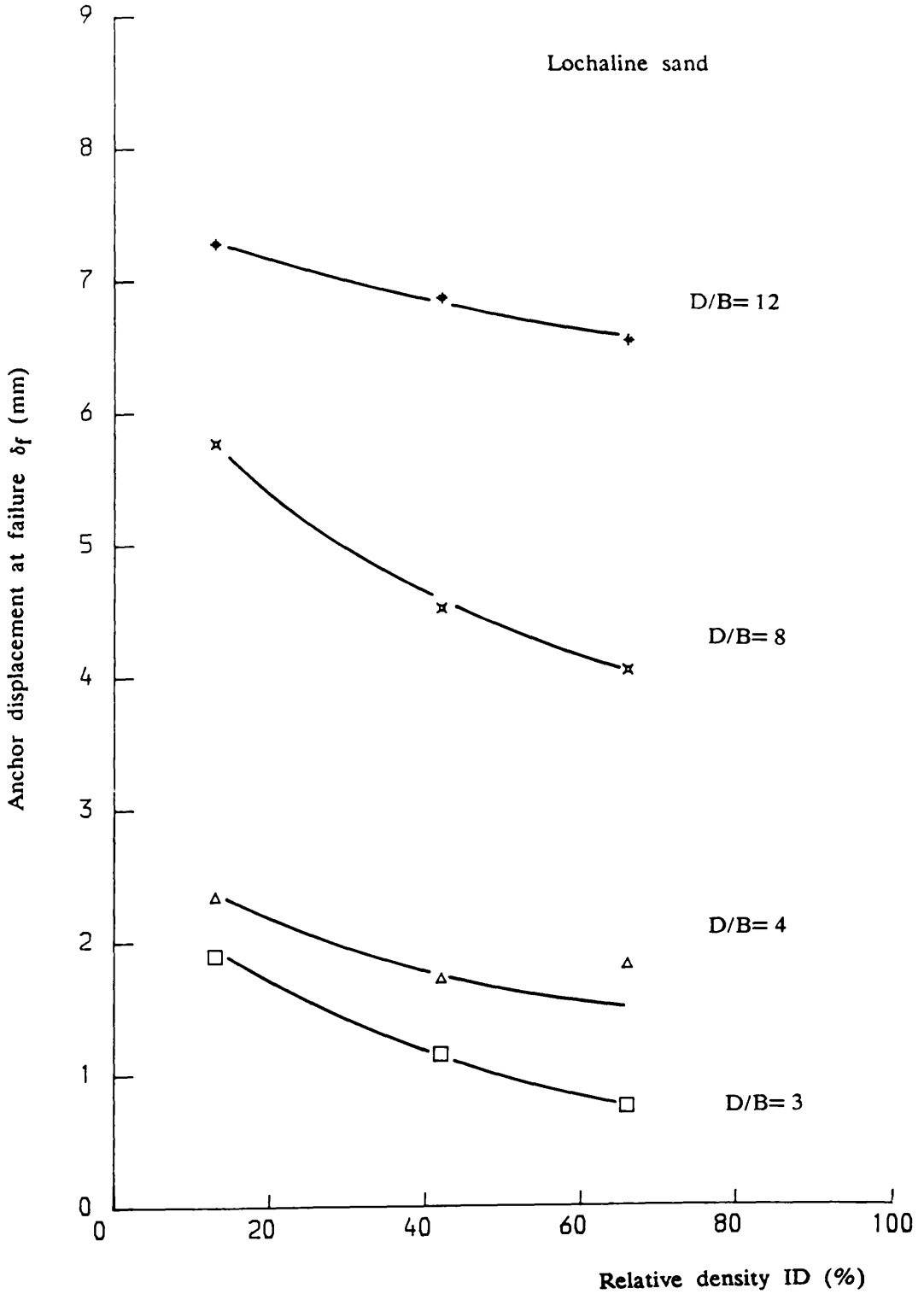


Fig. 5-6 Typical anchor movement to failure relative density relationship.

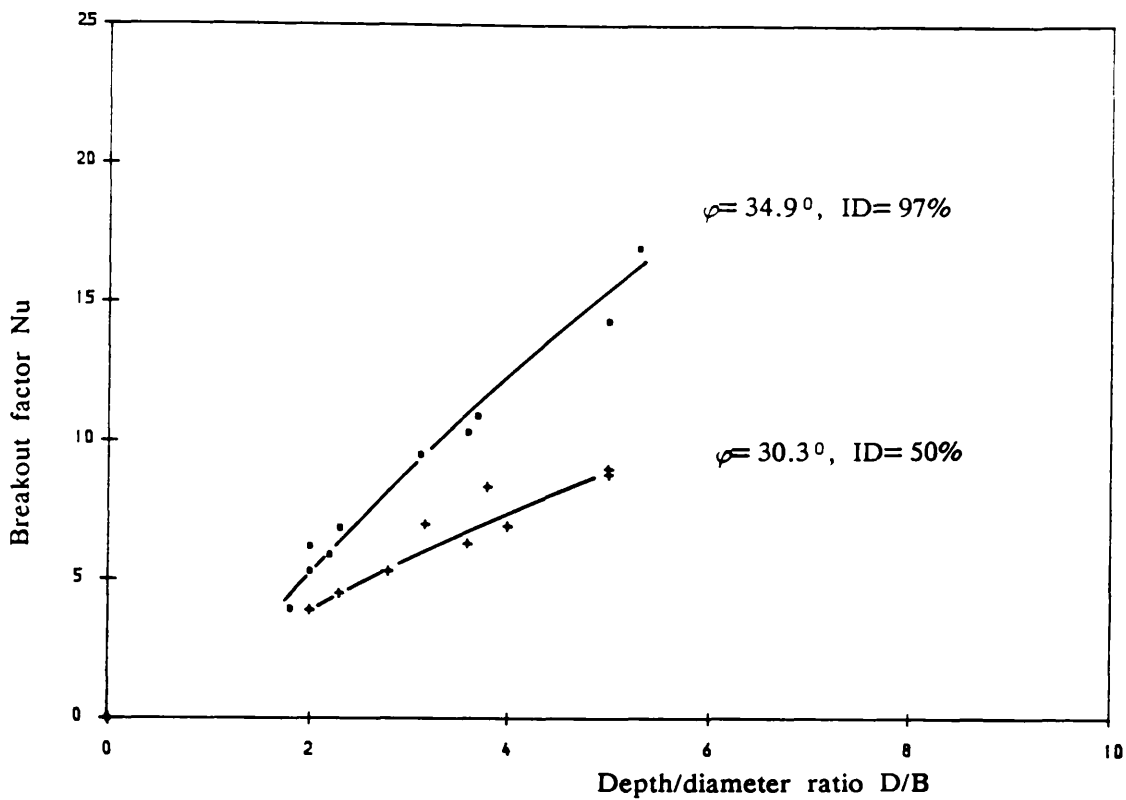


Fig. 5-7 Breakout factor vs depth/diameter ratio for shallow plate anchors embedded in Ballotini.

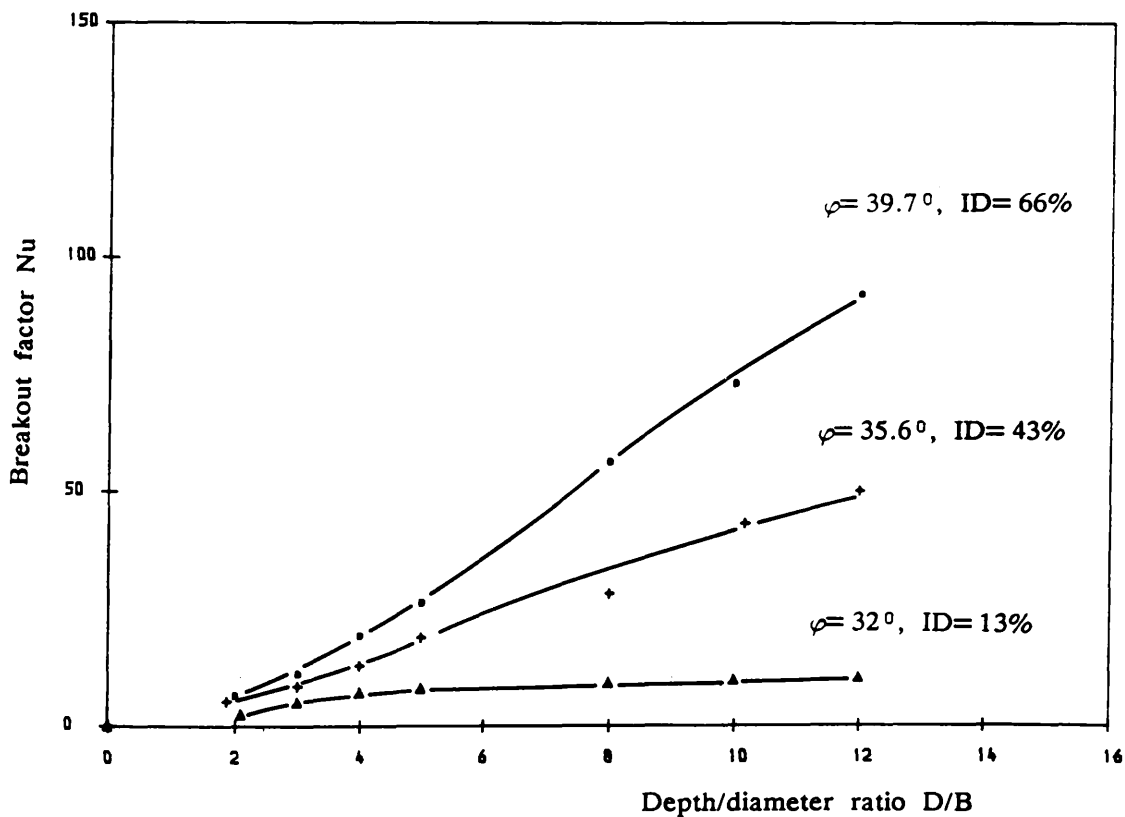


Fig. 5-8 Breakout factor vs depth/diameter ratio for plate anchors embedded in Lochaline sand.

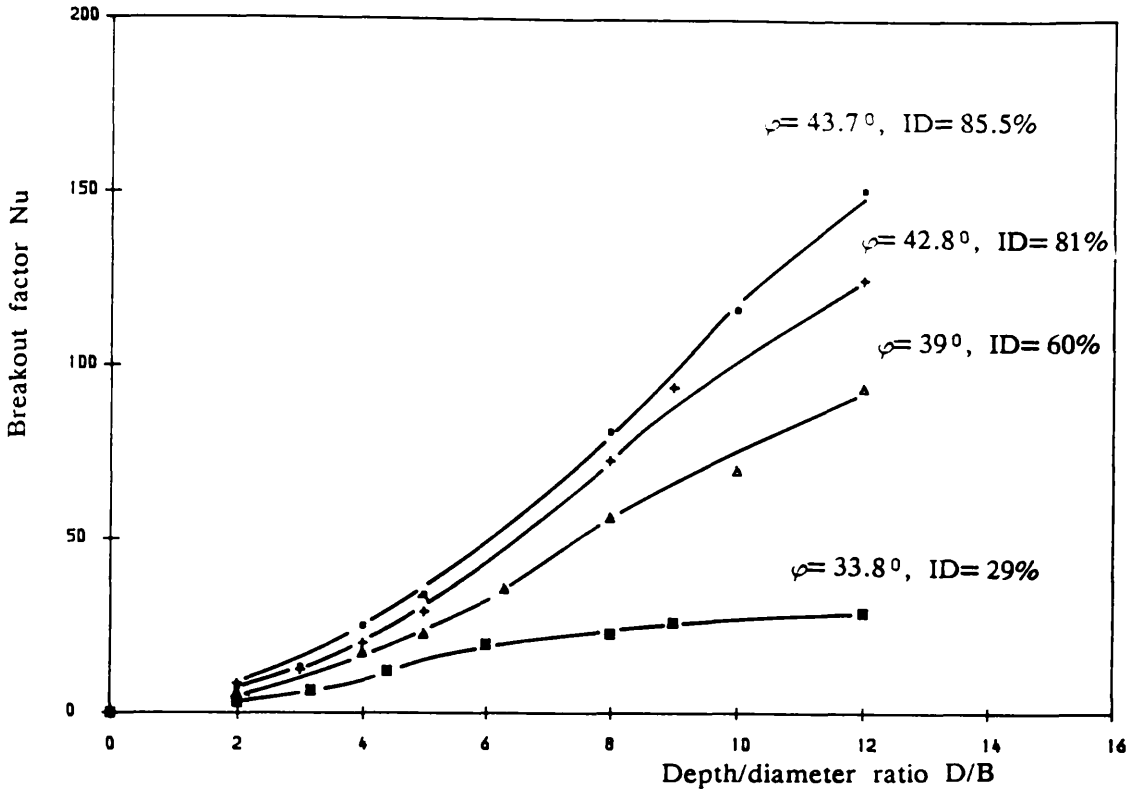


Fig. 5-9 Breakout factor vs depth/diameter ratio for plate anchors embedded in Leighton Buzzard sand.

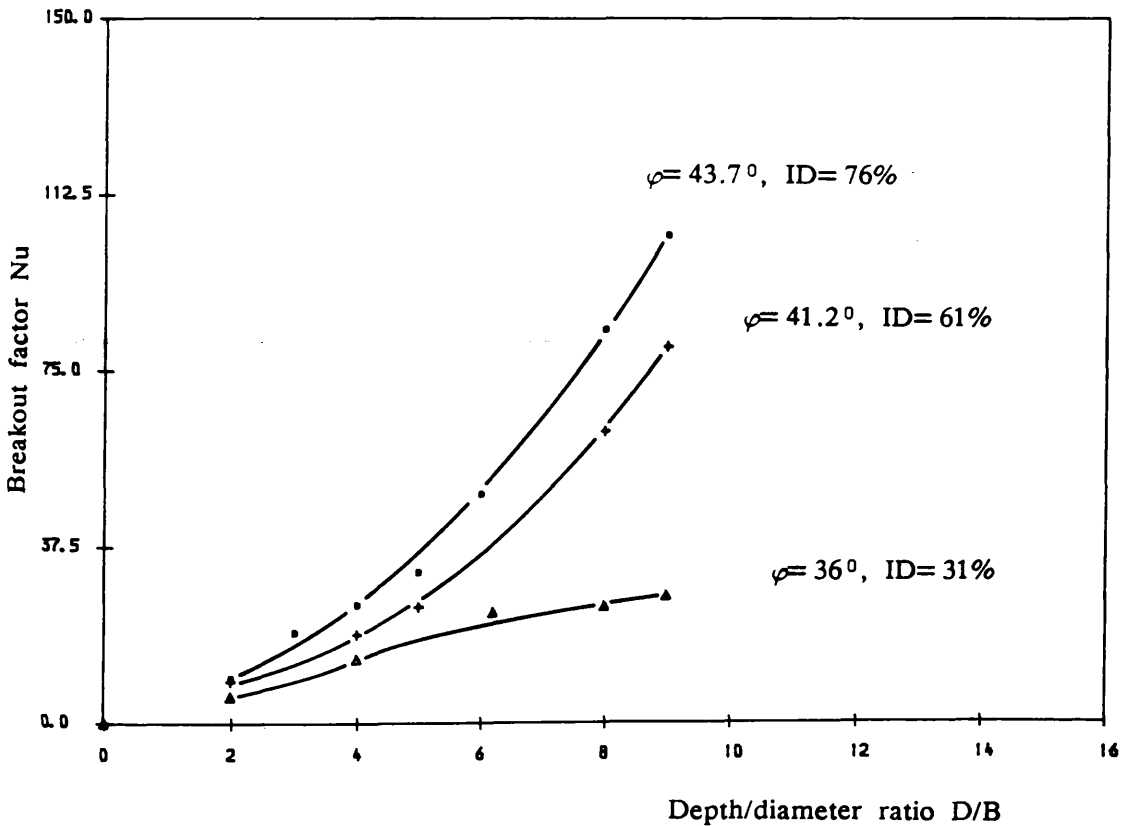


Fig. 5-10 Breakout factor vs depth/diameter ratio for plate anchors embedded in Douglasmuir sand.

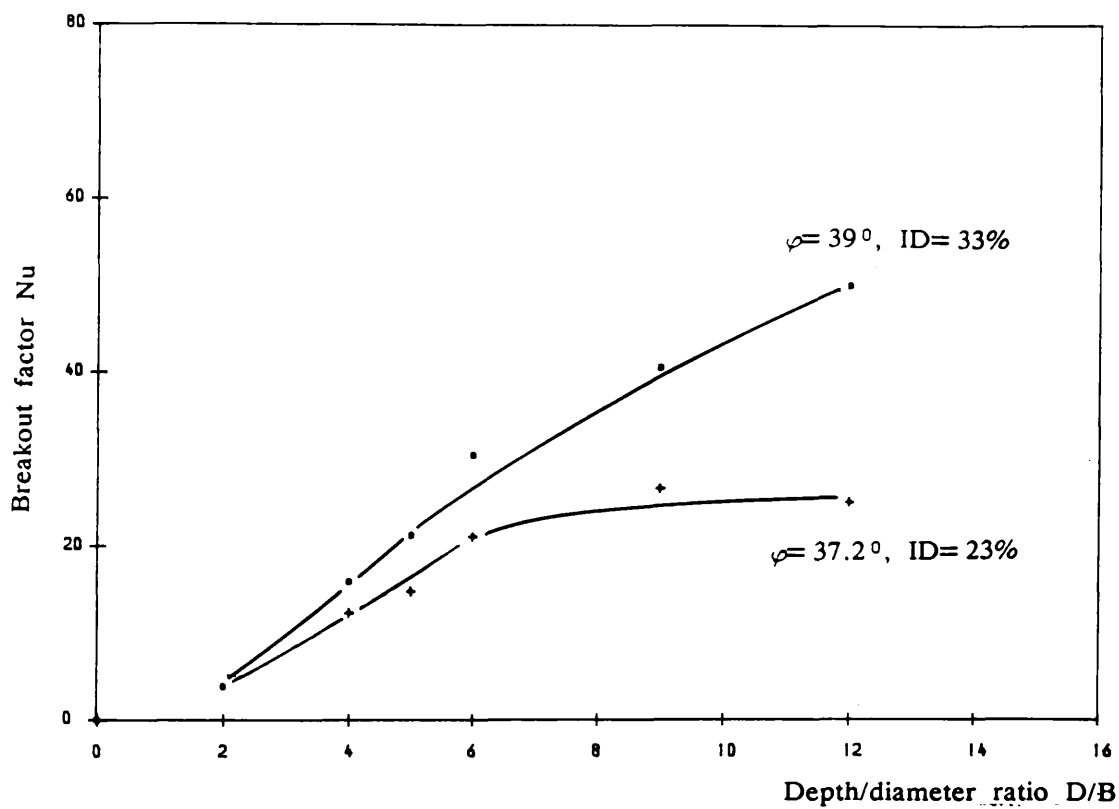


Fig. 5-11 Breakout factor vs depth/diameter ratio for plate anchors embedded in Hyndford sand.

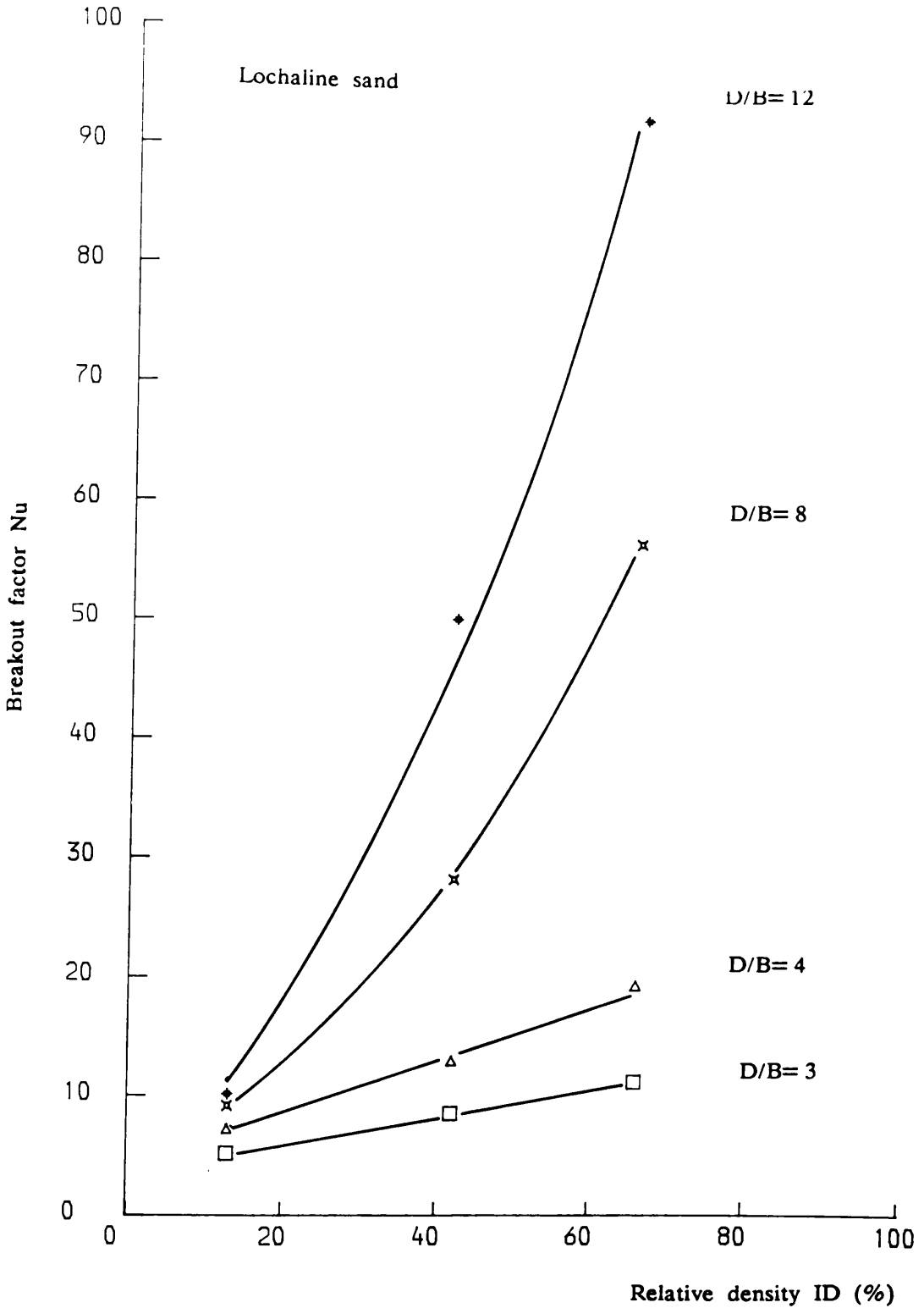


Fig 5-12 Breakout factor—relative density relationship for shallow and deep plate anchors.

5-2-4 Effect of grain size

The size of a cohesionless soil is generally defined by the " 50% finer than " size. This median grain size can be found from the conventional plot of the particle size distribution in fig. 3-1.

For the present investigation two sands having similar grading ($U=1.8$) and subrounded shape have been considered, a fine uniform Lochaline sand having an effective diameter (D_{50}) of 0.3 mm and a coarse uniform Leighton Buzzard sand having an effective diameter (D_{50}) of 0.8 mm. Pull out tests have been conducted on both sands at different relative densities and different depths as shown in figs. 5-8 & 5-9.

Fig. 5-13 & 5-14 depict the variation of breakout resistance with relative density for shallow and deep anchors respectively. It can be observed that an almost similar breakout factor is attained in both sands over the range of D/B considered. For example, at a relative density of 50%, the breakout factors at $D/B=3$ and $D/B=12$ are equal to 9.25 and 62.0 in Lochaline sand and 8.75 and 64.0 in Leighton Buzzard respectively. This observation suggests that plate anchors behave similarly in both sands.

Since cohesionless soils can have the same angle of internal friction ϕ for different relative densities (ID), and the same relative density for different angles of internal friction, it can be asserted that the breakout factor is also a function of the angle of internal friction. Fig. 5-15 shows a correlation of the breakout factor and frictional angle, the points on the graph being the breakout factors obtained for the sands placed at the same relative density (ID = 40% & 60%). This figure shows a close correlation for the two sands over the range of D/B considered.

However, small differences in the breakout factor still exist and may be attributed to the fact that although the two sands have the same shape and grading, they are still different in roundness and sphericity which as shown in chapter 3 led to a slight disparity in the relationship between φ and ID. From the above, it can be concluded that the grain size causes no differences in the breakout factor when the anchor is embedded in sands having similar shape and grading.

Although the literature is abundant on work on the pull out resistance of plate anchors regarding the effect of overburden pressure, depth of embedment, etc..., nevertheless the influence of grain size on the uplift resistance has not received much attention. The present results show clearly that the grain size has no influence on the value of the uplift resistance factor obtained from model anchor tests in sands having similar shape and grading, thus confirming the observations made regarding the effect of grain size on the failure shape (chapter 7). The effect of grain size on pull out of a model plate anchor may be regarded as similar to the same effect on the penetrometer test. Gibbs & Holtz (1957) considered a similar problem in regard to the penetrometer test in a fine and a coarse sand of similar grading. They found that the penetration resistance was the same in the two sands for the same relative density and the same overburden pressure. More recently, Roa & Venkatesh (1985) showed that the behaviour of a short pile embedded in a uniform sand and subjected to an uplift load is independent of soil particle size.

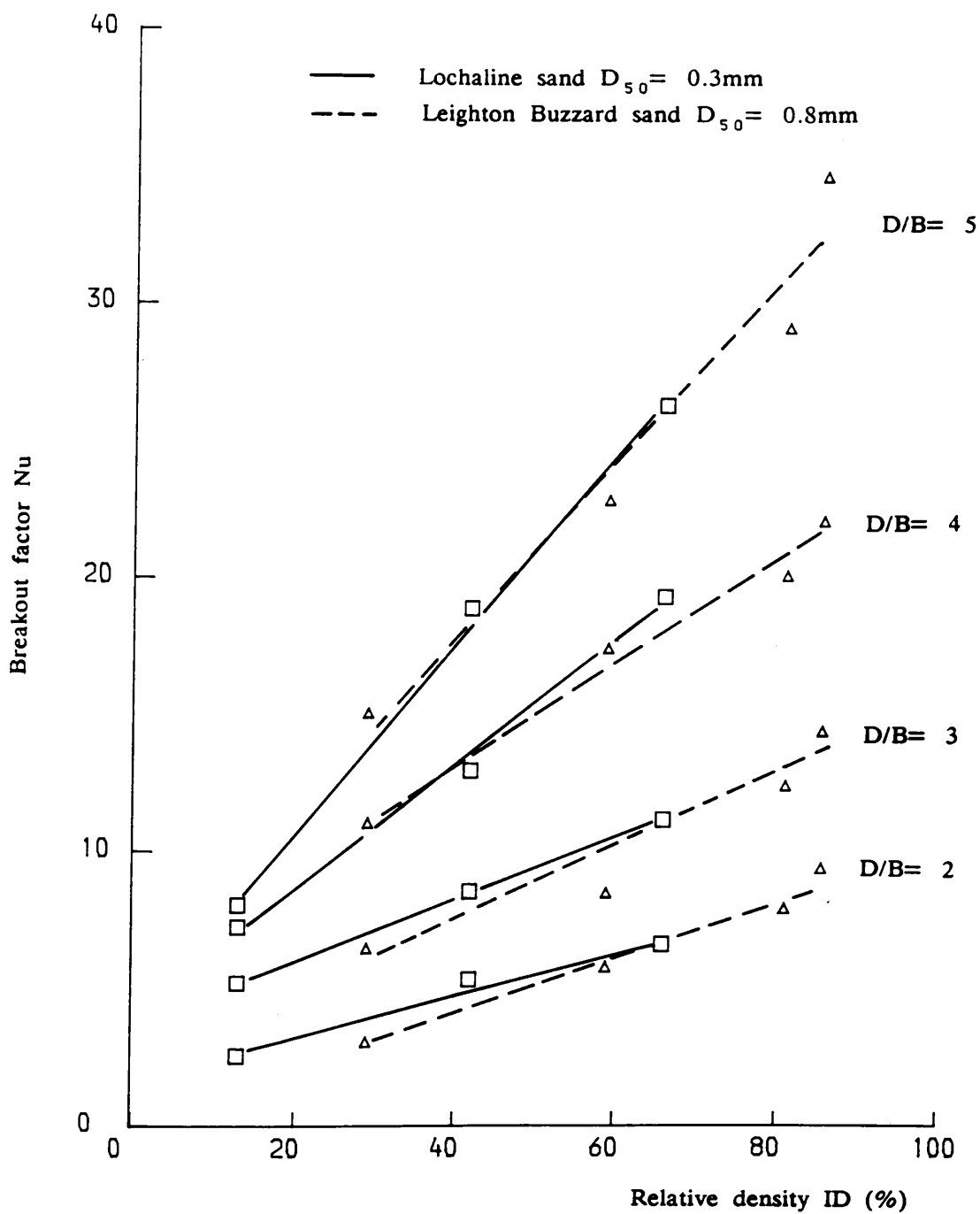


Fig. 5-13 Breakout factor vs relative density for shallow anchors: Grain size diameter (D_{50}) effect.

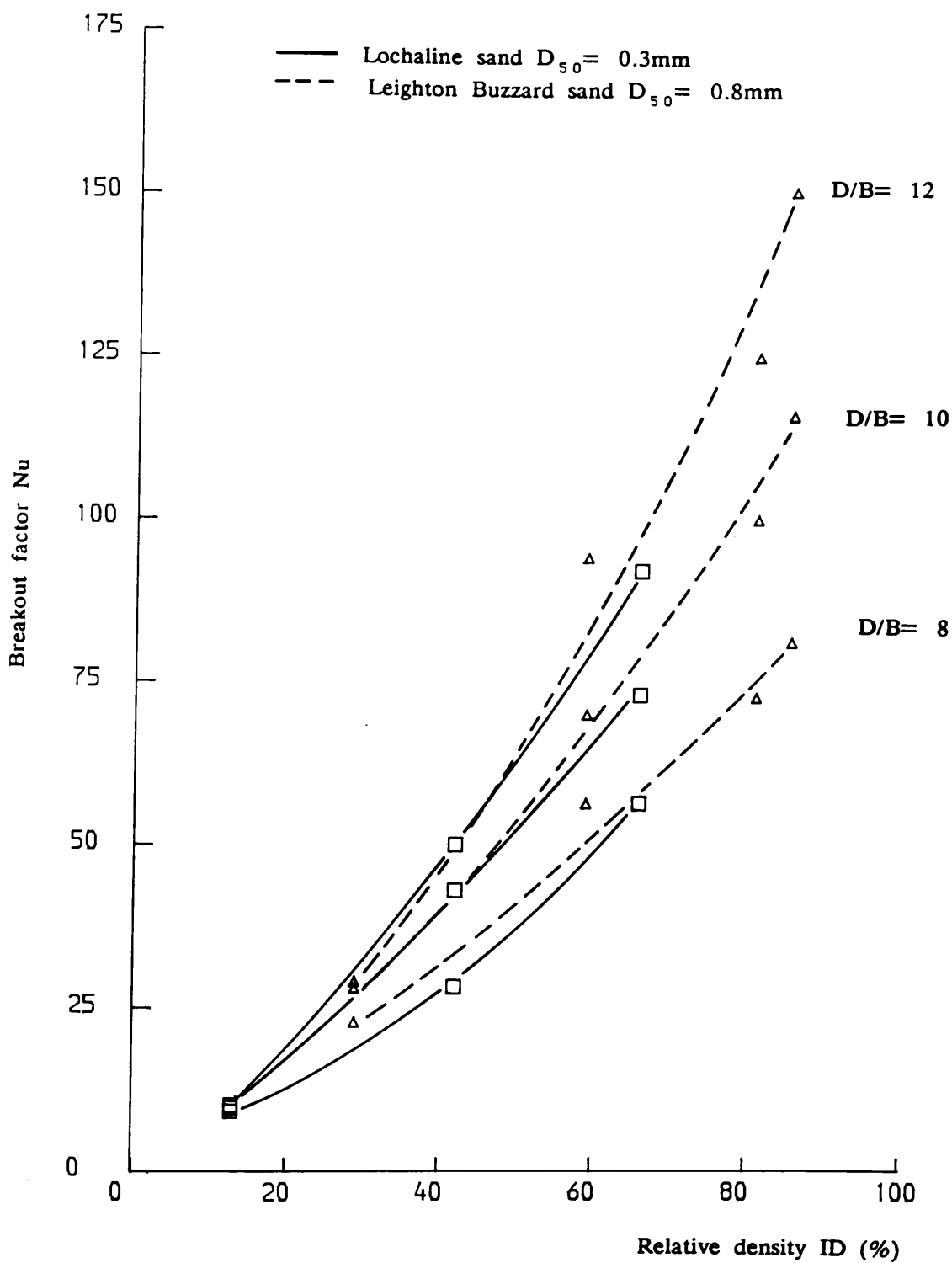


Fig. 5-14 Breakout factor vs relative density for deep anchors: Grain size diameter (D_{50}) effect.

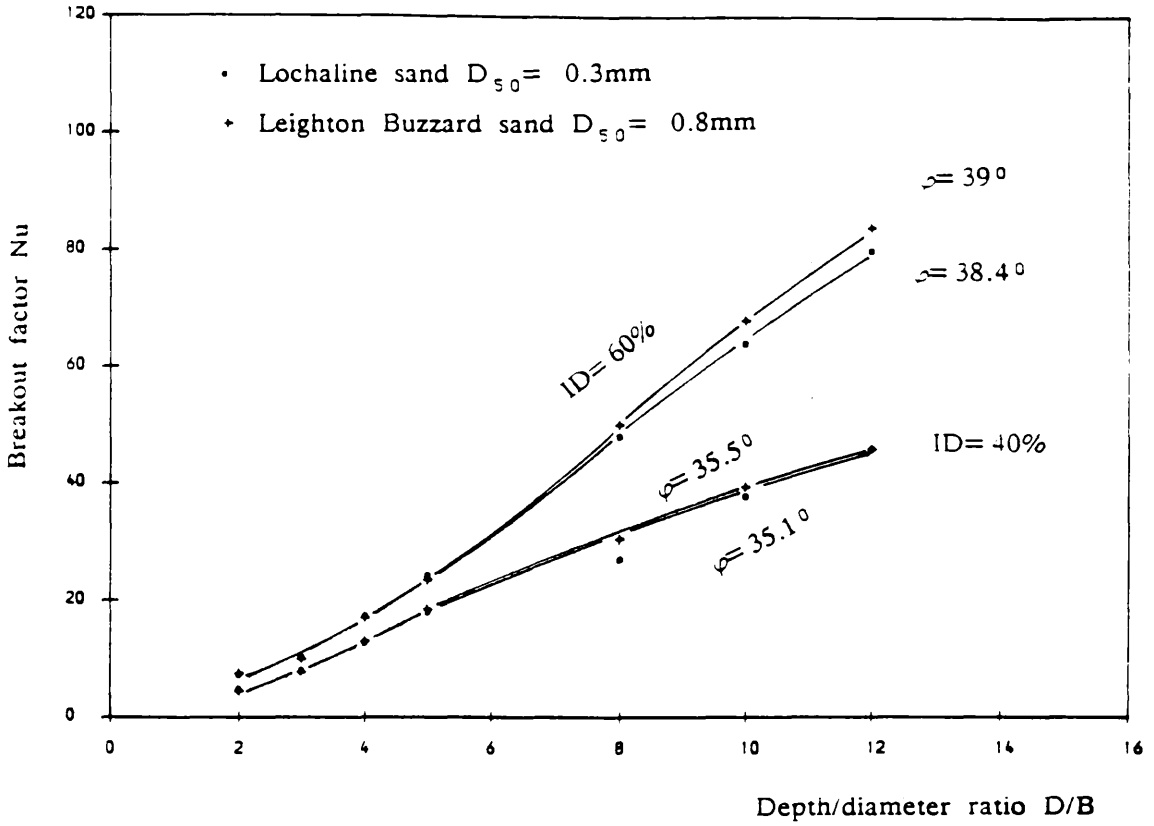


Fig. 5-15 Breakout factor—depth/diameter ratio relationship at the same relative density.

5-2-5 Effect of grain shape

The influence of particle shape on the breakout factor was investigated by considering three granular materials with particles in the coarse to medium sand range and with similar size and grading. In the discussion of the results herein, descriptive terminology such as subangular or subrounded is used to describe the particle shape and is fully explained in chapter 3. The materials include Ballotini (glass beads) with smooth rounded shape and an effective diameter (D_{50}) of 0.8mm. Due to the difficulty of obtaining this material in large quantities pull out tests were performed in the shallow range only. Leighton Buzzard sand which has been described in the previous section and Douglasmuir sand which has a subangular shape and an effective diameter (D_{50}) of 0.8mm were also used. Pull out tests in the three sands have been carried out at different relative densities and at different depth / diameter ratio as shown in figs. 5-7, 5-9 & 5-10.

Breakout factors versus relative density for shallow and deep anchors are plotted in fig. 5-16 & 5-17. The data show a marked increase in the breakout factor with increase of angularity of the particles and relative density, with Ballotini exhibiting the least increase. At a relative density of 65%, Douglasmuir sand with subangular particles registered breakout factors which were higher than the values recorded for the rounded and subrounded sand. This increase in angularity shows also that for example at $D/B=2.0$ and a breakout factor of say 5.0 (shallow range) there is a spread in relative density from 30% to 85%, and at $D/B=9.0$ and a breakout factor of 70.0 (deep range) there is a spread in relative density from 59% to 66% (without Ballotini). These observations suggest that grain shape can drastically affect the uplift behaviour of a plate anchor.

Since the particle shape influences both the breakout factor and the friction

angle, it can be postulated that the breakout factor is also a function of the shear strength of the sand. This is confirmed by the correlation of Nu values and friction angles shown in fig. 5-18 at ID=70%.

The present tests suggest that the breakout factor Nu is affected by particle shape. Pull out resistance at a particular relative density increases with the angularity of the particles. The increase in the breakout factors, which is similar to the increase in friction angle, indicates that it is affected by relative density and shear strength of the sand which is highly dependent on angularity. Therefore, relative density or angle of internal friction correlations with breakout factors obtained for a particular sand are not necessarily applicable to sand with different particle shape and can be misleading and result in conflicting values. Because angularity influences both the deformability of the sand and the breakout factor, the error in using a theoretical equation which includes ϕ or ID to predict the breakout resistance may be compounded. For example, consider an equation developed for an average sand that is used to predict the breakout resistance of an angular sand. First, for the same relative density the angular sand will deform considerably more than the average sand. The greater angularity of the particles will cause a larger breakout resistance factor. Secondly, pull out resistance will be computed for a material denser than actually exists. Accordingly, the breakout prediction developed for an average sand would lead to an underestimation of the magnitude of the breakout factor Nu for the angular sand.

It can be concluded that, at a given relative density, the breakout factor of a plate anchor embedded in sands having similar size and grading increases with angularity. However, no direct relationship was found between the angularity and the breakout factor Nu.

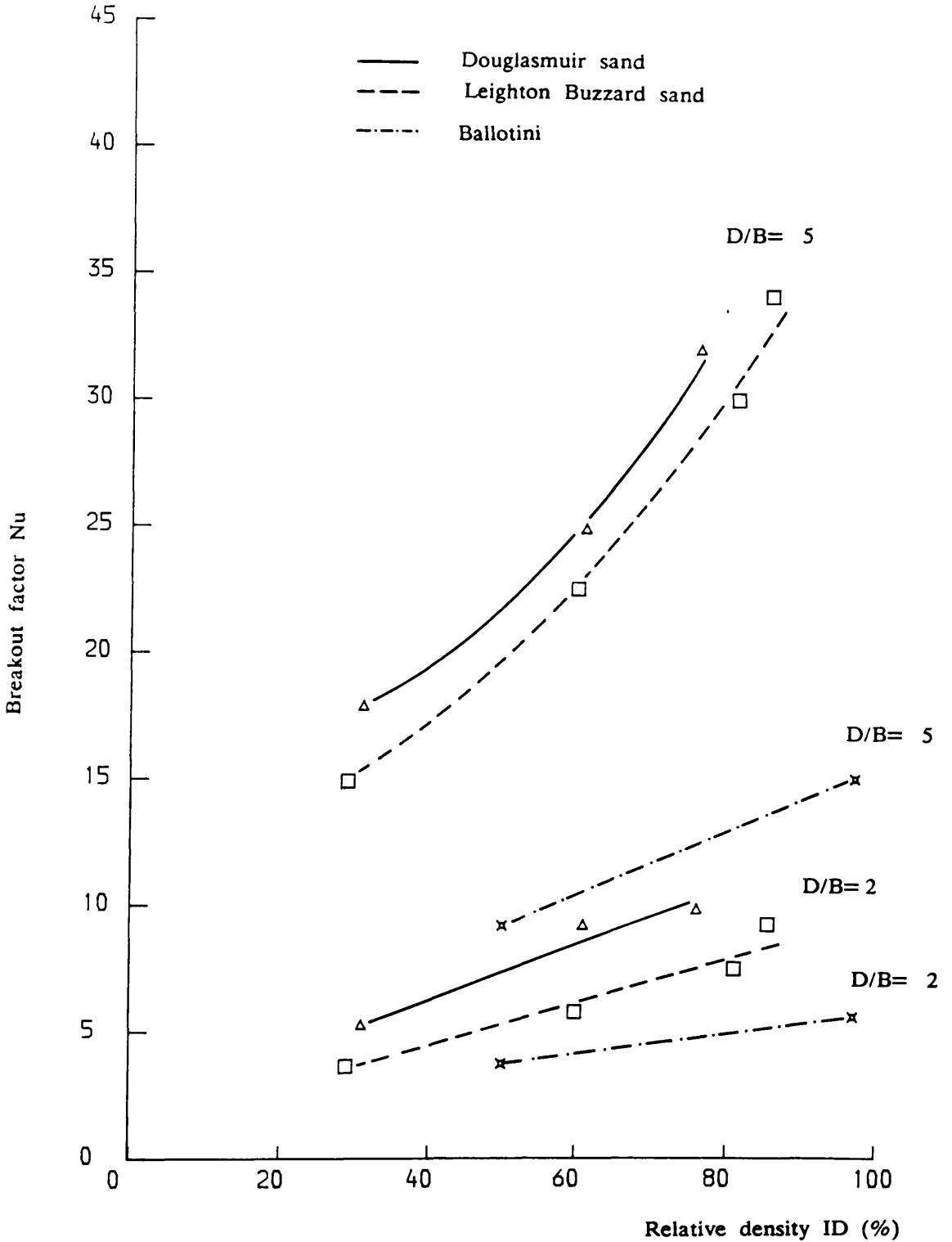


Fig. 5-16 Breakout factor vs relative density for shallow anchors: Grain shape effect.

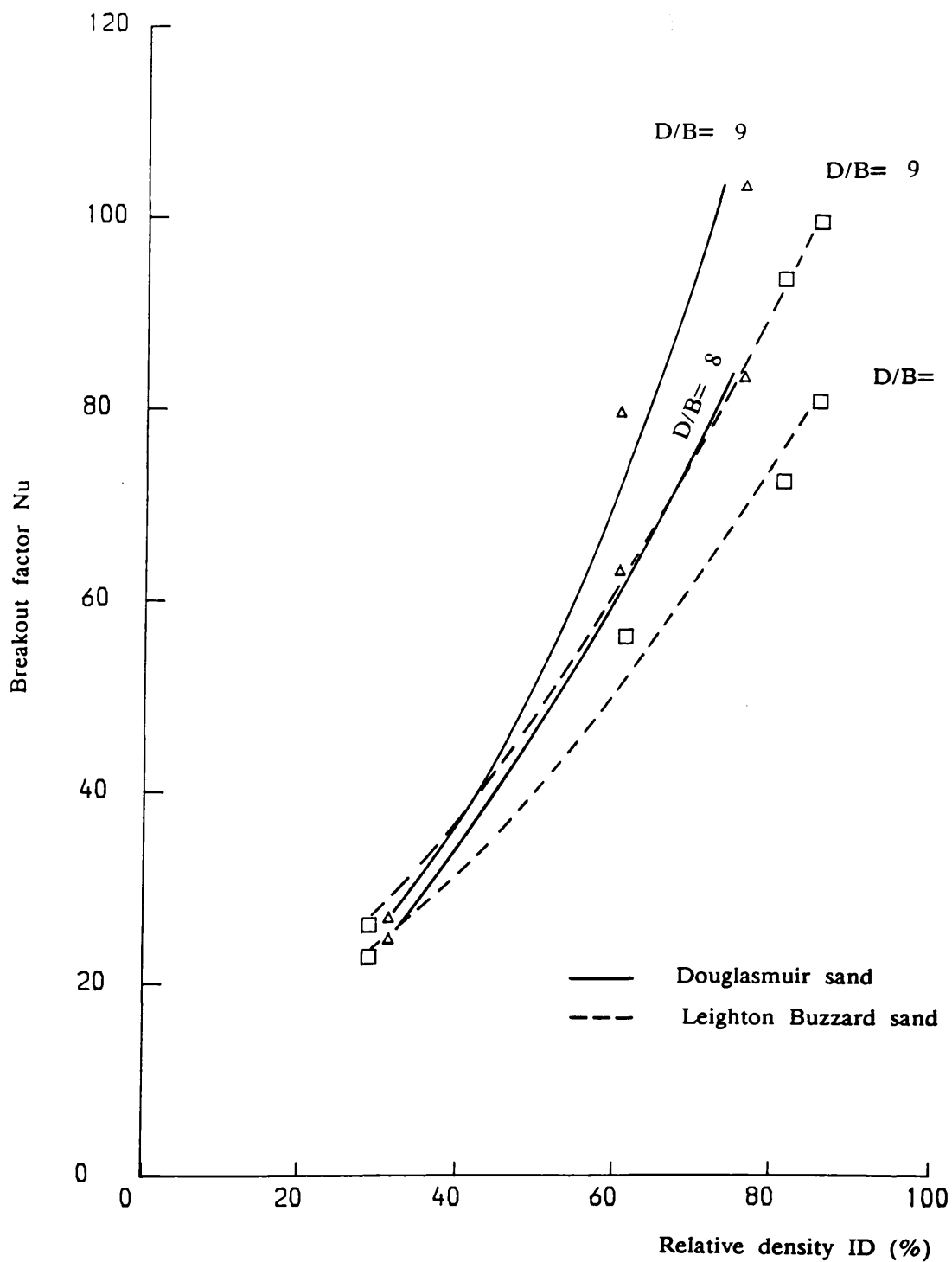


Fig. 5-17 Breakout factor vs relative density for deep anchors: Grain shape effect.

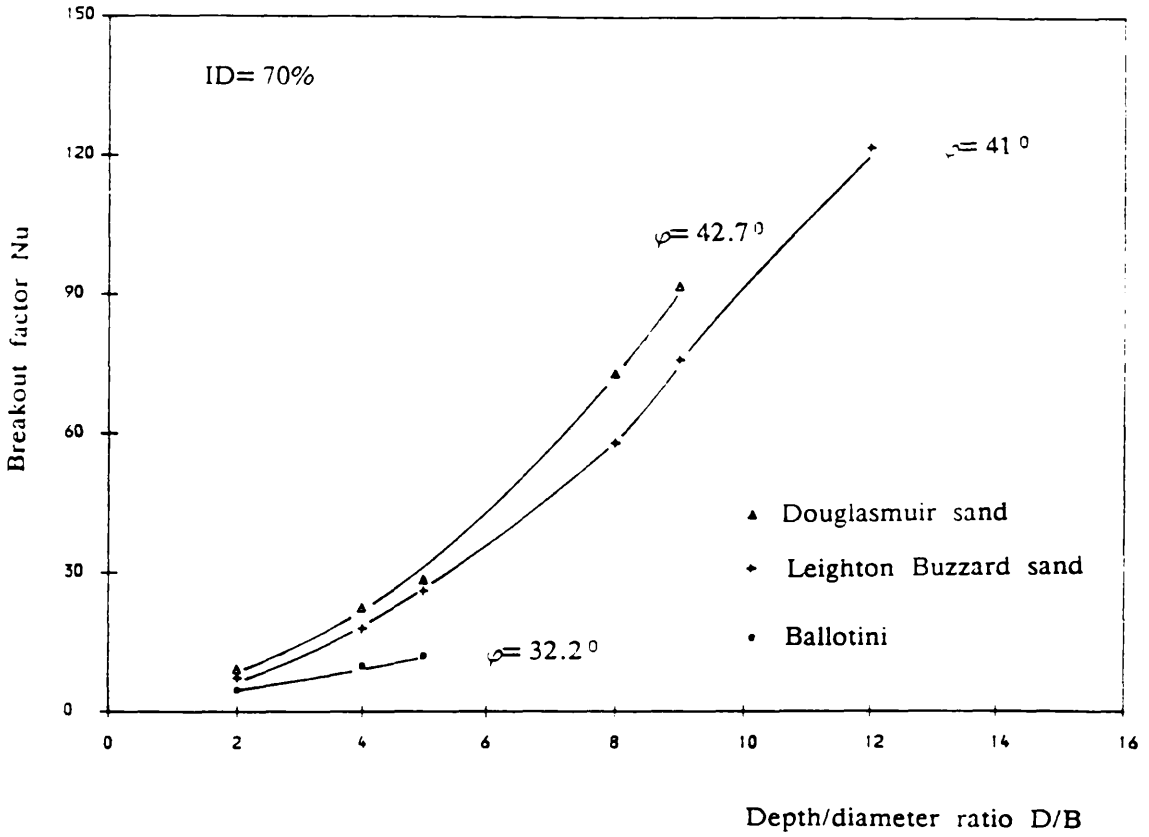


Fig. 5-18 Breakout factor—depth/diameter ratio relationship at the same relative density.

5-2-6 Effect of grading

This section discusses the effect of grading on the pull out resistance. In the present investigation soil grading is defined by the coefficient of uniformity $U = D_{60}/D_{10}$, found from the particle size distribution, where D_{60} and D_{10} are the mesh sizes through which 60 per cent and 10 per cent of the sand pass respectively. The discussion of the present results generally follows along similar lines as in section 5-2-5.

The effect of varying the coefficient of uniformity on the pull out resistance was investigated by carrying out pull out tests on a well graded Hyndford sand with $U = 5.5$ and a uniform Douglasmuir sand with $U = 1.8$. Both sands had a similar size ($D_{50} = 0.8\text{mm}$) and particle shape (subangular). Tests have been conducted on a wide range of relative densities and depth to diameter ratios, and the resulting breakout factors are shown in fig. 5-10 & 5-11.

Figs. 5-19 & 5-20, portray the breakout resistance versus relative density relationship for shallow and deep anchors respectively. The data show a tendency towards an increase in the breakout resistance factor with decreasing uniformity at a given relative density. For example, at a relative density of 65% the breakout factor in the shallow range ($D/B = 5.0$) increases from 27.25 to 39.5 (31% difference) and from 83 to 113 (26.5% difference) in the deep range ($D/B = 9.0$). Conversely at $D/B = 5.0$ and $Nu = 25$ there is a spread in relative density from 40% to 60% and from 54.5% to 64.5% at $D/B = 9.0$ and $Nu = 80$.

It is apparent that a better distribution of particle sizes produces a better interlocking between particles and hence give a higher angle of internal friction. On the other hand it also influences the breakout factor as has been shown in fig.

5-19 and fig. 5-20 , therefore it can be postulated that the breakout factor is also influenced by the shear strength of sand. This is substantiated by the correlation of N_u values and friction angles shown in fig. 5-21 at $ID=65\%$.

The present tests indicate that the breakout factor N_u is affected by the soil grading. Pull out resistance at a given relative density increases with the decrease in uniformity, however, this change depends upon the alteration caused by grading on the relative density and angle of internal friction relationship. Similar to the conclusions reached in the previous section relative density or angle of internal friction correlations with breakout factors obtained for a particular sand are not automatically applicable to sand with different grading and can result in an underestimation of the breakout factors in a well graded sand.

A review of previous work on pull out testing on plate anchors was made in chapter 2 but no information was found as to the effect of grading alone on the breakout resistance. The present investigation shows that at a given relative density, the breakout resistance of a plate anchor embedded in sands having similar size and shape increases with increasing coefficient of uniformity. However, no direct relationship was found between the uniformity and the breakout resistance. The same characteristic was reported by Ostermayer & Sheele (1978) for grading effect, in a paper dealing with prestressed ground anchors where it was found that the ultimate load holding capacity increased with the coefficient of uniformity.

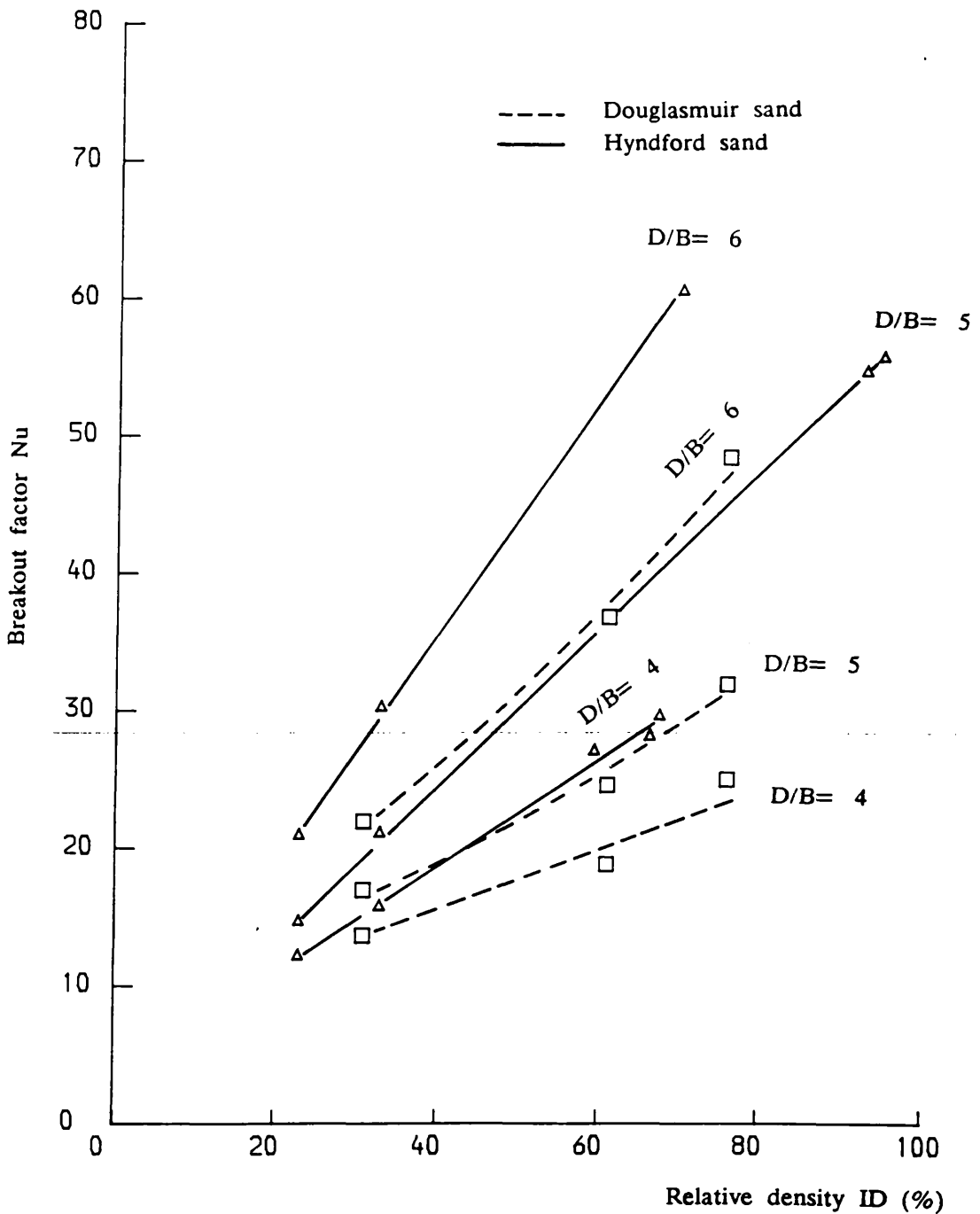


Fig. 5-19 Breakout factor vs relative density for shallow anchors: Grading effect.

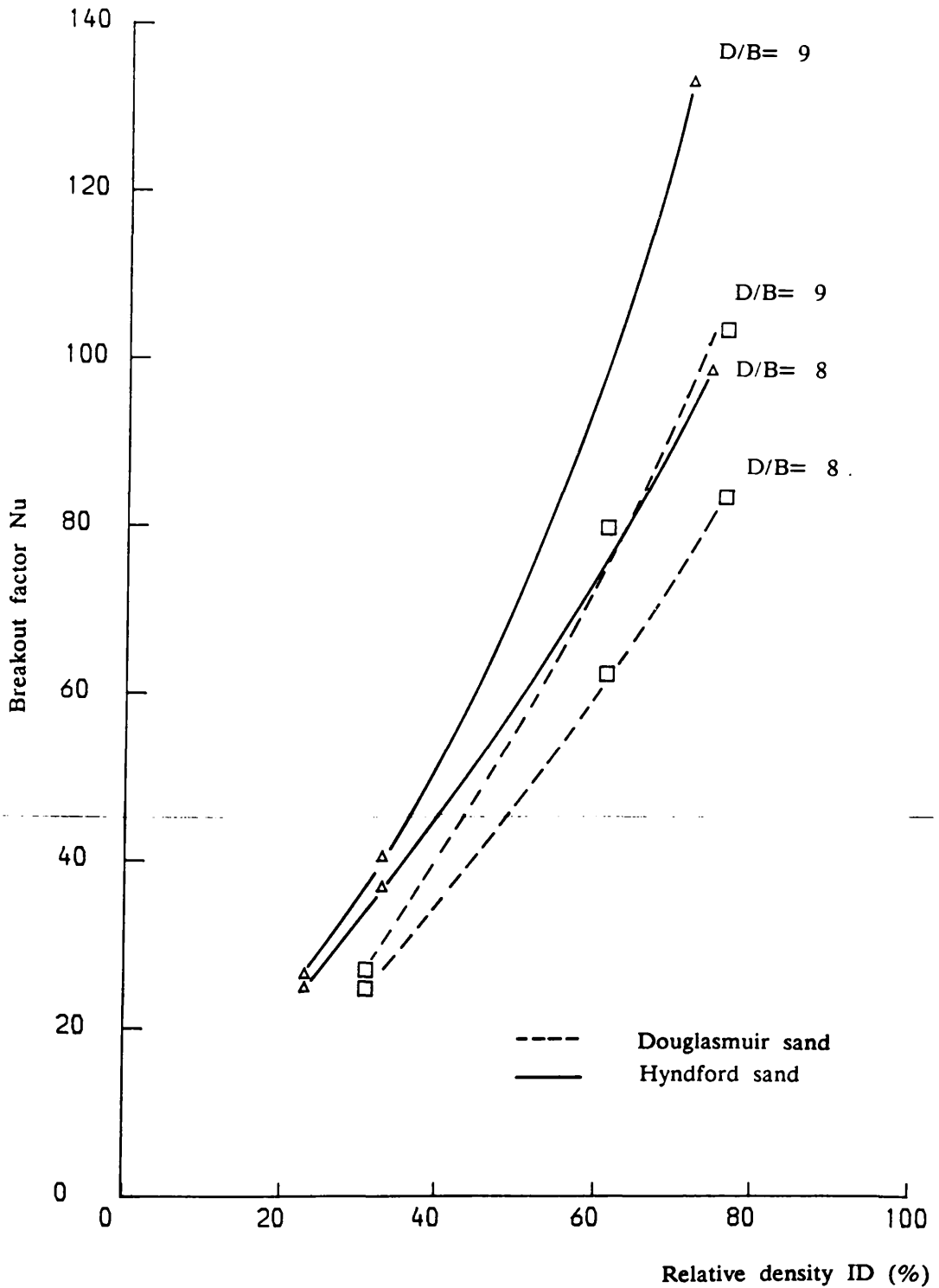


Fig. 5-20 Breakout factor vs relative density for deep anchors: Grading effect.

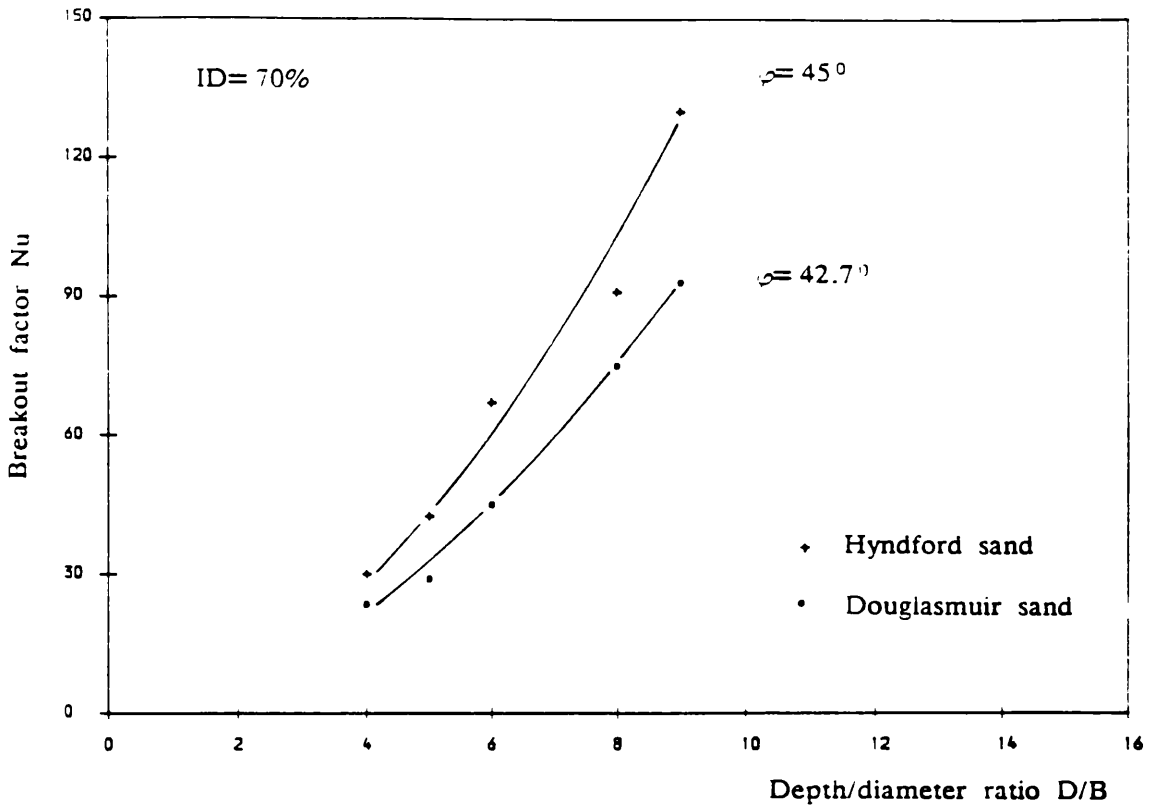


Fig. 5-21 Breakout factor—depth/diameter ratio relationship at the same relative density.

5-2-7 Summary

The causes of the variations of the uplift resistance with each of the factors (ID, φ , grain size, grain shape and grading) have been investigated and their relative importance assessed.

Relative density, angle of internal friction and depth of embedment were found to have an important effect on the pull out resistance. These factors have already been the object of investigation by previous researchers. However, the principal aim of the present research was to study the effect of grain size, grain shape and grading on the pull out resistance.

From the present results, it appears that the breakout factor is not solely a function of overburden pressure, relative density or angle of internal friction but is also a function of soil characteristics. The following conclusions can be drawn:

- 1- If the sands have the same grain size distribution, the breakout factor is greater for subangular than subrounded sand at a given relative density.
- 2- If the sands have the same mean diameter D_{50} and shape, the breakout factor is greater for well graded sand than uniform sand at a given relative density.
- 3- For the above cases, it was found that no direct relationship exists between the pull out resistance, grain shape and grading.
- 4- Tests on sands having similar grading and shape but different grain size (D_{50}) demonstrated that there was no difference in the breakout factor, which was therefore independent of the grain size.

5-4 COMPARISON OF PRESENT RESULTS WITH PREVIOUS THEORIES

A comparison of some of the present test results with the predicted values of anchor uplift resistance from some of the theories reported in chap. 2 is presented in this section.

In fig. 5-22 predictions from Balla's (1961) theory are plotted for two densities of sand corresponding to the experimental values tested in Leighton Buzzard sand (i.e. $\phi = 42.8^\circ$, 33.8° and $ID = 81\%$, 29% respectively). Balla's theory gives a breakout factor at $D/B = 3.0$ for loose sand ($\phi = 33.8^\circ$) of the order of 91% of the value for dense sand ($\phi = 42.8^\circ$), compared with the experimental results which gave 45%. This confirms the argument by Sutherland (1965, 1988) that Balla's theory is insensitive to changes in ϕ and therefore sand density. This might be due to the narrow range of sand condition tested by Balla ($\phi = 36^\circ - 38^\circ$) where the influence of the variation in density was not observed. For dense sand ($\phi = 42.8^\circ$) the percentage of Balla's theoretical prediction to the present experimental value at $D/B = 3.0$ is 74% while that of the loose sand is 151%. This shows that Balla's theory underestimates the mobilized load in dense cohesionless soils and overestimates it in loose cohesionless soil.

Matsuo's (1967) theory is plotted for the shallow anchor range ($D/B \leq 6$) in fig. 5-23 for two different sands, Leighton Buzzard ($\phi = 39^\circ$) and Hyndford ($\phi = 39^\circ$). It can be observed that in both cases Matsuo's theory overestimates the ultimate uplift loads. At small values of D/B ($D/B \leq 3$) the theoretical values overpredict the experimental ultimate uplift capacities by as much as 337% in Hyndford sand and 224% in Leighton Buzzard. For D/B values between 3 and 6 overestimation of the experimental ultimate uplift capacities averaged 124% in the well graded sand and 115% in the uniform sand.

Meyerhof & Adams' (1968) theory is shown in fig. 5-24a & 5-24b for both shallow and deep anchors. In dense Leighton Buzzard sand ($\phi = 43.7^\circ$) their semi-empirical analysis shows good agreement with the experimental values up to $D/B = 8$ beyond which the theoretical loads fall below the experimental values. This confirms the argument by Carr (1970) and Maddocks (1978) that for anchor systems installed at greater depth the sliding surfaces as defined by Meyerhof and Adams theory were not observed to occur and consequently results tend to be underestimated. In dense Douglasmuir sand (subangular grains, $\phi = 43.7^\circ$), the ultimate capacity is underestimated. In the loose state (fig. 5-24a) the theoretical values were found to be higher than the experimental values.

Vesic (1971) and Tagaya et al (1988) predictions are shown in fig. 5-25 and 5-30 respectively. Very poor correlation was found between the theoretical values and the present experimental results (Lochaline sand, $\phi = 39.7^\circ$, 32° and $ID = 66\%$, 13% respectively), all theoretical values of N_u were far below the experimental ones. This suggest that both theories are insensitive to the variations of ϕ and ID .

Figs. 5-27a and 5-27b show a comparison between the predictions of Fadl's (1981) approximate analysis and some of the author's experimental results. It can be seen from fig. 5-27a that Fadl's predictions over the whole range of D/B values in Leighton Buzzard sand ($\phi = 43.7^\circ$, $ID = 85.5\%$) and Lochaline sand ($\phi = 39.7^\circ$, $ID = 66\%$) are in good agreement with the test results. However, ultimate uplift loads are underestimated in the loose state. From fig. 5-27b, it can be observed that Fadl's predictions did not give a good correlation when sands having different characteristics (shape and uniformity) were considered. Similar conclusions can be drawn from figs 5-28a & 5-28b, where Saeddy's (1987) predictions are plotted against the experimental results in Leighton Buzzard sand ($\phi = 43.7^\circ$, $ID = 85.5\%$) and Douglasmuir sand ($\phi = 43.7^\circ$, $ID = 76\%$).

Murray & Geddes (1987) predictions (equilibrium method) are shown in fig. 5-29. Poor correlation was found between theoretical values and the present test results ($\varphi=39^\circ$ & 36°). This can be attributed to the fact that the above theory was derived from tests on subrounded sand and was based on a slip line field extending to the ground surface for both shallow and deep anchors at all densities.

Figs. 5-26 & 5-31 show the finite element predictions of Rowe & Davis (1982) and Vermeer & Sutjiadi (1985) respectively. It can be seen that both methods gave very conservative predictions. Koutsabeloulis & Griffiths (1989) finite element approach is plotted in fig. 5-32. Unlike the two previous theories, this approach seems to be sensitive to the variations of φ and gives by far the best estimation of N_u for a finite element approach.

The Frydman & Shiham (1989) predictions are applied to the case of a sand with subangular shape and a sand with a subrounded shape. The results are shown in fig. 5-33. This figure indicates that the breakout factor in the subrounded sand sand is predicted reasonably well. However, in the case of the subangular sand the same approach appear to overpredict the experimental results. The source of the difference is due to the fact that two different type of sands have been tested. The grain shape effect associated with such tests has been explained in section 5-2-5.

The above discussion indicates the importance of the grain shape and the uniformity in addition to relative density or φ for prediction of ultimate uplift loads when considering different sands. It is also believed that the assumption of a unique failure surface for all sands is also not valid (see chapter 7). The spread of data derived from testing four different sands and theoretical predictions suggests that equations developed for all cohesionless soils under all conditions are not valid.

5-4 COMMENTS

The above discussion indicates the importance of grain shape and uniformity in addition to other parameters (D/B, ID, φ , stress history) on the ultimate uplift load. This has been shown by comparing the breakout factors of anchors embedded in sand with similar φ values or similar ID and also by comparing the author's experimental results with some of the theories presented in chap.2, which often produced results compatible only with the particular tests conditions and materials for which they were derived and when applied to different situations such as the present investigation yielded unsatisfactory results. It is presently well understood that the nature of the soil uplift resistance phenomena at play above the plate anchor depends on the volume change characteristics (and therefore relative densities) of the given sand at its density: yet, whichever type of failure is postulated, punching, local or general it cannot escape notice that the formulae are established in terms of φ values. Burmister (1948) stated that:

" The concept of relative density was introduced to bring the behaviour characteristics of soils on a common basis in consistent and practically useful relationships and to provide a tool for communications between engineers".

Ezquivel-Diaz (1967) followed this line and suggested the inclusion of the relative density in any theoretical analysis of the pull out resistance. Fadl (1981) and Saeddy (1987) did so and formulated equations which showed good agreement with some of the past and present experimental results. However, their interpretation is at fault in attempting to consider all sands within a single $\varphi = f(\text{ID})$ function. A glance at fig. 3-6 shows that the universality of the relation between φ and ID, ever consciously denied, but always implicitly employed, does not prevail. Obviously for a given sand there is a very close correlation between φ and ID, moreover, for two sands that are quite similar (e.g. Lochaline sand and Leighton Buzzard sand) as regards the relationship $\varphi = f(\text{ID})$, there continues to be a single close correlation

between φ and ID, so that if any phenomenon is dependent on φ it is simultaneously correlatable to ID.

Recognising the significance placed on the correlation of relative density or the angle of internal friction with engineering properties, the question arises : Do granular soils at the same φ or ID have the same properties? Tests on sands having different particle shape and grading indicate that granular soils at the same relative density can have drastically different engineering properties. Therefore, the use of relative density or the angle of internal friction criteria in any theoretical analysis, without considering the particle shape or uniformity, can result in poor or misleading predictions of ultimate uplift load.

In conclusion it would appear from the present investigation that the differences in the breakout factor are due to soil type, suggesting that the breakout factor, angle of internal friction, relative density relationship are not universal for all sands. It is not surprising that this relationship varies for different sands. According to classical soil mechanics theory, the uplift capacity of plate anchors embedded in cohesionless soils is very dependent on φ and ID, and a universal friction angle, relative density relationship, valid for all sands, does not exist.

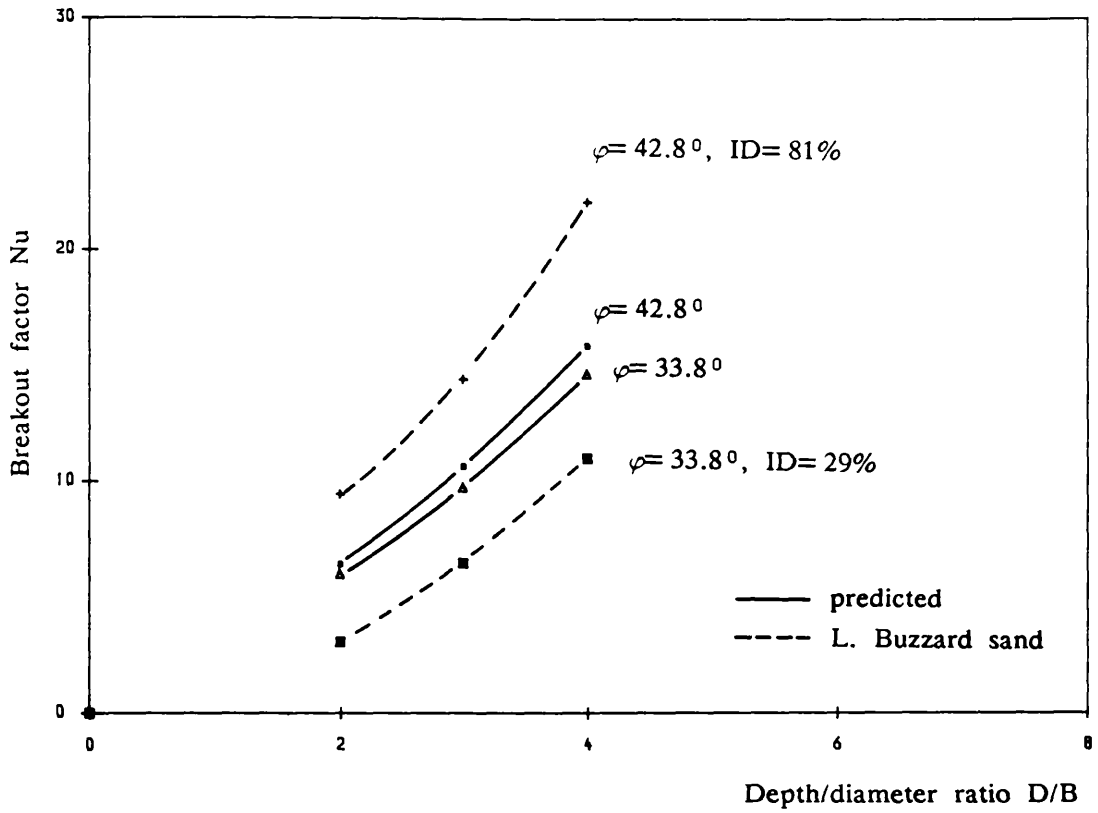


Fig. 5-22 Comparison of Balla's (1961) predictions with present test results.

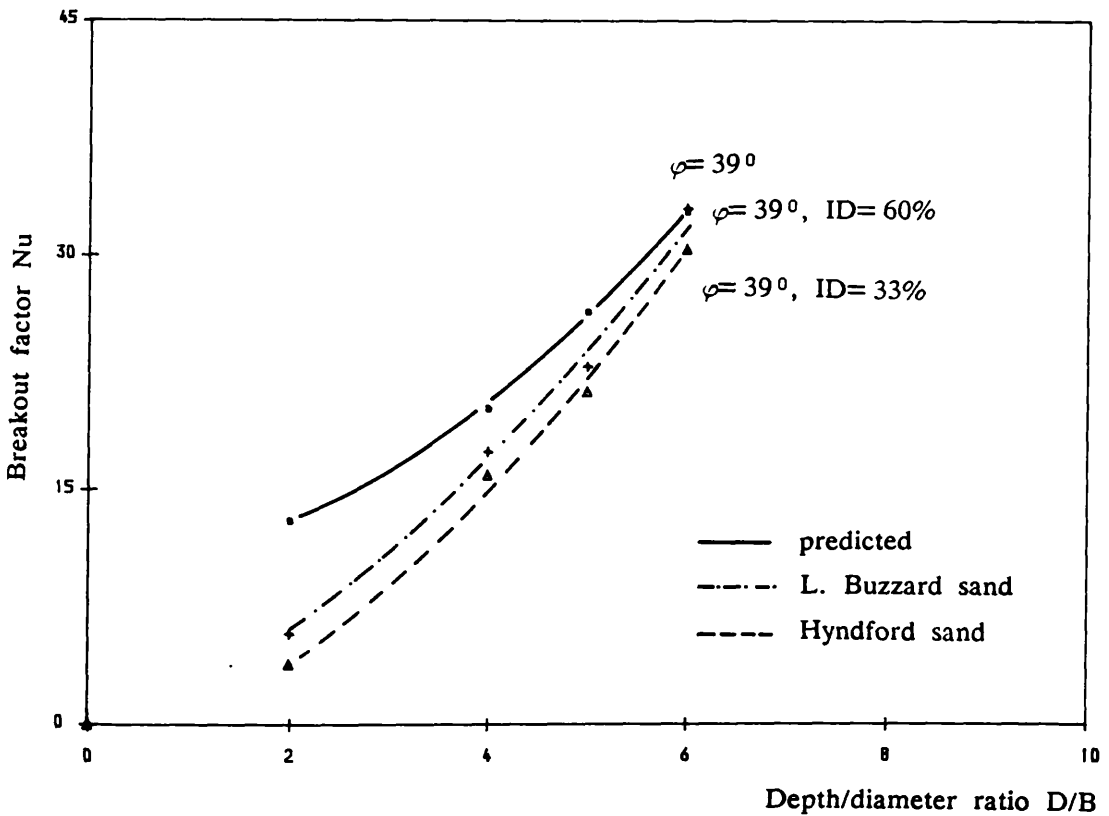


Fig. 5-23 Comparison of Matsuo's (1968) predictions with present test results.

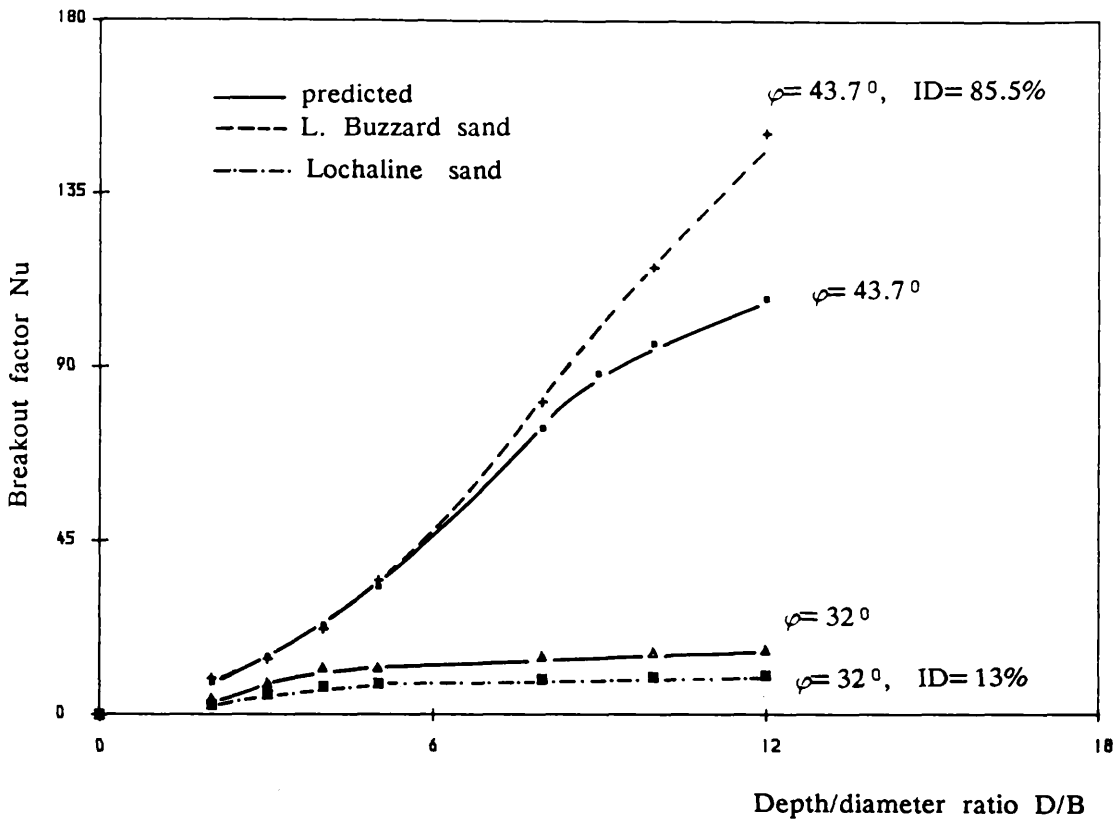


Fig. 5-24a Comparison of Meyerhof and Adams' (1968) predictions with present test results.

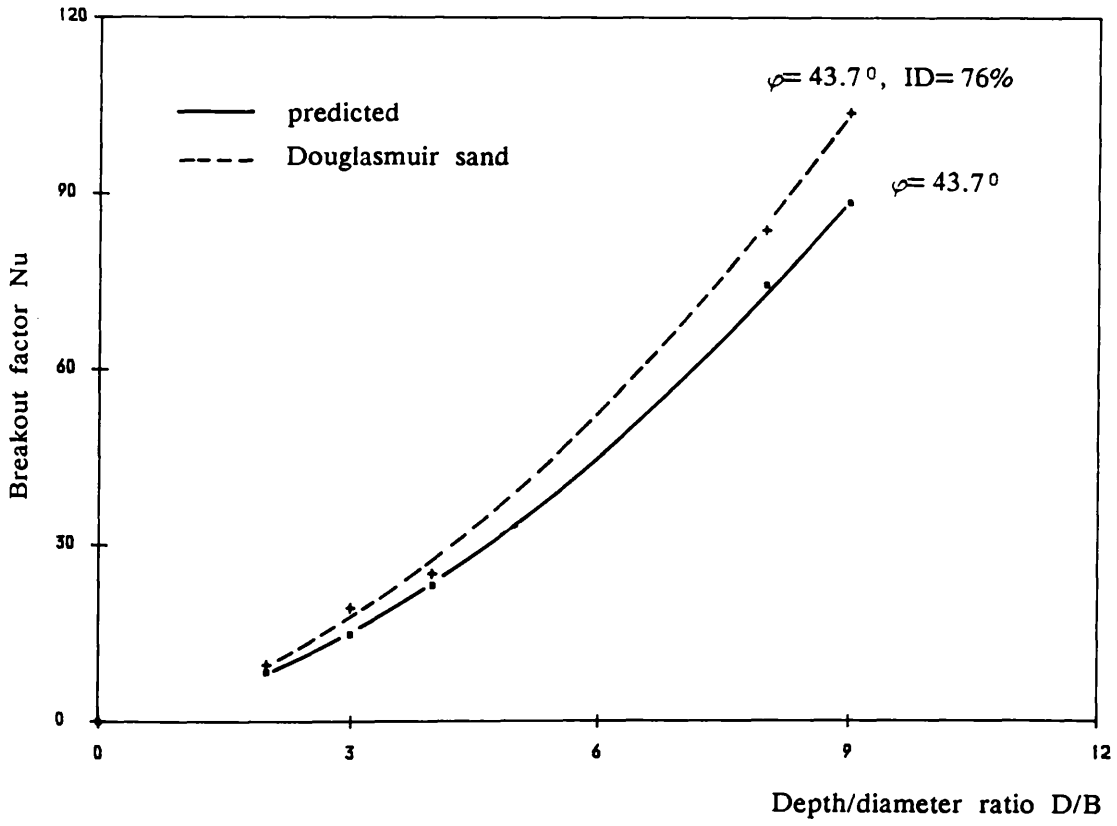


Fig. 5-24b Comparison of Meyerhof and Adams' (1968) predictions with present test results.

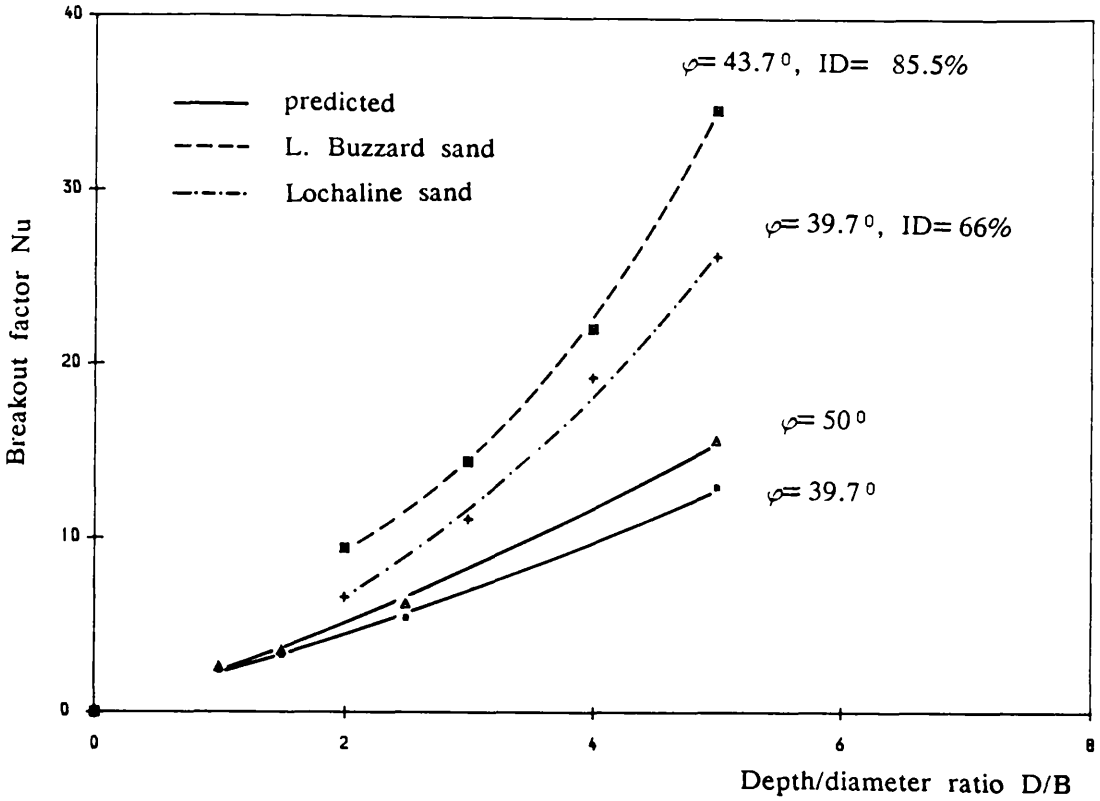


Fig. 5-25 Comparison of Vesic's (1971) predictions with present test results.

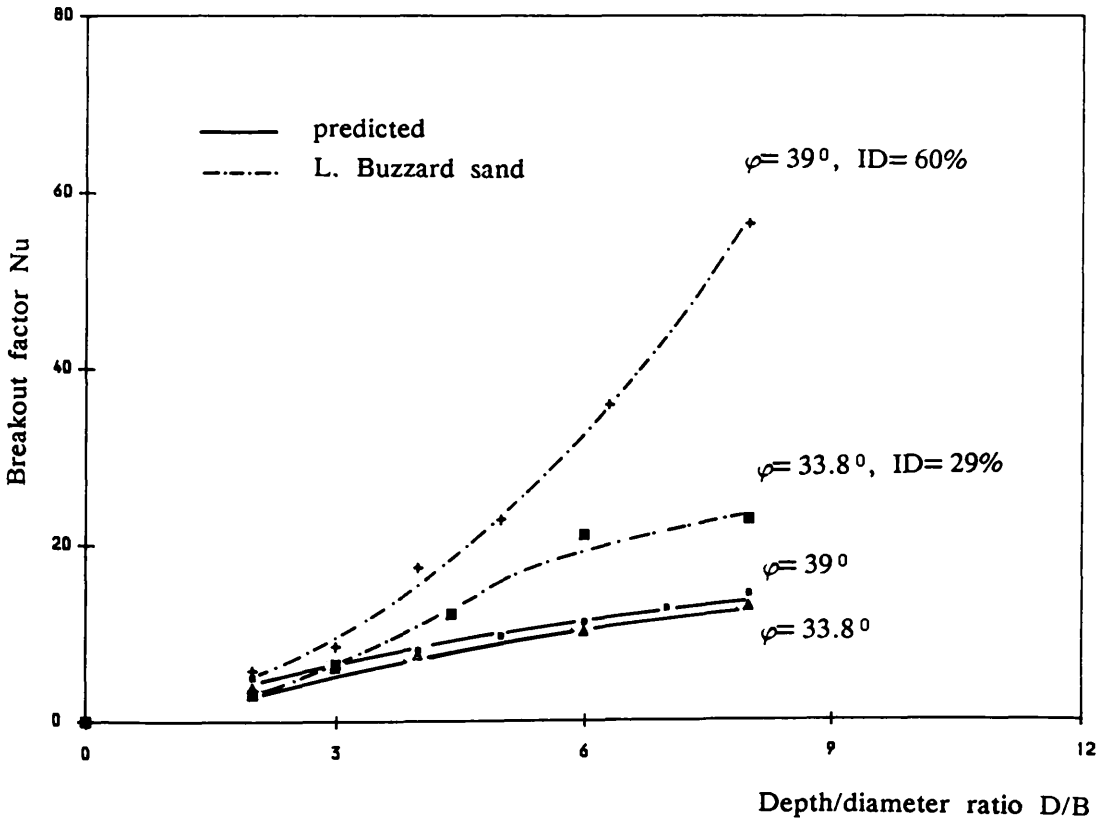


Fig. 5-26 Comparison of Rowe & Davis (1982) predictions with present test results.

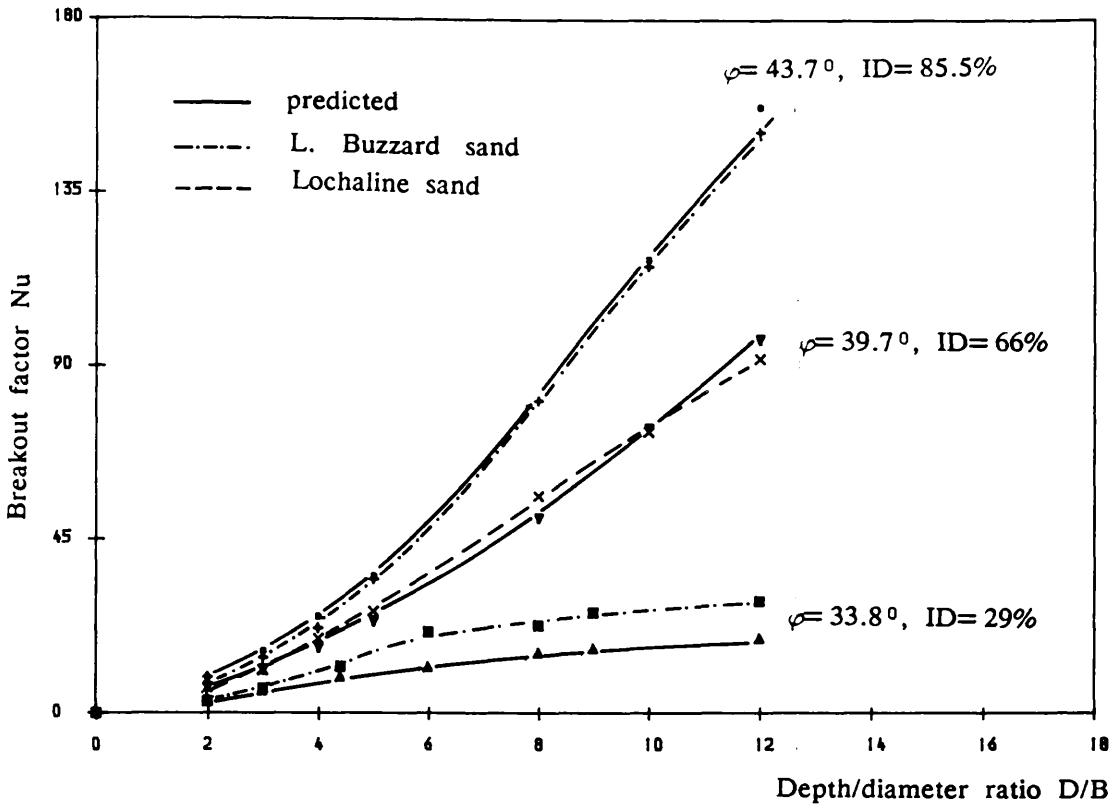


Fig. 5-27a Comparison of Fadl's (1981) predictions with present test results.

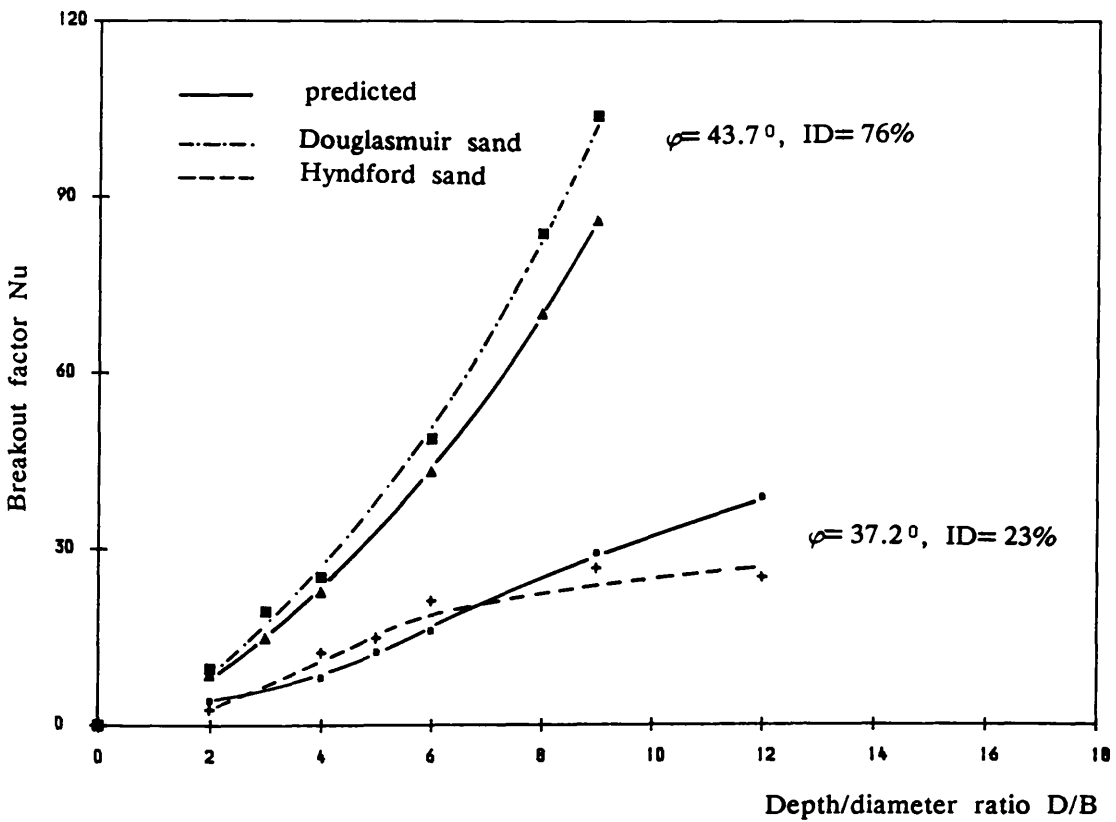


Fig. 5-27b Comparison of Fadl's (1981) predictions with present test results.

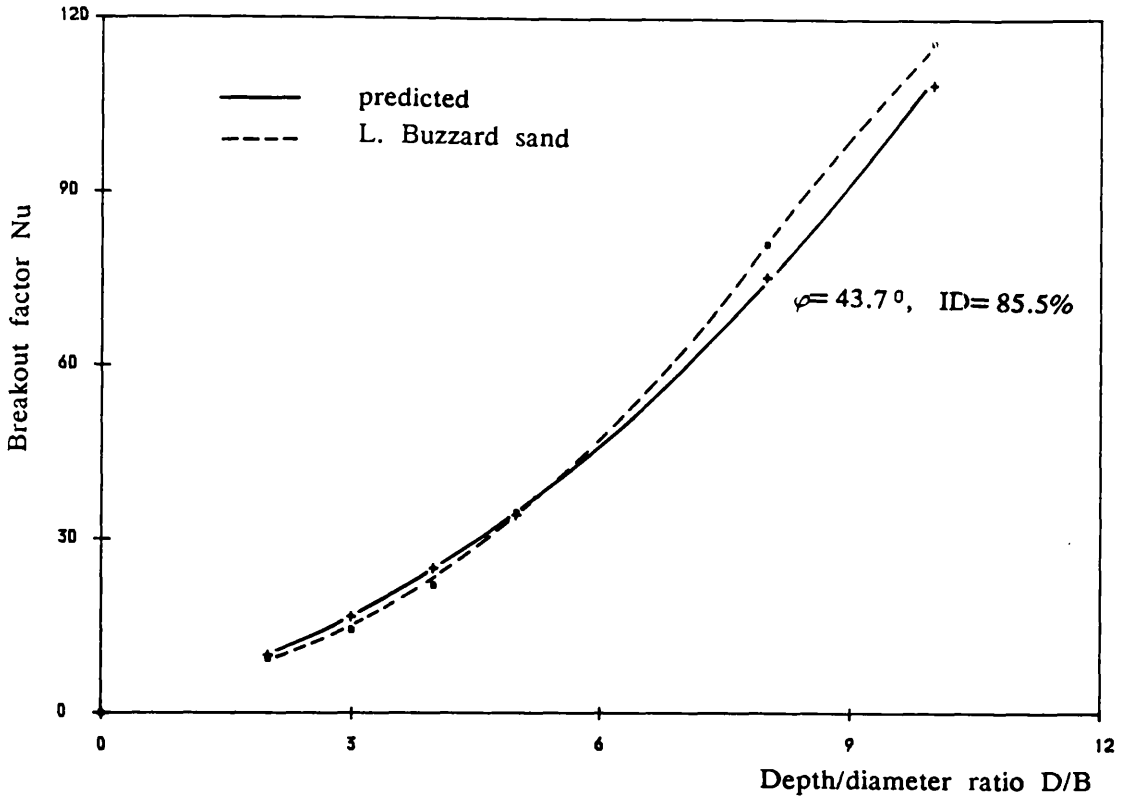


Fig. 5-28a Comparison of Saeddy's (1987) predictions with present test results.

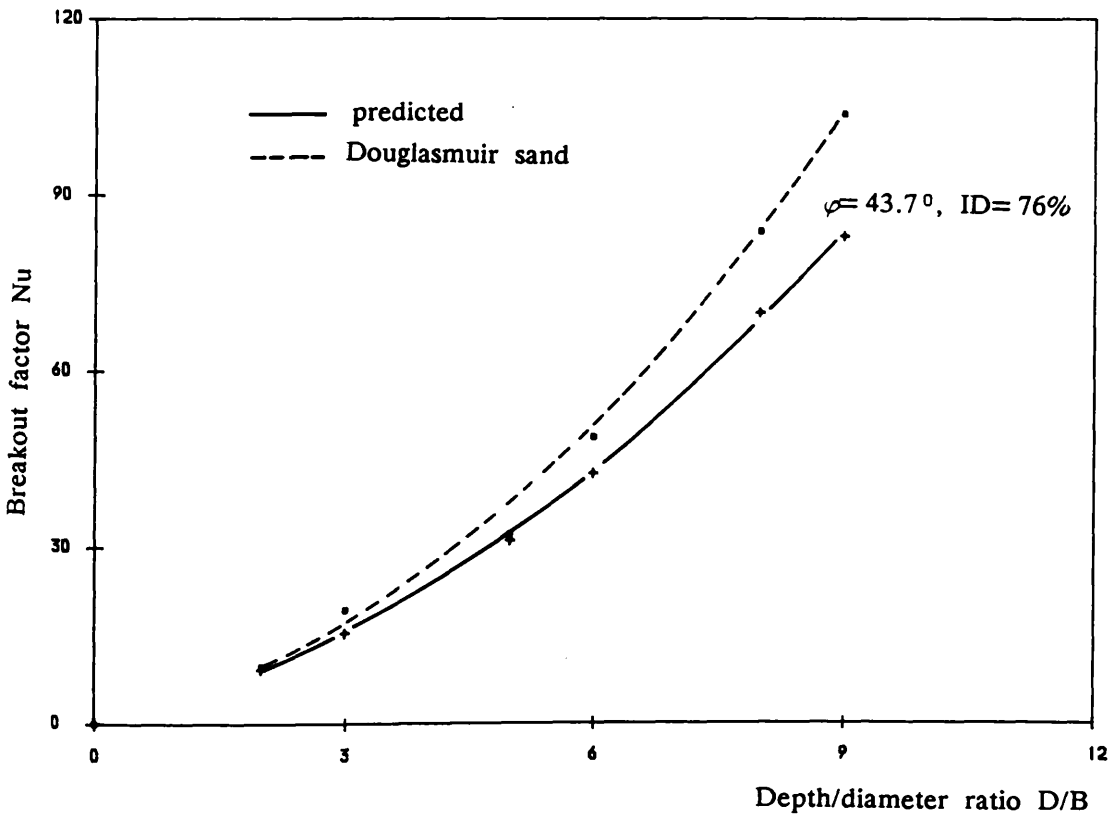


Fig. 5-28b Comparison of Saeddy's (1987) predictions with present test results.

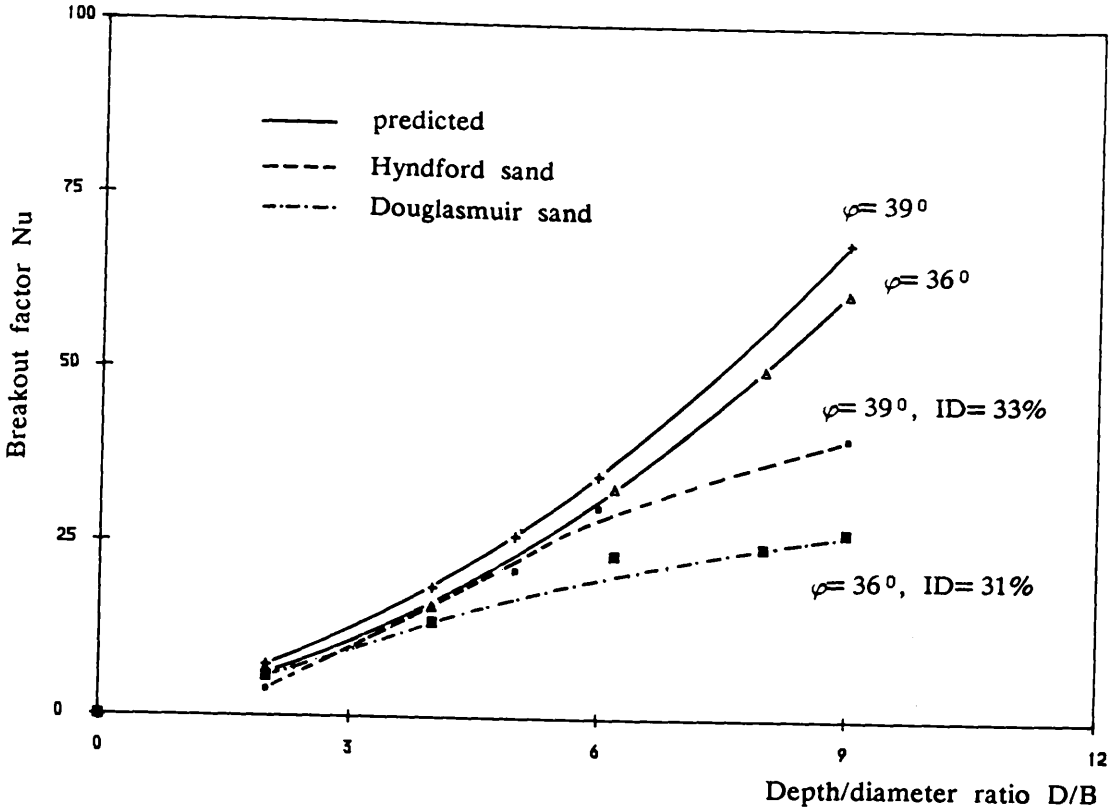


Fig. 5-29 Comparison of Murray & Geddes (1987) predictions with present test results.

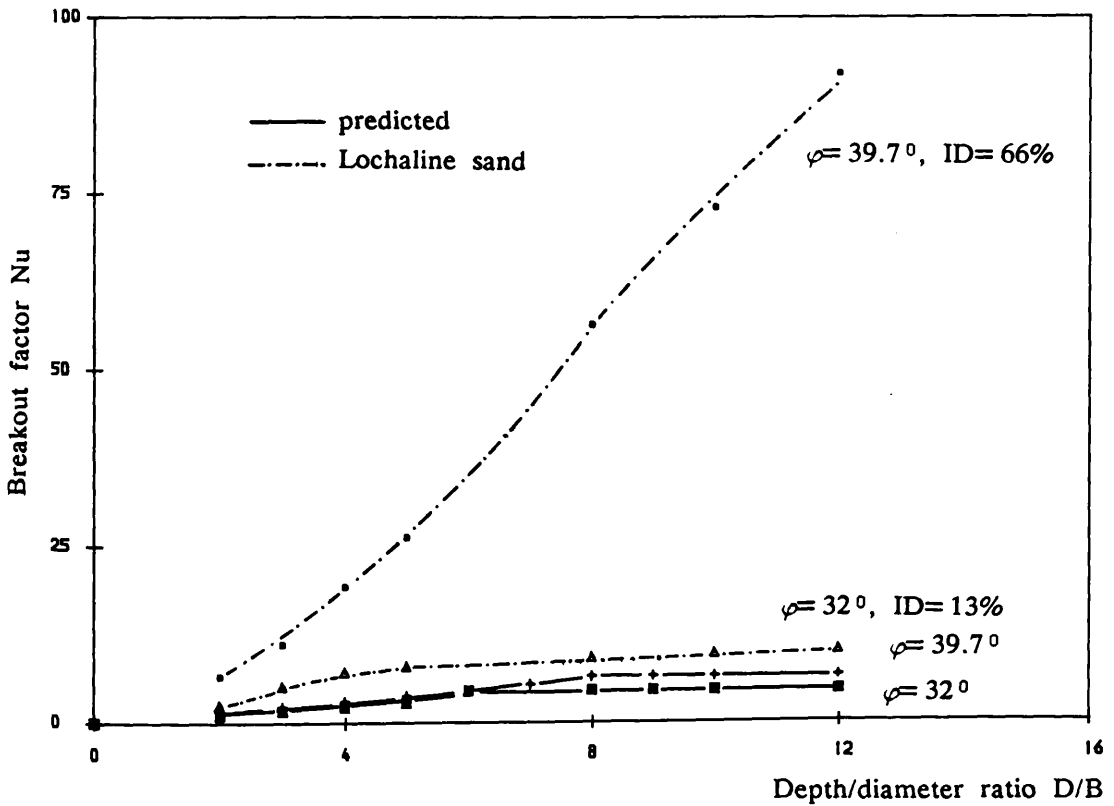


Fig. 5-30 Comparison of Tagaya et al (1988) predictions with present test results.

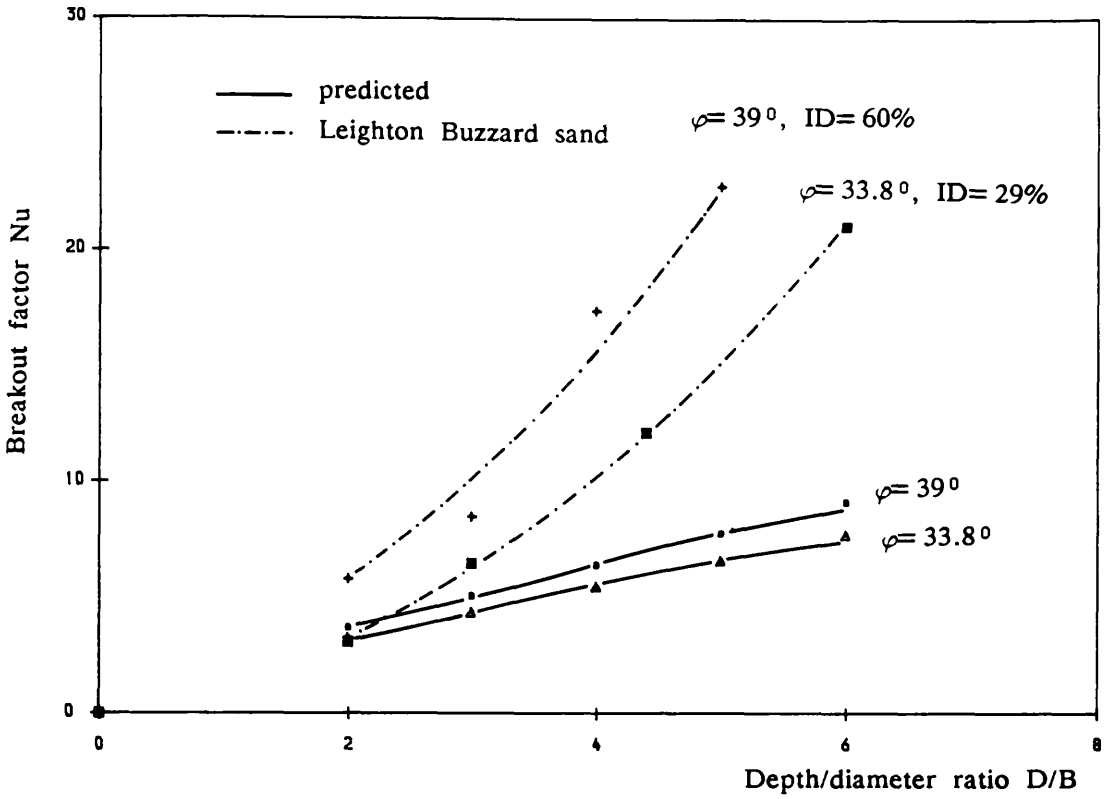


Fig. 5-31 Comparison of Vermeer & Sutjiadi (1985) predictions with present test results.

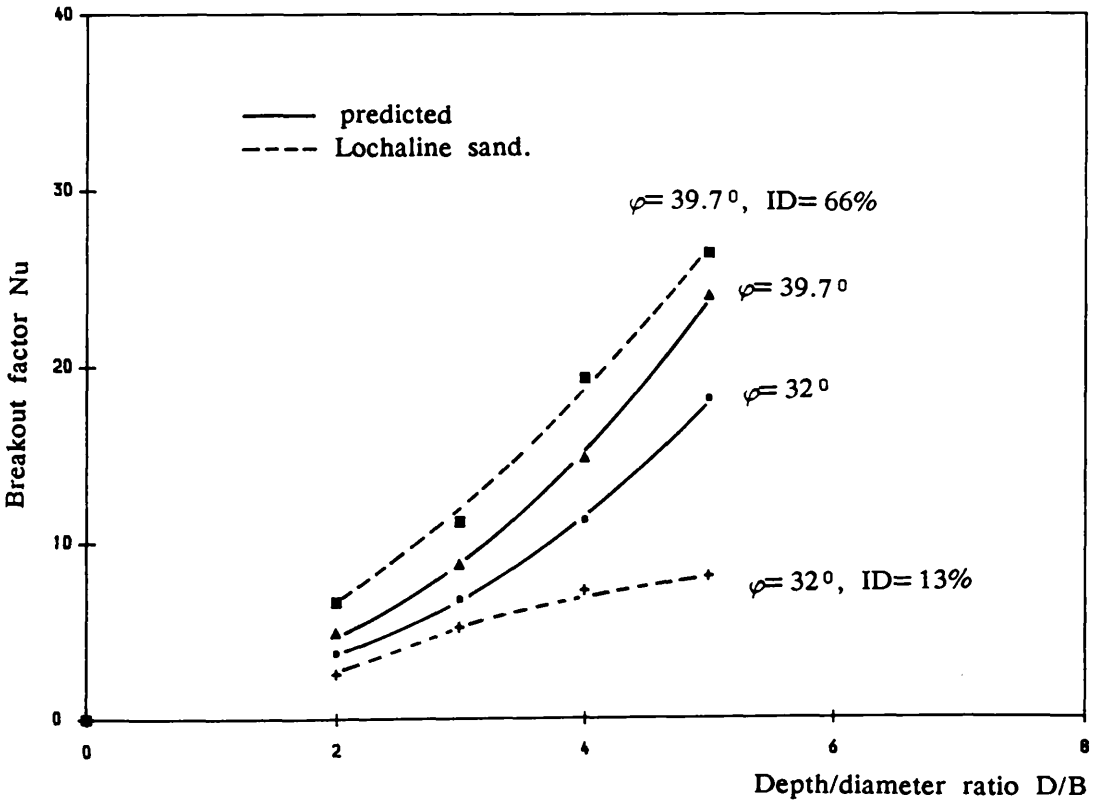


Fig. 5-32 Comparison of Koutsabeloulis & Griffiths (1989) predictions with present test results.

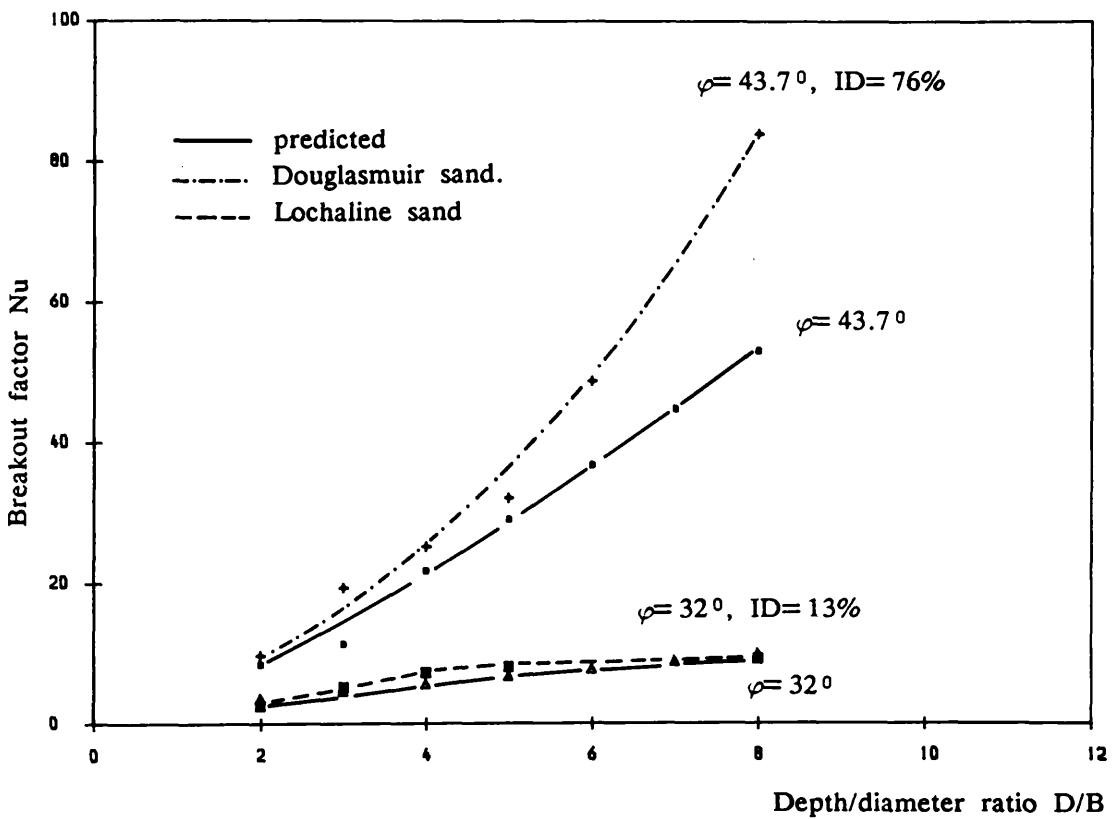


Fig. 5-33 Comparison of Frydman & Shaham (1989) predictions with present test results.

Chapter 6

THE STEREO PHOTOGRAMMETRIC METHOD FOR OBTAINING DISPLACEMENT AND STRAIN FIELDS

6-1 INTRODUCTION

Engineering testing often involves the measurements and analysis of displacements or deformations in materials under various types of loading conditions. For many problems in soil mechanics it is by no means trivial to establish the shape of the displacement field. It is especially important to know the characteristics of the displacement field in order to relate it to the relevant soil mechanics parameters such as ϕ , ψ etc... . In the literature several successful methods have been described for performing such measurement.

In the present investigation, stereo-photogrammetry, a technique by which geometrical information is derived from a pair of negatives or photographs, has been used. Although its best known application is in topographic mapping, it is being applied to an increasing extent to a variety of scientific and engineering measurements.

In this chapter a literature review of the different methods is given as well as a description of the technique used in the present investigation.

6-2 LITERATURE REVIEW

The various techniques used for measuring displacement may be divided into five groups, depending on the method employed for recording the soil movements, as follows:

6-2-1 Direct measurement

This technique involves displacement transducers embedded in the soil mass, which are able to record the local displacement directly. Eggestad (1964) has used specially made variable inductance transducers to monitor the sand movements below a footing, Carr (1970) has used embedded mechanical gauges capable of sensing horizontal or vertical soil displacements. A particular disadvantage of the method, such as the lack of a practical way of checking its accuracy was reported. The fact that the transducer embedded in the material (soil mass) is a foreign object, and hence interference is unavoidable, reduces the reliability of the results. Furthermore, a large number of transducers are necessary in order to obtain representative information on a displacement field, but this will inevitably result in a substantial alteration of the material properties. However, the use of telemetric cell gauges (Prange, 1971) minimises to a certain degree the influence introduced by the presence of the connections by transmitting the signal out of the soil mass.

6-2-2 Photographic technique

The use of photography in model studies is claimed to have been introduced to soil mechanics by Kurdyumov in 1891 (Malyshev, 1971). The method involved time exposure photographs of the indentation by a model footing in a sand bed

contained in a glass sided tank, where the actual slip surfaces in the sand mass could be defined as the boundary between the sharp (in focus) and the blurred (out of focus) parts of the photographs. Since that time, a number of different methods have been developed involving photography coupled with various measuring devices. The above mentioned method has been widely used by many investigators. Qualitative information about the displacement patterns may be obtained from this technique, but no quantitative analysis is possible. The time exposure photography method does not distinguish clearly the amounts of movement within the disturbed zone and it is not possible to measure the magnitude of the displacements within the disturbed zone.

6-2-3 X-rays technique

This technique involves radiographic recording of embedded lead markers. Gerber (Tchebotarioff*, 1954), (Bourdeau & Recordon, 1988) pioneering this method as early as 1929, used x rays to observe the total movement of embedded small lead spheres in his tests on footings on sand, taking two radiographs on the same film, one before and one after the application of the load to the footing. Since then, this technique has been dramatically improved by the Cambridge University Group (Roscoe et al, 1963). James (1972) pointed out that the sharpness of the image, which affects the accuracy of the measurements, depends on the model thickness. At points which are far from the centre of the image, the markers are less clear than at the centre. This is due to divergence of the X-rays as they penetrate greater distance near the edges of the image than at the centre. This method can only provide information about the displacements at the points where the lead shot are placed. Such information may not be sufficiently representative (in the case of a high displacement gradient).

* (After Maddocks, 1978)

6-2-4 Other methods

An extended use of the Moire method has been used for the investigation of the strain state in foundation beds by Nikitin & Nesmelov (1973) who superimposed the positive of an initial photograph (before loading) to the negatives of successive photos at different stages of the test, producing a Moire pattern in transmitted light. The accuracy of the method using irregular gratings is claimed to be approximately the same as when using regular gratings (10^{-4} for a spacing of 0.02mm). Recently, new sophisticated techniques have been introduced such as the optographic trace recording. This technique was introduced at the University of Braunschweig (FRG) in 1980 in the field of optimization and humanization of industrial manufacturing process. It has been modified by Feeser (1984) for use in geotechnical testing (fig. 6-5). This method is intermediate between X-ray photography and stereo photogrammetry but it is less suitable for use in sand grains. Pater & Niewenhuis (1987) have used a method related to the well known speckle interferometry to assess the deformation of a sand surface during cone penetration, using double exposure photographs made on high resolution film. The displacement between exposures was determined with the aid of the interference pattern that is formed by directing a laser beam through the negatives. The technique of laser speckle interferometry is not easy to use since the interference pattern cannot be obtained very clearly (sand grains rotate easily and there is always a loss of coherence between successive pictures). Wood (1984) used a photoelastic technique to obtain the state of stress of crushed glass in a conventional shear box. However, the technique can only be used with materials that possess photographic properties (crushed glass, glass discs), so the technique has the immediate disadvantage that it cannot be used with any real soils.

6-2-5 Stereo photogrammetry technique

This method, which was developed by Butterfield et al (1970), is based on the fundamental principles of conventional stereo photogrammetry. Close range photography techniques yield global information, on both components of displacement, throughout cross sectional areas; i.e, the number of possible measurements is limited only by the resolution of the photographs. High density displacement information allows the comprehensive analysis of strains. Also, since the photographs represent a permanent record of the event, information may be obtained from them at any time following their exposure. Typically, a test material is housed in a rectangular container and is visible, in cross section, through transparent glass plates which constitute one side of the container. Successive photographs of the model are taken by a fixed camera as the test progress. When two photographs, including a relative displacement of the soil particles with respect to a fixed object, are viewed together as a stereoscopic pair, a three dimensional image with distinct topography will be perceived. The test material may or may not contain targets for measurements at discrete points. If targets are not present, it becomes necessary for the materials to have sufficient texture to form a discernable surface for photogrammetric measurement. Photogrammetry has a number of inherent features which can be advantageous when considering the technique for specific applications. Butterfield et al (1970), Andrawes (1976) and Welsh (1985) listed the following advantages:

- 1- Remote, non contacting measurement can be made.
- 2- No embedded markers are used.
- 3- The photographs provide a permanent record which can be remeasured at a later date.

- 4- Measurement can be made with the object in situ.
- 5- Conventional standard equipment available for stereo photogrammetry can be used directly.
- 6- Efficiency of measuring the displacements in the areas of large discontinuities or high displacement gradients since every particle can be individually traced.

6-3 REVIEW OF PREVIOUS WORK

6-3-1 Laboratory based studies

The application of close range photogrammetry to soil mechanics problems is not a new concept. Turpin (1958) measured soil movements around a laterally loaded pipe which was a scale model of a piling. Two non metric 4.5 inch Crown graphic cameras with 135mm focal length lens were used. The object distance was 56 cm. Image coordinates were measured with a Kern Dkm 1 theodolite. Three dimensional movements of glass beads on the soil's surface were determined with a probable error of 0.25-1.0 mm. El-Beik (1973) determined three dimensional deformation in soil models undergoing centrifugal testing (fig. 6-3). Two Zeiss UMK 10/1318 cameras were used. An 800 × 600 mm soil surface area on a centrifuge was photographed from 1.5 m. The subject was moving at 45 m/s and had to be flash stopped. Stereophotographs of soil models subjected to steadily increasing gravitational forces were recorded and measured in a modified Kelsh stereoplotter. Spot height measurements at between 9 and 20 points enabled settlements/heave curves to be constructed (fig. 6-4). From these graphs the nature of the failure of the soil models could be determined and used to predict the behaviour of the soil in practice. Wickens & Barton (1971) used motion parallax

to compute movements in a model of an excavated rock slope. A 2.4m by 1.2m cross section of the model was photographed through a 25 mm thick glass plate. A 50 mm grid was etched inside the glass. A Santoni A camera was used at a 2.4 m photographic distance. A Zeiss (Pulfrich) stereocomparator was used to measure the parallax at grid points and at the soil immediately adjacent. The first use of photogrammetry for the analysis of planar displacements in soil was reported by Butterfield & al (1970), the technique involving taking single photographs, from the same camera position, of a glass sided tank which contained the soil under investigation. Photographs were taken before and after the sand within the tank was subjected to movement by a moving wall or wedge situated in the tank. The photographs were taken on fine grain film with a 35 mm camera (55 mm lens) at about 1 m range. By examination of the photographs in an analogue stereoplotter, the relative height of features could be measured and displacement contour diagrams produced (fig. 6-1). Maddocks (1978) used the same technique to assess the field displacement occurring when a static or dynamic pull out load was applied to a ground anchor. An aerial photography camera with either a 360 mm or 135 mm lens has been used. A Zeiss Stecometer was used to analyse the results from a consecutive pair of negatives and contours of strains and displacements were subsequently produced. Davidson et al (1981) used stereo-photogrammetry to monitor the deformation of sand around a cone penetrometer tip, and a Fotocartigrafo Nistri model VI stereoplotter was used to measure the different displacements (figs. 6-2a & 6-2b). Wong & Vonderohe (1978a, 1978b, 1981) used similar techniques to measure displacements of sandy soils around tunnel models (fig. 6-6), using a Kodak, bellows type, press camera with a 20 × 25 cm format and a 305 mm length Ektar lens for the photography, and a Wild STK stereocomparator for the Stereoscopic coordinate measurements. Desrues et al (1985) used the motion parallax technique to find the localization of deformation on dry sand (fig. 6-8) in

a true triaxial apparatus and a biaxial apparatus. A Stecometer type C has been used to define the shear band propagation. Cichy et al (1987) monitored the zone of interaction between soil and structure in a shear box (200 mm × 200 mm × 100 mm) having a frontal glass side. A Linhoff chamber, plate (90 mm × 120 mm) and a Stecometer type C have been used to present the displacement fields (fig. 6-7).

6-3-2 Field based studies

This technique is also relevant to the measurement and monitoring of large features in the field (for example, rock faces, landslides, retaining walls). The use of close range photogrammetry for monitoring earth and rockfill dams has been discussed by Moore (1973). He described the use of a Wild P30 phototheodolite for monitoring the three dimensional displacements of the Llyn Brianne rockfill dam, in mid Wales, during several stages of construction. By using a Wild A7 stereoplotter, measurements were taken at over 80 targets, at different levels of fill. The results indicated a range of displacements varying from 0.1 to 0.6 m (fig. 6-9). Brandenberger (1974) discussed the use of photogrammetry as part of a dam deformation monitoring programme in Quebec (Canada). Data was acquired using a Wild P30 photo - theodolite from geodetically surveyed control points on the downstream side of the dam face. From photo coordinates measured on a monocomparator, the ground coordinates of 17 common test points on the dam face were computed. Bozozuk et al (1978) used the same technique to record the movements of previously driven piles during the installation of 116 concrete piles in marine clay. A Wild P-31 camera was used to take photographs of the piles as they were driven over a certain period of time. A Zeiss Jena stereocomparator 1818 was employed for the photogrammetric analysis. Veress & Sun (1978) used a modified KA-2 aerial camera to monitor the deflection of a gabion wall which was

over 400 m long and varied from 2m to 18m in height. Photographs were obtained from fixed control points up to 1000 m from the wall. Over 100 target points were observed on an analytical plotter and ground coordinates computed.

6-4 STEREO-PHOTOGRAMMETRIC METHOD

6-4-1 General description of the method

This method utilizes the basic principles of conventional aerial stereo-photogrammetry where two photographic negatives, paper prints or glass plates of a stationary object are taken by a camera mounted in an aeroplane. The two photographs are taken from different positions during flight (fig. 6-11). A stereoscopic image of the object can be reconstructed from the two photographs if they are positioned in a stereo projector (as shown in figs. 6-11 & 6-12). The height of the object in the stereo image is caused by the difference in location of the corresponding points in the two plates, which is called X-parallax.

In the present investigation, although the camera is stationary and the objects, the soil particles, are moving as the photographs are taken, X-parallax is produced in a very similar manner to that produced in aerial photogrammetry. When soil particles are photographed, from a fixed camera position, before and after displacement, their simultaneous projection produces a stereo image. The particles appear to be elevated above a datum reference level formed from the image of the stationary background field (i.e. points of zero displacements). The elevation is proportional to the displacement of the particle which can be scaled by reference to an object included in photographs which moves by a known amount. Although the general planar displacement of the particle has two components U_1 and U_2 (fig.

6-12), it is only the U_2 component parallel to the viewing base line which gives rise to an elevated image. In order to measure the second displacement component U_1 , the two photographs are rotated through 90° such that the U_1 direction becomes parallel to the viewing base line.

The general displacement field however contains an infinite number of soil particles moving in different directions with various magnitudes of displacements. Thus if two photographs of such a field are viewed stereoscopically they will yield a three-dimensional optical model.

6-4-2 Recording the displacement field

An accurate and complete photographic record of the displacement field should fulfill the following conditions:

-1- A set of static reference marks should be recorded in the photographs. This is necessary to determine the datum level for height measurement in the stereo image. In the present investigation an orthogonal grid was scored for this purpose on the inside face of the glass side of the box. This grid was formed of equal squares $25\text{mm} \times 25\text{mm}$ for shallow anchors and $30\text{mm} \times 30\text{mm}$ for deep anchors.

-2- The camera used should have a good quality lens capable of producing sharp negatives so that the objects in the pair of photos are easily fused when viewed stereoscopically. In displacement field work the overlap is 100% and the movement of particles between photos will be recorded through the same part of the lens. Any distortion by the lens will produce similar errors in successive photos and the measurement of the parallax between points will not be significantly in error.

For a high degree of accuracy a plate camera capable of taking glass plates or large size negatives is preferable. In the present study a Hassebald 500 LM camera fitted with an 80 mm lens, capable of producing a 55mm by 55mm negative, was used. A clear relief image is enhanced if the photos contain contrasts between adjacent objects. Careful illumination of the model can improve the texture of the surface and the quality of the photos. Two floodlights were positioned at an angle of 45° with respect to the camera sand bed axis. The camera had a black screen (with only the lens protruding) to minimize unwanted reflections in the glass window. The camera position was approximately 0.5 m from the edge of the model in the case of shallow anchors and 0.8 m from the model in the case of deep anchors.

- 3- The camera should be fixed in position relative to the stationary parts of the model so that the optical axis is perpendicular to the plane of displacements. If the camera moves between photos this will become apparent, when a pair of photos is viewed stereoscopically, by differences in parallax between points in the model which are known not to have moved. Andrawes (1976) stated that the error introduced by a tilt of the camera of 2° from the perpendicular will introduce an average error of about $\pm 1\%$ in the value of the contours. In this study the camera has been mounted on a rigid pedestal and the pictures were taken with the help of a remote control device so that the camera was not touched during the test.

- 4- All photogrammetric work is dependent on the stability of the film which is used to make the photographs. Plates are considered to be the most accurate but are expensive, and an economical solution is the use of high resolution film. The negatives of the film or plate should be used in the photogrammetric work to avoid introducing errors due to enlarging or printing negatives. In this investigation large negatives, 55mm by 55mm each, were used to record the displacement fields. A

black and white Kodak technical pan film type 6415 with an extremely high resolving power has been used to take the photographs.

6-4-3 Measurement of the displacement field

Measurement of parallax, and therefore of planar displacement, can be made using any one of the following pieces of apparatus:

- 1- Mirror Stereoscope.
- 2- Stereoplotter.
- 3- Stereocomparator

The least accurate measurements of parallax are produced by using the mirror stereoscope. A high quality stereoplotter, when properly adjusted, can provide very accurate measurements of displacements. An increasingly common approach, when a numerical output is required, involves the use of a stereocomparator for measurement. The advantages of this type of measuring equipment include the possibility of accepting any principal distance, any base/distance ratio and any orientation, since the model is formed analytically. Many of the shortcomings of conventional stereoplotting instruments are solved by using a stereocomparator. In the present study, a Zeiss Jena Stecometer type c precision comparator in stereo mode has been used. It incorporates stereoscopic viewing of the photos to enable the operator to achieve the highest accuracy of measurement of parallax. The photos or negatives may be placed in the Stecometer without great emphasis on their relative orientation as this is dealt with in the analysis of the measurements.

6-4-4 The measuring principles of the Zeiss Jena Stecometer

The Stecometer is composed of two main parts: The optical system and the photo carriage (figs. 6-12a & 6-12b).

The optical system consists of the eyepieces and photo illumination system mounted above the photo carriages and the optical carriage situated below the photo carriages. The optical system of the eyepieces and the optical carriage moves as a single unit but can only move in the y direction as illustrated in figs. 6-12a & 6-12b. This allows the operator to scan both photos together in the y direction only. The measuring marks are therefore always at the same fixed spacing in x and are always parallel to the eyebase of the operator.

The photo carriage allows both photos to be moved together in the x direction using shaft B and permits the independent movement in y of the left photo relative to the right photo using shaft C. The independent movement in the x direction of the right photo relative to the left photo is achieved using shaft D. The rotations of the four shafts A, B, C and D are counted and converted to the measured movements in the x and y directions. The principle of the method is basically to align two identical points. The photo in the right cannot be moved independently in y so both must be scanned together in y using shaft A (Y_r control) to pick up the point in the right photo. The measuring mark is then seen on the point in the right photo. Once the same point is seen in both left and right photos, shaft C (P_y control) is used to align the two points in y and then a measuring mark appears over the point in the left photo as well as the right. The operator views the three dimensional image and aligns the measuring marks until they merge. The procedure for alignment in the x direction is that the point in the left photo must be picked up by using shaft B (X_l control) so that the measuring mark is on the point in the left photo. To complete the alignment in x direction shaft D (P_x control) is used to bring the point on the measuring mark. The alignment is an iterative procedure requiring the use of the four controls to locate the points, eliminate the y parallax and measure accurately the x parallax and vice versa.

6-5 OUTPUT FROM THE ZEISS STECOMETER

The output from the Stecometer consists of the measurement made by counting the rotations of the four control shafts. The measurements for a single point in the two photos are recorded as X_1 , Y_r , P_x and P_y and this information is numbered consecutively for successive points. The zero values in the X_1 and Y_r registers fix the position of the axes to which all x and y measurement are referred. The orientation of the photos in the Stecometer is not of a prime importance and will not affect the definition of the values X_1 , Y_r , P_x and P_y which relate the positions of identical points in the two photos to the commonly defined x and y axes. The quantities X_r and Y_1 which are not measured are obtained from the equations:

$$X_r = X_1 + P_x \quad \dots\dots\dots (6-1)$$

$$Y_1 = Y_r + P_y \quad \dots\dots\dots (6-2)$$

where the coordinates for the first negative (Y_1) are formed by adding the y parallaxes to the corresponding Y_r coordinates and for the second (X_r) by adding the x parallaxes to the X_1 coordinate. In displacement field work the vertical and horizontal axes of the model as recorded in the photos are oriented parallel to the x and y axes of the Stecometer. The measured parallaxes are therefore due to vertical and horizontal movements in the model. At the start of measurement the reference marks (grid intersections) which are known not to have moved are examined. The P_x and P_y values measured at these points represent the zero parallax condition and if all subsequent P_x and P_y measurements are related to this zero condition then the measured P_x and P_y values are the parallaxes in the negatives and therefore the displacements in the model in the vertical and horizontal directions are measured at the scale of the negatives. Referring to the above

equations for measurements made on a point that has not moved, the absolute P_x and P_y values are zero and the coordinates of the points in the two photos are identical. For all points where there have been movements, P_x and P_y will have non zero values and this will give rise to two sets of coordinates (X_l, Y_l) and (X_r, Y_r) separated by the amounts of movement P_x and P_y in the x and y directions. The investigation described in this section has related all movements to the first negative (left hand) so that the contour diagrams represent the movement that points will undergo during the interval between the two photos.

6-6 MEASUREMENT OF DISPLACEMENT

The major movements in the anchor model occur parallel to the vertical axis and therefore the negatives were set up in the instrument so that the vertical axis shown in the negatives was parallel to the x axis of the instrument. This dramatized the apparent relief when the pair was viewed stereoscopically. The negatives were placed on the photo holders which are mounted in the photo carriages and they can be rotated through 360° and locked in any desired position. Viewed stereoscopically there will be no y parallax as the measuring marks are tracked from one side of the photo to the other along the vertical axis marked when the negatives are accurately aligned. The vertical relief in the three dimensional image now seen is due to vertical movements in the model and the x and y parallaxes measured in the instrument will be the vertical movements in the model measured at the scale of the photos. In the negatives the grid appears as a distinct white colour "datum" surface from where the measuring mark can be driven towards the elevated sand particles. The first measurements were of the identifiable points (grid intersections) to establish the overall scale of the photos, the P_x and P_y values corresponding to zero x and y parallax. The measurements were made

point by point along steep slopes, peaks, depressions and breaks in the relief. If the whole displacement field is to be reproduced there must be an interpolation between the measured points. It was found that measurements at approximately 500 points for shallow anchors and 1000 points for deep anchors gave good reproduction of the images viewed. The measurements of all the points throughout the field took around 3 hours for shallow anchors and around 5 hours for deep anchors. Measurements made with the Stecometer are subject to an operator error due mainly to the tiredness of the eyes. To reduce the possibility of this error becoming significant the author from time to time checked back on points which had been measured previously. Readings on the same points did not vary by more than 15 microns during the measuring procedure.

6-7 COMPUTER PROCESSING OF DATA FROM THE STECOMETER

The author has developed a computer program which processed all the data given by the stereocomparator and plotted all the required diagrams using the UNIRAS package (UNIMAP). The measurements made in the Stecometer are from points which are randomly spaced throughout the field. These measurements are used by the program to calculate the values of the vertical and horizontal displacements which occur in the field at the position of the nodes of a regular grid which covers the whole field. The fields of the vertical and horizontal displacement components are then plotted. The displacement component values are combined to give the resultant displacements at the nodes of the grid and they are also used to derive the strains throughout the field.

6-8 STRAINS COMPUTATION

The strains are calculated from the values of the vertical and horizontal

displacement at the nodes of the grid. Each element of the grid is considered to be a square element (12.5×12.5 mm for shallow anchor and 15.0×15.0 mm for deep anchor). The vertical and horizontal strains are calculated through the centre of the element. The following assumptions (James, 1972) apply:

- 1- Displacements vary linearly across each element which in turn assumes that the sand in every element strains uniformly.
- 2- Changes in the geometry of the system during testing have a negligible effect on the calculated strains.
- 3- Compressive strains are assumed to be positive.

The shear strain is defined as the angular distortion at the centre of the element taken from the top right hand quarter of the element and is calculated from the appropriate vertical and horizontal displacements of the four corners of the element. All the strain values are assigned to the centres of the elements and the coordinates of the nodes of the grid containing the strains are redefined to these positions. The nodal points of each element are numbered proceeding in a counterclockwise direction around the element in the order 1, 2, 3 and 4 (see fig. A).

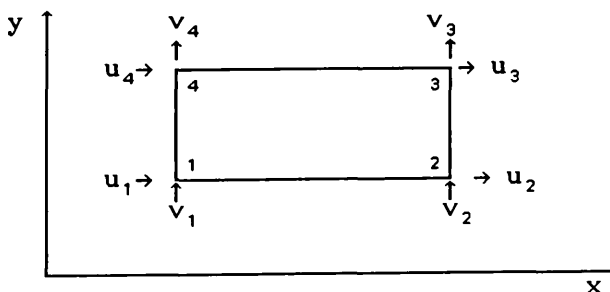


Fig. A Numbering convention for the nodal points

The following equations were derived:

$$\epsilon_x = \frac{(u_1 + u_4) - (u_2 + u_3)}{2x} \dots\dots\dots(6-3)$$

$$\epsilon_y = \frac{(v_1 + v_2) - (v_3 + v_4)}{2y} \dots\dots\dots(6-4)$$

$$\gamma_{xy} = [((v_2 - v_1) + (v_3 - v_4))/2x] + [((u_4 - u_1) + (u_3 - u_2))/2y] \dots\dots\dots(6-5)$$

The principal strains ϵ_1 and ϵ_3 are determined, in terms of the strain components ϵ_x , ϵ_y and γ_{xy} from the following equation which may be derived from Mohr's circle of strain shown in fig. 6-14a.

$$\epsilon_{1,3} = 0.5 (\epsilon_x + \epsilon_y) \pm [(\epsilon_y - \epsilon_x)^2 + (\gamma_{xy})^2]^{\frac{1}{2}} \dots\dots(6-6)$$

the maximum shear is given by:

$$\gamma_{max} = [(\epsilon_y - \epsilon_x)^2 + (\gamma_{xy})^2]^{\frac{1}{2}} \dots\dots\dots(6-7)$$

6-9 ERRORS AND ACCURACY

The main sources of errors in measuring the displacement field using the stereophotogrammetric technique are:

- 1- Movement of the camera during successive photographs
- 2- Distortion of the photographic films
- 3- Camera lens distortion
- 4- Geometric changes in the apparatus during testing

Taking these errors in turn as they apply to this particular study they may be

evaluated as follows:

- 1- No error was anticipated from this source since the camera was mounted on a rigid pedestal and was operated using a cable release in order to avoid any pressure on the camera that might have caused it to move.
- 2- No significant errors were expected from the film distortion as large size negatives were used directly in the Stecometer.
- 3- Although a sharp image is necessary, the quality of the camera lens is not of prime importance. Since any slight distortion of the image will occur in the same parts of the field for each successive photograph, the relative displacement (i.e. the difference) will not be appreciably in error.
- 4- The deflection of the glass side of the box was monitored during preliminary testing see plates 6-1 & 6-2 by fixing very sensitive displacement transducers to the front of the glass at different points. The transducers were connected to a data logger. It was found that the deflection averaged 0.015 mm. The normal earth pressure acting against the glass, which may cause an additional deflection, is very low for the problem studied, therefore the anticipated error from the likely relative movement of the grid network due to glass deflection is almost nil.

6-10 UPLIFT TESTING PROCEDURE

In the present investigation a push up test was chosen rather than pull out test for the following reasons:

- 1- The push up test is more convenient since there is no anchor shaft to create problems during sand deposition.
- 2- It was found that the difference between the push up tests and the pull out test for the same dimension of anchor and depth of sand is not significant (Fadl, 1981, Zakaria, 1986).

The apparatus (fig. 6-15 and plate 6-4) consisted of a wooden box, 600 cm by 300 cm in plan and 400 cm depth. The front viewing face of the box was designed to allow a 6 mm thick glass to slide in and out. Sufficiently stiff bracing for this glass face was obtained on the bottom and sides of the tank by the use of thin U metal plates. It was restrained against the frame by bolts screwed through tapped holes in the front of the box. A semi circular brass bush with 5 mm inside diameter was fixed in the base at the centre of the box immediately behind the glass face. Two semi circular brass discs 50 mm and 45 mm diameter and 13 mm thick were used for shallow and deep anchors respectively and were welded to the upper end of 5 mm diameter shafts. The shafts were 400 mm long, their diameters having been reduced to 5 mm from the middle to the upper end in order to be pushed through the bush. The bottom end of the shaft was fixed to a load cell which in turn was fixed to the base plate of a 1 ton Whykeham Farrance multispeed machine. A Sangamo transducer was also fixed to the base plate to record the displacement of the plate anchor. The load cell and the LVDT were connected to a data logger and a plotter in order to monitor the different stages of the test.

In order to minimize any increase in glass friction due to the grid, the inner face of the glass was cleaned with Genklene before each test. The half anchor was then positioned at the centre of the box. The friction between the bush and the anchor shaft, the anchor and the glass was reduced by smearing the anchor shaft and the front of the half anchor with silicone grease. In each test it was ensured that the half anchor remained completely in contact with the glass face so that the development of a gap between the half anchor and the glass face was kept to the minimum.

The sand was placed in layers of 30 mm thickness until the required depth was reached, a rectangular hopper, 650 mm by 300 mm in plan and 300 mm in depth, being used to produce a rain of sand grains and therefore achieve medium to dense densities. Details of the technique have already been given in chapter 3. The loose state was obtained by pouring the sand from a bucket into the box layer by layer, horizontal lines at 30 cm vertical spacings, marked round the box, assisting the placement and final levelling of the sand. After placing the sand the push out test was performed. Photographs were taken at regular upward displacements.

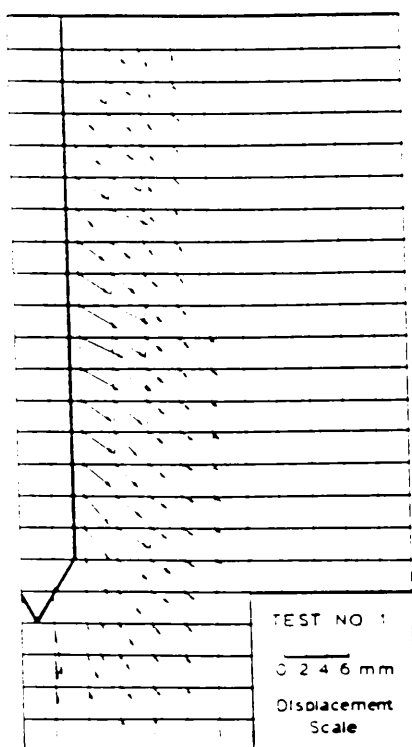


Fig. 6-2a Displacement Directions Around a Cone Penetrometer in Loose Sand (after Davidson & al, 1981).

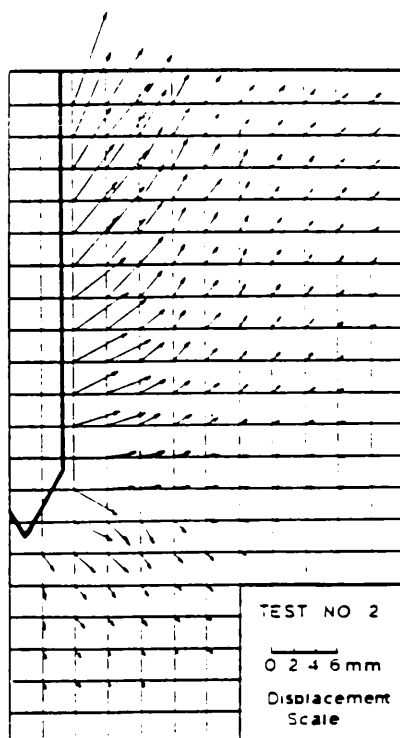


Fig. 6-2b Displacement Directions Around a Cone Penetrometer in Dense Sand (after Davidson & al, 1981).

Fig. 6-5 Displacements Around a Constricted Cone in Loose Sand (ID= 35%) (After Feeser, 1986).

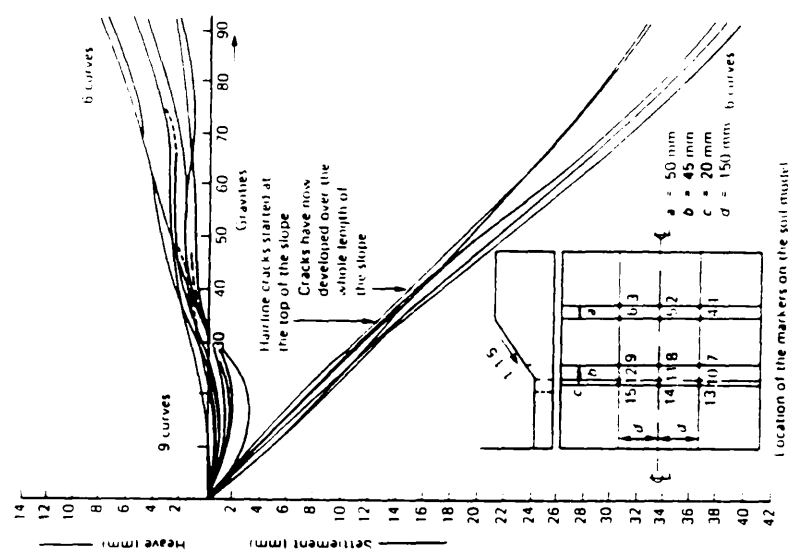
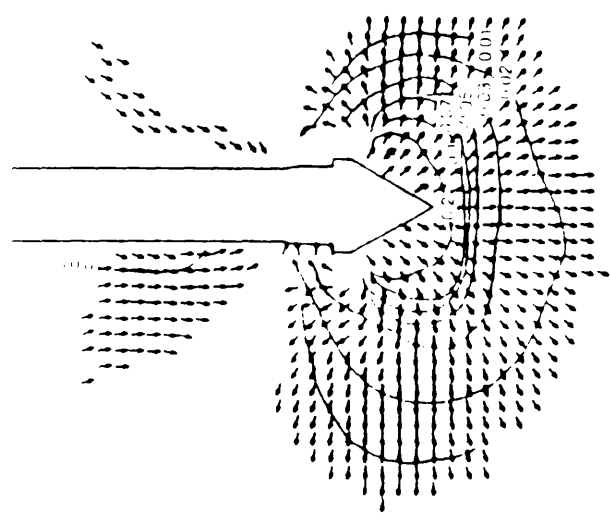


Fig. 6-3 Design of a heavy Centrifuge to Incorporate a Pair of Zeiss (Jena) UMK 10/1318 Cameras (After El-Beik, 1973).

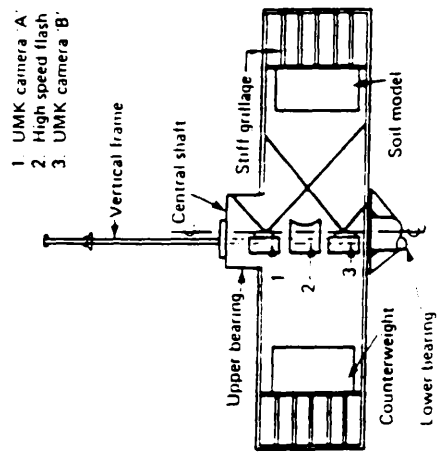


Fig. 6-4 Settlements/Heave Gravity Curves of Recompacked embankment in Keuper Marl Failure (After El.Beik, 1973).

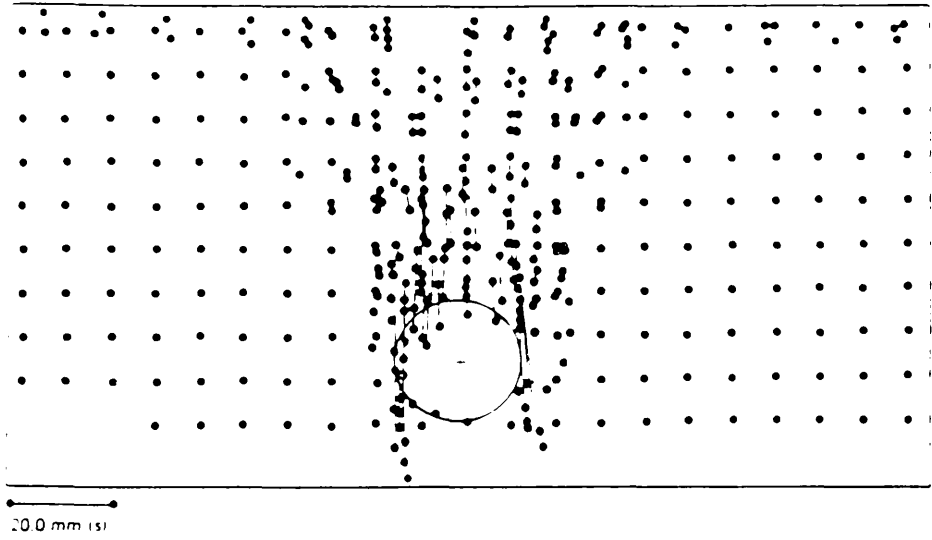


Fig. 6-6 Movement Vectors of Sand Particles Around a Tunnel Model Produced by The Time Parallax Method (After Wong & Vonderohe, 1978 & 1981).

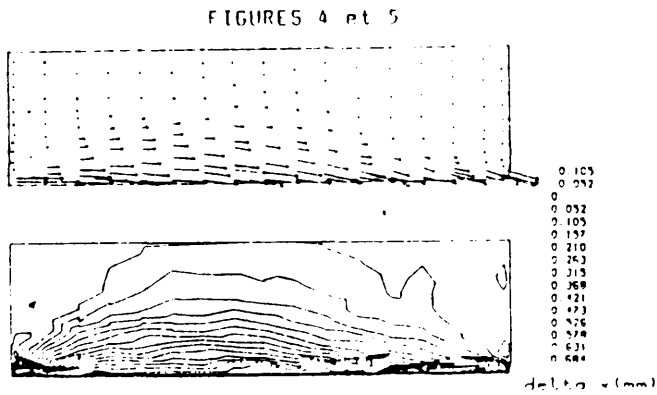


Fig. 6-7 Displacement fields and horizontal displacements contours of a dry sand in a shear box (After Cichy et al, 1987).

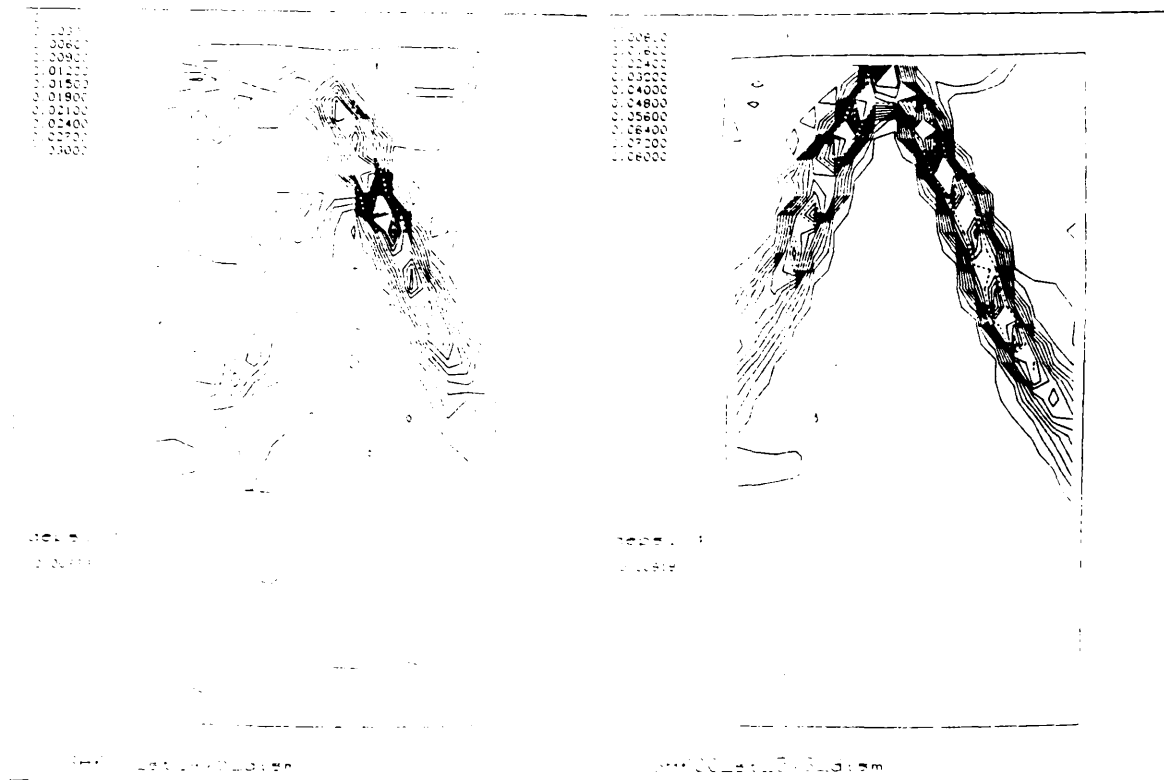


Fig. 6-8 Shear band propagation in a triaxial sample of dry sand (after Desrues et al, 1985).

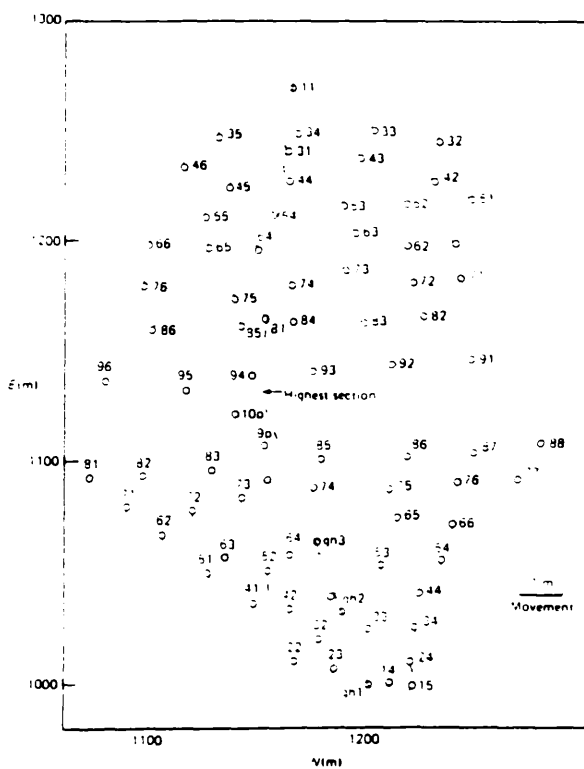


Fig. 6-9 Vector Diagram showing Horizontal Displacements of Targeted Points on Llyn Brianne Dam (After Moore, 1973).

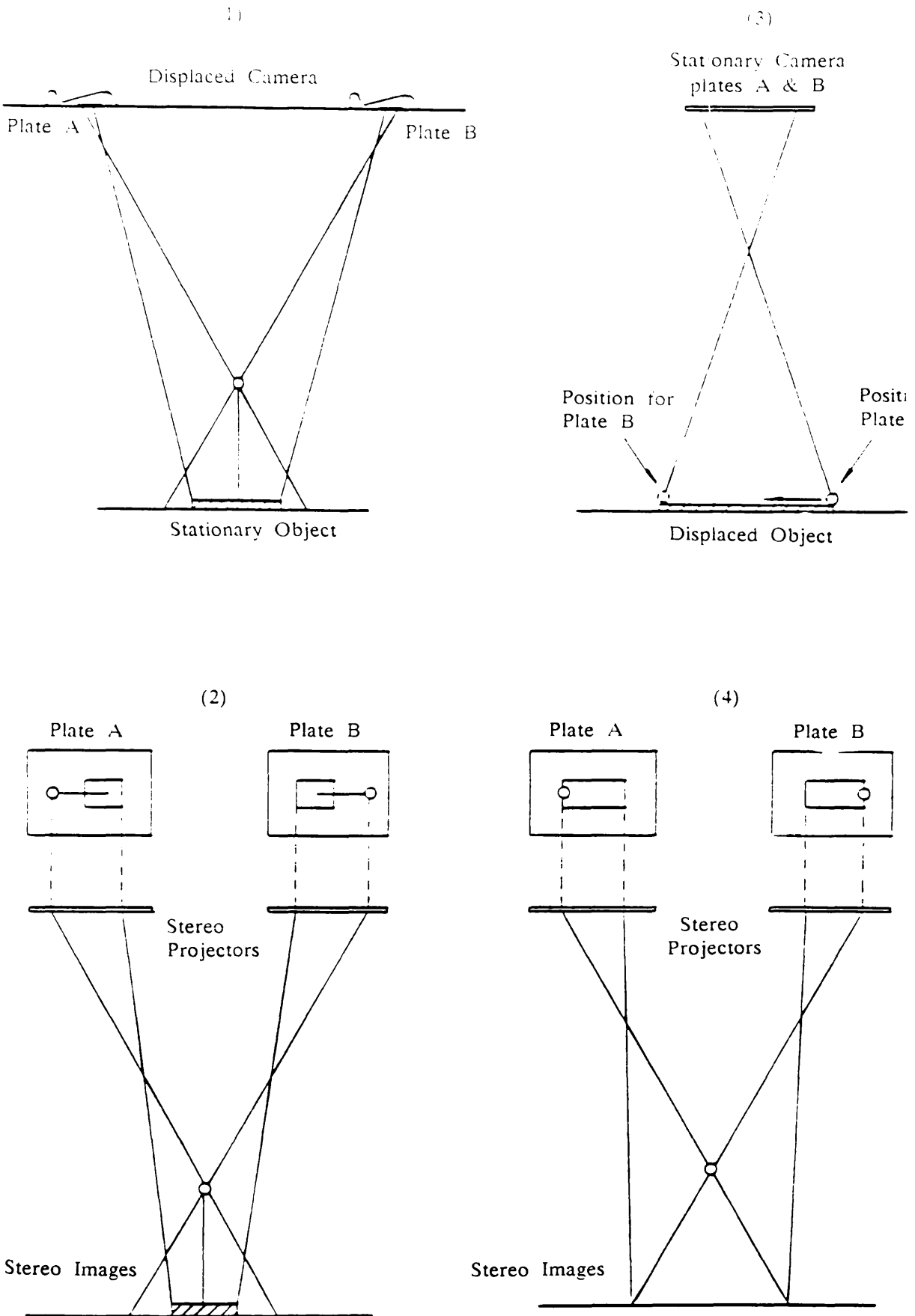


Fig. 6-10 Stereo images (After Andrawes, 1976).

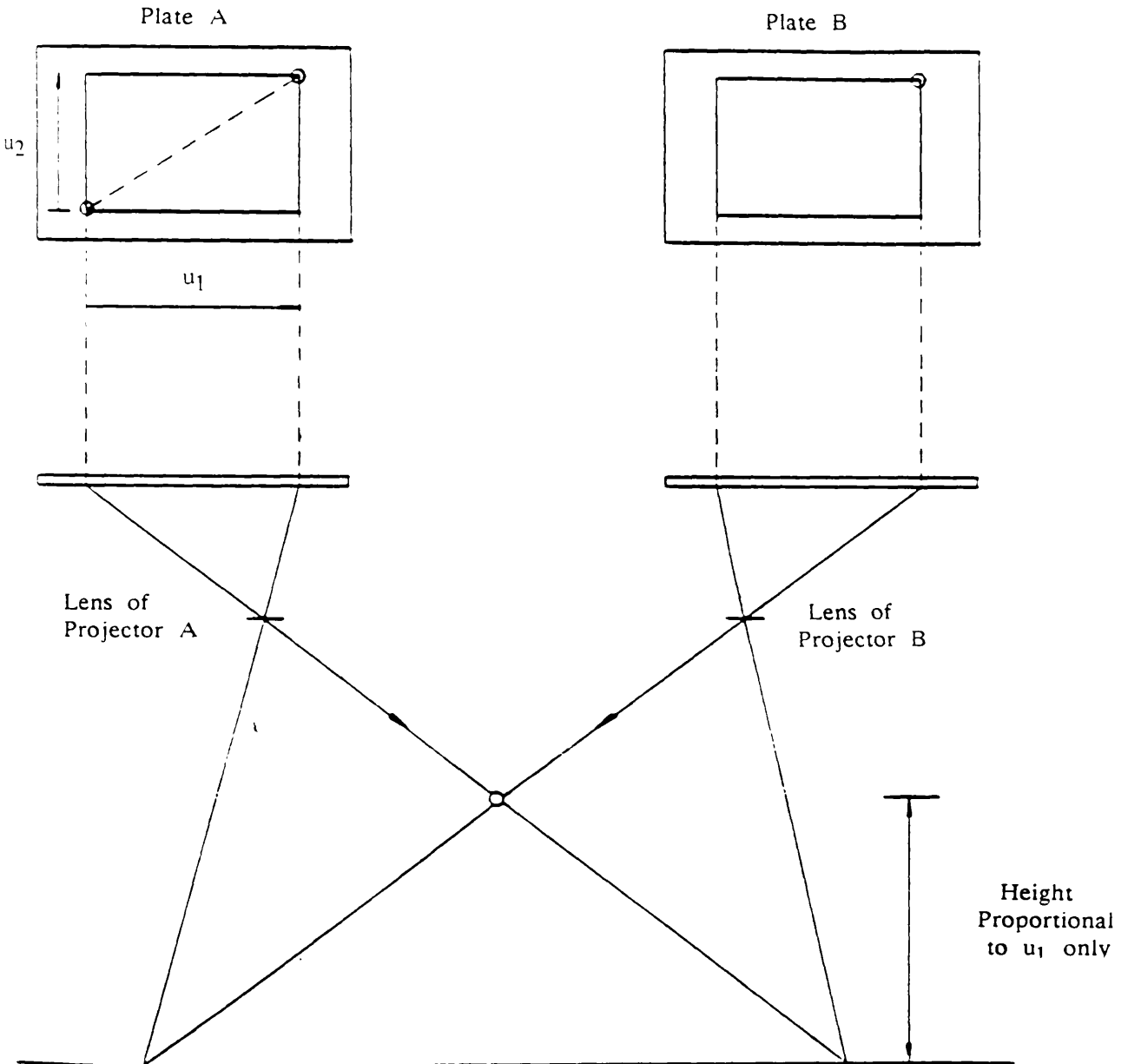


Fig. 6-11 General two-dimensional displacement (after Andrawes, 1976).

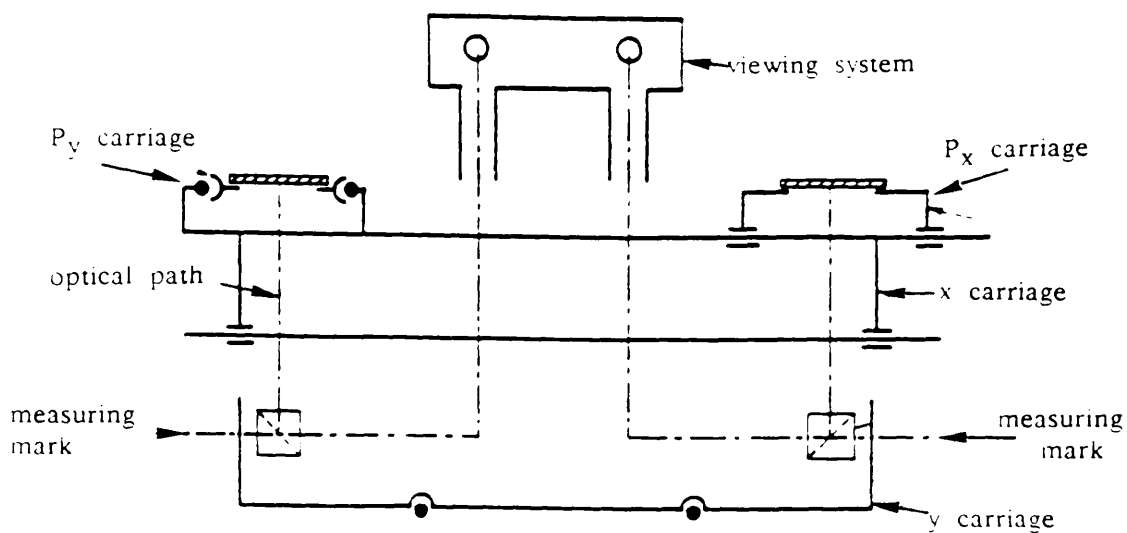


Fig. 6-12a Optical and measuring systems of the Zeiss Stecometer.

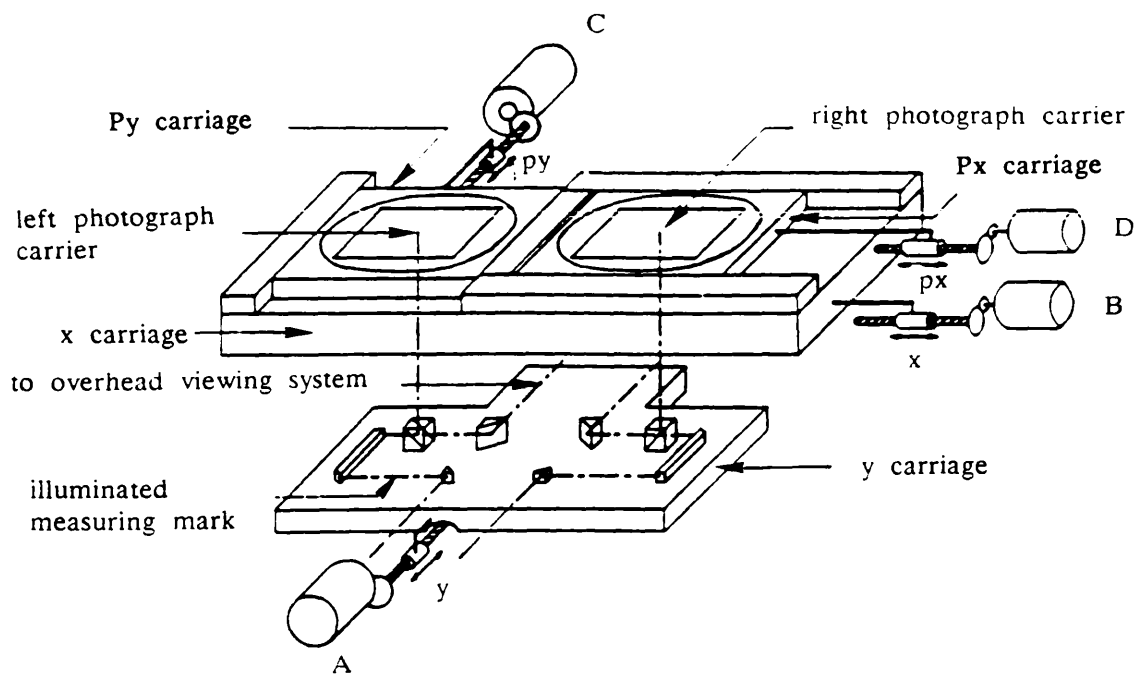


Fig. 6-12b Optical and measuring systems of the Zeiss Stecometer.

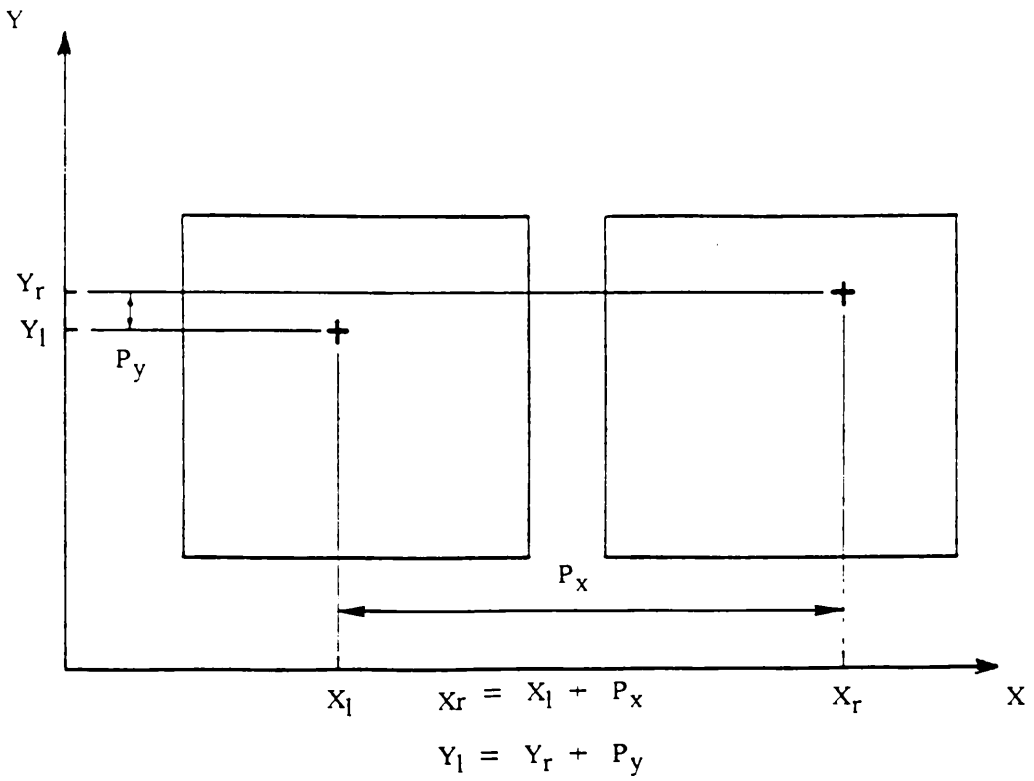


Fig. 6-13 Relationships between the quantities measured in the Stecometer.

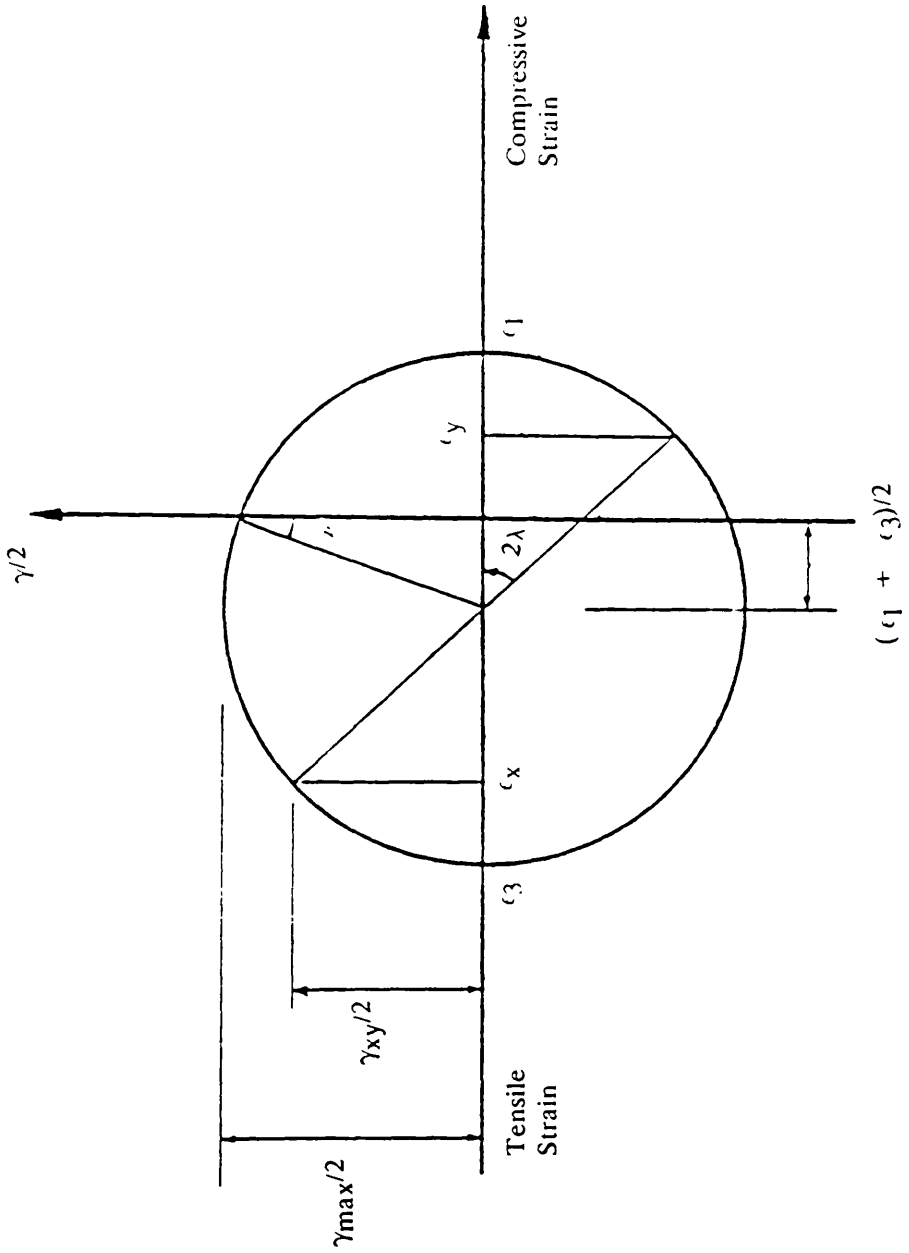


Fig. 6-14 Mohr's circle of strain

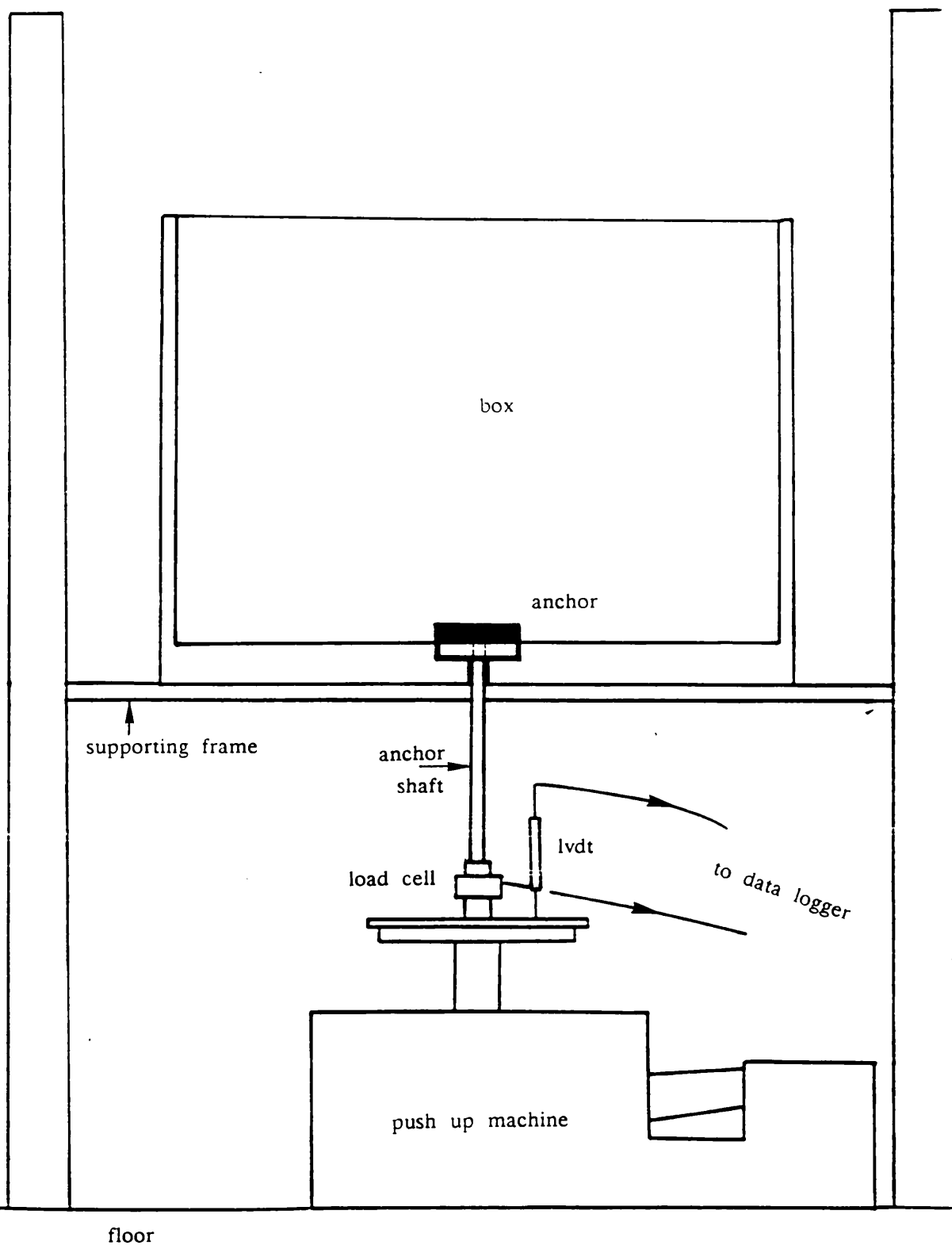


Fig. 6-15 Stereo-photogrammetric test set up.



Plate 6-1 Transducers position.

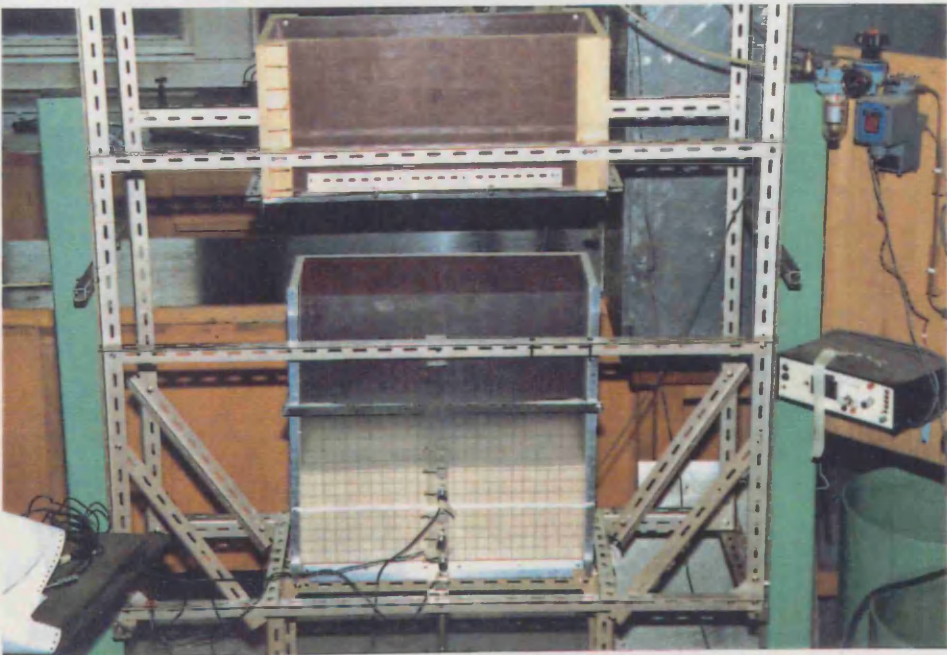


Plate 6-2 Glass deflection monitoring.

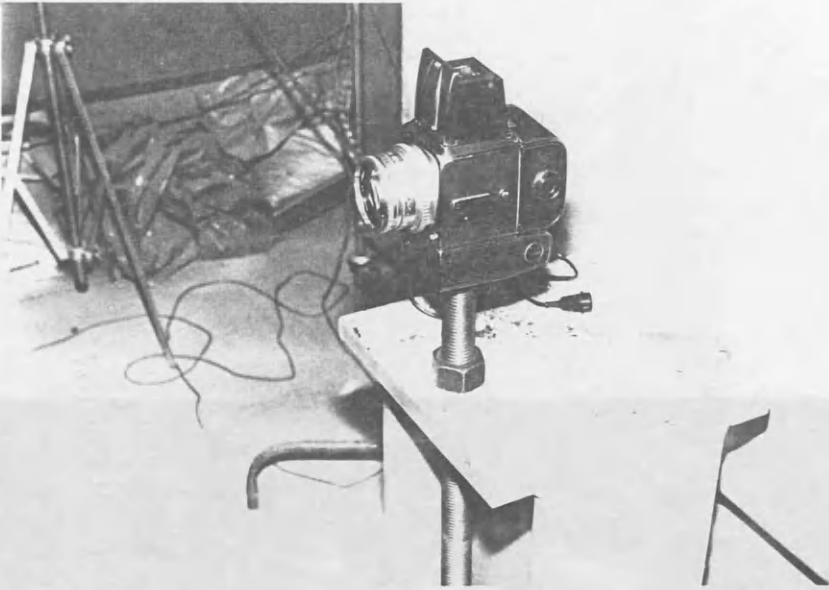


Plate 6-3 Hasselblad 500 LM camera.

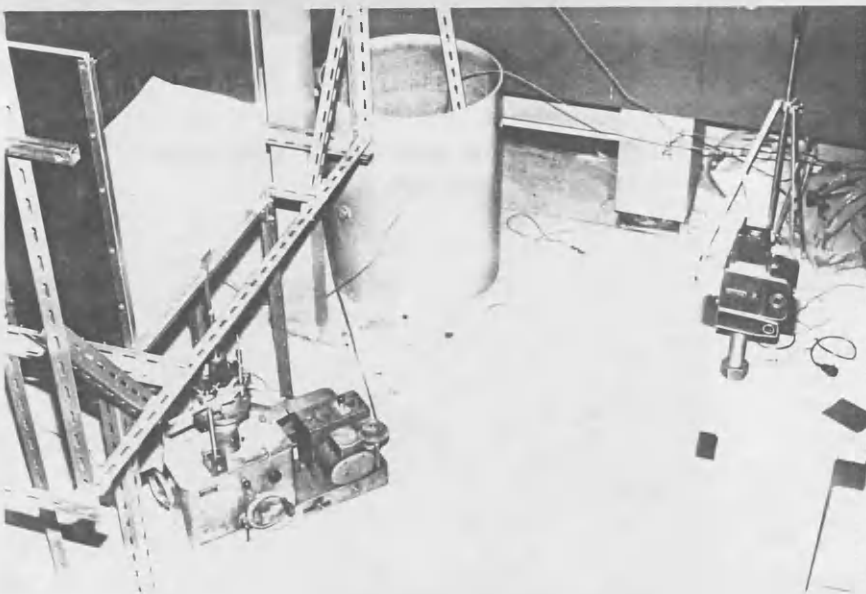
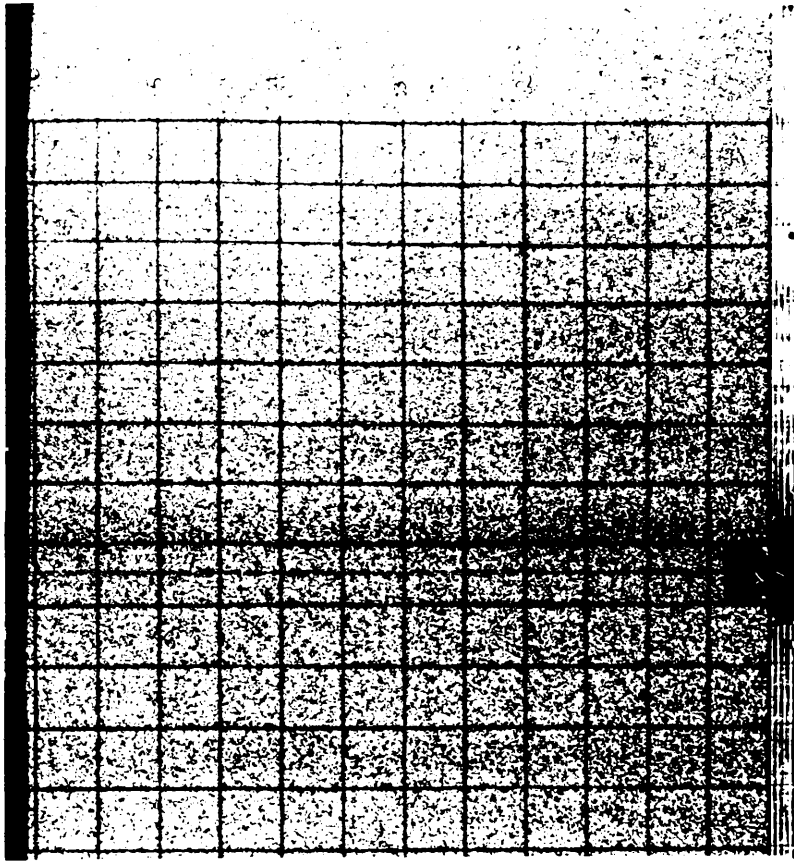


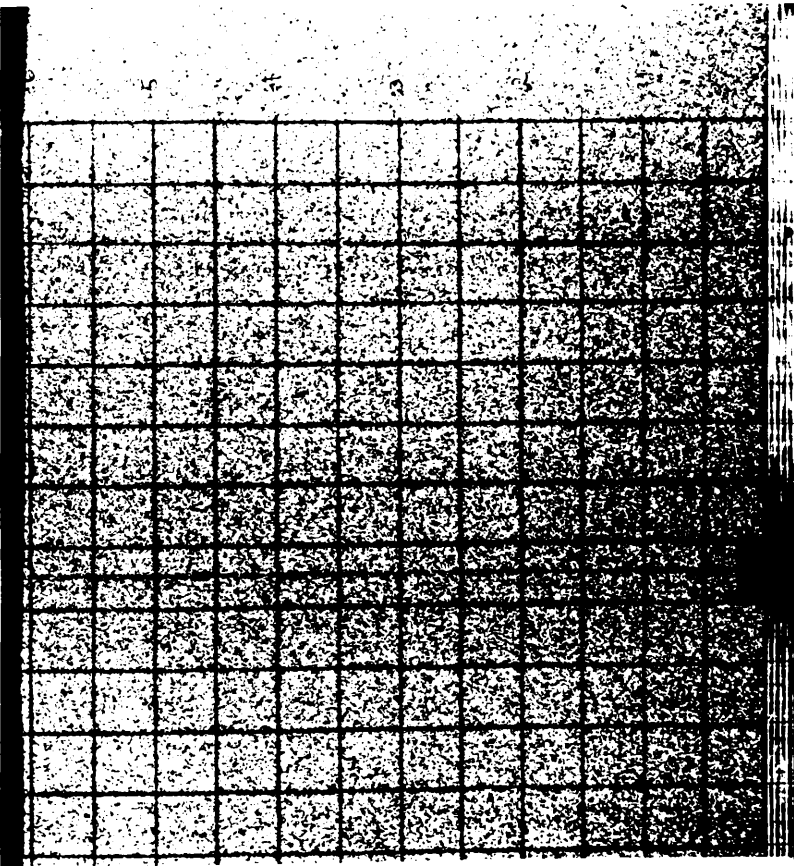
Plate 6-4 Stereo-photogrammetric set up.



Plate 6-5 Zeiss Jena stecometer type C
and data logging system.



(b)



(a)

Plate 6-6 Stereo-pair: model (a) before and (b) after a displacement increment.

Chapter 7

DISCUSSION OF THE STEREO PHOTOGRAMMETRIC TEST RESULTS

7-1 INTRODUCTION

Rupture layers in cohesionless soils are characterised by local increases in space between particles, which according to the normal relationship between voids ratio and strength, result in a relative weakness in the layer. It is also this decrease in density which leads to a clear record of the whole displacement field occurring at a given load. The purpose of these photogrammetric tests was to observe the extent of the zone of disturbed sand caused by uplift loading of a plate anchor. As has been explained previously, several techniques have been used to record and monitor the displacements of sand grains. However, the stereo-photogrammetric method was deemed to be the most accurate and therefore was used in this investigation. The main object of the tests conducted by the author was to examine the effect of relative density, depth of embedment, grain shape, grain size and grading of a cohesionless soil on the form of the zone of disturbed sand. Anchors buried at depth/diameter ratio $D/B = 4$ & 8 have been tested for this purpose. During each test a sequence of eight photographs was taken, the first prior to pushing, the remainder at approximately 1.0 mm upward displacement intervals.

The interaction between the anchor plate and the surrounding sand has been monitored throughout the loading, up to the post-failure of the plate anchor. The displacements of the sand resulting from this interaction have been measured

accurately and the development of these displacements is presented. In each test a large quantity of data is generated. The interaction between the anchor and the sand is represented by:

- 1- A set of displacement diagrams which show the displacement of the plate anchor and the surrounding sand that occurs during loading. In this case the contours are given in mm.

- 2- A corresponding set of shear strain diagrams which show the strain developed in the sand surrounding the anchor during loading. In this case the strains are given in (%).

The displacement diagrams and the shear strain diagrams are derived from the displacement fields measured in the Stecometer for each displacement increment. Due to the large amount of data accumulated only essential increments are herein reported. A typical load versus displacement curve is given in fig. 7-1. It shows a smooth peak followed by a softening stage. The numbers on the curve are the serial numbers of the photographs.

To enhance the work of presentation the soil anchor interaction is covered in three separate sections:

- 1- Shallow anchors
- 2- Deep anchors
- 3- Effect of grain size, grain shape and grading

7-2 DISCUSSION OF THE RESULTS

7-2-1 Uplift tests, shallow anchors $D/B=4$

7-2-1-1 Loose state, L. Buzzard sand

When the anchor is subjected to loading the load is transmitted to the sand surrounding it. The deformations occurring in the sand were observed and recorded. Figs. 7-2 to 7-13 show the displacements and strains for the different increments of the applied load. They show the zones of the bed that responded to the applied load and the variations in the response within this zone.

At the first stage of loading, anchor displacement $\delta=0.8$ mm, approximately 30% of the maximum load, the resulting deformations and strains of the sand are presented in figs. 7-2 to 7-5. The zone of sand responding to the above increment is confined to the area just around the plate anchor. The magnitudes of displacements of the sand immediately above the plate is nearly equal to the upward movement of the rigid plate. The strains, at this stage, occur mainly around the plate anchor. The sand is suffering vertical compaction.

For $\delta=1.8$ mm (50% of the maximum load) the resulting deformations of the sand are shown in figs. 7-6 to 7-9. It can be seen that the sand immediately above the plate anchor is displaced vertically upwards, the sand to the side of the plate suffering only very small components of both vertical and horizontal displacements. The zone where most of the displacement occurs does not exceed $2.0 \times B$ above the level of the plate and $0.25 \times B$ to the side of the plate. However, the displacements suffered by the grains were larger than during the

previous increment. At this stage a very small cavity was observed to form below the anchor as it moved upwards. The strain diagram suggests that the sand immediately above the plate still suffers vertical compaction, but with a slight lateral expansion.

Near failure, $\delta = 3.6\text{mm}$, the resulting deformation of the sand is shown in figs. 7-10 to 7-13. The zone of the bed responding to this increment of the load is slightly bigger than that responding to the previous increment. Displacements mainly occur $2.25 \times B$ above the level of the plate anchor and do not exceed $0.125 \times B$ to the side of the plate anchor. The magnitude of displacements gradually decreases from the plate to the sand surface and the discontinuity becomes indistinct, the local shear failure is much clearer. The fact that in this increment the anchor movement disturbed only a small area of sand, although with larger displacements, shows that the plate anchor started to punch through the soil mass without encountering any resistance. It has been noticed that 55% of the anchor displacement occurred during the application of the final 25% of the maximum load.

7-2-1-2 Dense state, L. Buzzard sand

The deformations of the sand surrounding the plate anchor are presented in fig. 7-14 to 7-25.

For $\delta = 1.8\text{ mm}$, figs. 7-14 to 7-17, the sand above the plate anchor is displaced upwards, the zone of sand affected in this way continues to increase until it extends outwards from the perimeter of the plate anchor to reach the surface of the sand. The zone of sand suffering displacement extends all the way above the plate and extends approximately to $1.5 \times B$ to the side of the plate

anchor. Fig. 7-17 shows that the shear is developing above the edge of the plate anchor along a surface extending vertically. The strains in the zone directly above the plate reached smaller values due to the fact that the soil mass, in this zone, was displaced uniformly.

For $\delta = 2.7$ mm, Figs. 7-18 to 7-21, the zone of sand responding to this increment of load is much greater than that responding to the previous increment. It extends approximately from $0.125 \times B$ to $2.0 \times B$ to the side of the plate anchor, and a clear discontinuity of displacements can be seen in fig. 7-20. The vertical displacement diminishes as the distance above the plate increases, but the amount of movement is much greater than for $\delta = 1.8$ mm. The horizontal displacements are insignificant and occur mainly above the side of the plate. It was observed that at this stage the sand has begun to fall into the cavity left below the plate anchor as it rises. The shear has continued to develop and is extending in a generally vertical direction upward from the edge of the plate anchor. The immediate effect of this propagation is depicted in fig. 7-21.

Near failure, $\delta = 3.2$ mm figs. 7-22 to 7-25, the zone of sand above the anchor suffering vertical displacements continued to grow larger. However, the zone responding to this increment of load does not appear to increase. The horizontal displacements still have low values and occur above the edge of the plate. The discontinuity of displacements evident in the previous increment now appears much clearer. The shearing in the sand has continued to develop along the surface of rupture where the strains have reached their maximum values. However, in the area directly above the plate anchor the strains are still at their lower values.

7-2-2 Uplift tests, deep anchors $D/B=8$

7-2-2-1 Loose state, L. Buzzard sand

The deformations of the sand surrounding the plate anchor are presented in fig. 7-26 to fig. 7-41 for each of the upward displacement increments reported herein.

For the first increment, $\delta = 1.8$ mm, the resulting deformations and shear strains of the sand are presented in fig. 7-26 to fig. 7-29. The measurable displacements caused by this increment are confined to a zone of sand that extends $2.65 \times B$ above the plate anchor, and remains almost undisturbed to the side. The displacements are essentially vertical. The magnitude of the displacement of the sand immediately above the plate is nearly equal to the vertical movement of the plate anchor. Fig. 7-29 shows that the shear strains occur mainly around the plate anchor.

At failure, increment $\delta = 3.6$ mm, the resulting deformations of the sand are shown in fig. 7-30 to 7-33. It can be seen that the zone of the bed responding to this increment is similar to the one in increment 1. However, larger vertical displacements occurred in this area, suggesting that the plate anchor punches through the soil in a bearing capacity type of failure, thus limiting the anchor capacity. At this stage, there is very little evidence of compaction of the sand above the plate anchor. The shear failure is fully developed in the vertical upward direction and occurs mainly around the plate anchor.

7-2-2-2 Dense state, L. Buzzard sand

The deformations and strains of the sand surrounding the plate anchor are presented in figs. 7-34 to 7-41 where each increment of load corresponding to a vertical anchor displacement of 1.8 mm and 3.6 mm is examined.

In the first increment, $\delta=1.8$ mm figs. 7-34 to 7-37, the anchor plate and the sand immediately above it are moving together vertically upwards and penetrate the overlying sand. However, the upward displacement of sand diminishes as the distance above the plate increases. A zone of sand extending outwards from the perimeter of the plate anchor is taking form, however this zone stops at $2.0 \times B$ above the plate anchor and $1.0 \times B$ to the side. Measurable displacement still occurs at $4.5 \times B$ above the plate where vertical movements predominate. The strain diagram highlights the development of a local shear which is taking place above the edge of the plate anchor. The presence of a core of soil with very low strains just above the plate suggests that the sand within this zone is lifted as a rigid body.

For $\delta=3.6$ mm, figs. 7-38 to 7-41, the anchor plate and the sand immediately above it are still moving together, the zone of sand responding to this increment of load is much greater than that responding to the previous increment. The zone of sand extending outwards from the perimeter of the plate anchor stops at $3.65 \times B$ above it and extends to $1.2 \times B$ to the side of the plate, and clear discontinuity of displacement is evident in this case. However, the zone of sand suffering measurable displacement extends to $5.65 \times B$ above the plate. The vertical displacement of sand above the anchor body diminishes as the distance above the plate anchor increases, and vertical displacements within this zone

predominate over the smaller horizontal displacements. The local shear has continued to develop, extending in a vertical direction upward from the edge of the plate. At this stage the load has not yet reached its maximum value. The low strained core of sand has been reduced as the soil above the plate started to yield, and it is clear that the shear failure is developing along the side of this core. The strained area above the plate increased slightly.

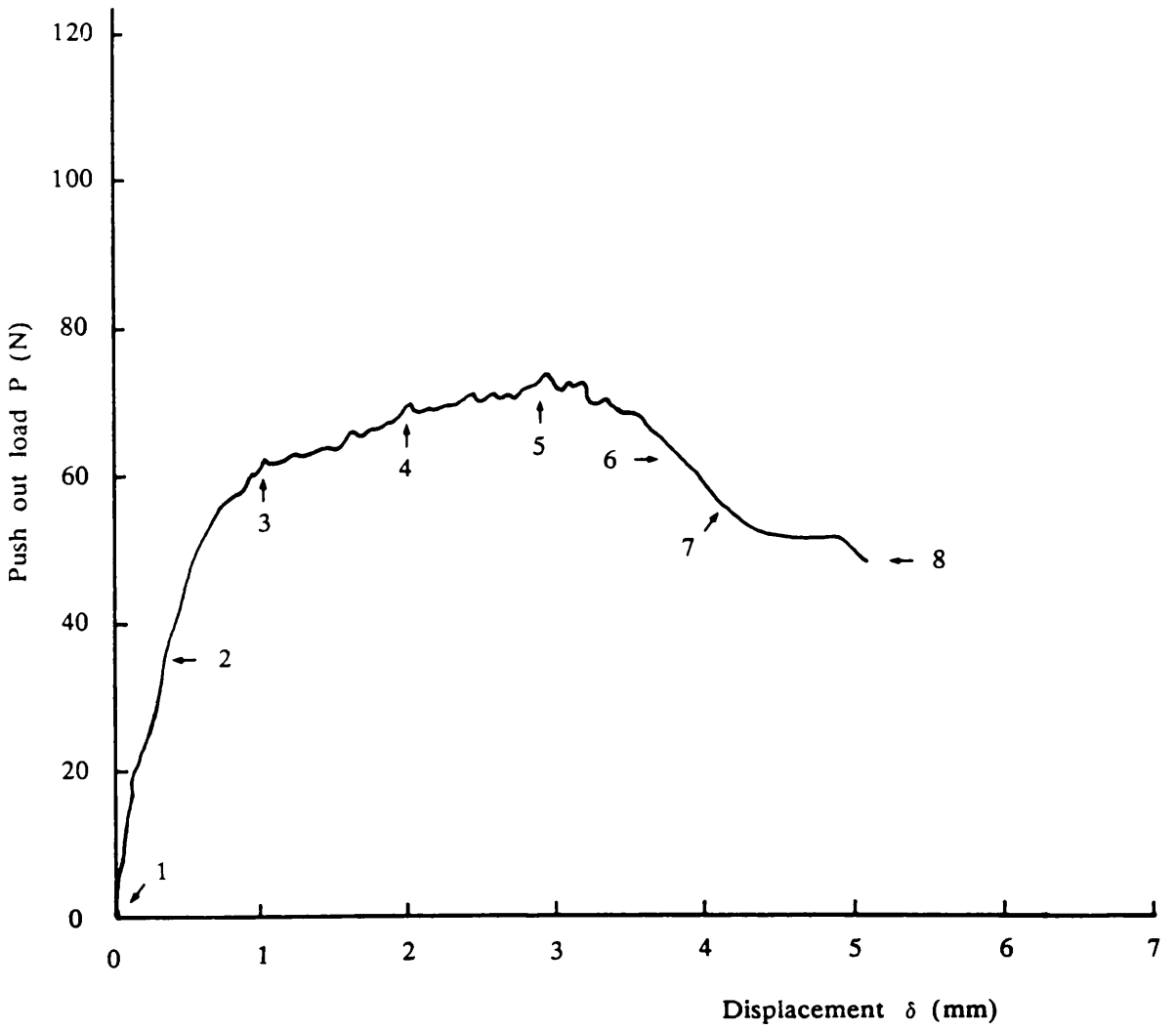


Fig. 7-1 Typical load vs displacement curve in Lochaline sand, $D/B = 4$, $ID = 75\%$.

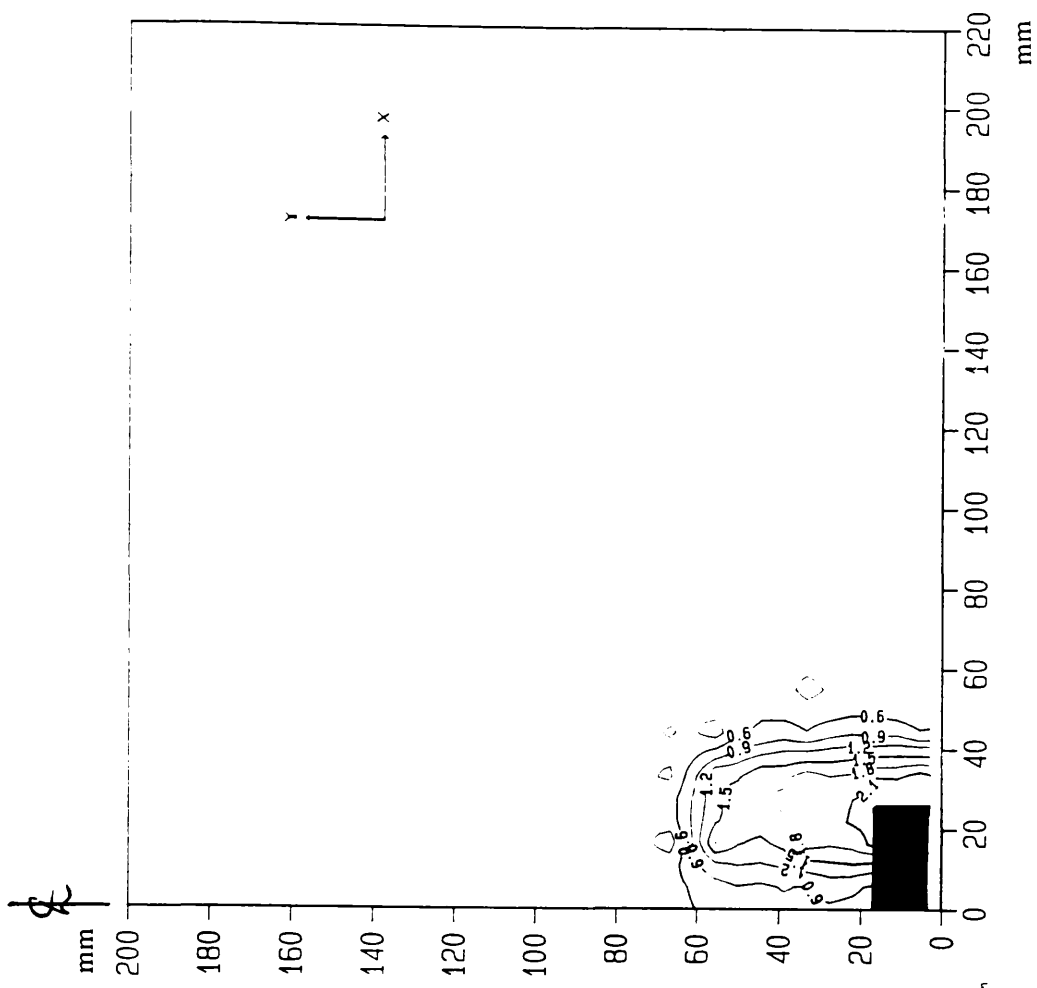


Fig. 7-5 Contours of maximum shear strain in Leighton buzzard
 $D/B = 4$, $ID = 15\%$, $\delta = 0.8$ mm.

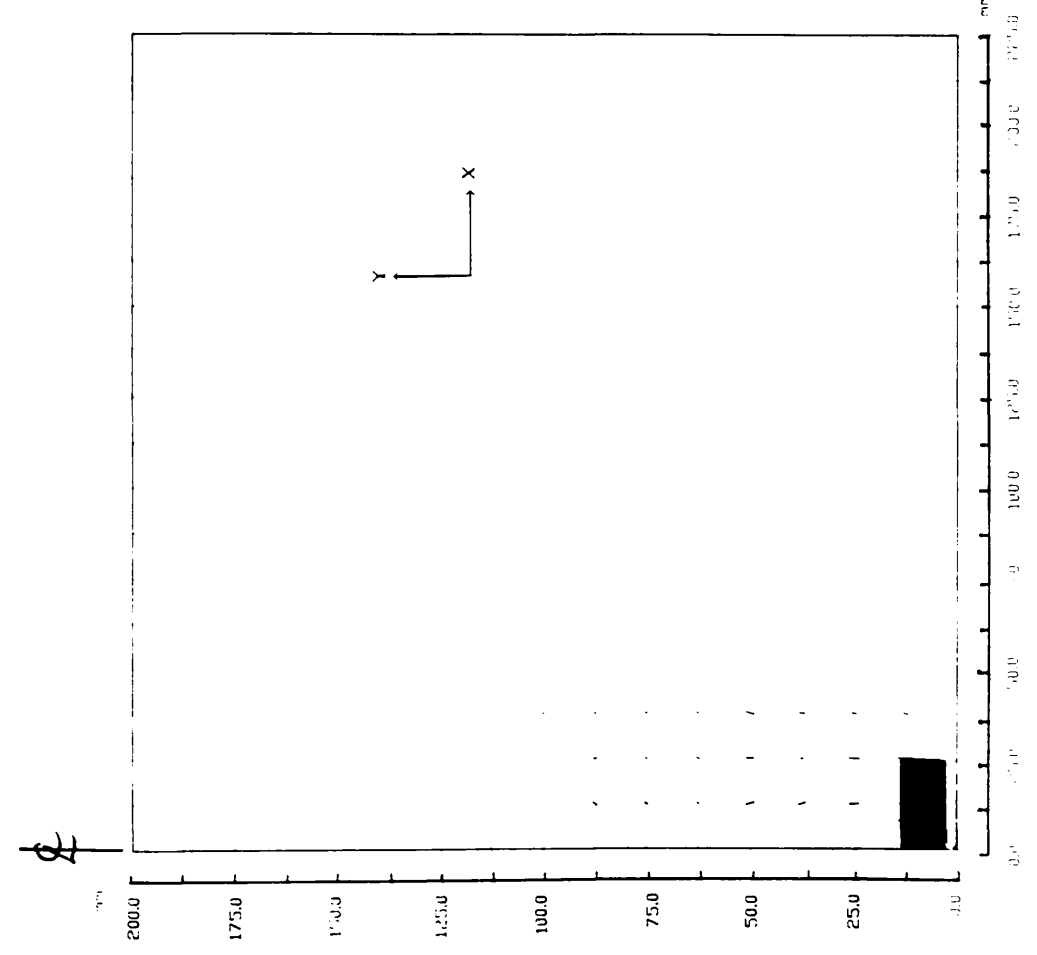


Fig. 7-4 Displacement fields in Leighton buzzard sand
 $D/B = 4$, $ID = 15\%$, $\delta = 0.8$ mm.

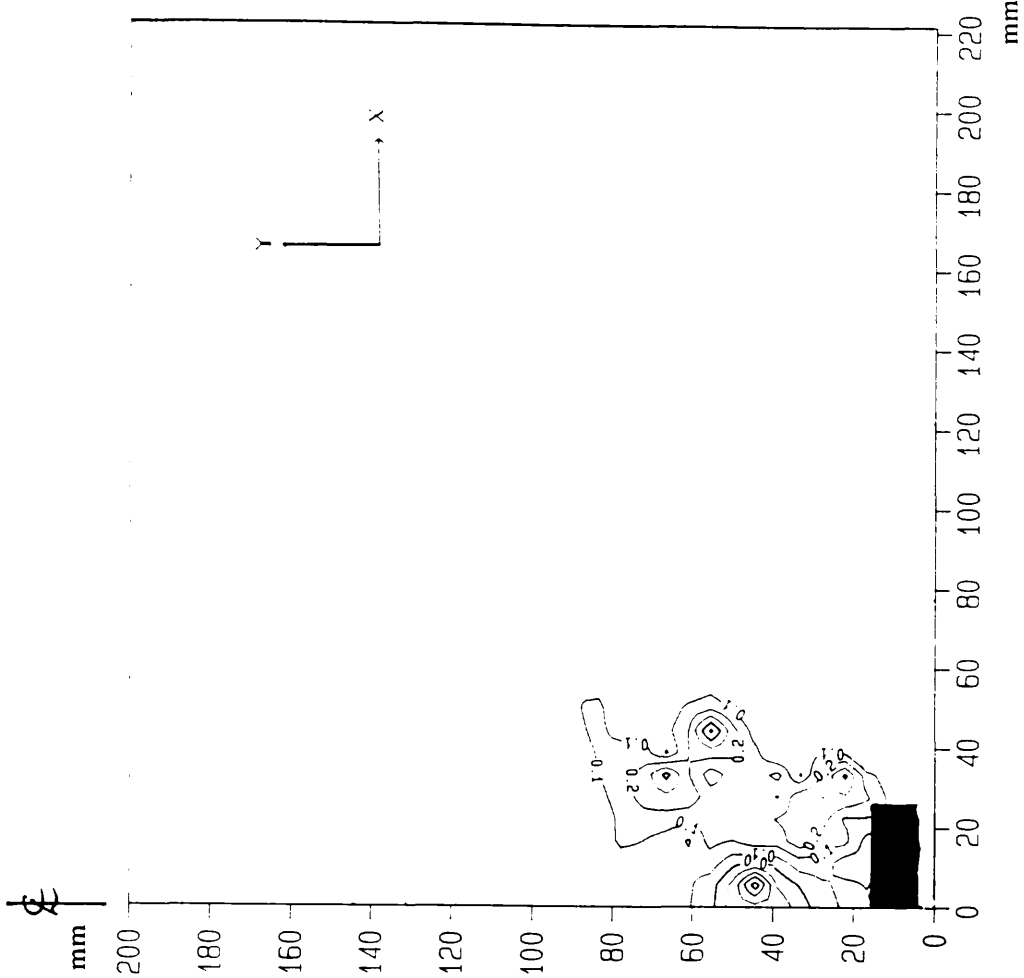


Fig. 7-7 Contours of horizontal displacements in Leighton Buzzard sand, $D/B=4$, $ID=15\%$, $\delta=1.8$ mm.

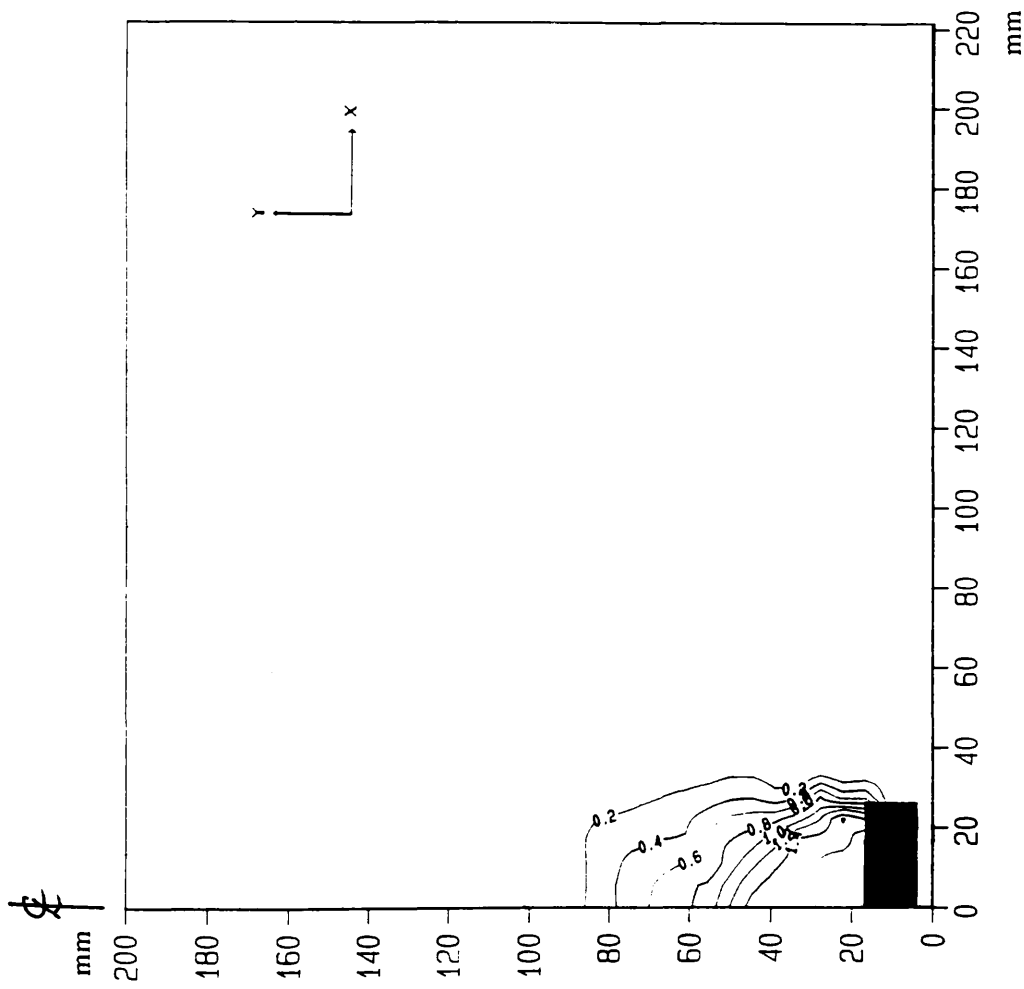


Fig. 7-6 Contours of vertical displacements in Leighton Buzzard sand, $D/B=4$, $ID=15\%$, $\delta=1.8$ mm.

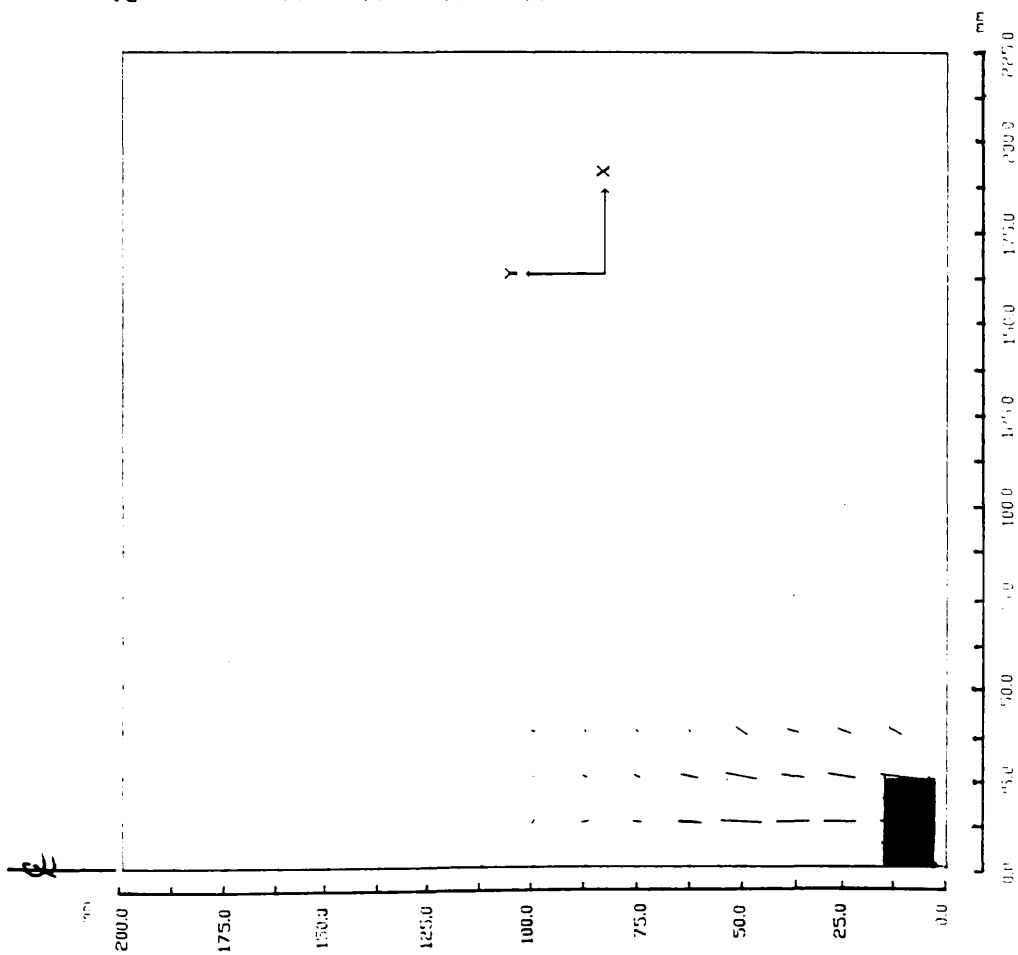


Fig. 7-8 Displacement fields in Leighton buzzard sand

$D/B = 4$, $ID = 15\%$, $\delta = 1.8$ mm.

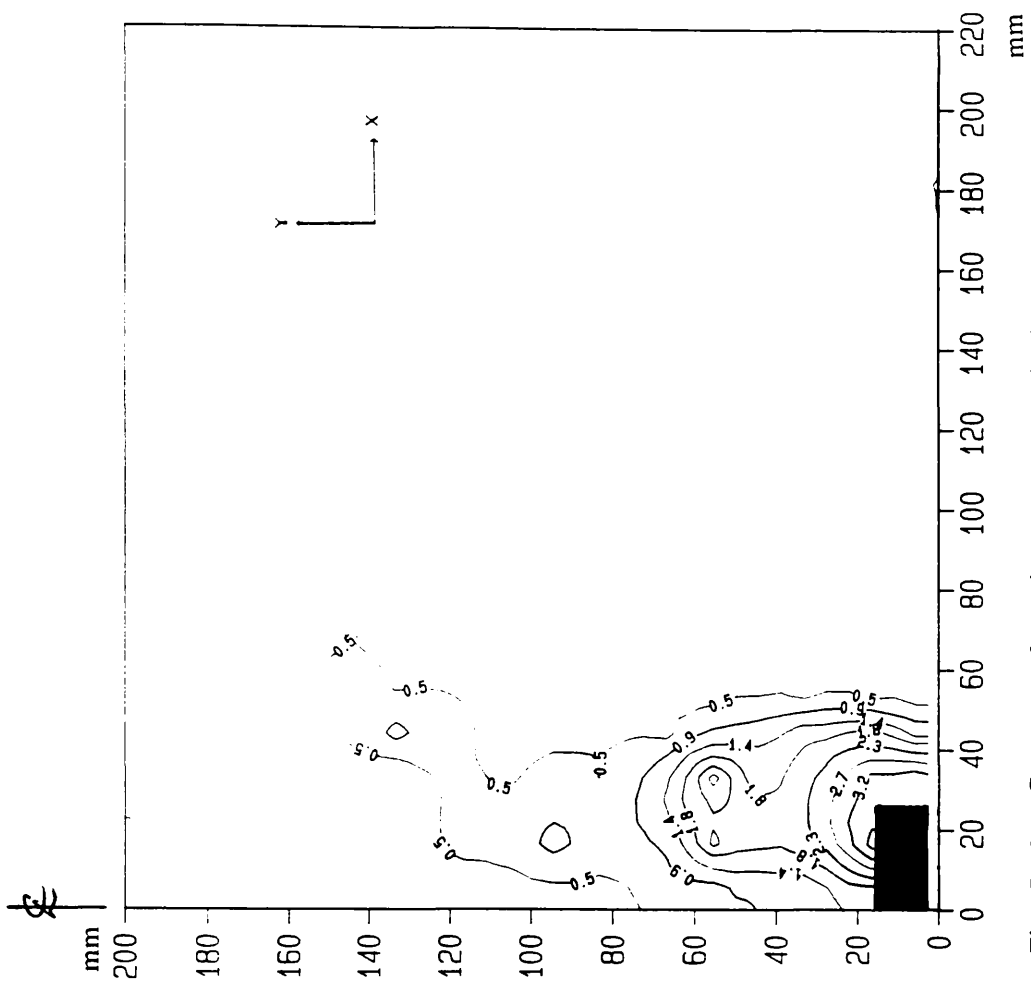


Fig. 7-9 Contours of maximum shear strain in Leighton buzzard

$D/B = 4$, $ID = 15\%$, $\delta = 1.8$ mm.

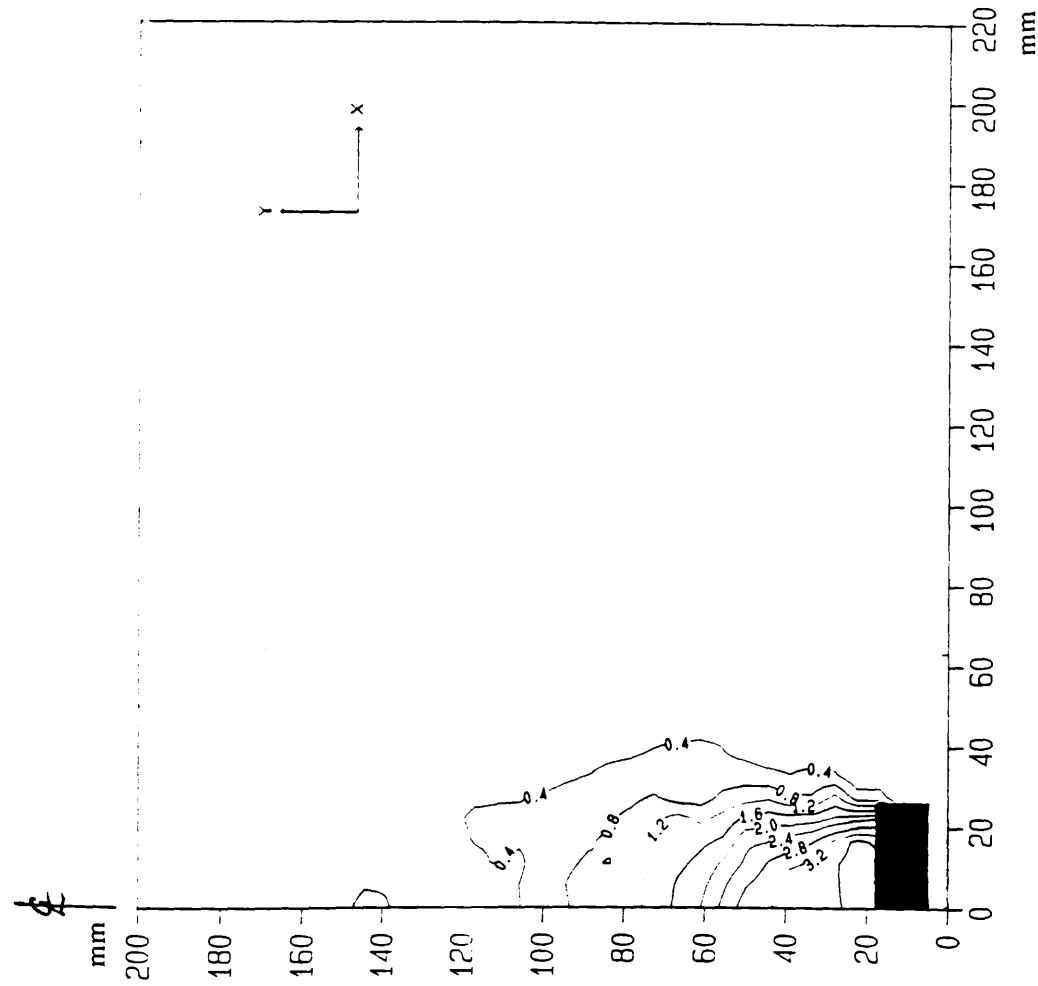


Fig. 7-10 Contours of vertical displacements in Leighton Buzzard sand, $D/B=4$, $ID=15\%$, $\delta=3.6$ mm.

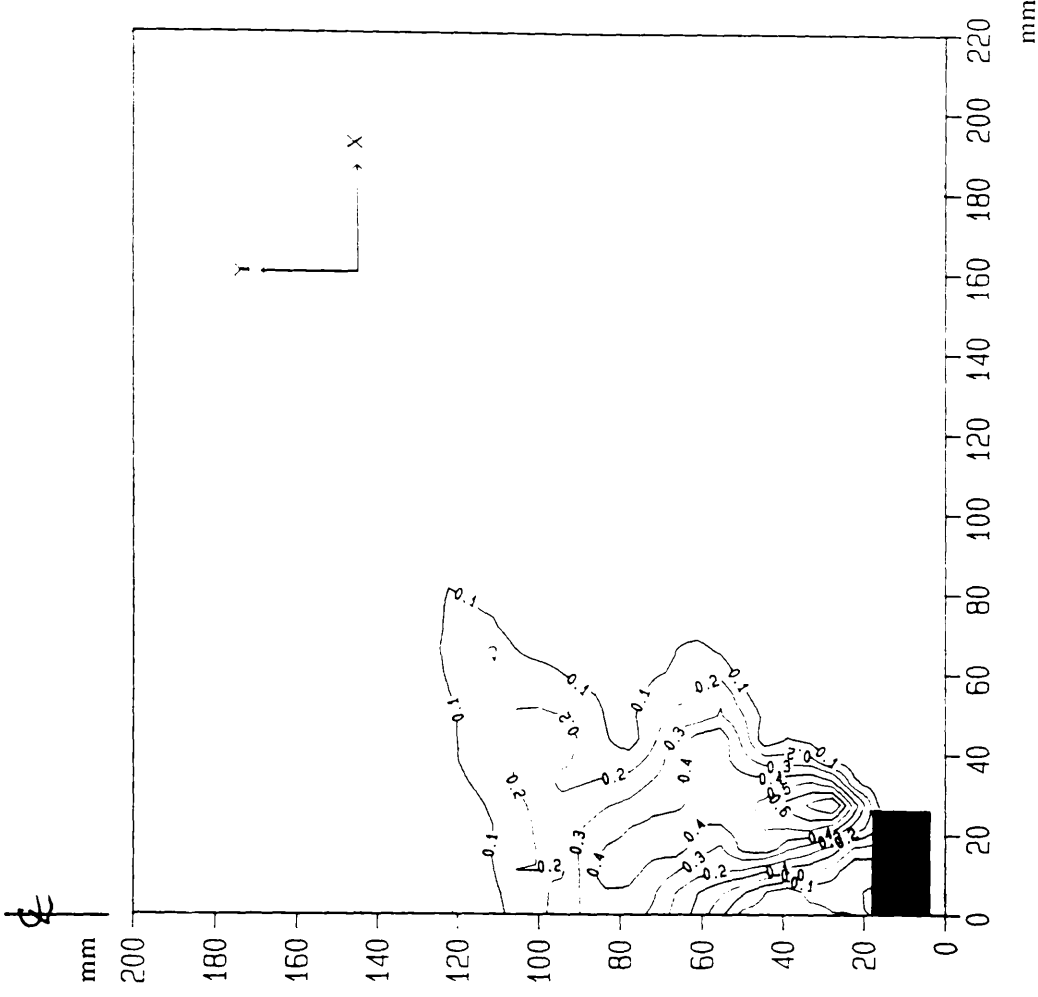


Fig. 7-11 Contours of horizontal displacements in Leighton Buzzard sand, $D/B=4$, $ID=15\%$, $\delta=3.6$ mm.

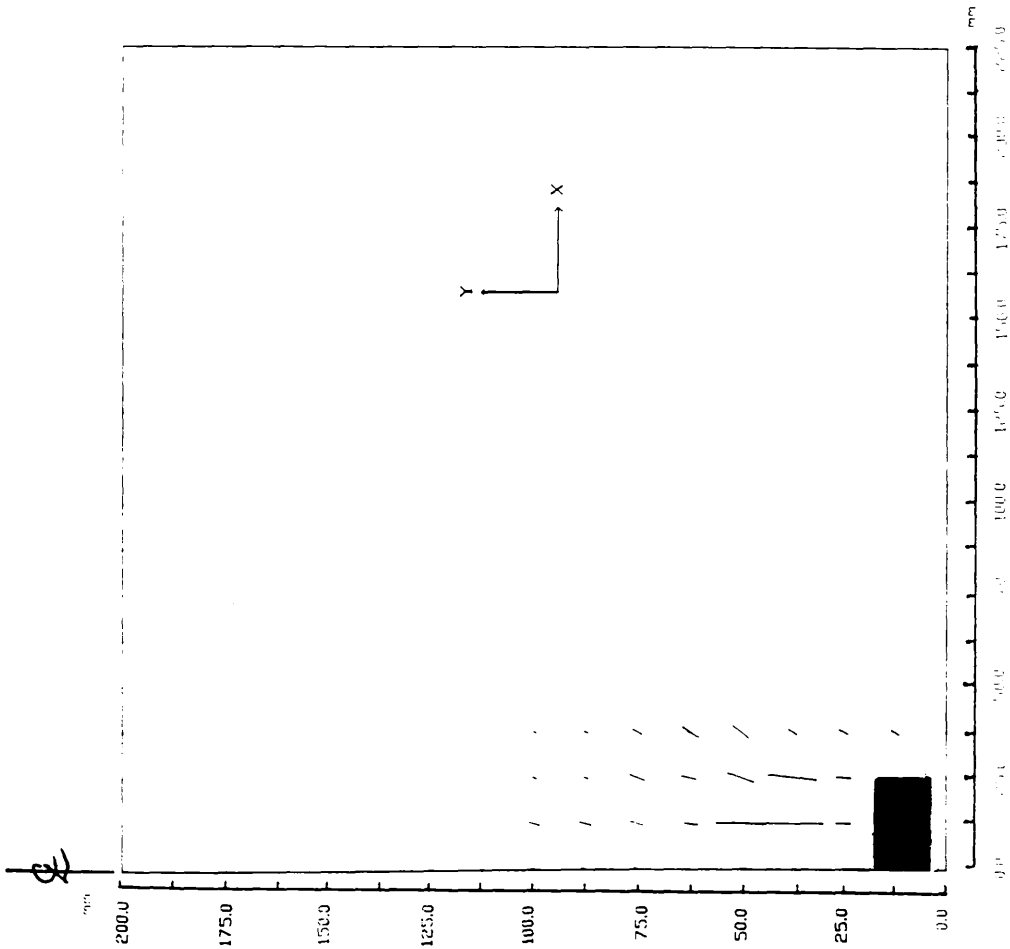


Fig. 7-12 Displacement fields in Leighton buzzard sand

D/B= 4, ID= 15%, $\delta= 3.6$ mm.

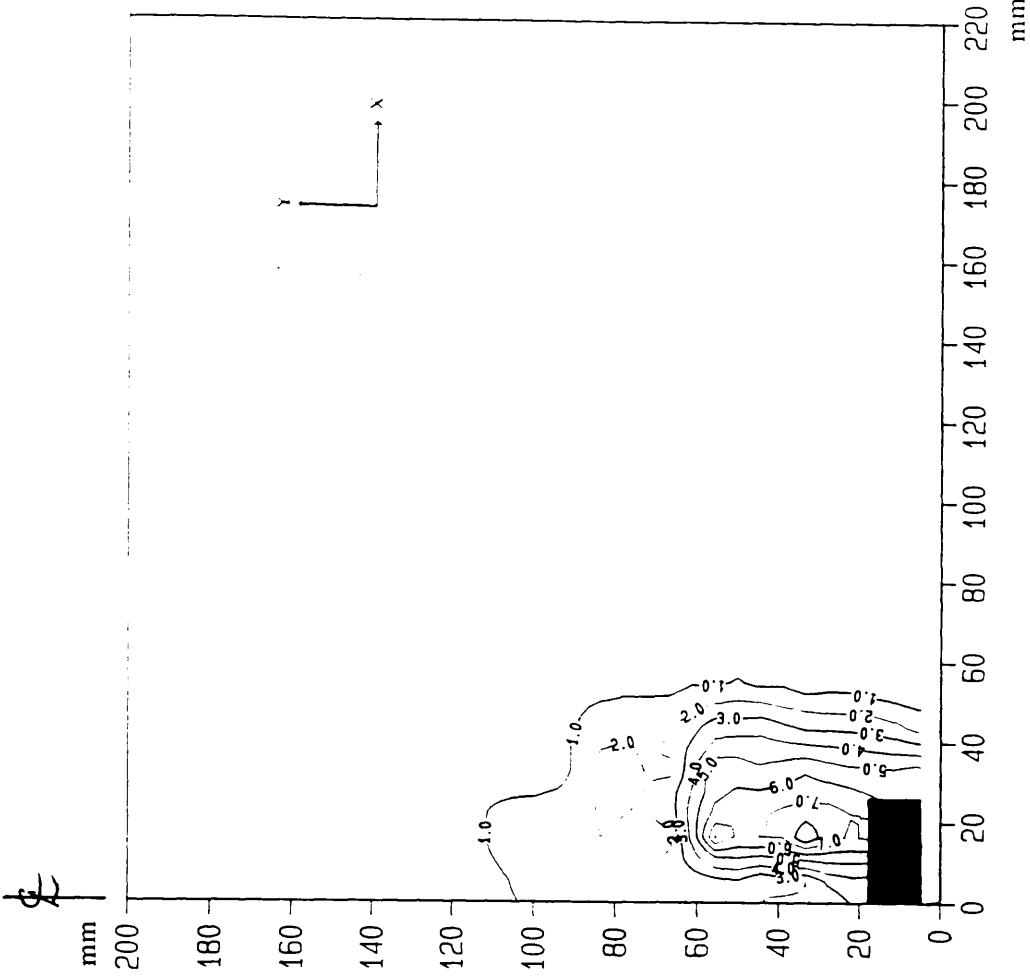


Fig. 7-13 Contours of maximum shear strain in Leighton buzzard

D/B= 4, ID= 15%, $\delta= 3.6$ mm.

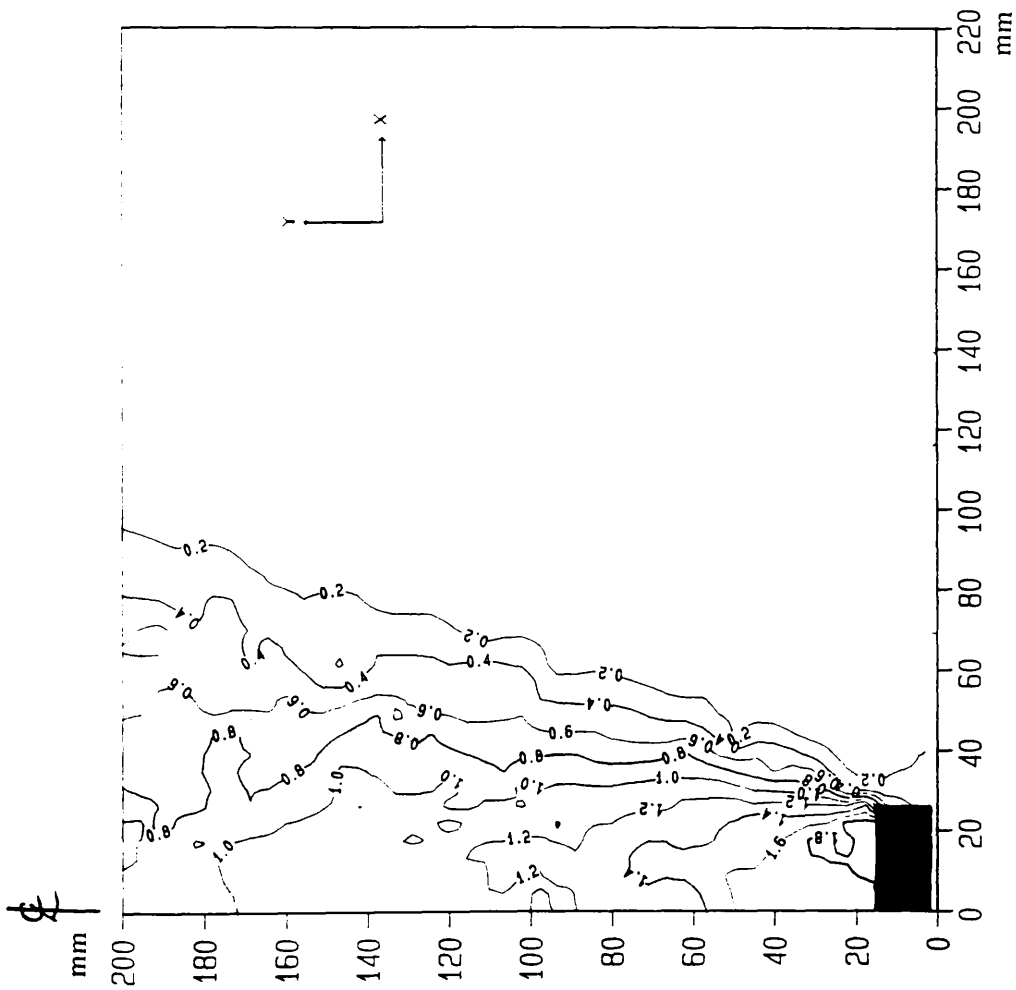


Fig. 7-14 Contours of vertical displacements in Leighton Buzzard sand, $D/B=4$, $ID=75\%$, $\delta=1.8$ mm.

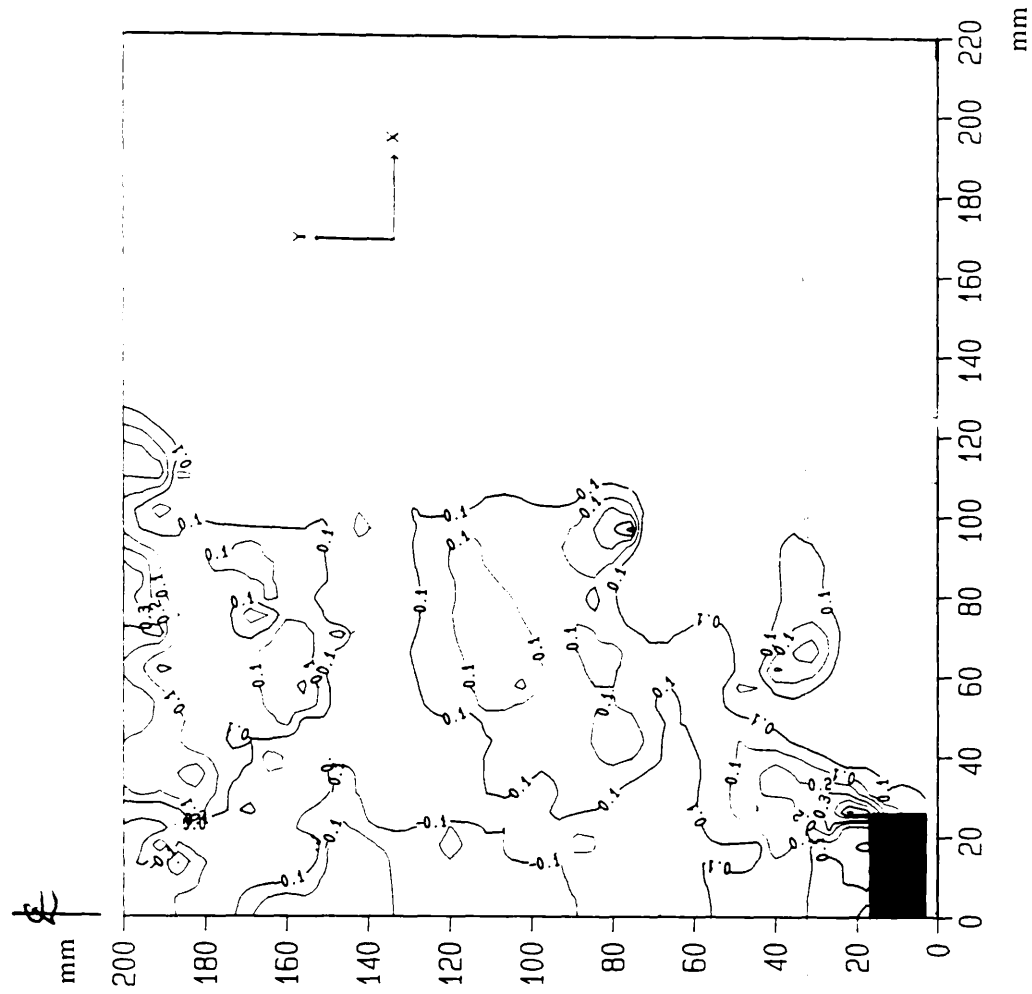


Fig. 7-15 Contours of horizontal displacements in Leighton Buzzard sand, $D/B=4$, $ID=75\%$, $\delta=1.8$ mm.

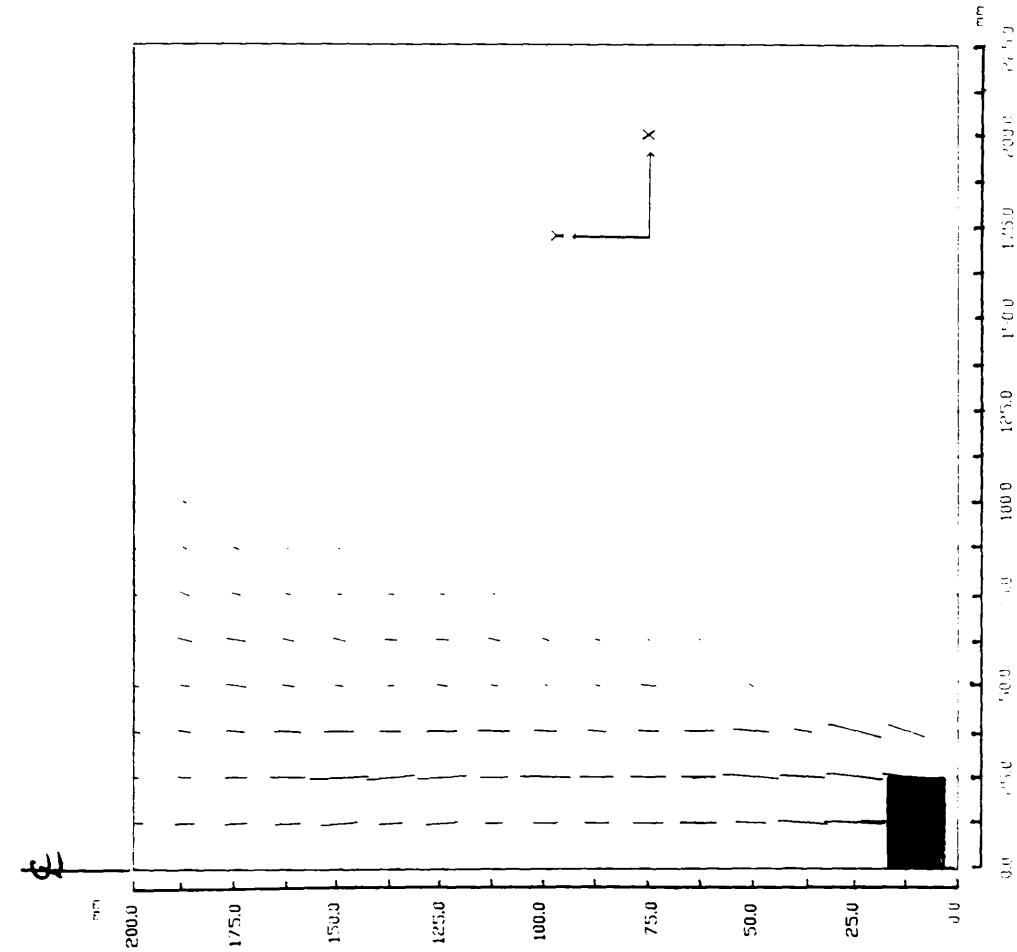


Fig. 7-16 Displacement fields in Leighton buzzard sand

D/B= 4, ID= 75%, δ = 1.8 mm.

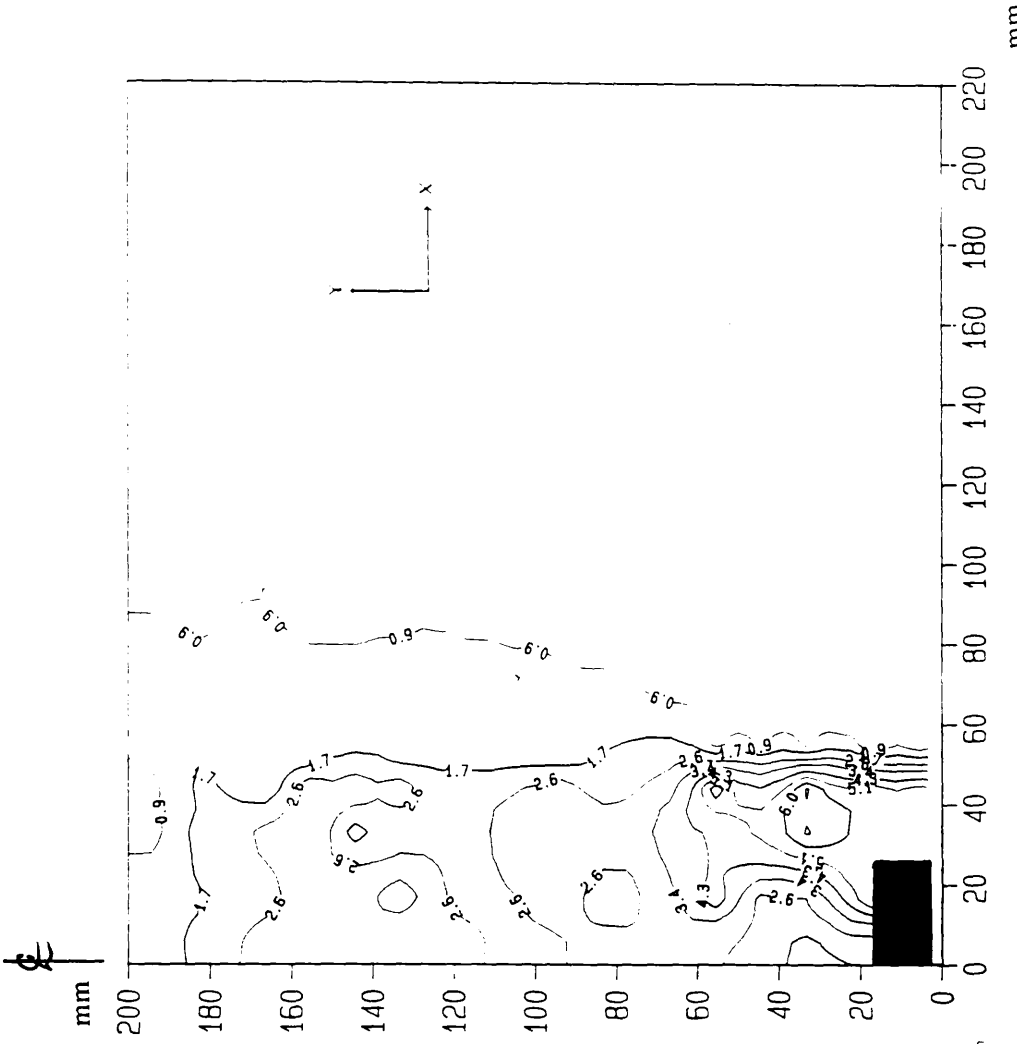


Fig. 7-17 Contours of maximum shear strain in Leighton buzzard

D/B= 4, ID= 75%, δ = 1.8 mm.

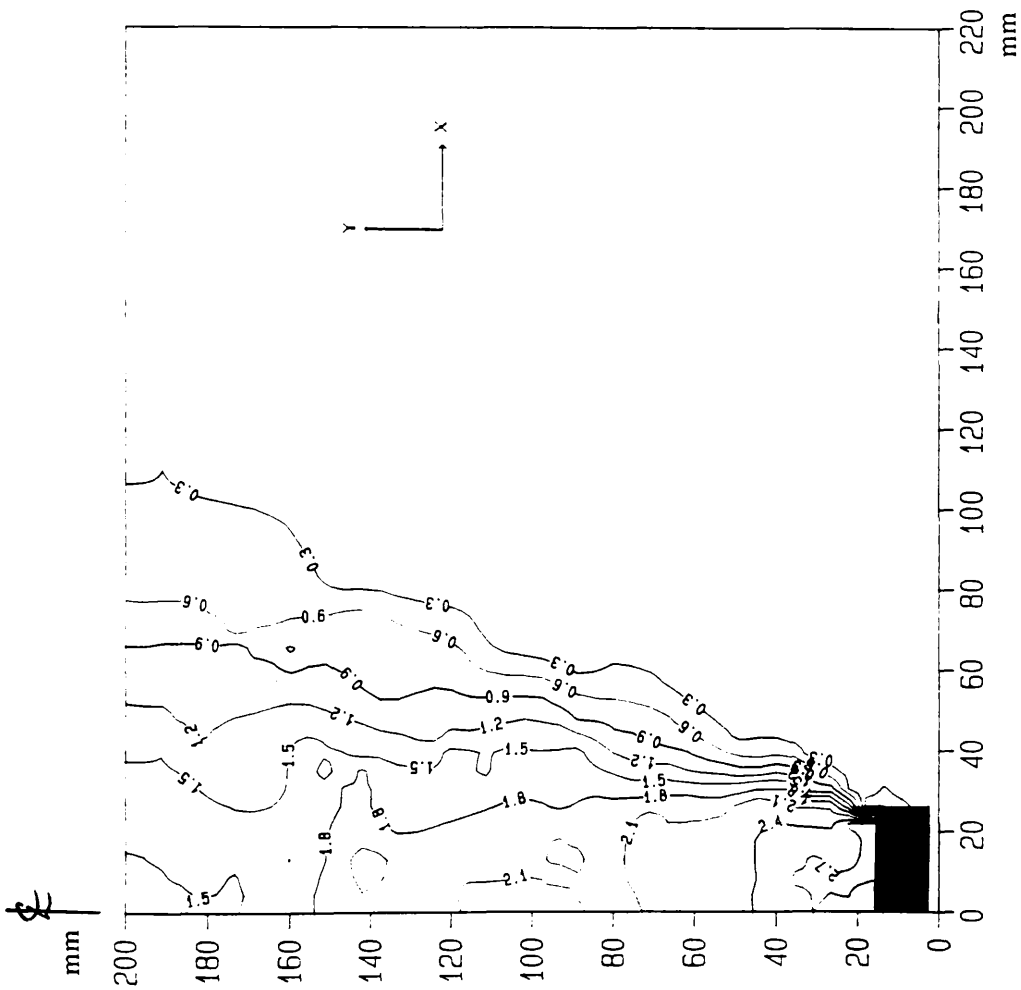


Fig. 7-18 Contours of vertical displacements in Leighton Buzzard sand, $D/B=4$, $ID=75\%$, $\delta=2.7$ mm.

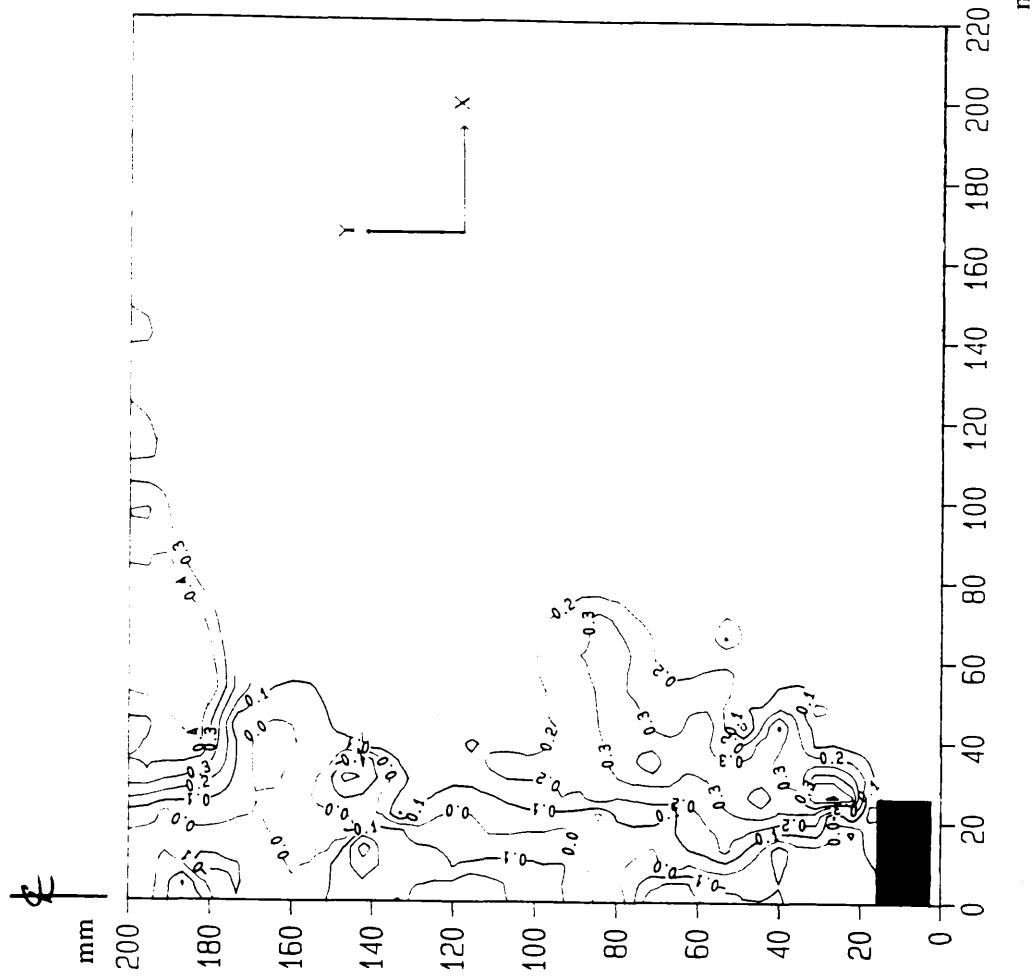


Fig. 7-19 Contours of horizontal displacements in Leighton Buzzard sand, $D/B=4$, $ID=75\%$, $\delta=2.7$ mm.

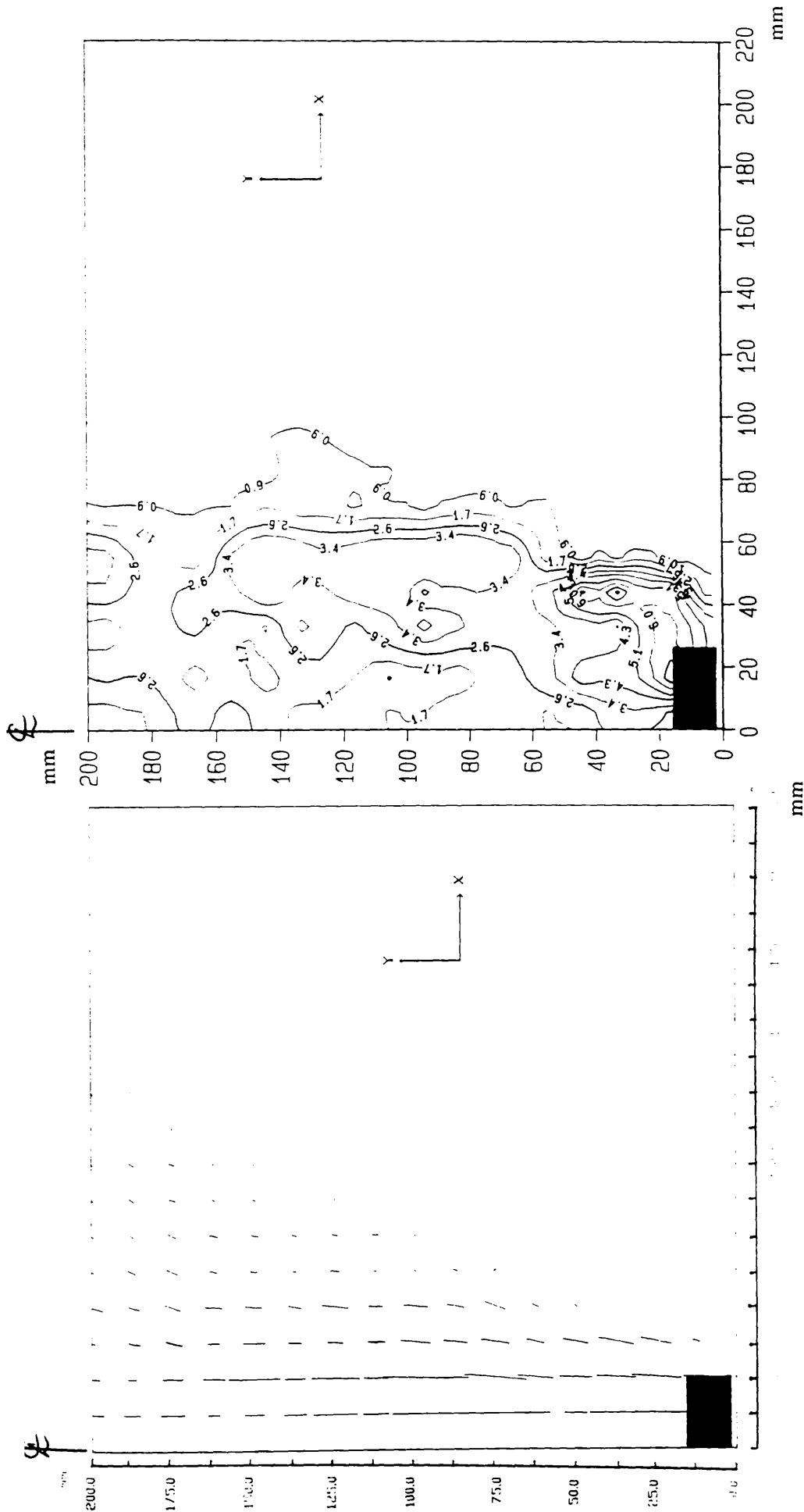


Fig. 7-20 Displacement fields in Leighton buzzard sand
D/B= 4, ID= 75%, $\delta= 2.7$ mm.

Fig. 7-21 Contours of maximum shear strain in Leighton buzzard
D/B= 4, ID= 75%, $\delta= 2.7$ mm.

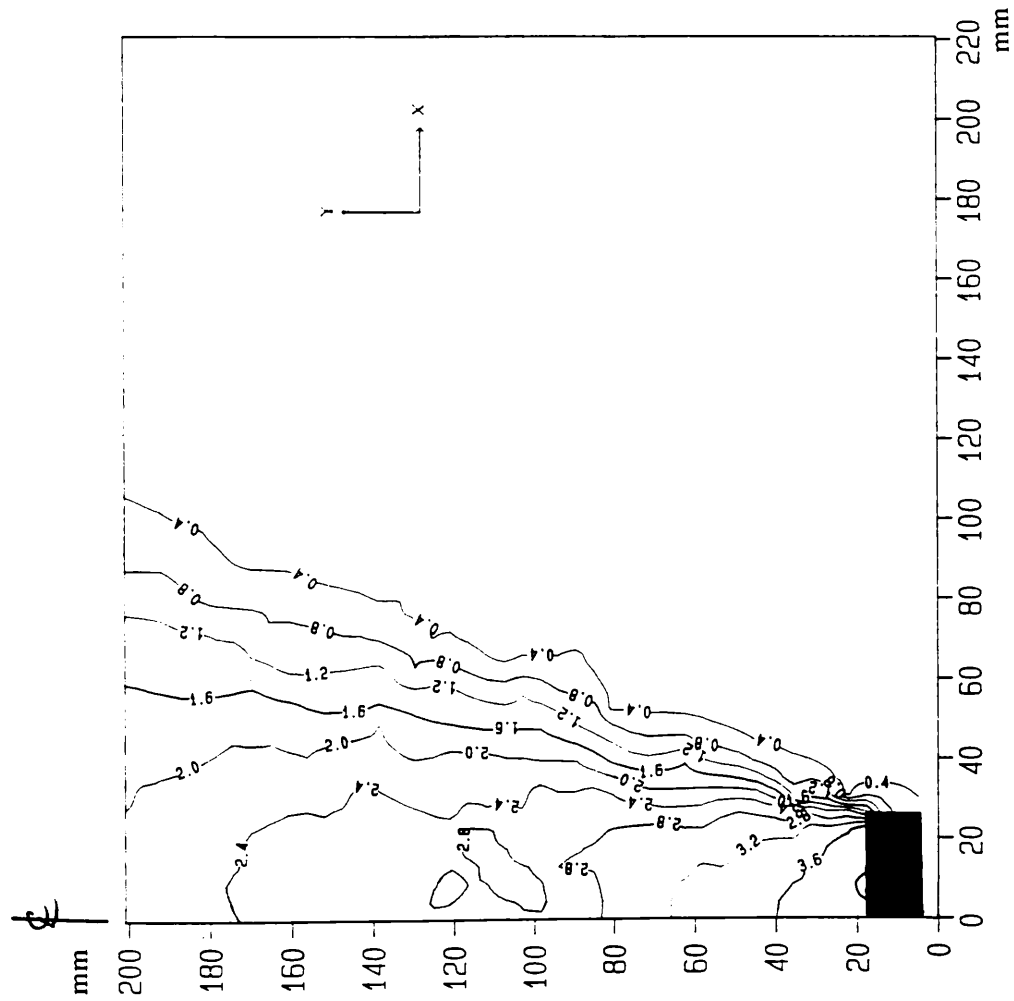


Fig. 7-22 Contours of vertical displacements in Leighton Buzzard sand, $D/B=4$, $ID=75\%$, $\delta=3.6$ mm.

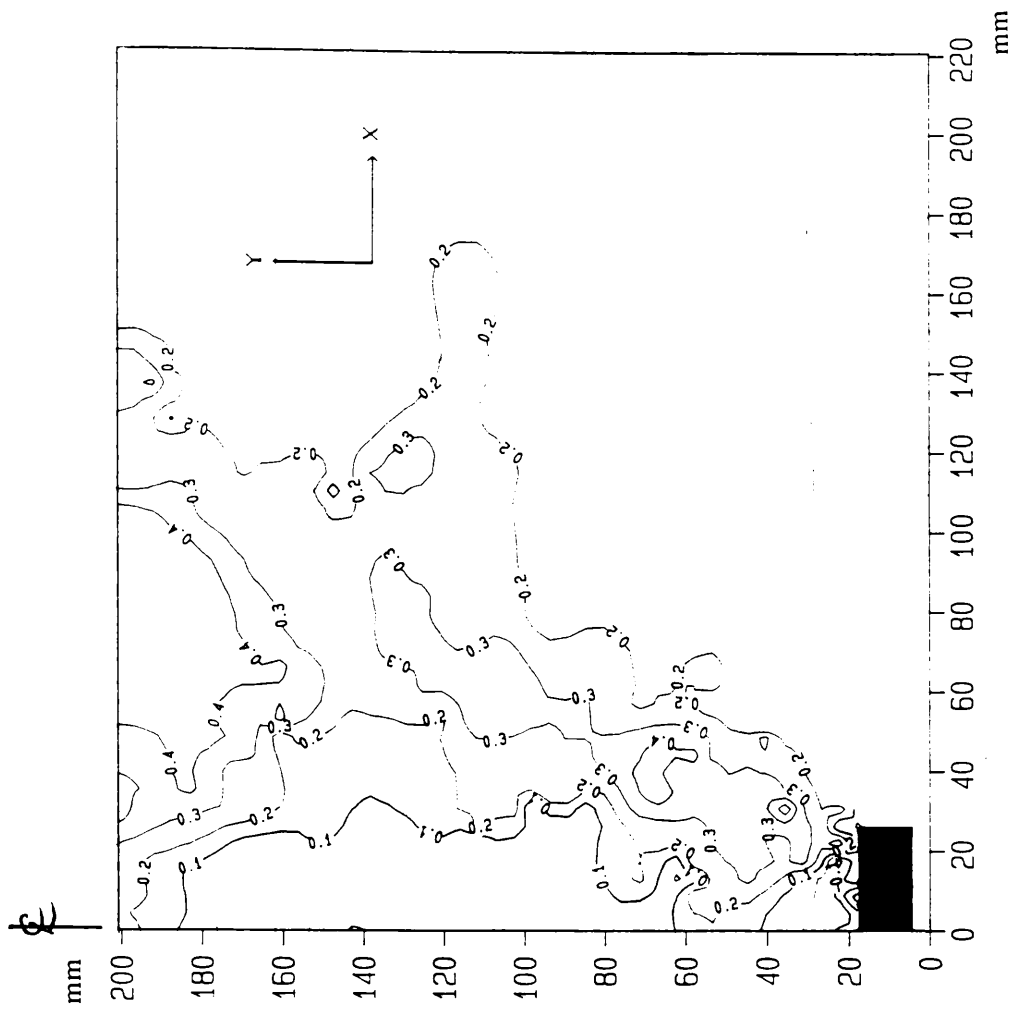


Fig. 7-23 Contours of horizontal displacements in Leighton Buzzard sand, $D/B=4$, $ID=75\%$, $\delta=3.6$ mm.

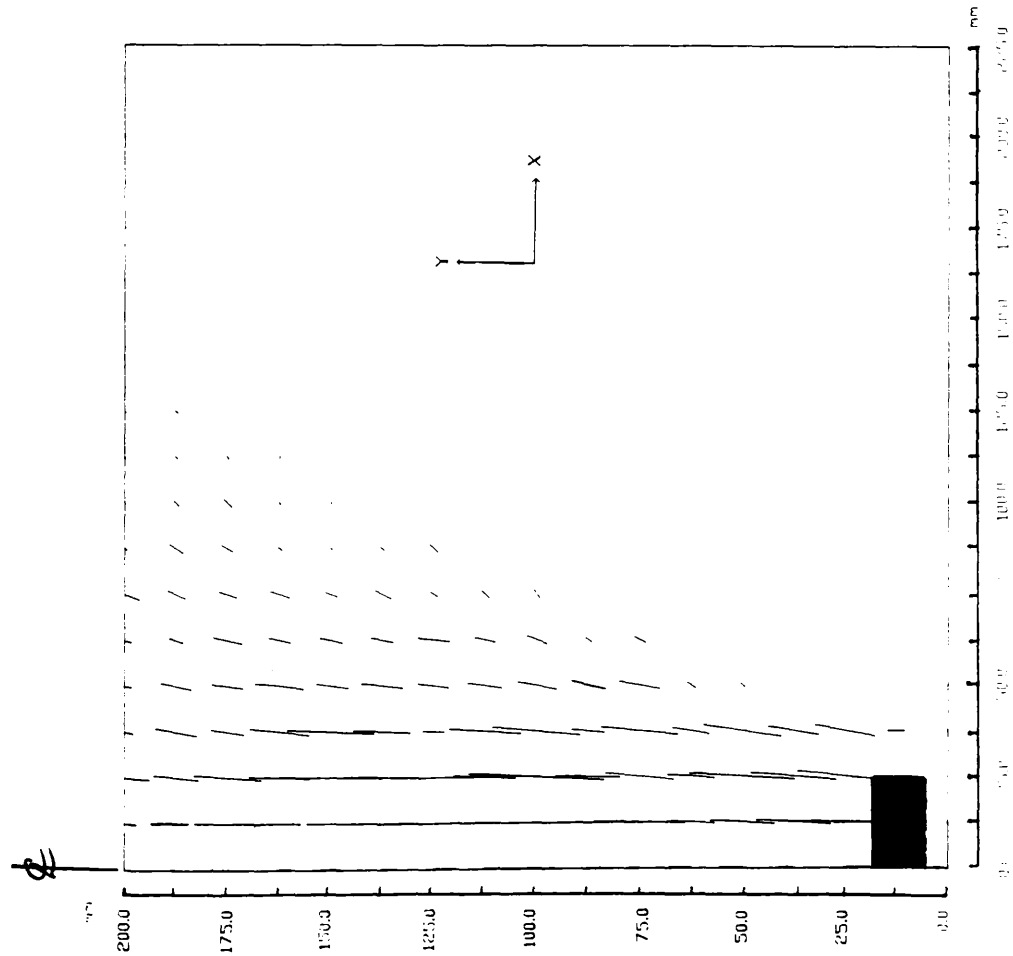


Fig. 7-24 Displacement fields in Leighton buzzard sand

$D/B=4$, $ID=75\%$, $\delta=3.6$ mm.

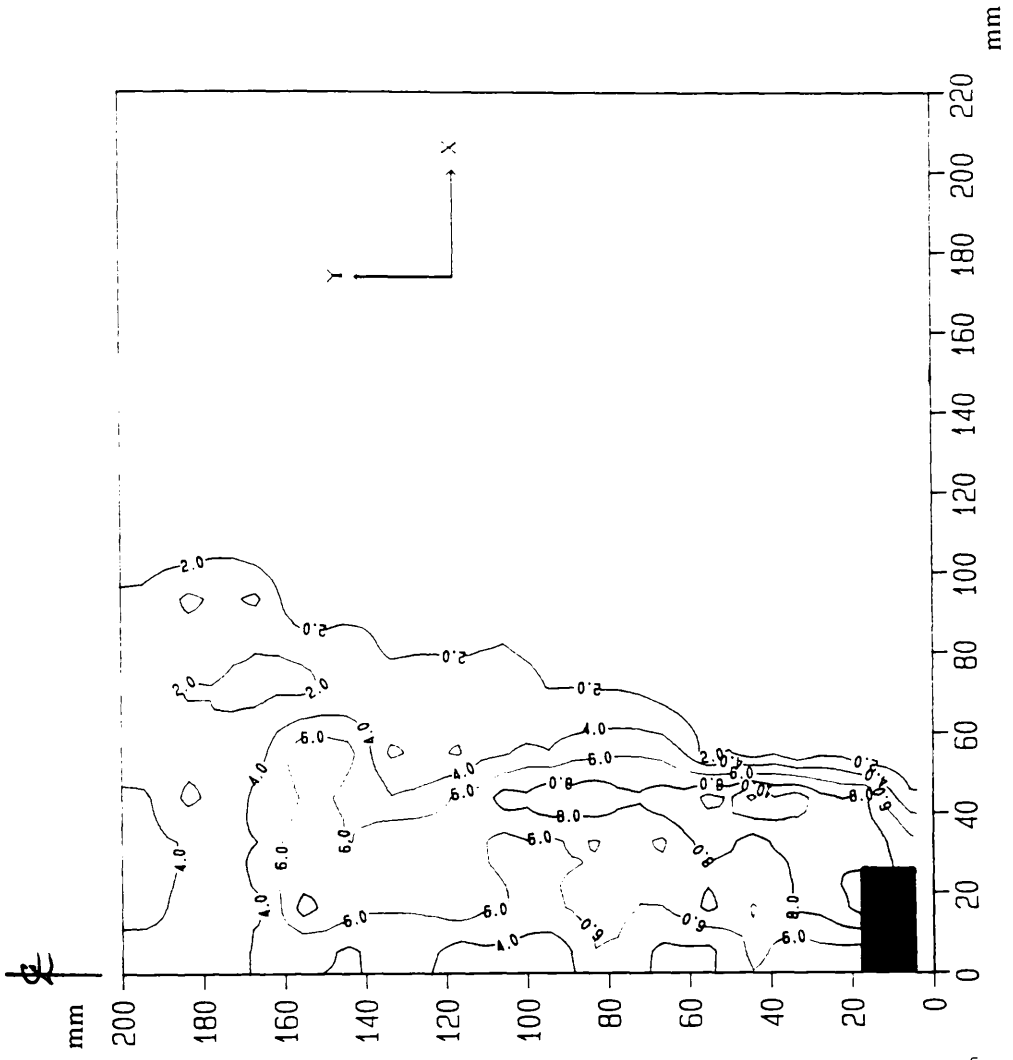


Fig. 7-25 Contours of maximum shear strain in Leighton buzzard

$D/B=4$, $ID=75\%$, $\delta=3.6$ mm.

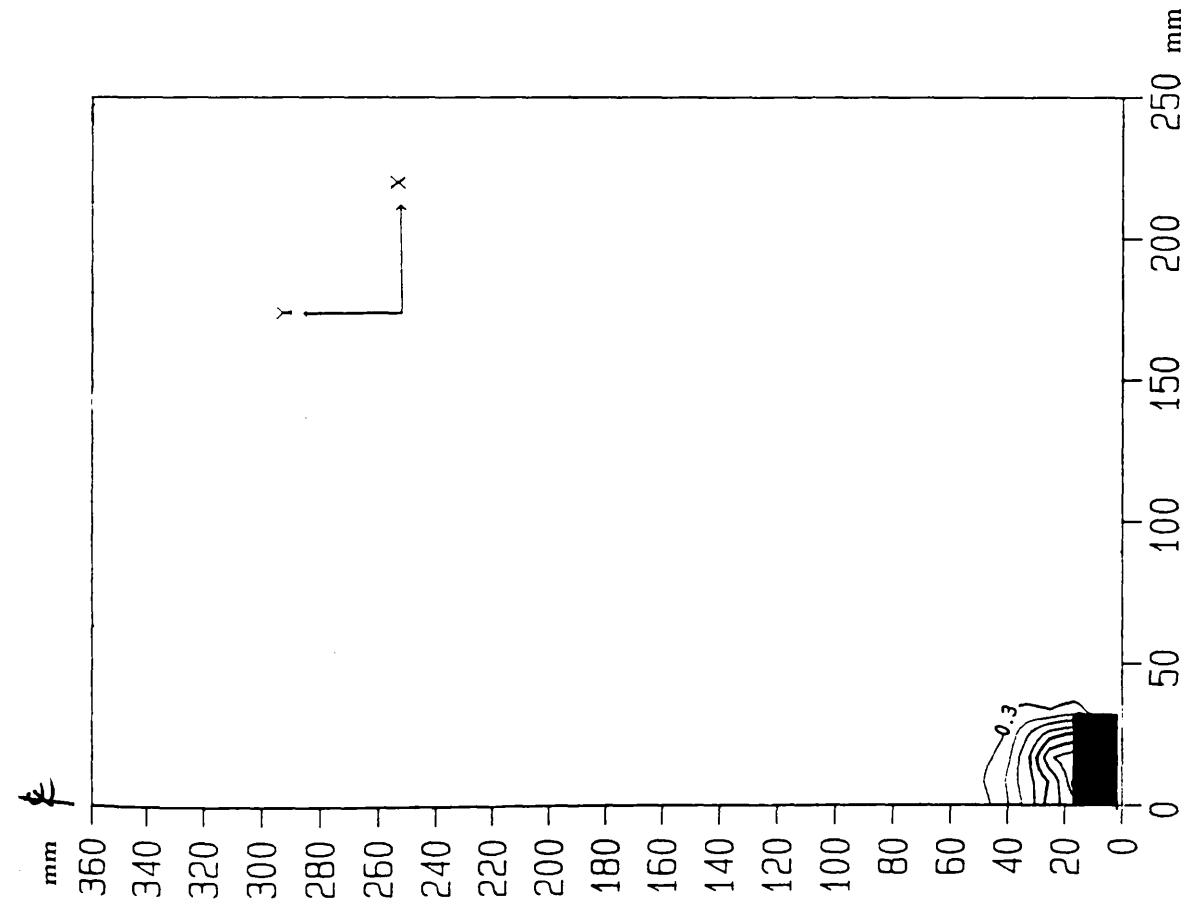


Fig. 7-26 Contours of vertical displacements in Leighton Buzzard sand, $D/B=8$, $ID=15\%$, $\delta=1.8$ mm.

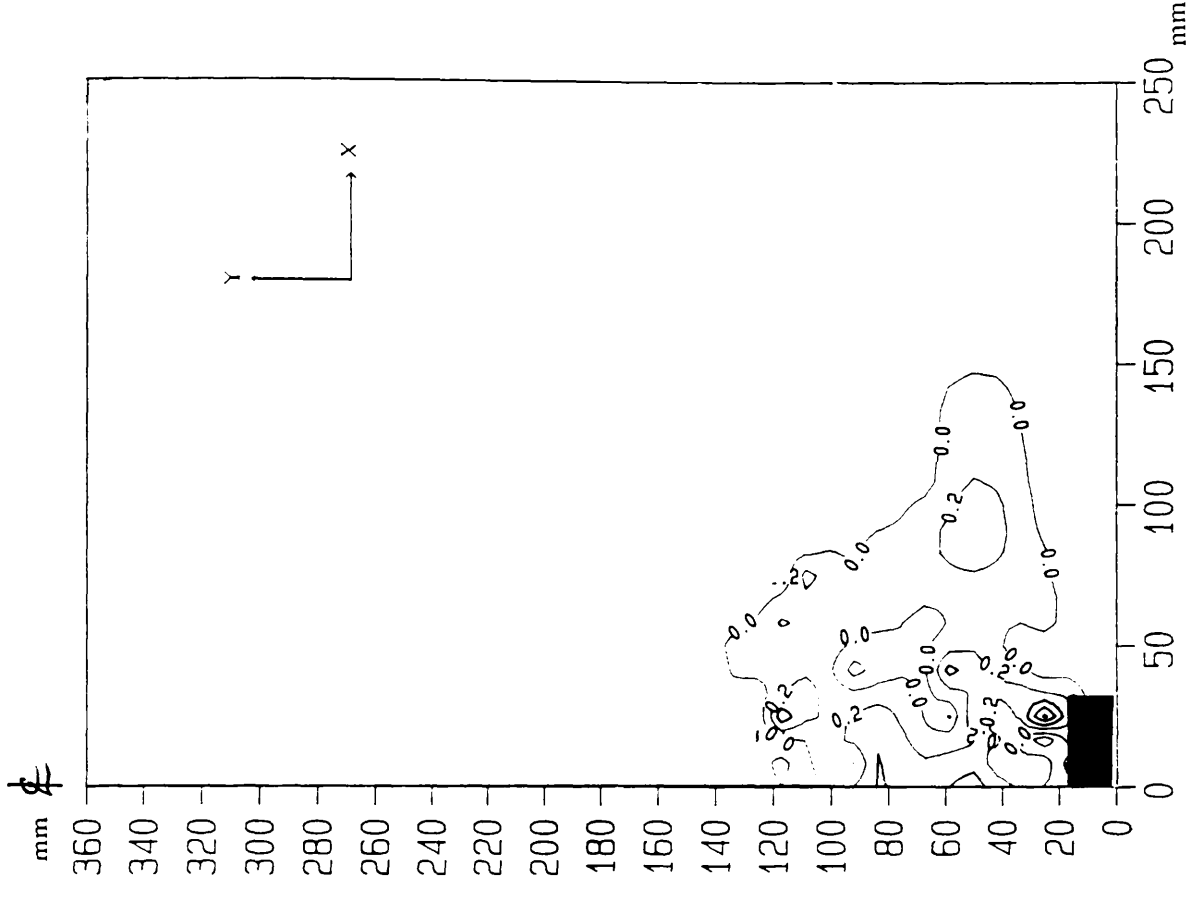


Fig. 7-27 Contours of horizontal displacements in Leighton Buzzard sand, $D/B=8$, $ID=15\%$, $\delta=1.8$ mm.

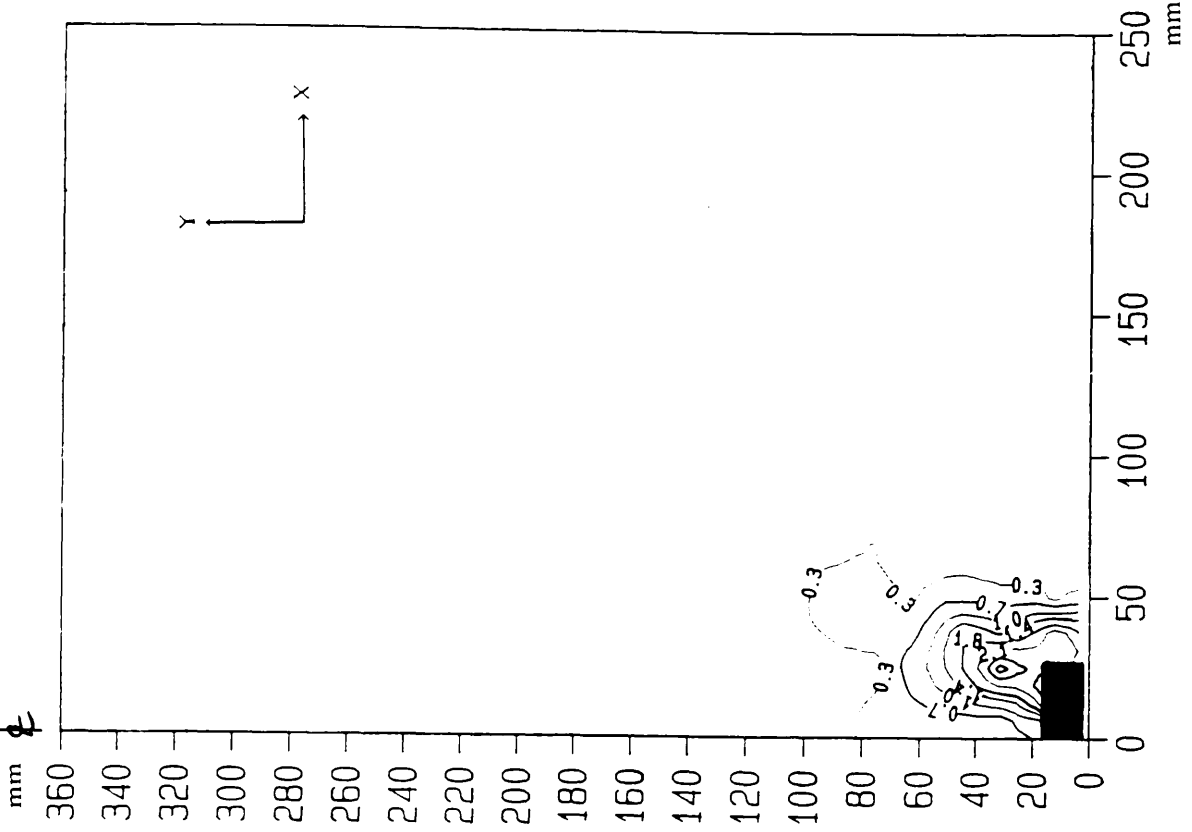


Fig. 7-29 Contours of maximum shear strain in Leighton buzzard
 $D/B = 8$, $ID = 15\%$, $\delta = 1.8$ mm.

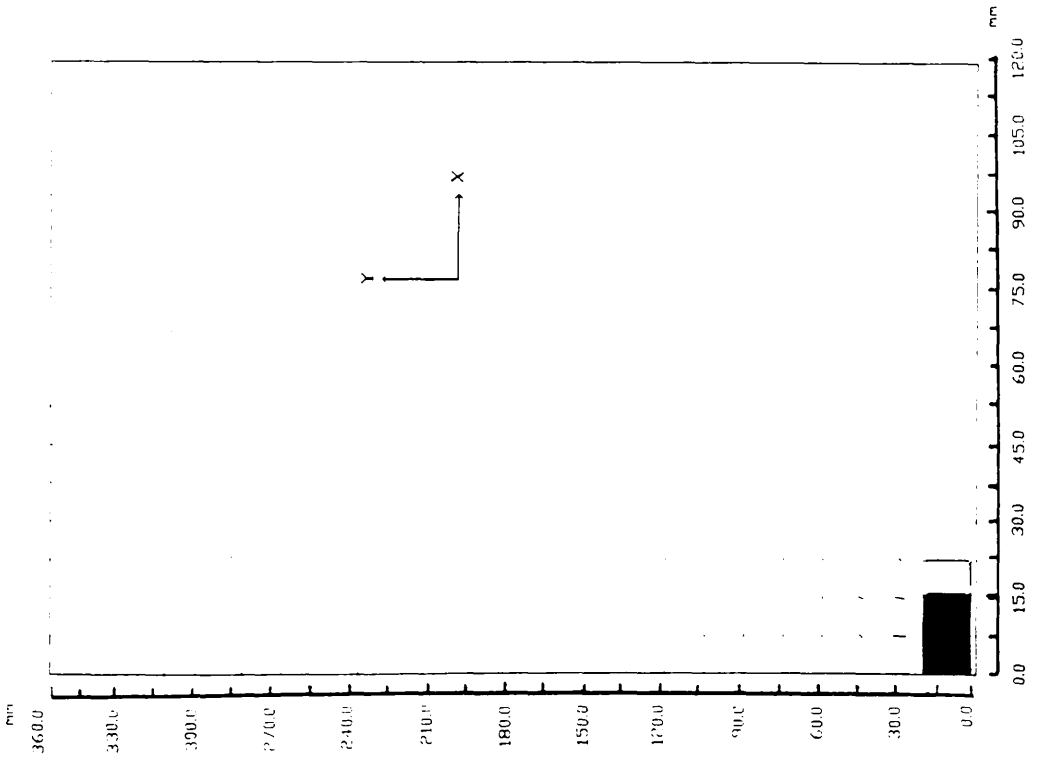


Fig7-28 Displacement fields in Leighton buzzard sand
 $D/B = 8$, $ID = 15\%$, $\delta = 1.8$ mm.

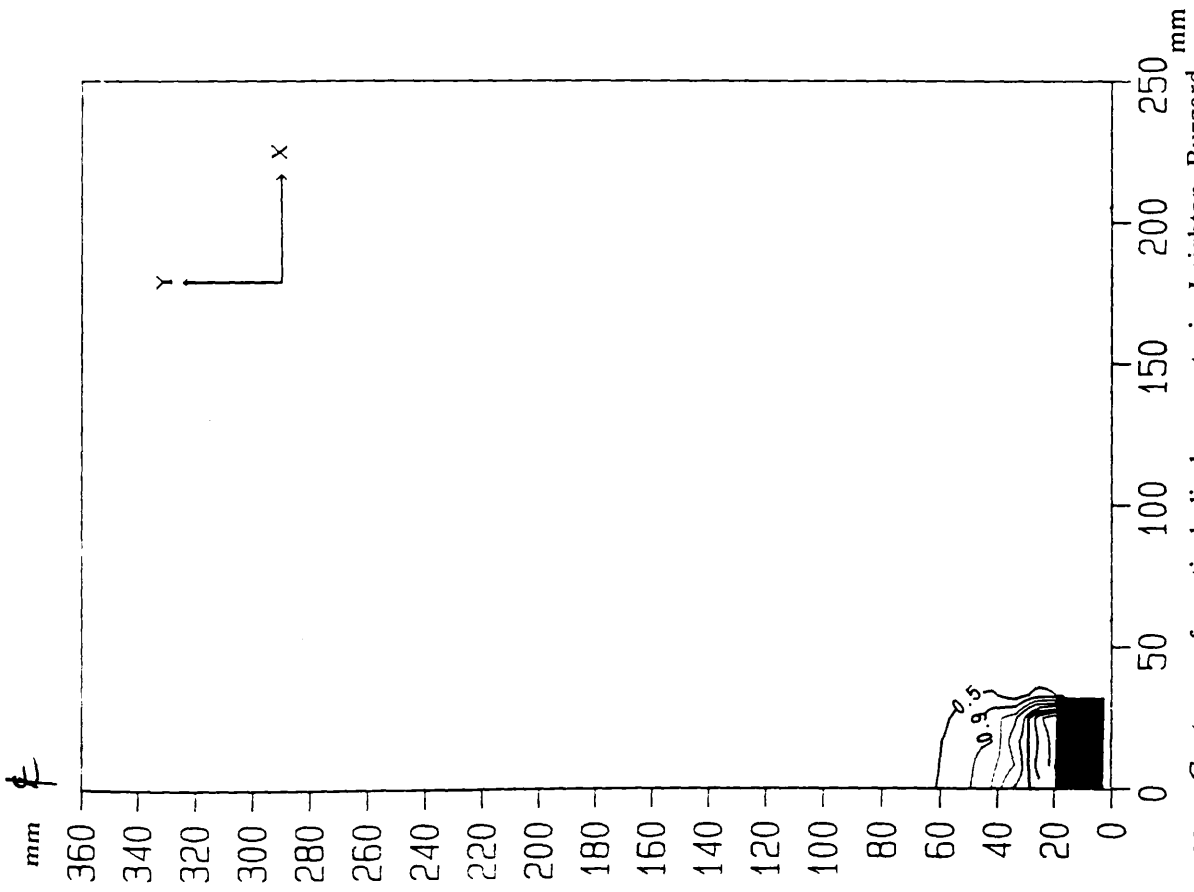


Fig. 7-30 Contours of vertical displacements in Leighton Buzzard sand, $D/B=8$, $ID=15\%$, $\delta=3.6$ mm.

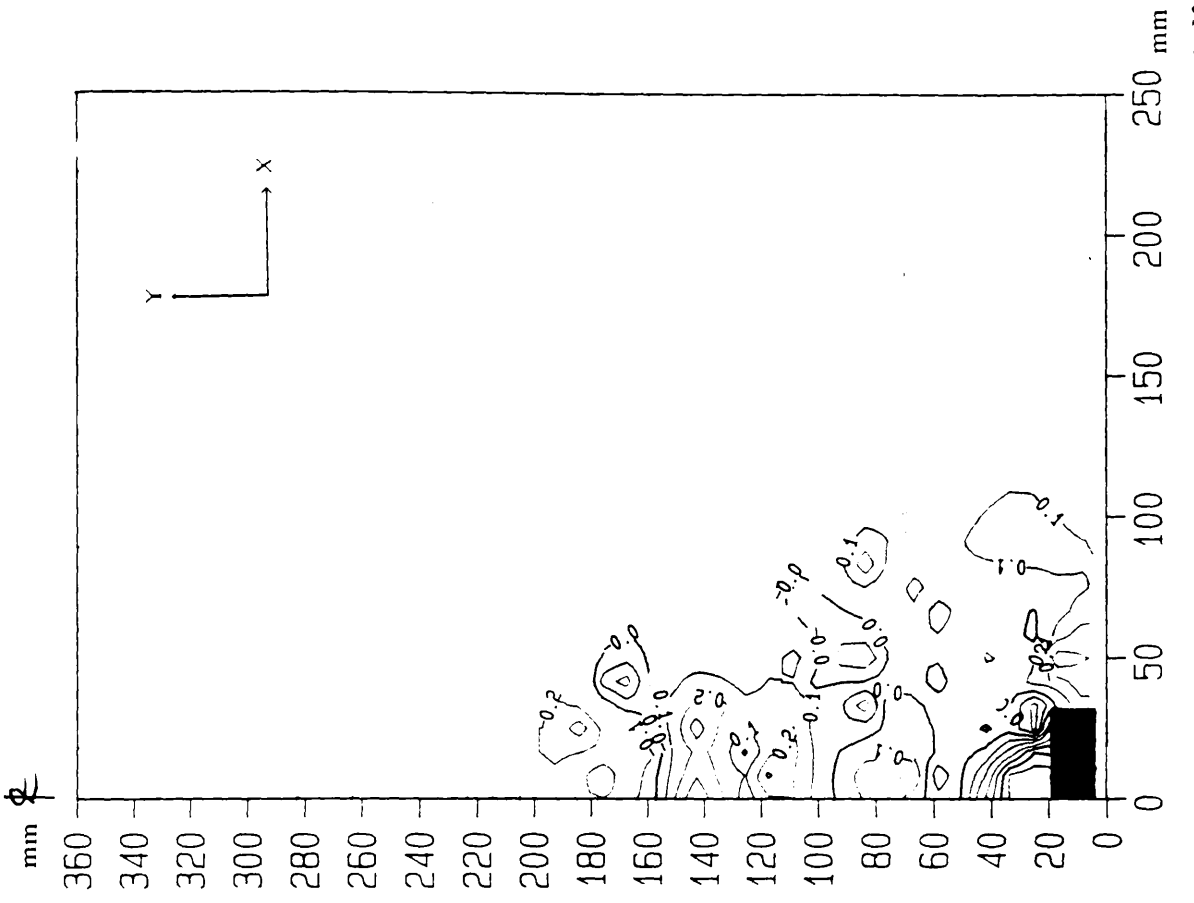


Fig. 7-31 Contours of horizontal displacements in Leighton Buzzard sand, $D/B=8$, $ID=15\%$, $\delta=3.6$ mm.

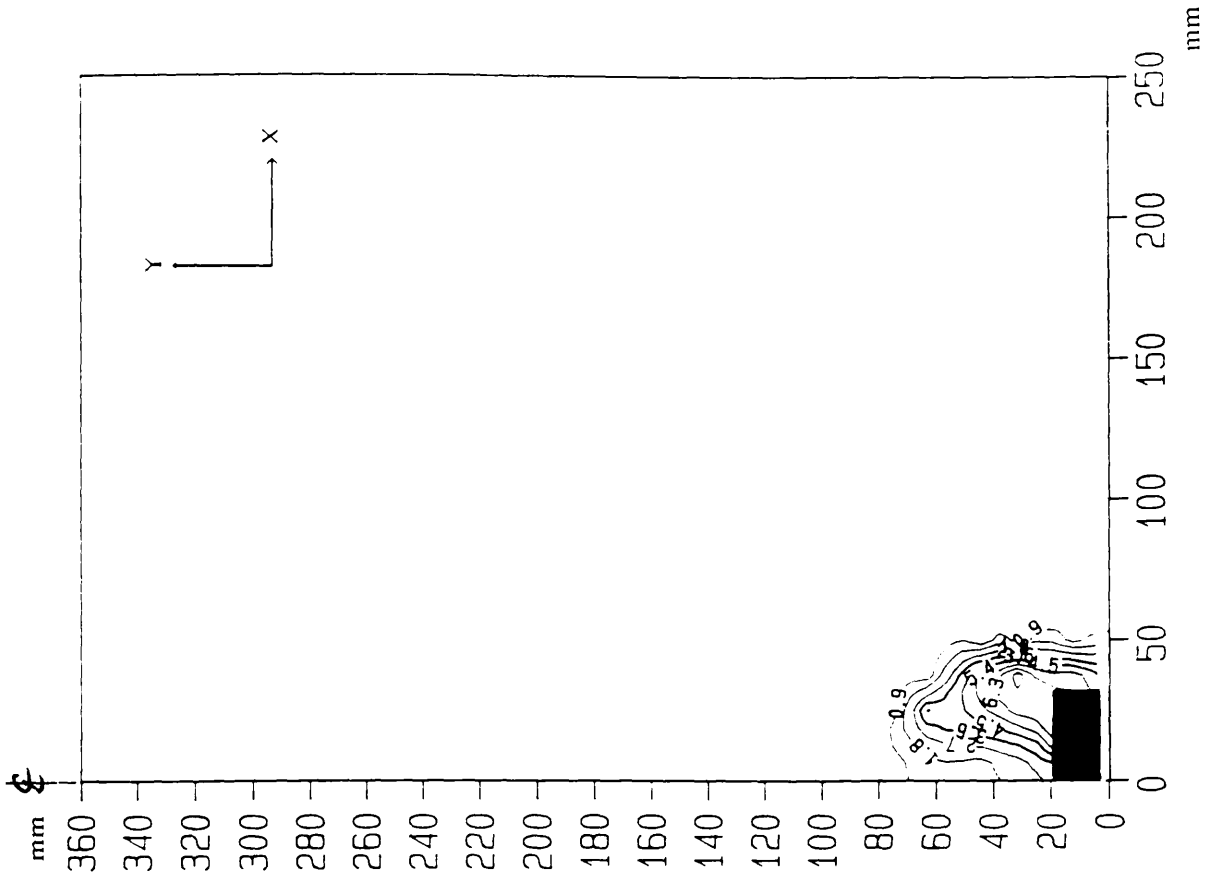


Fig. 7-33 Contours of maximum shear strain in Leighton buzzard
 D/B = 8 , ID= 15% , δ = 3.6 mm.

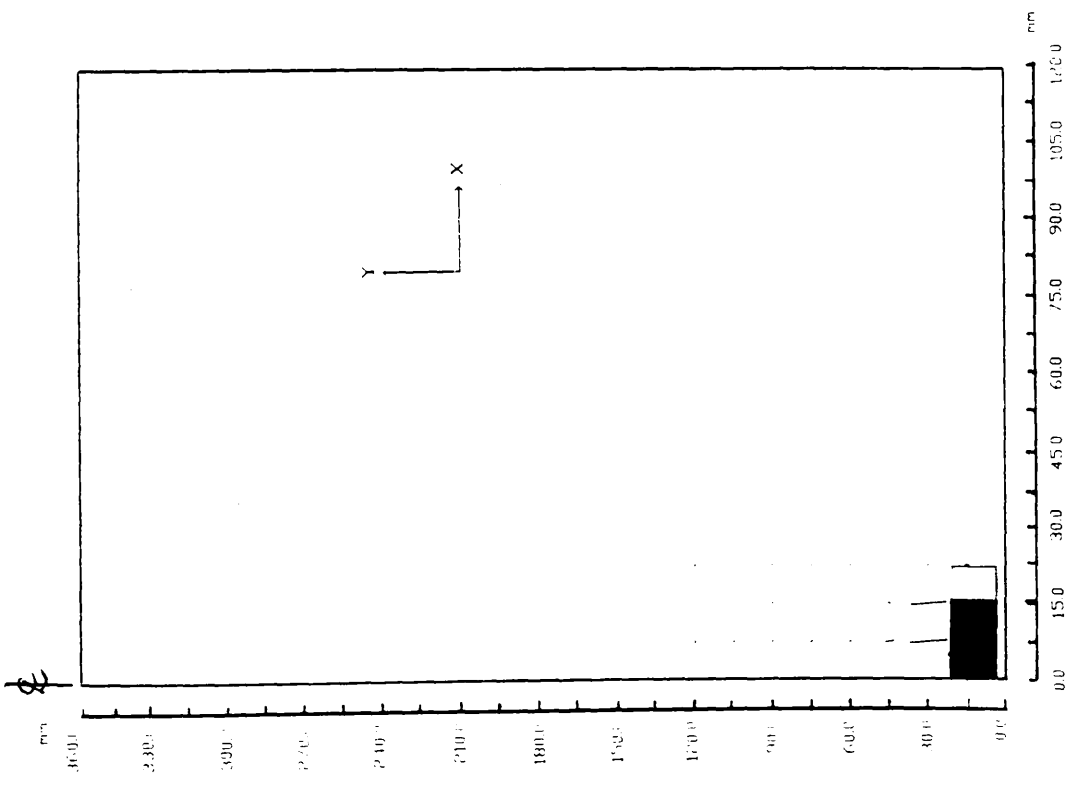


Fig. 7-32 Displacement fields in Leighton buzzard sand
 D/B= 8 , ID= 15% , δ = 3.6 mm.

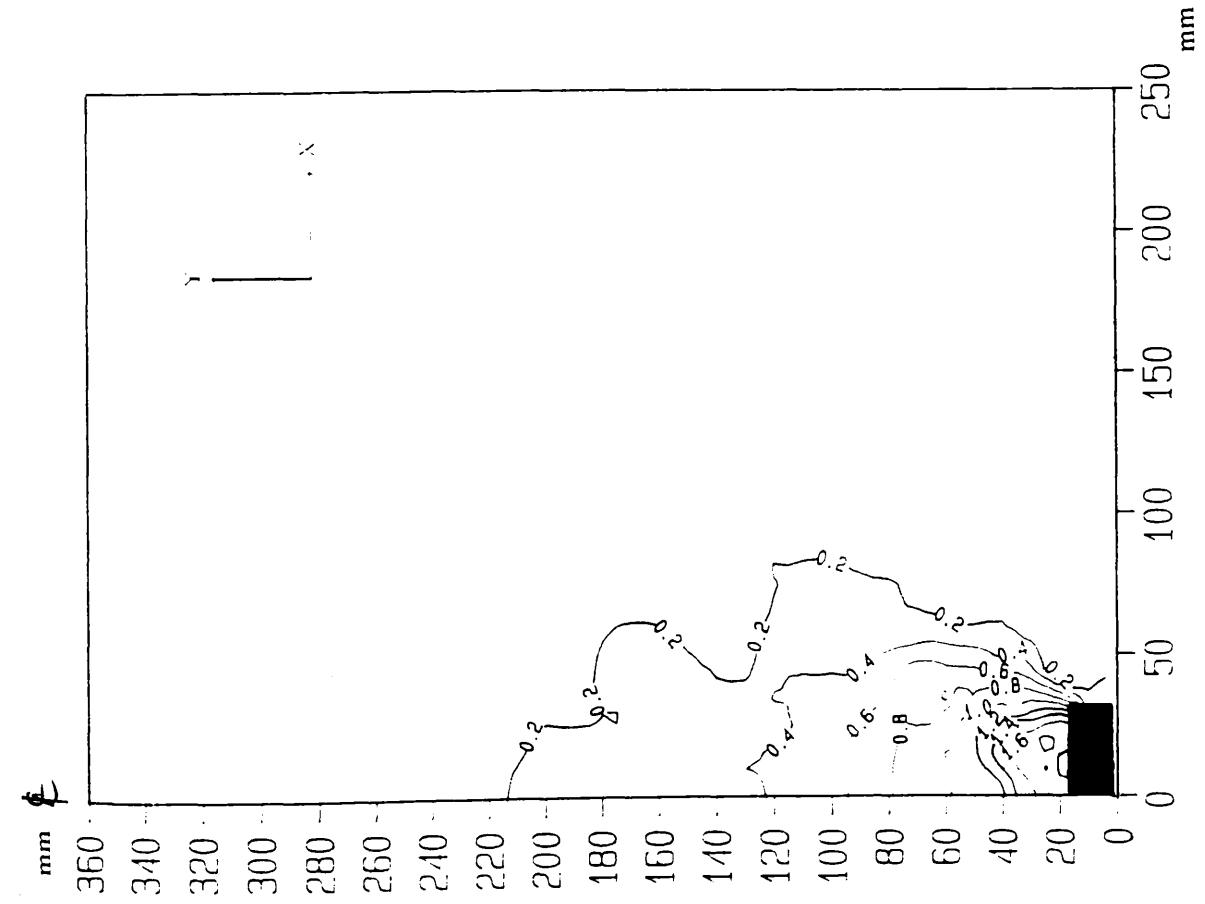


Fig. 7-34 Contours of vertical displacements in Leighton Buzzard sand, $D/B=8$, $ID=75\%$, $\delta=1.8$ mm.

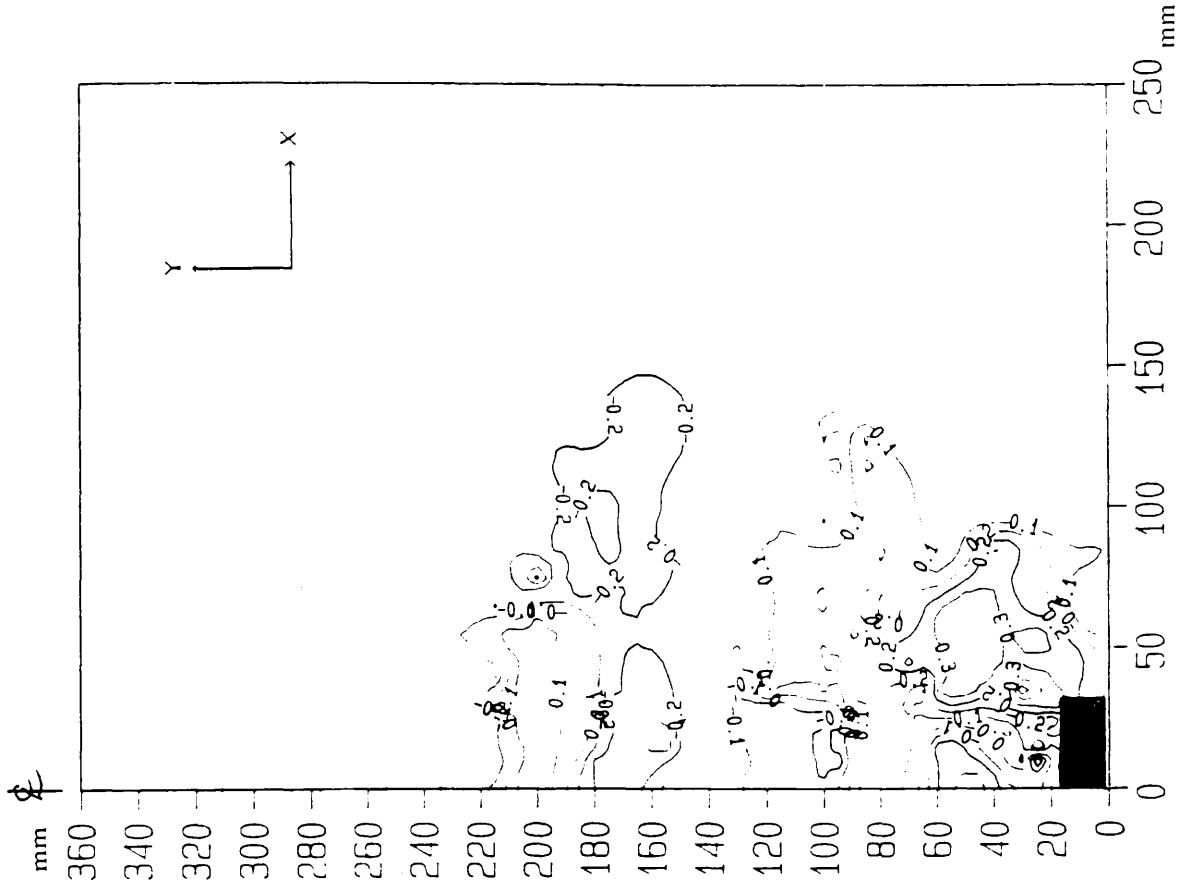


Fig. 7-35 Contours of horizontal displacements in Leighton Buzzard sand, $D/B=8$, $ID=75\%$, $\delta=1.8$ mm.

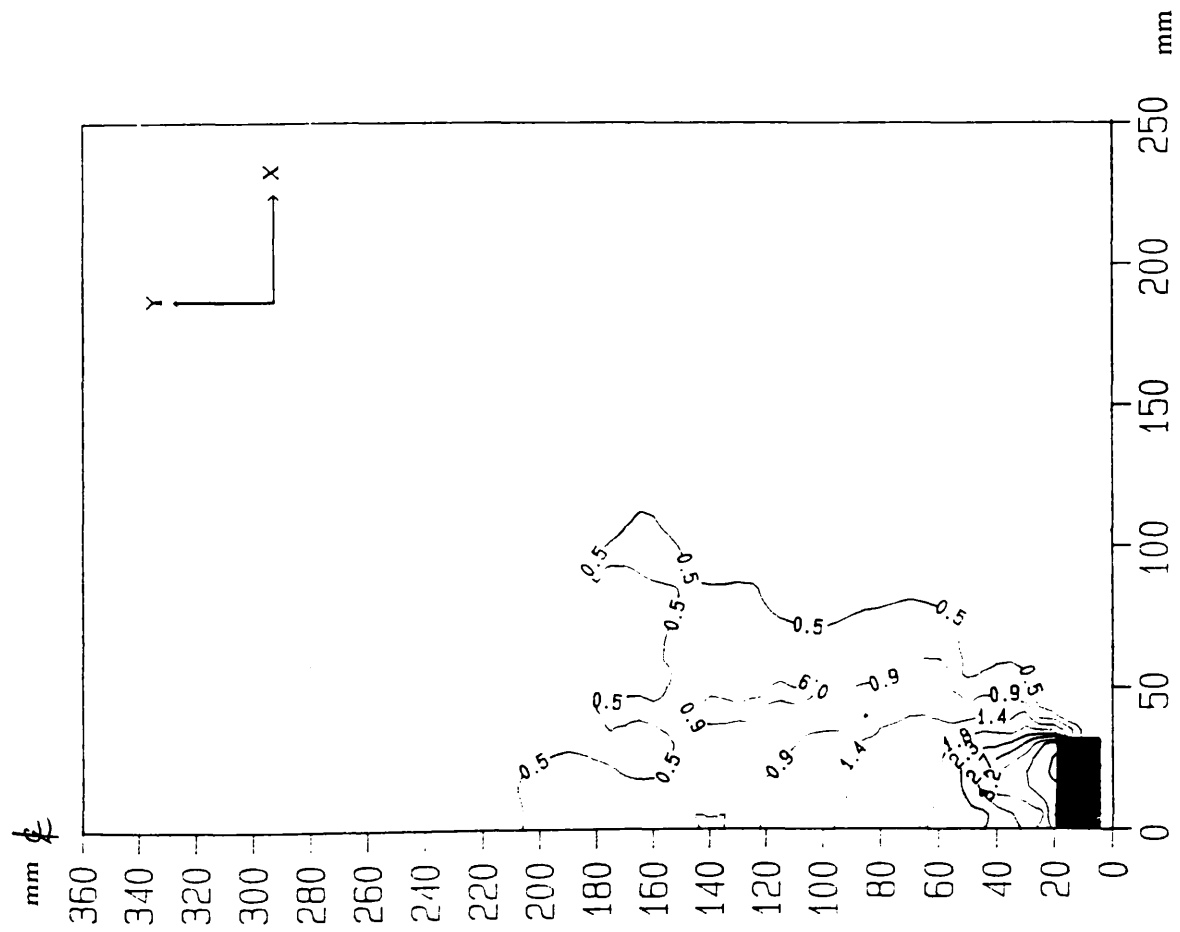


Fig. 7-38 Contours of vertical displacements in Leighton Buzzard sand, $D/B=8$, $ID=75\%$, $\delta=3.6$ mm.

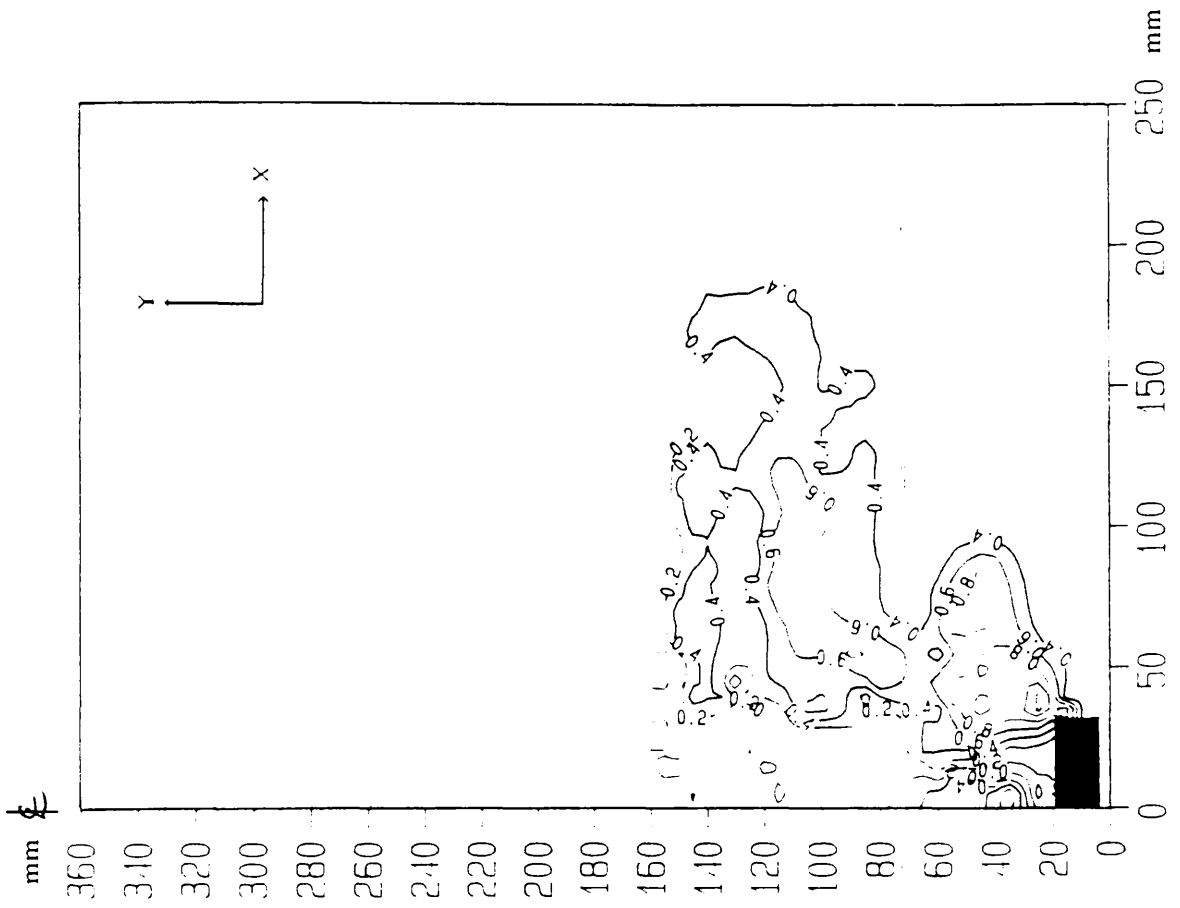


Fig. 7-39 Contours of horizontal displacements in Leighton Buzzard sand, $D/B=8$, $ID=75\%$, $\delta=3.6$ mm.

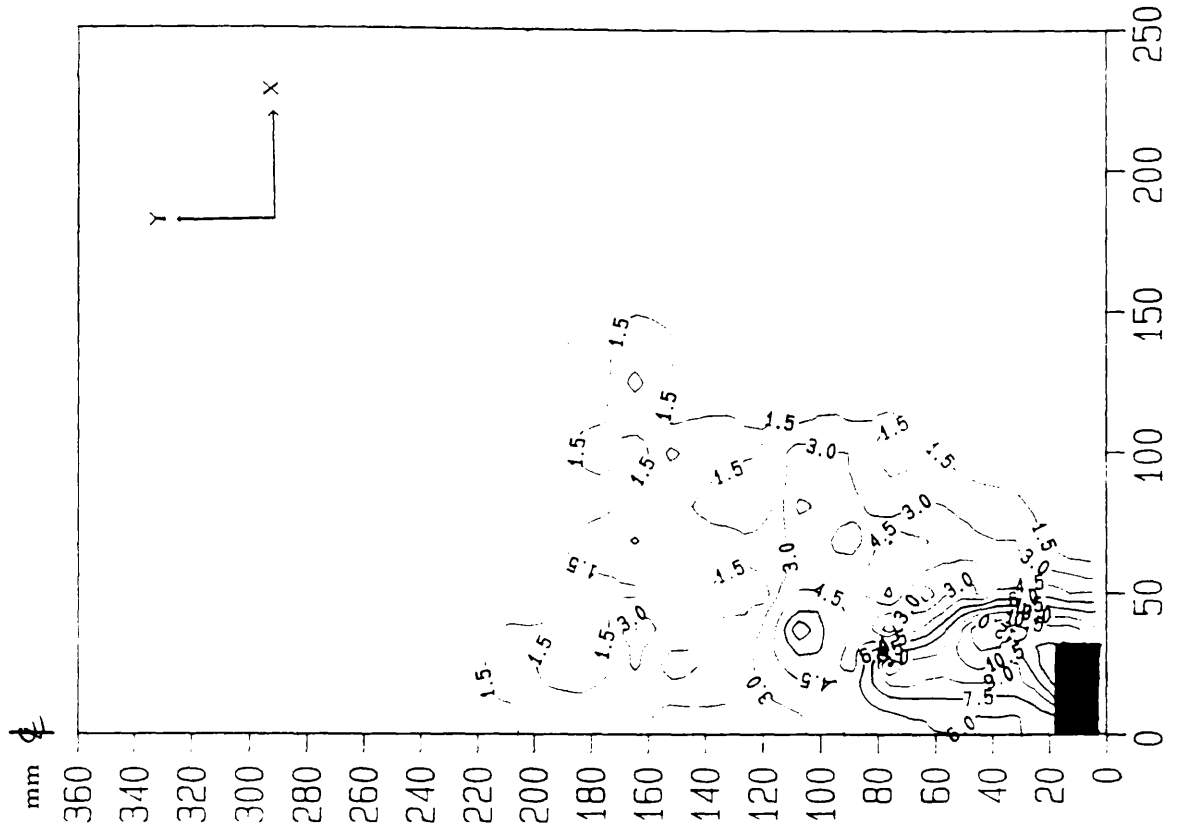


Fig. 7-41 Contours of maximum shear strain in Leighton buzzard
 $D/B = 8$, $ID = 75\%$, $\delta = 3.6$ mm.

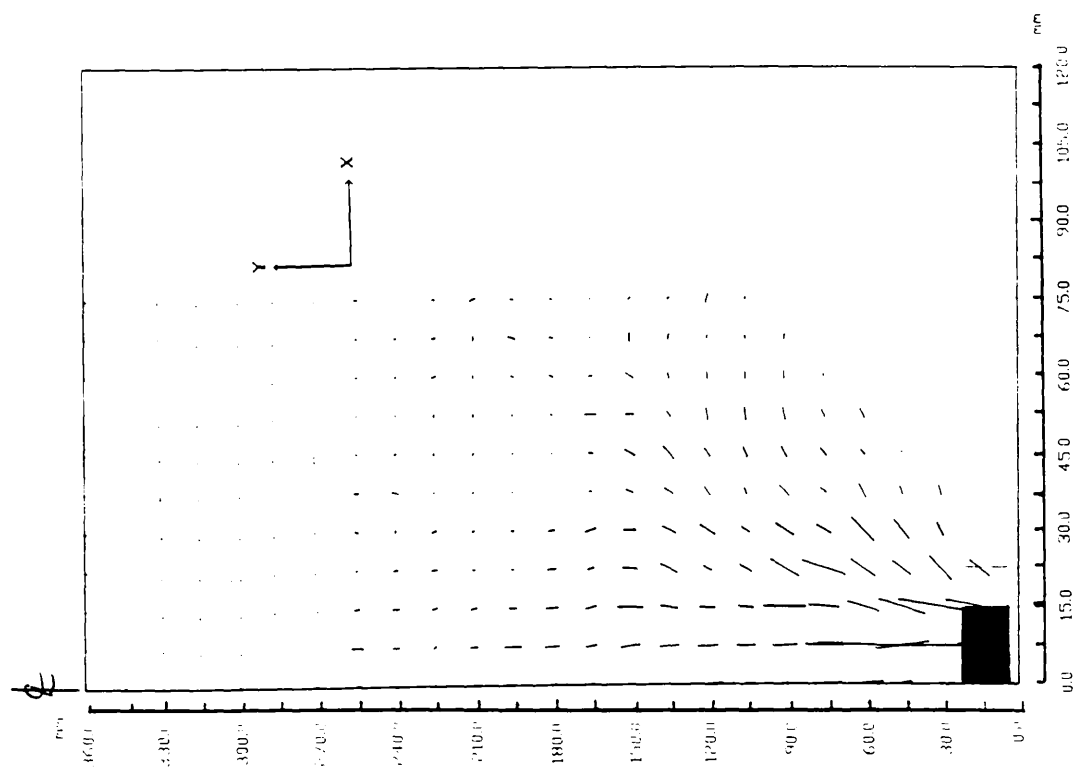


Fig. 7-40 Displacement fields in Leighton buzzard sand
 $D/B = 8$, $ID = 75\%$, $\delta = 3.6$ mm.

7-2-3 Effect of grain size, grain shape and grading

The main object of the present section is to present the separate effects of grain size, grain shape and grading on the form of the displaced soil mass. Due to the large amount of data accumulated and also for the sake of clarity, only displacement fields at failure are presented. The test procedure is identical to the one described in chapter 5. In the course of the present testing a technical complication arose as it was found difficult to achieve similar relative densities for all the sands. However, this difficulty was overcome by trial and error testing. All the photogrammetric tests have been conducted at relative densities of 15% (loose) and 75% (dense) and at depth/diameter ratios $D/B = 4$ and 8 .

7-2-3-1 Grain size

For the present investigation two sands which differed only with respect to grain size, namely Lochaline sand (fine) and Leighton Buzzard (coarse), are used, and other factors affecting the pull out capacity being kept constant. Figs. 7-42 to 7-49 depict the deformation fields occurring in the loose and dense state with shallow and deep anchors. A closer look at these figures shows that the photogrammetric tests give more or less similar results for both sands. Although the sands are descriptively different (fine vs coarse), they are indeed identical in the face of the phenomenon at play. Based on these results it is possible to conclude that for sands having similar shape and grading, the shape of the displaced sand mass is independent of the grain size at a given depth and relative density.

7-2-3-2 Grain shape

Stereophotogrammetric tests were made in two sands, each having grains of a

different known shape but with similar size and grading. The two sands used were Leighton Buzzard (subrounded) and Douglasmuir (subangular). The effect of the grain shape on the zone of disturbed sand is illustrated in fig. 7-50 to fig. 7-57 where the displacement fields occurring at failure in dense and loose state are shown.

Considering, firstly, the dense state, figs. 7-52 & 7-53 show that at shallow depth the zone of sand suffering displacement for both materials extends all the way above the plate anchor to reach the ground surface. However, in the case of Leighton Buzzard sand this zone radiated from $0.25 \times B$ to $2.0 \times B$ to the side of the plate anchor whereas in Douglasmuir it radiated from $0.25 \times B$ to $2.75 \times B$. For a deep anchor, the mode of failure is totally different as it is more local. Figs 7-56 and 7-57 show that the zone of sand suffering measurable displacement spread out to $5.6 \times B$ above the plate anchor in Leighton Buzzard whereas in Douglasmuir this zone came to a stop $6.0 \times B$ above the plate. Another feature is also observable and is a characteristic of a local shear failure, a zone of sand spreading from $0.0 \times B$ to approximately $1.2 \times B$ outwards from the perimeter of the plate anchor and stopping $3.65 \times B$ above it can be seen in Leighton Buzzard whereas in Douglasmuir this zone is much wider as it radiates from $0.0 \times B$ to $1.5 \times B$ to the side of the plate anchor and stops $3.35 \times B$ above it.

In the loose state, fig. 7-50 and 7-51, it can be seen that at shallow depth the displacements in Leighton Buzzard have mainly occurred $2.0 \times B$ above the plate anchor and $0.25 \times B$ laterally whereas in Douglasmuir sand the disturbed area extended $2.0 \times B$ above the plate and radiated $0.75 \times B$ to its side. For deep anchors, figs. 7-54 and 7-55, the upward displacement at failure yielded a localisation of the deformation which extended in the subangular sand $2.65 \times B$

above the plate and $0.35 \times B$ in the lateral outward direction whereas in the subrounded sand this zone of disturbance was confined to $2.65 \times B$ above the plate without disturbance of the sand at its side.

It is clear that the observations made in the present experiment study show that the extent of the displaced sand mass at a given depth and relative density is substantially influenced by the grain shape.

7-2-3-3 Grading

In order to study the influence of the above parameter on the shape of the slip line, two sands having similar size and shape have been used, namely Douglasmuir sand (uniform) and Hyndford sand (well graded). It should be pointed out that testing in Hyndford sand took place only in the loose state as it has been found difficult to obtain a dense state which would have allowed a valid comparison.

Test results obtained for shallow and deep anchors are presented in fig. 7-58 to 7-61. Examination of these figures reveals that although the same general features exist, the sands behave differently during the uplift. The extent of the sands responding to the loading of a shallow anchor (at failure) is depicted in figs. 7-58 and 7-59 where it can be seen that in the case of Hyndford sand the zone of disturbed sand extends $2.0 \times B$ above the plate anchor and $1.25 \times B$ in the laterally outward direction whereas in Douglasmuir sand this zone is restricted to $2.0 \times B$ above the plate and $0.75 \times B$ laterally. Figs. 7-60 and 7-61 show the displacement fields occurring at greater depth. It can be seen that the zone of sand suffering displacement in the well graded sand extends $3.0 \times B$ above the plate anchor and radiates $0.5 \times B$ to its side whereas in the uniform sand the measurable

displacements are confined to a zone of sand extending $2.65 \times B$ above the plate and $0.35 \times B$ to its side.

It is clear from the present tests that the difference in grading is responsible for a distinct change in the extent of the zone of disturbance.

7-3 Comments

The information displayed in the previous sections gives a detailed and comprehensive picture of the interaction between a plate anchor and, respectively, a bed of loose and dense sand with shallow and deep anchor. Generally, when the load is applied the anchor resists it by bearing against the overlying sand which is effectively continuous over the plate

In the case of a shallow anchor embedded in loose sand, the displacement of the plate is accompanied by a punching shear failure as the load on the anchor increases. The sand above the plate is compacted until the uplift load reaches approximately 75% of its maximum. The displacement of the sand is predominantly vertical but with very small magnitudes. The zone of disturbed sand extends over a limited distance vertically above the perimeter of the plate anchor. A number of previous researchers (Clemence & Veesaert, 1977; Fadl, 1981) have assumed a unique curved shape (reaching the ground surface) with a small angle of inclination to make allowance for the fact that a loose sand was under investigation. Others have assumed a cylindrical failure shape. However, the present investigation shows that the present mode of failure is of a local type of failure and is reflected by the formation of a small frustrum of cone above the plate anchor. It is obvious that this type of failure is a characteristic of an anchor embedded at the critical depth

and indeed it is the case as $D/B=4.0$ represents the transition depth in loose sand. For deep anchors embedded in loose sand, the sand above the plate anchor is compacted as it resists the initial loading. The failure surface is essentially vertical and limited to a short distance above the anchor, and similar results have been reported by Fadl (1981). Nevertheless, it was observed that depending on the type of sand the displacement of the plate anchor is accompanied by either a punching or a local shear failure. Furthermore, it was found that grain shape and grading can dramatically affect the extent of the displaced sand mass as has been demonstrated in the previous section.

In the case of a shallow anchor embedded in dense sand, uplift loading causes a large zone of the sand bed to deform. The sand above the plate suffers predominantly vertical upward displacement and is compacted as it resists the initial loading. As the uplift load increases, the anchor moves upwards and the sand above suffers more vertical displacements, the sand near the anchor plate being displaced laterally. Shear strains develop vertically upwards, and further loading causes more upward movement of the anchor and the sand above it, although the zone of disturbed sand remains the same. The shearing of the sand is more prominent along the rupture lines. The shape of the failure surface is defined by the shape of the boundary of the disturbed zone of sand (i.e. a frustrum of cone). This finding is compatible with those obtained by earlier investigators such as Carr (1970), Fadl (1981), Sarac (1989). The assumption of a curved surface presumes that a cone of failure will always occur (Murray & Geddes, 1987), which generally is not the case. These assumptions are reasonable for a shallow anchor under certain conditions, but are not applicable to a deep anchor. Deep anchors, which are defined as those which develop their maximum load without disturbance of the ground surface, have been investigated. In the early stages of the loading,

compaction of the sand above the plate anchor takes place. The increasing uplift load causes further movement of the anchor and the sand above it, and at this stage the sand is also moving laterally. The magnitude of the displacements in the sand above the plate varies and is largest directly above the plate. Further loading causes more upward movement of the anchor and the sand above it. The zone of sand which has been disturbed is much greater and does not reach the ground surface, and intense shearing is taking place immediately above the plate anchor. It has also been observed that a wedge of sand or elastic wedge (for both shallow and deep anchors) as referred to by Maddocks (1978) and Stewart (1988) is apparent on top of the plate anchor. As the anchor moves upwards the sliding which develops on the sloping surfaces of the wedge of sand reduces the vertical upward displacement of the sand overlying the wedge and gives it a lateral displacement which permits the upward movement of the anchor. A consequence of this is that, near the plate anchor, sand that has been displaced by the upward movement of the plate anchor begins to move downwards as it recovers from the passage of the plate. This behaviour agrees with that observed by Carr (1971) and Maddocks (1978). Kupferman (1974), Meyerhof & Adams (1968) reported that in dense sand the failure surface curved outwards from the anchor perimeter and then became vertical and extended to the ground surface. The displacements described by those two authors, taken from tests with relatively low values of D/B , appear to combine characteristics of the shallow and deep modes of behaviour. Meyerhof and Adams identified the outer boundary of blurring in their time exposure photographs as a failure surface. This is not strictly correct as this boundary marks the border between sand that has moved and sand that has remained stationary. Time exposure photography does not accurately represent the relative displacements within the mass of sand that has displaced and the outer boundary of movement is not necessarily the surface on which sliding first developed. From the present investigation, for both

cases of shallow and deep anchors, it was found that angularity of the grains and grading influenced the extent of sand disturbance whereas grain size did not have any effect.

The prediction of the inclination of the failure surfaces has received a great deal of attention especially in shallow anchors. Most of the theories presented in chapter 2 were based on these slip lines. For example Balla (1961) considered that the failure surface met the ground surface at $(\pi/4 - \varphi/2)^0$; in this case the apex angle is $(\pi/2 - \varphi/2)^0$. Murray & Geddes (1987) assumed an apex angle of 2φ . A third possible assumption for the apex angle is based on the consideration that the inclination is a function of φ and ID (Fadl, 1981); in this case the apex angle is equal to $0.5 M$ where M is given in sec. 2-11 (chap.2). Let's consider two types of dense sand (ID=75%) used in the present investigation, at ID=75% the subrounded sand has an angle of shearing resistance (φ) of 41.5^0 whereas for the subangular sand φ is equal to 45.7^0 . The inclination of the shear band as given by Balla (1961) and Murray & Geddes (1987) would be $(\pi/4 - \varphi)^0 = 23^0$ and $\varphi/2 = 22^0$ respectively in the subrounded sand and $(\pi/4 - \varphi)^0 = 19.5^0$, $\varphi/2 = 25.5^0$ in the subangular sand. Using Fadl's axisymmetric expression the inclination would be equal to 27^0 in the subrounded sand and 30^0 in the subangular sand. The estimated inclinations for each of the three assumed mechanisms given previously show that a large discrepancy can occur for the same problem. In view of what is stated above, it appears obvious that a unique failure surface for all the sands cannot exist. Very recently Frydman & Shaham (1989) stated that:

" It is not possible, on the basis of existing data, to identify which of the failure mechanisms best describes the pull out of horizontal anchors. Clarification of this point may be possible by testing models in an artificial soil for which the φ values are such that the predicted shear plane indications are significantly different".

The present tests results give an answer to the above statement by showing clearly that a universal form of failure surface does not exist and also provide an explanation as to why the prediction of the inclined surfaces can be at fault. In the present investigation grain shape was found to substantially affect the form of the zone of displaced sand mass both in the loose or dense state with shallow and deep anchors, and in the present context the subangular sand always yielded a wider surface. Similarly, Arthur & Dunstan (1982) on their work on rupture layers in granular media reported that the orientation of a rupture layer was related to the grain shape. Equally as important, it was found that, in loose soil, grading can have drastically the same effect. A less marked effect was found when varying the grain size. The present investigation shows that it is reasonable to assume that there will be distinct differences in the extent of disturbance caused by relative density, depth of embedment, grain shape and grading. Different soil characteristics will require different failure mechanisms, and there is no rational basis to establish these ruptures in a general manner.

Similar to the conclusions made by Hanna et al (1972), it was found that the magnitude and direction of the sand displacements were regulated to a large extent by the anchor embedment depth, and the sand relative density.

It was found that the stereo photogrammetric technique can yield accurate measurements and it is possible by measuring both the vertical and horizontal displacements within the sand bed to establish the relative displacements occurring throughout the bed for any increment of displacement of the anchor. It is therefore possible to build up information on displacements in the sand bed increment by increment throughout the loading and displacement of the anchor.

2

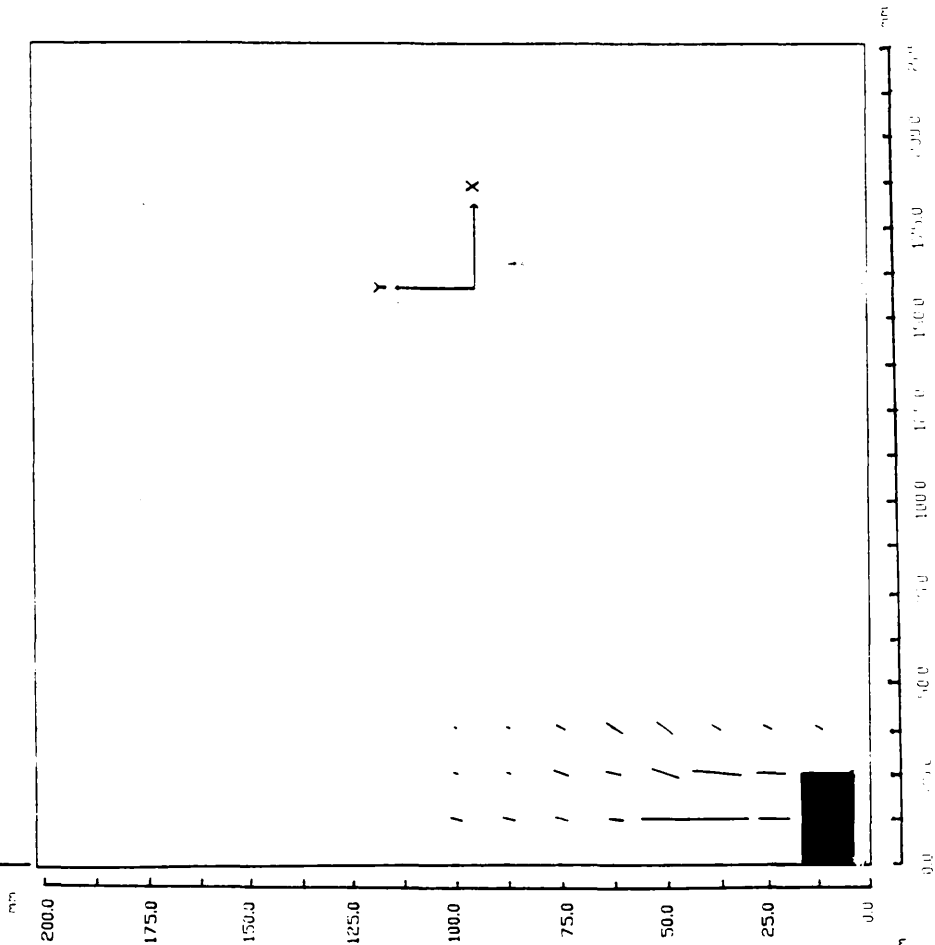


Fig. 7-43 Displacement fields in Leighton buzzard sand

D/B = 4, ID = 15%, $\delta = 3.6$ mm.

17

3

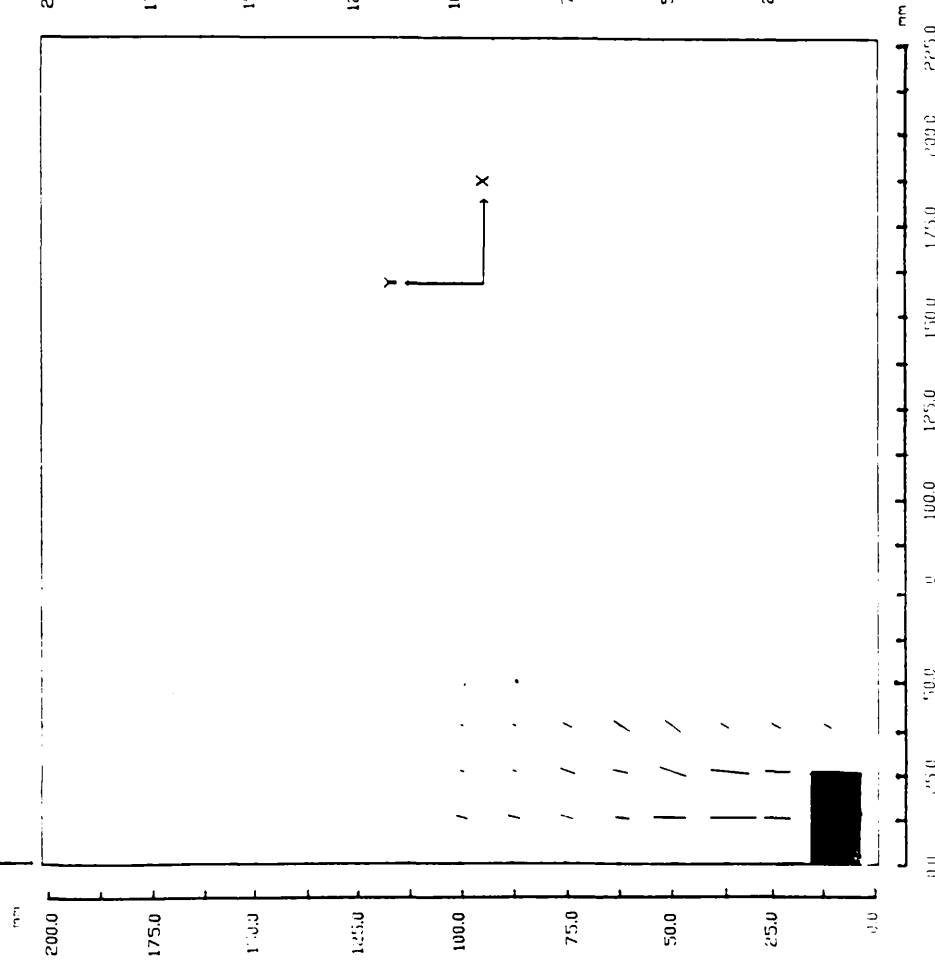


Fig. 7-42 Displacement fields in Lochaline sand

D/B = 4, ID = 15%, $\delta = 4.5$ mm.

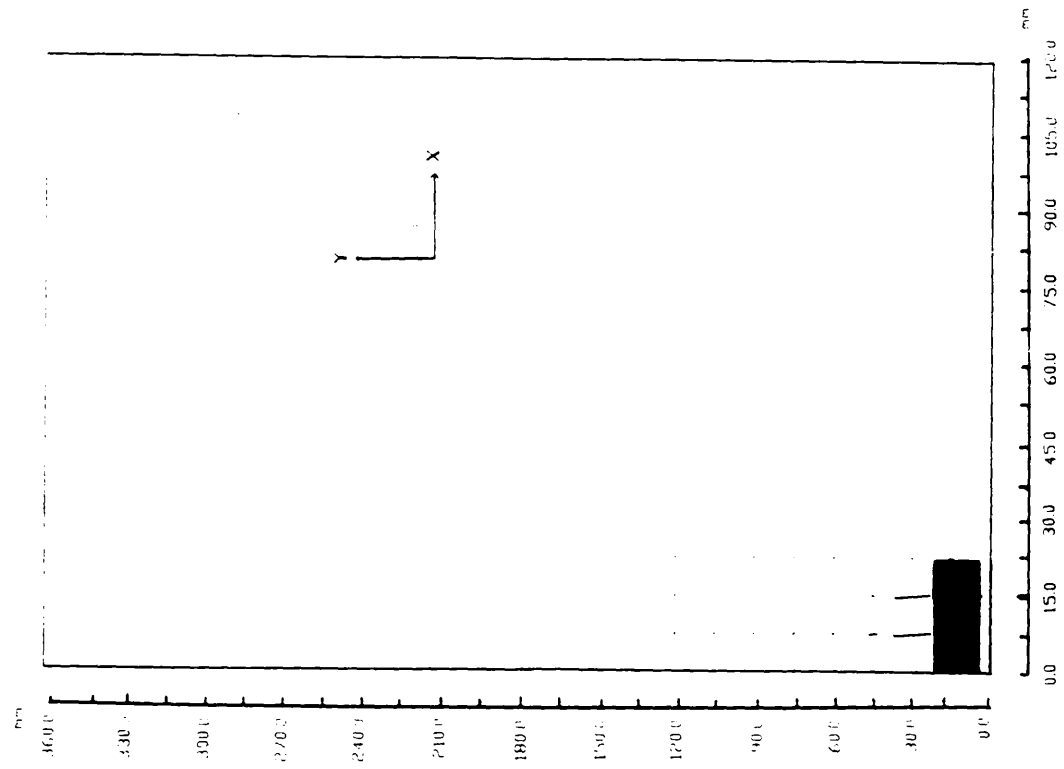


Fig. 7-45 Displacement fields in Leighton Buzzard sand, $D/B=8$, $ID=7\%$, $\delta=3.6$ mm.

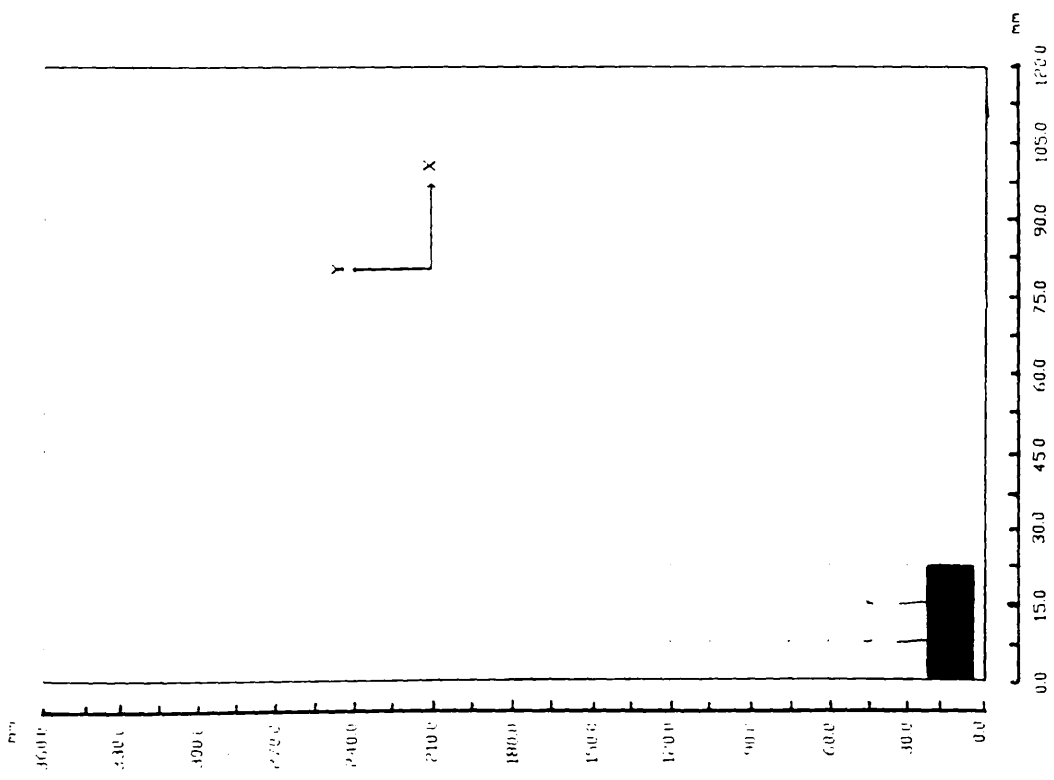


Fig. 7-44 Displacement fields in Lochaline sand $D/B=8$, $ID=15\%$, $\delta=4.0$ mm.

⊕

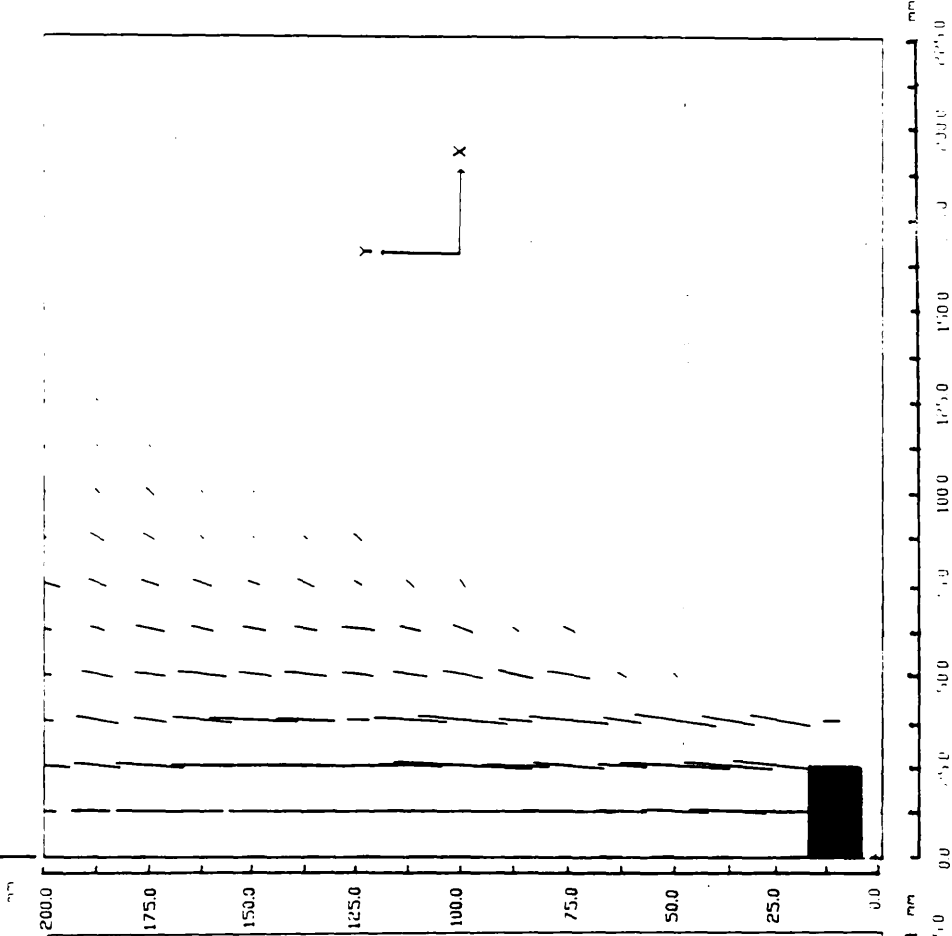


Fig. 7-47 Displacement fields in Leightons Buzzard sand, $D/B=4$, $ID=75\%$, $\delta=3.2$ mm.

⊕

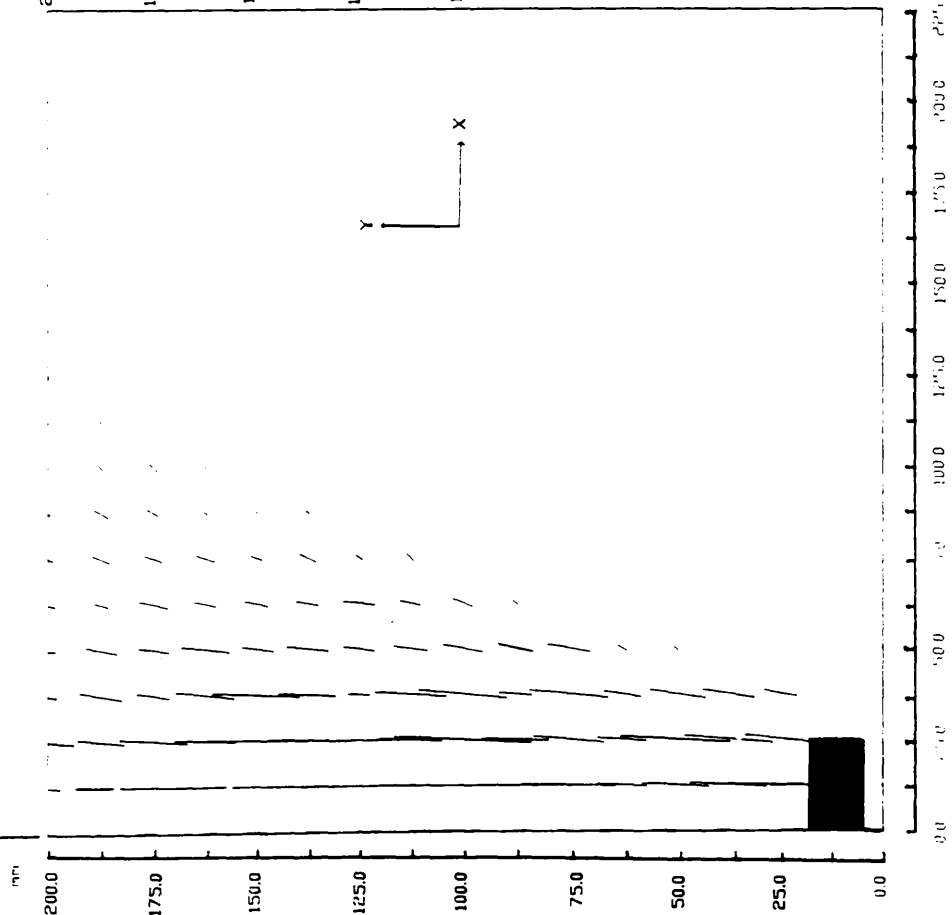


Fig. 7-46 Displacement fields in Lochaline sand $D/B=4$, $ID=75\%$, $\delta=3.5$ mm.

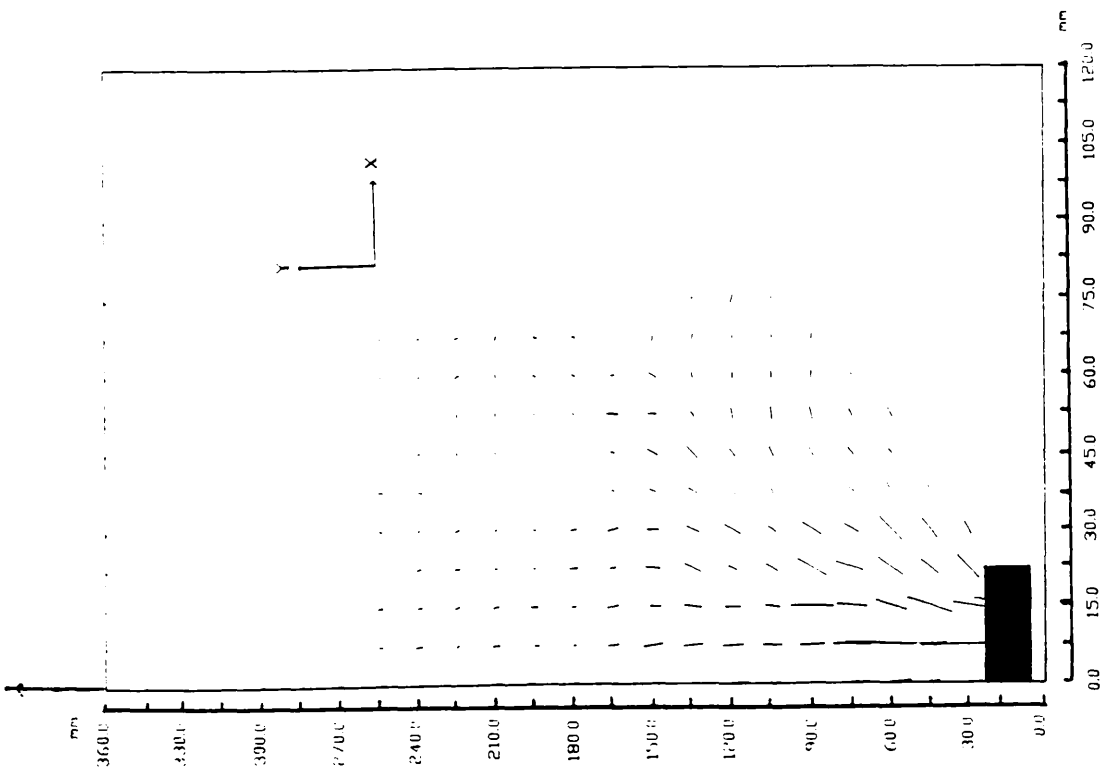


Fig. 7-48 Displacement fields in Lochaline sand
 $D/B=8$, $ID=75\%$, $\delta=5.0$ mm.

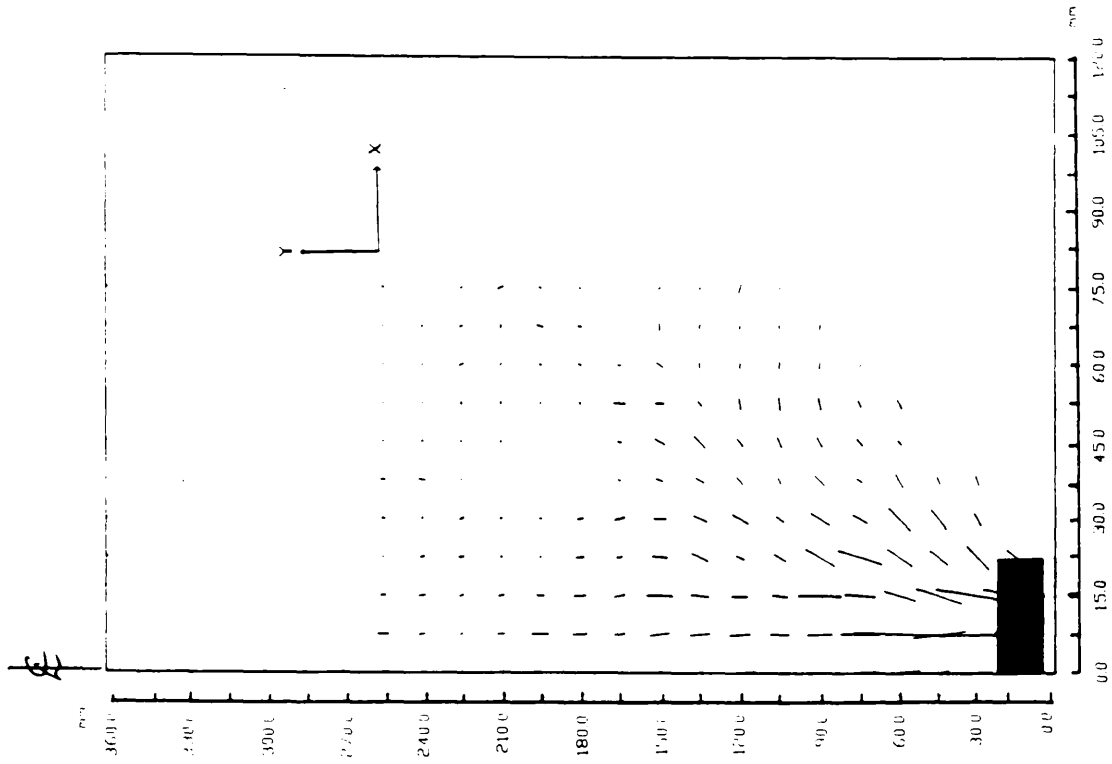


Fig. 7-49 Displacement fields in Leighton Buzzard
sand, $D/B=8$, $ID=75\%$, $\delta=3.6$ mm.

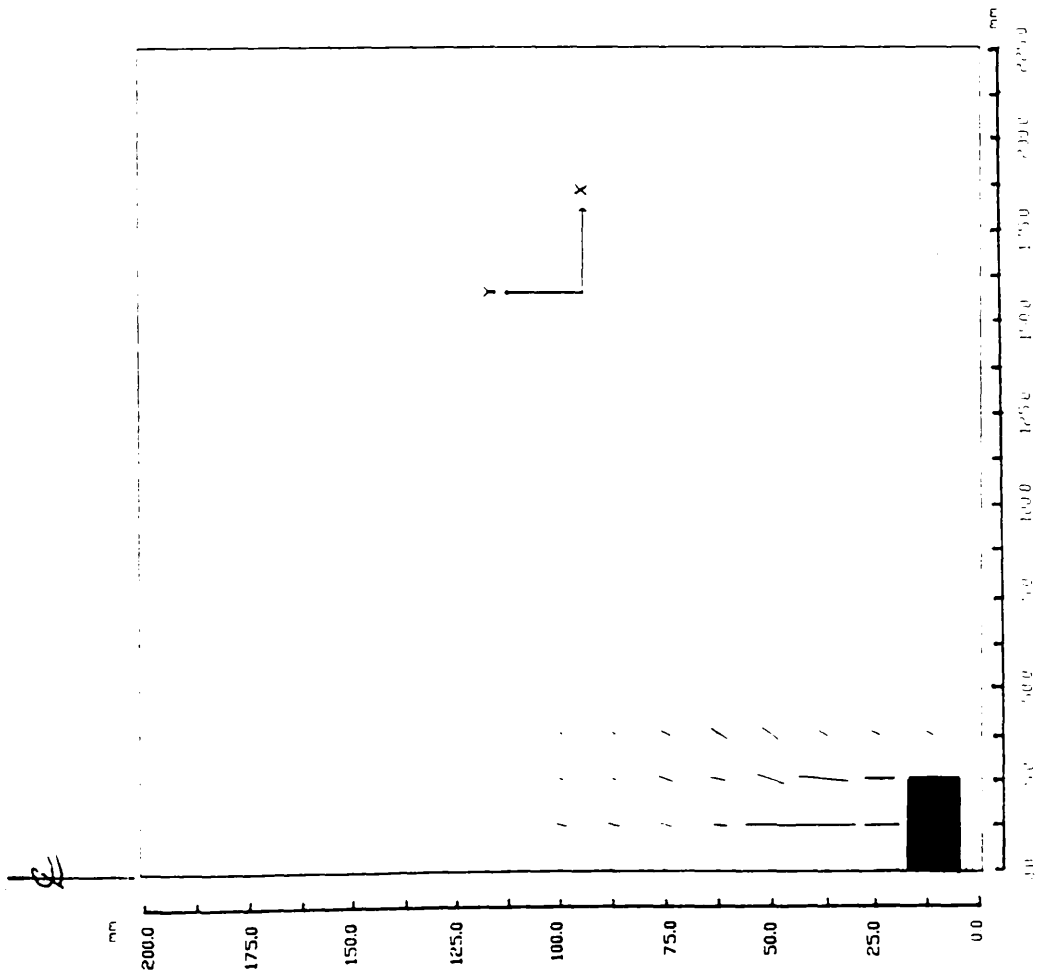


Fig. 7-50 Displacement fields in Leighton buzzard sand

$D/B = 4$, $ID = 15\%$, $\delta = 3.6$ mm.

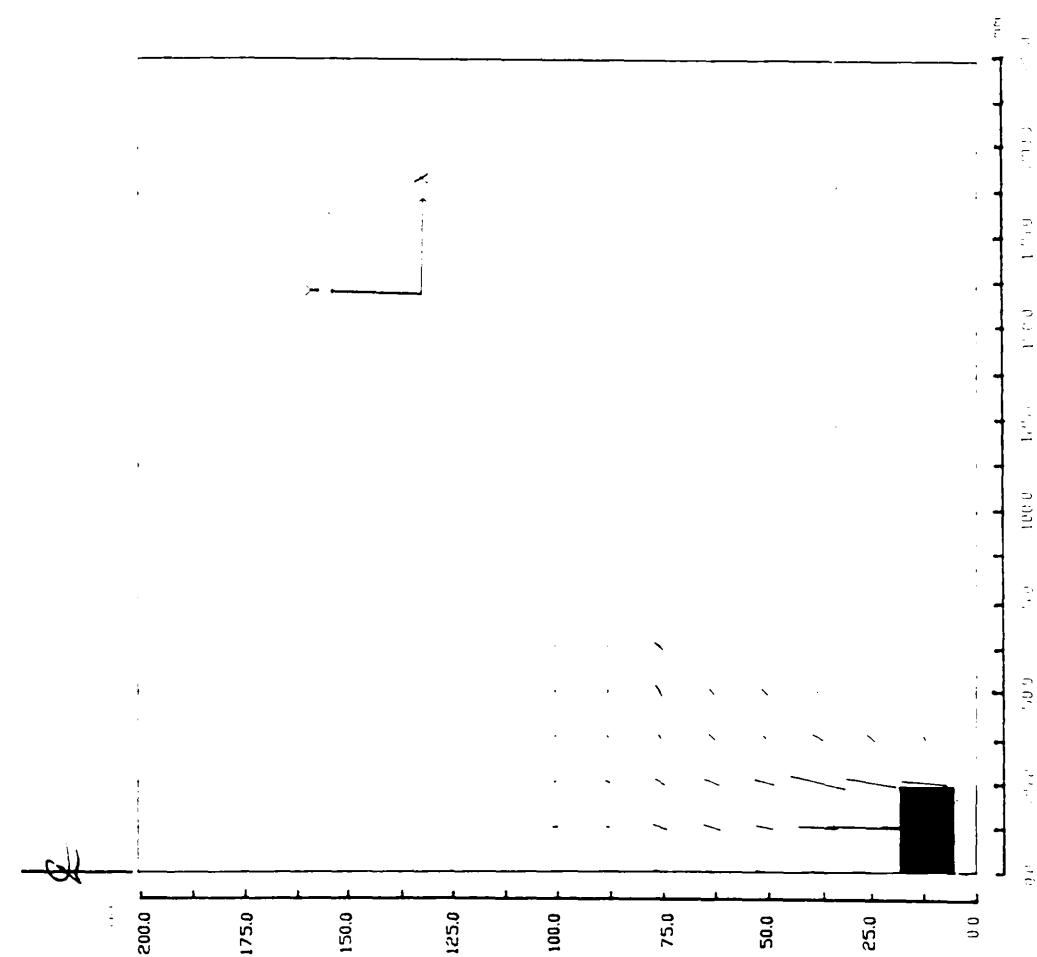


Fig. 7-51 Displacement fields in Douglasmuir sand

$D/B = 4$, $ID = 15\%$, $\delta = 4.5$ mm.

2

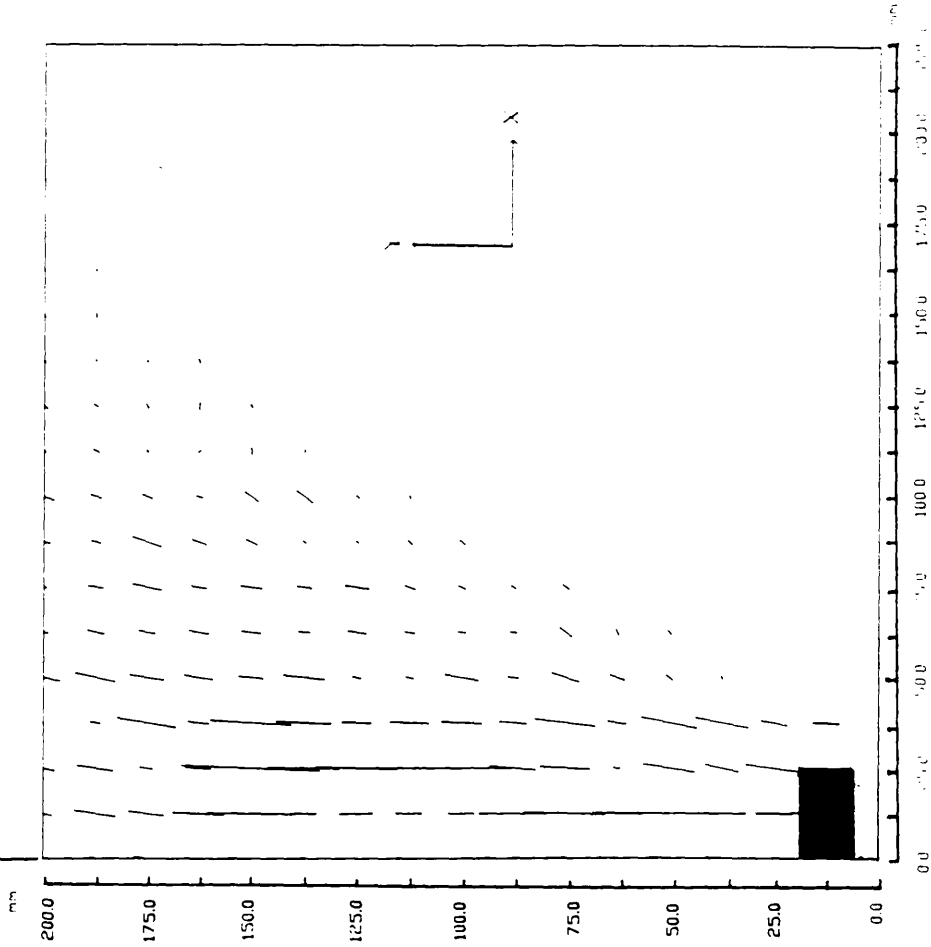


Fig. 7-53 Displacement fields in Douglasmuir sand

$D/B = 4$, $ID = 75\%$, $\delta = 4.0$ mm.

2

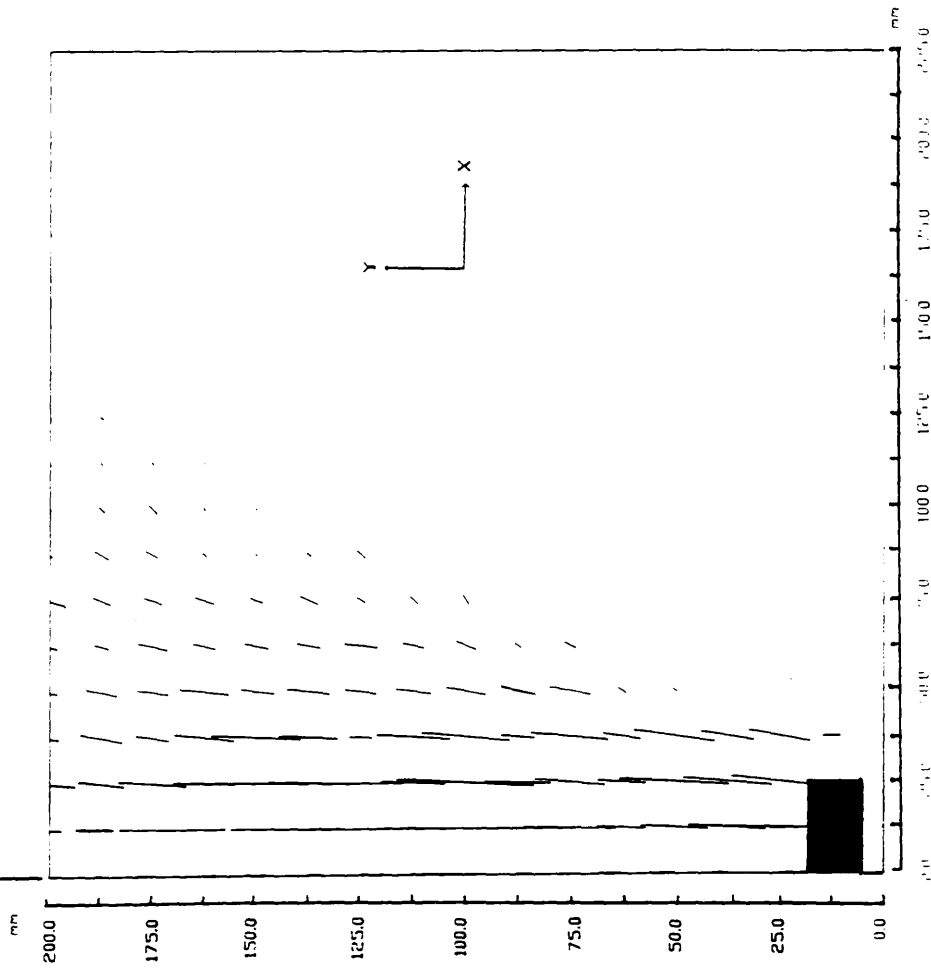


Fig. 7-52 Displacement fields in Leighton Buzzard sand

$D/B = 4$, $ID = 75\%$, $\delta = 3.2$ mm.

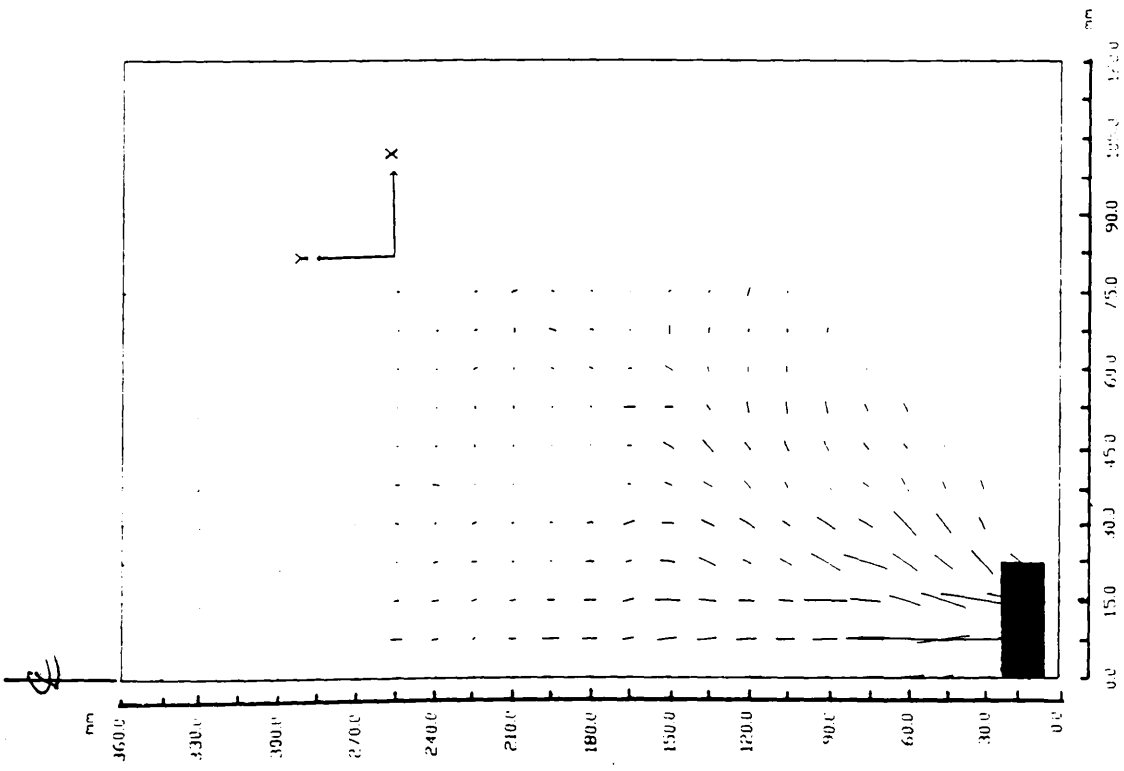


Fig. 7-56 Displacement fields in Leighton Buzzard sand
 $D/B = 8$, $ID = 75\%$, $\delta = 3.6$ mm.

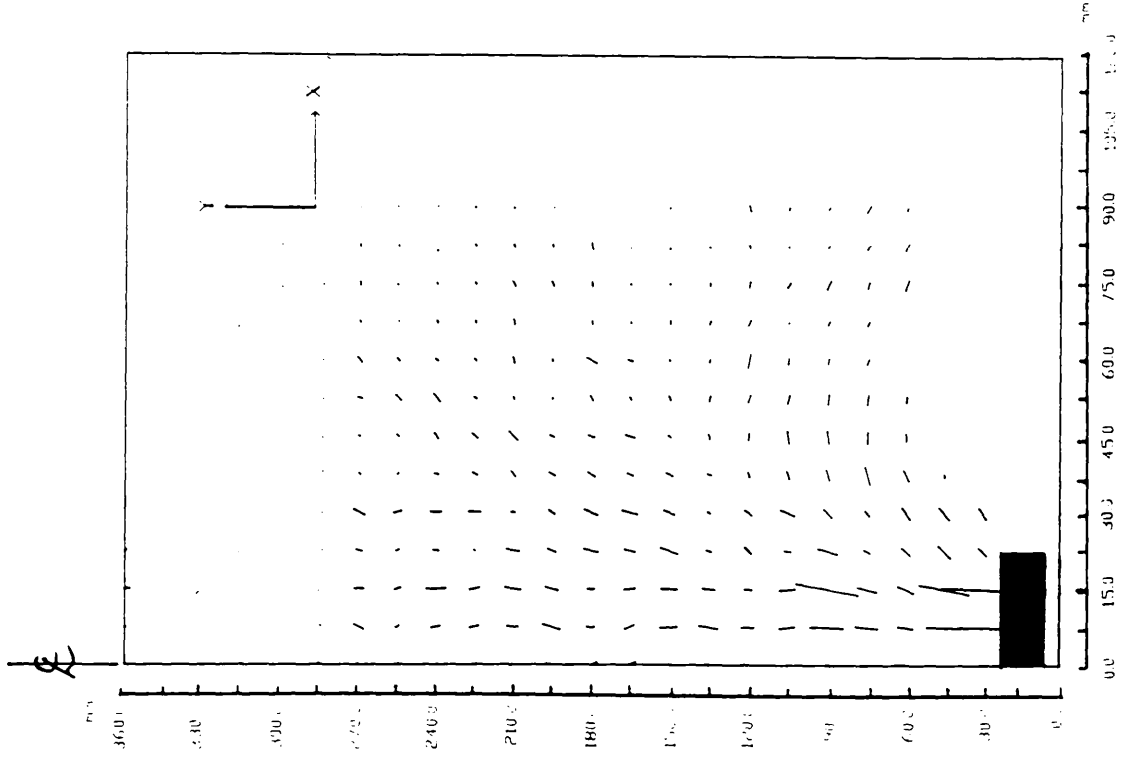


Fig. 7-57 Displacement fields in Douglasmuir sand
 $D/B = 8$, $ID = 75\%$, $\delta = 5.0$ mm.

2

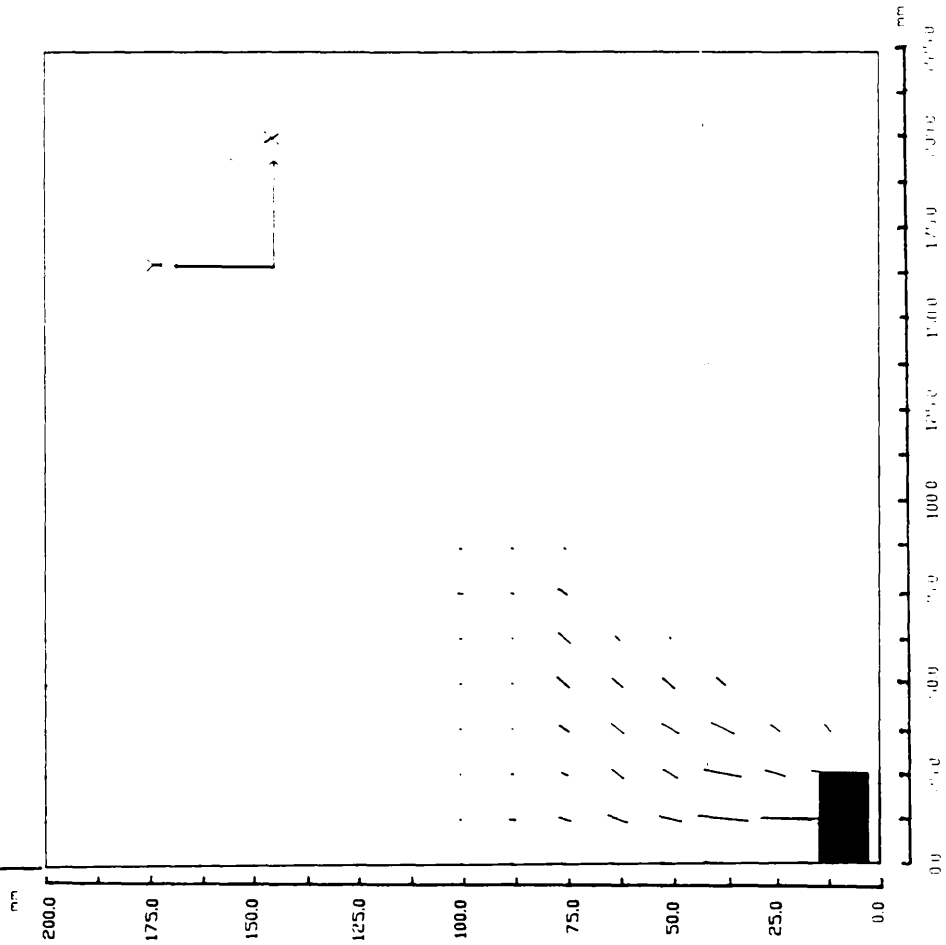


Fig. 7-59 Displacement fields in Hyndford sand
 $D/B = 4$, $ID = 15\%$, $\delta = 4.0$ mm.

2

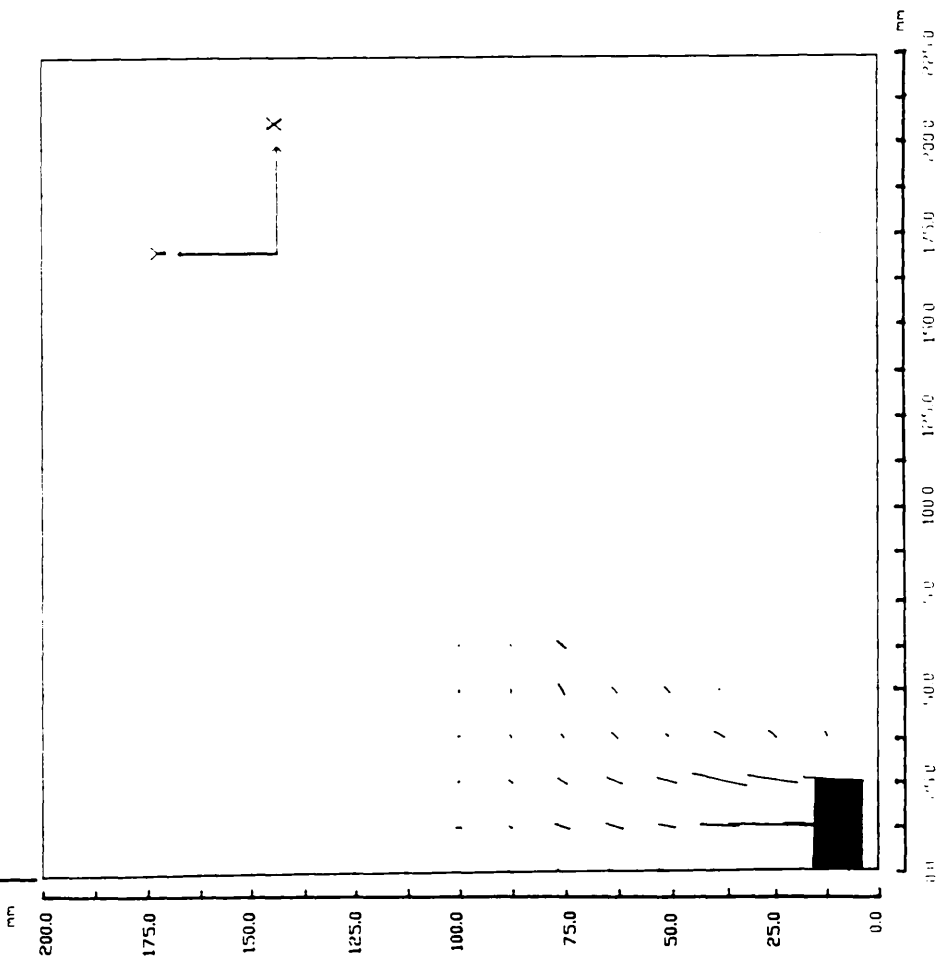


Fig. 7-58 Displacement fields in Douglasmuir sand
 $D/B = 4$, $ID = 15\%$, $\delta = 4.5$ mm.

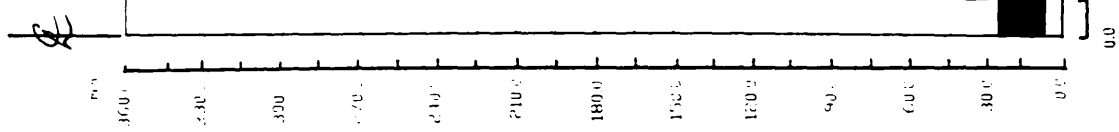


Fig. 7-61 Displacement fields in Hyndford sand
 $D/B = 8$, $ID = 15\%$, $\delta = 6.0$ mm.

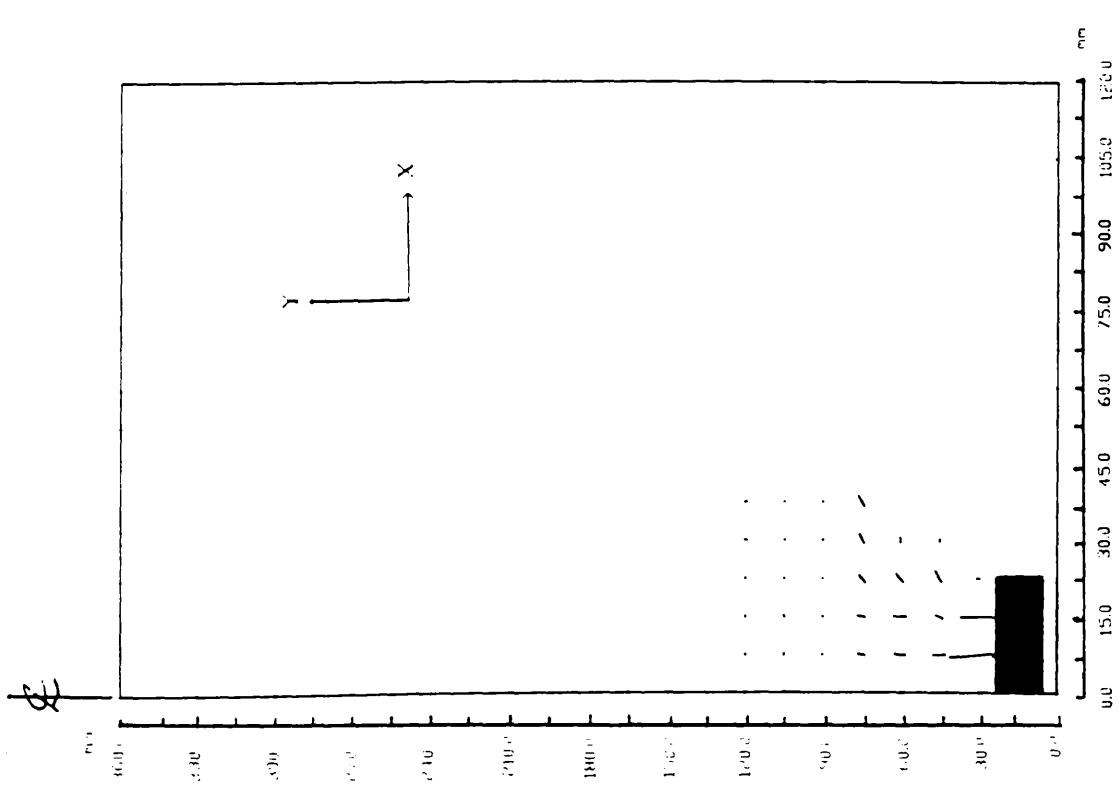


Fig. 7-60 Displacement fields in Douglasmuir sand
 $D/B = 8$, $ID = 15\%$, $\delta = 5.0$ mm.

Chapter 8

PLATE ANCHORS BURIED IN TWO LAYERED SAND:
EXPERIMENTAL AND THEORETICAL INVESTIGATION.

8-1 INTRODUCTION

During the past few years, various theories on vertical circular anchor pull out capacities have been reported by many investigators such as Meyerhof & Adams (1968), Fadhil (1981), Murray & Geddes (1987), Tagaya et al (1988), etc... . These theories were all based on homogeneous soil conditions either in the model tests or in the prototypes.

To the best of the author's knowledge, studies of the pull out capacity of an anchor embedded in two layered sand are non-existent. Since this particular problem has not received much attention, no literature review which has a direct relevance to the present problem is available. It is however worth mentioning the work done by Stewart (1985) on a related problem in which a model anchor study was carried out in a clay overlain by sand. It was found that the cohesionless soil overlay significantly increased the ultimate uplift capacity of the plate anchor compared with its value when embedded in clay alone. This increase in uplift capacity is due to two main factors. The first is the additional overburden pressure which converts the original shallow anchor into a deeper anchor. The second is the mobilization of the frictional resistance of the overlays. However, Sutherland (1988) pointed out that in practice there would be little real benefit on uplift capacity by placing a cohesionless material overlay on an anchor embedded in clay, as a large displacement is required to mobilize the shear strength of the overlays. A more

sensible solution would be to place the anchor on the surface of the clay.

The present chapter is intended to give an insight into a case which is often encountered by practising engineers. Experimental work carried out by the author and reported herein has indicated that the presence of multi layered sands can have a dramatic effect on the ultimate uplift capacity.

The present investigation is limited to the shallow anchor range ($D/B \leq 5$) in two layered sand (see fig. 8-1). A dimensionless parameter, the upper thickness ratio, is introduced. It is defined as the ratio of upper layer thickness to anchor diameter, $\lambda = H/B$. Upper layer thickness ratios λ ranging from 1 to 4 have been investigated with D/B varying from 2 to 5. As has been explained previously a shallow anchor may be defined as one in which the effect of the surface above the anchor plays a major part in the behaviour of the soil under uplift pressure and exhibits a general shear failure. The present chapter is divided into three main sections.

- 1- Stereo photogrammetric tests.
- 2- Theoretical solution.
- 3- Experimental investigation.

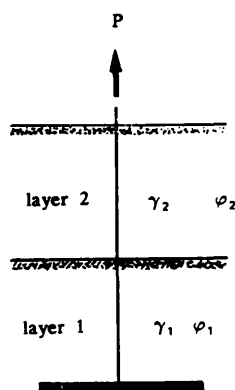


Fig. 8-1 Plate anchor under vertical uplift load in two layered sand.

8-2 STEREO PHOTOGRAMMETRIC TESTS

A series of stereophotogrammetric tests were carried out to assess the form of the failure surface zone when layers of different densities were present. Anchors, diameter= 50 mm, buried at depth/diameter ratio $D/B= 4$ and 6 have been tested for this purpose. During each test a sequence of six or eight photographs was taken, the first prior to pushing, the remainder at 0.5 mm upward displacement intervals. Due to the large amount of data accumulated, only two increments are herein reported. Particle movements are presented using the first (no pushing), intermediate and last negatives. The testing procedure is fully explained in chapter 5.

8-2-1 Two layered soil, $D/B= 4$, $\lambda= 1$

Figs. 8-2 to 8-9 show the displacements and strains for the different incremental displacements. Zones of sand that responded to the increment are depicted.

For $\delta= 1.5$ mm, the resulting deformations and strains of the layered sands are presented in figs. 8-2 to 8-5. The zone of sand responding to this increment extended slightly outward from the perimeter of the plate anchor without reaching the ground surface. Vertical displacements within this zone predominate over the smaller horizontal displacements. From fig. 8-4 it can be seen that a soil mass of roughly truncated conical shape in the lower layer is pushed into the upper layer. Fig. 8-5 shows that shear is developing above the edge of the anchor plate along a surface extending vertically. However the strains in the zone directly above the plate anchor are at their low values.

For $\delta=3.2\text{mm}$, the zone of sand responding to this increment is much greater. The discontinuity of displacements is much clearer and it can be seen that the actual failure zone has reached the ground surface without a reduction in the angle of inclination α . As in the case of the homogeneous bed, the sand immediately above the plate anchor is displaced vertically upwards but the amount of vertical displacement diminishes as the distance above the plate anchor increases. However, it was found that the displacements suffered in the loose area were relatively smaller than the displacements suffered in the same area in a homogeneous dense bed. The shear has continued to develop vertically upward from the edge of the plate anchor (see fig. 8-9).

8-2-2 Two layered sands, $D/B=6$, $\lambda=2$

The deformations of the sand surrounding the anchor plate are presented in fig. 8-10 to 8-17 showing the displacements and strains in the sand for each of the upward displacement increments.

An incremental vertical displacement, $\delta=1.4\text{ mm}$, of the plate anchor produces measurable displacements in a zone of the sand bed which extends distances of $5.7 \times B$ above and $0.75 \times B$ to the side of the plate anchor. The sand within this zone suffers vertical displacements with negligible horizontal displacements. The development of a soil mass of a truncated conical shape in the lower layer is already noticeable and this penetrates the overlying loose sand. Shear is developing above the edge of the plate anchor along a surface extending vertically and with a small strained area directly above the plate anchor.

At increment , $\delta=3.2\text{ mm}$, approaching failure the extent of the zone of

the bed responding to this increment is much greater. Measurable displacements occur up to the ground surface above the plate anchor and $0.25 \times B$ to $1 \times B$ to the side. Vertical displacements within this zone predominate over smaller horizontal displacements. The vertical displacements of the sand diminish as the distance above the plate anchor increases. However, at some distance above (loose area) it appears that a large zone of sand suffered very small vertical displacements. The displacement field diagram of fig. 8-16 shows that the diameter of the soil mass of a roughly truncated cone reduces as it penetrates the weak layer. The shear failure is fully developed from the edges of the plate anchor but with a concentration of the highest maximum shear strains in the dense area.

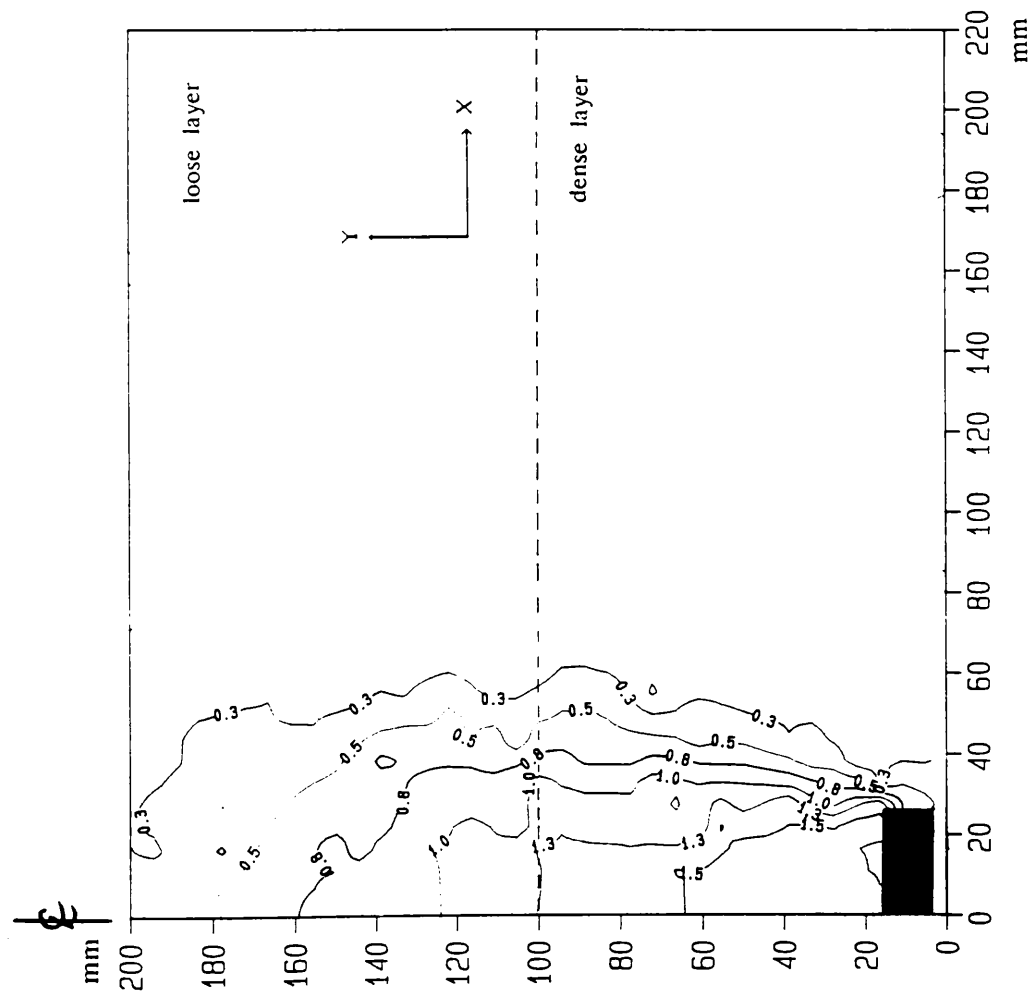


Fig. 8-2 Contours of vertical displacements in a two layered subrounded sand. $D/B=4$, $\lambda=1$, $\delta=1.5\text{mm}$

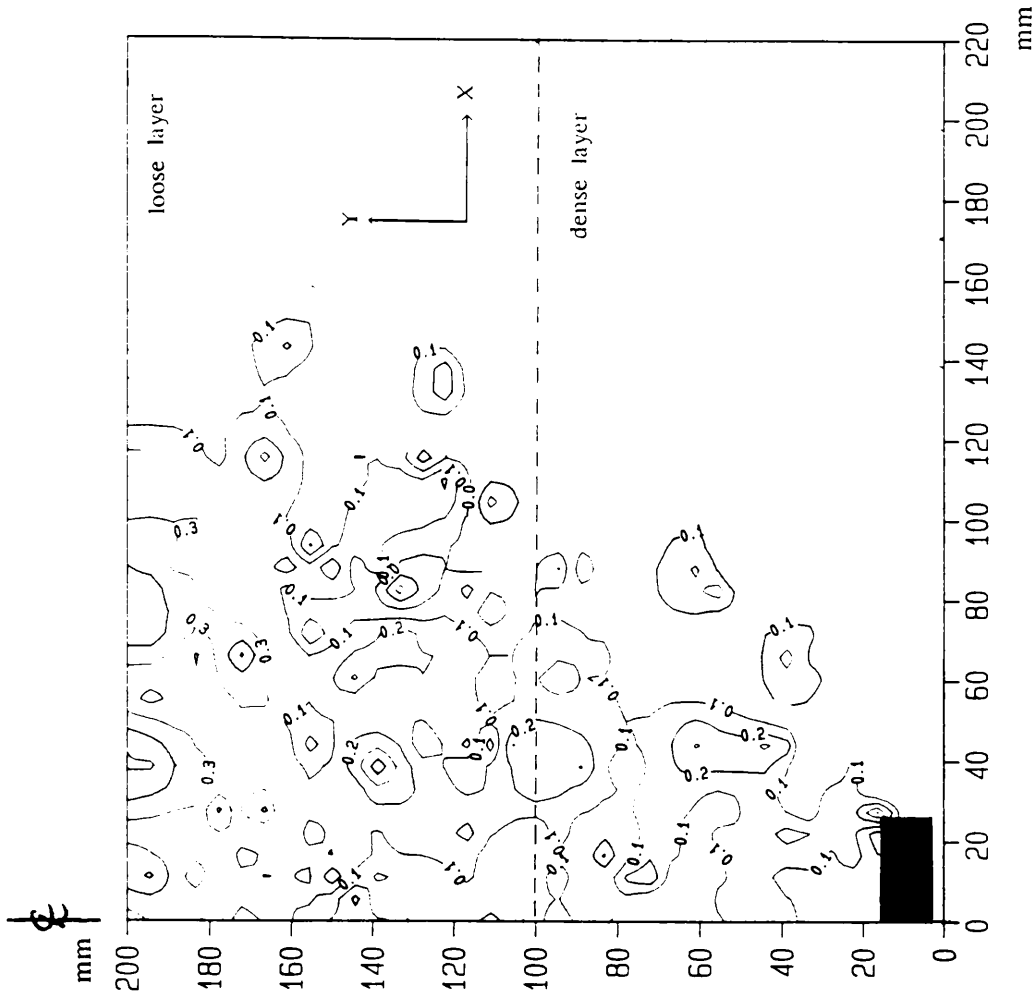


Fig. 8-3 Contours of horizontal displacements in a two layered subrounded sand. $D/B=4$, $\lambda=1$, $\delta=1.5\text{mm}$

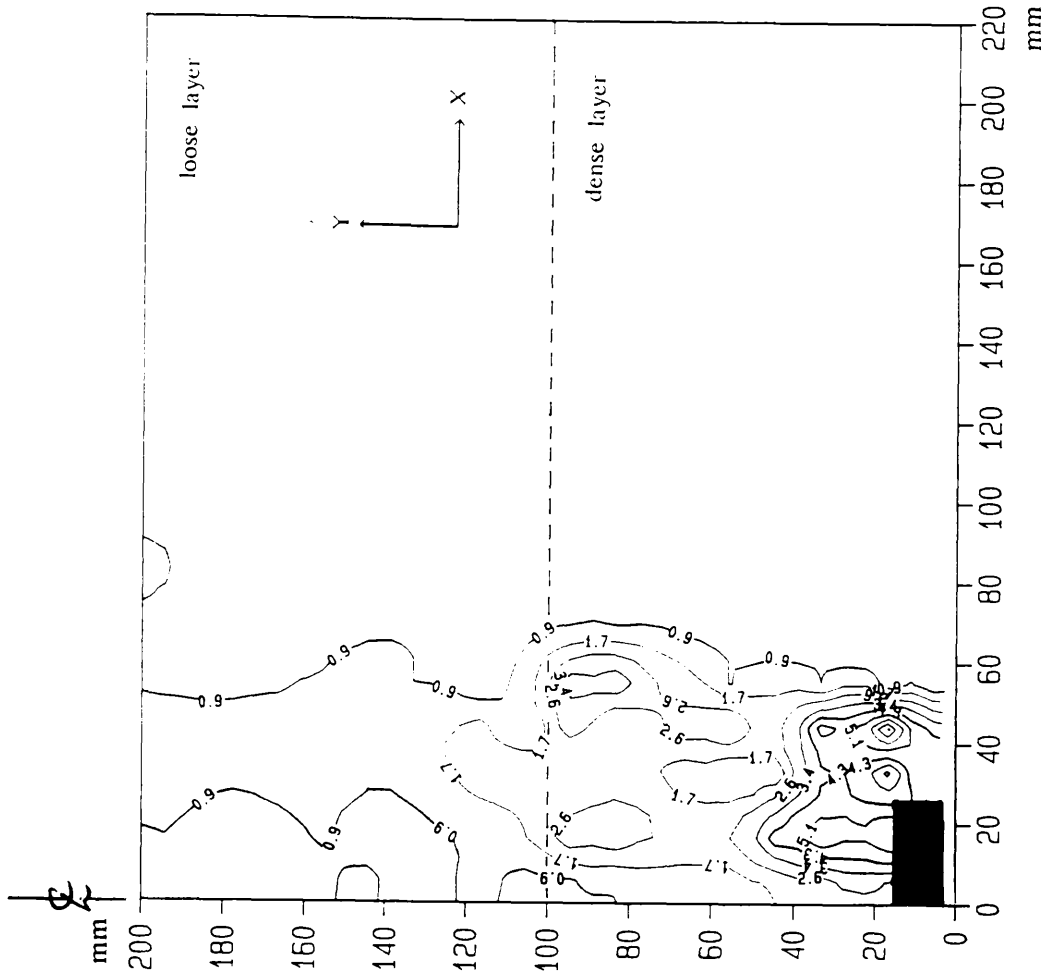


Fig. 8-5 Contours of maximum shear strain in a two layered subrounded sand. $D/B=4$, $\lambda=1$, $\delta=1.5\text{mm}$

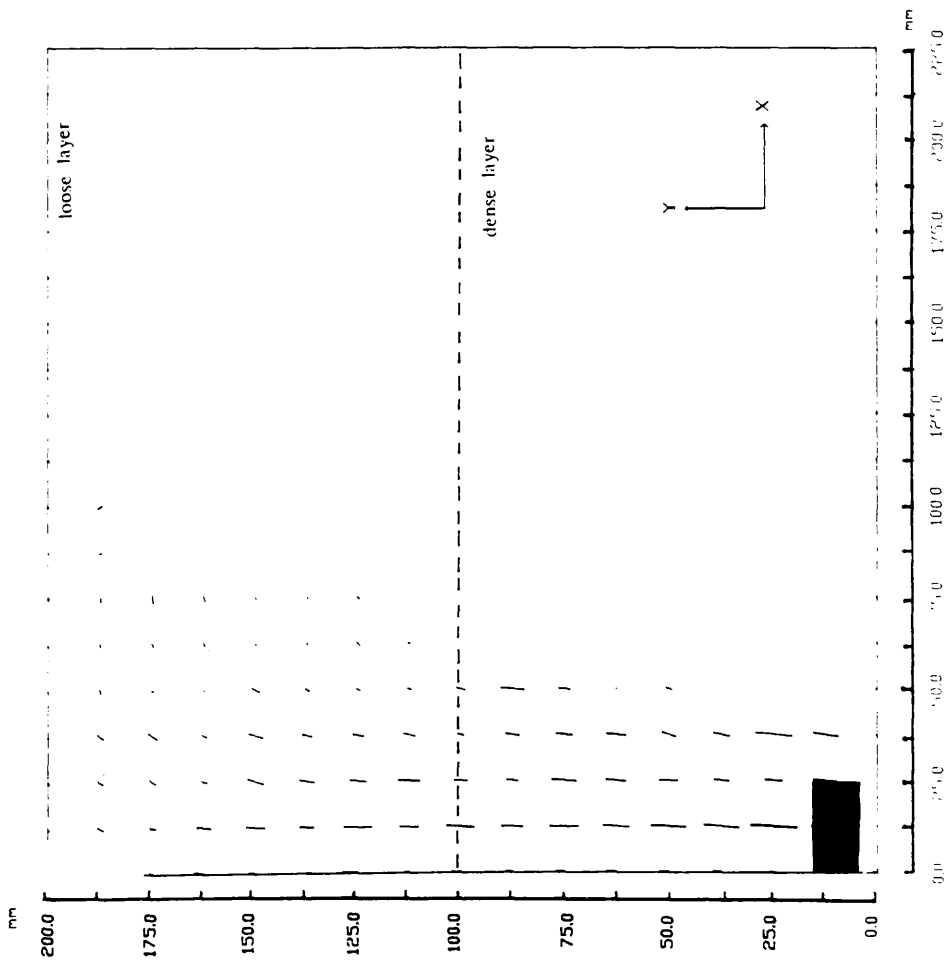


Fig. 8-4 Displacement fields in a two layered subrounded sand. $D/B=4$, $\lambda=1$, $\delta=1.5\text{mm}$

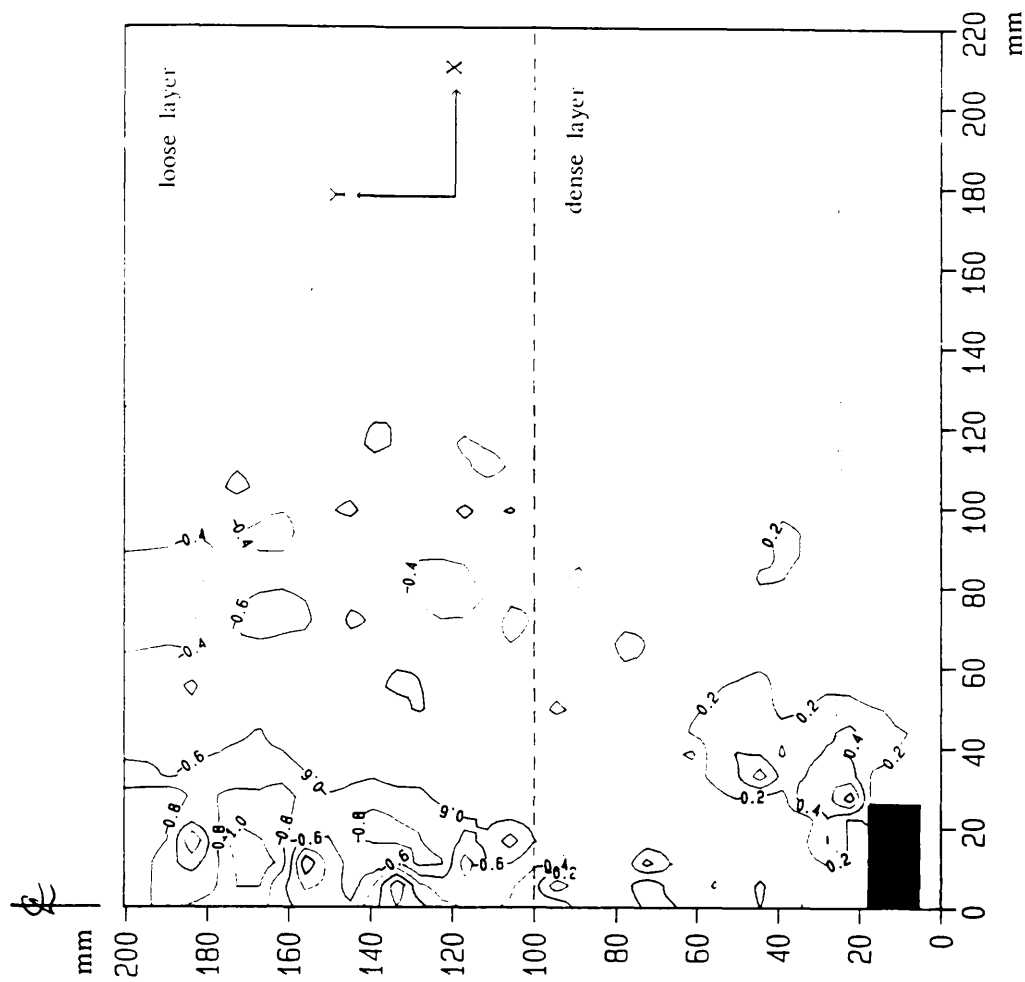


Fig. 8-7 Contours of horizontal displacements in a two layered subrounded sand. $D/B=4$, $\lambda=1$, $\delta=3.2$ mm.

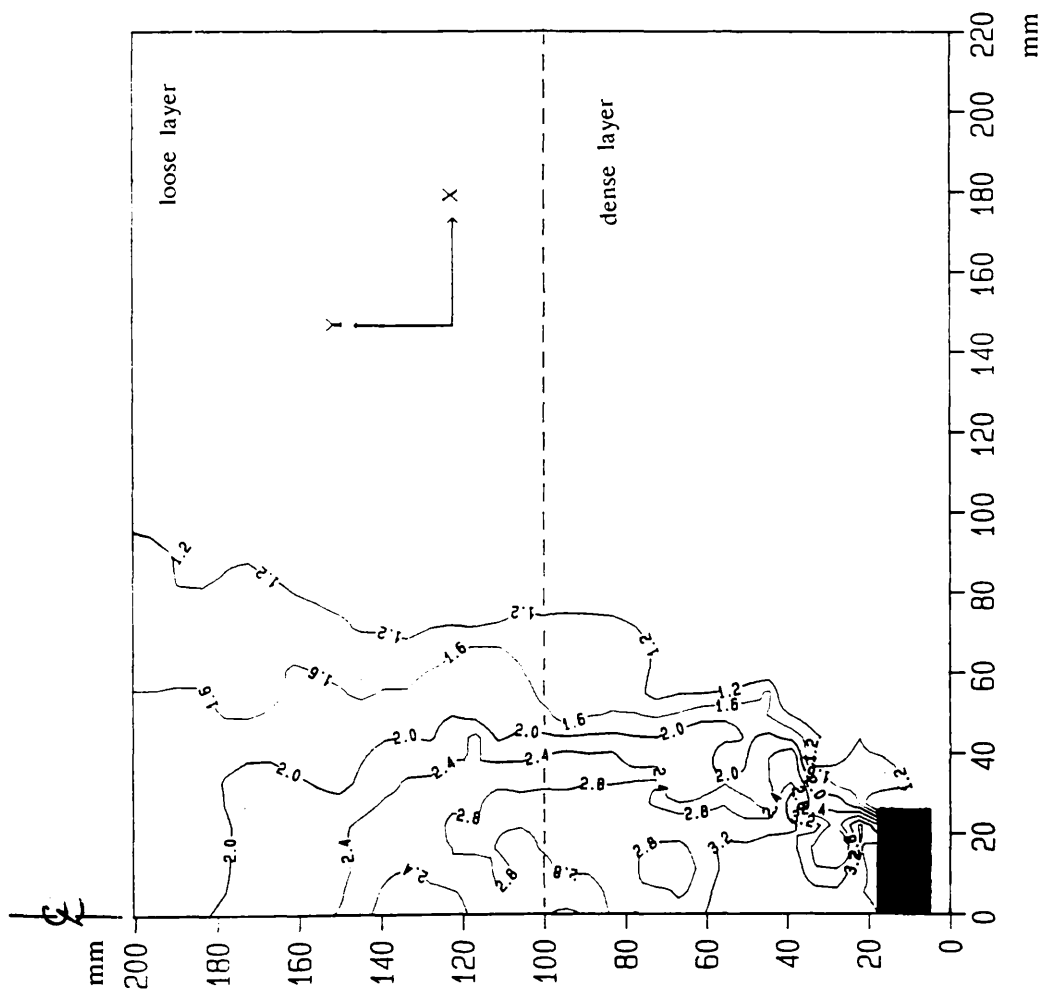


Fig. 8-6 Contours of vertical displacements in a two layered subrounded sand. $D/B=4$, $\lambda=1$, $\delta=3.2$ mm.

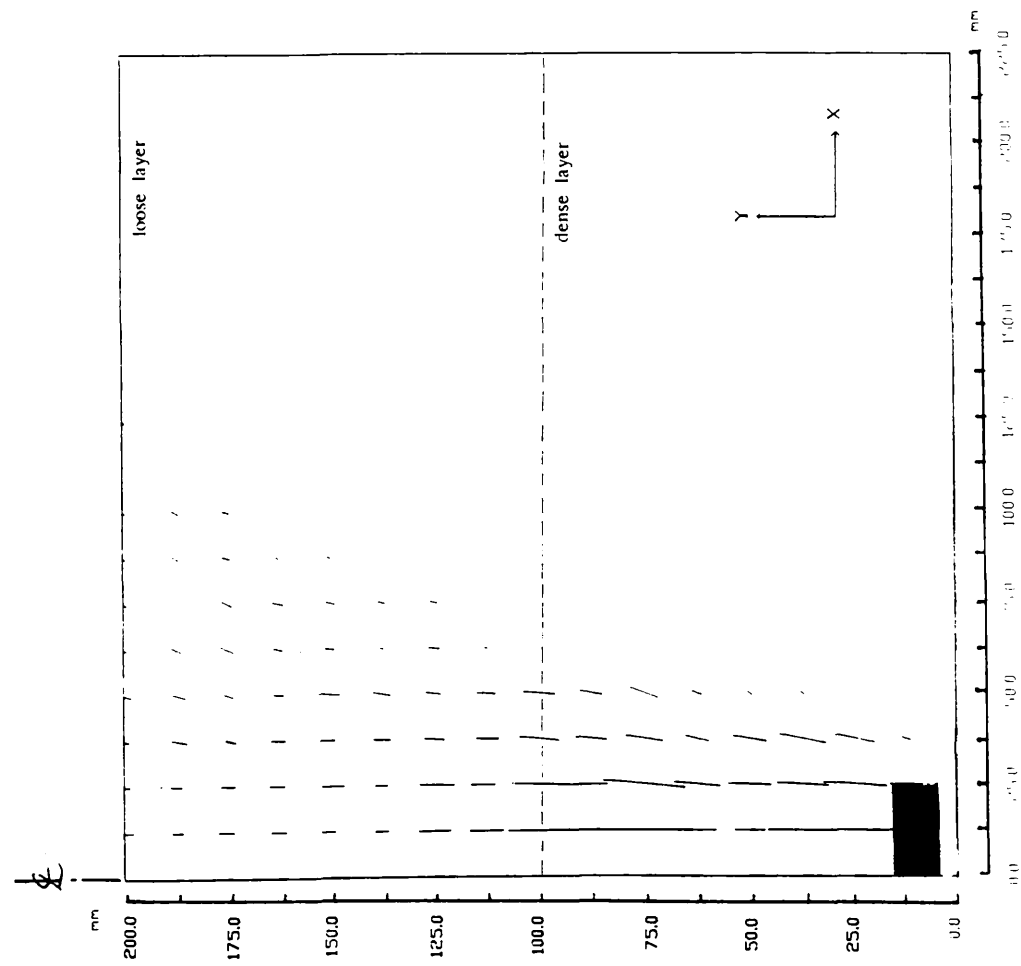


Fig. 8-8 Displacement fields in a two layered subrounded sand. $D/B=4$, $\lambda=1$, $\delta=3.2$ mm.

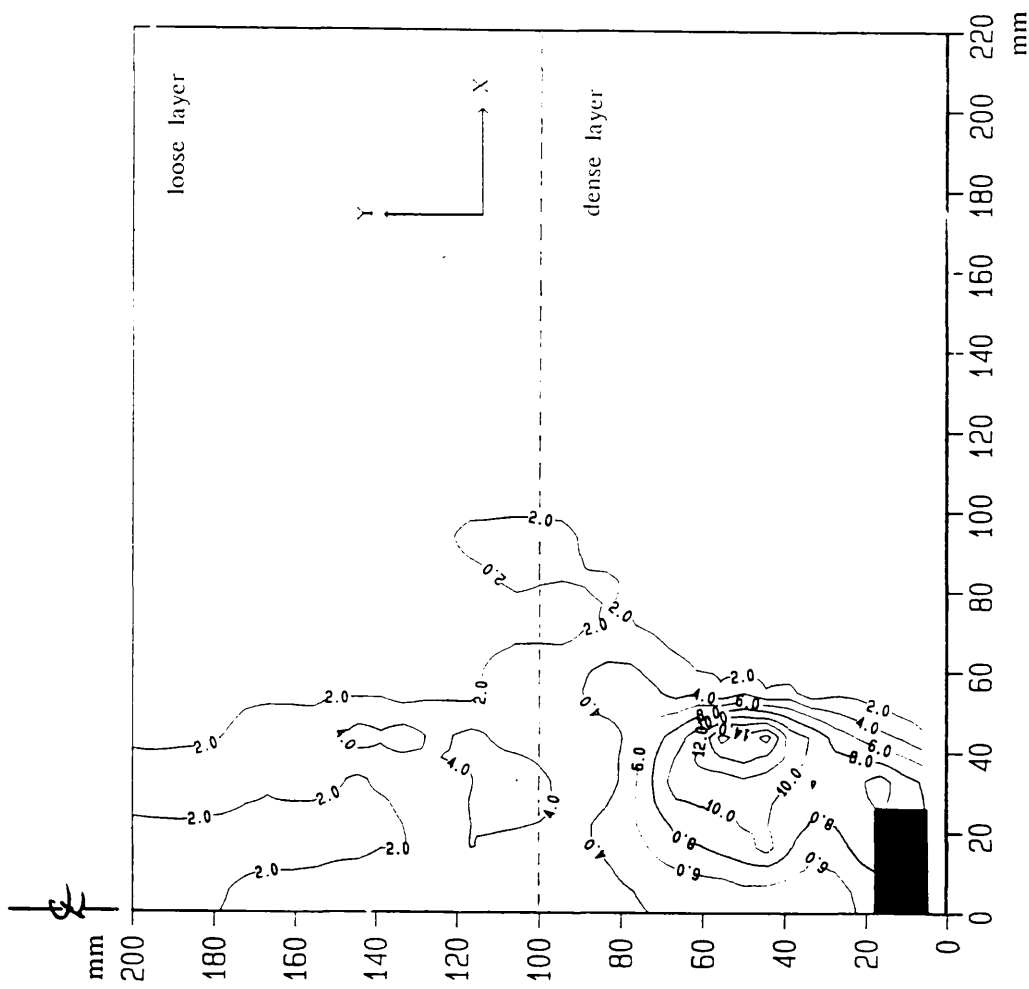


Fig. 8-9 Contours of maximum shear strain in a two layered subrounded sand. $D/B=4$, $\lambda=1$, $\delta=3.2$ mm

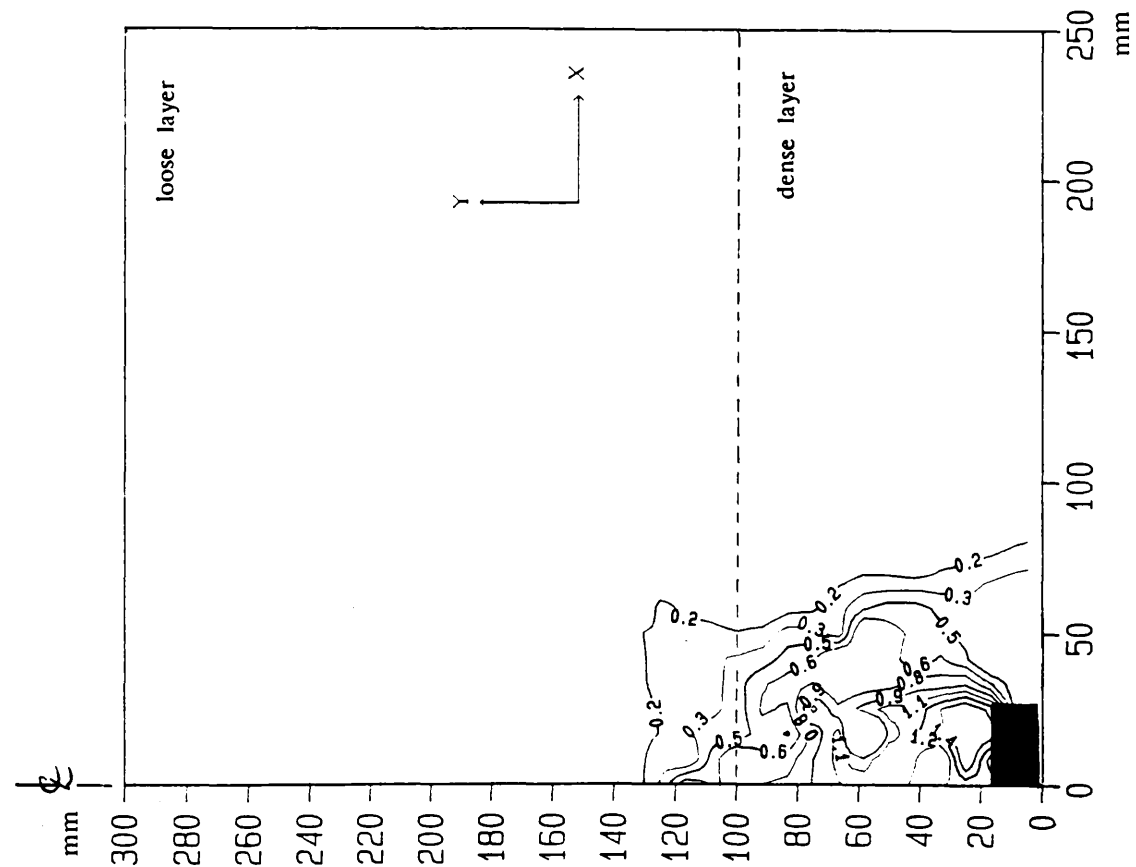


Fig. 8-10 Contours of vertical displacements in a two layered subrounded sand. $D/B=6$, $\lambda=2$, $\delta=1.4\text{mm}$.

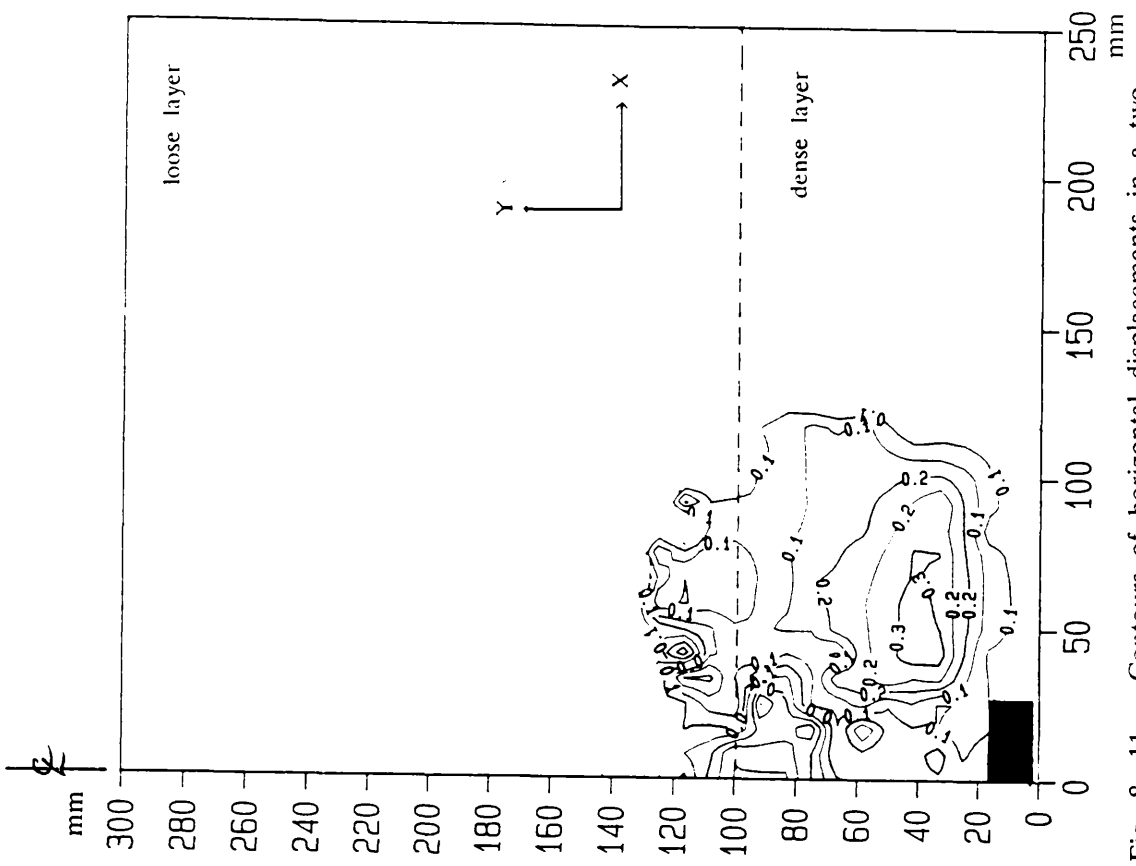


Fig. 8-11 Contours of horizontal displacements in a two layered subrounded sand. $D/B=6$, $\lambda=2$, $\delta=1.4\text{mm}$.

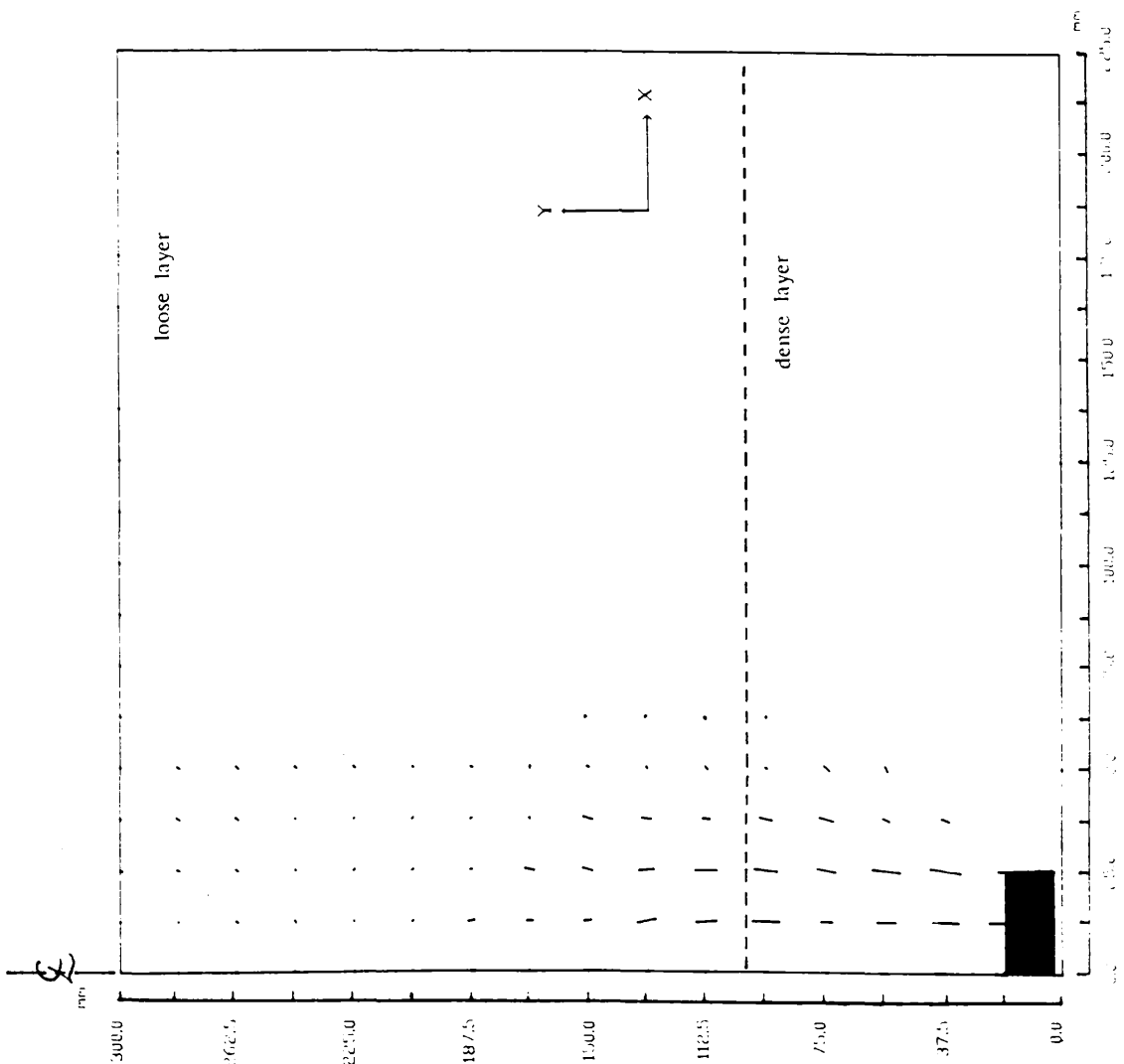


Fig. 8-12 Displacement fields in a two layered subrounded sand. $D/B=6$, $\lambda=2$, $\delta=1.4\text{mm}$.

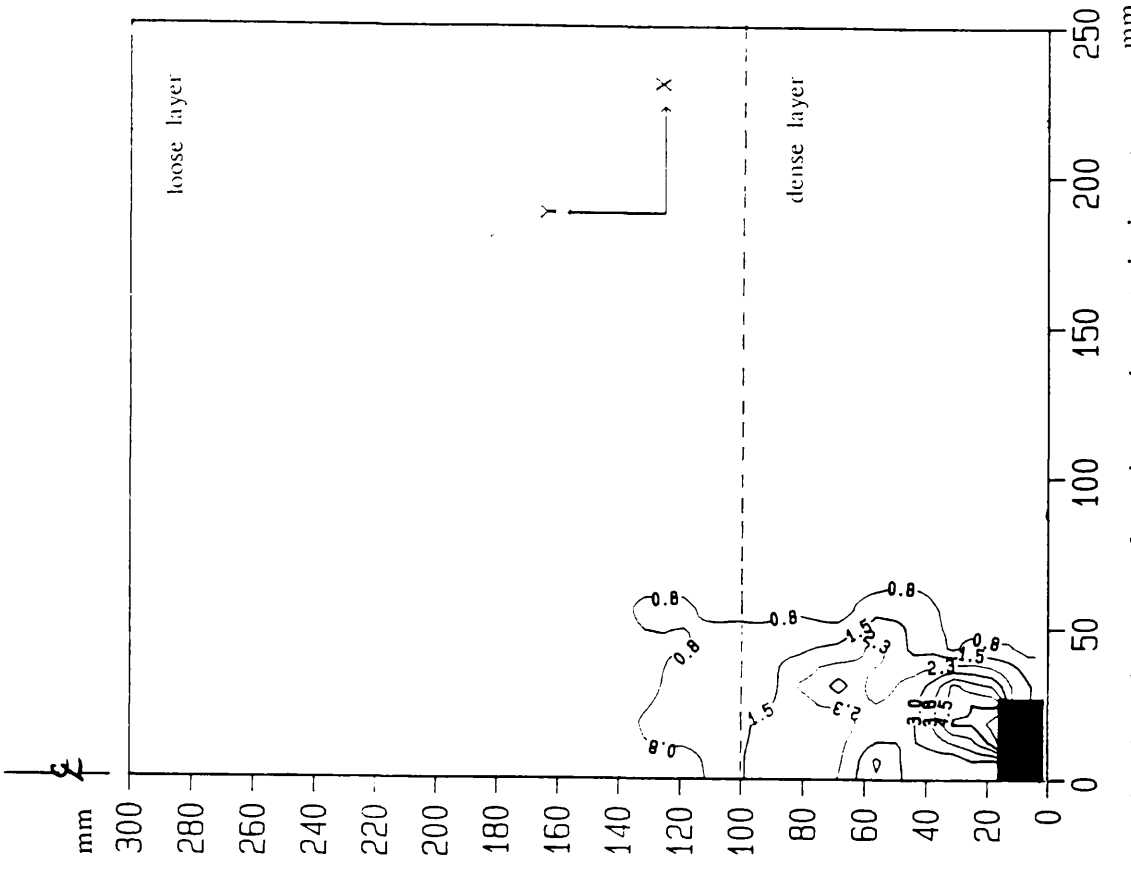


Fig. 8-13 Contours of maximum shear strain in a two layered subrounded sand. $D/B=6$, $\lambda=2$, $\delta=1.4\text{mm}$

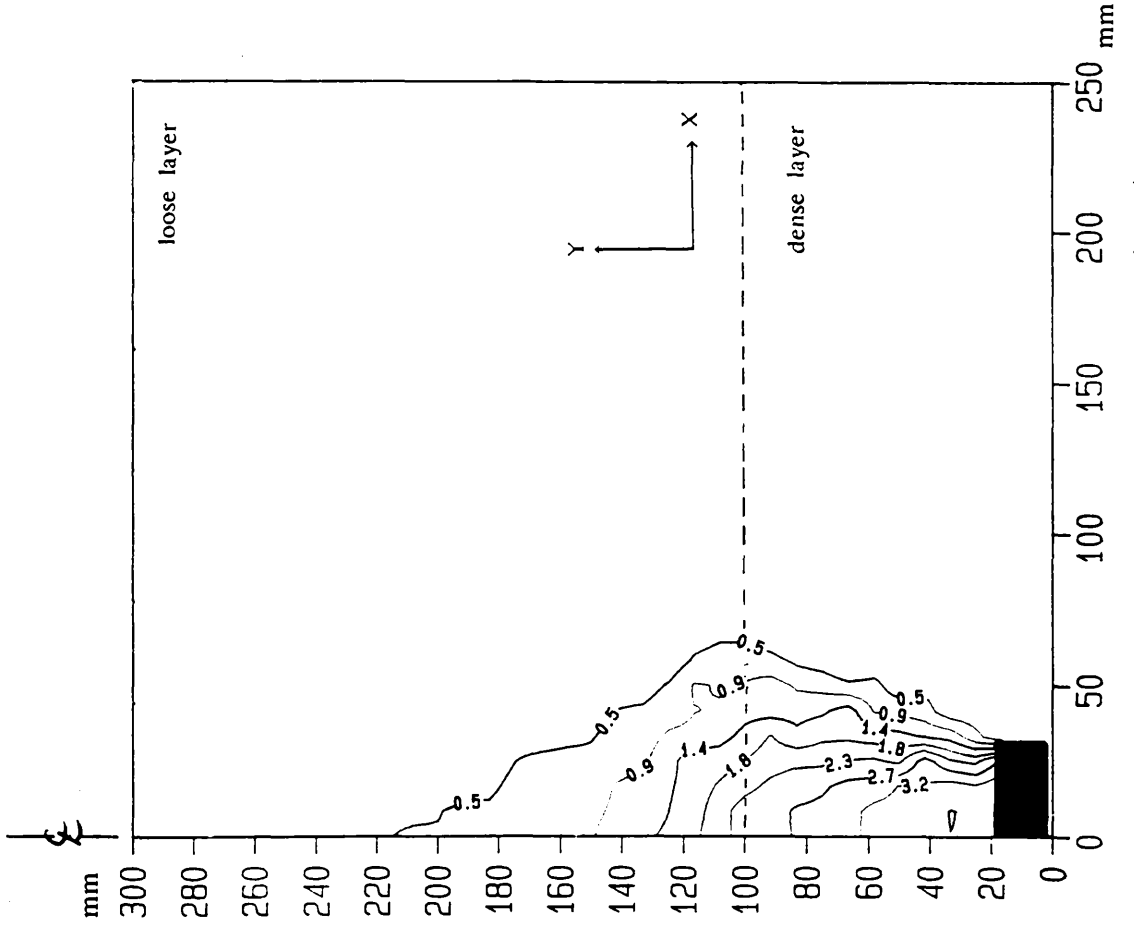


Fig. 8-14 Contours of vertical displacements in a two layered subrounded sand. $D/B=6$, $\lambda=2$, $\delta=3.2\text{mm}$

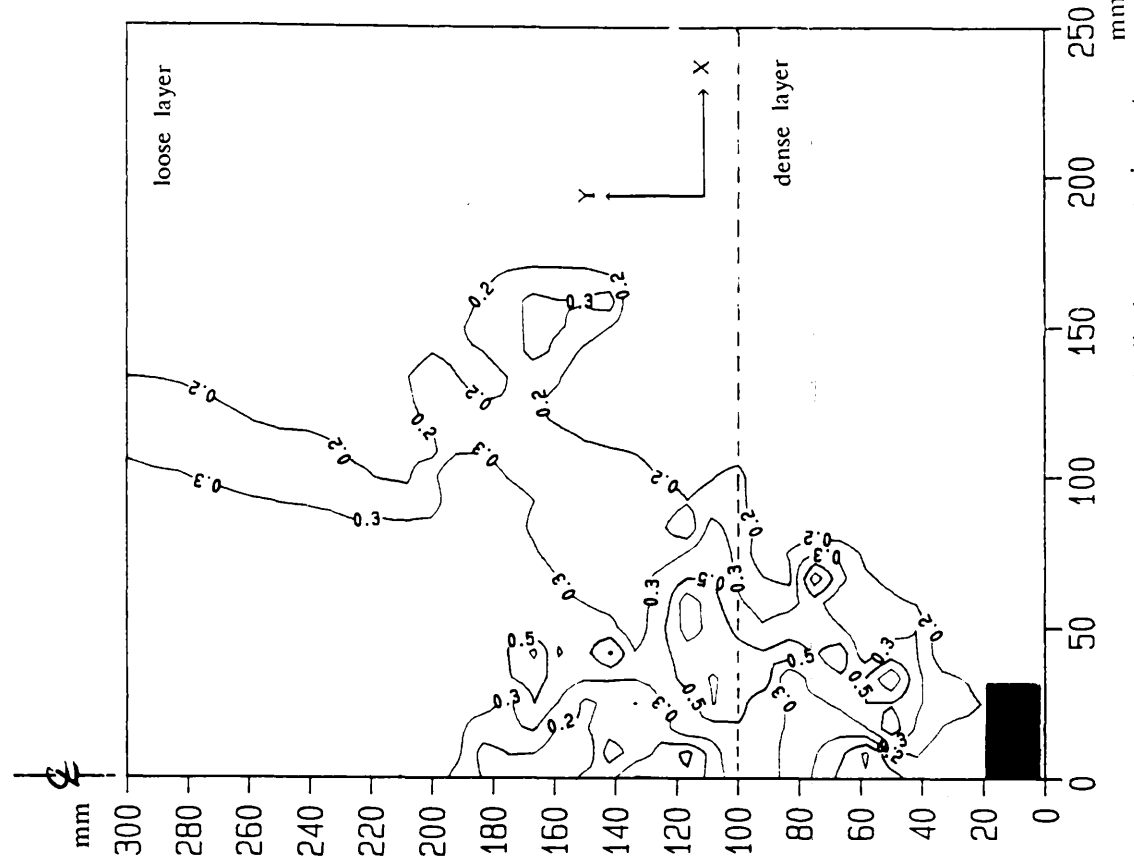


Fig. 8-15 Contours of horizontal displacements in a two layered subrounded sand. $D/B=6$, $\lambda=2$, $\delta=3.2\text{mm}$

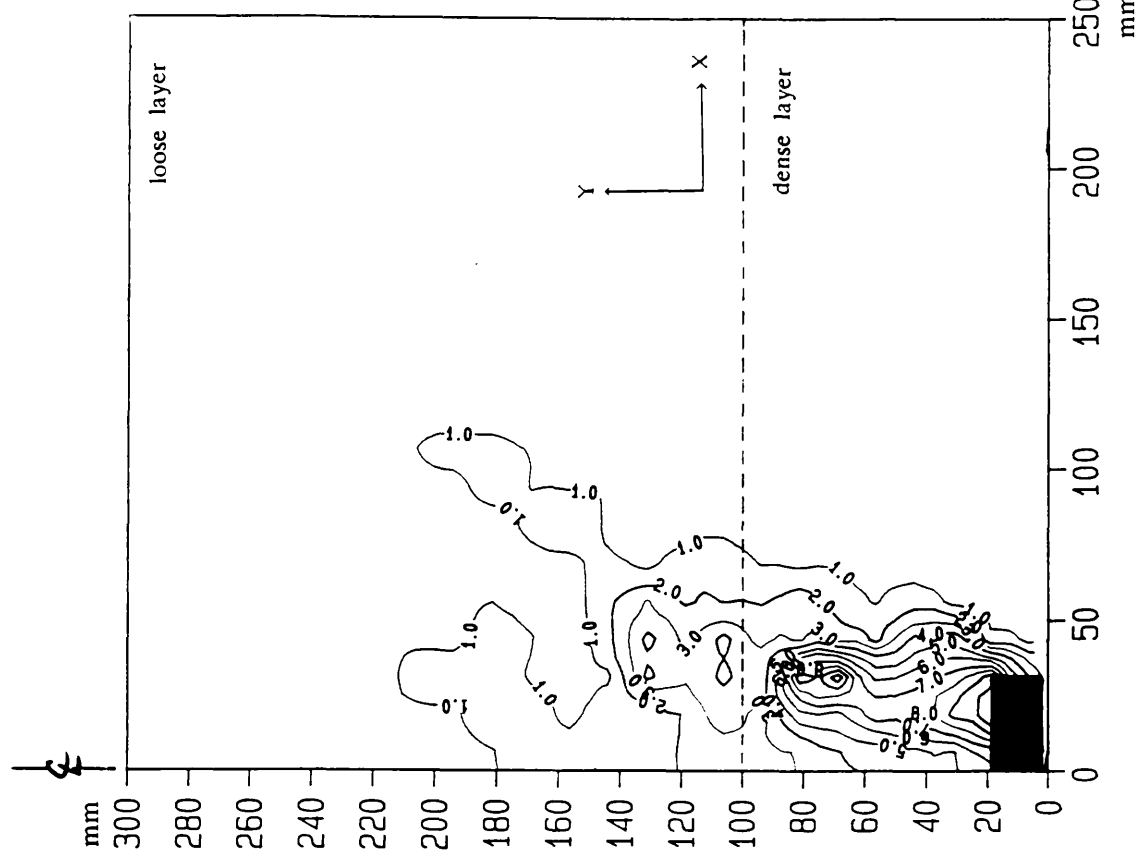


Fig. 8-17 Contours of maximum shear strain in a two layered subrounded sand. $D/B=6$, $\lambda=2$, $\delta=3.2\text{mm}$

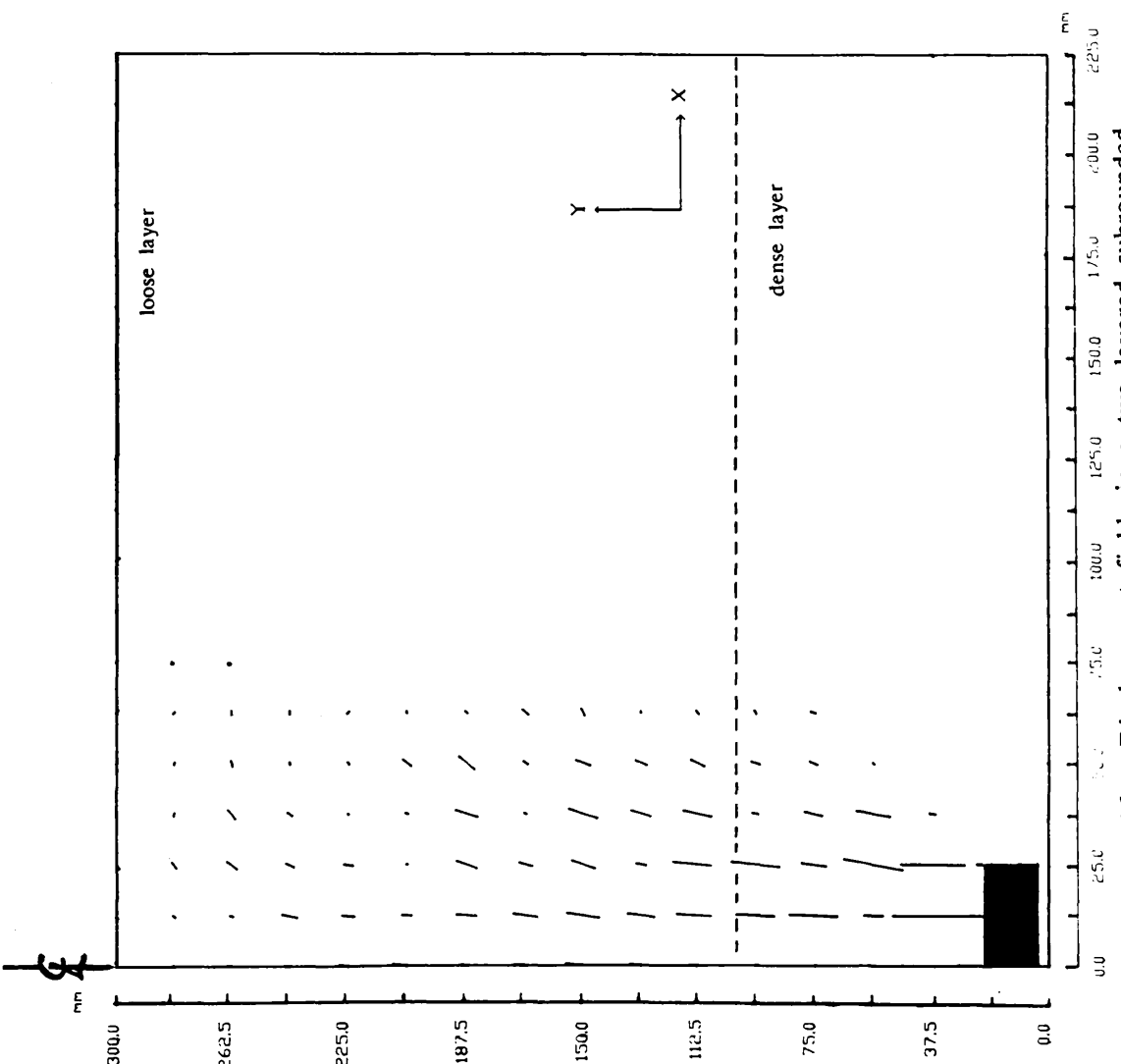


Fig. 8-16 Displacement fields in a two layered subrounded sand. $D/B=6$, $\lambda=2$, $\delta=3.2\text{mm}$

8-3 THEORETICAL APPROACH

Although numerous theories pertaining to the pull out capacities of plate anchors in a homogeneous bed have been put forward, no attempt appears to have been made to quantify the anchor pull out load in a two layered sand. In the present section a theoretical attempt is made to account for the thickness and strength of the overburden in a two layered sand. From the earliest studies on soil mechanics problems ultimate methods of analysis involving the use of some failure criteria for the soil have been increasingly used. The most commonly used condition is that failure will occur at a point in a soil mass when the shear stress reaches a limiting value dependent on the normal stress (Coulomb, 1776). These solutions are usually based on failure surfaces either assumed or derived from a hypothetical condition. Solutions of this type have been used to provide answers with acceptable accuracy to a great variety of problems in homogeneous soils. Considerably less work has been published on shear failure in a two layered soil.

The formulation of an exact theoretical solution in soil mechanics is not easy, especially in the case of a layered soil with different shear strength properties which do not obey Mohr-Coulomb failure criterion and do not fail simultaneously along a given failure surface area. Therefore, the researcher has to rely, to a large extent, on the observed mode of failure and experimental results to produce a simple and rational procedure for use by the practising engineer in design.

The method proposed herein is based on Fadl's approximate method (1981) for a homogeneous sand bed and on the observed mode of failure. Since rigorous solutions of most of the problem in soil mechanics are very complicated the need for simplified procedures is necessary (Terzaghi, 1956).

The assumptions made in developing the present method are as follows:

- 1- The soil within each layer is isotropic and cohesionless.
- 2- Full frictional resistance is developed along the failure surface.
- 3- For a shallow anchor, the shape of the failure surface has been simplified to a straight line generator with an inclination α with the vertical as shown in fig. 8-18. In case 2 the inclined failure surface makes an angle α with the vertical through the anchor edges up to the interface with the first layer of dense sand and in the rest of the layers (medium or loose) the angle of inclination is reduced to α^* .

α and α^* are defined in terms of relative density ID and angle of shearing resistance φ by Fadl (81).

8-3-1 DETERMINATION OF THE ULTIMATE UPLIFT LOAD

The uplift load of an anchor in a two layered sand can be given as the sum of:

1. The self weight of the anchor.
2. The weight of soil within the failure surface.
3. The resultant shear resistance developed along the failure surface in the direction of loading i.e. the axis of the anchor.

The uplift resistance can be written as:

$$P = G + W + T \dots\dots\dots(8-1)$$

where, P= Ultimate uplift resistance.

G= Weight of the anchor.

W= Weight of soil within the failure surface.

T= Vertical shear resistance along the failure surface.

In case 2 the failure surface consists of two parts. Initially the failure surface is inclined, making an angle α with the vertical through the anchor edge, but as the surface reaches the weaker layers the shear resistance is then mobilised along a surface inclined at α^* .

i) Soil weight

For the calculation of the soil weight inside the failure cone, the volume is found by revolving the straight sliding surface around the anchor axis as shown in fig. 8-19

$$W = \gamma \int_0^D \pi (B/2 + x)^2 \tan \alpha \, dh \dots\dots\dots(8-2)$$

where, γ = unit weight of soil.

D= Depth of embedment of plate anchor.

B= Plate anchor diameter.

dh is any depth from the surface of the soil, $dh = dx / \tan \alpha$ where α is the inclination of the failure surface from the vertical direction.

and $\alpha = 0.25 [(1 + \cos^2 \phi) ID + (1 + \sin^2 \alpha)] \phi \dots\dots\dots(8-3)$

ii) Shearing resistance along the failure line

Matsuo (1967) presented a relationship similar to Kotter's equation in a rectangular coordinate system, which describes the variation of the shear stress on a rupture line or failure surface. This differential equation represents the plane stress condition for the failure surface within the soil mass which is assumed by Matsuo to be in a state of plastic equilibrium. Although the problem of uplift resistance of a circular plate anchor is an axisymmetric stress condition in three dimensions the assumed plane stress condition for the sliding surface was calculated on the three dimensional sliding surface. This is due to the absence of a method which can exactly represent the three dimensional stress condition. Matsuo (1967) presented the following differential equation.

$$\partial p / \partial S + 2p \cdot \tan \phi \partial \theta / \partial S = \gamma \sin \theta \dots\dots\dots(8-4)$$

Where p is the resultant shearing resistance acting on the sliding surface and S the arc length of the rupture plane. Fadl's approximate method assumes that the failure shape has the form of a straight line generator inclined at α through the edges of the plate anchor, therefore in this case the term $\partial \theta / \partial S$ is equal to zero. Taking the component of the resultant shear force in the direction of loading P i.e. in the vertical direction (Matsuo, 67 and Fadl, 81).

$$P = \gamma (y - D) \sin \alpha \dots\dots\dots(8-5)$$

where $y = h$ or h^* (Fig. 8-20)

The total vertical component of the resultant shearing resistance T acting on the sliding surface which is formed by the revolution line around the axis of the anchor is given by:

$$T = \int_0^D D \tan \alpha \int_0^{2\pi} P (B/2 + x) ds d\beta \dots\dots\dots(8-6)$$

where, $h = x/\tan\alpha$ and $ds = dx/\sin\alpha$

8-3-1-1 Two layered soil, $2 \leq D/B \leq 5$, $\lambda=1$

i) Soil weight:

This is divided into two parts, the first part being the weight of soil in the dense layer, the second part the weight of soil in the medium or loose layer.

The weight of soil in part 1 is given by:

$$W_1 = \gamma_1 \int_0^{(D-H)\tan\alpha} \pi (B/2 + x)^2 dh \dots\dots\dots(8-7)$$

Where $\gamma_1 =$ unit weight of dense soil.

$H =$ thickness of the upper layer

$h =$ is any depth from the interface weak/dense layer.

Integrating and rearranging equation 8-7 gives:

$$W_1 = \gamma_1 \pi (D-H) \left[1/3 (D-H)^2 \tan^2\alpha + 1/2 B (D-H)\tan\alpha + B^2/4 \right] \dots\dots(8-8)$$

The weight of soil in part 2 is given by :

$$W_2 = \gamma_2 \int_0^{H\tan\alpha} \pi (S + x)^2 dh \dots\dots\dots(8-9)$$

where $\gamma_2 =$ unit weight of medium or loose state.

$$S = B/2 + (D-H)\tan\alpha$$

Integrating and rearranging the above equation gives the following:

$$W_2 = \gamma_2 \pi H \left[1/3 H^2 \tan^2\alpha + S H \tan\alpha + S^2 \right] \dots\dots\dots(8-10)$$

ii) Shearing resistance along the failure line

The total vertical component of the shearing resultant T acting downwards on the sliding surface is formed by the revolution of the inclined line (fig. 8-20) around the axis of the anchor and is obtained by integrating over the whole failure surface.

The shearing resistance in part 1 is given by T_1 :

$$T_1 = \int_0^{(D-H)\tan\alpha} \int_0^{2\pi} P_1 (B/2 + x) dsd\beta \dots\dots\dots(8-11)$$

where $P_1 = \gamma_1 [(D-H) - h] \sin\alpha \dots\dots\dots(8-12)$

integrating and rearranging equation 8-11 gives:

$$T_1 = \pi \gamma_1 (D-H)^2 \tan^2\alpha [1/3 (D-H) + B/2 \tan\alpha] \dots\dots\dots(8-13)$$

the shearing resistance in part 2 is given by T_2 :

$$T_2 = \int_0^{H\tan\alpha} \int_0^{2\pi} P_2 (S + x) dsd\beta \dots\dots\dots(8-14)$$

where $P_2 = \gamma_2 (H-h) \sin\alpha \dots\dots\dots(8-15)$

integrating and rearranging equation 8-14 gives:

$$T_2 = \gamma_2 \pi H^2 \tan^2\alpha [(D-H) + 1/3 H + B/2 \tan\alpha] \dots\dots\dots(8-16)$$

The total uplift resistance can be written as follow:

$$P = G + W_1 + W_2 + T_1 + T_2 \dots\dots\dots(8-17)$$

8-3-1-2 Two layered soil, $2 < D/B \leq 5$, $1 < \lambda \leq 4$

In this case two parts are also considered. The first part considers the dense layer which has 1 to 3 anchor diameter thickness ($D-H$) with $2B \leq H \leq 4B$ see figs. 8-19 and 8-20, the second part considers the weakest layers (medium or loose) where there is a reduction of the angle of inclination as noticed experimentally. The method of calculation is the same as in case 1. Equations 8-8 and 8-13 are still valid. However in part 2 the angle of inclination α is replaced by the reduced angle α^* . The following equations have been derived for part 2.

i) Soil Weight

The weight of soil in part 2 is given by:

$$W^*_2 = \gamma_2 \int_0^{H \tan \alpha^*} \pi (S + x)^2 dh^* \dots\dots\dots(8-18)$$

where $S = B/2 + (D-H)\tan\alpha$
 $dh^* = dx/\tan\alpha^*$

integrating and rearranging equation 8-18 gives:

$$W^*_2 = \gamma_2 \pi H [1/3 H^2 \tan^2\alpha^* + S H \tan\alpha^* + S^2] \dots\dots(8-19)$$

ii) Shearing resistance along the failure surface

The shearing resistance in part 2 is given by T^*_2 :

$$T^*_2 = \int_0^H \tan\alpha^* \int_0^{2\pi} P_4 (S + x) ds^* d\beta \dots\dots\dots(8-20)$$

where $P_4 = \gamma_2(H-h^*)\sin\alpha^*$
 $ds^* = dx/\sin\alpha^*$

integrating and rearranging equation 8-20 gives:

$$T^*_2 = \gamma_2 \pi H^2 \tan \alpha^* \left[B/2 + 1/3 H \tan \alpha^* + (D-H) \tan \alpha \right] \dots (8-21)$$

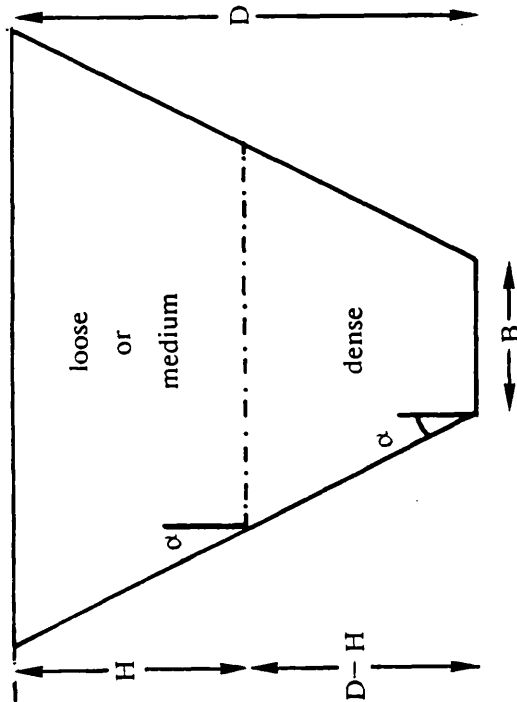
The total uplift resistance is given by:

$$P^* = G + W_1 + W^*_2 + T_1 + T^*_2 \dots (8-22)$$

CASE 1

$$2 \leq D/B \leq 5$$

$$\lambda = 1$$



CASE 2

$$2 \leq D/B \leq 5$$

$$2 \leq \lambda \leq 4$$

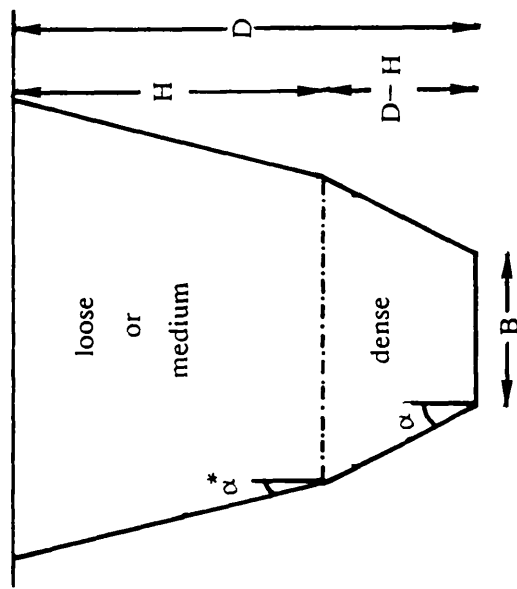
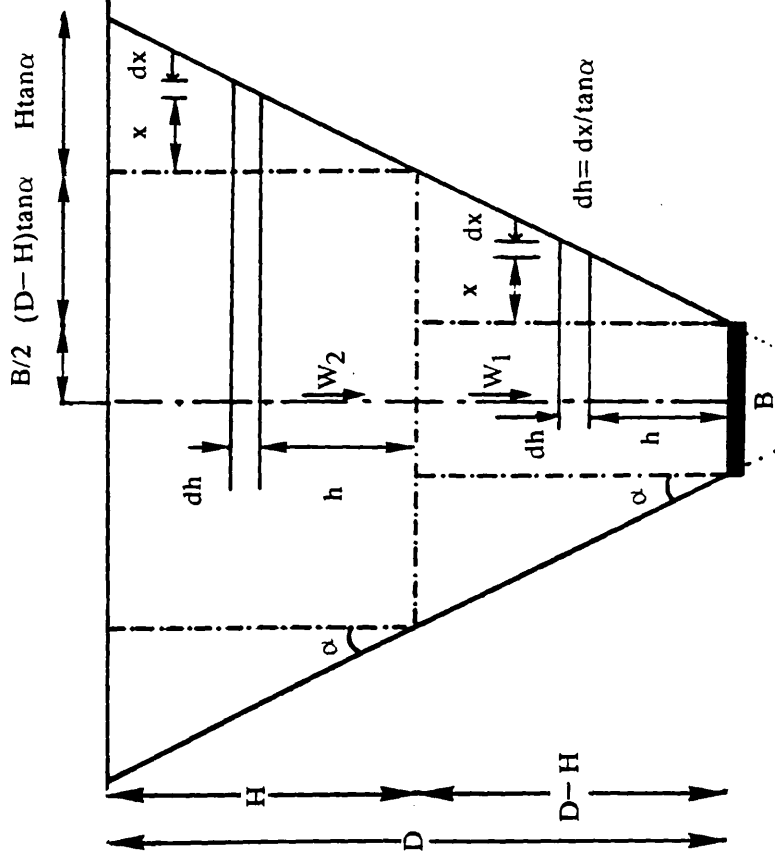


Fig. 8-18 Suggested failure surfaces for a vertical shallow anchor embedded in a two layered subrounded sand.

CASE 1

$2 \leq D/B \leq 5$

$\lambda = 1$



CASE 2

$2 \leq D/B \leq 5$

$2 \leq \lambda \leq 4$

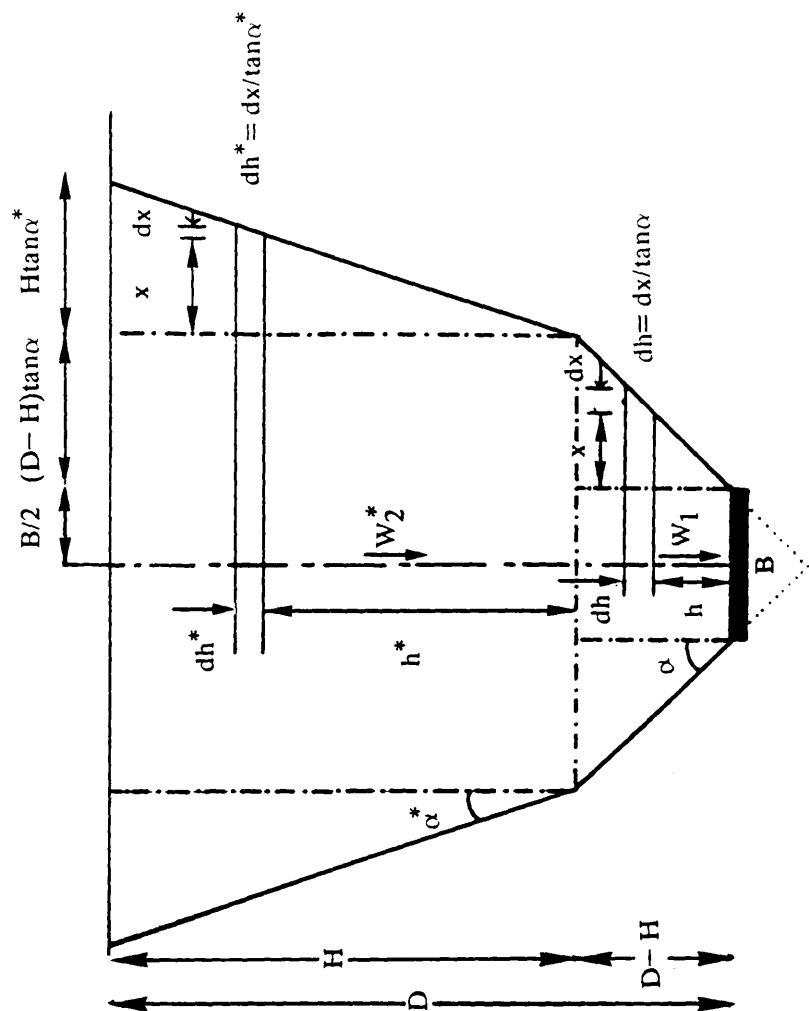
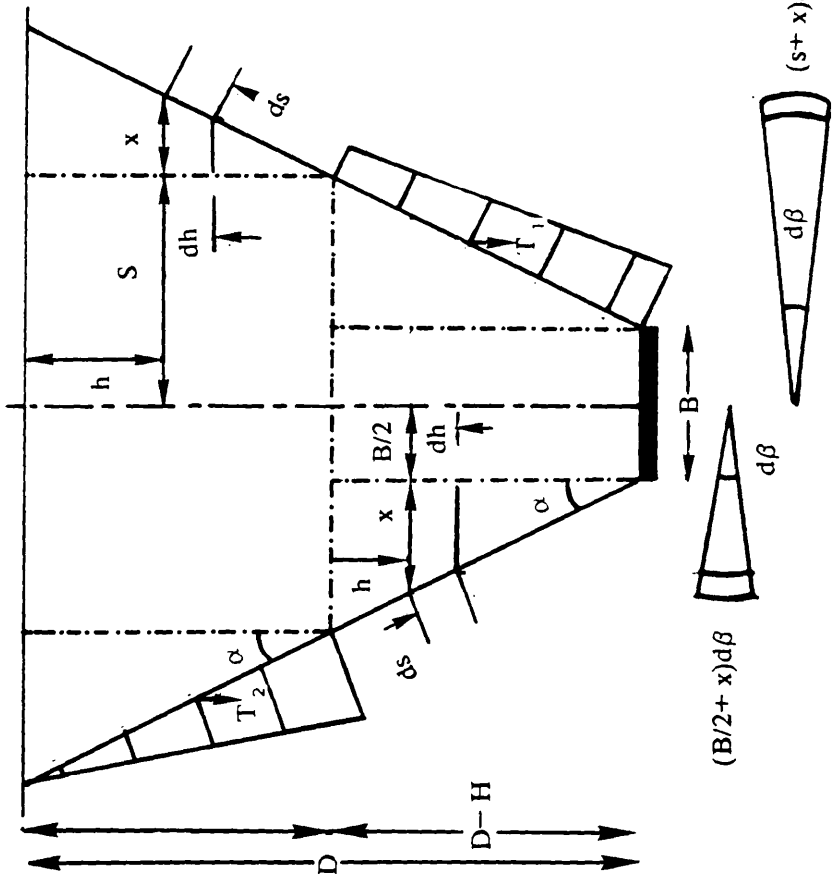


Fig. 8-19 Soil weight of vertical shallow anchor embedded in a two layered subrounded sand.

CASE 1

$2 \leq D/B \leq 5$

$\lambda = 1$



CASE 2

$2 \leq D/B \leq 5$

$2 \leq \lambda \leq 4$

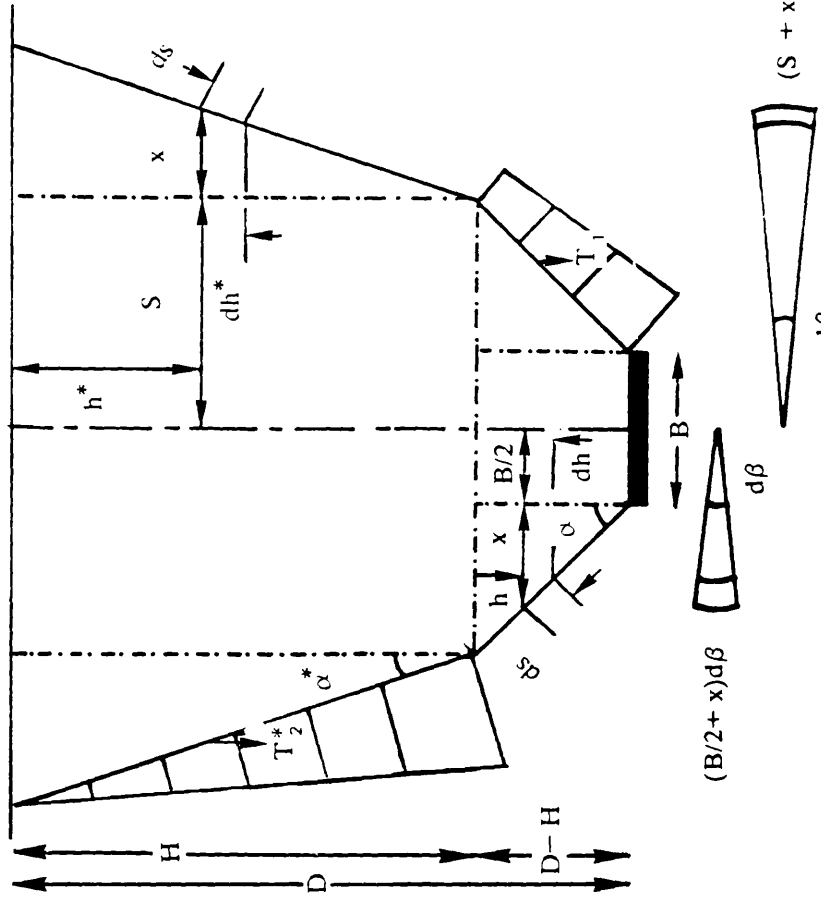


Fig. 8-20 Distribution of shear resistance for a vertical shallow

8-4 EXPERIMENTAL INVESTIGATION

In this section, experimental results on model scale anchors are presented and discussed. The investigation was carried out using the same test set up described in chapter 4. The sand used for the model anchor tests was Leighton Buzzard whose properties are described in chapter 3. The different unit weights of the layers above the plate anchor were as follows: 17.28, 16.57 and 15.63 Kn/m^3 corresponding respectively to relative densities of 85.5%, 61% and 29%. The load tests were carried out to obtain experimental evidence concerning the effect of a layered soil on the load displacement relationship. The two layered soil for this test series consisted of a layer of loose or medium sand overlying a dense stratum (see fig. 8-1).

The loose and medium state were achieved by changing the size of the sieve apertures. After preparing the dense state the hopper was lifted down, the sieve plate with 4 mm apertures diameters was unscrewed and another plate with 7 or 10 mm diameter of apertures was then fixed. The hopper was lifted back to the chosen height and the sand was then poured into the container. The pull out tests were carried out on an anchor embedded at a depth D in a combination of layers of sand. The thickness of each layer was increased to a certain proportion of the anchor diameter and in this investigation it was increased from 1 to 4 anchor diameters. A total of twenty pull out tests were carried out in which ten were with a loose upper layer and the remainder with a medium upper layer. The pull out test was carried out in the same way as explained in chapter 4. The test results are summarised in tables 8-1 & 8-2

Fig. 8-21 shows the load displacement relationship for an anchor embedded in a sand bed where λ is equal to 1. It can be seen that the ultimate pull out

load remains the same whether the upper layer is loose or medium. This suggests that for this particular case ($\lambda=1$) the ultimate pull out load is independent of the state of the weak layer as it would appear that the dense layer is providing most of the strength. This is in a sense confirmed by the stereo photogrammetric tests where it has been shown that the presence of a weaker layer has no influence on the form of the failure surface.

However, when the thickness of the upper layer (loose or medium) was increased ($2 \leq \lambda \leq 4$) a different phenomenon occurred as the load displacement relationship was, as expected, found to be dependent on the nature of the upper layer. In fig. 8-22 for the particular case of $\lambda=2$ and $D/B=4$ it can be seen that two distinct curves representing a loose upper layer and a medium upper layer lay between the homogeneous upper and lower layer soils. This observation suggest that the load displacement relationship is governed by the density state of the upper layer, the weaker the upper layer, the lower is the ultimate uplift load.

Another feature is depicted in fig. 8-22, where the upper and lower limits shows a typical load displacement curve of a plate anchor (load control test) embedded in a homogeneous bed. In this case the ultimate uplift load is always taken as the stage load which occurred immediately before failure (Fadl, 1981). However, in the case of a layered soil a distinct peak load is visible which is rather unusual for a load controlled test. This behaviour could be explained by the fact that the load transferred from the anchor to the sand started at the beginning to breakout the dense layers of sand, and, once the weaker layers (medium or loose) had been reached less force was required to breakout the soil and consequently a drop in the pull out load occurred. This latter observation goes alongside the information obtained from the stereo photogrammetry where it has been shown that the presence of a weak layer above a dense layer influenced the behaviour of the soil under uplift load.

Typical test results of the variation of the ultimate capacity with increasing thickness of the loose or medium layer above the dense stratum are shown in fig. 8-23 for different depth/diameter ratios D/B . It is observed that the ultimate uplift load decreases with the increase in the upper thickness ratio, λ , to a minimum value which is close to that obtained for the same D/B ratio in a homogeneous soil deposit at the same density as the upper layer. As expected the results show that the ultimate uplift capacity increased with increasing depth of embedment to anchor diameter ratio D/B .

8-5 COMPARISON OF THEORETICAL AND EXPERIMENTAL RESULTS

The predicted ultimate pull out loads are compared with the experimental results obtained from the present model tests. The comparison covered a range of shallow anchors embedded in interbedded layers of sand.

This theoretical approach is based on Fadl's approximate method for shallow anchors where it is assumed that a truncated cone of failure subtending an angle α from the direction of loading is taking place. In the present research two cases have been investigated and are referred to as case 1 and case 2 (see fig. 8-19) and take into account the different combination of layers of sand. The general formula has been modified in order to take into consideration the effect of a combination of layers of sand of different densities on the maximum pull out load.

Tables 8-1 & 8-2 show the comparison between the experimental model test results of vertical anchors and the predicted maximum pull out loads. A reasonable agreement was found between the predicted and the observed pull out values. The mean value of P_{the}/P_{exp} is 0.94, this shows that the modified method of calculation is satisfactory and can be applied successfully to a problem in which a plate anchor ($D/B \leq 5.0$) is embedded in interbedded layers of subrounded sand.

8-6 CONCLUSIONS

The salient observations and important conclusions drawn from the present chapter are summarized in this concluding section.

-1- The test results show that the ultimate uplift load of a plate anchor embedded in a two layered uniform subrounded sand is dependent on the depth of embedment, the thickness of the upper layer and the relative strength of the different layers.

-2- At $\lambda=1$ and for a given D/B ratio, there was no difference between pulling a plate anchor from a dense/medium bed or a dense/loose bed.

-3- For a given D/B ratio and $1 < \lambda \leq 4$, a dense/medium bed gives a greater uplift than a dense/loose bed.

-4- The mode of failure of the shallow anchor is function of the upper layer thickness ratio λ .

-5- An approximate design theory for the ultimate uplift load of a plate anchor embedded in a two layered uniform subrounded sand has been developed based on the observed mode of failure.

-6- The proposed approximate solution compared to the author's test results showed a reasonable agreement over the range of D/B and λ investigated.

D/B	λ	D (mm)	B (mm)	P_{exp} (N)	δf (mm)	P_{the} (N)	$\frac{P_{the}}{P_{exp}}$
2	1	75.00	37.50	12.00	1.225	11.20	0.93
3	1	112.5	37.5	28.50	1.275	28.25	0.99
3	2	112.5	37.5	21.5	1.600	19.40	0.90
4	1	150.0	37.5	54.50	1.525	56.80	1.04
4	2	150.0	37.5	52.00	0.975	46.90	0.90
4	3	150.0	37.5	48.50	1.375	45.20	0.93
5	1	187.5	37.5	111.5	1.895	103.5	0.93
5	2	187.5	37.5	87.65	2.045	86.50	0.99
5	3	187.5	37.5	79.80	2.285	74.20	0.93
5	4	187.5	37.5	82.50	2.298	78.35	0.95

**Table 8-1 Summary of experimental and theoretical results
in a two layered subrounded sand, upper thickness
layer = medium state.**

D/B	λ	D (mm)	B (mm)	P_{exp} (N)	δf (mm)	P_{the} (N)	$\frac{P_{the}}{P_{exp}}$
2	1	75.00	37.50	12.00	1.250	10.80	0.90
3	1	112.5	37.5	28.50	1.150	27.40	0.96
3	2	112.5	37.5	15.30	1.875	14.50	0.95
4	1	150.0	37.5	54.50	1.725	55.75	1.02
4	2	150.0	37.5	45.80	1.125	40.45	0.88
4	3	150.0	37.5	34.70	2.150	30.20	0.87
5	1	187.5	37.5	111.5	1.965	101.7	0.91
5	2	187.5	37.5	80.30	2.125	75.40	0.94
5	3	187.5	37.5	63.70	2.475	58.00	0.91
5	4	187.5	37.5	50.15	2.975	48.65	0.97

**Table 8-2 Summary of experimental and theoretical results
in a two layered subrounded sand, upper thickness
layer = loose state.**

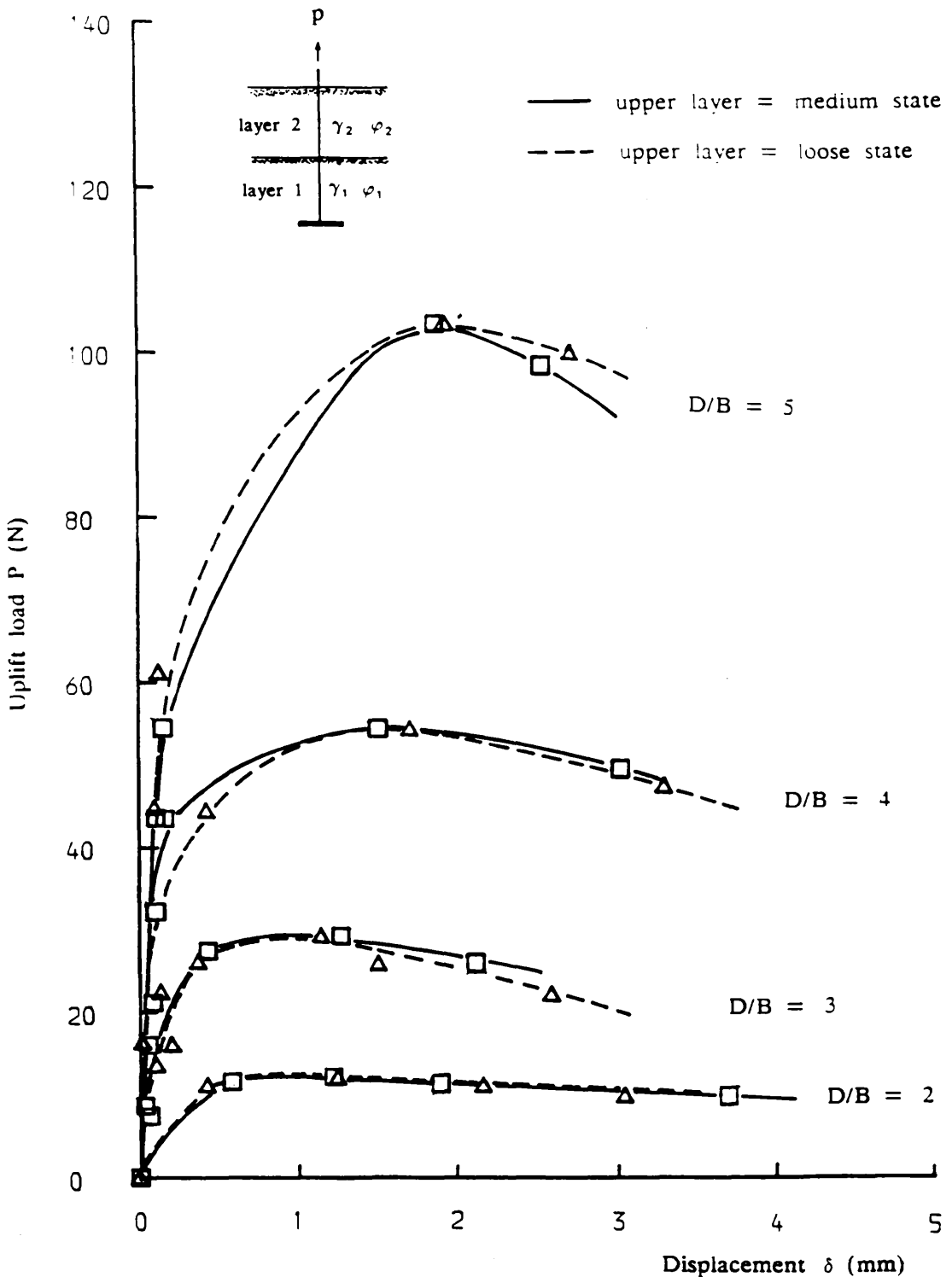


Fig. 8-21 Load-displacement relationship for a plate anchor embedded in a two layered subrounded sand, $\lambda=1$

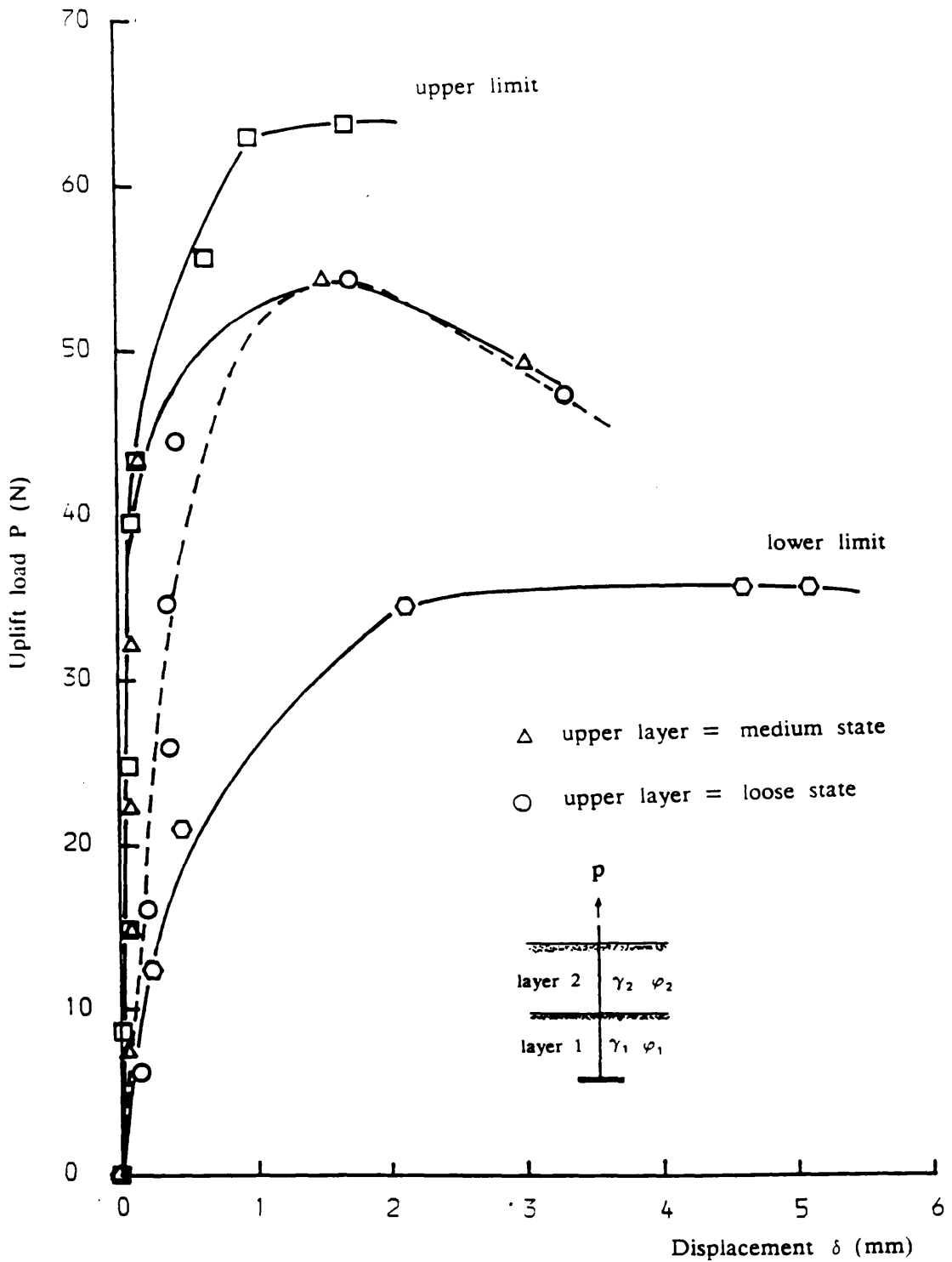


Fig. 8-22 Typical load-displacement relationship for a plate anchor embedded in a two layered subrounded sand, $\lambda=2$, $D/B=4$.

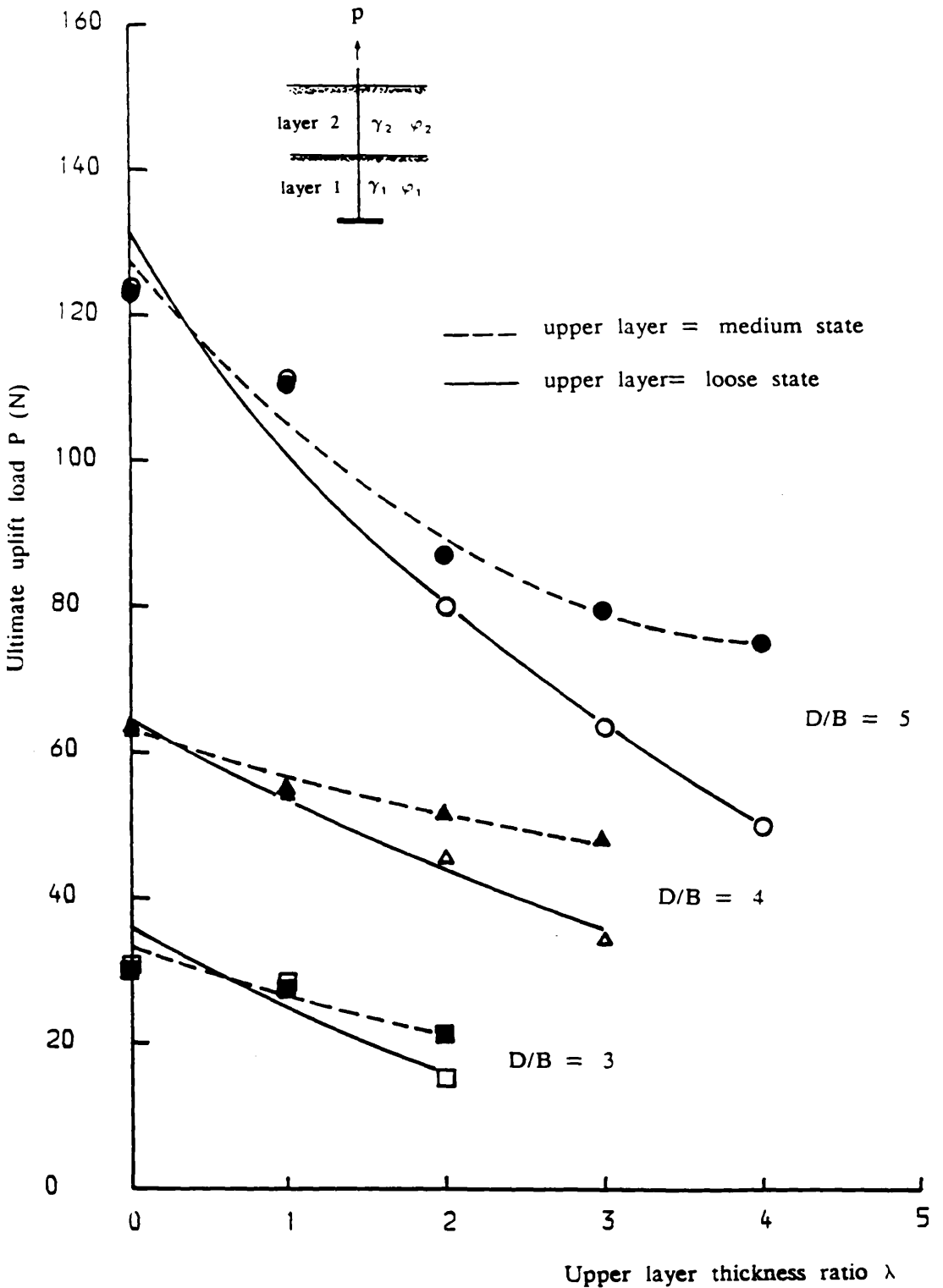


Fig. 8-23 Ultimate uplift capacity versus upper layer thickness ratio.

Chapter 9

DESIGN CONSIDERATIONS

9.1 INTRODUCTION

This section presents and discusses the use of the results of the present investigation in the estimation of the breakout factor of plate anchors embedded in cohesionless soil.

The present investigation has attempted to provide a better understanding of embedded anchor behaviour and formulate a design method for estimating anchor static loading. It is accepted that its main limitation is the lack of field scale data. Although it is anticipated that the presently observed trends and resulting design procedure will apply to larger scale behaviour, the links can be satisfactorily established only by a comprehensive programme of large scale testing.

At the present time, using plate anchors in a similar manner to the tension piles of the Hutton TLP (Tetlow et al, 1983) is not a practical proposition. The quoted maximum uplift resistance of the largest embedment anchor (270 Tonnes in sands, McCormick 1979) is considerably less than the uplift force for a single Hutton pile (1140 Tonnes). The principal use for plate anchors offshore will continue to be in the provision of single surface or sub-surface moorings. However, onshore they can be used over a large variety of projects.

9.2 DESIGN PROCEDURE

In the design of anchorage systems, the present practice is to carry out an

assessment of the pull out capacity using established empirical formulae. This may be supplemented by full scale tests at the site of the proposed embedments which, though expensive, provide valuable information. However, the ability to make the correct theoretical assessment is essential. Section 5-4 showed that most of the theories developed in the last decade were inadequate and not completely rigorous when evaluating the pull out capacity of a plate anchor embedded in different types of sand.

In the present section a design procedure for plate anchors embedded in cohesionless soil and subjected to static loading is presented, Design charts are shown in Fig. 9-1 to 9-3 and are divided into three categories as follows:

- 1- Uniform sand, rounded to well rounded shape.
- 2- Uniform sand, subrounded shape.
- 3- Uniform sand, subangular shape.

An extensive reference survey of the greatest possible number of pull out resistance data in different sands has been undertaken, the aim of which was to assemble the characteristics of the sands used and the range of N_u values attained in the different studies. This type of exercise is always made difficult by the fact that many of the publications lack details (such as relative density, shape, etc...) which are essential if useful evaluations are to be made. However, it was felt that sufficient information was available to put forward a design method taking into account parameters such as grain shape in addition to relative density and angle of internal friction. The design procedure is based on the cases quoted in tables 4-1 to 4-5 and table 9-1 which comprise relevant data available in the literature and emanating from well established laboratories. The data refer to samples tested in laboratory conditions only. Publications which failed to disclose the precise

conditions of the tests have been disregarded. The observed range of relative density (ID) and angle of internal friction (φ) varied from 7% to 35% and 30° to 45° respectively.

Habitually, in a field investigation, prior to anchor design and installation, estimation of soil properties would often be based on the results of in-situ sounding tests such as the SPT, values of φ would then commonly be estimated by translating the blow counts to relative density, using one of the existing correlations (e.g. Gibbs & Holtz, 1957; Bazaraa, 1967). Alternatively, the blow count may be related to φ (De Mello, 1971). In both cases, only approximate estimates of φ should be expected, and these are affected by many factors including profile variability, stress history of the site, etc... .

Bearing in mind that in practice the engineer is more familiar with SPT or CPT charts, it was felt that the design charts (figs. 9-1 to 9-3) should be presented in an analogous manner. Figs. 9-1 to 9-3 show the plot of the dimensional breakout factor N_u and φ against ID for depth to diameter ratio (D/B) ranging from 2 to 5 for category 1, from 2 to 12 for category 2 and from 2 to 9 for category 3. A visual classification of the grain characteristics and a knowledge of the grain size distribution are required to make the choice of the relevant chart. The proposed method should be regarded and used as a guideline only, it is not intended to suggest that these charts are representative values for all sands but rather that their use may lead to reasonable pull out capacity estimates. For final design field tests may be performed to confirm design assumptions and hence give a more reliable value of the ultimate capacity.

In the following sections, the author demonstrates the use of the method in the prediction of the breakout factor in relation to the available published data and gives a calculation of a plate anchor ultimate load through an example.

9.3 COMPARISON WITH PUBLISHED DATA

The design curves given are checked with other test results. The comparison is intended to cover shallow and deep anchors, and model tests as well as field tests. The parameters necessary to carry out the comparison are the angle of internal friction, relative density, grading and shape of the grains. In some papers details such as relative density and shape were not mentioned but from the description of the state of the sand and the value of φ a reasonable assumption could be made. This information is used in the design chart to predict the ultimate uplift capacity. To the best of the author's knowledge model and field tests results in rounded or well rounded sand are non existent, therefore a comparison is made only in subrounded and subangular sands.

9.3.1 Comparison with model and field tests in subrounded sand

Balla (1961), and Bemben & Kupferman (1975) model tests are plotted in fig. 9-4 & 9-5, and as shown the agreement is reasonable.

Breakout factors evaluated from test results on model anchors conducted by Harvey & Burley (1973) and Clemence & Veesaert (1977) are plotted in fig. 9-6 & fig. 9-7, and it can be seen that the values of breakout factors from the design curves are in excellent agreement with the experimental values.

Fig. 9-8 show the breakout factors obtained from model test by Murray & Geddes (1987). The proposed design curve indicates a reasonable agreement, a slight overestimation averaging 12% was found. The model test results reported by Das & Jones (1982) and Zakaria (1986) are shown in fig. 9-11 & figs. 9-9 & 9-10, from which it can be seen that the proposed method is in excellent agreement with the experimental values.

Stewart's (1988) model test results are plotted against the predicted values in fig. 9-12, and it can be seen that good agreement is obtained in the dense state. However, in the medium state the predicted values are rather conservative at greater depth ($D/B \geq 8$).

The field tests carried out at Sizewell nuclear power station, on the Suffolk coast (U.K.), at two different densities and reported by Sutherland (1965) are plotted together with the prediction of the design curve and are illustrated in fig. 9-13. It can be seen that the correlation is very good for both densities.

Cragg (1985) reported field uplift tests on circular footings performed at Essa transformer station, Ontario (Canada), the range of depth to diameter ratio varying from 3 to 7. The resulting breakout factors and the proposed design curve are plotted in fig. 9-15, and a reasonable agreement was found.

Shaheen et al (1987) conducted field tests on single fluke anchors at a depth to diameter ratio varying from 1 to 7. The testing site was located on the coast of Northeastern Massachusetts (USA). The ensuing breakout factors are shown in fig. 9-14 and compared to the proposed design curve. It can be observed that the predictions are conservative at shallower depth, and higher at greater depth. Andreadis (1979) compared circular and fluke anchor breakout factors and showed that the fluke anchor displayed relatively higher breakout factors at shallower depths and lower resistance at greater depths. The present prediction follows the same line and hence confirms Andreadis findings.

The breakout factors obtained from model tests by Saeddy (1971) are shown in fig. 9-16 where it can be seen that the predictions compare favourably with the experimental results.

In the light of the previous comparisons, it can be concluded that the

proposed design curves predict the ultimate uplift capacity of a plate anchor embedded in a subrounded sand with reasonable accuracy.

9.3.2 Comparison with model tests in subangular sand

Nicolaides et al (1987) model test results are illustrated in fig. 9-17, and a good agreement with the prediction is found. However, in the case of Das & Jin-kaun (1987) plotted in the same figure a slight overestimation of the pull out capacity is found when compared with the predictions. Results reported by Trautmann (1985) show a reasonable agreement with the predicted values.

Despite the considerable number of test results documented the author was unable to find a report mentioning field test results on subangular or angular sand. Most of the reports lacked details which are essential if useful evaluations of the test results are to be made.

It can be concluded that the proposed design curves were found to predict the ultimate uplift capacity of model anchors embedded in subangular sand with a reasonable accuracy.

9.3.3 Comparison with other field tests

Yokel et al (1982) reported field uplift tests on plate anchors carried out around Washington D.C. (USA), in which the range of depth to diameter ratio varied from 4.0 to 7.0. The resulting breakout factors N_u are shown in fig. 9-18 together with the present predictions, and a large discrepancy can be observed. It should be noted that for the sake of comparison the author has assumed the sand to be subangular. Yokel et al (1982) reported that prior to testing 6 m of overburden

was removed, and this can explain the relatively high breakout factor attained on the site as being the result of overconsolidation. Hanna & Carr (1971) showed that the maximum uplift loads developed in overconsolidated beds led to large increases over the uplift load developed in normally consolidated beds. A threefold increase over the maximum load in a normally consolidated bed at an overconsolidation ratio of 8 has been reported.

The ϕ values given by Yokel et al (1982) were derived from the SPT " N " values, and did not show whether the site soil was overconsolidated or normally consolidated. Nixon (1982) in his state-of-the art report indicated that it would be very difficult to establish the stress history of a site from field SPT " N " values. More recently, Jamiolkowski et al (1988) pointed out that the existing SPT correlations are applicable only to normally consolidated sands and their use in other sands (overconsolidated deposits) might cause misleading results. Hanna & Carr (1971) stressed the fact that a large scatter would result between predictions and field measurements if the initial stress system in the soil is not taken into account. However, there is no reliable method of assessing the in-situ stress within a sand mass, although attempts to infer an overconsolidation ratio from SPT results are at a preliminary stage of validation (Jamiolkowski et al, 1988), and until a reliable method is developed which is capable of defining the soil with respect to its stress history, the uncertainty will continue to exist. The reason for the apparent discrepancy observed in fig. 9-17 has been explained and shown to be due to the stress history of the soil. Fig. 9-17 also shows the limitation of the proposed design charts and highlights the complexity of the problem associated with such correlations

In the 28th Rankine lecture, Sutherland (1988) presented over 20 field uplift tests on belled piers from different sites in the United States of America

(Konstantinidis et al, 1987; Tucker, 1987). The piers were up to 5.2 m deep and 1.14 m wide and covered a range of D/B values from 1.38 to 5.0. Information was given on unit weight and angle of friction of each test. These results are reproduced in fig. 9-19. In order to be able to compare those results with the present predictions, the author assumed firstly that all the sands were subrounded and secondly subangular. The upper and lower limit changed accordingly, these limits are plotted in fig. 9-19 and it would appear that the comparison of these field test results with the predicted values is reasonable over the range of friction angles investigated. There are few anomalous results due probably to the assumptions made but despite this the average of the belled pier results is close to the predicted values.

9.4 EXAMPLE OF DESIGN

In the design of anchors, as with any foundation problem, it is necessary to know some properties of the soil. These properties include the grain shape which can be easily assessed with a portable microscope, grading, angle of internal friction φ , sand density γ and the relative density ID which can be obtained from penetration tests in boreholes. Other parameters are the anchor depth D and the anchor diameter B.

Ultimate loads are calculated, for the purpose of illustrating the design procedure for anchors embedded in a uniform subrounded sand, the same procedure is valid for the subangular and the rounded sand.

The following properties of the sand are assumed:

$\gamma = 16.90 \text{ Kn/m}^3$, $\varphi = 40^\circ$, ID = 73%, Shape:subrounded.

Case 1 Shallow anchors

Taking D/B = 2 and B = 750 mm, from fig. 9-2 Nu corresponding to $\varphi = 40^\circ$

and $D/B = 2$ is equal to 7.0.

Hence, the ultimate pull out load given by $P = N_u \cdot \gamma \cdot D \cdot \pi/4 \cdot B^2$ is equal to

$$P = 7.0 \times 16.90 \times 1.5 \times 3.14/4 \times 0.075^2 = 0.783 \text{ Kn}$$

The additional forces to be added are the shaft and the anchor plate weight. However, in the present case these additional forces are neglected and are considered to be on the safe side.

Case 2 Deep anchors

Taking $D/B = 12$ and $B = 750$ mm, from fig. 9-2 N_u corresponding to $\varphi = 40^\circ$ and $D/B = 12$ is equal to 110. Hence $P = 73.88$ Kn.

The design example has been done on the basis of the curves and information available from the extensive testing done in the present research and literature survey. In practice much less information would be available, but by estimating the necessary factors from site investigation results it should be possible to arrive at a reasonable estimate of the uplift capacity of a plate anchor.

Sand	ID (%)	φ ($^{\circ}$)	Shape	Grading	Range of D/B ratio	Range of Breakout Factors	Sources	Laboratories
Sizewell	95	45	subrounded	uniform	1 to 5	4.8 to 36.9	Sutherland (1965)	Glasgow University
	33	31			1 to 5	2.5 to 11.0		
Chatahooche	61	41.3	subangular	uniform	1.5 to 9.8	7.6 to 87.4	Ezquivel Diaz (1967)	Duke University
	7	32.8			1.5 to 9.8	1.5 to 6.1		
Bush farm Borough green	73	42	subangular subrounded	uniform uniform	2 to 12	12 to 177	Andreadis (1981)	London University
	66	37			2 to 12	6 to 123		
Leighton Buzzard	85	41.5	subrounded	uniform	1 to 12	3.8 to 146.3	Fadl (1981)	Glasgow University
	50	36.5			1 to 12	3.2 to 56.6		
	25	33.6			1 to 12	2.5 to 17.5		
Dansk normal sand	108	37.7	rounded	uniform	1 to 3.5	3.6 to 15	Ovesen (1981)	Danish Geotechnical Institute
	61	32.3			1 to 3.5	7.3 to 8.1		
	36	29.5			1 to 3.5	2.2 to 5.8		

Table 9-1 Test details of some previous investigators.

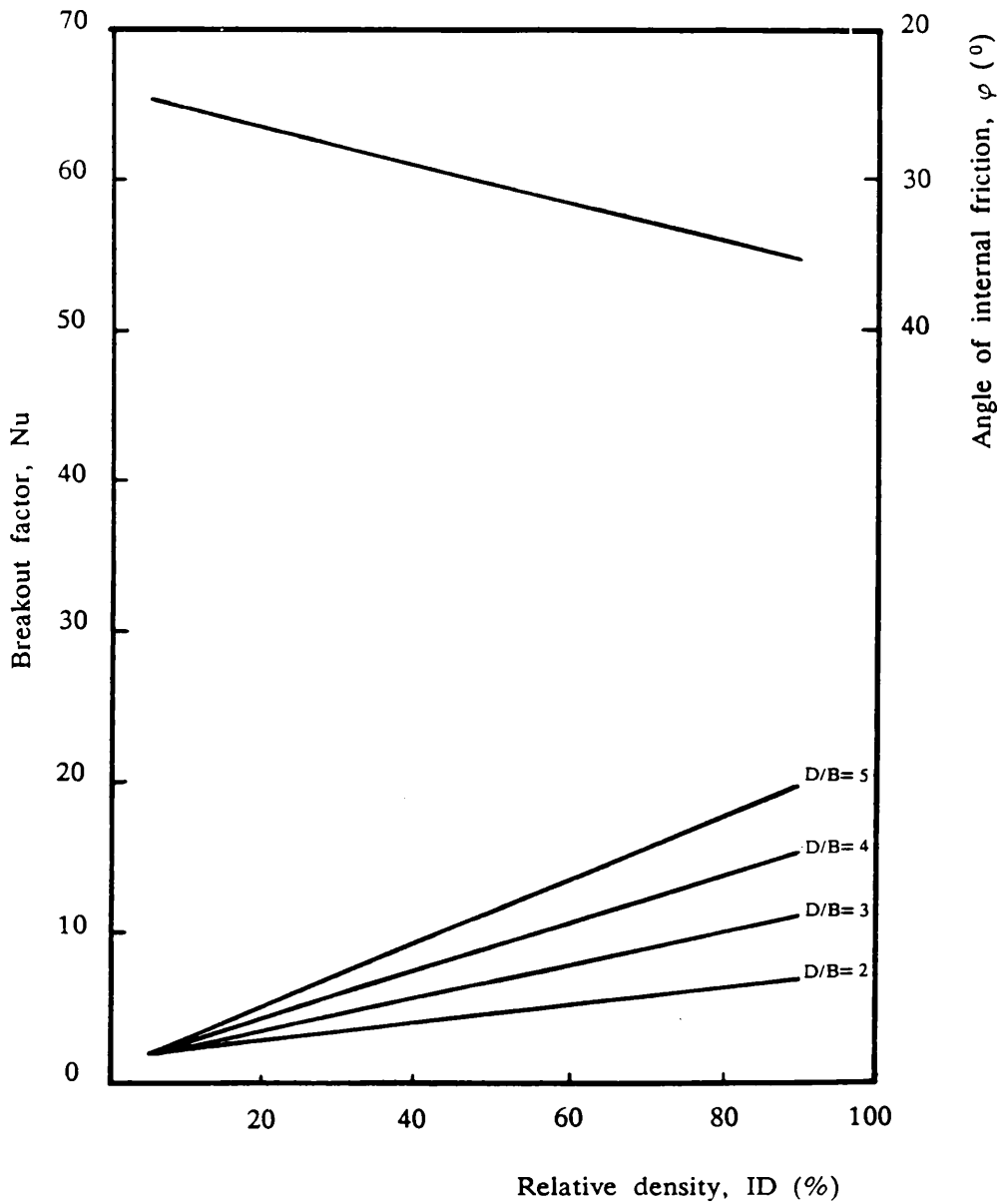


Fig. 9-1 Design chart for uniform rounded to well rounded sand (shallow anchors).

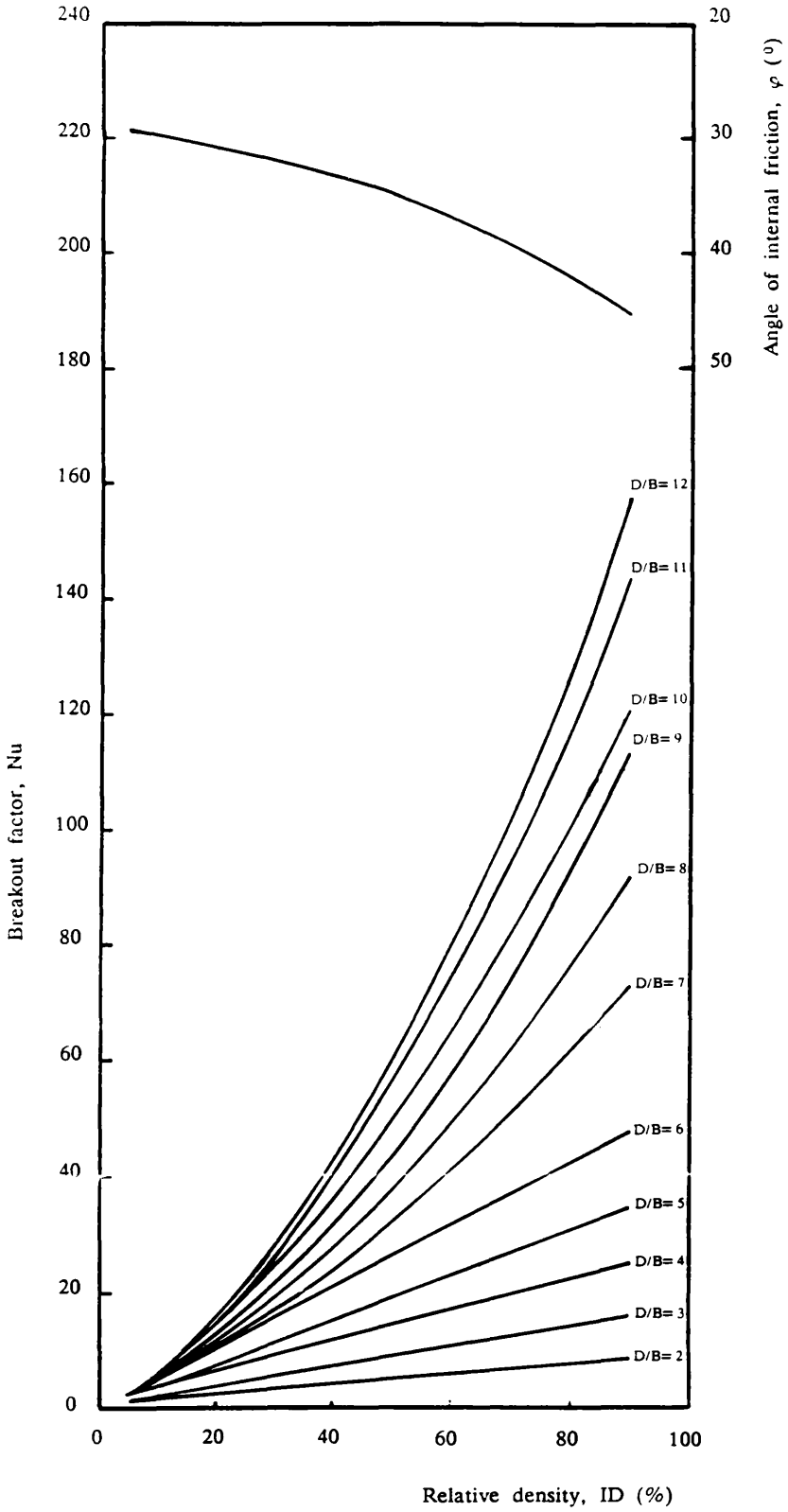


Fig. 9-2 Design chart for uniform subrounded sand.

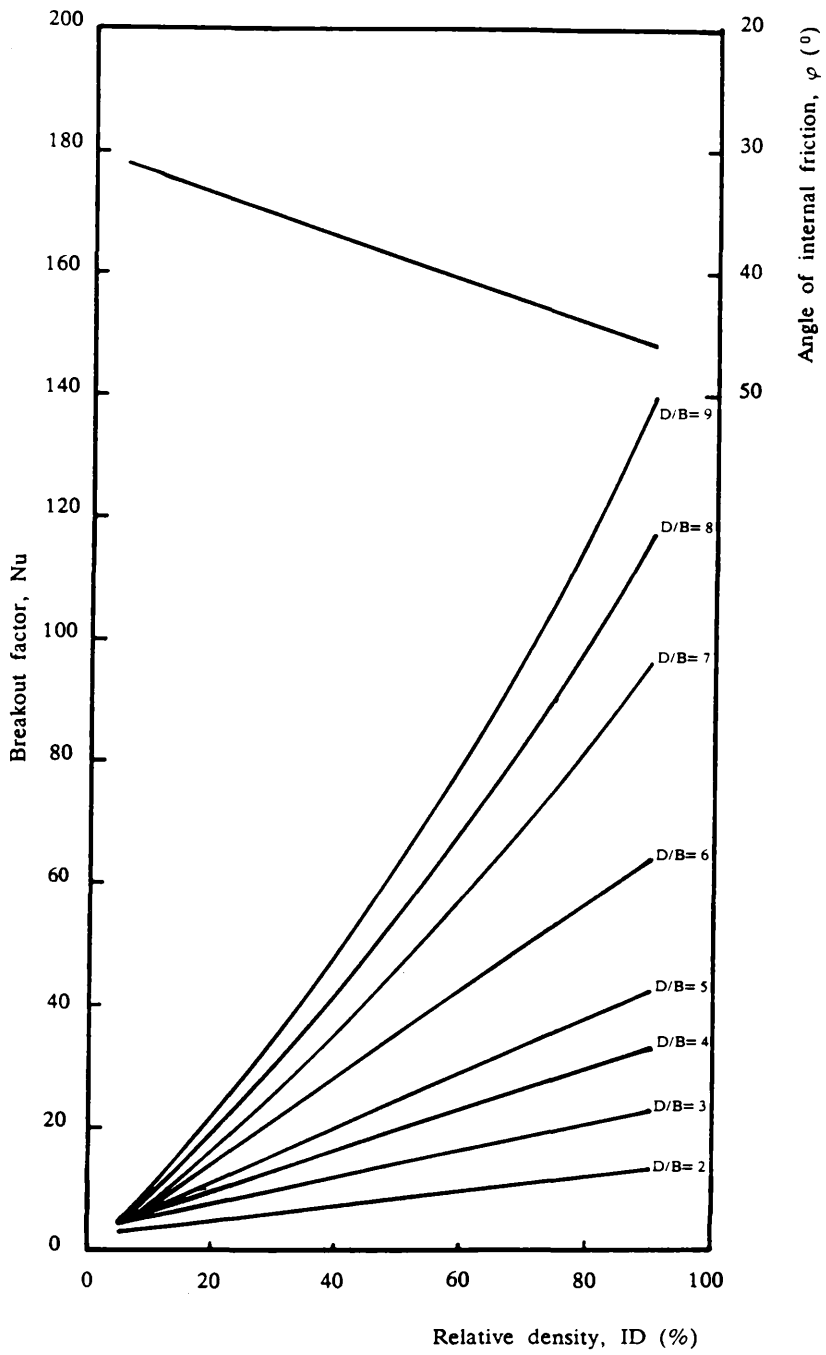


Fig. 9-3 Design chart for uniform subangular sand.

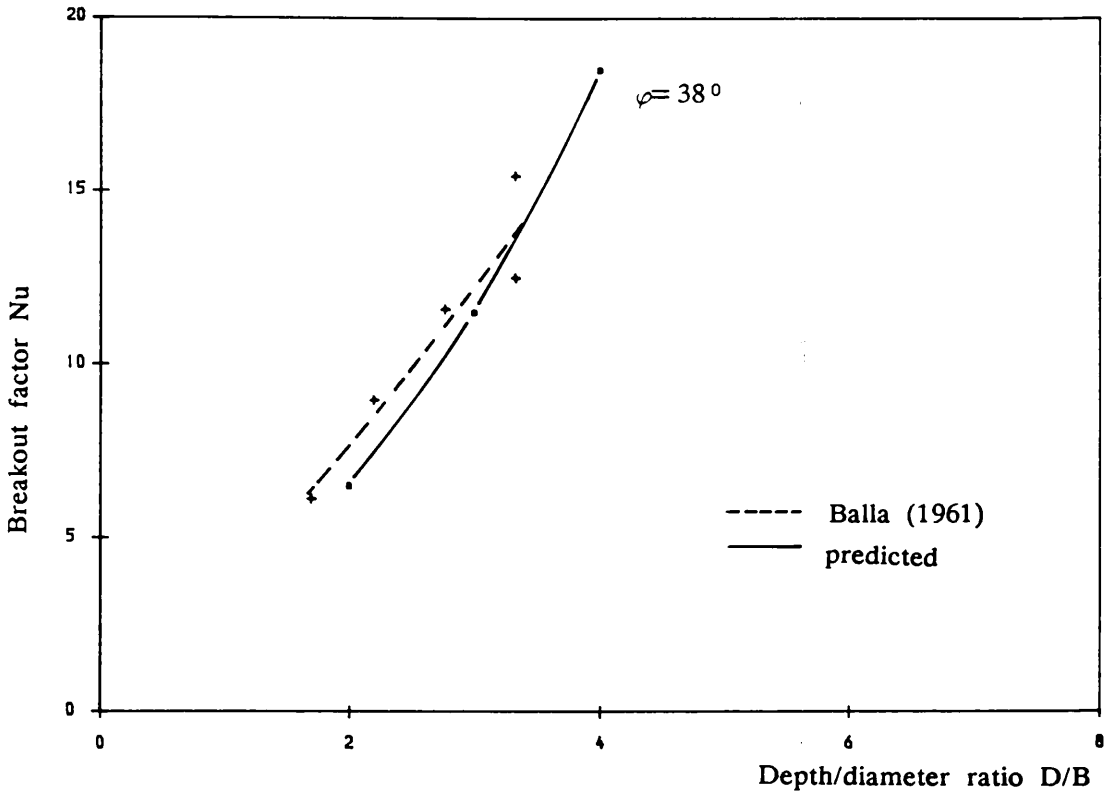


Fig. 9-4 Comparison of Balla (1961) model test results and present predictions.

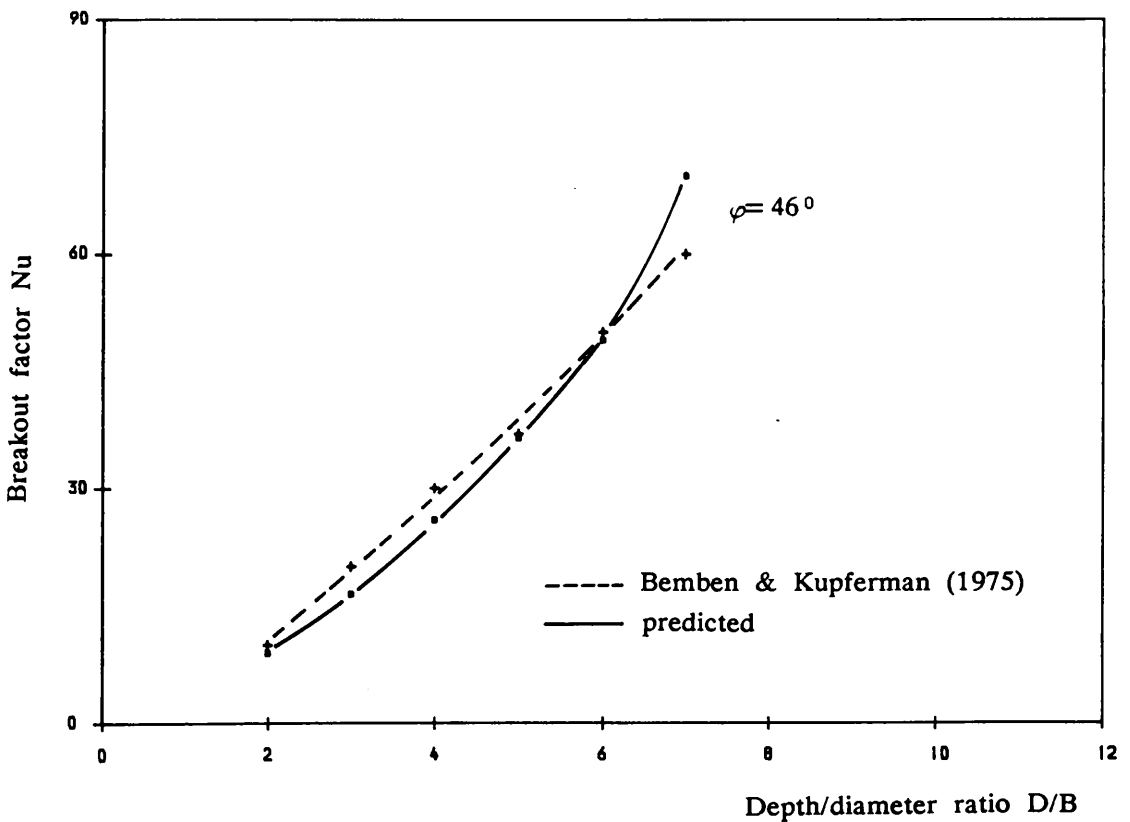


Fig. 9-5 Comparison of Bemben & Kupferman (1975) model test results and present predictions.

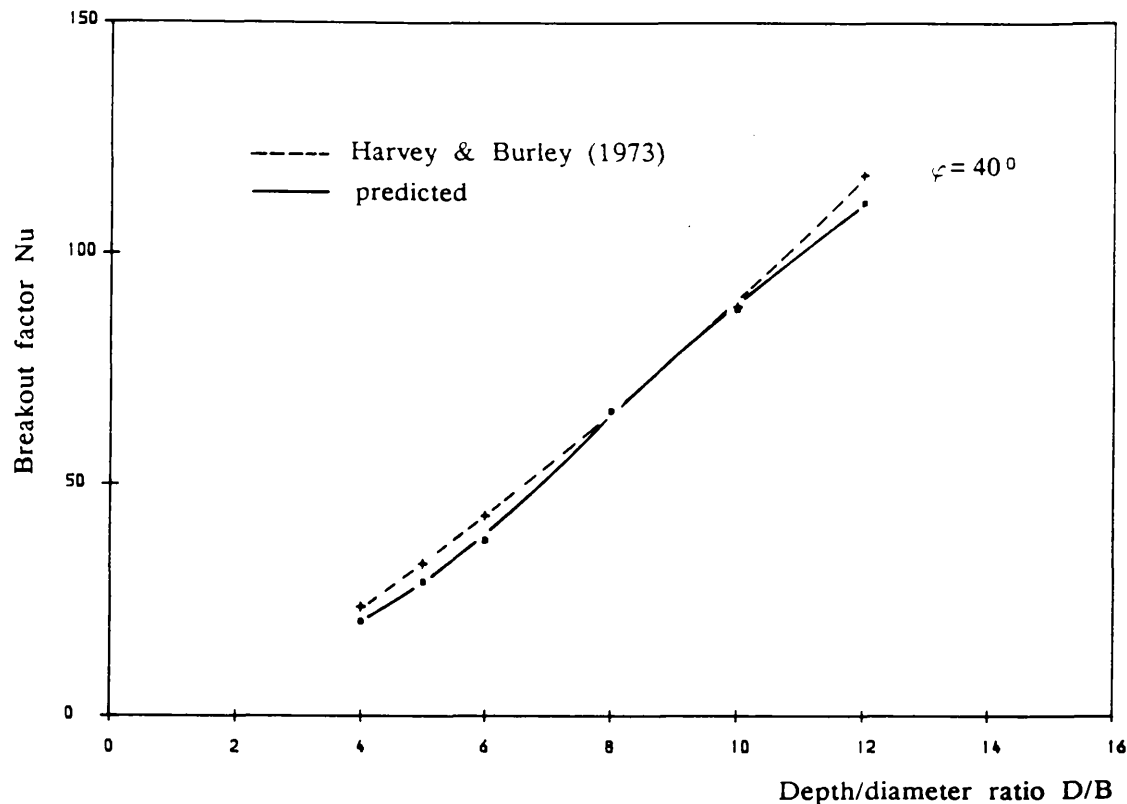


Fig. 9-6 Comparison of Harvey & Burley (1973) model test results and present predictions.

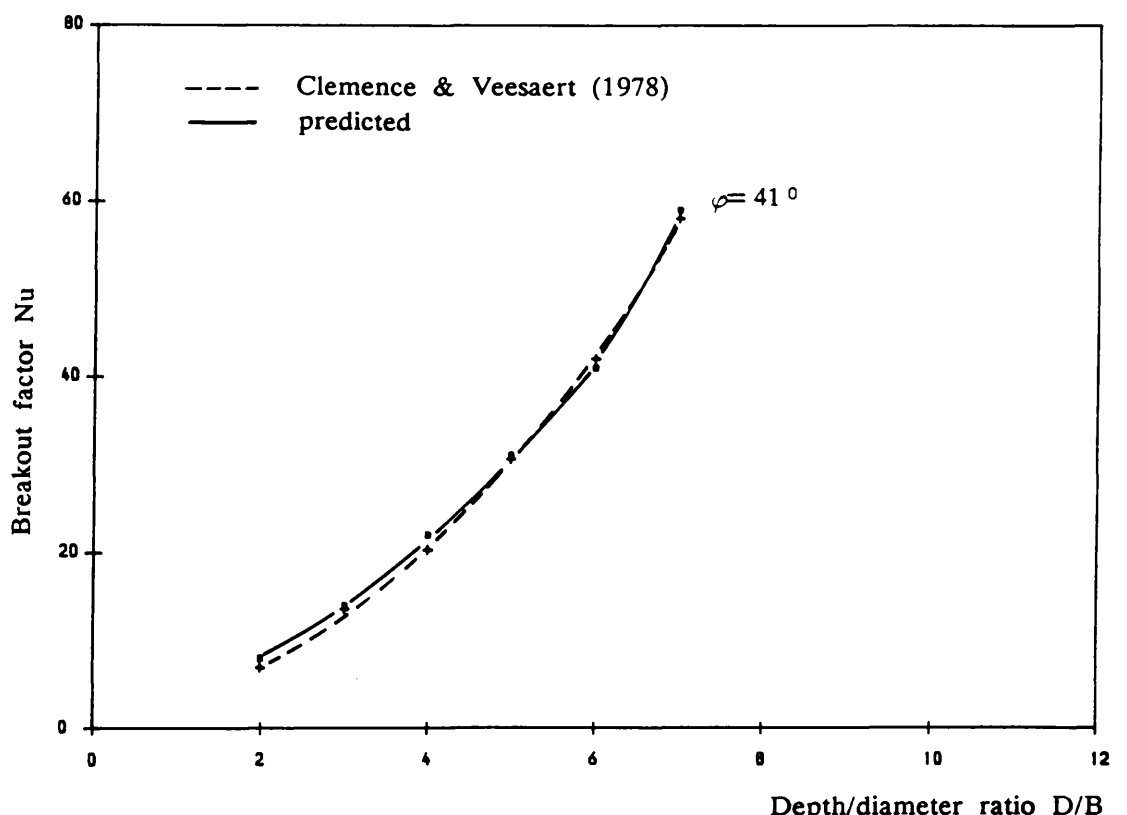


Fig. 9-7 Comparison of Clemence & Veesaert (1978) model test results and present predictions.

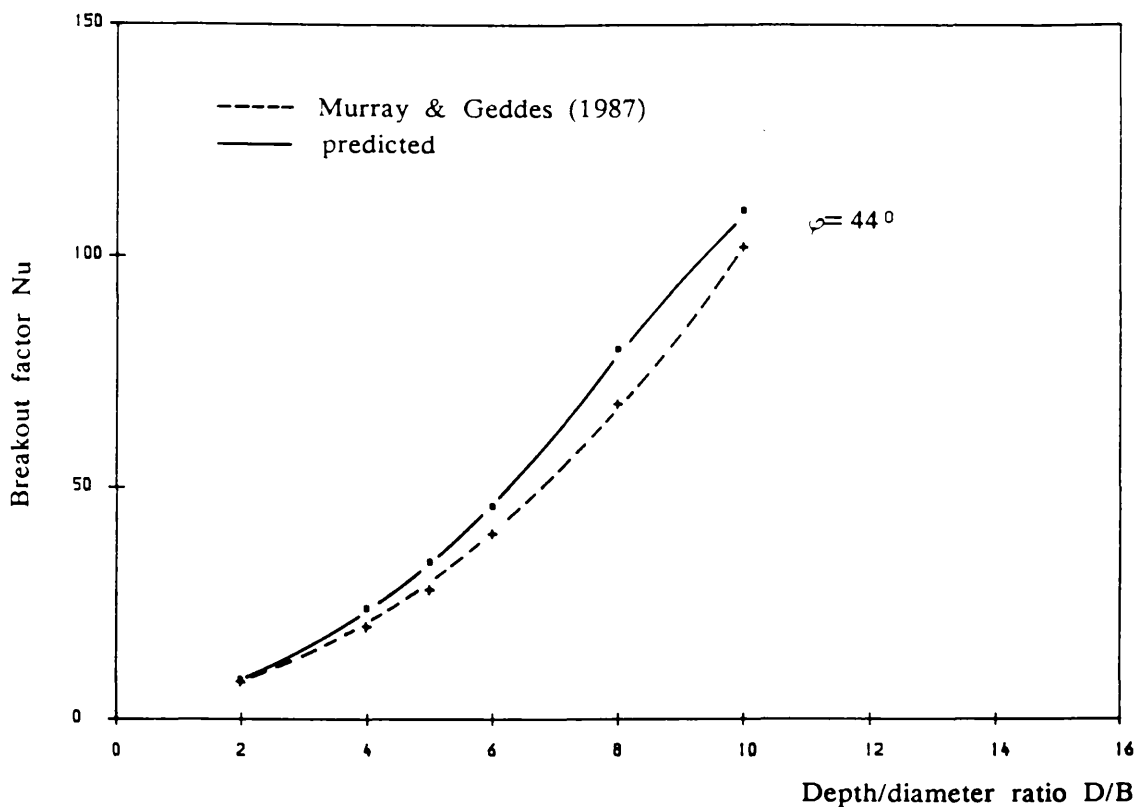


Fig. 9-8 Comparison of Murray & Geddes (1987) model test results and present predictions.

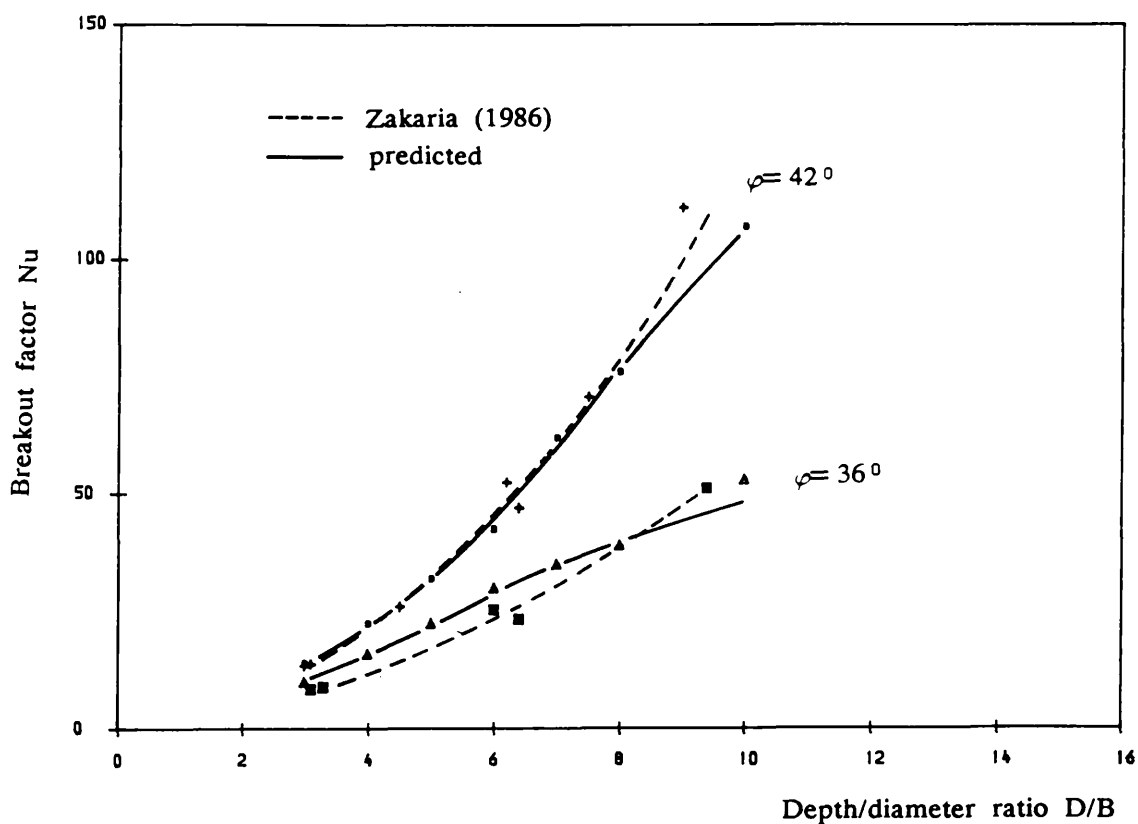


Fig. 9-9 Comparison of Zakaria (1986) model test results and present predictions.

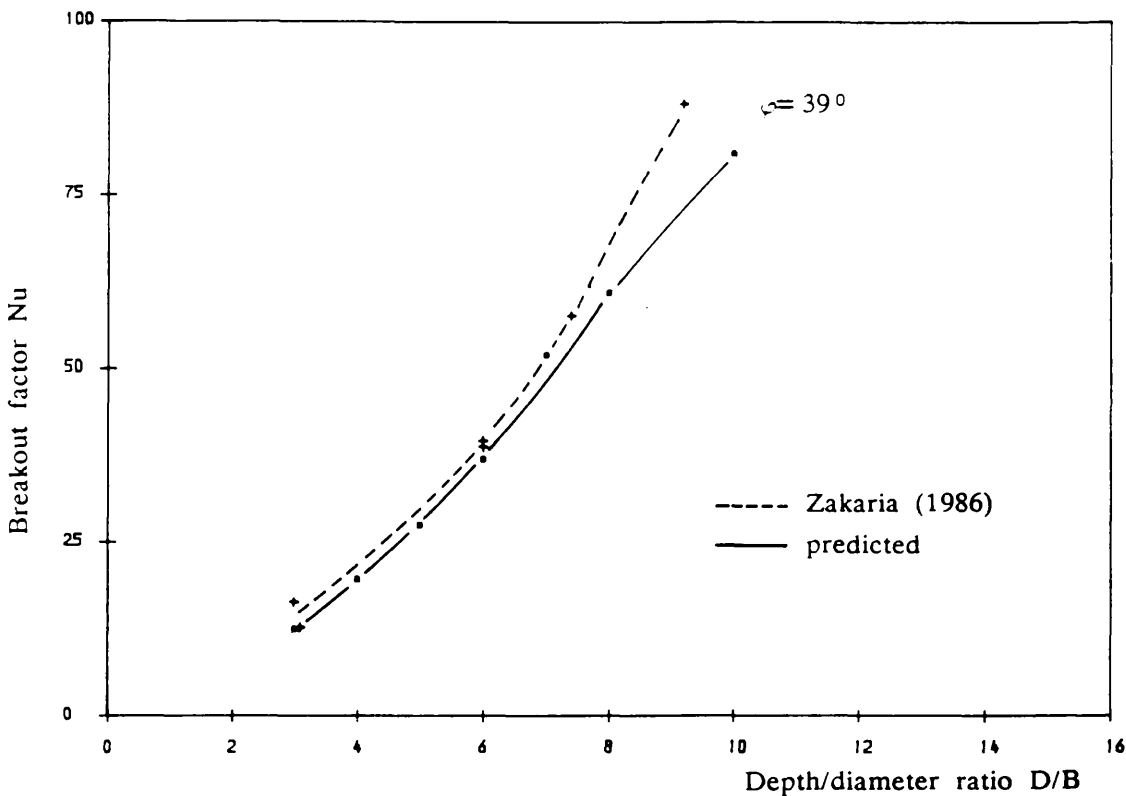


Fig. 9-10 Comparison of Zakaria (1986) model test results and present predictions.

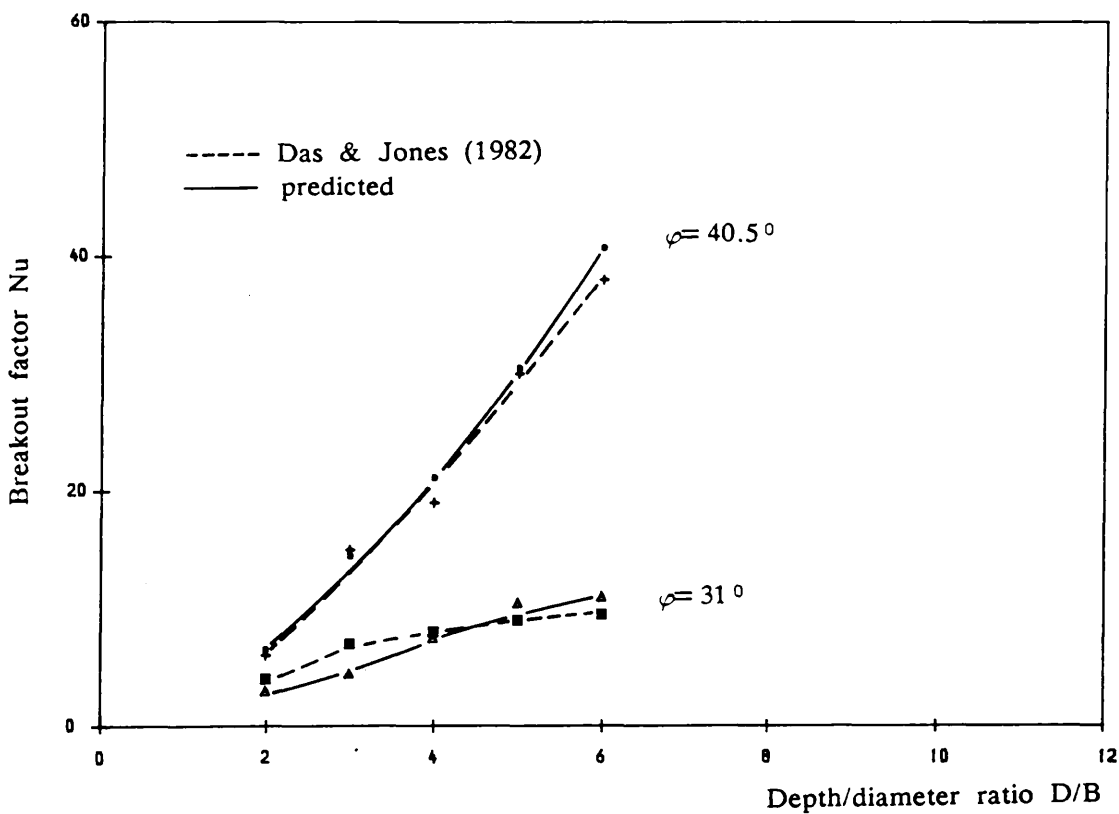


Fig. 9-11 Comparison of Das & Jones (1982) model test results and present predictions.

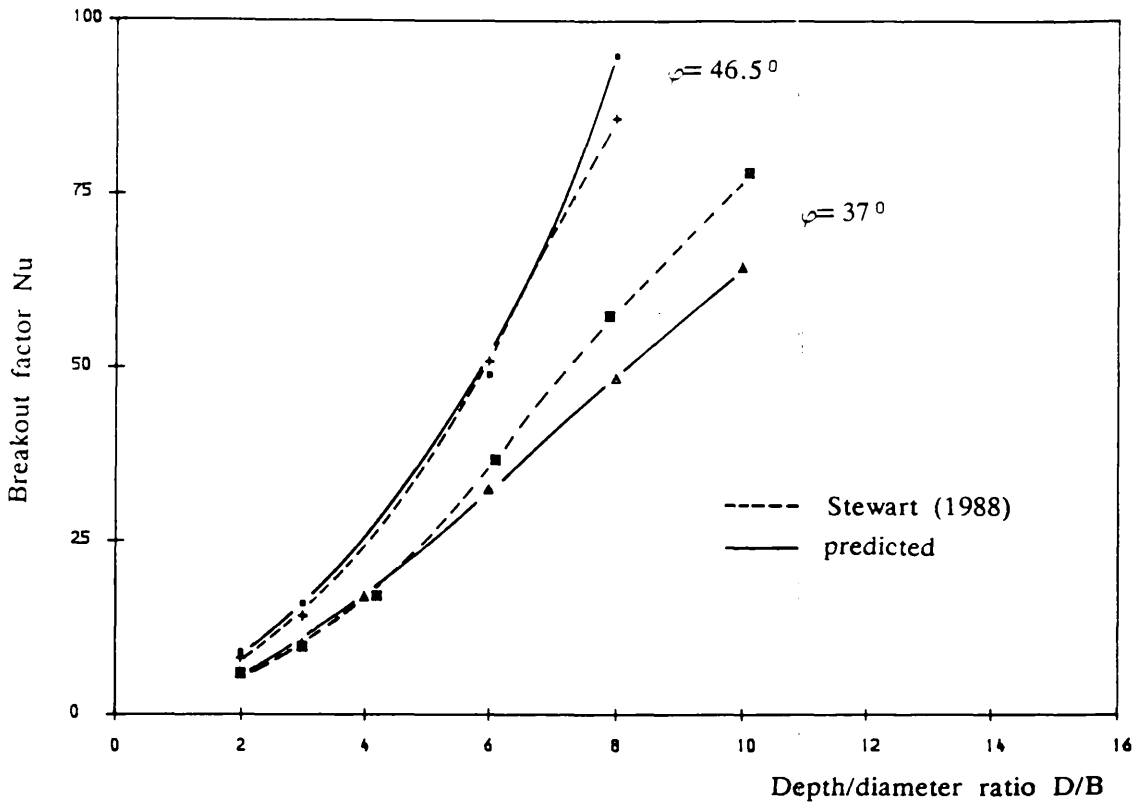


Fig. 9-12 Comparison of Stewart (1988) model test results and present predictions.

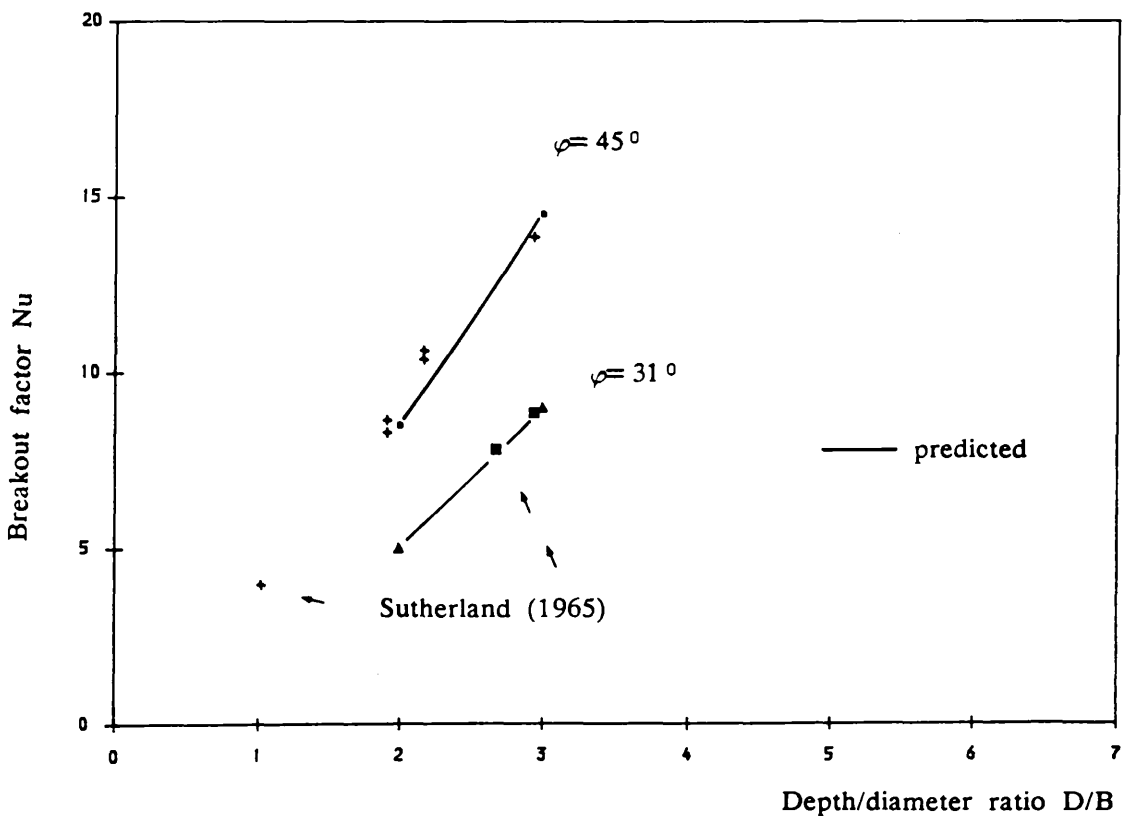


Fig. 9-13 Comparison of Sutherland (1965) field test results and present predictions.

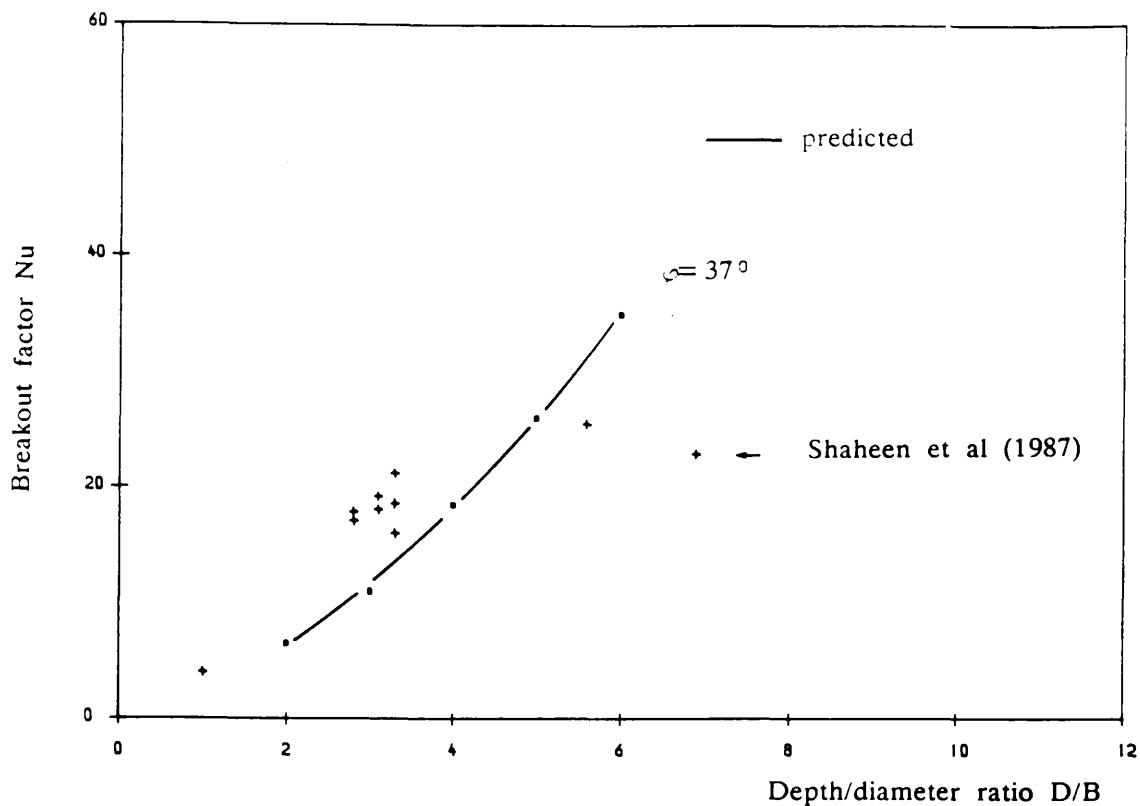


Fig. 9-14 Comparison of Shaheen et al (1987) field test results and present predictions.

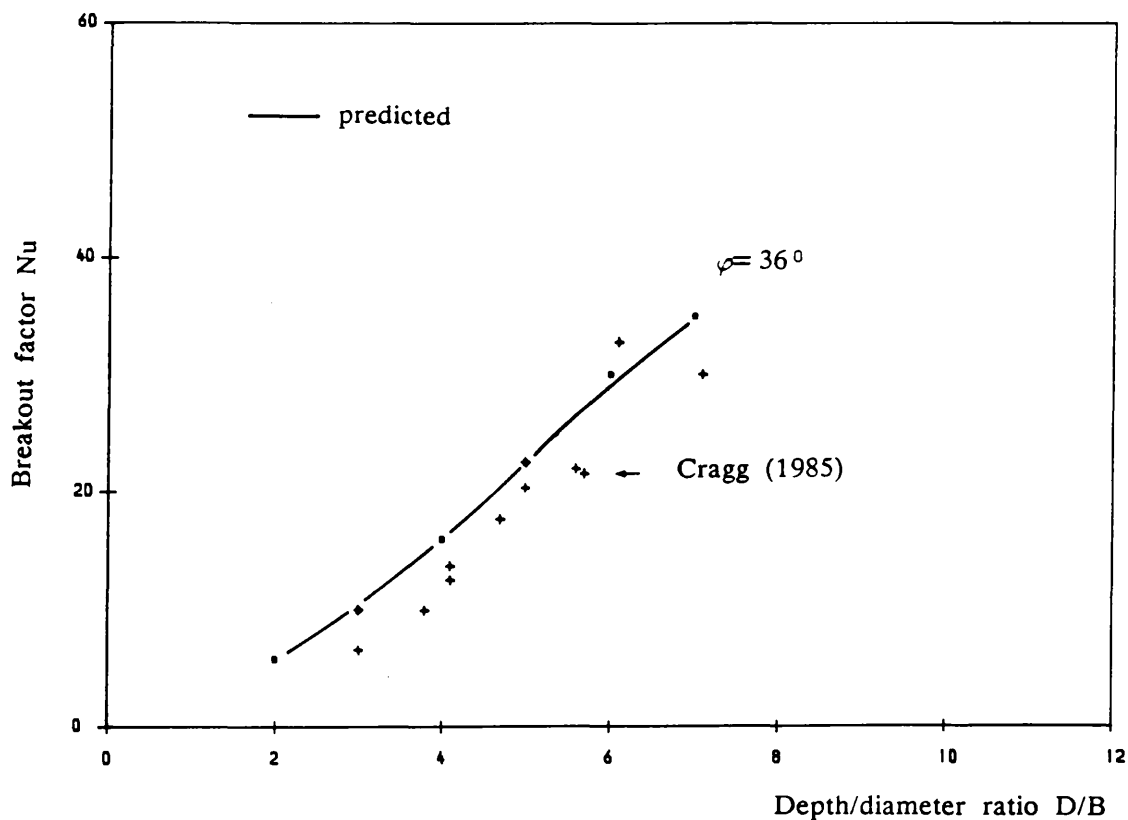


Fig. 9-15 Comparison of Cragg (1985) field test results and present predictions.

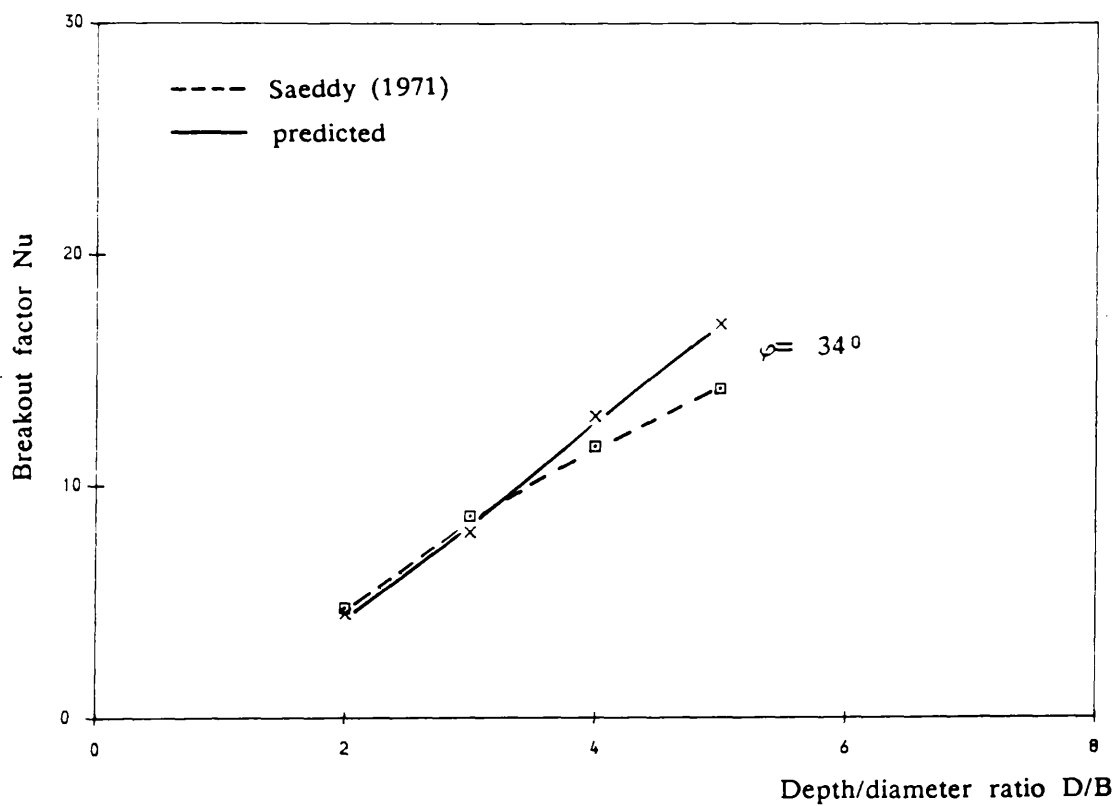


Fig. 9-16 Comparison of Saeddy (1971) model test results and present predictions.

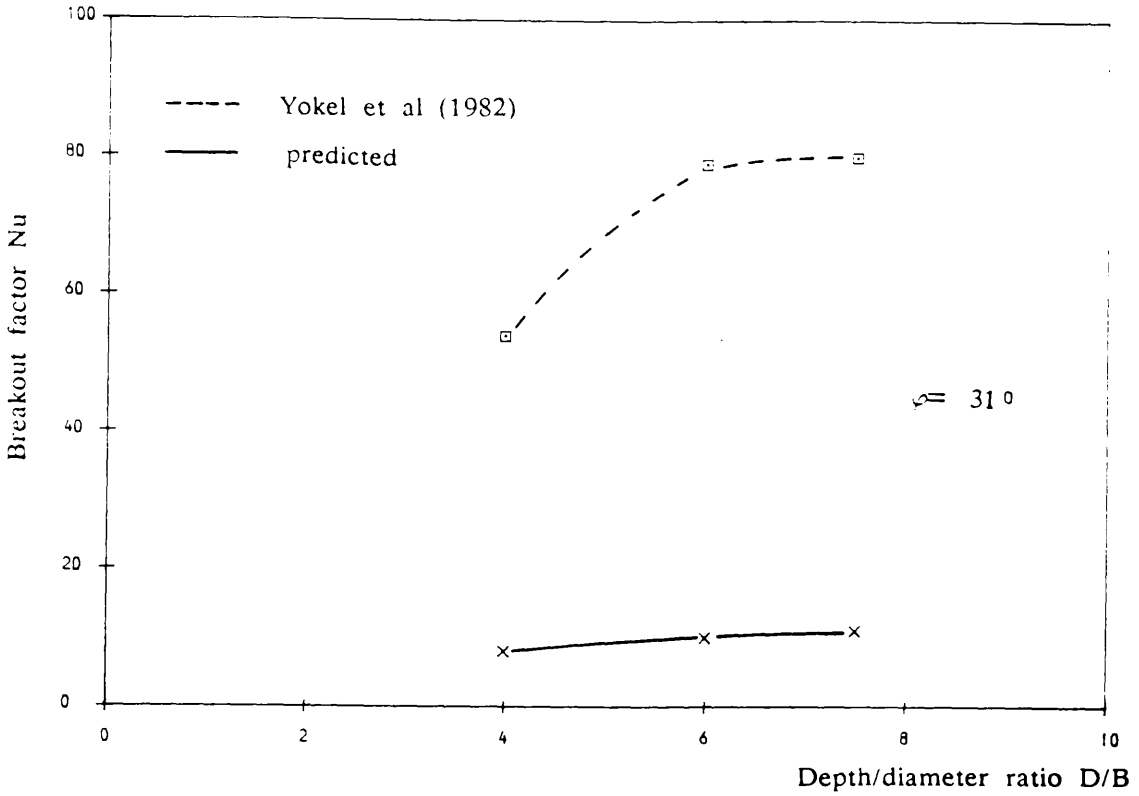


Fig. 9-17 Comparisons of Yokel et al (1982) field test results and present predictions.

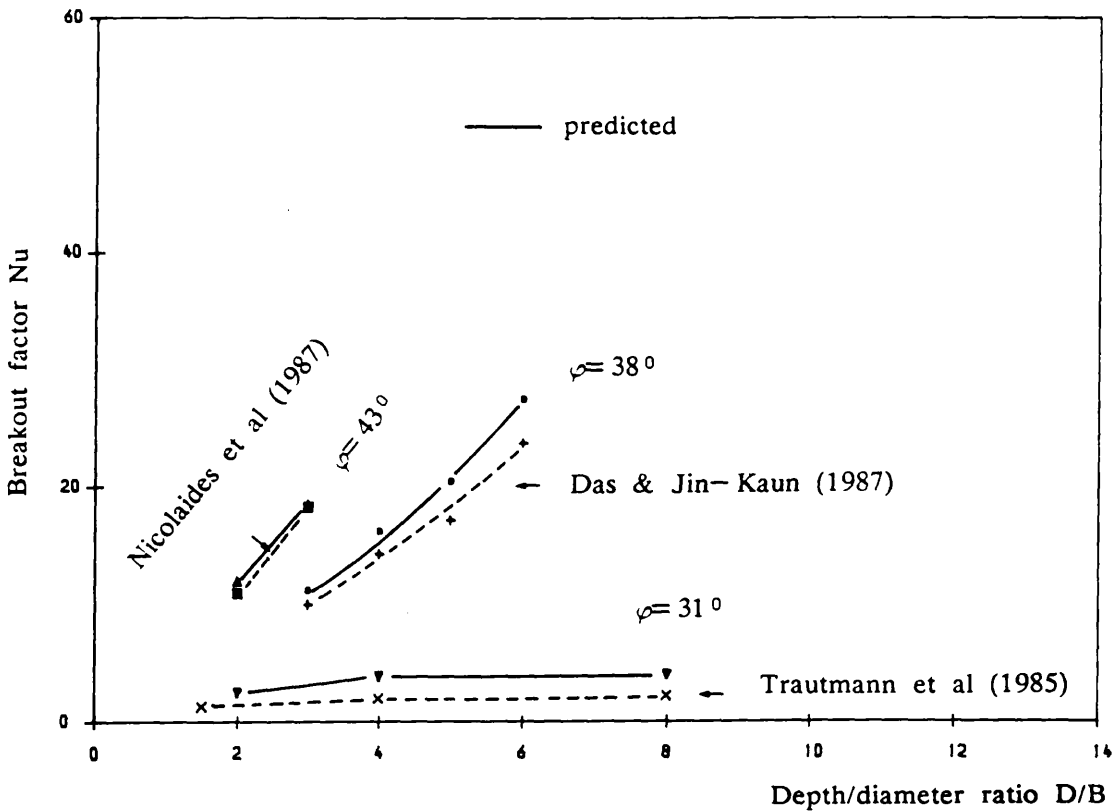


Fig. 9-18 Comparison of Das & Jin-Kaun (1987), Nicolaides et al (1987) and Trautmann et al (1985) model test results and present predictions.

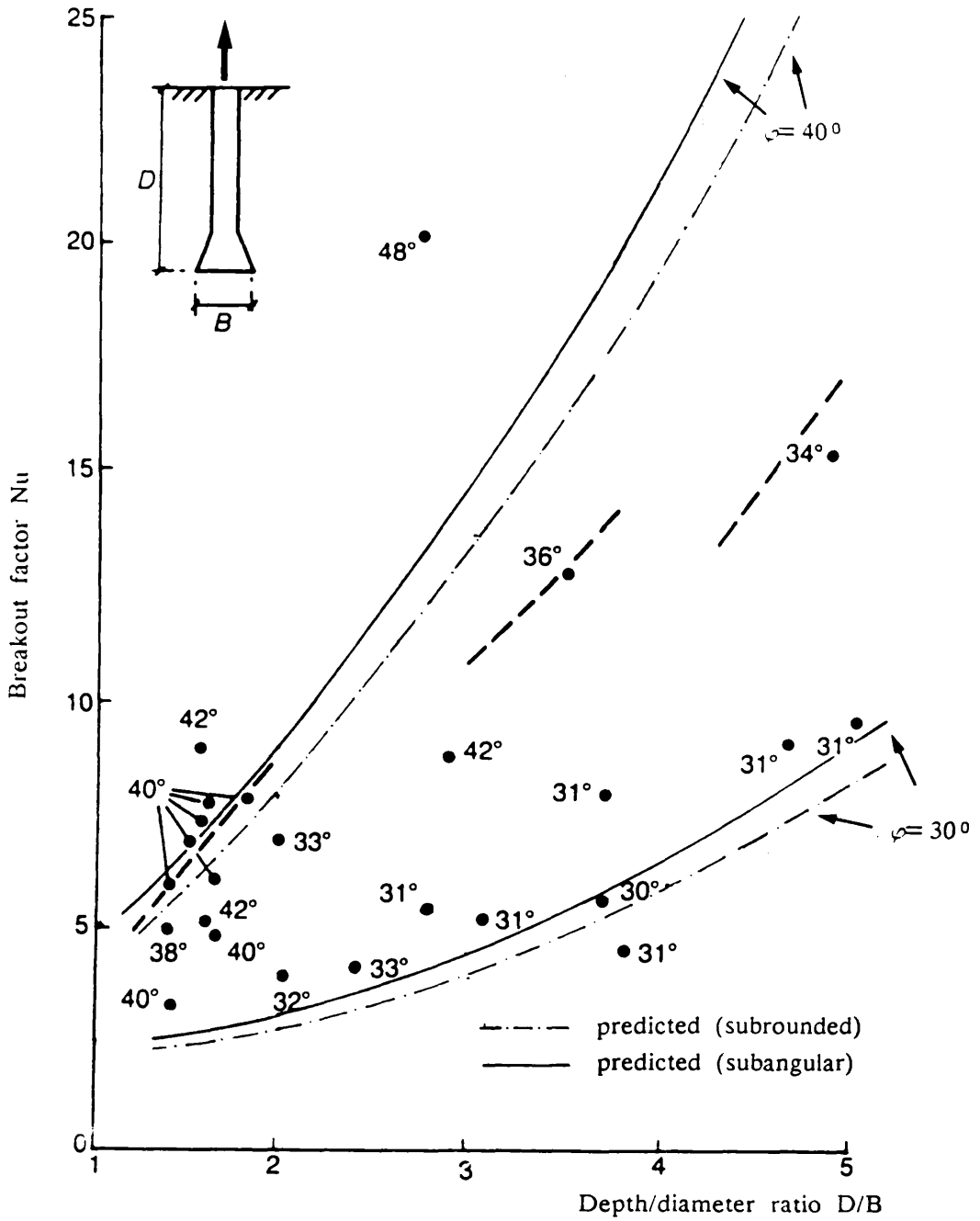


Fig. 9-19 Comparison of field test results as Compiled by Sutherland (1988) and present predictions.

Chapter 10

CONCLUSIONS

10-1 GENERAL

The various deductions made or conclusions drawn from the current investigation are summarised in the following sections. Although a considerable amount of knowledge has been accumulated through previous and present research efforts, more information, achieved using further investigation, is needed before soil anchor interaction can be understood more comprehensively. A few lines of further investigation, believed to be instructive for the improvement and advancement of the knowledge of plate anchors behaviour are suggested herein.

10-2 CONCLUSIONS

(1) A research programme on the effect of sand properties on the behaviour of plate anchors subjected to uplift loading has been undertaken in which a series of load tests were performed on vertically installed plate anchors. From the test results obtained, an insight has been gained into the performance of plate anchors, embedded in different type of sands at different relative densities and at various depths. The effect of a layered system on the plate anchor response has also been assessed.

Recognising that well documented plate anchor test data is of considerable engineering significance it is expected that the test results presented in this thesis will provide a useful reference document for future investigators in this field.

(2) The apparatus and measurement equipment used in this investigation worked satisfactorily throughout the test period. When checked the repeatability of the results was good.

(3) Static loading test

The following conclusions are made with respect to the results from static loading tests

(i) Homogeneous bed

(a) The anchor displacements at ultimate loads increase with D/B ratio resulting in larger displacement for deep anchors. Nevertheless these displacements decrease with increase of density, yielding higher uplift loads.

(b) The maximum uplift load or breakout factor is significantly dependent on the relative density (ID).

(c) The ultimate load or breakout factor increases with D/B and the rate of increase is higher in the shallow anchor range.

(d) If the sands have similar mean diameter D_{50} and grading the breakout factor is greater for subangular than subrounded sand at a given relative density.

(f) If the sands have the same mean diameter D_{50} and shape, the breakout factor is greater for well graded sand than uniform sand at a given relative density.

(g) For case d & f, it was found that no direct relationship exists between the pull out resistance, grain shape, and grading.

(h) Tests on sands having similar grading and shape but different grain size (D_{50}) demonstrated that there was no difference in the breakout factor which was thus independent of the grain size.

(i) An empirical design procedure based on the combined use of present and past data has been presented. Reasonable agreement was found with results from previous investigators.

(ii) Two layered sand bed

(a) The test results show that the ultimate uplift load of a plate anchor embedded in a two layered uniform subrounded sand is dependent on the depth of embedment, the thickness of the upper layer and the relative strength of the different layers.

(b) At $\lambda=1$ and for a given D/B ratio, there was no difference between pulling a plate anchor from a dense/medium bed or a dense/loose bed.

(c) For a given D/B ratio and $1 < \lambda \leq 4$, a dense/medium bed gives a greater uplift than a dense/loose bed.

(d) An approximate design theory for the ultimate uplift load of a plate anchor embedded in a two layered uniform subrounded sand has been developed based on the observed mode of failure.

(e) The observed approximate solution compared to the author's test results showed a reasonable agreement over the range of D/B and λ investigated.

(4) Stereo photogrammetric tests

With reference to the results of stereo photogrammetric tests the following conclusions can be drawn:

- (a) The mode of failure of a plate anchor embedded in a homogeneous sand is controlled by the relative depth of embedment and the relative density of the surrounding soil.
- (b) For sands having similar grading and shape, the zone of displaced sand mass was found to be independent of grain size diameter.
- (c) Grain shape and grading can dramatically affect the extent of the disturbed sand for shallow and deep anchors.
- (d) The predictions of failure surfaces is a very complex problem. However, the present test results show why there is such a large discrepancy in their predictions.
- (e) The mode of failure of a shallow anchor embedded in a two layered sand is a function of the upper layer thickness ratio (λ).
- (g) It was found that the stereo photogrammetric technique can yield accurate measurement, it is possible by measuring both the vertical and horizontal displacements within the sand bed to establish the relative displacements occurring throughout the bed for any increment of anchor displacement.

10-3 SUGGESTIONS FOR FUTURE WORK

-1- The role of the present work in design practice is still limited due to the fact that all correlations between breakout factor and engineering parameters have been established on very clean normally consolidated sands; therefore neglecting possible influence of factors such as: overconsolidation, sand structure, ageing, slight cementation, etc... Studies of these parameters will indeed throw more light on the soil anchor interaction problem.

-2- Design and construction of foundations on soft clay layers is rather difficult. Under this circumstance, various types of soil improvement technique are used amongst them being the construction of stone columns. Study of the uplift behaviour of a plate anchor embedded in a granular trench made in a soft clay will give an insight into a problem which may be encountered in practice.

-3- Investigation of the plate anchor behaviour in a three layered sand and deep anchor behaviour in a two layered sand. This is a logical extension to the work carried out in the present thesis.

-4- The effect of sand properties on the behaviour of a single, vertical, plate anchor has been investigated in the tests described. Of equal importance is the behaviour of a single inclined plate anchor and a group of plate anchors embedded in different types of sand.

-5- Analysis of the model situations using the finite element technique should be developed. The results of the model tests provide the data against which the analysis can be checked. If satisfactory procedures can be developed for the models the method may be extended to the prototype situation.

REFERENCES

- Abu-Taleb, M.G.A. (1974). "The behaviour of anchors in sand". Ph.D Thesis. Sheffield University, Sheffield (England).
- Akroyd, T.N.W. (1957). "Laboratory testing in soils engineering". Soils Mechanics Ltd.
- Al-Hussaini, M. (1983). "Effect of particle size and strain conditions on the strength of crushed basalt". Canadian Geotechnical Journal. Vol. 20 (4), pp. 706-717.
- Andrewes, K.Z. (1976). "The use of stereo photogrammetry for measuring displacement fields". S R C Report. Strathclyde University, Glasgow (Scotland).
- Andrewes, K.Z. & Butterfield, R. (1973). "The measurement of planar displacement of sand grains". Geotechnique 23, No 4, pp 571-576.
- Andreadis, A. (1979). "Uplift resistance of embedded sea bed anchors". Ph.D Thesis. Queen Mary College, London University (England).
- Andreadis, A & Harvey, R.C. (1981). "A design procedure for embedded anchors". Applied Ocean Research. Vol. 3, No 4, pp 177-182.
- Andreadis, A., Harvey, R. C. & Burley, E. C. (1981). "Embedded anchor response to uplift loading". Proc. ASCE, Jour. Geotech. Engng. Div. Vol. 107, No GT 1, pp 59-78.
- Arthur, J.R.F. & Dunstan, T. (1982). "Rupture layers in granular medium". IUTAM Conf. Deformation and Failure of Granular Materials, Delft (Netherland), pp 453-459.
- Balla, A. (1961). "The resistance to breaking out of mushroom foundations for pylons". Proc. 5th Int. Conf. Soil Mech. Fdn. Engng, Paris (France). Vol. 1, pp 569-576.
- Baker, W.H. & Kondner, R. L. (1966). "Pull out load capacity of a circular earth anchor buried in sand". Highway Research record 108. National Academy of Sciences, pp 1-10.
- Bazaraa, A.R.S.S. (1967). "Use of the standard penetration test for estimating settlements of shallow foundations on sand". Ph.D Thesis. University of Illinois, Urbana (USA).
- Been, K. (1981). "Non destructive soil bulk density measurements by X-ray attenuation". Geotechnical Testing Journal. No 4, pp. 169-176.
- Bemben, S.M. & Kupferman, M. (1975). "The vertical holding capacity of marine anchor flukes subjected to static and cyclic loading". Proc. 7th Annual. Off. Tech. Conf., Houston (USA). pp 363-374.
- Bishop, A.W. & Henkel, D.J. (1962). The measurement of soil properties in the triaxial test. 2nd edition, Publ. by Edward Arnold.
- Bobbit, D.E. & Clemence, S.P. (1987). "Helical anchors: application and design criteria". Proc. 9th Southeast Asian Geotech. Conf., Bangkok (Thailand), pp 105-120.

Bourdeau, P.L. & Recordon, E. (1988). "Application de la radiographie a l'etude des deformations en mecanique des sols". Conf. Int. "Mesures et essais en Genie civil", Lyon-Villeurbanne (France), vol. 2, pp 387-396.

Bozozuk, M., Van wijk, M.C. & Fellenius, B.H. (1978). "Terrestrial photogrammetry for measuring pile movements". Canadian Geotechnical Journal. Vol. 15 (4), pp 596-599.

Brandenberger, A. J. (1974). "Deformation measurements of power dams". Photogrammetric Engineering. Vol. 40 (9), pp 1051-1058.

Burmister, D.M (1948). Proceeding American for Testing and Materials, Vol. 48, pp. 1249-1268.

Butterfield, R. & Andrawes, K.Z. (1970). "An air activated sand spreader for forming uniform sand beds". Geotechnique 20, pp 97-100.

Butterfield, R., Harkness, R.M. & Andrawes, K. Z. (1970). "Stereo photogrammetric method for measuring displacement fields". Geotechnique 20. No 3, pp 308-314.

Carr, R.W. (1970). "An experimental investigation of plate anchors in sand". Ph.D Thesis. Sheffield University, Sheffield (England).

Carr, R.W. & Hanna, T.H. (1971). "Sand movement measurement near anchor plates". Proc. ASCE, J. Soil Mech. Fdns Div. Vol. 97, No SM5, pp. 833-840

Cichy, W., Boulon, M. & Desrues, J. (1987). "Etude experimentale stereo photogrammetric des interfaces sols-foundations a la boite de cisaillement direct". 4ieme Coll. Franco-Polonais de Mec. des Sols Appliquee, Grenoble (France). pp 311-325.

Clemence, S.P. & Veesaert, C.J. (1977). "Dynamic pull out resistance of anchors in sand". Proc. Inter. Symp. Soil Structure-Interaction, Rourkee (India). Vol. 1, pp 389-397.

Coulomb, C.A. (1776). "Essai sur une application des regles de maximis et minimis a quelques problems de statique relatifs a l'architecture". Memoires de Mathematiques et de Physiques. Academie Royale des Sciences. Vol. 7, Paris (France).

Cragg, C.B.H. (1985). "Field uplift tests in cohesionless soils". Report 85-186-K. Ontario Hydro Research Division.

Cragg, C.B.H., Krishnasamy, S.G. & Radhakrishna, H.S. (1986). "Uplift design of transmission tower foundations in sand, a probabilistic approach". Inter. Symp. Probabilistic Methods Applied to Electric Power Systems, Toronto (Canada). pp 1-11.

Danziger, F.A. Pereira Pinto, R. & Danziger, B.R. (1989). "Uplift load tests on grillages for guyed towers in Itaipu transmission system". Proc. 12th Int. Conf. Soil Mech. Fdn. Engng, Rio Janeiro (Brasil). Vol. 2, pp 1193-1196.

Das, B. M. & Jones, A. D. (1982). "Uplift capacity of rectangular anchors in sand". Transportation Research Record 884. pp 54-58.

Das, B.M. & Yang Jin- Kaun (1987). "Uplift of model group anchors in sand". Foundations for transmission line towers, Geotech. Special Publ. No 8. New York (USA): ASCE, pp 57-71.

- Davie, J.R. (1973). "Behaviour of cohesive soils under uplift forces". Ph.D Thesis. Glasgow University (Scotland).
- Davidson, J.L., Mortensen, R.A. & Barreiro, D. (1981). "Deformations in sand around a cone penetrometer tip". Proc. 10th Inter. Conf. Soil Mech. Fdn. Engng., Stockholm (Sweden). Vol. 2, pp 467-470.
- De Beer, E. (1965). "Influence of the mean normal stress on the shearing strength of sand". Proc. 6th Int. Conf. Soil Mech. Fdn. Engng., Montreal (Canada). Vol. 1, pp 165-169.
- De Mello, V.F.B. (1971). "The standard penetration test". Proc. 4th Pan American Conf. Soil Mechs. Fdn. Engng., San Juan (Puerto Rico), Vol.1, pp. 1-86.
- Desrues, J., Lanier, J. & Stutz, P. (1985). "Localisation of the deformation in tests on sand samples". Engineering Fracture Mechanics. Vol. 21, No 4, pp 909-921.
- Dickin, E.A. (1973). "Influence of grain shape and size upon the limiting porosities of sand". Evaluation of relative density and its role in geotech. projects involving cohesionless soil, ASTM STP 523. pp 113-120.
- Dickin, E.A. (1988). "Uplift behaviour of horizontal anchor plates in sand". Proc. ASCE, Journal Geotech. Engng. Vol. 114, No 11, pp
- Eggestad, A. (1964). "Deformation measurements below a model footing on the surface of dry sand". Norwegian Geotechnical Institute, publ. No 58, pp 29-35.
- El-Beik, A.H.A (1973). "Photogrammetry in centrifugal testing of soil models". Photogrammetric Record. Vol. 7 (41), pp 538-554.
- El Rayes, M.K. (1965). "Behaviour of cohesionless soils under uplift forces". Ph.D Thesis. Glasgow University, Glasgow (Scotland).
- Esquivel-Diaz, R.F. (1967). "Pull out resistance of deeply buried anchors". M.Sc Thesis. Duke University, North Carolina (USA).
- Fadl, M.O. (1981). "The behaviour of plate anchors in sand". Ph.D Thesis. Glasgow University, Glasgow (Scotland).
- Feeser, V. (1984). "Optographic trace recording: a new method of strain measurement in geotechnical testing". Geotechnique 34. No 2, pp 277-281.
- Frydman, S. & Shaham, I. (1989). "Pull out capacity of slab anchors in sand". Canadian Geotechnical Journal. Vol. 26 (3), pp 385-400.
- Gerrard, C.M. & Cameron, D.A. (1988). "Inclined uplift capacity of various ground anchors". Proc. 5th Austr.-New Zealand Conf. Geomech., Sydney (Australia), pp 497-502.
- Gibbs, H.J. & Holtz, W.G. (1957). "Research on determining the density of sands by spoon penetration testing". Proc. 4th Inter. Conf. Soil Mech. Fdn. Engng., London (England). Vol. 1, pp 35-39.
- Ghosh, S.K. (1988). Analytical Photogrammetry. Pergamon Press (2nd Ed.).
- Hanna, T.H. & Carr, R.W. (1971). "The loading behaviour of plate anchors in normally and overconsolidated sands". Proc. 4th Conf. Soil Mech. Fdn. Engng., Budapest (Hungary), pp 589-600.

- Hanna, T.H., Sparks, R. & Yilmaz, M. (1972). "Anchor behaviour in sand". Proc. ASCE, Jour. Soil Mech. Fdn. Div. Vol. 98, No SM11, pp 1187-1208.
- Hanna, T.H. (1982). Foundations in tension, ground anchors. Trans. Tech. Publ. No 6.
- Holubec, I. & d'Appolonia, E. (1973). "Effect of particle shape on the engineering properties of granular soils". Evaluation of relative density and its role in geotech. projects involving cohesionless soil, ASTM STP 523. pp 304-318.
- Harvey, R.C. & Burley, E. (1973). "Behaviour of shallow ground anchorages in cohesionless sand". Ground Engineering. Vol. 6 (5), pp 48-55.
- Harvey, R.C. Andreadis, A. & Tsangarides, S.N. (1980). Discussion on "Uplift testing of model drilled shafts in sand". Proc. ASCE, Journ. Geotech. Engng. Div. No GT5, pp. 575-579.
- James, J.P. (1967). "Stress displacement relationship for sand subjected to passive pressure". Ph.D Thesis. Manchester University, Manchester (England).
- James, R.G. (1972). "Determination of strains in soils by radiography". Lectures notes CUED/C-Soils/LN 1(a). Cambridge University.
- Jamiolkowski, M., Ghionna V.N, Lancelotta, R. & Pasqualini, E. (1988). " New correlations of penetration tests for design practice". Penetration Testing 88, ISOPT I. Orlando (USA), Vol. 1, pp. 263-296.
- Karal, K. (1982). "Anchors for wave energy converters". Proc. 2nd Inter. Symp. Wave Energy Utilization, Trondheim (Norway), pp 211-228.
- Kerr, N. (1976). "A self burying anchor of considerable holding power". Proc. 8th Annual Off. Tech. Conf., Houston (USA), pp 447-458.
- Kolbuszewski, J.J. (1948a). "An experimental study of the maximum and minimum porosities of sands". Proc. 2nd Int. Conf. Soil Mech. Fdn Engng., Rotterdam (Netherlands). Vol. 1, pp 158-167.
- Kolbuszewski, J.J. (1948b). "General investigation of the fundamental factors controlling the loose packing of sands". Proc. 2nd Int. Conf. Soil Mech. Fdn Engng., Rotterdam (Netherlands). Vol. 2, pp 47-49.
- Kolbuszewski, J.J. & Jones, R.H. (1961). "The preparation of sand samples for laboratory testing". Proc. Midland Soil Mech. Fdn. Engng. Soc., Vol. 4, pp 107-123.
- Kolbuszewski, J.J. & Frederick (1963). "The significance of particle shape and size in the mechanical behaviour of granular materials". Proc. Eur. Conf. on Settlement Computation, Wiesbaden (West Germany). p 139
- Konstantinidis, B., Pacal, A.J. & Shively, A.W. (1987). "Uplift capacity of drilled piers in desert soils". Foundations for transmission towers, Geotech. Special Publ. No 8. New York: ASCE, pp. 128-141.
- Koutsabeloulis, N.C. & Griffiths, D.V. (1989). "Numerical modelling of the trap door problem". Geotechnique 39. No 1, pp 77-89.
- Kovacs, W.D. & Yokel, F.Y. (1979). "Soil and rock anchors for mobile homes—state of the art". Report NBS Building Science Series 107. National Bureau of Standards, Washington D.C. (USA).

- Krumbein, W.C. (1941). "Measurement and geological significance of shape and roundness of sedimentary particles". Journ. Sedimentary Petrology. Vol. 11, pp 64-72.
- Kulhawy, F.H., Kozera, D.W. & Withlam, J.L (1979). "Uplift testing of model drilled shafts in sand". Proc. ASCE, Journ. Geotech. Engng. Div. No GT1, pp. 31-47.
- Kulhawy, F.H. (1985). "Uplift behaviour of shallow soil anchors—an overview". Proc. ASCE, uplift behaviour of anchor foundations in soil, Detroit (USA), pp 1-25.
- Kulhawy, F.H., Trautmann, C.H. & Nicolaides, C.N. (1987). "Spread foundation in uplift: experimental study". Foundations for transmission line towers, Geotech. Special Publ. No 8. New York (USA):ASCE, pp 96-109.
- Kupferman, M. (1974). "The behaviour of embedded marine anchor flukes subjected to static and cyclic loading". Ph.D Thesis. Massachussets University, Amherst (USA).
- Larsen, P. (1989). "Suction anchors as an anchoring system for floating offshore constructions". Proc. 21st Annual Off. Tech. Conf., Houston (USA). Vol. 2, pp 535-540.
- Low, K.S (1986). "Pile-anchor response to monotonic and repeated loadings". Ph.D Thesis. Sunderland Polytechnic, Sunderland (England).
- Maddocks, D.V. (1978). "The behaviour of model ground anchors installed in sand and subjected to pull out and repeated loading". Ph.D Thesis. Bristol University, Bristol (England).
- Malyshev, M.V. (1971). "Slip lines and displacement paths of particles in a cohesionless medium". Soil Mech. and Fdn. Engng. Vol. 6, pp 379-386. Translated from Osnovaniya, Fundamenty i mekhanika Gruntov.
- Mariupolskii, L.G. (1965). "The bearing capacity of anchor foundations". Soil Mech. and Fdn. Engng. Vol. 2, No 1, pp 26-32. Translated from Osnovaniya, Fundamenty i mekhanika Gruntov.
- Matsuo, M. (1967). "Study of the uplift resistance of footings (I)". Soils & Foundations. Vol. 7, No 4, pp 1-37.
- Matsuo, M. (1968). "Study of the uplift resistance of footings (II)". Soils & Foundations. Vol. 8, No 1, pp 18-48.
- Meyerhof, G.G. (1951). "The ultimate bearing capacity of foundations". Geotechnique 2. No 4, pp. 301-333.
- Meyerhof, G.G. & Adams, J.D. (1968). "The ultimate uplift capacity of foundations". Canadian Geotechnical Journal. Vol. 5 (4), pp 225-244.
- Moore, J.F.A. (1973). "The photogrammetric measurement of constructional displacements of a rockfill dam". Photogrammetric Record. Vol. 7 (42), pp 628-648.
- Morin, J. (1988). "Density of granular materials derived from X-ray photographs: calibration, reliability and recommended procedures". Canadian Geotechnical Journal. vol. 25, pp. 488-499.
- Morota, (1989). Personal Communication.

- Murray, E.J. & Geddes, J.D. (1987). "Uplift of anchor plates in sand". Proc. ASCE, Jour. Geotech. Engng., Vol. 113, No 3, pp 202-215.
- Nair, D. & Duval, P.S. (1982). "Design Concepts and strategies for guyed tower platforms". Proc. 3rd Inter. Conf. Behaviour of Offshore Structures, Cambridge, Massachusetts (USA). Vol. 2, pp 123-146.
- Nikitin, V.M. & Nesmelov, N.S. (1973). "Experimental investigation of the strain state of foundation beds by the Moire method". Soil Mech. and Fdn. Engng., Vol. 3, pp 187-191. Translated from Osnovaniya, Fundamenty i mekhanika Gruntov.
- Nixon, I.K. (1982). "SPT, state-of-the art report". Proc. 2nd Eur. Symp. Penetration testing, ESOPT II. Amsterdam (Netherlands), Vol. 1, pp. 3-24.
- Ostermayer, H.D. & Scheele, F. (1978). "Research on ground anchors in non cohesive soils". Revue Francaise de Geotechnique, No 3, pp 92-97.
- Ovesen, N.K. (1962). "Cellular cofferdams, calculation methods and model tests". Danish Geotech. Institute, Bulletin 14, Copenhagen (Denmark).
- Ovesen, N.K. (1981). "Centrifuge tests of the uplift capacity of anchors". Proc. 10th Inter. Conf. Soil Mech. Fdn. Engng., Stockholm (Sweden). Vol. 1, pp 717-722.
- Pater, C.J. & Nieuwenhuis, J.D. (1987). "Method for measuring the deformations of sand". Geotechnique 38. No 4, pp 581-585.
- Ponniah, D.A. (1984). "Behaviour of plate anchors in cohesive soils under static and cyclic loads". Ph. D Thesis. Glasgow University (Scotland).
- Powers, M.C. (1953). "A new roundness scale for sedimentary particles". Journ. Sedimentary Petrology. Vol. 23, No 2, pp 117-119.
- Prange, B. (1971). "The state of telemetry in soil mechanics". Proc. Roscoe Memorial Symposium, Cambridge (England), pp 476-488.
- Rao, K.S.S. & Venkatesh, K.H. (1985). "Uplift behaviour of short piles in uniform sand". Soils & Foundations. Vol. 25, No 4, pp 1-7.
- Rittenhouse, G. (1943). "A visual method of estimating two-dimensional sphericity". Journ. Sedimentary Petrology. Vol. 13, No 2, pp 79-81.
- Rocha, M. (1957). "The possibility of solving soil mechanics problems by the use of models". Proc. 4th Inter. Conf. Soil Mech. Fdn. Engng., London (England). Vol. 1, pp 183-188.
- Roraas, H. & Hagen, O. (1989). "Method for design, construction, and setting of very high capacity anchors". Proc. 21st Annual Off. Tech. Conf., Houston (USA). Vol. 2, pp 585-598.
- Roscoe, K.H., Arthur, J.R.F. & James, R.G. (1963). "The determination of strains in soils by an X-ray method". Civ. Engng. and Publ. Work Rev., pp 1009-1012.
- Roscoe, R.H. (1968). "Soils and model tests". Journ. Strain Analysis. Vol. 3, No 1, pp 57-64.
- Rowe, R.K. & Davis, E.H. (1982). "The behaviour of anchor plates in sand". Geotechnique 32. No 1, pp 25-41.

- Saeddy, H.S. (1971). "Analytical and experimental stability of earth anchors". Ph.D Thesis. Oklahoma State University (USA).
- Saeddy, H.S. (1975). "Analytical determination of anchor capacity in sand". Proc. 1st Baltic Conf. Soil Mech. Fdn. Engng., Gdansk (Poland). Vol. 3, pp 199–212.
- Saeddy, H.S. (1987). "Stability of circular vertical earth anchors". Canadian Geotechnical Journal. Vol. 24, pp 452–456.
- Sahota, B.S. (1979). "The breakout behaviour of a suction anchor embedded in a granular soil". M. Phil Thesis, Robert Gordon's Institute of Technology, Aberdeen (Scotland).
- Sarac, Dz. (1989). "The uplift capacity of shallow buried anchor slabs". Proc. 12th Int. Conf. Soil Mech. Fdn. Engng., Rio Janeiro (Brasil). Vol. 2, pp 1213–1216.
- Shaheen, W.A., Chang, C.S. & Demars, K.R. (1987). "Field evaluation of plate anchor theories in sand". Proc. 19th Annual Off. Techn. Conf., Houston, Texas (USA). Vol. 1, pp 521–530.
- St John, H.D. (1980). "A review of current practice in the design and installation of piles for offshore structures". OT-R-8002. Department of Energy, Offshore Research & Development.
- Stewart, W. (1985). "Uplift capacity of circular plate anchors in layered soil". Canadian Geotechnical Journal. Vol. 22, pp. 589–592.
- Stewart, W. (1988). "Plate anchors in sand under static and cyclic loads". Ph.D Thesis. Glasgow University, Glasgow (Scotland).
- Stewart, W.P., True, D. & Jones, T. (1989). "Deep embedment plate anchors". Proc. 21st Annual Offshore. Techn. Conf., Houston, Texas (USA). Vol. 2, pp 575–584.
- Sutherland, H.B. (1965). "Model studies for shaft raising through cohesionless soil". Proc. 6th Int. Conf. Soil Mech. Fdn. Engng., Montreal (Canada). Vol. 2, pp 410–413.
- Sutherland, H.B., Finlay, T.W. & Fadl, M.O. (1982). "Uplift capacity of embedded anchors in sand". Proc. 3rd Int. Conf. Behaviour of Offshore Structures, Cambridge, Massachusetts (USA). Vol. 2, pp 451–463.
- Sutherland, H.B. (1988). "Uplift resistance of soils". 28th Rankine Lecture. Geotechnique 38, No 4, pp 491–516.
- Tagaya, K., Tanaka, A. & Aboshi, H. (1983). "Application of finite element method to pull out resistance of buried anchor". Soils & Foundations. Vol. 23, pp 91–104.
- Tagaya, K., Scott, R.F. & Abshi, H. (1988). "Pull out resistance of buried anchor in sand". Soils & Foundations. Vol. 28, No 3, pp 114–130.
- Taylor, R.J. (1982). "Interaction of anchors with soil and anchor design". Report TN-1627. Naval Civil Engng. Lab., Port Hueneme, California (USA).
- Terzaghi, K. (1956). Theoretical soil mechanics. John Wiley edition.

- Trautmann, C.H., O'Rourke, T.D. & Kulhawy, F.H. (1985). "Uplift force displacement response of buried pipe". Proc. ASCE, Jour. Geotech. Engng. Vol. 111, No 9, pp 1061-1076.
- Trautmann, C.H., Kulhawy, F.H. & O'Rourke, T.D. (1985). "Sand density for laboratory studies". Geotechnical Testing Journal. No 8, pp 159-165
- Trautmann, C.H. & Kulhawy, F.H. (1988). "Uplift load displacement behaviour of spread foundations". Proc. ASCE, Jour. Geotech. Engng. Vol. 114, No 2, pp 168-184.
- Tsangarides, S.N. (1978). "The behaviour of ground anchors in sand". Ph.D Thesis. Queen Mary College, London University (England).
- Tucker, K.D. (1987). "Uplift capacity of drilled shafts and driven piles in granular soils". Foundations for transmission line towers. Geotech. Special Publ. No 8. New York (USA): ASCE, pp. 142-159.
- Turpin, K.L. (1958). "Soil movements around a circular pile". Photogrammetric Record. Vol. 5, No 12, pp 24-32.
- Vaid, Y.P. & Negussey, D. (1984). "Relative density of pluviated sand samples". Soils & Foundations. Vol. 24, No 2, pp 101-105.
- Vallerga, B., Seed, H.B., Monithmith, C. & Cooper, R.S. (1957). "Effects of shape, size and surface roughness of aggregate particles on the strength of granular material". ASTM, Special Techn. Publ. STP 212. pp. 63-74.
- Veress, S. & Sun, L. (1978). "Photogrammetric monitoring of a gabion wall". Photog. Engng. and Remote Sensing. Vol. 44, No 2, pp 205-211.
- Vermeer, P.A. & Sutjiadi, W. (1985). "The uplift resistance of shallow embedded anchors". Proc. 11th Int. Conf. Soil Mech. Fdn. Engng., San Francisco (USA). Vol. 3, pp 1635-1638.
- Vesic, A.S. (1971). "Breakout resistance of objects embedded in ocean bottom". Proc. ASCE, Journ. Soil Mech. Fdns. Div. Vol. 97, No SM 9, pp 1183-1205.
- Vesic, A.S. (1972). "Expansion of cavities in infinite soil mass". Proc. ASCE, Journ. Soil Mech. Fdns. Div. Vol. 98, No SM 3, pp 265-29166.
- Vesic, A.S. (1975). "Principles of pile foundation design". Soil Mechanics series. No 38, School of Engineering, Duke University (USA).
- Wadell, H. (1935). "Volume, shape and roundness of quartz particles". Journal of Geology. Vol. 43, pp 250-280.
- Walker, B.P. & Whitaker, T. (1967). "An apparatus for forming uniform beds of sand for model foundation tests". Geotechnique 17. No 2, pp 161-167.
- Wang, M.C., Demars, K.R. & Nacci, V.A. (1978). "Applications of suction anchors in offshore technology". Proc. 10th Annual Off. Techn. Conf., Houston, Texas (USA), pp 1311-1320.
- Weikart, A.M. & Clemence, S.P. (1987). "Helix anchor foundations-Two case histories". Foundations for transmission line towers. Geotech. Special publ. No 8. New York (USA):ASCE, pp. 72-80.
- Welsh, N. (1986). "Photogrammetry in engineering". Photogrammetric Record. Vol. 12, No 67, pp 25-44.

- Wickens, E.H. & Barton, N.R. (1971). "The application of photogrammetry to the stability of excavated rock slopes". Photogrammetric Record. Vol. 7, No 37, pp 46-54.
- Wong, K.W. & Vonderohe, A.P. (1978a). "Measurement of displacements around tunnel models by motion parallax". Inter. Archives of Photogrammetry. Vol. 22 (5), pp 12-21.
- Wong, K.W. & Vonderohe, A.P. (1978b). "Photogrammetric measurement of displacements around tunnels in sandy soils". Proc. 44th Annual Meeting Amer. Soc. Photog. Washington DC (USA), pp 373-389.
- Wong, K.W. & Vonderohe, A.P (1981). "Planar displacement by motion parallax". Photog. Engng. and Remote Sensing. Vol. 47, No 6, pp 769-777.
- Wood, D.M (1984). "Experiments with crushed glass". CUED/D-Soils TR161. Cambridge University (England).
- Yokel, F.Y., Chung, R.M., Rankin, F.A. & Yancey, C.W.C. (1982). "Load-displacement characteristics of shallow soil anchors". NBS building Science Series 142. National Bureau of Standards, Washington DC (USA).
- Zakaria, I.B. (1986). "The effect on the uplift resistance of anchors of ground disturbance during placing". M.Sc Thesis. Glasgow University (Scotland).
- Zelasko, J.S., Krizek, R.J. & Tuncer, B.E. (1975). "Shear behaviour of sands as a function of grain characteristics". Proc. 7th Eur. Conf. Soil Mech. Fdn. Engng. Istanbul (Turkey). Vol. 1, pp 55-63.

APPENDIX I

I-a TRANSFORMATION OF COORDINATES

It is often necessary to establish the relationship between two coordinate systems in order to transfer a number of points from one to the other. There are numerous methods of transformation for use in three dimensional problems, simplified versions of which are applicable to two dimensional space. The effect of transformation of a body can be a simple change in location and attitude (i.e., without any change in shape and in size) or a complex one (i.e., change in both shape and size) or something in between, e.g., variation in size with no change in shape.

I-a-1 Three dimensional transformation

This is known as similarity transformation, it involves translations, rotations and a scale change. The three dimensional transformation involving no change in shape is symbolized by:

$$X = sM^T X + T_0 \quad \dots\dots\dots(II)$$

where $X = [x \ y \ z]^T$ coordinates after transformation

$X = [x \ y \ z]^T$ coordinates before transformation

$T_0 = [T_x \ T_y \ T_z]^T$ vector of three shifts indicating

the x, y, z coordinates of the origin of the

x, y, z system

$M =$ an orthogonal three angle rotation matrix

$s =$ scale factor

The primary rotation, (Ω) transforms the axes y z into the positions y_Ω and z_Ω , respectively (see Fig. 1a). This is expressed by the rotation matrix M_Ω .

$$M_\Omega = \begin{bmatrix} 1 & 0 & 0 \\ 0 & \cos\Omega & \sin\Omega \\ 0 & -\sin\Omega & \cos\Omega \end{bmatrix} \dots\dots\dots(12)$$

The coordinates of any point P in this, primary rotated, x_Ω , y_Ω , z_Ω system are:

$$\left. \begin{aligned} x_\Omega &= x \\ y_\Omega &= y \cos\Omega + z \sin\Omega \\ z_\Omega &= -y \sin\Omega + z \cos\Omega \end{aligned} \right\} \dots\dots\dots(13)$$

The second rotation (Φ) transforms the axes x_Ω and z_Ω into the position $x_{\Omega\Phi}$ and $z_{\Omega\Phi}$, respectively (see fig. 1b). This is expressed by the rotation matrix M_Φ .

$$M_\Phi = \begin{bmatrix} \cos\Phi & 0 & -\sin\Phi \\ 0 & 1 & 0 \\ \sin\Phi & 0 & \cos\Phi \end{bmatrix} \dots\dots\dots(14)$$

The coordinates of the same point P in the twice rotated $x_{\Omega\Phi}$, $y_{\Omega\Phi}$, $z_{\Omega\Phi}$ system are:

$$\left. \begin{aligned} x_{\Omega\Phi} &= x_\Omega \cos\Phi - z_\Omega \sin\Phi \\ y_{\Omega\Phi} &= y_\Omega \\ z_{\Omega\Phi} &= x_\Omega \sin\Phi + z_\Omega \cos\Phi \end{aligned} \right\} \dots\dots\dots(15)$$

The tertiary rotation (K) next transforms the axes $x_{\Omega\Phi}$ and $y_{\Omega\Phi}$ into positions $x_{\Omega\Phi K}$, and $y_{\Omega\Phi K}$, respectively (see Fig. 1c). This is expressed by the rotation matrix M_K .

$$M_K = \begin{bmatrix} \cos K & \sin K & 0 \\ -\sin K & \cos K & 0 \\ 0 & 0 & 1 \end{bmatrix} \dots\dots\dots(16)$$

The coordinates of the same point P now in the final, thrice rotated, $x_{\Omega\Phi K}$, $y_{\Omega\Phi K}$, $z_{\Omega\Phi K}$ system are:

$$\left. \begin{aligned} x_{\Omega\Phi K} &= x_{\Omega\Phi} \cos K + y_{\Omega\Phi} \sin K \\ y_{\Omega\Phi K} &= -x_{\Omega\Phi} \sin K + y_{\Omega\Phi} \cos K \\ z_{\Omega\Phi K} &= z_{\Omega\Phi} \end{aligned} \right\} \dots\dots\dots(17)$$

The final effect of all the three rotations is then expressed by the rotation matrix M as used in eq. 11, M^T being its transpose.

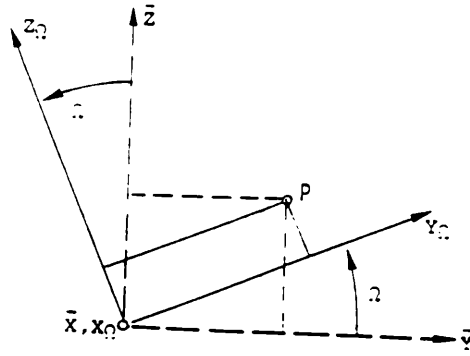
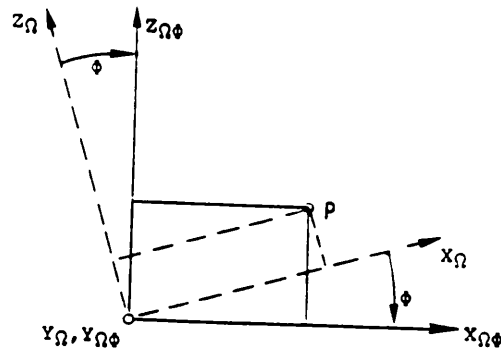
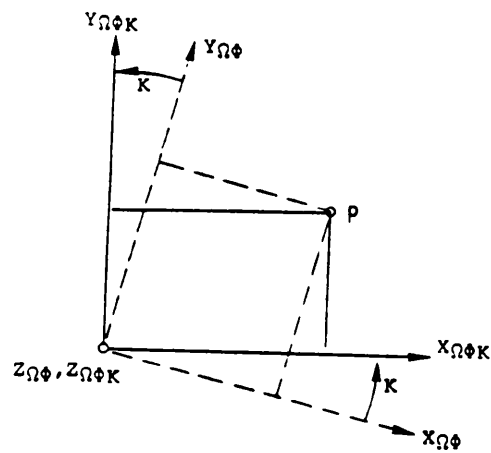
$$M = M_{\Omega} \cdot M_{\Phi} \cdot M_K \dots\dots\dots(18)$$

The elements of this rotation matrix can be expressed in various ways:

$$M^T = \begin{bmatrix} m_{11} & m_{21} & m_{31} \\ m_{12} & m_{22} & m_{32} \\ m_{13} & m_{23} & m_{33} \end{bmatrix} \dots\dots\dots(19)$$

or

$$M^T = \begin{bmatrix} \cos\phi \cos K & -\cos\phi \sin K & \sin\phi \\ \cos\Omega \sin K & \cos\Omega \cos K & -\sin\Omega \cos\phi \\ +\sin\Omega \sin\phi \cos K & -\sin\Omega \sin\phi \sin K & \\ \sin\Omega \sin K & \sin\Omega \cos K & \cos\Omega \cos\phi \\ -\cos\Omega \sin\phi \cos K & +\cos\Omega \sin\phi \sin K & \end{bmatrix} \dots (110)$$

Fig. Ia Primary Rotation, Ω Fig. Ib Secondary Rotation, ϕ Fig. Ic Tertiary Rotation, κ

Appendix II

